Cathodoluminescence Studies of Feldspars and Apatites from the Coldwell Alkaline Complex

by

Jian Xiong

CATHODOLUMINESCENCE STUDIES

OF

FELDSPARS AND APATITES FROM

THE COLDWELL ALKALINE COMPLEX

BY JIAN XIONG

A THESIS SUBMITTED IN PARTIAL FULFILMENT OF THE

REQUIREMENT FOR THE DEGREE OF

MASTER OF SCIENCE

SUPERVISOR: Dr. R.H. MITCHELL

DEPARTMENT OF GEOLOGY

LAKEHEAD UNIVERSITY

THUNDER BAY, ONTARIO

CANADA

MAY 1995

Lakehead University
OFFICE OF GRADUATE STUDIES & RESEARCH

TITLE OF THESIS: CATHODOLUMINESCENCE STUDIES OF FELDSPARS AND APATITES FROM THE COLDWELL ALKALINE COMPLEX

NAME OF STUDENT: JIAN XIONG

DEGREE AWARDED: M.Sc.

* * * * * * * * * * * * * * * * * * * *

This thesis has been prepared
under my supervision
and the candidate has complied
with the Master's regulations.

R.H. McKee

Signature of Supervisor

May 5, 1995

Date

To my wife, Julie Selway, for all her love and support.

CATHODOLUMINESCENCE STUDIES OF THE COLDWELL ALKALINE COMPLEX

Abstract

The Coldwell alkaline Complex is located on the north shore of Lake Superior, and consists of three Centers representing three magmatic episodes. Center I consists of gabbro, and layered and unlayered ferro-augite syenite. Center II consists of alkalic biotite gabbro, miaskitic nepheline syenite, amphibole nepheline syenite, perthitic nepheline syenites and recrystallized nepheline syenites. Center III consists of magnesio-hornblende syenite, ferro-edenite syenite, contaminated ferro-edenite syenite, and quartz syenite.

The textures and compositions of the feldspars and apatite from these three Centers were examined using cathodoluminescence (CL) and the scanning electron microscope (SEM). All of the colours described in the text refer to cathodoluminescence colours. The feldspars in Center I consist of light blue to light violet blue, optically homogeneous alkali feldspar; braid microperthite and incipient perthite; and irregular vein or patch perthite. The irregular vein and patch perthite contain light violet blue cryptoperthitic patches, light blue exsolved albite and dull blue exsolved K-feldspar. During late-stage fluid-induced alteration, these feldspars were replaced by violet secondary albite and purple secondary K-feldspar; and were coarsened by a deuteric antiperthitic rim. The Fe-rich antiperthitic rim consists of deep red secondary albite and brown secondary K-feldpsar. The later dominates in the upper series of the layered and unlayered syenites. The homogeneous alkali feldspar crystallized at high temperatures ≥700°C, exsolved into microperthite at 650-550°C and formed irregular vein and patch perthite at 520-420°C. Late-stage fluid-induced replacement and deuteric coarsening occurs at

relatively low temperatures 500-300°C.

The feldspars in Center II consist of light blue or light bluish grey oligoclase; light violet blue homogeneous alkali feldspar; and irregular vein or patch perthite. A few oligoclase crystals are mantled by a light blue alkali feldspar rim. Most of the irregular vein and patch perthite contain light blue exsolved albite and dull blue K-feldspar host; and some of them contain light violet blue to light violet unexsolved alkali feldspar patches in the core, and violet blue to dull blue cross hatched microcline along the margin. During late-stage fluid-induced deuteric alteration, the alkali feldspar was replaced by light violet blue to light violet secondary albite or dull blue to dark brown secondary K-feldspar along the margins; and the alkali feldspar was coarsened by a red to deep red secondary albite rim. The oligoclase crystallized at high temperatures 800-750°C, and the homogeneous alkali feldspar crystallized at ≥710-620°C. The perthite texture and the unexsolved alkali feldspar patches may have formed at 600-450°C. The K-feldspar host may have transformed to the cross-hatched microcline at ≈300°C. The deuteric coarsened and replaced secondary feldspar formed at low temperatures <350°C.

In the recrystallized nepheline syenites of Center II, the feldspar crystals are usually mantled with a relict core and a light violet blue recrystallized alkali feldspar rim. The relict cores usually are light blue albite or light violet homogeneous alkali feldspar.

The feldspars in Center III consist of zoned plagioclase crystals with light greenish blue andesine-oligoclase cores and light violet blue to light blue oligoclase-albite rims; light blue to blue homogeneous alkali feldspar, K-rich feldspar, braid microperthite and oscillatory zoned alkali feldspar; irregular vein perthite consisting of light blue to light violet exsolved albite and dull blue K-feldspar host; and regular to irregular vein antiperthite consisting of dull blue to dark blue exsolved K-feldspar and dull red to deep red albite host. Most irregular

vein antiperthite grains reveal alternating dull red, violet and deep red oscillatory zones. During late-stage fluid-induced alteration, most light blue to blue original alkali feldspar were coarsened by a deuteric antiperthite rim which consists of red secondary albite and dark brown secondary K-feldspar. The plagioclase crystallized at high temperatures about 900-750°C, the homogeneous alkali feldspar crystallized at ≥725-520, and the K-rich feldspar crystallized at 580-450°C. The microperthitic texture may have formed at 650-420°C, and the perthite and antiperthite textures may have formed at non-equilibrium temperatures about 520-350°C. The deuteric coarsened antiperthitic rim formed at temperatures <350°C.

The apatite crystals in the Coldwell complex exhibit a variety of CL textures which include: (1) uniform light pink to pink grains; (2) growth zones with a small brownish pink core and light pink to pink rims; (3) light pink to pink alternating oscillatory zones; (4) mantled grains with light pink to pink cores and brownish pink reaction rims. Some of the reaction rims are overgrown by light pink and yellow secondary apatite.

The light pink and pink CL colours in the apatite crystals are dominantly caused by Eu^{2+} activation, the brownish pink CL colour is dominantly caused by Dy^{3+}, Sm^{3+} and Pr^{3+}, and the yellow luminescent secondary apatite is characteristic of Dy^{3+} and Tb^{3+} activation. The brownish pink apatites have higher contents of total REE and Si than the light pink apatites. The yellow or light pink secondary apatites have relatively low contents of total REE and Si. The apatite crystals in the Coldwell complex are characterized by LREE-enrichment which is caused by the coupled substitution of $2Ca^{2+}+P^{5+}\rightleftarrows(REE^{3+}+REE^{2+})+Si^{4+}$. The Si content in the apatite crystals increase from Center I through Center II to Center III.

Acknowledgements

I would like to thank many people who assisted during the research for this thesis. I am grateful to Dr. Mitchell, my supervisor, for his academic guidance and patience while proofreading many copies of my thesis. Dr. Platt and I had many thought provoking thesis discussions. Dr. Kissin encouraged me to attend Lakehead University.

I would like to thank Al MacKenzie of the Lakehead University Instrumentation Laboratory for teaching me how use to the scanning electron microprobe and providing technical support. Anne Hammond and Reino Viitala made thin sections for this research.

I would also like to thank my wife, Julie Selway for supporting me and proofreading my thesis.

TABLE OF CONTENTS

LIST OF FIGURES

CHAPTER 1

CHAPTER 2

CHAPTER 3

CHAPTER 4

CHAPTER 5

5.1 Feldspars in the layered ferroaugite syenites, Center I

6.3 Recrystallized nepheline syenites, Center II

CHAPTER 7

7.1 Feldspars in the magnesio-hornblende syenite, Center III

7.2 Feldspars in the ferro-edenite syenite, Center III

CHAPTER 8

CHAPTER 9

CHAPTER 10

10.4 Apatites in the syenites, Center III

LIST OF TABLES

CHAPTER 1

THE NATURE OF CATHODOLUMINESCENCE AND INSTRUMENTATION

1.1. Introduction

Many natural minerals and synthetic crystals emit luminescence light due to irradiation by a high energy source, such as ultraviolet light, x-rays, electrons and ions. These luminescence crystals (or minerals) commonly contain impurities, or activator ions, (e.g., transition elements or REE) or have lattice defects (e.g., the dislocations). The impurity or defect is called the luminescence center and their host crystal (or mineral) is called a phosphor. Generally, luminescence light emission is produced by electron transitions within a crystal. The excited electrons lose their excess energy when they return to their initial ground state in the form of photons. The electron transitions in many luminescence materials are involved with the luminescence centers. If the luminescence is produced by an electron beam irradiation, it is called cathodoluminescence. If the luminescence is excited by light, such as ultraviolet light, it is called photoluminescence. Cathodoluminescence usually emits light in the visible range (about 400 to 700 nm, corresponding to about 3.1 to 1.8 eV), but sometimes it can be found in the ultra-violet (UV) and infra-red (IR) region.

Cathodoluminescence (CL) is a useful method for studying petrographic textures in geological samples (Smith and Stenstrom, 1965; Marfunin, 1979; Marshall, 1988; Remond et al, 1992). In general, CL analysis performed with an optical CL microscope can be

divided into two areas of study: microscopy and spectroscopy. In the former, luminescence images of interested regions of the sample can be displayed by a CL optical microscope; in the latter, a CL spectrum corresponding to a selected area of the sample can be obtained by a light spectrophotometer. In CL spectra, different luminescence colours are represented by luminescence peaks occurring at certain wavelengths with certain intensities. CL spectra provide important information, such as the identity of the activator ions (e.g., transition elements or REE) in the host mineral or the presence of lattice defects in the crystal. This information benefits the petrographic study of geological samples.

1.2. The theory of cathodoluminescence

1.2.1. Interaction of the electron beam with the surface of the crystal

When a primary electron beam irradiates a crystal (or solid) surface, some of the incident electrons may penetrate the surface and travel to some depth in the crystal, while other electrons are reflected from the crystal surface. The penetrating electrons lose their energy by elastic and inelastic collisions with the lattice ions along the electron trajectories, generating back-scattered electrons, secondary electrons, Auger electrons, x-rays and cathodoluminescence. This process is illustrated schematically in Fig. 1-1a.

When the incident electrons reach and penetrate the surface of a conductor, the activator ions in the crystal are excited by

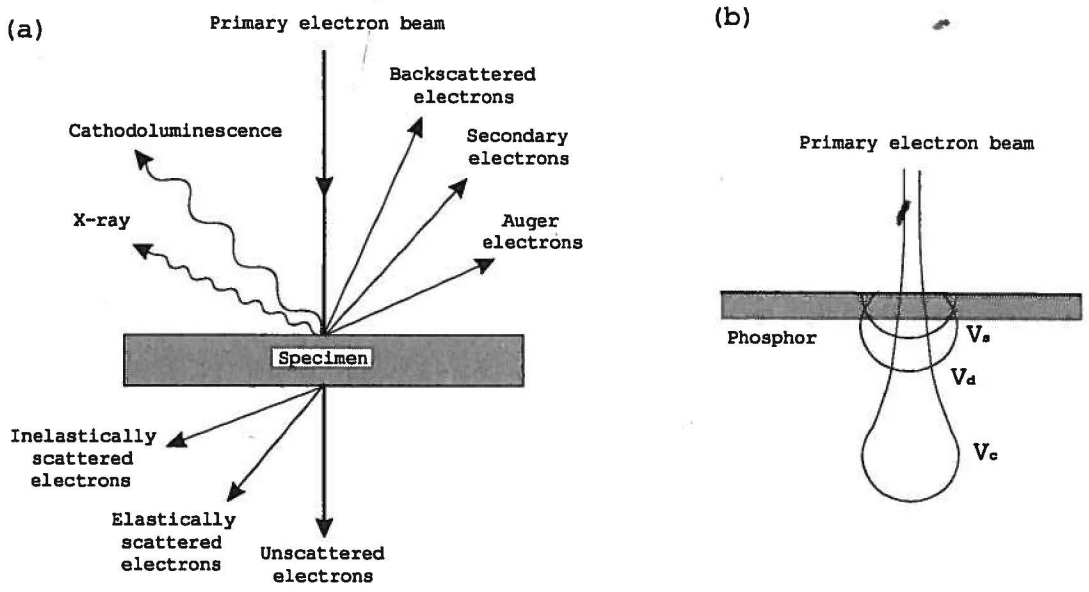

Fig. 1-1. (a) Schematic diagram of types of the major interactions due to electron beam interaction with a solid (After Yacobi and Holt, 1990); (b) Schematic representation of types of the plasmas in a phosphor. The V_s is the secondary electrons plasma. The V_d is a plasma which is generated by activator ions (direct excitation). The V_c is a plasma which is generated by mobile electrons and holes (indirect excitation) in the crystal (After Ozawa, 1990).

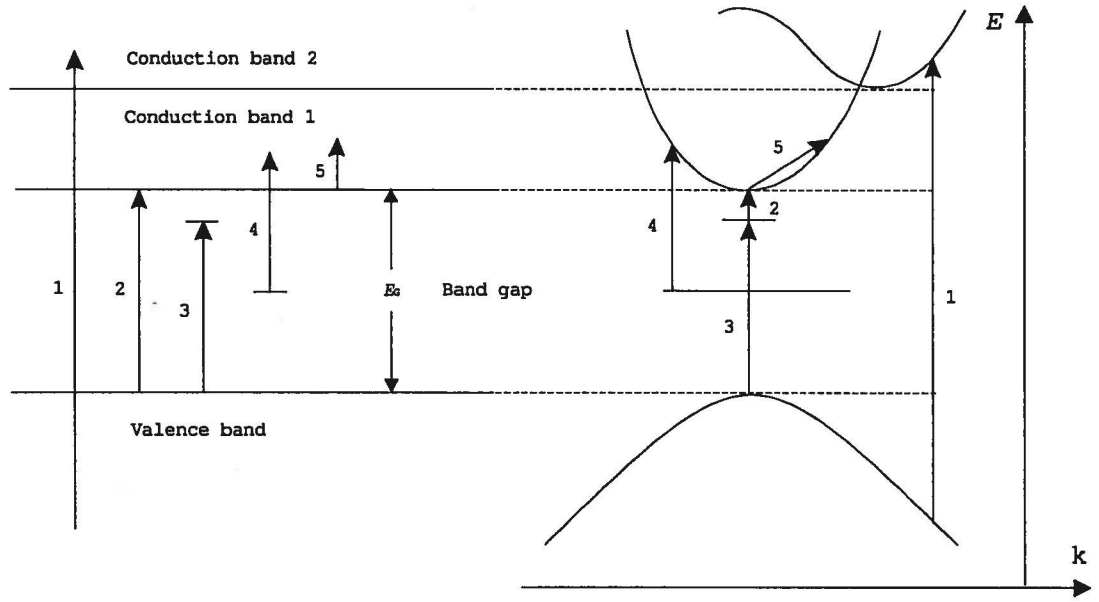

Fig. 1-2. Characteristic types of optical transitions shown both for the flat-band model and for the energy (E) vs wave vector (k) plot. (1) Excitation from the valence band to the higher energy conduction band, (2) excitation across the band gap, (3) exciton formation, (4) excitation from impurities (activator ions), (5) free-carrier excitation (After Bube, 1992).

secondary electrons and electron-hole pairs. According to the incident electron scattering hypothesis (Ozawa, 1990), the incident electrons penetrate the surface of the crystal and excite the lattice ions in the crystal which are assumed to generate a plasma with a volume V_d (Fig. 1-1b). The volume V_d is defined by the energy of the incident electrons. If the activator ions in the crystal are only excited by the plasma (V_d), all CL data must be explained by this plasma model, but CL is generated by a plasma which has a volume greater than the volume V_d.

The electron plasma also produces electron-hole pairs in the final step of the energy loss process within the crystal. These electron-hole pairs are mobile carriers inside the crystal and can leave the volume V_d. Some of these mobile carriers are recombined with the activator ions generating a plasma with a volume V_c. This volume V_c is defined by the migration distance of the electrons and the holes. The volume V_c is always greater than volume V_d (Fig. 1-1b).

Therefore, the activator ions in the crystal are excited by both plasmas: plasma V_d (direct excitation) and the mobile carriers plasma V_c (indirect excitation). Both plasmas giving rise to the same characteristic activator luminescence which cannot be distinguished by the luminescence spectrum alone (Ozawa, 1990). However, the concentration dependence curve (CD) of luminescence intensity (I) of the activator ions may provide more information on the different types of excitation (see the next section).

For semiconductors and insulators, crystals are covered with a

layer of surface-recombination (SR) centers of mobile electrons and holes. If the incident electrons can not penetrate the SR layer, the crystal shows no luminescence, or shows a faint luminescence which is due to the direct excitation of the activator ions (V_d). If the incident electrons penetrate through the SR layer, the crystal shows an intense luminescence which is produced by the recombination of the electron-hole pairs of the activator ions in the crystal volume (V_c) below the SR layer of luminescence (Ozawa, 1990).

The process of incident electron interaction with the surface of the crystal, may be much more complicated than the above assumptions, such as the surface-bound electrons effect. However, an ordinary industrial phosphor study only assumes that the cathodoluminescence is generated by the incident electron beam which reaches and penetrates the crystal surface generating secondary electrons and the electron-hole pairs of activator ions in the crystal.

1.2.2. Interpretation of cathodoluminescence by band theory

Phosphors and semiconductors luminescence processes can be interpreted by the band theory of solid state physics. In band theory application to cathodoluminescence, the CL emission spectra can be divided into intrinsic and extrinsic luminescence (Holt, 1974; Marfunin, 1979; Yacobi and Holt, 1990; Remod et al., 1992).

Intrinsic luminescence

The intrinsic luminescence emission is a fundamental or edge emission. The luminescence emission peak may have a near Gaussian-shape and photon energy $h\nu = E_g$ (Fig. 1-2). This is a result of the electron transitions from the conduction band to the valence band. By definition in solid state physics, properties of materials which are associated with electrons excited across band gaps at room temperature are called intrinsic. Intrinsic luminescence emission is produced by the inverse of the mechanism responsible for the fundamental absorption edge (Fig 1-2, inverse route 2). This intrinsic luminescence is also called self-activated luminescence.

The electron transitions between the conduction band and the valence band can be divided into direct and indirect transitions. A direct transition is represented by a vertical line across the narrowest part of the energy gap when the extreme of conduction and valence bands occur at same wave vector (k). This transition only produces a photon (Fig. 1-3a). According to quantum theory, the direct transition yields a straight line with an energy intercept of E_{gd} (direct band gap) on the plot of a^2 (absorption constant) vs $\hbar\omega_{pt}$ (photon energy) diagram (Fig 1-3a, insert diagram). Thus the direct band gap is given by $E_{gd} = \hbar\omega_{pt}$.

An indirect transition occurs when the two extremes of the conduction and valence bands have different wave vectors (k). So that a transition from the top of the valence band to the bottom of the conduction band requires a change of both energy and wave vector by the participating phonon ($\hbar\omega_{pn}$) (Fig 1-3b). The indirect

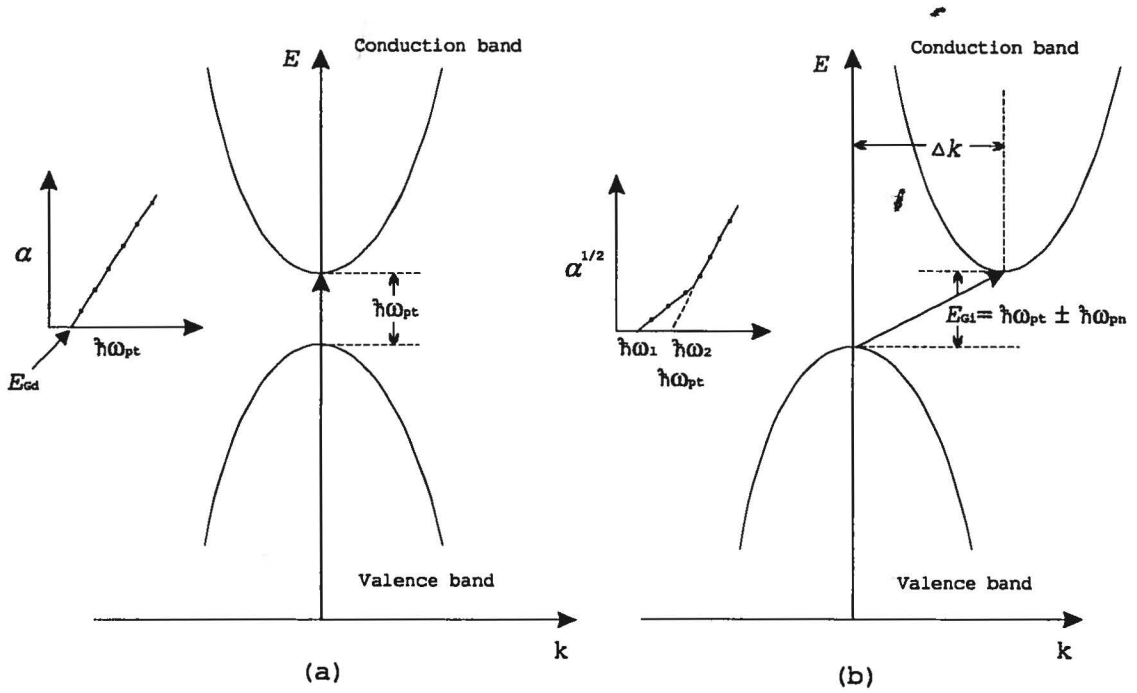

Fig. 1-3. Direct and indirect electron transitions between the valence band and the conduction band. (a) direct transition; (b) indirect transition. Inserts show the variation of absorption constant with phonon energy expected for each type of transition (After Bube, 1992).

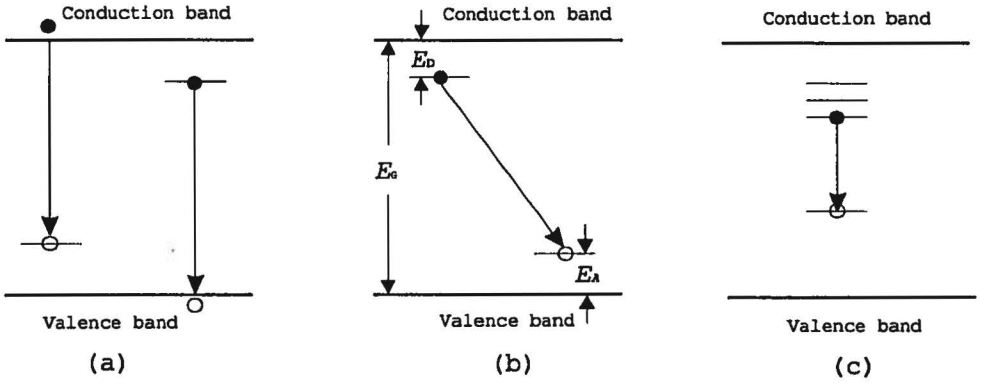

Fig. 1-4. Electron transition model for extrinsic luminescence. (a) Classical model; (b) pair-recombination model; (c) recombination within the atomic levels of an impurity ion (After Bube, 1992).

transitions are second-order processes with a smaller absorption constant than for the direct transition. A plot of $a^{1/2}$ vs $\hbar\omega_{pt}$ gives two straight line segments with intercepts on the energy axis of $\hbar\omega_1$ and $\hbar\omega_2$ as indicated in Fig. 1-3. Thus the indirect band gap is given by $E_{ai} = (\hbar\omega_1 + \hbar\omega_2)/2$, and the participating phonon energy is given by $\hbar\omega_{pn} = (\hbar\omega_2 - \hbar\omega_1)/2$.

1.2.3. Extrinsic luminescence

Extrinsic luminescence emission is dominated by the impurities (activator ions) energy levels in the material at room temperature as defined by solid state physics. Because the luminescence is caused by impurities (activator ions) or other defects in the material, the luminescence emission peaks are characteristic of the particular impurity (activator ion). Thus extrinsic luminescence is due to the electron transitions within the forbidden energy gap of the localized impurity energy level.

Luminescence occurring through impurities associated with the recombination of electrons and holes can be described by one of three models in Fig 1-4 (Bube, 1992). (1) The classical model involves the recombination between a free carrier, either an electron or hole, with a trapped carrier of the opposite charge (Fig 1-4a). If the free carrier is an electron, the model is known as the Klasens-Schoen model, whereas if the free carrier is a hole, the model is known as the Lambe-Klick model. These processes account for most of the observed cases of the luminescence.

(2) The pair recombination model (the Williams-Prener model),

this transition involves a donor-acceptor pair recombination (Fig 1-4b). The donor refers to an impurity which can contribute electrons to the conduction band, and the acceptor refers to an impurity which can borrow electrons from the valence band thus producing holes in the valence band. At a shallow energy level (which is commonly associated with trivalent and pentavalent impurities), the donor is usually trapped just below the bottom of the conduction band, whereas the acceptor is trapped slightly above the top of the valence band. The donor-acceptor also can be trapped at a deep energy level (within the band gap). The energy of the transition at a deep level is much smaller than that at a shallow level, and may result in the emission of photons in the visible and near-infrared ranges in some wide band-gap materials (Yacobi and Holt, 1990). The wave function of the electron trapped at the upper level must appreciably overlap the function of the hole trapped at the lower level for a large probability of a transition occurring (Bube, 1992). This pair-recombination model accounts for the majority of the observed cases of high-efficiency luminescence.

(3) The recombination within the atomic levels of an impurity (Fig. 1-4c), the excitation and emission is due to an electron transition within the atomic levels of the crystal. The electron transition has no necessary involvement of the crystal itself except as its energy levels are perturbed by the crystal field. As a result of this type perturbation, the energy levels of the f-d orbitals of the impurities (activator ions) are usually separated by crystal field splitting. The inner shell of the impurities

(activator ions) usually has an incomplete configuration, such as in REE ions and transition metal elements.

1.2.4. Direct and indirect excitation mechanisms in CL

In an industrial phosphors study, the direct and indirect excitations of the activator ions by the electron beam irradiation were developed not on the basis of the band structure theory, but on the mechanisms of the migration of the electrons and holes in the crystal. The direct and indirect excitations of activator ions by incident electron beam have been studied by Ozawa (1990) in industrial phosphors. The direct excitation and indirect excitation by the electron beam irradiation can be distinguished by the shape of the concentration dependence (CD) curve in the diagram of the concentration vs. the luminescent intensity (I) of the activator ions in the crystal. If the activator ions in the crystal are directly excited by incident electrons, the CD curve has an unit straight line slope at low concentrations of the activator ions where the self-concentration quenching mechanisms are not involved (Fig 1-5). The unit slope of the CD curve indicates no crystal size effect for the direct excitation.

If the activator ions in the crystal are indirectly excited by incident electrons, the luminescence is produced by radioactive recombination of mobile electrons and holes. The mobile electrons and holes in the crystal, which can be produced by a high energy source of irradiation, e.g. an electron beam, has energy greater than the band gap energy E_g. Thus the activator ions are excited by

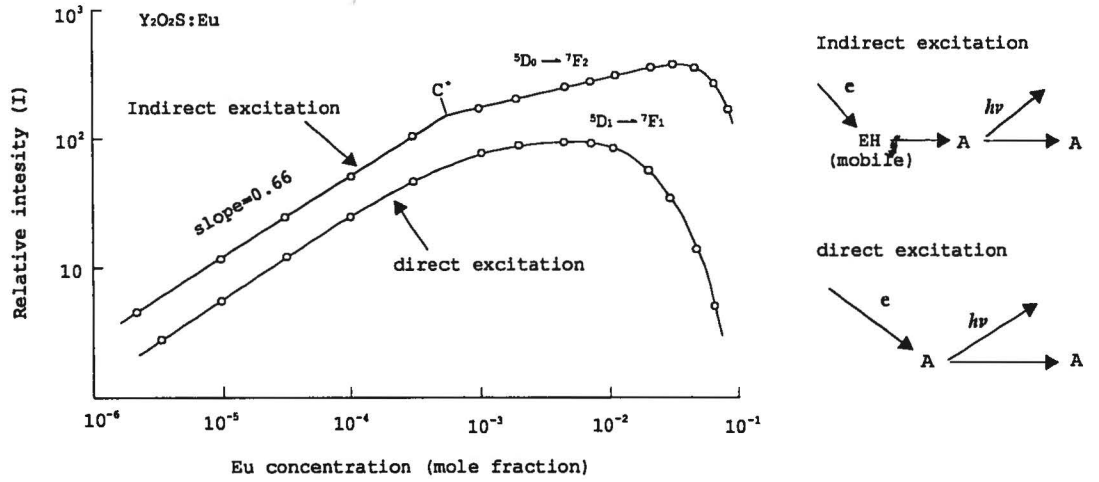

Fig. 1-5. Difference in concentration dependence (CD) curves with types of excitation mechanisms of activator ions (Eu) by incident electrons. The direct excitation exhibits no crystal size effect and the CD curve has a slope of unity. The indirect excitation exhibits crystal size effect and the CD curve has two slopes with an inflection point at C* (After Ozawa, 1990).

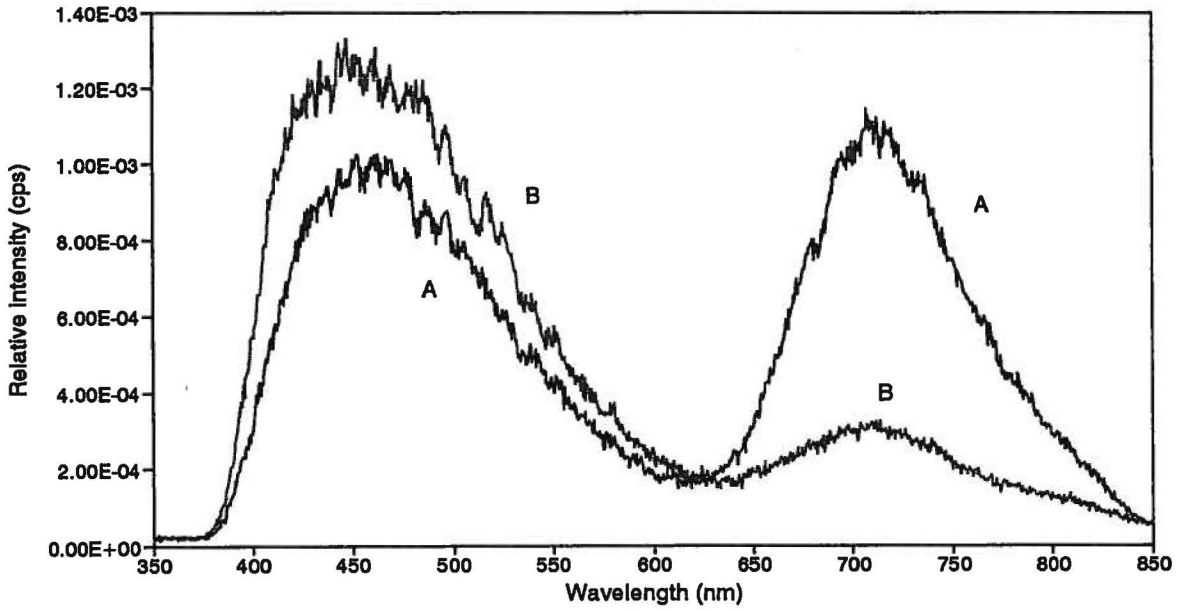

Fig. 1-6. Intensity of the luminescence peak is depended on the primary electron beam energy. (A) is obtained under 10 keV, 0.8 Am. (B) is obtained under 15 keV, 0.8 Am, both CL spectra are from same area of a feldspar sample.

these electrons and holes at internal recombination centers. The CD curve has two slopes with an inflection point at C^* (Fig. 1-5). The value of C^* depends on the crystal size, because C^* corresponds to the average electron and hole migration distance which is proportional to the crystal size.

Thus direct and the indirect excitations can be distinguished for the ordinary cathodoluminescence study. The direct excitation usually produces a weaker luminescence intensity than the indirect excitation (Fig. 1-5), because recombination of the mobile electrons and holes at activator ions results a high efficiency luminescence.

1.3. Instrumentation of cathodoluminescence

1.3.1. Cathodoluminescence equipment

The Luminoscope (ELM-2B) is designed to mount directly onto the stage of an optical microscope, therefore, the user can quickly alternate between transmitted light and cathodoluminescence. The system uses a cold cathode electron gun as the source of the electron beam. The electron beam bombards the surface of a polished thin section in a vacuum chamber at a pressure of less than 50 millitorr.

A light spectrophotometer (1681B Minimate) manufactured by SPEX industries Inc. (1988) is attached to the Luminoscope system. The 1681B Minimate is a 0.22 meter, double dispersion grating spectrometer which is fully computer controlled by DM-3000 computer software to perform wavelength scans and record spectra. The

furnished software provides a full range of data manipulation capabilities, such as background subtraction, smoothing, subtraction of spectra, and system transmission correction, etc.

1.3.2. Cathodoluminescence operating conditions

a. Electron beam voltage and beam current

In geological samples, the optimal set up beam voltage and beam current may vary with the sample studied. Usually, a low voltage darkens the luminescence, and therefore produces low intensity CL spectral peaks. A higher beam voltage brightens the luminescence, but has a higher risk of damage to the samples. Mariano (1988) obtained CL spectra of feldspars under 8.5-15 keV beam voltage and 0.3-0.6 mA beam current. The spectra of apatites were obtained under 6-17 keV beam voltage and 0.1-0.8 mA beam current (Mariano, 1988). Telfer and Walker (1978) used 10 keV beam voltage and an electron beam current density of $2uA\ cm^{-2}$ to study plagioclase from lunar and terrestrial samples.

In this study, the spectra for most feldspars and apatites were obtained under 10 keV beam voltage and 0.7-0.8 mA beam current. It is very important to stabilize the electron beam voltage throughout the whole experiment, because variation in the beam voltage can cause changes in the CL colour and peak intensity. Figure 1.6 shows that the intensity of CL peak is significantly effected by the beam voltage. The two feldspar spectra are obtained under a beam voltage of 10 keV and 15 keV with the same beam current (0.8 mA) from the same area within the sample. Under 10 keV (Fig. 1-6, spectrum A),

the feldspar reveals light violet blue luminescent colour with both the intensity of the blue peak and the red peak nearly the same. When the beam voltage is increased to 15 keV (Fig. 1-6, spectrum B), the luminescence colour changes to light blue. In the CL spectrum B, the intensity of the blue peak is only increased slightly, but the intensity of the red peak is decreased dramatically.

b. Electron beam diameter

The size of the electron beam diameter effects power density of the electron beam. When the electron beam is sharply focused on the samples, the beam has a higher power density which produce a brighter luminescence. However, since the beam only covers a small area on the surface of the samples, it will easily damage the samples by heat accumulating in the samples. In this study, a moderate beam size of 5x8 mm was found suitable for producing the desired intensity of CL, and covering a large area. For most of the CL microphotography, a large beam diameter (such as 8x12 mm) was used.

c. Peak resolution and sensitivity

The resolution and sensitivity of CL peaks is controlled by the width of the entrance slit and the exit slit of the spectrophotometer at a certain energy level of the incident electron beam. The entrance slit is set between the fibre optic probe and the spectrophotometer, the exit slit is set between the

spectrophotometer and the photomultiplier detector. Normally, the size of the exit slit is the same as that of the entrance slit (or slightly larger). Small slits provide better resolution but lower intensity peaks.

Fig. 1-7 shows spectra from an apatite obtained using different width slits. When the spectrum is obtained using the large slits (5 mm) (Fig. 1-7a), the luminescent peaks have a higher intensity than those obtained using the small slits (2.5-0.25 mm) (Fig. 1-7b,c,d). However, the peak resolution is relatively poor using the larger slits, e.g., the Dy^{3+} peak at 567 nm is not well resolved. When the spectrum is obtained using the smallest slits 0.25 mm (Fig. 1-7d), most of the luminescent peaks have a relatively low intensity. However, the resolution for most of the peaks are much better, e.g., the Dy^{3+} peak is well resolved at 569 and 579 nm.

The slits of 5 mm or 2.5 mm width are used in most of this study to produce an intensity in the range of nE-3 to nE-4 cps, that satisfies both of the resolution and sensitivity requirements for all of the peaks.

It should be noted that varying the size of the slits can cause the peaks to shift slightly by a few nm's of wavelength. When the size of the slits is increased from 0.25 mm to 1.25 mm to 2.5 mm and to 5 mm (Fig. 1-7), the peaks shift, e.g., the Sm^{3+} peak shifts from 600 nm to 599 nm to 598 nm and to 593 nm respectively. This instrumentational shift must not be misinterpreted as being caused by different activators or different electron transitions in the crystal field.

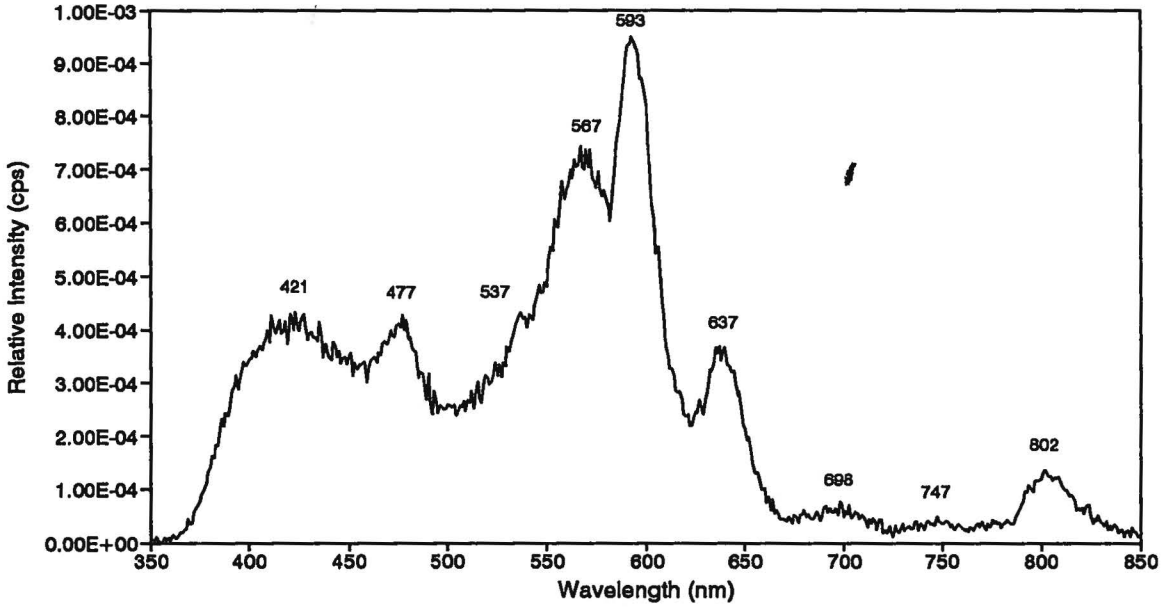

Fig. 1-7a. CL spectrum of an apatite is obtained by using 5 mm entrance and exit slits. CL conditions: 8 keV, 0.8 Am, magnification 10×10.

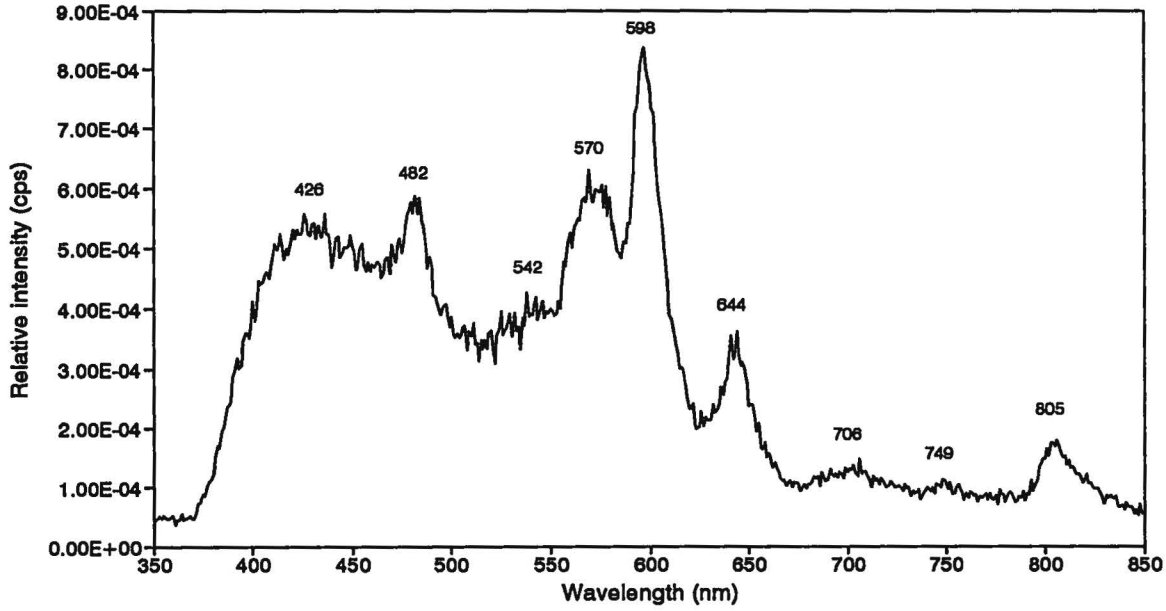

Fig. 1-7b. CL spectrum of the apatite is obtained by using 2.5 mm entrance and exit slits. CL conditions: 8 keV, 0.8 Am, magnification 10×10.

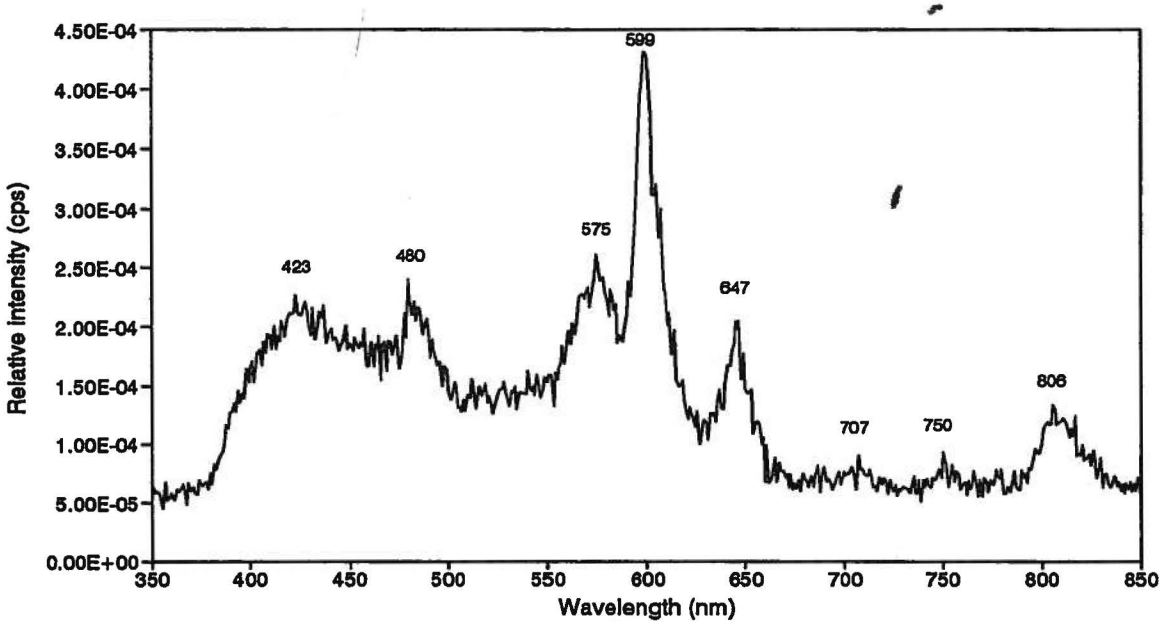

Fig. 1-7c. CL spectrum of the apatite is obtained by using 1.25 mm entrance and exit slits. CL conditions: 8 keV, 0.8 Am, magnification 10×10.

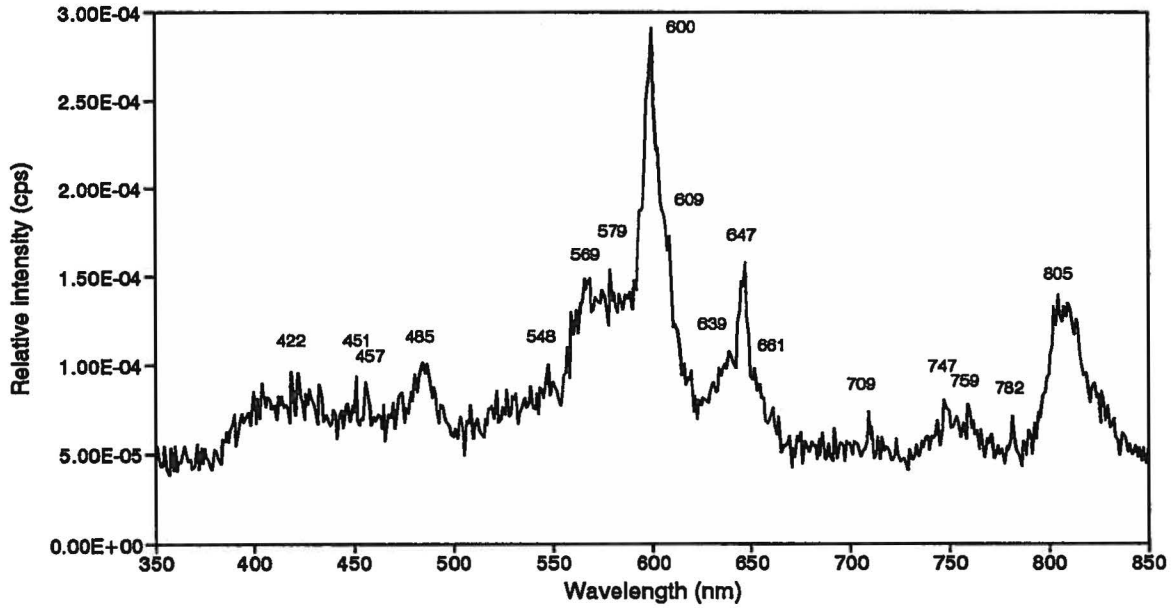

Fig. 1-7d. CL spectrum of the apatite is obtained by using 0.25 mm entrance and exit slits. CL conditions: 8 keV, 0.8 Am, magnification 4×10.

d. Other data acquisition parameters are as followings:

Wavelength scanning from 350 to 850 nm

Increment 0.8-1.0 nm

Integration time 0.2-0.3 sec

1.3.3. Cathodoluminescence spatial resolution

The spatial resolution of CL emission depends on the diameter of the fibre optic probe in the ocular and the magnification of the objective. The fibre optic probe is normally arranged so that input light is located in the objective focal plane. One attempts to sample the CL from a single crystal whose diameter is slightly larger than that of the fibre optic probe.

When the spectra were obtained in this study, a 1250 microns diameter fibre optic probe was used and the objective magnification was 10×. Therefore, the light from an area of 125 microns (1250/10) diameter will be sampled.

1.3.4. Cathode-ray output

The cold cathode electron gun basically consists of a cathode and an anode. When the gas pressure in the chamber of the electron gun has reached a suitable range for a certain electron voltage, a discharge will take place between the cathode and the anode (Luminoscope Instruction Manual, 1988). The discharge is made up of positive ions travelling generally in the direction of the cathode, and electrons travelling generally in the direction of the anode. The electrons pass through a small aperture in the anode then are

focused by a magnetic coil and form an electron beam.

Since the cathode and the anode are metallic and mainly consist of Fe, Cr, Ni and Cu, a high fraction of the metal atoms will be in the excited state. As gas ionizations occur in the cathode-ray tube, there is a recombination of these metal ions with the electrons. The result of this process is the emission of a complex multiline spectrum in the region between 375 and 475 nm. Figure 1-8 shows spectral distribution of the cathode-ray tube output lines in the region between 350 and 850 nm. The spectrum is obtained by the fibre optic probe which is directly set next to the lead glass window of the vacuum chamber after all of the optical lenses are removed (Fig. 1-9a). These cathode-ray tube output lines should be subtracted from the spectra of the samples. The procedure may require a least-squares deconvolution program to simulate these lines of output because they increase with time of spectrum acquisition.

However, the cathode-ray tube output lines are usually concealed by the background of the most sample spectra, when the spectra are obtained by the fibre optic probe sitting in the normal ocular lens position of the polarizing microscope (Fig. 1-9b).

1.4. Cathodoluminescence photographic techniques

1.4.1. Instrumentation of the photography system and operating conditions

The Photoautomat MPS45 is a fully automatic system used in this study of CL photography. The system consists of the MPS45

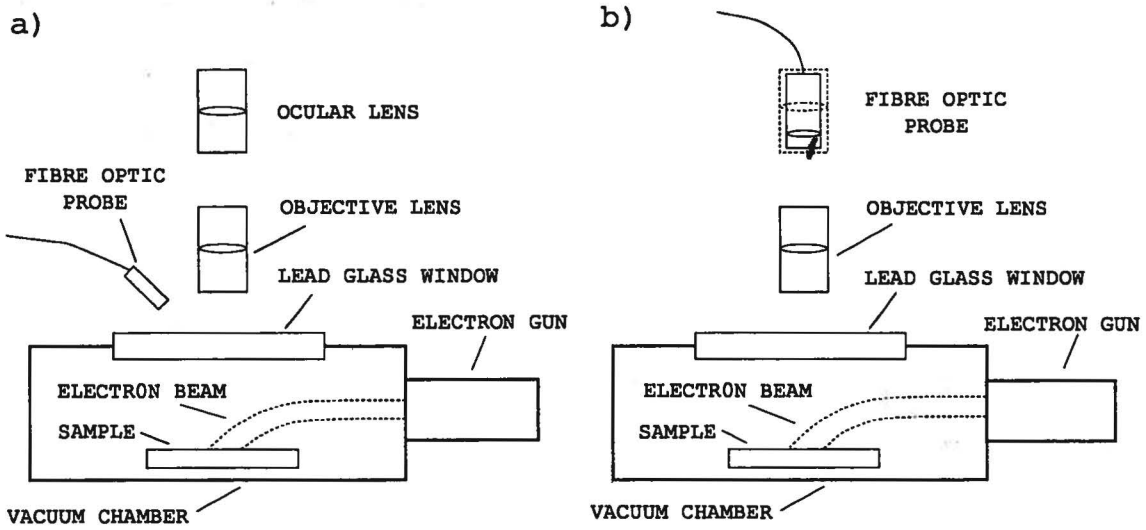

Fig. 1-8. Spectral distributions of the Cathode-ray tube output. CL conditions: 8 keV, 0.8 Am.

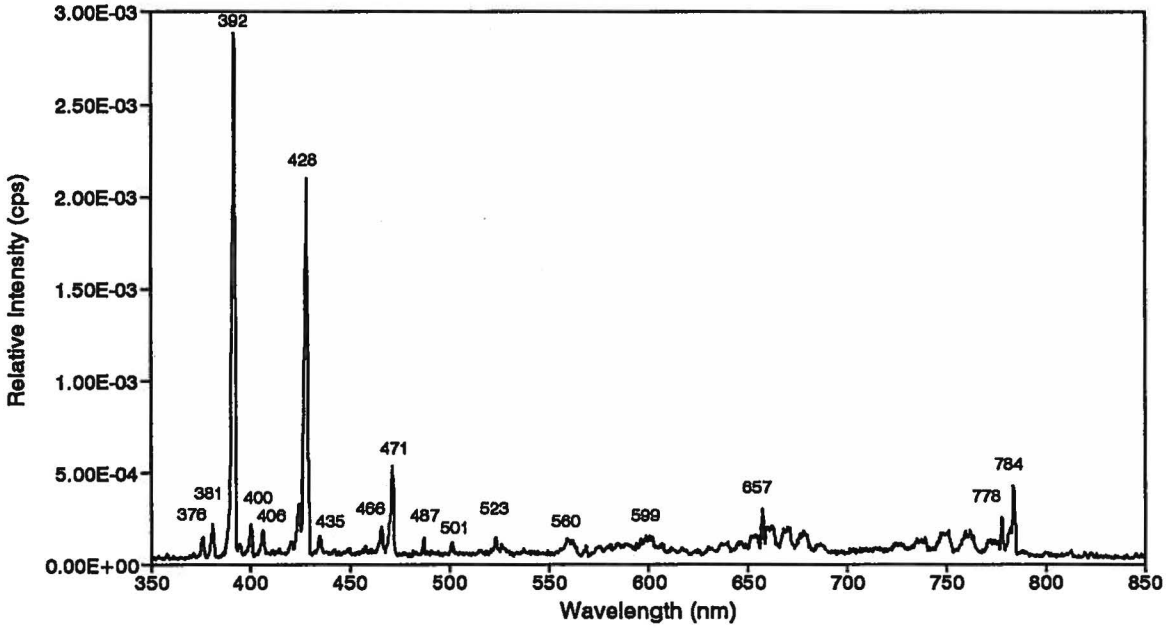

Fig. 1-9. Schematic arrangement of the fibre optic probe for CL microscope. (a) The fibre optic probe is set directly next to the lead glass window of the vacuum chamber. (b) The fibre optic probe is set in the normal ocular lens position.

Photoautomat, a shutterpiece, a 35 mm magazine, a photo-eyepiece (10×), and a Leitz microscope.

The Photoautomat is set at a condition of reciprocity failure correction (switching LINEAR/NORMAL switch to LINEAR) for colour film, and the DF/NORMAL switch is set to NORMAL for bright CL field exposure. The individual compensation is set as a standard exposure for all photography (i.e. CAL. is set at 1) and the exposure time is set on automatic mode. When the CL field is too dark, the exposure mode is set on manual and the exposure time is estimated individually for each picture.

These photographic conditions are the same for the transmitted light and polarized light photography.

1.4.2. The focusing of CL pictures

Unlike transmitted light (TrL) and polarized light (PoL) photography, the CL photographic image has a much lower light intensity making it difficult to see a clear picture of the subject in the focusing telescope. The CL focusing distance is also not the same as for the TrL and PoL image.

The best way to focus a CL picture is by using the micropores in the sample to focus the picture. The micropores are very small holes that usually occur in minerals or at the interstices between minerals. The micropores usually fill up with the polishing compounds and have a very bright greenish blue luminescence. When the picture is in focus, most of the micropores will have a clear singular image (not multiple images) in the field of view.

Another problem is heat effect. When a sample has a very low CL intensity, it may require a longer exposure time, and heat will be accumulated in the sample by prolonged electron beam bombardment. This heat may cause the epoxy to "bubble" which will cause the picture to be out of focus. This can be avoided by changing to a higher film speed.

1.4.3. CL picture exposure time and film speed

The Photoautomat automatically controls the CL picture exposure time which ranges from a few seconds to a few minutes depending on the CL intensity of different minerals, and the film speeds under certain magnifications of the microscope. For brightly luminescing minerals, such as the feldspars (light blue CL colour) under 10x4 magnification, the best range of exposure time is 30 sec to 1 min for ASA 400 (Konica) film. This produces an almost true CL colour and with good colour resolution. A higher speed film (ASA 1000, Kodak Ektar) is used when the mineral has a very low CL intensity with a dark CL field in the view, or for a higher magnification (10×10) image. The best range of the exposure time is 1 to 2 min. However, the CL colour may be distorted as it appears more orange-red in comparison with the CL colour which was observed under microscope.

CHAPTER 2

REVIEW OF LUMINESCENCE CENTERS IN FELDSPARS

2.1. Introduction to cathodoluminescence in feldspars

Feldspars from different types of rocks usually exhibit four different CL colours: purple, light blue, green and red. Although, the origin of the luminescent colour is controversial, the luminescence colour of feldspar is attributed to the excitation of activator ions in the crystal field, to the lattice defect centres in Si-O-Al groups or to the intrinsic luminescence. For feldspars, CL provides a great deal of petrographic information, especially in cases of fluid induced alteration and deuteric coarsening.

2.2. REE activation in feldspars

2.2.1. Eu^{2+} activation in feldspars

Laud et al. (1971) synthesized the alkaline earth feldspars: $CaAl_2Si_2O_8$ (anorthite), $SrAl_2Si_2O_8$ (triclinic Sr-plagioclase) and $BaAl_2Si_2O_8$ (celsian and metastable hexacelsian) with Eu^{2+} (2 mole %). Under cathode-ray irradiation, the CL emission of Eu^{2+}-activated Ca-feldspar occurs in the blue region with a broad peak centered at 470 nm (Fig. 2-1a), the emission of Eu^{2+}-activated Sr-feldspar also occurs in the blue region with a broad peak centered at 465 nm. The emission of Eu^{2+}-activated Ba-feldspar (celsian and hexacelsian) occurred in the ultraviolet region and very weakly in the blue-green region with a narrow peak at 375 nm and a broad peak at 500 nm, respectively (Fig. 2-1a).

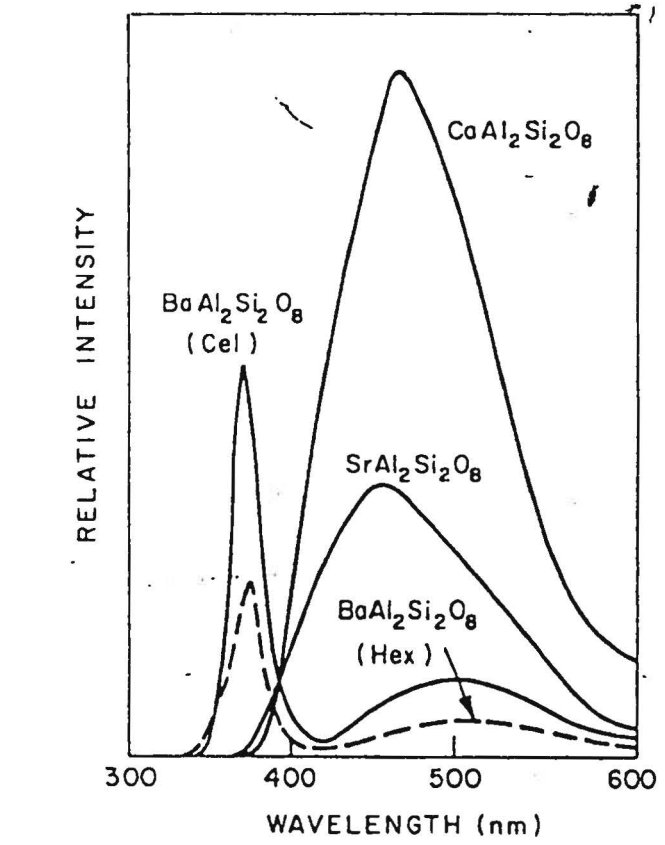

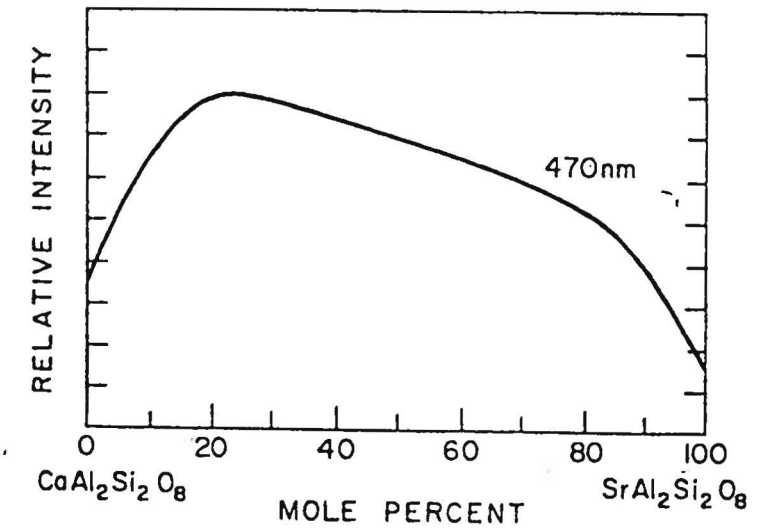

Fig. 2-1. a. CL spectra of Eu^{2+}-activated $CaAl_2Si_2O_8$, $SrAl_2Si_2O_8$ and $BaAl_2Si_2O_8$. b. Relative peak intensity vs. composition in the system $CaAl_2Si_2O_8$:Eu^{2+}-$SrAl_2Si_2O_8$:Eu^{2+} (From Laud et al., 1971).

In the Eu^{2+}-activated $CaAl_2Si_2O_8$-$SrAl_2Si_2O_8$ solid solution series, Laud et al. (1971) found that the luminescence peak position of Eu^{2+} activator did not significantly changes as a function of the composition, since the end members of the Eu^{2+}-activated Ca-feldspar and Sr-feldspar have nearly the same peak position. However, the relative intensity of the emission peaks is a function of their composition. The intermediate members have higher luminescence intensities than their end members (Fig. 2-1b), e.g., the feldspar with 75 mole% $CaAl_2Si_2O_8$, and 25 mole% $SrAl_2Si_2O_8$ have a more intense maximum luminescence peak at 470 nm, than the end members.

In the Eu^{2+}-activated $BaAl_2Si_2O_8$-$SrAl_2Si_2O_8$ solid solution series, similar results were also observed by Laud et al. (1971), the relative intensity increases with Ba^{2+} concentration up to 35 mole% $BaAl_2Si_2O_8$, and then the intensity decreases to 70 mole% $BaAl_2Si_2O_8$. With continued increase in the Ba^{2+} concentration, the luminescence almost ceases.

Since the spectra of the Eu^{2+}-activated Ba-feldspar show two peaks at 375 nm (26.67 cm^{-3}) and 500 nm (20.00 cm^{-3}), Laud et al. (1971) suggested that this may be due to a splitting of the 5*d* energy level of the Eu^{2+} ions in the crystal field. However, the reason for the increasing luminescence intensity in these intermediate members of the solid solutions is not clear. It may be caused by an increased efficiency of the Eu^{2+} ions activation, or by an improvement in the energy transfer mechanism between the host and the activator ions.

Mariano et al. (1973, 1975) also studied Eu^{2+} as an activator in

plagioclase ($Na_{1-x}Ca_2Al_{1+x}Si_{1-x}O_8$). They obtained a CL spectrum of a synthetic anorthite crystal with approximately 200 ppm of Eu^{2+} which yielded a deep blue luminescence with a broad emission band at approximately 420 nm (Fig. 2-2). They also noted that the luminescence colour of the Eu^{2+}-activated synthetic anorthite is darker than the blue luminescence exhibited in terrestrial and lunar feldspars. Although Eu^{2+} is an activator in synthetic feldspars, Mariano (1978) considered that the concentration of europium is insufficient to cause activation in a natural feldspar host. In synthetic feldspars, n×100 ppm of Eu is necessary to produce the blue luminescence, but europium has never been observed above n×10 ppm in a natural feldspar host.

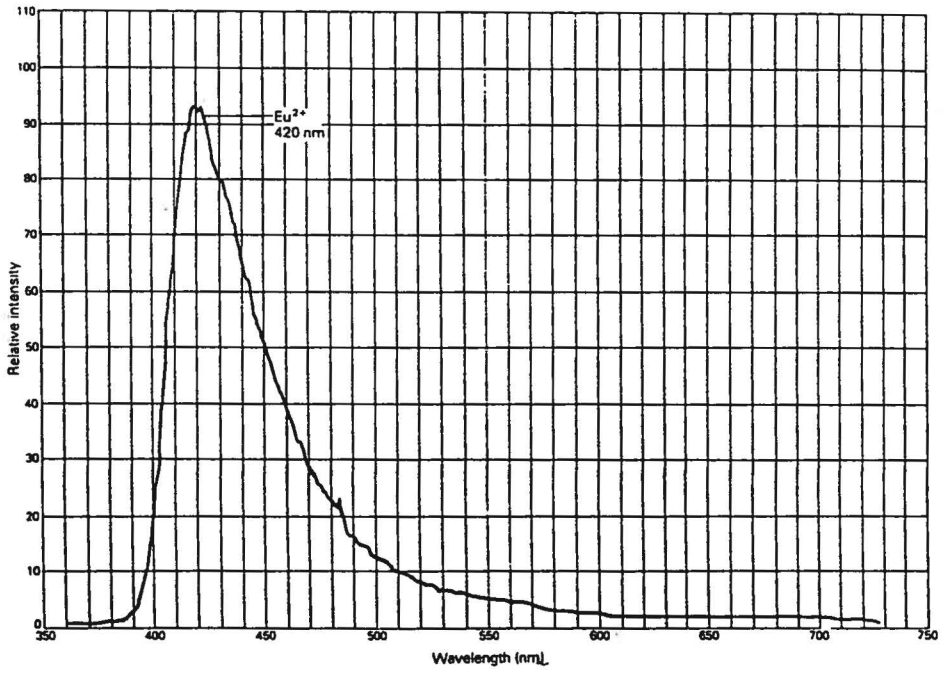

Fig. 2-2. CL spectrum of Eu^{2+} (about 200 ppm) doped synthetic anorthite. This Eu^{2+}-activated synthetic anorthite exhibited a deep blue luminescence. (From Mariano, 1988).

2.2.2. Ce^{3+} activation in feldspars

Laud et al. (1971) also synthesized the feldspars: $CaAl_2Si_2O_8$ (anorthite), $SrAl_2Si_2O_8$ (triclinic Sr-plagioclase), and $BaAl_2Si_2O_8$ (celsian and metastable hexacelsian) with 1 mole Ce^{3+}. The spectrum of the Ce^{3+}-activated anorthite consists of a narrow band in the ultraviolet region with peak at 355 nm, and a broad, weak band in the visible blue-green region with peak at 490 nm (Fig. 2-3a). Ce^{3+}-activated Sr-feldspar produced a narrow band in the green region a with peak at 530 nm. Ce^{3+} doped Ba-feldspars were inert to cathode-ray excitation.

In the Ce^{3+}-activated $CaAl_2Si_2O_8$-$SrAl_2Si_2O_8$ solid solution series, Laud et al. (1971) found that the Ce^{3+} emission peaks for both end members are present in the intermediate members without any shift in the peak positions. The luminescence intensity is a function of composition (Fig. 2-3b), e.g., for the peak at 530 nm, the luminescence intensity increases with decreasing Ca-feldspar content in the solid solution series. In the Ce^{3+}-activated $BaAl_2Si_2O_8$-$SrAl_2Si_2O_8$ solid solution series, the luminescence peak intensities in the intermediate members are higher than their end members.

Laud et al. (1971) assumed that the separation of emission peaks in the spectrum of the Ce^{3+}-activated Ca-feldspar is caused by the Ce^{3+} ion splitting in the crystal field. In the Ca-feldspar and Sr-feldspar end members, the Ce3+ ions may occupy in two different sites because the CL spectra are different. However, in intermediate members, the Ce^{3+} ions probably occupy in both sites,

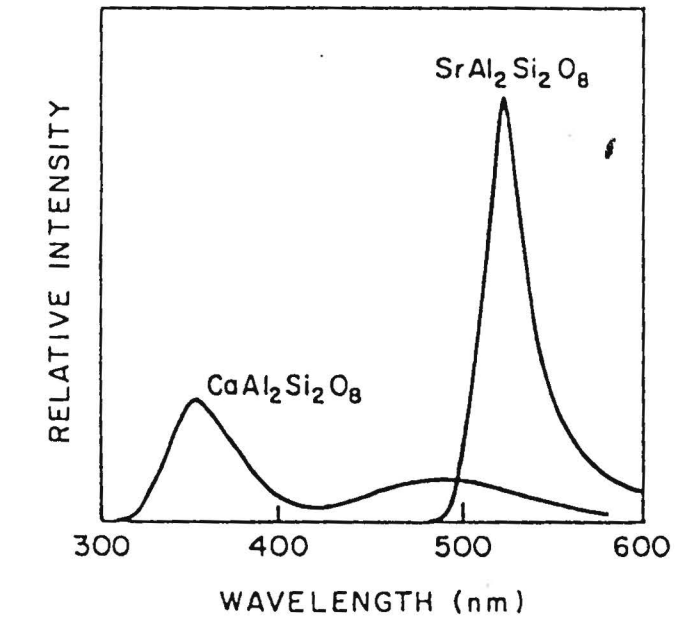

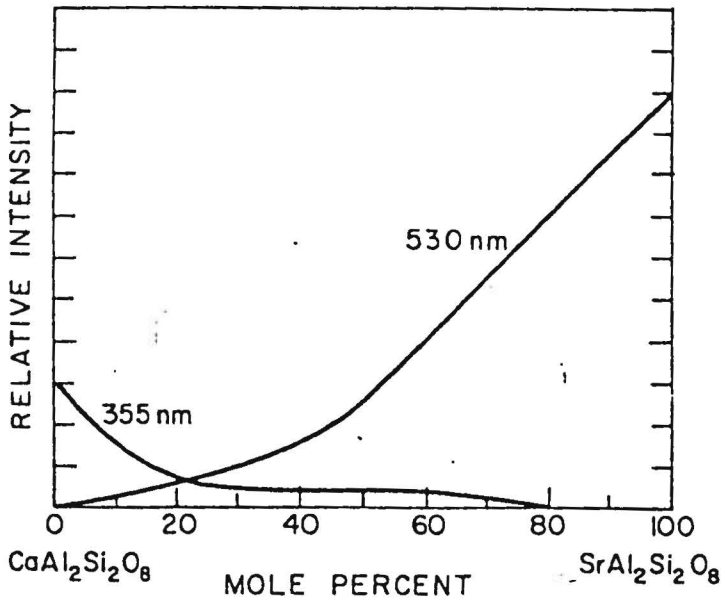

Fig. 2-3. a. CL spectra of Ce^{3+}-activated $CaAl_2Si_2O_8$ and $SrAl_2Si_2O_8$. b. Relative peak intensity vs. composition in the system $CaAl_2Si_2O_8$:Ce^{3+}-$SrAl_2Si_2O_8$:Ce^{3+}. (From Laud et al., 1971).

because the CL spectra are combined by both end members emission peaks.

2.3. Transition elements activation in feldspars

2.3.1. Ti^{4+} activation in feldspars

A light blue CL emission of feldspars has been observed by many authors. The emission spectrum includes a broad band with a peak wavelength of about 450 (±10) nm. This emission band is attributed to Ti^{4+} impurity which intensifies some weak intrinsic CL emission in UV and the blue region of feldspars (Mariano, 1988). This suggestion is based on studies of titanium impurities in silicates. The CL spectra of SiO_2 and several silicates exhibit broad bands which extend from the UV region into the blue part of the visible region. This emission band is associated with SiO_4 groups or the Si-O bond and can be intensified by a titanium impurity. Titanium intensification in silicate phosphors acts as an activator and contributes to the anomalously high electronic polarization of the oxygen ion (O^{2-}), in the field adjacent to the titanium ion (Ti^{4+}) (Mariano, 1988). The titanium impurity in a silicate also produces a structural perturbation which may distort the normal host crystals, because Ti prefers to be in octahedral coordination with O, as compared with the normal tetrahedral coordination of Si with O.

Mariano et al. (1978) reported synthetic labradorite and anorthite with 0.1 wt.% of Ti^{4+} impurity gives blue luminescence with a broad band at 460 (±10) nm. This emission band is similar to

the Ti^{4+}-activated synthetic silicate phosphor. Mariano (1988) illustrated a synthetic labradorite with 0.2 wt.% of TiO_2 exhibits light blue luminescence with a broad peak centered at about 470 nm (Fig. 2-4).

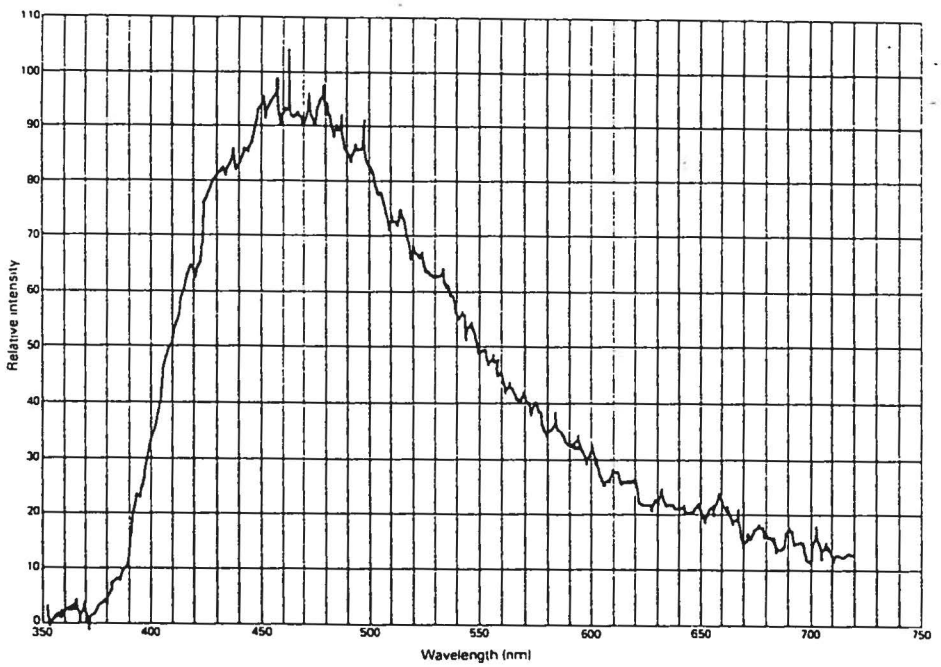

Fig. 2-4. CL spectrum of Ti^{4+} (0.2 wt.% TiO_2) doped synthetic labradorite. The synthetic labradorite exhibited a light blue luminescence. (From Mariano, 1988).

In natural feldspar, Mariano (1978, 1988) also showed that the microcline in fenite veins from granite-Cerro Impaoto, Estado Bolivar, Venezuela exhibits a light blue luminescence, and the CL spectrum consists of a high blue peak at about 420 nm and a low red peak at about 710 nm. In gneiss from Kangankunde Carbonatite, Malawi, the plagioclase exhibits a light blue luminescence with a broad band centred at about 500 nm. In quartz latite porphyry from

Mt. Fubilan of OK Tedi, New Guinea, an orthoclase phenocryst exhibits a light blue luminescence, and the CL spectrum consists of a low blue peak at about 450 nm and a high red peak at about 700 nm (Fig. 2-5). The blue luminescence peak in the CL spectra of these natural feldspars is comparable to the blue peak in the CL spectrum of the synthetic labradorite.

Hutcheon et al., (1978) reported all plagioclase (anorthite) in the Allende meteorite shows blue luminescence, and there was no correlation of CL intensity with Ti concentration (<50-340 ppm). However, they found a strong negative correlation between CL intensity and the Na and Mg concentrations.

Sippel and Spener (1970) observed broad luminescence bands centered at 450 and 559 nm in lunar feldspar. They found that the blue peak (450 nm) shows a variability in peak position and shape and which does not correlate with composition. Sippel and Spener (1970) suggested that more than one luminescence center may be involved in producing the blue luminescence peak.

Rae and Chambers (1988) studied the relationship between blue luminescent feldspars and their Ti contents in the North Qorôq center, South Greenland. They reported that the unmetasomatised perthitic feldspar (sample 46297), from the North Qorôq center, exhibited a pale blue luminescence colour, and in comparison, a sample of granular syenite (sample 77-22), from Klokken intrusion, which has suffered minimal water-rock interaction, showed a strong blue luminescence. CL spectra of both samples are illustrated by Rae and Chambers (1988). In these feldspars, CL spectra are not

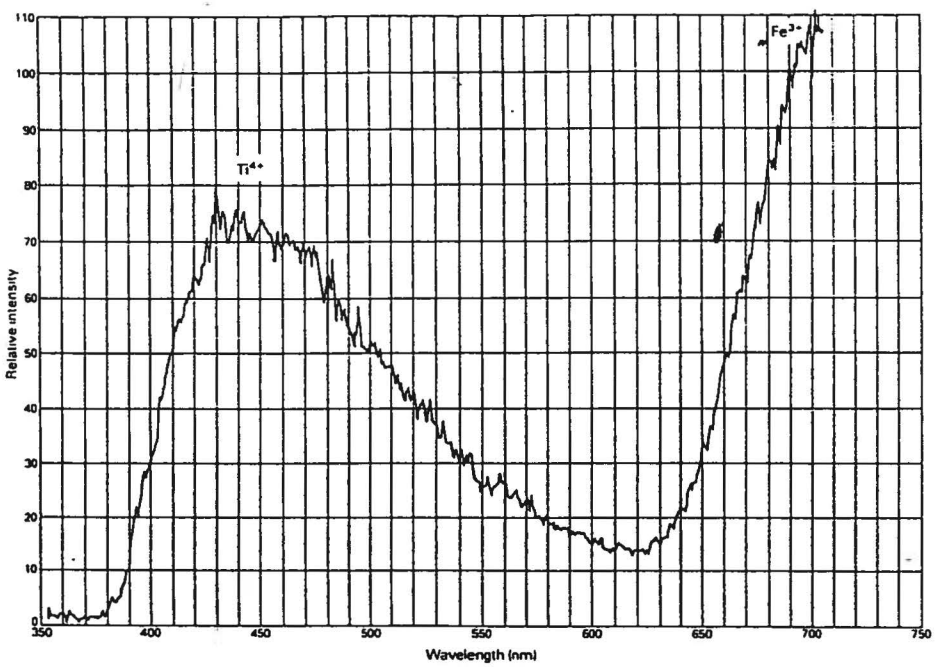

Fig. 2-5. CL spectrum of an orthoclase phenocryst from Mt. Fubilan quartz latite porphyry of Ok Tedi, Guinea. The CL spectrum consists of a broad band peak at about 440 nm which is attributed to lattice defects produced by substitution Ti^{4+}, and a peak at about 700 nm which is typical of Fe^{3+} activation. This orthoclase crystal exhibited a light blue luminescence (From Mariano, 1988).

compatible with the luminescence colours which are described by Rae and Chambers (1988). CL spectrum of the pale blue luminescent perthitic feldspar did not shown any blue peak at about 450 nm and only showed a very high red peak centred at about 750 nm. CL spectrum of the strong blue luminescent granular syenite only showed a very weak blue peak centered at about 450 nm and a very high red peak centered at about 750 nm. Rae and Chambers (1988) interpreted that is because the red emission is in the near infra-red thus making it very difficult for the human eye to detect (the human eye picks up little above 650 nm and is at its most sensitive in the blue-green region of the spectrum). Even if this were true, the CL spectrum of the perthitic feldspar still does not represent

what is called the pale blue luminescence colour, because the relative luminescence intensity at 650 nm is higher than it is at 450 nm.

Despite the contradiction of the luminescence colour with the CL spectra, Rae and Chambers (1988) also used an ion probe to analyzed 38 feldspar samples, as Ti was below the electron microprobe detection limit. They found that the concentration of Ti ranged from 3 to 389 ppm, and distribution of the Ti was heterogeneous within each sample. No correlation was evident between intensity of the blue peak and concentration of the Ti and other elements analyzed. Therefore, Rae and Chambers (1988) believe that the blue luminescence in alkali feldspars is not activated by a Ti^{4+} substitution for Si^{4+}, but is a result of a defect centre which is completely unrelated to minor element concentrations. This hypothesis was also proposed by Geake et al. (1977), who suggested that the blue luminescence is probably due to lattice defects rather than to any particular activator.

2.3.2. Fe^{3+} activation in feldspars

Red luminescent feldspars were reported by several authors (Smith and Stenstron, 1965; Geake et al., 1973, 1977; Mariano, 1978) during the early studies of cathodoluminescence of geological materials. It was commonly suggested that the red luminescence, near the IR region, was due to an Fe^{3+} activator, with the Fe^{3+} occupying the tetrahedral Al^{3+} sites in the Al-O-Si framework.

Mariano (1978, 1988) showed that optical quality orthoclase, from

the Itrongay region, Madagascar, has a red luminescence with a broad band centered at about 700 nm (Fig. 2-6), and contains 0.29 wt.% of Fe (Mariano, 1988). Fe in this amber-yellow orthoclase is in the ferric state wite 2.56 wt.% Fe_2O_3 reported by Deer et al. (1966) based on chemical analyses. Thus the red luminescence peak at about 700 nm in this orthoclase is attributed to Fe^{3+} activation. Faye (1969) and Manning (1970) assigned Fe^{3+} ions in this orthoclase to the tetrahedral sites by use of optical absorption spectrum.

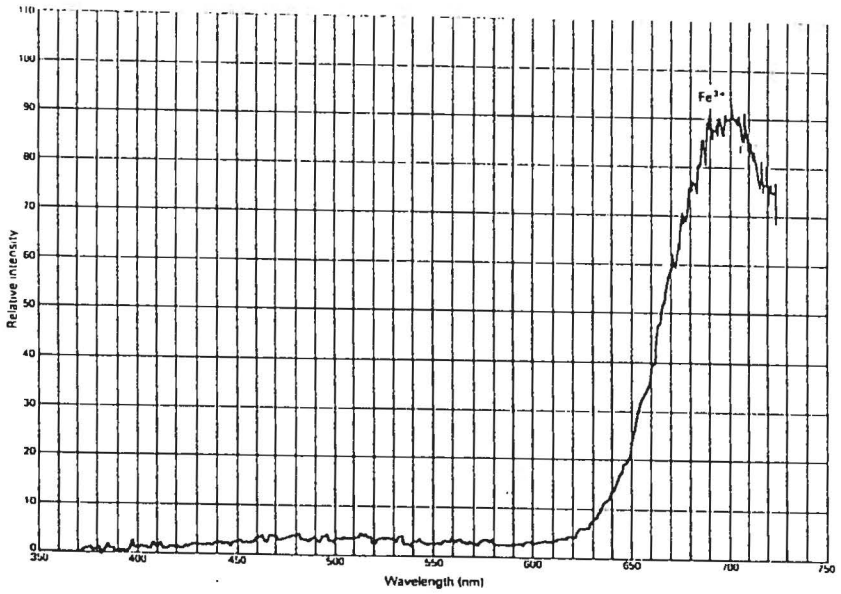

Fig. 2-6. CL spectrum of an orthoclase from Itrongay region, Madagascar. The orthoclase exhibited a red luminescence which is attributed to Fe^{3+} activation. (From Mariano, 1988).

For most terrestrial plagioclase which have an emission peak occurring in the near infrared region between 700 and 780 nm, it is assumed that this peak is produced by Fe^{3+} activation in the Al

sites (Geake et al., 1977). This was tested by doping a pure, synthesized anorthite with iron under oxidizing conditions, such that the iron would be expected occur as Fe^{3+}. Luminescence of the anorthite resulted in a strong emission peak at about 700 nm (Fig. 2-7). A similar spectrum of the a Fe^{3+} doped synthetic labradorite have been obtained by Mariano (1978, 1988) (Fig. 2-8).

Telfer and Walker (1978) reported that the red emission band occurs at about 680 nm in synthetic anorthite with 5190 mole ppm Fe^{3+}, and between 698 and 781 nm in natural plagioclase. By interpretation of the optical absorption spectra based on ligand field theory, Telfer and Walker (1978) confirmed that Fe^{3+} in plagioclase occupies the distorted tetrahedral sites (T-sites) (the largest T-sites are normally occupied by Al^{3+}) and assumed that the red emission band probably is from the lowest of the split energy levels. The Fe activator concentration level in natural plagioclase was found generally at about 1000 ppm. These Fe contents were confirmed by X-ray fluorescence analysis.

Recently, Rae and Chambers (1988) have found that in the North Qorôq centre, all of the red luminescent albites with an infrared peak centered at about 750 nm have significant Fe contents. They suggested a possible correlation between the infrared peak intensities and the Fe content. They also suggested that the red luminescence is the result of electronic transitions in the Fe^{3+} ion present as an impurity in the feldspar, and that Fe^{3+} is in tetrahedral coordination. This was confirmed by the excitation spectra which are the same as that of the red-infrared luminescing

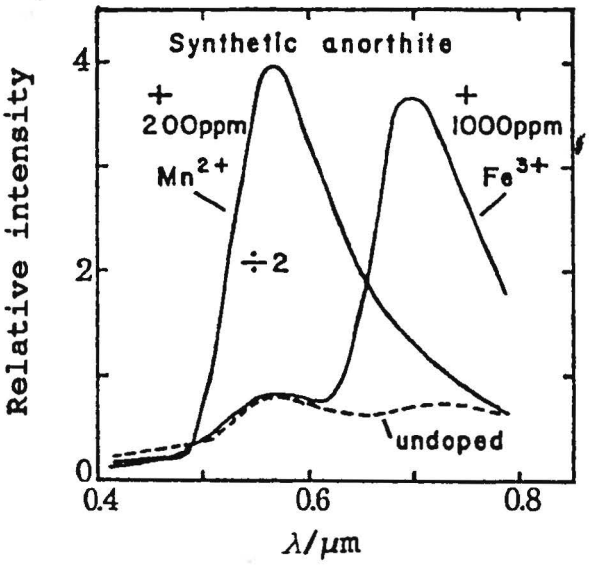

Fig. 2-7. CL spectra of Fe^{3+} and Mn^{2+} doped synthetic anorthite (Form Geak et al., 1973).

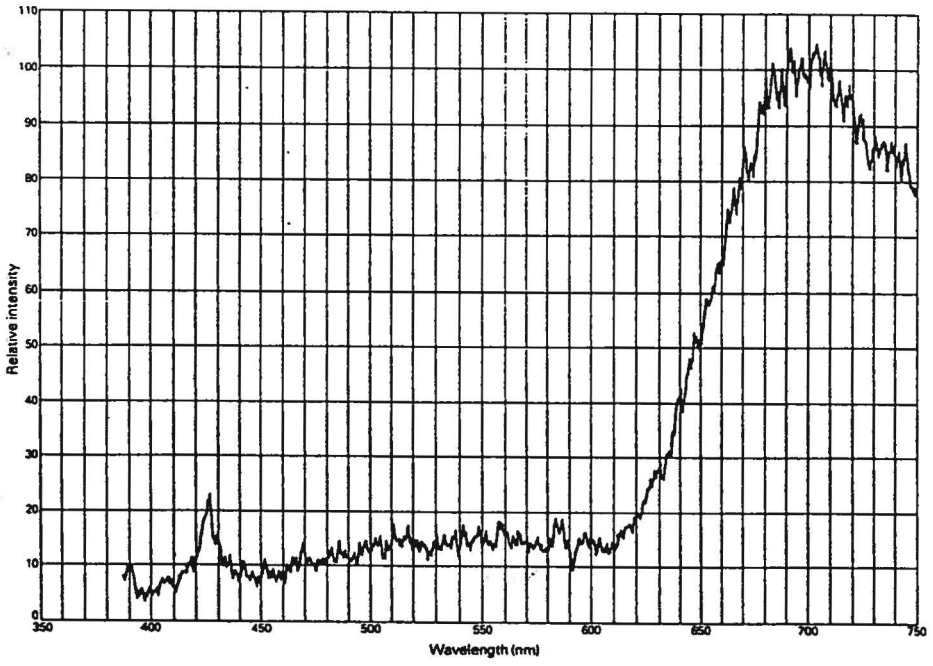

Fig. 2-8. CL spectrum of Fe^{3+} (0.18 wt.% Fe_2O_3) doped synthetic labradorite. The synthetic labradorite exhibited red luminescence with a broad band at about 700 nm (From Mariano, 1988).

plagioclase reported by Telfer and Walker (1978). There are no differences between the excitation spectra for the red luminescence albites (metasomatic syenite, sample 59751 and 59755), and the blue luminescence feldspars (unaltered perthite, sample 77-22 and 46297) in the North Qoroq centre and Klokken intrusion by Rae and Chambers (1988).

If the excitation spectra by Rae and Chambers (1988) are reliable, the red luminescence colour of the feldspars is due to Fe^{3+} activation, and the excitation spectra of orthoclase and plagioclase (red CL) represent the energy levels of Fe^{3+} ion splitting in the ligand field. Although the blue luminescent feldspars should not have the same excitation spectra as the red luminescent albite. The blue luminescence from feldspar crystals are commonly considered due to Ti^{4+} intensification or due to a defect center.

2.3.3. Fe^{2+} activation in feldspars

Fe^{2+} usually reduces the luminescence intensity by acting as a quencher in some minerals, such as carbonates. However, Mariano (1988) reported that Fe^{2+} is an activator for CL in plagioclase. A synthetic plagioclase containing ferrous iron exhibits a strong green luminescence with an emission peak at about 550 nm (Fig. 2-9). The synthetic plagioclase crystal is anorthite with a composition of $(Fe_{0.1}Ca_{0.9})Al_2Si_2O_8 \cdot nH_2O$. This crystal was examined by SEM and EDS point analysis which indicated that the crystal is a homogeneous grain and Fe is substitutional in the anorthite

lattice. A Mössbauer spectrum of this anorthite indicated that the Fe is mainly Fe^{2+}, and the estimated ratio of Fe^{3+}/Fe^{2+} is about 0.2.

The green luminescent peaks have been observed in many natural plagioclase, both terrestrial and lunar. Mariano (1988) argued that the green peak at about 550 nm in the plagioclase is due to Fe^{2+} activation rather than Mn^{2+} activation. These plagioclase commonly contain about 1 wt.% Fe content. The Fe is mostly in the ferrous state for the lunar plagioclases and no red emission peak was observed in the green luminescent terrestrial plagioclases.

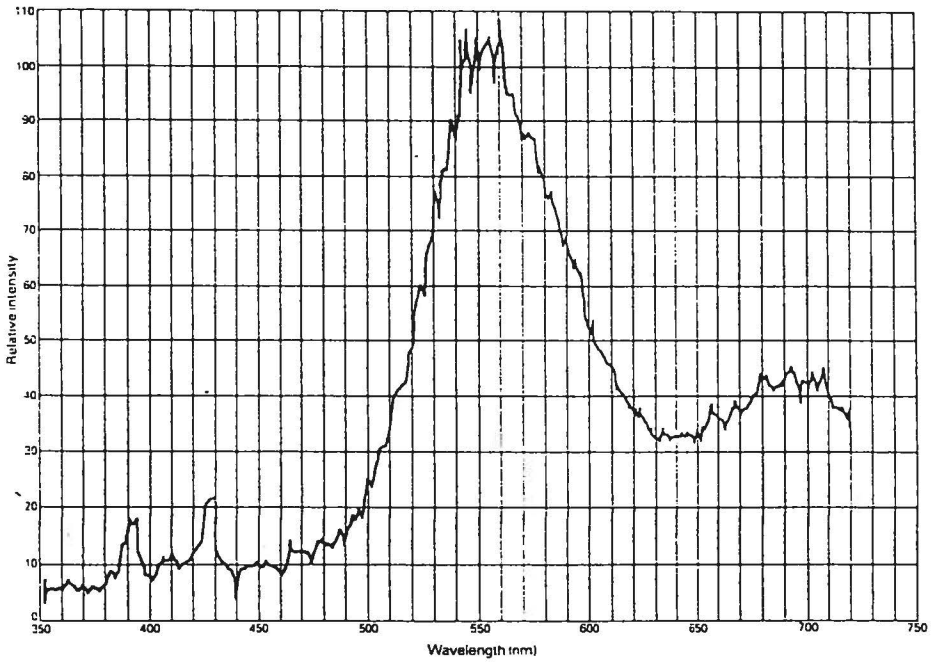

Fig. 2-9. CL spectrum of Fe^{2+} (2 wt.% FeO) doped synthetic plagioclase. The synthetic plagioclase exhibited green luminescence with high green peak at about 550 nm (Fe^{2+} activation) and a low red peak at about 700 nm (Fe^{3+} activation) (From Mariano, 1988).

Fe^{2+} (Mn^{2+}) activation in plagioclase from the plutonic complex of the Meissen massif, East Germany are reported by Wenzel and Ramseyer (1992). The dioritic plagioclase (andesine) exhibits a bluish-green luminescence, and CL spectra of this andesine consists of a low peak at 460 nm and a high peak at 750 nm. This dioritic plagioclase contains on average 1700 ppm Fe and 300 ppm Mn. In comparison the brown luminescent plagioclase of the monzonites, contain on average 1500 ppm Fe and <200 ppm Mn, and have a relatively lower green peak and a relatively higher red peak than that of the dioritic plagicolase. Thus, this is considered as a correlation between decreasing Mn contents and decreasing the peak heights at 560 nm from diorite to monzonite. They also assumed that the Fe^{2+} content of the dioritic plagioclase is higher than in the plagioclases of monzonites, because the dioritic plagicolases contain higher Fe, but have a lower red peak at 750 nm (lower Fe^{3+}). Therefore, Wenzel and Ramseyer (1992) concluded that the emission peak at 560 nm may be caused by both Fe^{2+} and Mn^{2+} activation.

2.3.4. Mn^{2+} activation in feldspars

Mariano (1978) reported that three synthetic labradorite samples with 0.02, 0.036 and 0.057 wt.% Mn^{2+} showed broad emission bands at 570 nm, and the luminescence intensities increased with the Mn contents. The greenish yellow luminescence colour of the natural plagioclases is considered to be due to Mn^{2+} activation. Mariano (1988) also reported a synthetic labradorite with 430 ppm MnO exhibited a yellow luminescence colour with a broad band centered

at 570 nm (Fig. 2-10).

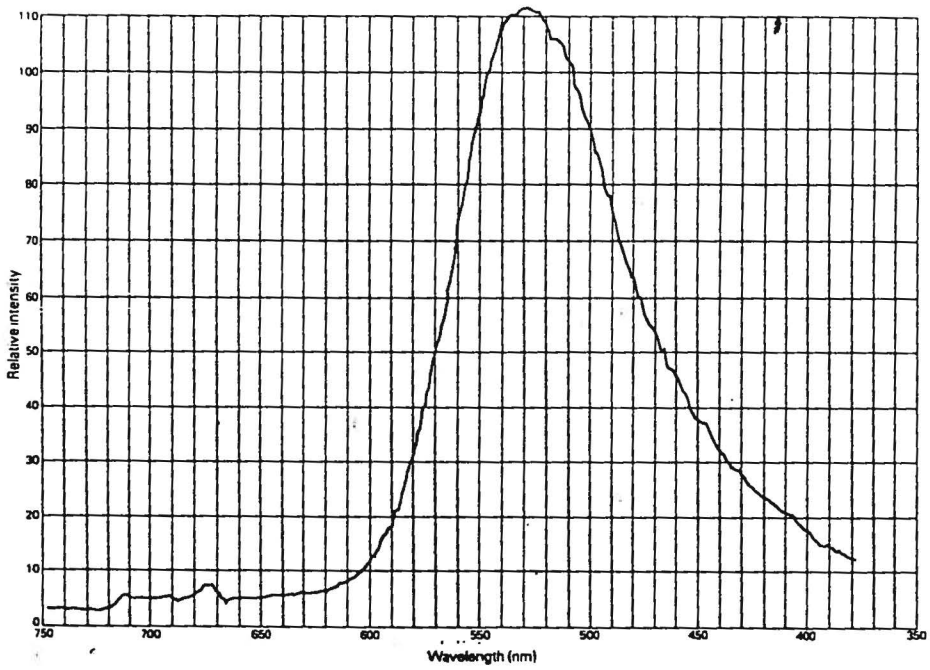

Fig. 2-10. CL spectrum of Mn^{2+} (430 ppm MnO) doped synthetic labradorite. The synthetic plagioclase exhibited yellow luminescence with a broad peak at about 570 nm (From Mariano, 1988).

Geake et al. (1977) reported that the emission spectra of lunar, meteorite, and terrestrial plagioclases showed three broad peaks at about 450, 560 and 700-780 nm. In lunar and meteorite plagioclases, the green peak at 560 nm is commonly higher than the blue peak (450 nm) and the red peak (700-789 nm). This green peak was attributed to Mn^{2+} activation and confirmed by Mn (200 ppm) doped synthetic anorthite which also has a strong emission peak at 560 nm (Geake et al., 1977). The excitation spectra of both the lunar and terrestrial plagioclases are the same as the synthetic Mn^{2+}-activated plagioclases and were characteristic of a d^5 electron

configuration. Thus Geake et al. (1977) suggested that Mn^{2+} is substituting mainly in the Ca^{2+} sites.

Telfer and Walker (1978) reported the green emission due to Mn^{2+} activation in plagioclase can be divided into two types: type I emitting an emission band at about 560 nm (terrestrial anorthite and synthetic anorthite); and type II emitting an emission band at about 580 nm (terrestrial oligoclase after heating). According to the excitation spectra of these two types of plagioclase, Telfer and Walker (1978) believed that the Mn^{2+} ions were mostly substituting for Ca^{2+} at the M-sites, but sometimes may also substitute for Al^{3+} in the tetrahedral sites (T-sites).

2.3.5. Cu^{2+} activation in feldspars

Cu^{2+} (0.0n wt.%) doped synthetic feldspar exhibits a blue luminescence with a peak at about 420 nm (Mariano, 1978).

2.3.6. Pb^{2+} activation in feldspars

Pb^{2+} activation in amazonites gives a broad luminescence band in the UV region at about 300 nm (Marfunin, 1979). This luminescence band was assigned to electronic transition of Pb^{2+} ion $^3P_1 \rightarrow {}^1S_0$ in a tetragonal crystal field.

2.4. Ga activation in feldspars

Ga activation in feldspars in the alkali syenitic rocks from Thor Lake, North West Territories are reported by Jorre and Smith (1988). The feldspars are red luminescent microclines and red

luminescent albites with blue luminescent albite margins. The CL spectrum of the red luminescent albite cores exhibit a broad band centered at about 710 nm, while the blue luminescent margins consisted of a sharp peak centered at 425 nm, a broad weak peak centered at about 480 nm, and a red peak centered at 710 nm. The red peak in the spectrum is due to contamination partially by red luminescent materials.

Jorre and Smith (1988) also presented a CL spectrum of a synthetic Ga-oligoclase (5.53 wt.% Ga) which consisted of a similar sharp peak centered at about 430 nm and a well developed broad peak centered at about 580 nm. They noted that the peak at about 425 nm is considered to be an artifact peak caused by the detector used in the study.

Jorre and Smith (1988) also reported that blue luminescent albite margins contain 0.08-0.4 wt.% Ga, while the red luminescent albite cores contain less than 0.06 wt.% Ga. The red luminescent microcline contained 0.02-0.06 wt.% Ga. They also noted these Ga analyses are not accurate considering the high analytical errors caused by a high peak/background ratio and low detection limits for Ga. Based on similar profiles of CL spectra of the synthetic Ga-oligoclase and blue luminescent albite margins, and the close spatial relationship between the cathodoluminescence colours and Ga concentrations, Jorre and Smith (1988) suggested that the blue luminescence from the albite margins is related to the Ga concentration.

Finch and Walker (1991) disagreed that the blue luminescence can

be related to the Ga concentration, as the gallium concentration increases from the blue luminescent core to the red luminescent rim in the Blå Måne Sø perthosite, South Greenland. An ion microprobe was used to measure the Ga concentration in the feldspars, and it was determined that there was 20 ppm Ga in the core and 50 ppm Ga in the rim. However, these Ga concentrations are far less that those of the gallium-rich feldspars in the Thor Lake. Finch and Walker (1991) concluded that Ga does not produce the blue luminescence in feldspars.

2.5. Interpreting CL observations for feldspars in alkaline rocks

The CL characteristics of activators in feldspars noted above were used by Mariano (1978, 1988) to study fenitization (metasomatism) in alkaline rocks. He found that fenitized feldspars showed red luminescence due to Fe^{3+} activation, and nonfenitized feldspars commonly showed blue luminescence. Red luminescence from feldspars due to Fe^{3+} activation may indicate a high alkalinity or strong oxidation conditions.

Subsequently, CL studies of syenites were carried out by Rae and Chambers (1988) who confirmed that red luminescence albite was found in all of the rocks affected by a late-stage fluid phase interaction, while blue luminescence was found in unaltered perthite. The red luminescence peak intensity increases with progressive action of the fluid phase, but it also may be related to an increase in the Fe concentration.

Recently, Finch and Walker (1991) found that the reddening of the

CL colours in alkali feldspars from the Blå Måne Sø perthosite unit may be correlated with an increase in microporosity. They suggested that the micropores may be formed by a direct interaction between the metasomatic fluid and the alkali feldspars. According to the oxygen isotopic ratios of the alkali feldspars, Finch and Walker (1991) suggested that the fluid was derived essentially from the magma itself with a small meteoric water component (possibly released from the feldspars themselves).

CHAPTER 3

CATHODOLUMINESCENCE PROPERTIES OF FELDSPAR AND APATITE AND OTHER MINERALS

3.1. Time-dependent change of luminescence intensity

When an electron beam bombards the surface of a sample, luminescence intensity and colour may change with time. The physical and chemical processes involved in this change are complicated, and are not well documented for feldspar and apatite, and other minerals. Time-dependent decrease or increase in luminescence intensity of minerals may be caused by the incident electrons interacting with the surface of the sample or by thermal agitation within the sample.

3.1.1. Time-dependent change of luminescence intensity in feldspar

Most of the feldspars in the syenites from the Coldwell alkaline complex have a stable luminescence intensity and colour relative to other minerals, e.g., sodalite and fluorite. When the electron beam irradiates the surface of a feldspar, the luminescence colour and intensity change only slightly over time. For the light violet blue luminescent, homogeneous alkali feldspar which consists of a blue peak at 465 nm and a red peak at 710 nm (Fig. 3-1a), the intensity of the blue peak at 465 nm drops slightly from 1.1×10^{-2} cps to 9.8×10^{-3} cps within 10 minutes, after which the intensity is stabilized at 9.8×10^{-3} cps (Fig. 3-1b). The intensity of the red peak at 710 nm drops slightly from 2.3×10^{-3} cps to 1.6×10^{-3} cps in

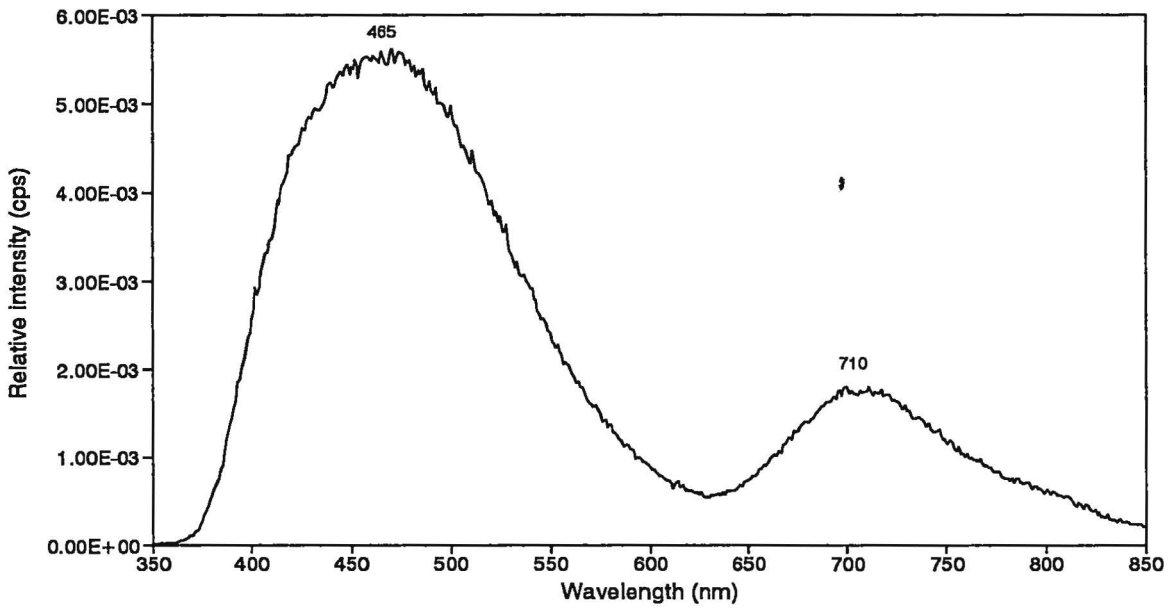

Fig. 3-1a. CL spectrum of the light violet blue luminescent homogeneous feldspar in syenite (sample C188) from Coldwell Complex. The CL spectrum consists of a blue peak at 465 nm and a red peak at 710 nm. CL conditions: 8 keV, 0.8 Am.

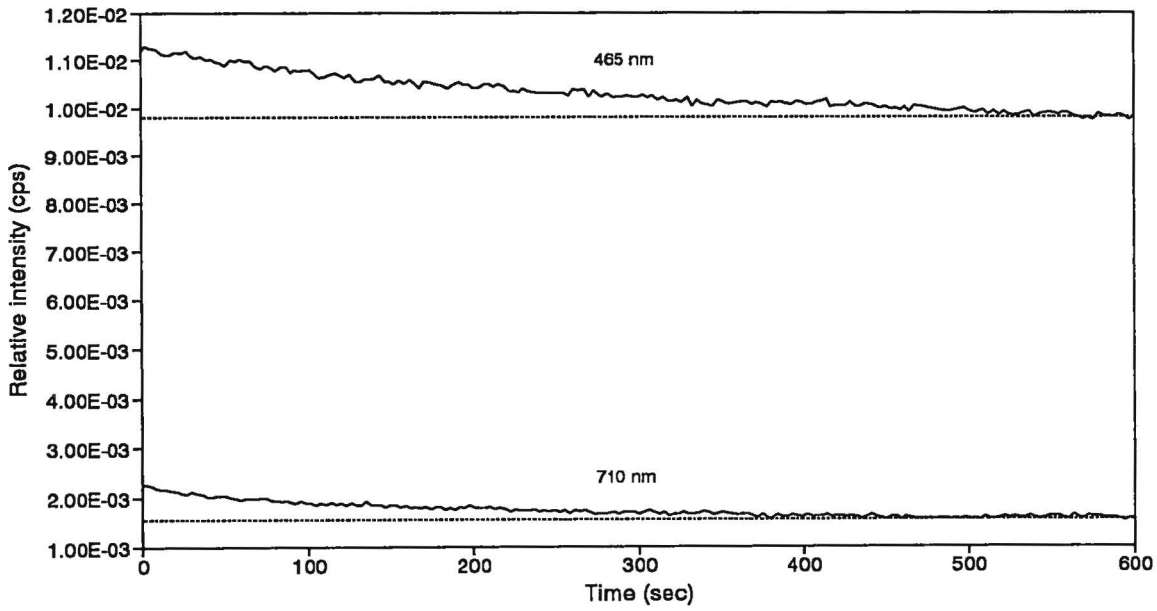

Fig. 3-1b. Time-dependent decrease of luminescence intensity curves of the light violet blue luminescent feldspar (sample C188) shown in Fig. 2-1a. CL conditions: 8 keV, 0.8 Am.

about 7.5 minutes, then the intensity is stabilized at 1.6×10^{-3} cps upon further irradiation. For the deep red luminescent secondary (deuteric coarsening) Na-feldspar which occurs at the margins of the alkali feldspar, the red luminescence peak usually spilts to two peaks at 702 and 718 nm (Fig. 3-2a). The intensity of the red peak at 702 nm drops from 6.9×10^{-3} cps to 4.6×10^{-3} in 5 minutes, then the intensity is stabilized at 4.6×10^{-3} cps upon further irradiation (Fig. 3-2b). The intensity of the red peak at 718 nm drops from 8.1×10^{-3} cps to 4.8×10^{-3} cps in 7 minutes, then the intensity is stabilized at 4.8×10^{-3} cpsupon further irradiation.

For the purple luminescent secondary K-feldspar which consists of a narrow blue peak at 425 nm and a red peak at about 710 nm (Fig. 3-3a). The intensity of the blue peak is increased gradually with time under electron beam irradiation (Fig. 3-3b).

Geake et al (1977) found that the intensity of red luminescence emission in plagioclase tends to decrease with time under the excitation beam, and they suggested that this was probably due to reducing conditions induced by the electron beam converting Fe^{3+} to Fe^{2+}.

Telfer and Walker (1978) found that the decay times of CL emission for Fe^{3+} luminescence centres (CL emission bands occur at about 680 to 781 nm) at room temperature were about three times shorter than the corresponding values obtained for Mn^{2+} centres (CL emission bands occur at about 560 nm) in both synthetic and natural plagioclases. Assuming that the electric dipole radiation occurs at tetrahedral sites (Fe^{3+} substituting for Al^{3+} in tetrahedral sites

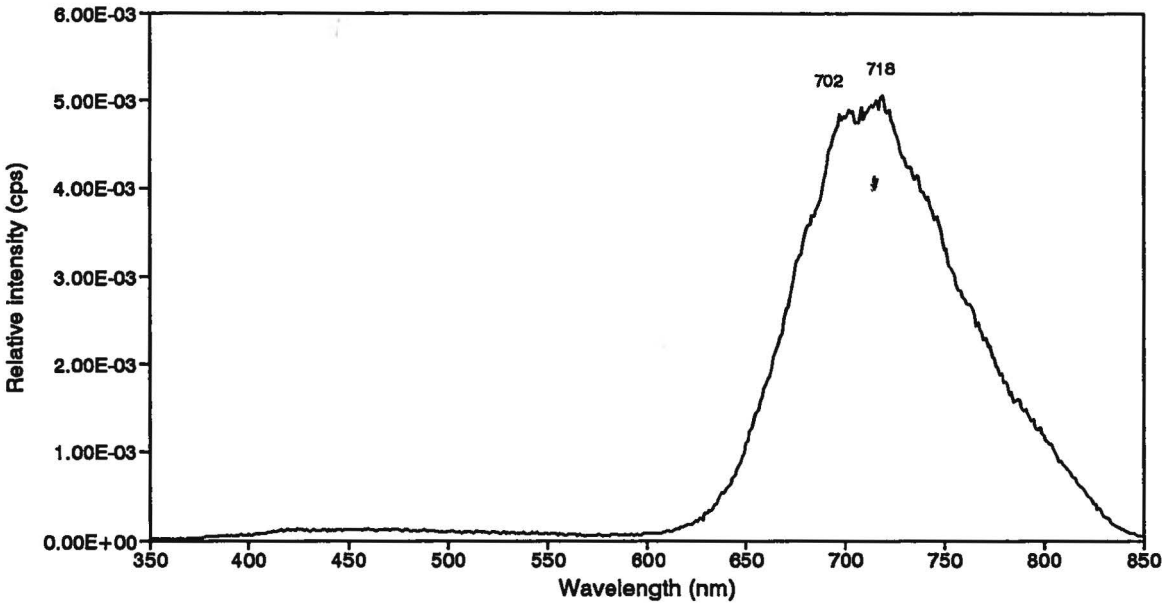

Fig. 3-2a. CL spectrum of the deep red luminescent secondary Na-feldspar in the syenites (sample C226) from Coldwell Complex. The red peak spilts into two peaks at 702 nm and 718 nm. CL conditions: 8 keV, 0.8 Am.

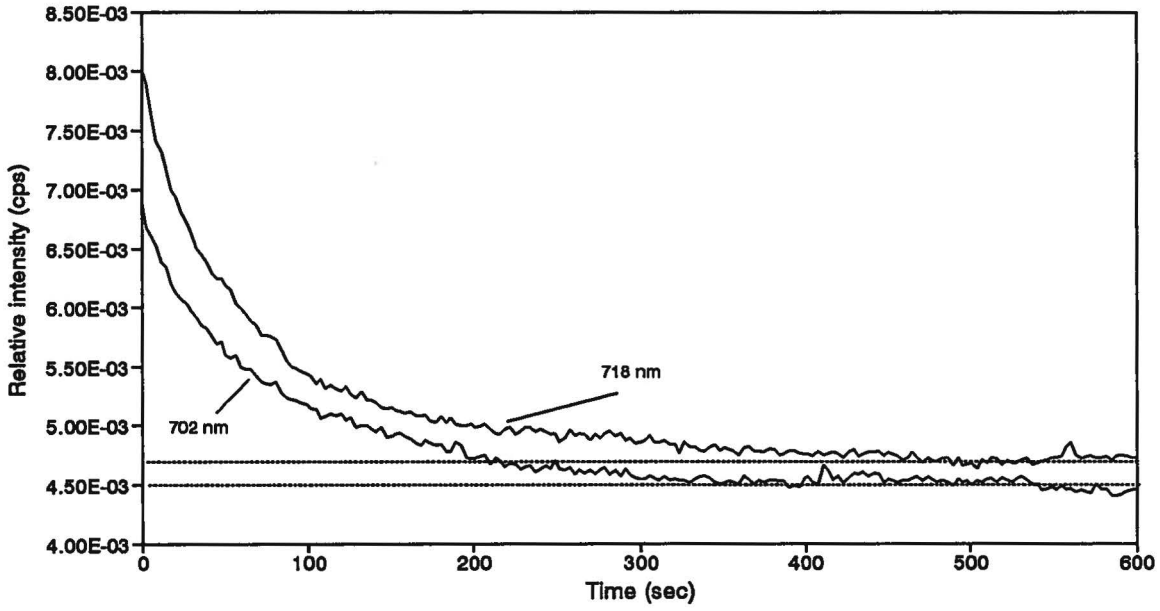

Fig. 3-2b. Time-dependent decrease of luminescence intensity curves of the deep red luminescent secondary Na-feldspar (sample C226) shown in Fig. 2-2a. CL conditions: 8 keV, 0.8 Am.

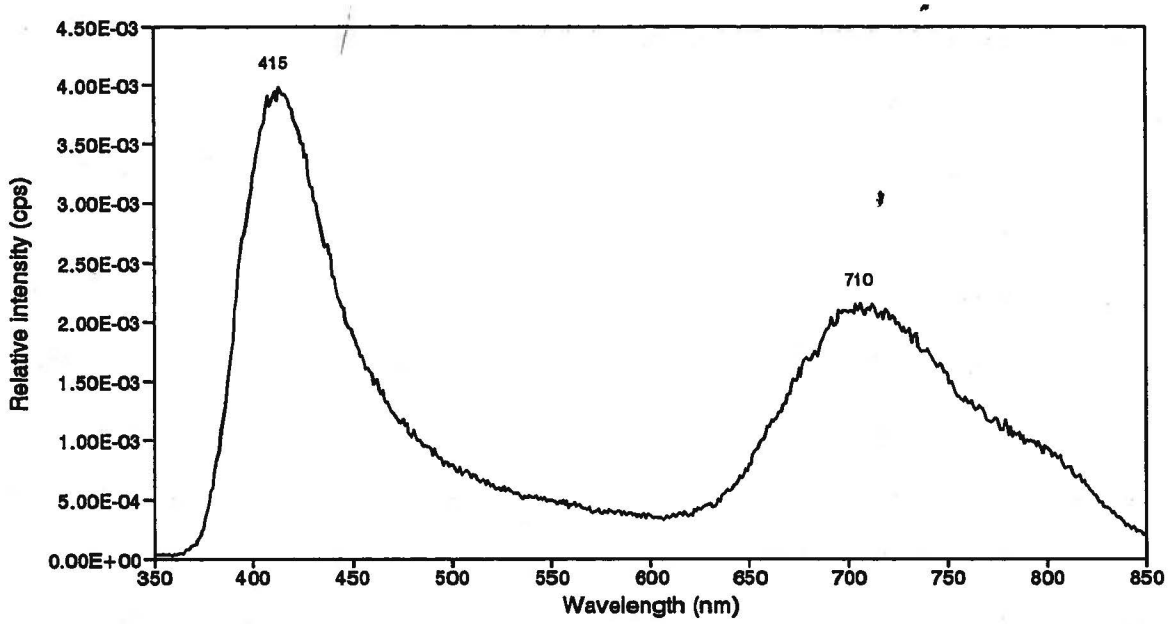

Fig. 3-3a. CL spectrum of the purple luminescent secondary K-feldspar in the syenites (sample C188) from Coldwell Complex. The spectrum consists of a blue peak at 415 nm and a red 710 nm. CL conditions: 8 keV, 0.8 Am.

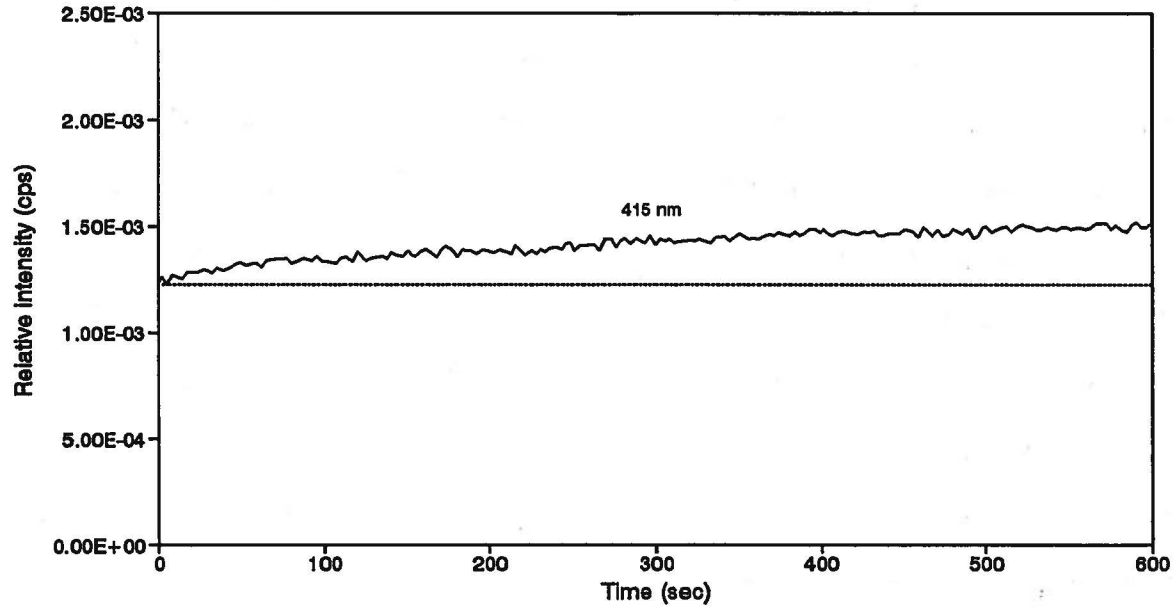

Fig. 3-3b. Time-dependent increase of luminescence intensity curves of the purple luminescent secondary K-feldspar (sample C188) shown in Fig. 2-3a. CL conditions: 8 keV, 0.8 Am.

of plagioclase), they suggested that shorter time decay could be attributed to the relative increase in the extent of metal-ligand orbital interaction, and an increase in allowedness (Fe^{2+}) of the luminescence transitions.

Time-dependent decrease of the red luminescent peak in the feldspar from Coldwell alkaline complex may indicate that the Fe^{3+} ions in the feldspar are converted to Fe^{2+} ions by the electron beam irradiation. However, the time-dependent decrease of the blue peak and time-dependent increase of the purple peak, may imply some unknown luminescence centers or processes occurring in the feldspar crystal when the luminescence is induced by electron beam irradiation.

3.1.2. Time-dependent change of luminescence intensity in apatite

As electrons irradiate the apatite surface, the luminescence colour and intensity of apatite changes with time. This is related to the orientation of the crystal lattice. When a section is cut parallel to the apatite c-axis, the luminescent intensity of the blue region with peak at 435 nm (Eu^{+2} activator) is stabilized over time (Fig. 3-4a,b). However, the intensity of the yellow-red region with a peak at 593 nm (Sm^{+3} activator) slightly increases over time (Fig. 3-4a,b). The resultant luminescent colour of the apatite remains stable as a light pink.

When a section is cut perpendicular to the c-axis, the luminescent intensity decreases rapidly with time for all of the peaks, e.g., the intensities of the peaks at 435 nm and 593 nm

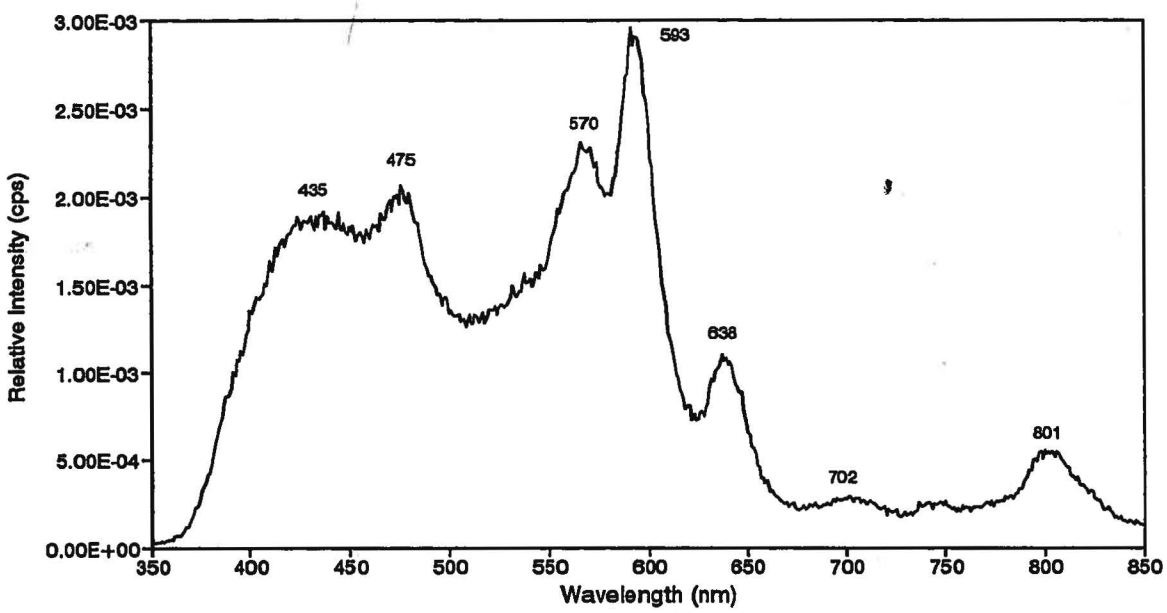

Fig. 3-4a. CL spectrum of the light pink luminescent apatite in the syenite (sample C188) from Coldwell Complex. The spectrum consists of narrow bands at 435 nm (Eu^{2+}-activator), and at 475 and 570 nm (Dy^{3+}-activator), and at 593, 638 and 702 nm (Sm^{3+}-activator). CL conditions: 8 keV, 0.8 Am.

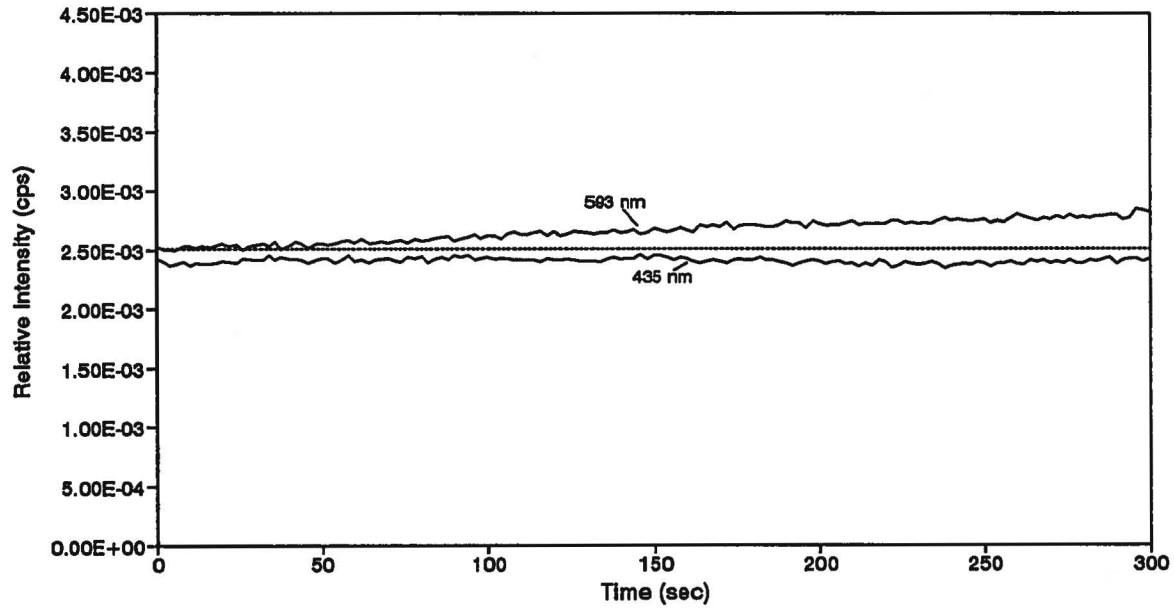

Fig. 3-4b. Time-dependent decrease and increase of luminescence intensity curves of the light pink luminescent apatite (sample C188) shown in Fig 2-4a. The apatite section is cut parallal to the c-axis. CL conditions: 8 keV, 0.8 Am.

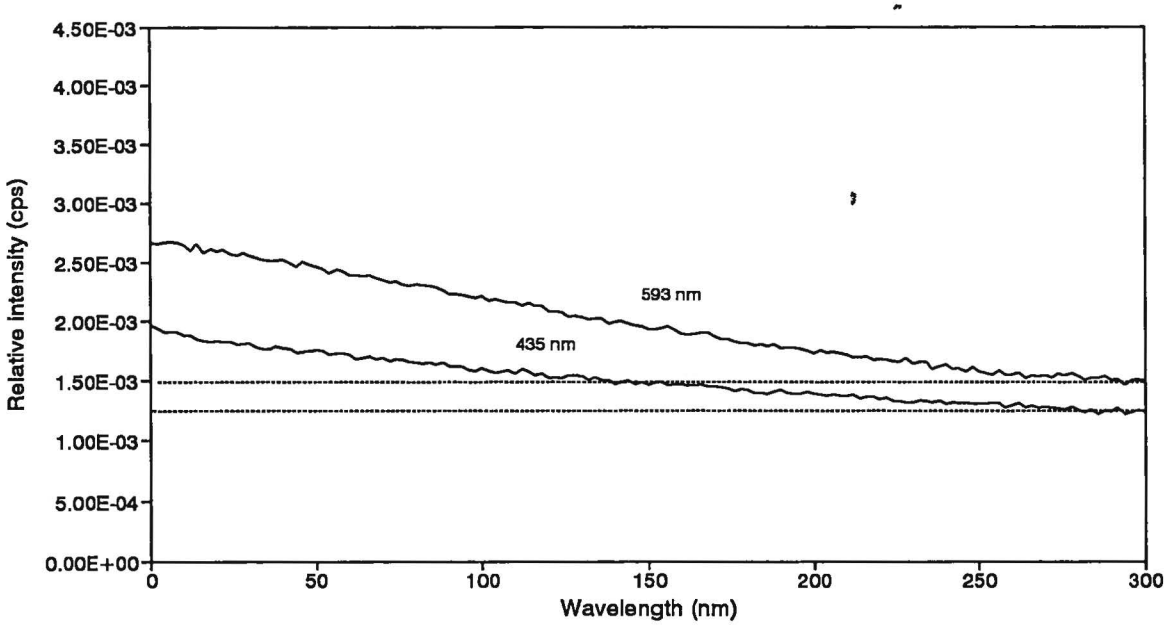

Fig. 3-4c. Time-dependent decrease of luminescence intensity curves of the light pink luminescent apatite (sample C188) shown in Fig. 2-4a. The apatite section is cut perpendicular to the c-axis. CL conditions: 8 keV, 0.8 Am.

decrease from 2.0×10^{-3} cps to 1.4×10^{-3} cps and from 2.7×10^{-3} cps to 1.5×10^{-3} cps, respectively (Fig. 3-4c). As the results, the luminescent colour of the apatite changes from light pink to dark pink. The time-dependent change of luminescence intensity is related to the orientation of the apatite lattice. The luminescence light from apatite is produced by electrons excitation of REE-activator ions in the apatite crystal field. The electric dipole of the REE-activator ions may have different orientations. e.g., the electric dipole in the $^7F_2$ energy level of the Eu^{3+}-activator ion in YVO_4 crystal has a polarized component along the c-axis at 6155.2 Å and a perpendicular component at 6193.8 Å (Brecher et al, 1967)(also see chapter on the luminescence spectra of REE-activated apatites).

3.1.3. Time-dependent decrease in luminescence intensity in sodalite and fluorite

The time decay of the CL intensity for sodalite and fluorite decreases dramatically over a very short time (within a minute). For all of the sodalite crystals and the most of the fluorite crystals, it is impossible to record reliable CL spectra. When an electron beam irradiates the sodalite crystal, the crystal first appears with a pink luminescence colour which quickly changes to a dark bluish grey luminescence colour as it starts to lose its luminescence. With continual irradiation, the sodalite crystal appears black or non-luminescence as it has totally lost its luminescence. In transmitted light, the colourless sodalite crystal changes to light pink and to purple.

When the electron beam irradiates the fluorite crystal, the crystal first appears with a light bluish grey luminescence colour, and it changes to dark grey as it starts to lose its luminescence. With continual irradiation, the fluorite crystal appears non-luminescence. In transmitted light, the colourless fluorite crystal changes to light purple and very dark purple.

3.2. Polarization of luminescence light from the feldspars

In the syenites from Coldwell complex, the luminescence emission light from some feldspars is polarized. This phenomena is usually revealed by a variation in luminescence intensity when the top polarizer of the optical microscope is rotated. In the syenite, the luminescence light from most homogeneous alkali feldspar and

perthite crystals is weakly polarized. However, the luminescence light from some feldspar crystals is strongly polarized. For emample, the Carlsbad twinned, fine-grained perthite from Neys Park, Center II may achieve almost complete extinction of the luminescence light when the top of polarizer of the optical microscope is rotated. As a result of polarization, one side of the twin exhibits light violet blue luminescence and the other side of the twin exhibits light blue luminescence (Fig. 6.2-1b).

Göre et al (1970) and Sippel (1971) recorded the polarization of luminescence light from several feldspar minerals. Smith and Stenstrom (1965) reported that the luminescence emission light from microcline is polarized, i.e., the intensity of the luminescence is a function of the orientation of the crystal lattice. They also noted that the cross-hatched twinning in the microcline is easily seen under CL because of the variation of the luminescence intensity as a function of the orientation.

In the syenites from Coldwell Complex, the polarization of the luminescence light from the feldspars is a function of the orientation of the crystal lattice. Thus the Carlsbad twinned feldspar crystals show different luminescence colours on each side of the twin under CL.

CHAPTER 4

GENERAL GEOLOGY OF THE COLDWELL COMPLEX

4.1. The tectonic setting

The Coldwell alkaline Complex is located on the north shore of Lake Superior (Fig. 4-1), and is the largest alkaline intrusion in North America. The complex intrudes into Archean metavolcanic and metasedimentary rocks of the Schreiber-White River belt (Mitchell and Platt, 1978, 1982). The complex is part of the Keweenawan volcanism (1087-1108 Ma) around the Lake Superior region and may be associated with the midcontinent rift system (1.1 Ga) in North America.

4.2. The petrology of the Coldwell Complex

The Coldwell alkaline Complex is divided into three centers (Fig. 4-1), which represent three distinct magmatic episodes (Mitchell and Platt, 1978, 1982). Center I rocks consist of gabbro together with layered and unlayered ferro-augite syenites. The most abundant rocks are saturated ferro-augite syenites which are associated with Fe-rich oversaturated peralkaline syenitic residua. The layered ferro-augite syenite can be divided into the lower and upper series syenites. The lower series syenites consist of alkali feldspar, olivine (Fa_{83-93}), ferro-augite ($Di_{50}Hd_{45}Ac_5$-$Di_5Hd_{90}Ac_5$), ilmeno-magnetite, and calcic amphiboles. The calcic amphiboles range in composition from hastingsitic hornblende through ferro-edenitic hornblende to ferro-actinolite. The upper series syenites consist

of alkali feldspar, olivine (Fa_{93}), acmitic-hedenbergite ($Di_5Hd_{90}Ac_5$-$Ac_{50}Hd_{50}$), aenigmatite, sodic-calcic amphiboles, REE-rich apatite and minor iron-titanium oxides. The sodic-calcic amphiboles range in composition from ferro-richterite to katophorite. The residual liquids produce K-feldspar, albite, REE-rich fluorite, calcite, quartz, aenigmatite, zircon, sodic-calcic amphibole (richterite) and alkali amphibole (arfvedsonite). The unlayered ferro-augite syenites are cumulates and generally have the same petrographic and mineralogical characteristics as the layered ferro-augite syenite unit.

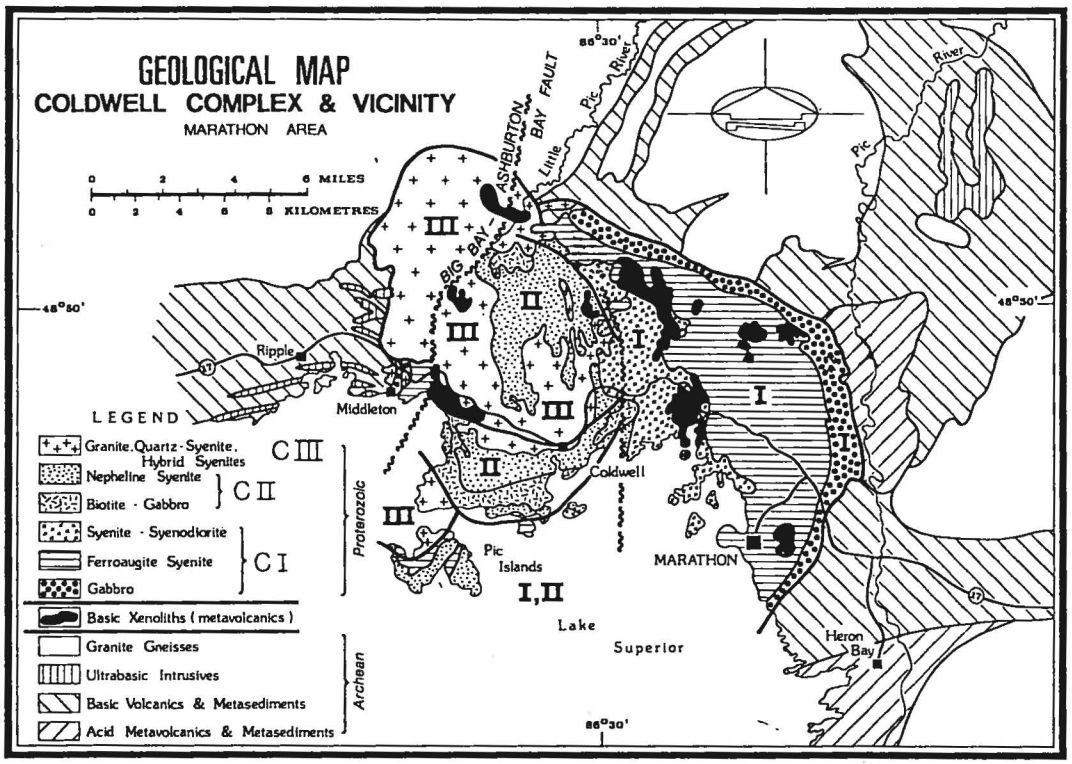

Fig. 4-1. Geological map of the Coldwell Complex and surrounding area (from Mulja and Mitchell, 1991)

Center II rocks consist of alkali biotite gabbro and undersaturated syenites which include miaskitic nepheline syenite, amphibole nepheline syenite and recrystallized nepheline syenite (Mitchell and Platt, 1982). The nepheline syenites consist of alkali feldspar, plagioclase, olivine (Fa_{74-77}), pyroxenes ($Ac_{10}Hd_{20}Di_{70}$-$Ac_{10}Hd_{75}Di_{15}$), calcic amphiboles, titaniferous biotite, nepheline, natrolite-boehmite, hydromuscovite, zeolites, sodalite, titanomagnetite, ilmenite, REE-rich apatite and minor calcite. The calcic amphiboles range in composition from magnesian hastingsitic hornblende to hastingsite and hastingsite hornblende (Mitchell and Platt, 1982; Mitchell, 1990), which are richer in Fe^{3+} than the amphiboles found in the Center I ferro-augite syenite (Mitchell and Platt, 1978).

Mitchell and Platt (1982) believed that the Center II nepheline syenites were emplaced as a hot, hydrous relatively unevolved magma during a period of cauldron subsidence, and subsequently fractionated towards an Fe-enriched hydrous residua. The abundant volatiles resulted in the formation of late-stage primary and deuteric minerals, and promoted extensive ion-exchange between fluids and feldspars. The recrystallized syenites formed at high temperatures during shearing associated with the intrusion. Mitchell and Platt (1982) suggest that the Center II nepheline syenites are derived by the extensive fractional crystallization of a mantle-derived alkali basaltic magma.

Center III syenites are associated with oversaturated residua, and four types of syenites have been recognized (Mitchell et al.,

1993). These are magnesio-hornblende syenite, ferro-edenite syenite, contaminated ferro-edenite syenite and quartz syenite. The magnesio-hornblende syenites mainly consist of alkali feldspar, plagioclase, calcic amphiboles, biotite and quartz, together with accessory minerals of magnetite, ilmenite, REE-bearing apatite, pyroxene, REE-bearing zircon, titanite, REE-bearing fluorite, calcite, pyrite and olivine.

The ferro-edenite syenites mainly consist of alkali feldspar, quartz, biotite, calcic-sodic amphiboles, magnetite-ilmenite, together with accessory minerals of REE-bearing apatite, titanite, pyroxene, REE-bearing fluorite, REE-bearing zircon, chevkinite, monazite, REE-fluorocarbonates, calcite, pyrochlore, columbite and allanite. The calcic-sodic amphiboles are mantled (or replaced) by alkali amphiboles along their margins during deuteric fluid-amphibole interaction.

The contaminated ferro-edenite syenites mainly consist of alkali feldspar, oligoclase, calcic amphiboles, biotite and minor quartz. The accessory minerals include REE-bearing apatite, magnetite, ilmenite, REE-bearing zircon, REE-bearing fluorite, pyroxene, REE-fluorocarbonates, chevkinite, pyrochlore, columbite, zirconolite, allanite and titanite.

The quartz syenites mainly consist of alkali feldspar, calcic-sodic amphiboles and minor quartz, together with accessory minerals of pyroxene (hedenbergite, $Wo_{44-49}Fs_{21-52}En_{4-30}$), REE-bearing apatite, REE-bearing zircon, chevkinite, columbite, pyrochlore, REE-fluorocarbonates, REE-bearing fluorite, magnetite, Nb-rutile,

allanite, monazite, fersmite and fergusonite.

Center III syenites are A-type granitoids, or metaluminous syenite and granites; and are characterized by significant negative Eu anomalies. The various syenite types represent multiple intrusions, contamination and brecciation during the closing stage of the magmatism at the Coldwell Complex (Mitchell et al., 1993) consider that all of the Center III syenites are derived by the extensive fractionation of a mantle-derived tholeiitic basalt magma.

CHAPTER 5

CATHODOLUMINESCENCE PROPERTIES AND COMPOSITIONS OF THE FELDSPARS IN FERROAUGITE SYENITES FROM CENTER I

5.1. Feldspar crystals in the layered ferroaugite syenites

5.1.1. Introduction

The layered ferroaugite syenites are located in the area near the south east margin of Center I. The detailed outcrop map and sample locations shown in Fig. 1. The layered ferroaugite syenites have been divided into a lower series (C35-C60) and an upper series (C63-C72) by Mitchell and Platt (1978). The basal portions of the lower series of syenites are located near the gabbros and meta-volcanics, and are characterized by well developed igneous layering. The mafic rich layers consist of olivine, diopside-hedenbergitic pyroxenes, amphibole, iron-titanium oxides and minor alkali feldspar, whereas the felsic bands are composed primarily of alkali feldspar. The upper series of syenites are essentially coares grained cumulates, which are distinguished from the lower series by weak igneous layering and the presence of aenigmatite and sodic amphiboles. The syenites consist of acmitic pyroxenes, amphiboles, fayalite, alkali feldspar and minor iron-titanium oxides (Mitchell and Platt, 1978). The detailed internal growth textures, CL characteristics and compositions of these feldspars are described in the following sections.

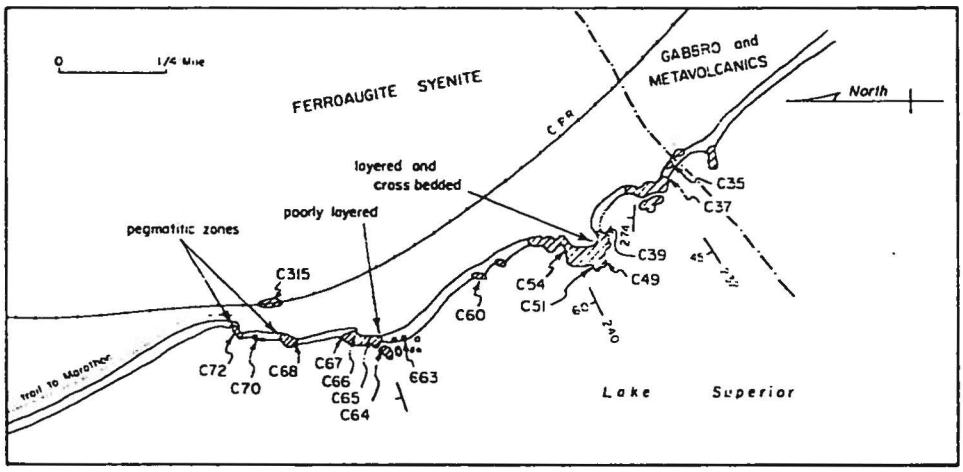

Fig. 5.1-1. Outcrop map of the south-eastern margin of the Coldwell complex, showing sample locations within the layered ferroaugite sequence (from Mitchell and Platt, 1978).

5.1.2. Feldspars in the lower series of the layered ferroaugite syenites

In the lower series of syenites, the feldspar crystals are mainly Carlsbad twinned, optically homogeneous alkali feldspar. However, some of them are weakly mantled by an incipient perthitic rim. The alkali feldspar crystals are replaced by secondary Na- and K-feldspars. These secondary feldspars commonly occur at the margin of the homogeneous alkali feldspar crystals or as irregular patches dispersed within the crystals. The secondary albite usually is clear, albite twinned crystal, whereas secondary K-feldspar has a turbid appearance. In samples from the base level of the lower sequence, the feldspar crystals are mainly homogeneous alkali feldspar, however some of them are intergrown with oligoclase and show replacement textures.

a. Intergrowths of alkali feldspar and oligoclase

Samples C35 and C37 are from the base level of the lower series where the syenites are in contact with gabbros and metavolcanic rocks. In the samples, most of the feldspar crystals are optically homogeneous alkali feldspar. However, some optically homogeneous plagioclase is also found in these samples which occur mainly at the margin of the optically homogeneous alkali feldspar crystals and partially replace the alkali feldspar crystals. The replacement textures are either lamellar-like intergrowths or myrmekites. The lamellar-like intergrowth textures are mainly found in sample C35 (Fig. 5.1-2a), and rarely in sample C37. The myrmekitic textures

(a)

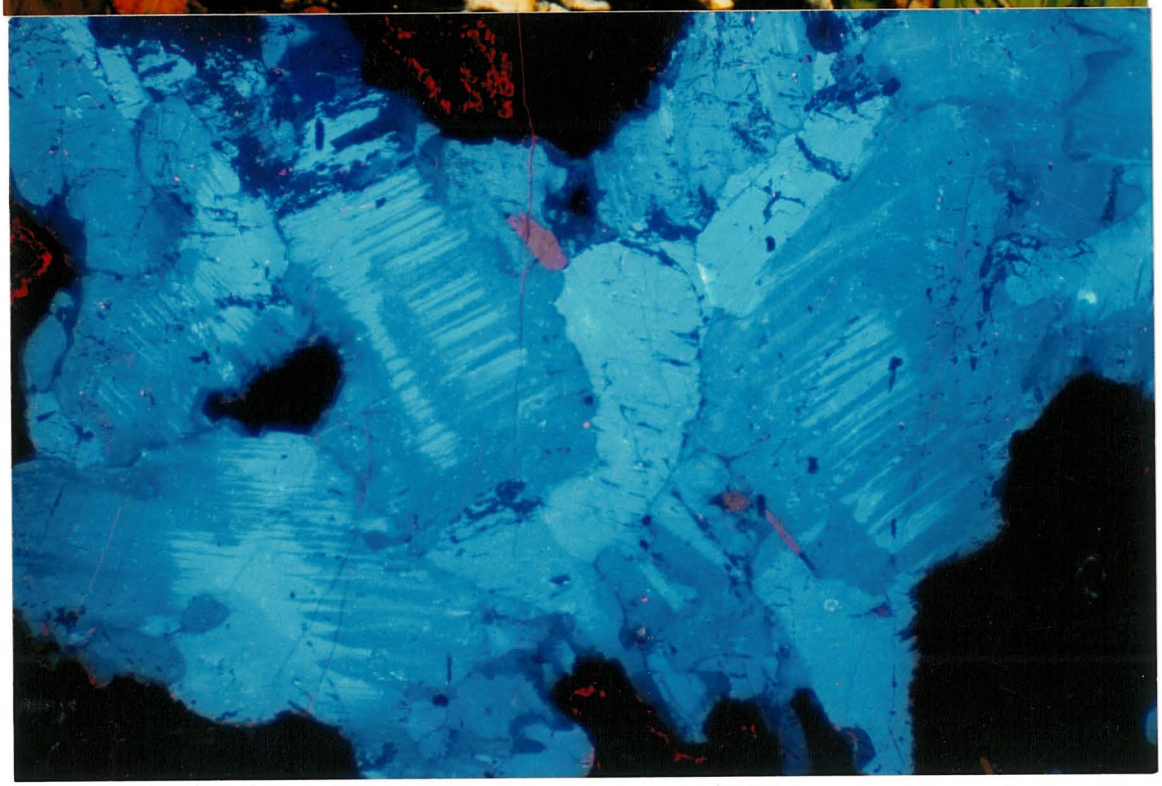

(b)

Fig. 5.1-2. Oligoclase replacement of homogeneous alkali feldspar in the lower series syenite (Sample C35), Center I. a. TrL. (Photographic conditions: 20s, ASA 25). b. CL. The light blue luminescent areas are the homogeneous alkali feldspar, and the dull blue luminescent areas are the oligoclase. Secondary feldspar (oligoclase-albite) exhibits a dark blue or dark purple luminescence along the margins of the oligoclase. Scale: 55 mm on photograph = 1 mm on thin section. (CL conditions: 10 kV, 0.8 Am. Photographic conditions: 30s, ASA 400).

are mainly found in sample C37.

Under CL, the optically homogeneous alkali feldspar crystals usually exhibit light blue luminescence, whereas the oligoclase crystals exhibit dull blue luminescence. For the lamellar-like intergrowth texture (Fig. 5.1-2b), CL clearly shown that the light blue luminescent alkali feldspar grains are replaced by the dull blue luminescent oligoclase along the margins. However, some of the light blue luminescent alkali feldspar crystals are penetrated by the dull blue luminescent oligoclase stripes through the centre of the crystals.

CL spectra of the light blue luminescent optically homogeneous alkali feldspar and the dull blue luminescent oligoclase are represented in Fig. 5.1-3. The light blue luminescent homogeneous alkali feldspar consists of a high blue peak centered at 461 nm and a weak red peak centered at 705 nm. The ratio of the intensities of the blue and red peaks (I_B/I_R) is about 10.5 (Fig. 5.1-3, spectrum A and Table 5.1-1). The dull blue luminescent oligoclase consists of a low blue peak centered at 461 nm and a very weak red peak centered at 705 nm, and the ratio of I_B/I_R is about 13.1 (Fig. 5.1-3, spectrum B and Table 5.1-1). Both of the spectra may contain a very weak infrared peak centered at about 800 nm. The light blue luminescent homogeneous alkali feldspar has a higher luminescent intensity than the dull blue luminescent oligoclase.

The oligoclase has been further affected by late-stage fluids. These metasomatic areas are present as narrow, irregularly-shaped dark blue or dark purple luminescent secondary oligoclase-albite

Table 5.1-1. Representative cathodoluminescence properties and compositions of feldspars in the lower series of the layered ferroaugite syenites from Center I, Coldwell Complex, Ontario

Occurrence of feldspar	Sample No./ Spectrum No.	Luminescence colour	Intensities (cps)					Compositions		
			Blue peak	(nm)	Red peak	(nm)	B/R ratio	Or	Ab	An
Lower series syenites:										
Homogeneous alkali feldspar	C35/A	Light blue	8.18E-03	(461)	7.83E-04	(705)	10.45	38-56	41-56	3-8
Oligoclase	C35/B	Dull blue	4.44E-03	(461)	3.40E-04	(705)	13.06	3-9	71-77	17-21
Secondary albite, margins	C35	Purple	N/A		N/A			2-8	77-86	12-16
Homo. alkali feldspar, core	C40/A	Light violet blue	4.10E-03	(466)	2.16E-03	(705)	1.90	32-42	54-62	4-6
Alkali feldspar	C40/B	Light blue	3.89E-03	(466)	1.50E-03	(708)	2.59	29-43	54-64	3-7
in incipient perthite rim	C40	Light violet	N/A		N/A			58-60	39-41	1
2nd. albite	C40	Dull blue-dull red	N/A		N/A			2-5	91-95	2-7
2nd. K-feldspar	C40	Purple	N/A		N/A			85-99	0-14	0-1
Homo. alkali feldspar, core	C47/A	Light violet blue	9.66E-03	(465)	3.73E-03	(708)	2.59	38-46	49-57	4-5
Homo. alkali feldspar, rim	C47/B	Light violet	6.28E-03	(465)	3.03E-03	(708)	2.08	50-59	38-49	1-3
2nd. albite	C47	Dull red	N/A		N/A			1-6	88-97	2-10
2nd. K-feldspar	C47	Purple	N/A		N/A			87-96	3-13	1
Homo. alkali feldspar	C53/A	Light violet blue	3.02E-03	(474)	1.02E-03	(700)	2.96	47-50	48-51	1-2
Secondary albite, margins	C53/B	Light violet	3.39E-04	(474)	6.48E-04	(700)	0.52	7-10	87-88	3-4
Secondary albite, margins	C53/C	Deep red	1.54E-04	(474)	3.24E-03	(714)	0.05	2	97	1
Secondary K-feldspar, margins	C53/D	Purple	2.50E-03	(414)	3.22E-04	(702)	7.76	87-99	4-7	1
Homo. alkali feldspar	C55/A	Light violet blue	9.75E-03	(463)	3.99E-03	(708)	2.44	40-49	48-56	2-4
Secondary albite, margins	C55/B	Violet	1.63E-03	(418)	2.72E-03	(709)	0.60	2-7	87-97	1-6
Secondary albite, margins	C55/C	Deep red	3.24E-04	(419)	3.46E-03	(709)	0.09	1-4	91-98	1-5
Secondary albite, margins	C55	Non CL	N/A		N/A			1	97-98	1-2
Secondary K-feldspar, margins	C55	Dull blue	N/A		N/A			87-99	0-12	0-1
Homo. alkali feldspar, core	C58/A	Light violet blue	4.93E-03	(471)	2.16E-03	(700)	2.28	35-36	59-61	4
Homo. alkali feldspar, rim	C58/B	Light violet	1.98E-03	(474)	1.30E-03	(700)	1.52	49	49	2

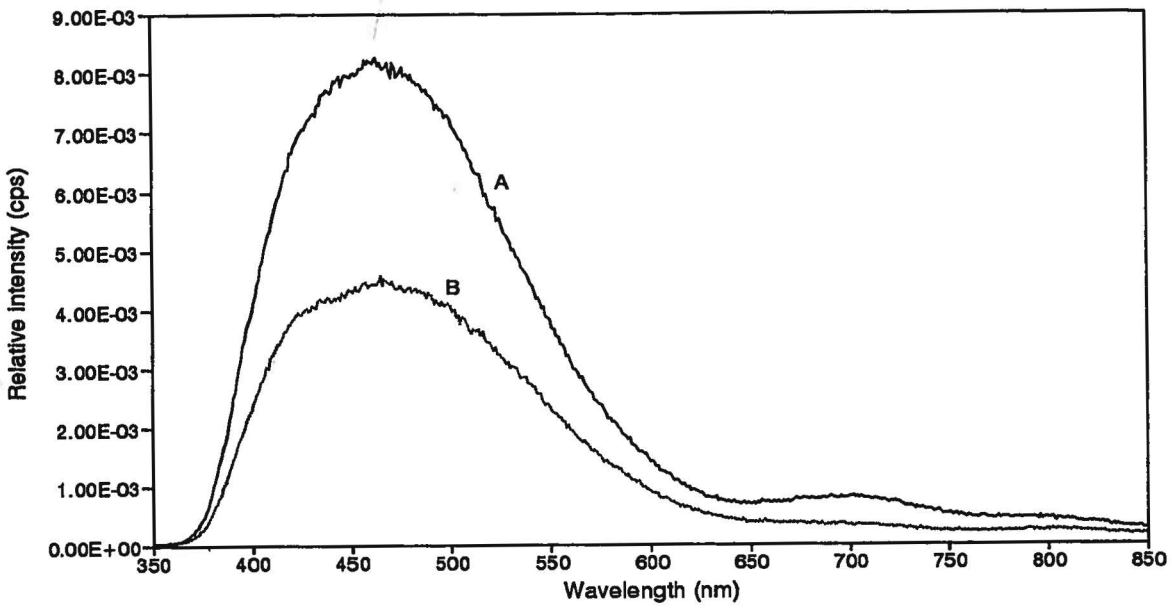

Fig. 5.1-3. CL spectra of the homogeneous alkali feldspar and the oligoclase in the lower series of the layered ferroaugite syenite (Sample C35), Center I. A-light blue luminescent homogeneous alkali feldspar. B-dull blue luminescent oligoclase. CL conditions: 10 kV, 0.8 mA.

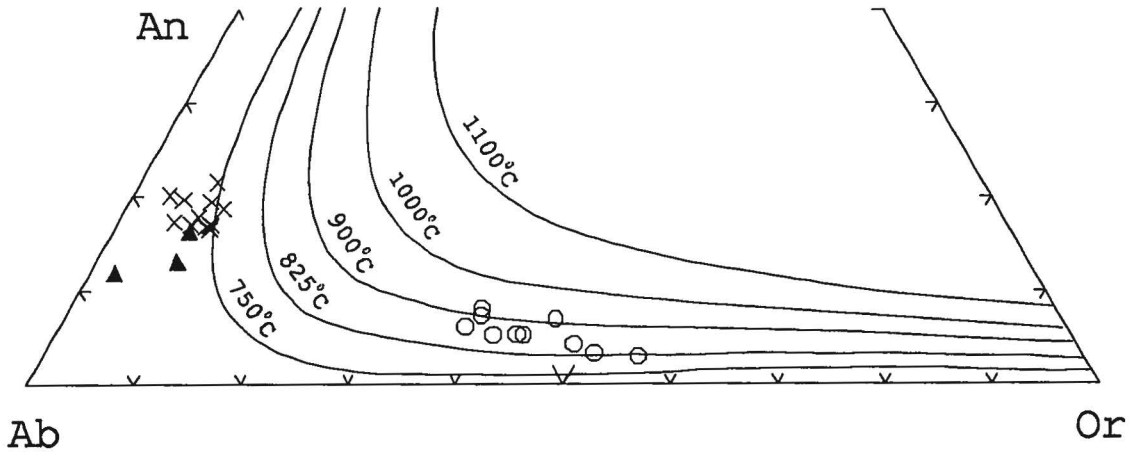

Fig. 5.1-4. The compositions of the feldspars in the layered ferroaugite syenite (Sample C35) plotted in the system Or-Ab-An.

The circles (o) are the light blue luminescent homogeneous alkali feldspar. The crosses (×) are the dull blue luminescent oligoclase.

The filled upper triangles (▲) are the dark blue or dark purple luminescent secondary feldspar (oligoclase-albite) which occurs along the margins of oligoclase. The isotherms are from Fuhrman and Lindsley (1988).

occurring at the margins of oligoclase crystals (Fig. 5.1-2b).

The light blue luminescent homogeneous alkali feldspar ranges in composition from $Or_{38-56}Ab_{41-56}An_{3-8}$, whereas the dull blue luminescent oligoclase range from $Ab_{71-77}An_{17-21}Or_{3-9}$ (Table 5.1-1, Fig. 5.1-4 and Appendix 1). The dark blue or dark purple luminescent secondary feldspar (oligoclase-albite) ranges in composition from $Ab_{77-86}An_{12-16}Or_{2-8}$. The secondary feldspar has relatively lower An contents than the oligoclase, which indicates that the Ca concentration has decreased and Na concentration has increased during the late-stage fluid-feldspar interaction. However, the secondary feldspar has relatively higher An contents than other secondary albites in Center I (see next sections). Thus the compositions of the secondary feldspars may be dependent on the compositions of the initial feldspar (oligoclase) which interacted with the late-stage fluids.

In the ternary-feldspar system, the compositions of coexisting feldspars are functions of crystallization temperature, thus the ternary-feldspar thermometer may be used to assess temperatures of equilibration and provide a valuable test for equilibrium between coexisting feldspar (Fuhrman and Lindsley, 1988). When the compositions of the alkali feldspars, oligoclases and secondary albites are plotted in the ternary-feldspar system, the crystallization temperatures of the homogeneous alkali feldspars are restricted to within a narrow range mainly between the 825 and 900 °C isotherms, whereas the oligoclase is distributed mainly below the 750 °C isotherm (Fig. 5.1-4). The different temperature

range of the crystallization provides further evidence that the oligoclase was not in equilibrium with the homogeneous alkali feldspars. The crystallization temperatures of the secondary feldspars (oligoclase-albite) also plot below the 750 °C isotherm, and are obviously not in equilibrium with the homogeneous alkali feldspar.

The replacement of alkali feldspar by oligoclase was also observed by Waldron and Parsons (1992) using transmission electron microscopy (TEM). In sample C37, they found that regular microtextures differ from those in the remaining layered syenites samples. Regular microtextures are defined by areas consisting of straight lamellae of low sanidine and albite-twinned oligoclase with a periodicity of about 500 nm. These cryptoperthites are equivalent to the light blue luminescent optically homogeneous alkali feldspars. The areas of the regular microtexture are cut by coarser lamellar (> 1 μm wide) albite-twinned oligoclase or large, irregularly shaped patches of albite-twinned oligoclase. These plagioclases correspond to the dull blue luminescent oligoclases. The periodicity (~500 nm) of the lamellae of the albite-twinned oligoclase in the regular microtexture is substantially larger than in the other samples (near 50 nm in the lower series), and the areas of the coarse oligoclase do not resemble Ab-rich ripples which are found in the rest of the samples (The term ripple refers to Ab-rich and Or-rich linear coherent cryptoperthites (about 10 μm) superposed on a regular microtexture). As ripples are not found in sample C37, Waldron and Parsons (1990) suggest that the

feldspars were affected by some process that did not involve the remaining augite syenite suite.

b. Optically homogeneous alkali feldspar

In samples C40, C47, and C58, feldspar crystals are lath-shaped, Carlsbad twinned, optically homogeneous alkali feldspar (Fig. 5.1-5a, -6a). The alkali feldspar crystals are partially replaced by some secondary feldspars at the margins or within the crystals during late-stage hydrothermal fluid-feldspar interaction. These secondary feldspars usually have a turbid, cloudy appearance and consist of secondary Na- and K-feldspar. Under CL, the optically homogeneous alkali feldspar crystals exhibit light violet blue luminescence in the centre of the crystals (Fig. 5.1-5b, -6b). This usually grades into light violet luminescence at the margin of the crystals. In sample C58 (Fig. 5.1-5b), CL also reveals that the optically homogeneous alkali feldspar crystals contain some irregular-shaped light violet luminescent bands within the crystals, these bands have sharp boundaries with the light violet blue luminescent alkali feldspar in the centre of the crystals.

CL spectra from the centre and margins of the homogeneous alkali feldspar crystals are represented in Fig. 5.1-7a. CL spectra of the light violet blue luminescent cores usually consist of high blue peaks at about 465-471 nm and low red peaks at about 700-708 nm with I_B/I_R ratios about 2.6-2.3 (Fig. 5.1-7a, spectrum A and Table 5.1-1). Although the total luminescence intensities (height of both the blue and red peaks) are relatively reduced in the margin of the

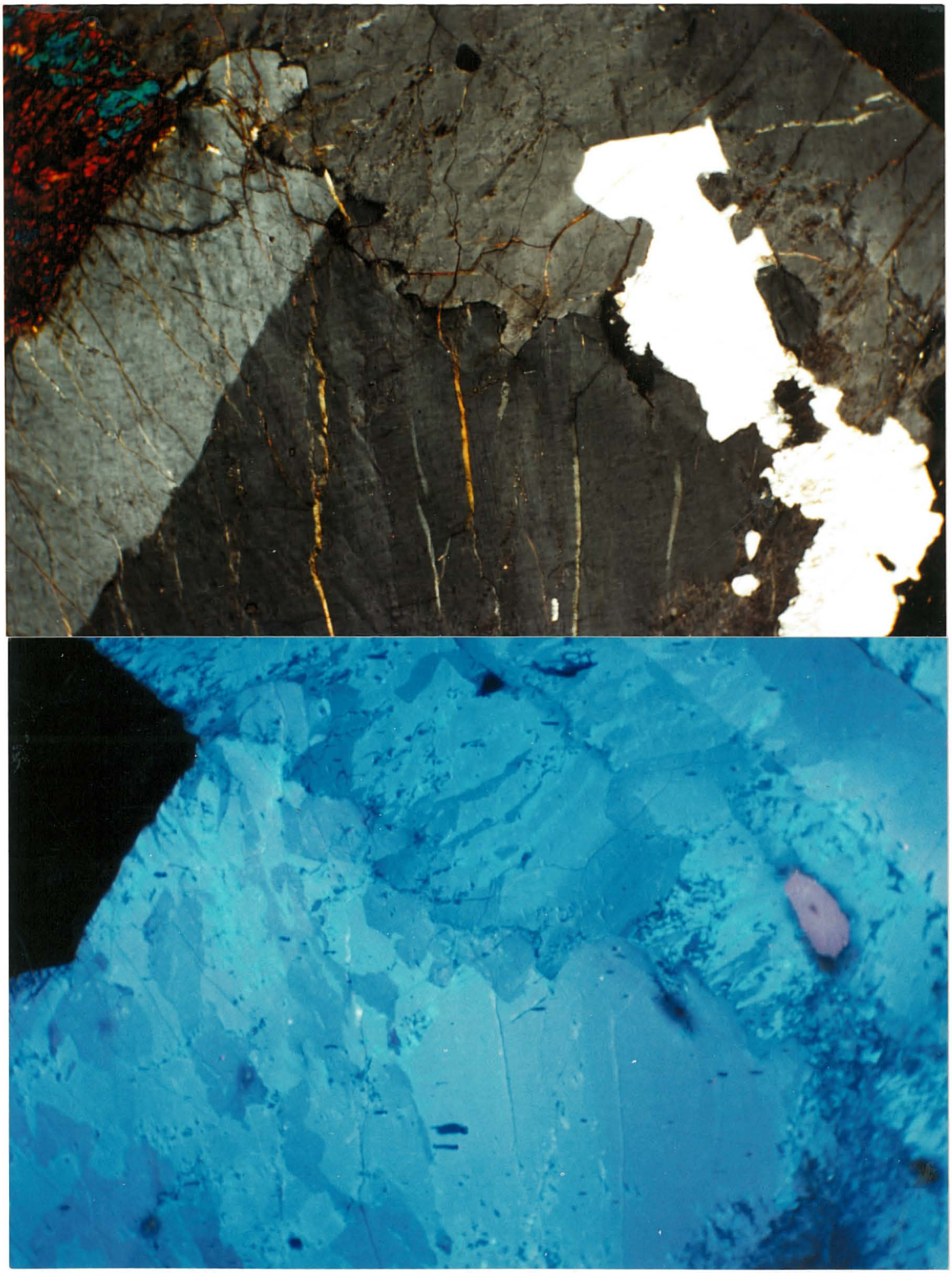

(a)

(b)

Fig. 5.1-5. Homogeneous alkali feldspar in the lower series syenite (Sample C58), Center I. a. TrL. The feldspar is optically homogeneous and Carlsbad twinned. (Photographic conditions: 15 s, ASA 25). b. CL. CL reveals that the feldspar is slightly mantled with a light violet blue luminescent core and a light violet luminescent rim. CL also reveals some irregular violet blue luminescent bands cross-cutting through the feldspar grains. Scale: 55 mm on photograph = 1 mm on thin section. (CL conditions: 10 kV, 0.8 Am. Photographic conditions: 1 m, ASA 400).

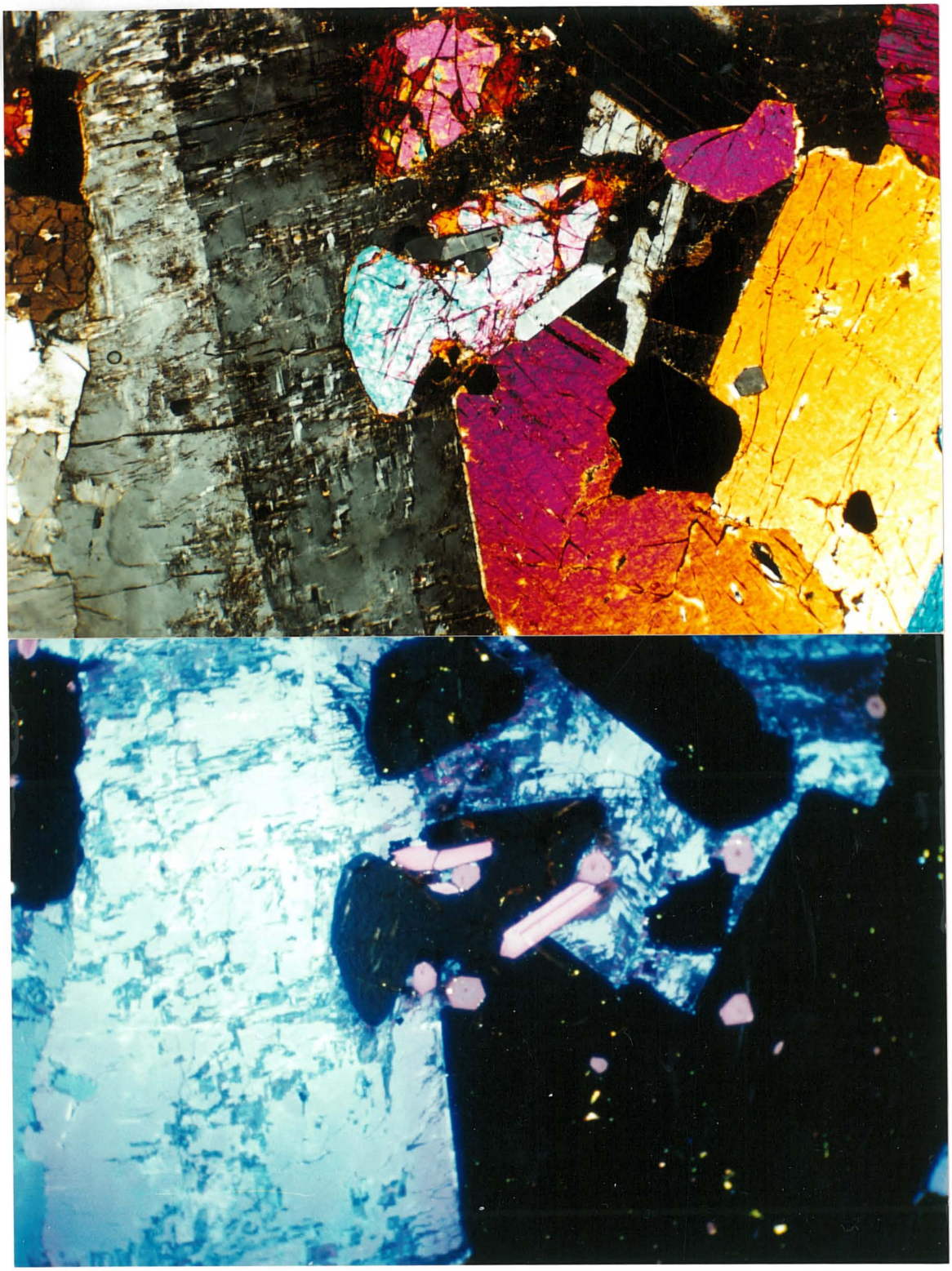

(a)

(b)

Fig. 5.1-6. Optically homogeneous alkali feldspar in the lower series syenite (Sample C47), Center I. a. TrL. The feldspar is optically homogeneous and Carlsbad twinned, and contains some turbid-looking areas which are secondary feldspars (Photographic conditions: 20s, ASA 25). b. CL. The homogeneous alkali feldspar exhibits light violet blue luminescence in the centre, and light violet luminesccence at the margins. Secondary albite exhibits dull blue or violet luminescence, and secondary K-feldspar exhibits purple luminescence. The pink luminescent crystals are apatite. Scale: 55 mm on photograph = 1 mm on thin section. (CL conditions: 10 kV, 0.8 Am. Photographic conditions: 1 m, ASA 400).

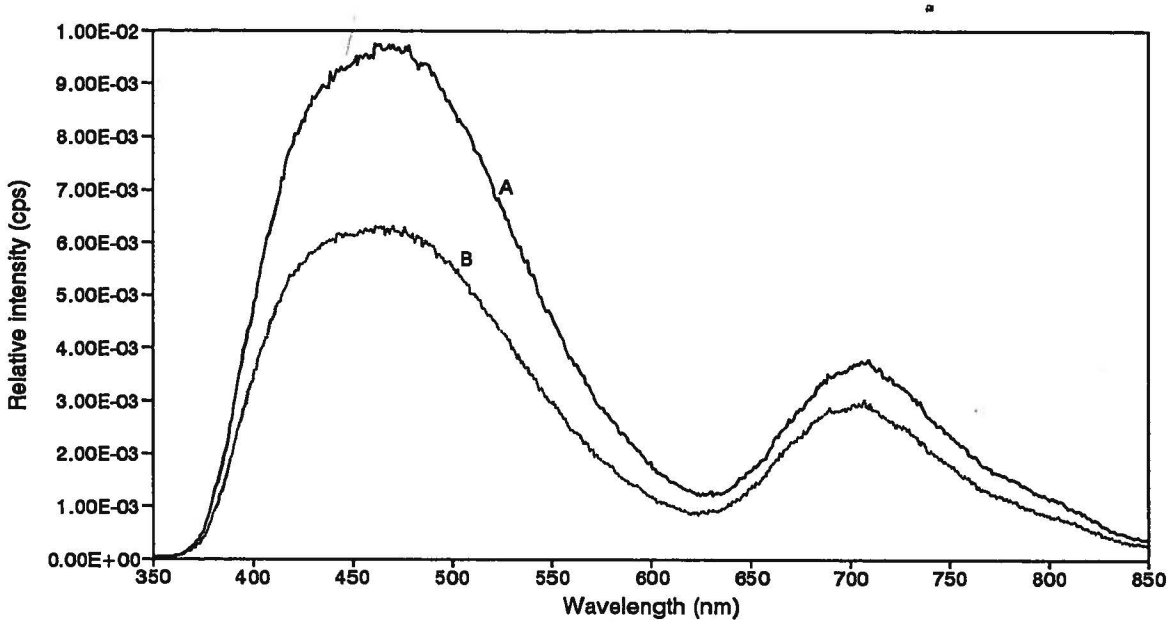

Fig. 5.1-7a. CL spectra of the homogeneous alkali feldspar in the layered ferroaugite syenite (Sample C47), Center I. The spectrum (A) is from the light blue luminescent alkali feldspar core, and the spectrum (B) is from the light violet luminescent alkali feldspar rim. CL conditions: 10 kV, 0.8 mA.

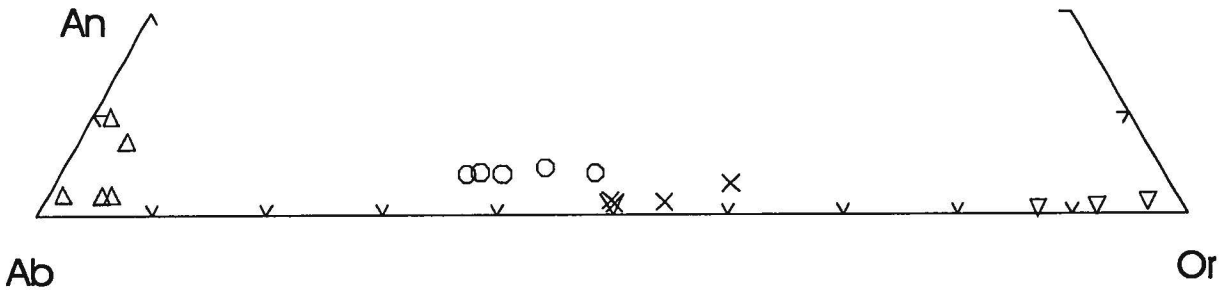

Fig. 5.1-7b. The compositions of the feldspars in the lower series of the layered ferroaugite syenites (Samples, C47 and C58) plotted in the system Or-Ab-An.

The circles (O) are light violet blue luminescent homogeneous alkali feldspar cores, and the crosses (×) are the light violet luminescent homogeneous alkali feldspar margins.

The upper triangles are (▵) the dull red luminescent secondary Na-feldspar, and the down triangles (▿) are the purple luminescent secondary K-feldspar at the margins.

crystals, the light violet luminescent rims also consist of high blue peaks at about 465-474 nm and low red peaks at about 700-708 nm. The ratios of I_B/I_R are about 1.5-2.1 (Fig. 5.1-7a, spectrum B and Table 5.1-1). The light violet blue luminescent centres have higher I_B/I_R ratios than the light violet luminescent margins.

In sample C47, the light violet blue luminescent homogeneous alkali feldspar core ranges in composition from $Or_{38-46}Ab_{49-57}An_{4-5}$, whereas the light violet luminescent margin is from $Or_{50-59}Ab_{38-49}An_{1-3}$ (Table 5.1-1, Fig. 5.1-7b and Appendix 1). In sample C58, light violet blue luminescent homogeneous alkali feldspar core ranges in composition from $Or_{35-36}Ab_{59-61}An_4$, whereas the light violet luminescent margin has a composition of $Or_{49}Ab_{49}An_2$ (Table 5.1-1, Fig. 5.1-7b and Appendix 1). In both of the samples, the Or contents increase while the An contents slightly decrease from the centre to the margin of the crystals.

In samples C44, C53 and C55, most of the homogeneous alkali feldspar crystals are strongly affected by late-stage hydrothermal fluids, and most areas within the crystals show turbid-looking areas which consist of secondary Na- and K-feldspars (Fig. 5.1-8a). Fresh, unaltered homogeneous alkali feldspar only occurs as irregular patches surrounded by secondary feldspars. These homogeneous alkali feldspar relict crystals exhibit light violet blue luminescence (Fig. 5.1-8b), and the CL spectra consist of high blue peaks at about 463-474 nm and low red peaks at 700-708 nm with I_B/I_R ratios about 2.4-3.0, and the feldspars range in composition from $Or_{40-50}Ab_{48-56}An_{1-4}$ (Table 5.1-1, Fig. 5.1-9 and Appendix 1). These

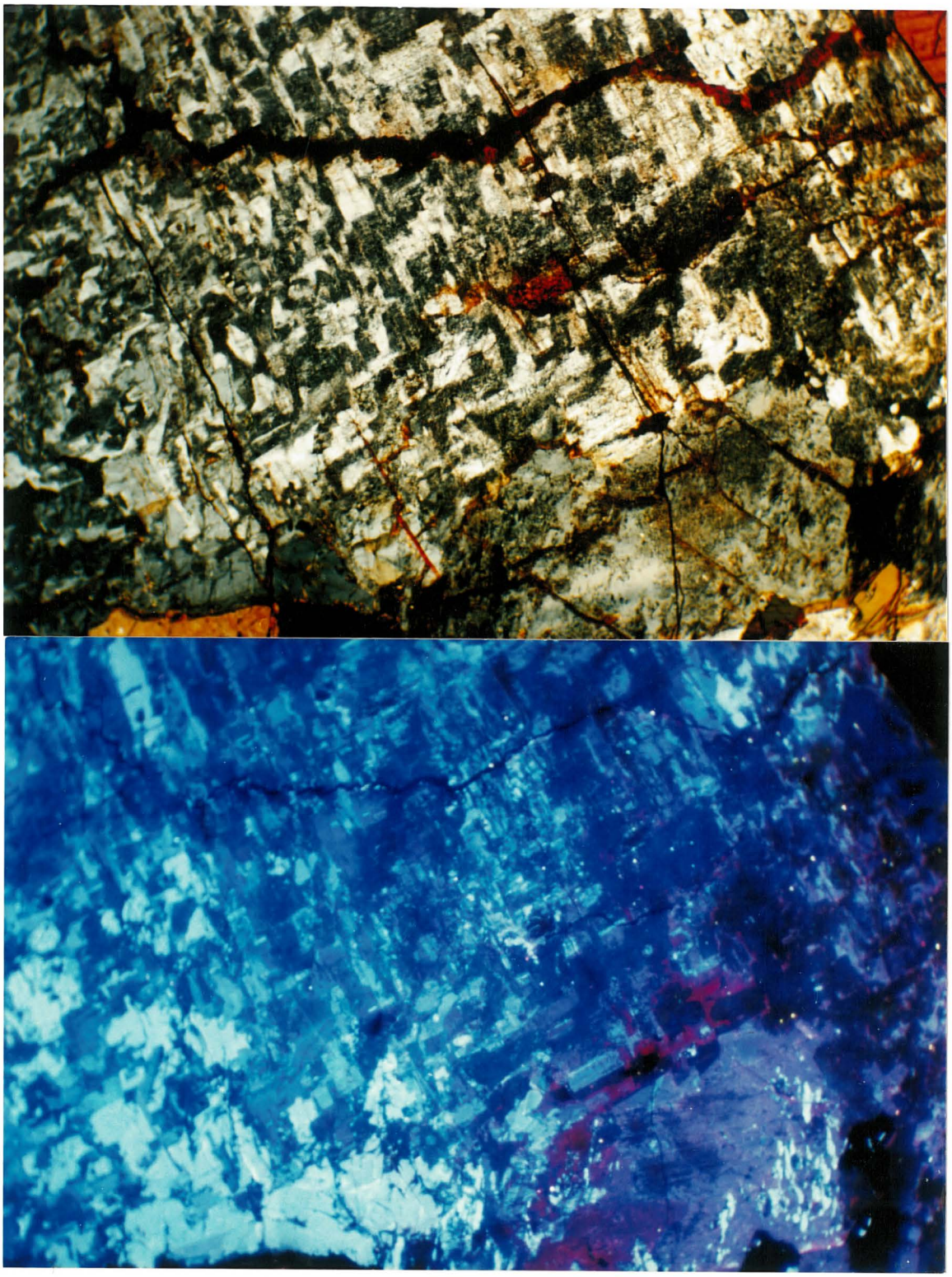

(a)

(b)

Fig. 5.1-8. Optically homogeneous alkali feldspar and secondary feldspars in the lower series syenite (Sample C53), Center I. a. TrL. The homogeneous alkali feldspar is altered by secondary albite (clear) and K-feldspar (turbid). (Photographic conditions: 20s, ASA 25). b. CL. The homogeneous alkali feldspar exhibits light violet blue luminescence. The secondary albite exhibits violet or deep red luminescence, and the secondary K-feldspar exhibits purple luminescence. Scale: 55 mm on photograph = 1 mm on thin section. (CL conditions: 10 kV, 0.8 Am. Photographic conditions: 2m, ASA 400).

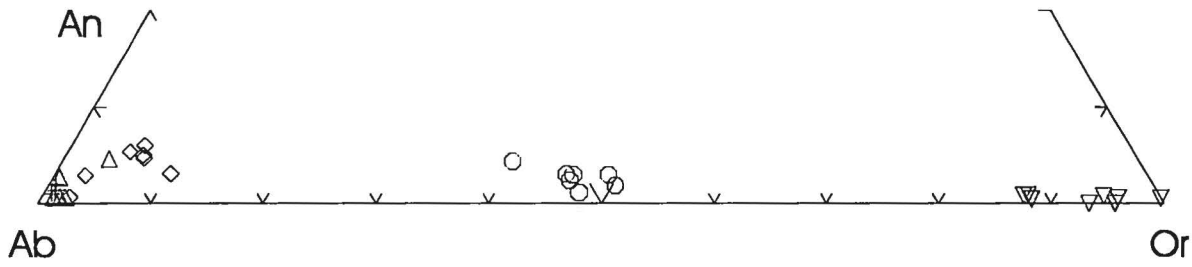

Fig. 5.1-9. The compositions of the feldspars in the lower series of the layered ferroaugite syenites (Samples C53 and C55) plotted in the system Or-Ab-An.

The circles (∘) are the light blue luminescent homogeneous alkali feldspars.

The down triangles (▿) are the purple luminescent secondary K-feldspars. The diamonds (◇) are the light violet and violet luminesecent secondary albites and the upper triangles (△) are the deep red luminescent secondary albites. The crosses (+) are the non luminescent secondary albites.

homogeneous alkali feldspar crystals have similar CL properties and compositions as those light violet blue luminescent alkali feldspar cores in samples C47 and C58, but the Or contents are slightly higher.

c. Optically homogeneous alkali feldspar mantled with incipient perthitic rim

In sample C40, some optically homogeneous alkali feldspar crystals are mantled by an incipient perthitic rim (Fig. 5.1-10a). The optically homogeneous alkali feldspar core exhibits light violet blue luminescence, and the incipient perthitic rim exhibits light blue luminescence and contains some light violet blue luminescent bands (Fig. 5.1-10b). CL spectra of both the light violet blue luminescent core and light blue luminescent rim consist of a high blue peak at 466 nm and a low red peak at about 705-708 nm (Fig. 5.1-11a), but the light violet blue luminescent core has a I_B/I_R ratio (1.9) relatively lower than the light blue luminescent rim (2.6) (Table 5.1-1). The light violet blue luminescent homogeneous core ranges in composition from $Or_{32-42}Ab_{54-62}An_{4-6}$. However, the light blue luminescent rim ranges in composition from $Or_{29-43}Ab_{54-64}An_{3-7}$, and the light violet blue luminescent bands within the rim range from $Or_{49-60}Ab_{39-49}An_1$ (Table 5.1-1, Fig. 5.1-11b and Appendix 1).

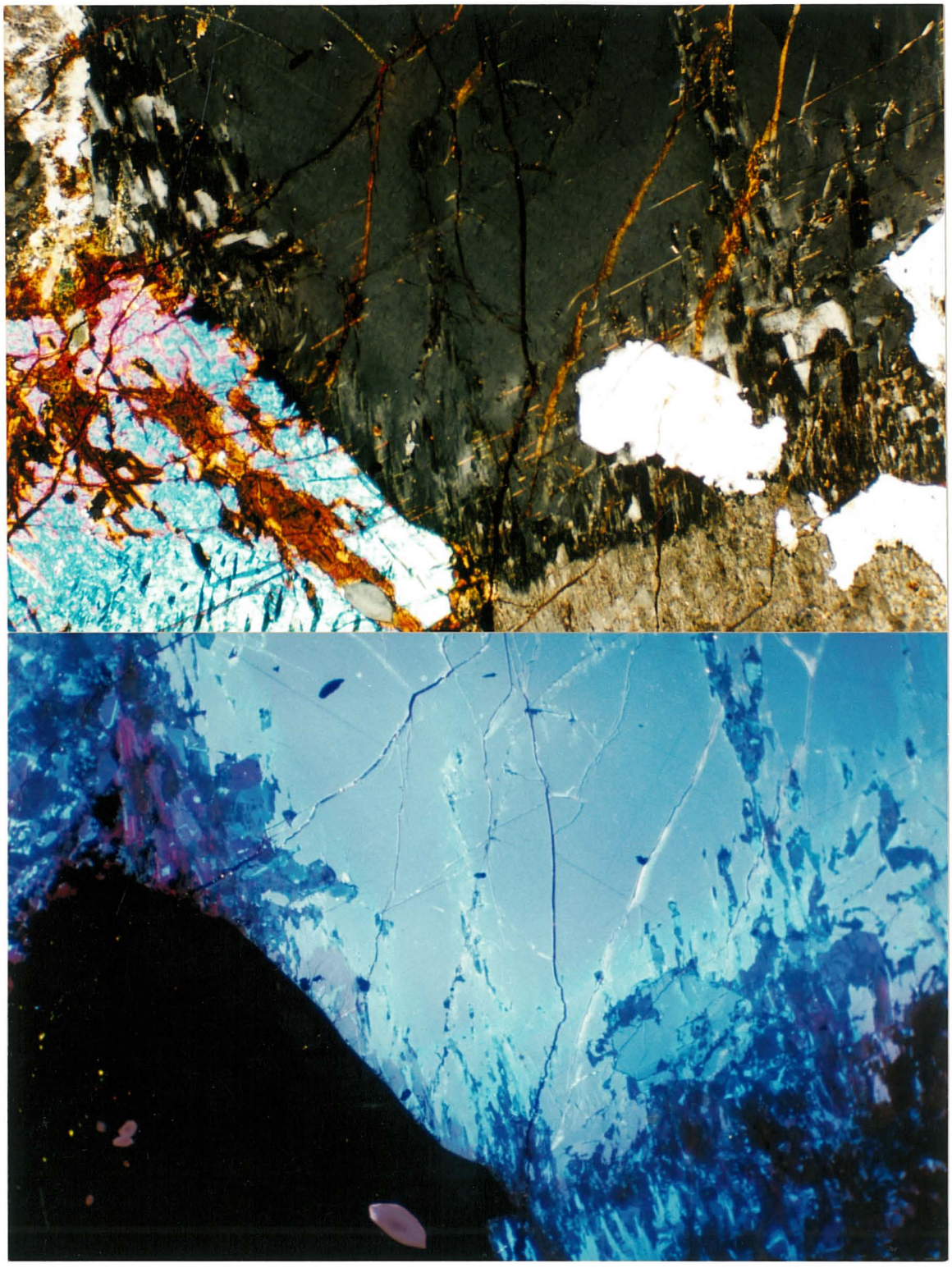

(a)

(b)

Fig. 5.1-10. Optically homogeneous alkali feldspar in the lower series syenite (Sample C40), Center I. a. TrL. The homogeneous alkali feldspar is slightly mantled with an incipient perthitic rim, and the rim is replaced by secondary feldspars which are turbid-looking. (Photographic conditions: 20s, ASA 25). b. CL. The homogeneous alkali feldspar core exhibits light violet blue luminescence. The incipient perthitic rim exhibits light blue luminescence and contains same light violet luminescent bands. Secondary albite exhibits dull blue, dull violet blue or dull red luminescence, whereas secondary K-feldspar exhibits purple luminescence. The pink luminescent crystals are apatites. Scale: 55 mm on photograph = 1 mm on thin section. (CL conditions: 10 kV, 0.8 Am. Photographic conditions: 40s, ASA 400).

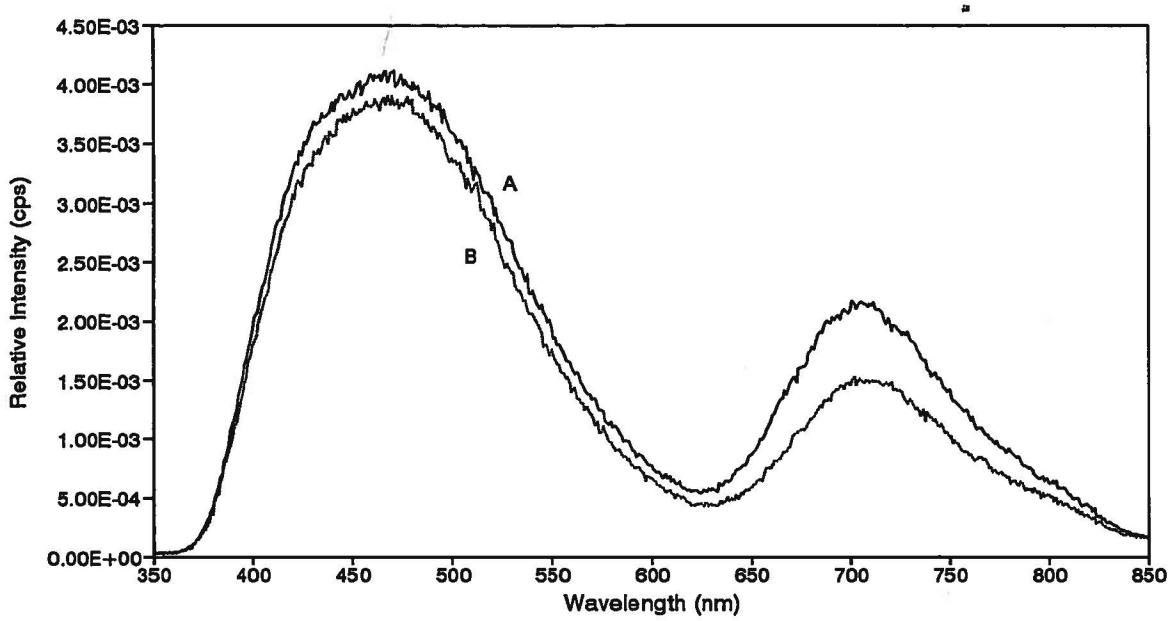

Fig. 5.1-11a. CL spectra of the alkali feldspars in the lower serise ferroaugite syenite (Sample C40), Center I. The spectrum (A) is from the light violet blue luminescent homogeneous alkali feldspar core. The spectrum (B) is from the light blue luminescent alkali feldspar in the incipient perthitic rim. CL conditions: 10 kV, 0.8 mA.

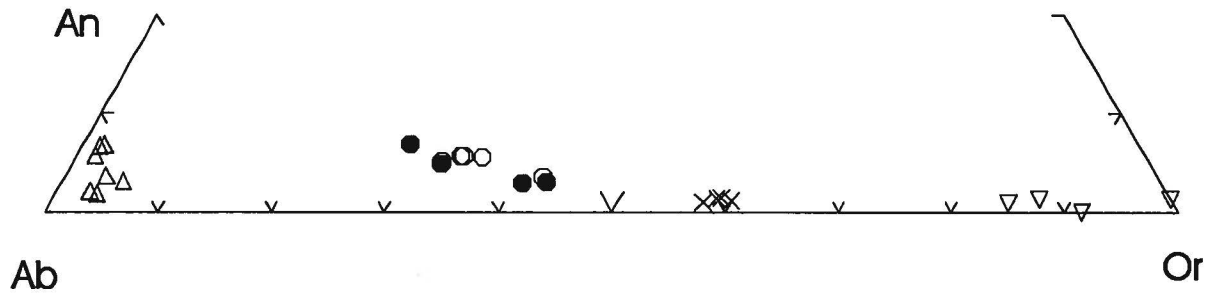

Fig. 5.1-11b. The compositions of the feldspars in the lower series of the layered ferroaugite syenites (Samples C40) plotted in the system Or-Ab-An.

The circles (O) are the light violet blue luminescent homogeneous alkali feldspar core. The filled circles (•) are the light blue luminescent alkali feldspar rim and crosses (×) are the light violet blue luminescent alkali feldspar bands in the rim.

The upper triangles are (▵) the dull blue, dull violet and dull red luminescent secondary Na-feldspars, and the down triangles (▿) are the purple luminescent secondary K-feldspars at the margins of the crystal.

5.1.3. Alkali feldspars in the upper series of the layered ferroaugite syenites

In the upper series of syenites, the feldspar crystals consist mainly of irregular vein or patch perthite and optically homogeneous alkali feldspar. However, a few individual albite grains are found in some samples. Most of these feldspar crystals are mantled by a deuteric coarsened antiperthitic rim, and some of them are mantled with an intermediate optically homogeneous mantle and an deuteric coarsened antiperthitic rim. Internal growth textures, CL characteristics and compositions of these alkali feldspars are described in the following sections.

a. Irregular vein perthite

In samples C63-C67, the alkali feldspar crystals are incipient irregular vein perthite or patch perthites. The perthites commonly consist of cryptoperthitic patches, Na-rich and K-rich feldspar exsolution lamellae and secondary K-feldspar within individual grains. Usually, the cryptoperthitic patches occur dominantly at the crystal margins, and these cryptoperthitic patches are exsolved gradually into Na-rich and K-rich feldspar lamellae along the patch margins (Fig. 5.1-12a, -13a, -14a). Also, there is no distinct boundary between the Na-rich and K-rich feldspar exsolution lamellae under transmitted light. The secondary K-feldspar usually occurs in fractures with a turbid or clouded appearance.

Under CL, the cryptoperthitic patches exhibit light greyish blue, light violet blue or light bluish violet luminescence (Fig. 5.1-

12b, -13b, -14b). The exsolved albite usually exhibits light blue luminescence, whereas the exsolved K-rich feldspar exhibits dull blue luminescence. CL spectra of the cryptoperthitic patches are shown in the Fig. 5.1-15a, spectra A to C. These spectra consist of high intensity blue peaks at about 457-464 nm and low intensity red peaks centered at about 707-711 nm. As the luminescence colours change from light greyish through light violet blue to light bluish violet, the intensities of the blue peaks are reduced, the intensities of the red peaks are increased, and the ratios of I_B/I_R change from 9.9 to 5.2 and 2.1, respectively (Table 5.1-2). The light blue luminescent exsolved albite consists of a very high blue peak at about 455 nm and a weak red peak centered at about 707 nm with a I_B/I_R ratio of about 18.9 (Table 5-2, Fig. 5.1-15a and spectrum D).

SEM/BSE image shows that the cryptoperthitic patches are strain-controlled microperthite, which is indicated by a microbraid texture of albite (dark grey) and K-feldspar (grey) lamellae in diagonal intergrowths (Fig. 5.1-16a). The braid microperthite grades into chemically homogeneous alkali feldspar (grey) near the deuteric coarsened antiperthitic rim. It then grades into irregular-shaped Na-rich feldspar (dark grey) or K-rich feldspar (light grey) in the centre of the crystals.

The light greyish blue, light violet blue or light bluish violet luminescent cryptoperthitic patches range in composition from $Or_{34-52}Ab_{47-64}An_{1-3}$ (Table 5.1-2, Fig. 5.1-17, Appendix 1). The light blue luminescent exsolved albite ranges in composition from

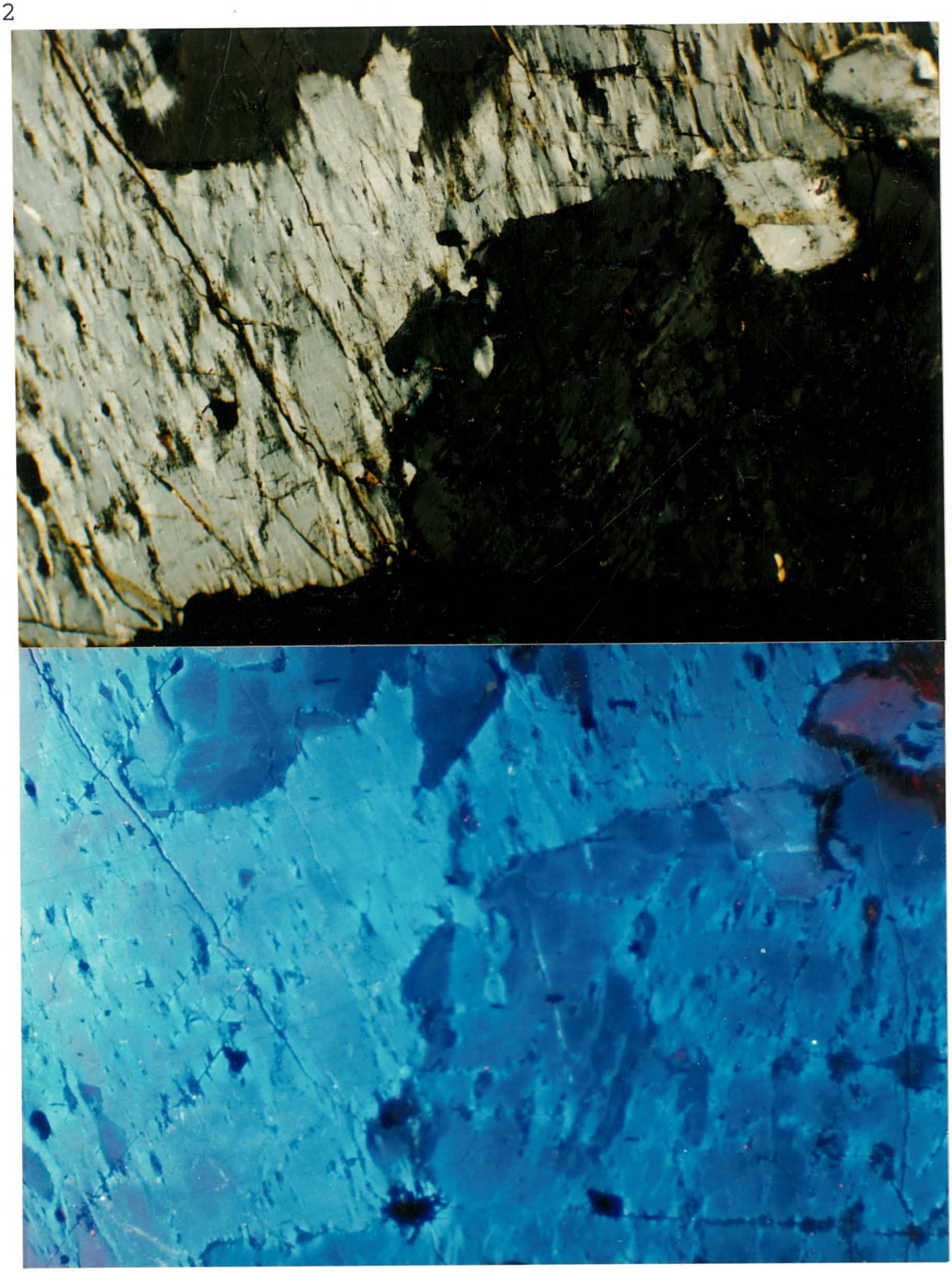

(a)

(b)

Fig. 5.1-12. Incipient irregular vein perthite in the upper series syenite (Sample C65), Center I. a. TrL. The perthite consists of cryptoperthitic patches and exsolved albite and K-feldspar. (Photographic conditions: 20s, ASA 25). b. CL. The cryptoperthitic patches exhibit light violet blue or light bluish violet luminescence. The exsolved albite exhibits light blue luminescence, whereas the exsolved K-feldspar exhibits dull blue luminescence. Scale: 55 mm on photograph = 1 mm on thin section. (CL conditions: 10 kV, 0.8 Am. Photographic conditions: 1m, ASA 400).

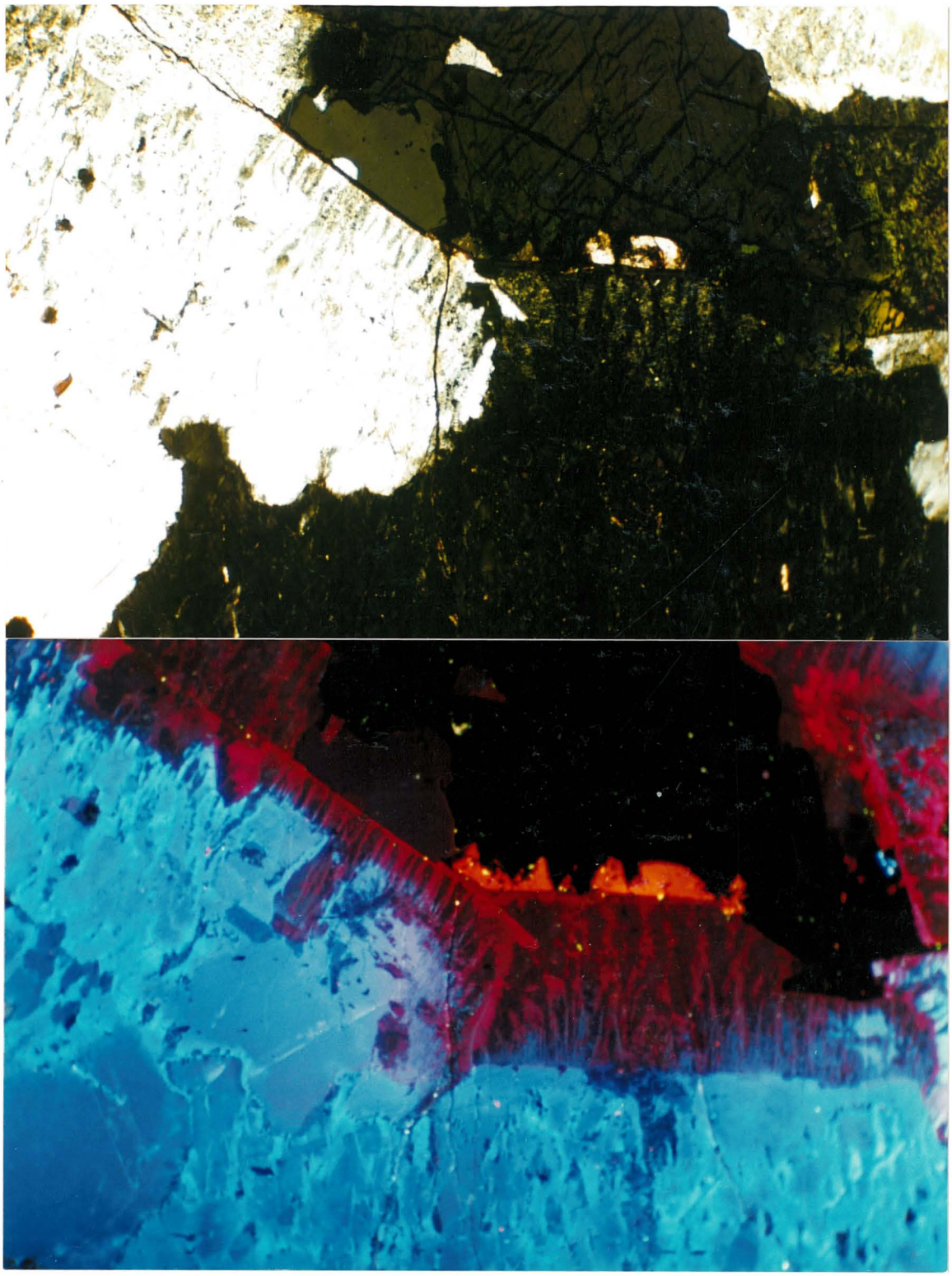

(a)

(b)

Fig. 5.1-13. Feldspars in the upper series syenite (Sample C65), Center I. a. TrL. The irregular vein perthite is mantled by a deuteric coarsened antiperthitic rim. (Photographic conditions: 10s, ASA 400). b. CL. The perthite consists of light violet blue or light bluish violet luminescent cryptoperthitic patches, light blue luminescent exsolved albite and dull blue luminescent exsolved K-feldspar. The deuteric coarsened antiperthitic rim consists of deep red luminescent secondary albite and brown luminescent secondary K-feldspar. Some dark brown luminescent quartz and orange luminescent calcite occur in the interstices between the deuteric coarsened antiperthitic rim and an amphibole grain. Scale: 55 mm on photograph = 1 mm on thin section. (CL conditions: 10 kV, 0.8 Am. Photographic conditions: 3m, ASA 400).

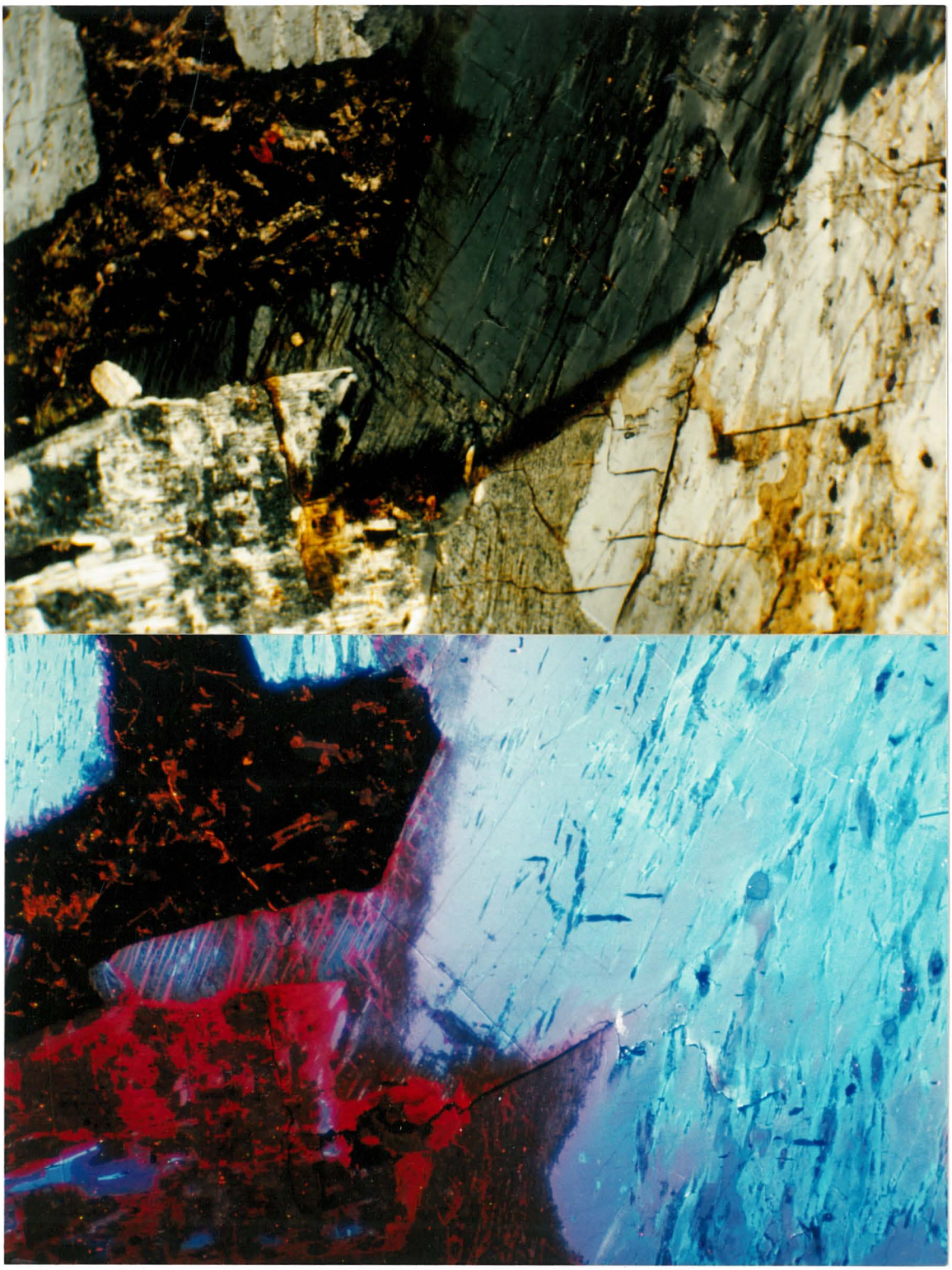

(a)

(b)

Fig. 5.1-14. Feldspars in the upper series syenite (Sample C65), Center I. a. TrL. The irregular vein perthite is mantled by a deuteric coarsened antiperthitic rim. (Photographic conditions: 15s, ASA 400). b. CL. The perthite consists of light violet blue or light bluish violet luminescent cryptoperthitic patches, light blue luminescent exsolved albite feldspar and dull blue luminescent exsolved K-feldspar. Some dark greenish blue luminescent irregular bands in the centre of the perthite are the secondary K-feldspars. In the deuteric coarsened antiperthite rim, the secondary albite exhihits deep red luminescence and secondary K-feldspar exhibits purple or brown luminescence. Scale: 55 mm on photograph = 1 mm on thin section. (CL conditions: 10 kV, 0.8 Am. Photographic conditions: 1m, ASA 400).

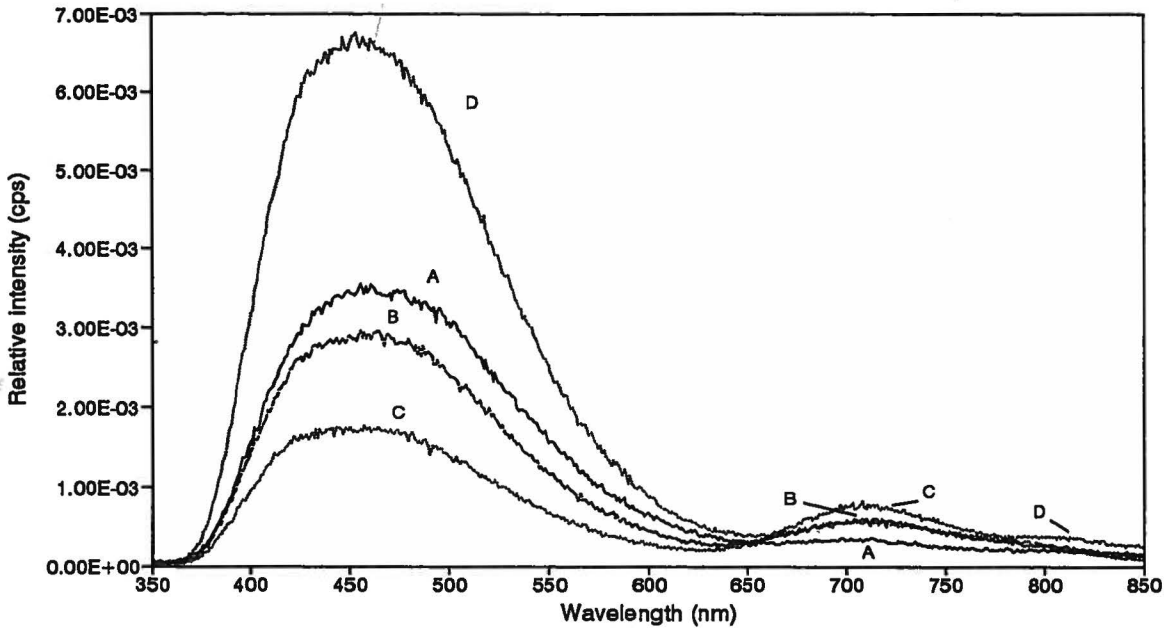

Fig. 5.1-15a. CL spectra of the cryptoperthitic patches and exsolved albite in the irregular vein perthite from the upper series of the layered ferroaugite syenites (Sample C65), Center I. Spectra (A), (B) and (C) are from the light greyish blue, light violet blue and light bluish violet luminescent patches, respectively. Spectrum (D) is from the light blue luminescent exsolved Na-rich feldspar. CL conditions: 10 kV, 0.8 mA.

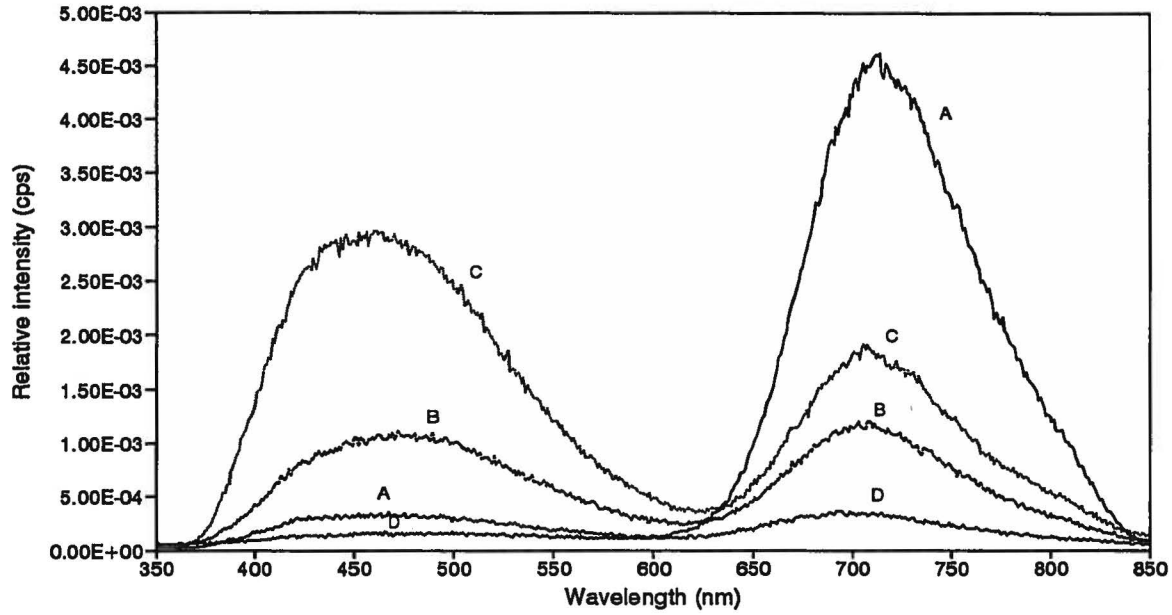

Fig. 5.1-15b. CL spectra of secondary feldspars from the deuteric coarsened antiperthitic rims in the layered ferroaugite syenite (Sample C65), Center I. The spectrum (A) is from the deep red luminescent secondary albite and the spectra (B), (C) and (D) are from the grey, violet blue and brown luminescent secondary K-feldspars, respectively. CL conditions: 10 kV, 0.8 mA.

Table 5.1-2. Representative cathodoluminescence properties and compositions of feldspars in the upper series of the layered ferroaugite syenites from Center I, Coldwell Complex, Ontario

Occurrence of feldspar	Sample No./ Spectrum No.	Luminescence colour	Intensities (cps)					Compositions		
			Blue peak	(nm)	Red peak	(nm)	B/R ratio	Or	Ab	An
Upper series syenites:										
Cryptoperthitic patches in perthite	C65/A	Light greyish blue	3.44E-03	(464)	3.48E-04	(707)	9.89			
	C65/B	Light violet blue	2.90E-03	(460)	5.55E-04	(711)	5.23			
	C65/C	Light bluish violet	1.78E-03	(457)	8.28E-04	(708)	2.14	34-52	47-64	1-3
Exsolved albite in perthite	C65/A	Light blue	6.57E-03	(455)	3.48E-04	(707)	18.91	1-10	87-97	1-5
Exsolved K-feldspar in perthite	C65	Dull Blue	N/A		N/A			61-82	17-38	1-3
2nd K-feldspar in fractures.	C65/B	Dull greenish blue	1.93E-03	(486)	2.96E-04	(704)	6.53	90-99	4-9	1
2nd. albite, antiperthite rim.	C65/A	Deep red	3.40E-04	(463)	4.60E-03	(713)	0.07	1-3	96-99	1
2nd. K-feldspar, antiperthitic rim	C65/B	Grey	1.08E-03	(473)	1.20E-03	(708)	0.89			
	C65/C	Violet blue	2.94E-03	(459)	1.92E-03	(708)	1.53	90-100	6-10	1
	C65/D	Brown	1.64E-04	(483)	3.49E-04	(701)	0.47	94-100	3-5	1
Homo. alkali feldspar, centre, core	C68/A	Light blue	1.10E-02	(447)	1.83E-03	(698)	6.01	27-36	63-72	1-2
- - -, intermediate, core	C68/B	Light violet blue	4.14E-03	(451)	4.19E-03	(698)	0.99	36-44	55-63	1
- - -, margin, core	C68/C	Light violet	5.24E-04	(452)	4.40E-03	(698)	0.12	40-41	59-60	1
Albite twinned albite, core	C68/A	Violet	2.48E-03	(413)	5.11E-03	(700)	0.49			
	C68/B	Violet-red	1.25E-03	(410)	5.73E-03	(700)	0.22	1-2	98-99	
2nd K-feldspar, albite core	C68	Brown	N/A		N/A			90-94	6-10	<1
2nd. albite, antiperthitic rim	C68	Deep red	N/A		N/A			1-2	97-99	<1
2nd. K-feldspar, antiperthitic rim	C68	Brown	N/A		N/A			84-92	7-16	0-1
Exsolved Na-albite, core	C72/A	Light blue	1.57E-02	(457)	7.73E-04	(704)	20.26	1-3	92-96	2-6
Exsolved K-feldspar, core	C72/B	Dull blue	3.99E-03	(458)	8.10E-04	(704)	4.92	66-72	27-33	1
Homo. alkali feldspar, mantle	C72/A	Light violet blue	4.82E-03	(460)	4.54E-03	(707)	1.06	48-50	49-52	1
	C72/B	Light violet	3.99E-03	(457)	3.14E-03	(707)	1.27	37-47	52-61	1
2nd. albite, antiperthitic rim	C72/A	Deep red	2.65E-04	(466)	6.53E-03	(711)	0.04	1-2	98-99	
	C72/B	Brown	1.06E-03	(463)	8.45E-04	(710)	1.25	90-92	7-9	1
2nd. K-feldspar, antiperthitic rim	C72/C	Grey	3.52E-04	(470)	4.15E-03	(711)	0.08	86-91	8-14	1

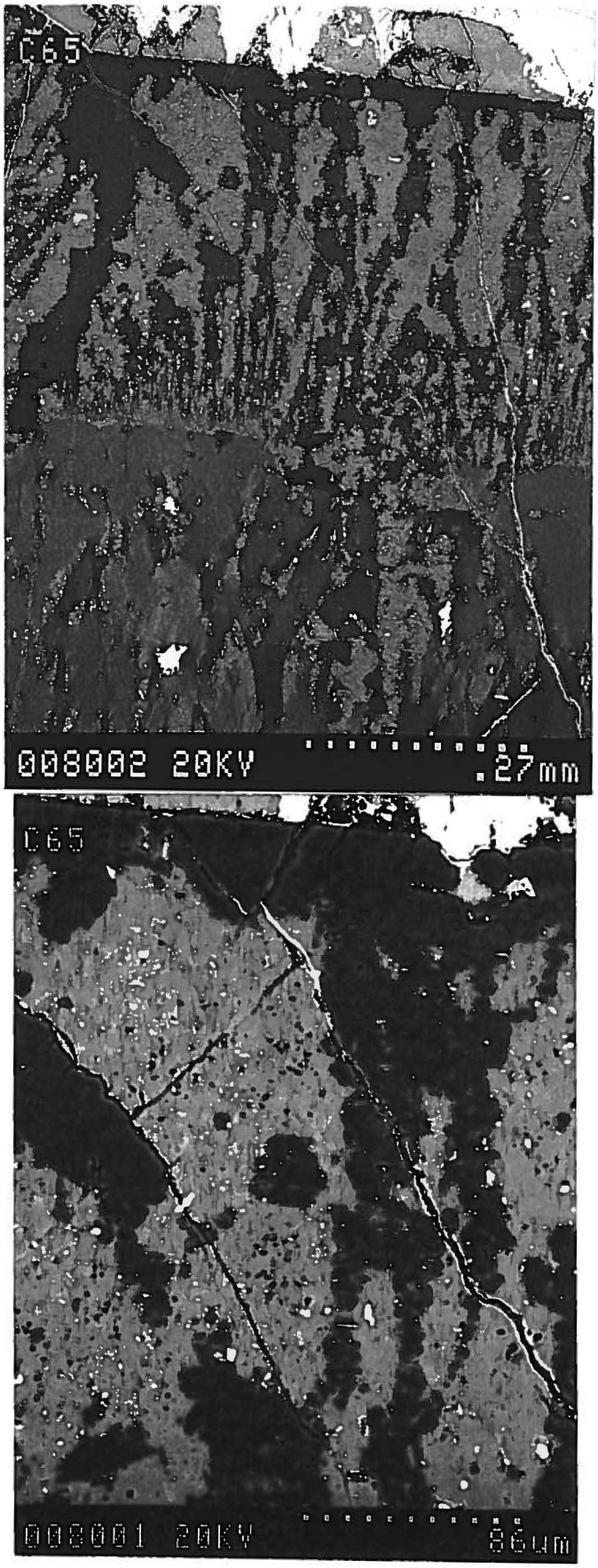

Fig 5.1-16. SEM/BSE micrograph of the irregular vein perthite and the deuteric coarsened anti-perthite rim in the upper series of the ferroaugite syenites (Sample C65), Center I. a. The irregular vein perthite (bottom) is mantled by the deuteric coarsened antiperthitic rim (top). Within the irregular vein perthite, the cryptoperthitic patches show a microbraid texture and grade into homogeneous feldspar along the contact with the deuteric coarsened anti-perthitic rim. These patches also grade into exsolved albite (dark grey) and exsolved K-feldspar (light grey), and are partially replaced by deuteric coarsened secondary albite (dark grey) and K-feldspar (light grey) at the rim of the crystal. b. The secondary albite (dark grey) and secondary K-feldspar in the deuteric coarsened antiperthitic rim. The white spots are the Fe-bearing minerals and the black spots are the micropores which are mainly distributed within the secondary K-feldspar.

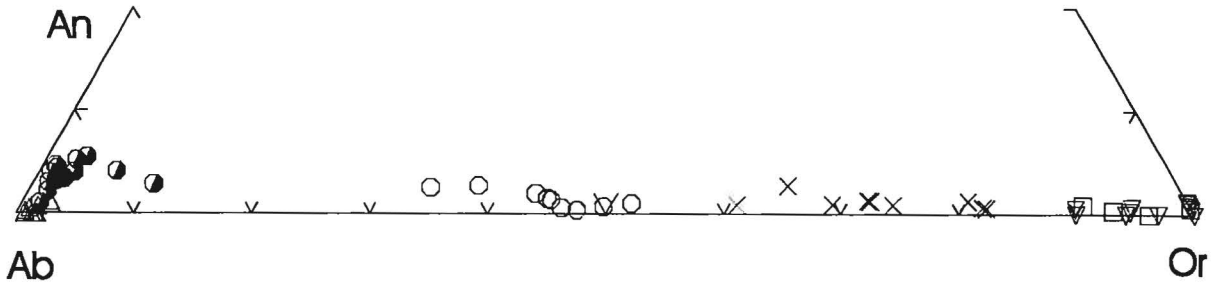

Fig. 5.1-17. The compositions of the feldspars in the upper series of the layered ferroaugite syenites (Sample C65) plotted in the system Or-Ab-An.

In the irregular vein perthite, the circles (O) are the light violet blue, light greyish blue and light bluish violet luminescent cryptoperthitic patches (braid microperthite). The crosses (×) are the dull blue luminescent exsolved K-feldspars and the half-filled circles (O) are the light blue luminescent exsolved albite at the margins of cryptoperthitic patches.

In the deuteric coarsened antiperthite rim, the upper triangles are (▵) the red luminescent secondary albite and the down triangles (▿) are the dull grey, violet blue and brown luminescent secondary K-feldspars.

The squares (□) are the dull greenish blue luminescent secondary K-feldspars in the fractures of irregular vein perthite.

$Ab_{87-97}Or_{1-10}An_{1-5}$, whereas the dull blue luminescent exsolved K-rich feldspars are from $Or_{61-82}Ab_{17-38}An_{1-3}$. The compositions of the cryptoperthitic patches a similar to those light violet luminescent homogeneous alkali feldspars in the lower series.

b. Irregular vein perthite mantled with a deuteric antiperthitic rim

In the feldspar crystals in contact with pyroxene and amphibole crystals, the incipient irregular vein perthite crystals are usually mantled by a deuteric coarsened antiperthitic rim (Fig. 5.1-13a, -14a). The incipient irregular vein perthite cores are the same as those perthite crystals which discussed in above (section a). However, in the deuteric coarsened antiperthite rims, the secondary albite exhibits a deep red luminescence (Fig. 5.1-13b, -14b), whereas the K-rich feldspar exhibits various luminescence colours such as grey, violet blue and brown. CL spectrum of the deep red luminescent secondary albite consists of a very low blue peak centered at about 463 nm and a very high red peak centered at about 713 nm with I_B/I_R ratio about 0.1 (Fig. 5.1-15b, spectrum A and Table 5.1-2). CL spectra of the grey, violet blue and brown luminescent secondary K-feldspars are also shown in Fig. 5.1-14a; spectra B-D. The peak positions and intensities of both blue and red peaks vary with their luminescence colours. As the luminescence colours change from grey through violet blue to brown, the ratios of I_B/I_R increase from 0.9 through 1.5 to 4.7 (Table 5.1-2).

SEM/BSE images (Fig. 5.1-16a) show the details of the deuteric

coarsened feldspar overgrowths at the edge of irregular vein perthite. The deuteric coarsened feldspars usually are strain-free antiperthites. However, near the contact with the irregular vein perthite, the deuteric coarsened feldspars are predominately secondary K-feldspar (light grey) intergrown with elongated strings or lenses of secondary albite (dark grey). With progression of the deuteric coarsening outwards, the secondary albite phase increases relative to the secondary K-feldspar phase to produce an antiperthitic texture. The secondary K-feldspar usually contains numerous micropores (black spots) and Fe-bearing minerals (white spots), but these rarely occur in the secondary albite (Fig. 5.1-16b). SEM/BSE image (Fig. 5.1-16a) shows that the irregular vein perthite was partially replaced by the secondary feldspars along the edge. The SEM/BSE image also shows that secondary K-feldspar (light grey with white spots) occurs in the edges of the braid microperthite (cryptoperthitic patche). In the CL image (Fig. 5.1-13b), the secondary K-feldspar is located in the dull greenish blue luminescent areas. However, this kind of replacement texture does not commonly occur in most samples.

The deep red luminescent secondary albite ranges in composition from $Ab_{96-99}Or_{1-3}An_1$ (Table 5.1-2, Fig. 5.1-17 and Appendix 1). The grey and violet blue luminescent secondary K-feldspars range from $Or_{90-100}Ab_{6-10}An_1$, whereas the brown luminescent secondary K-feldspar ranges from $Or_{90-100}Ab_{3-5}An_1$. The deep red luminescent secondary albite contains extremely high $KFeSi_3O_8$ contents (from 1.3 to 7.0 mole %), but the grey, violet and brown luminescent secondary K-feldspars

contain relatively lower $KFeSi_3O_8$ contents (from 0.5 to 2.3 mole %) (Appendix 1). However, in comparison with the feldspars in the irregular vein perthite, both secondary feldspars have higher $KFeSi_3O_8$ contents than the cryptoperthitic patches (about 0.5-1.6 mole %), the exsolved albite feldspar (about 0.3-2.0 mole %) and the exsolved K-feldspar (about 0.3-1 mole %) (Appendix 1).

c. Irregular vein perthite mantled by an intermediate optically homogeneous alkali feldspar mantle and a deuteric coarsened antiperthitic rim

In samp es C68 and C72, some of the irregular vein perthite is mantled by an intermediate optically homogeneous alkali feldspar mantle and a deuteric coarsened antiperthitic rim. The irregular vein perthite (core) consists of light blue luminescent exsolved albite and dull blue luminescent exsolved K-rich feldspar bands (Fig. 5.1-18a). CL spectrum of the light blue luminescent exsolved albite and dull blue luminescent exsolved K-rich feldspar are shown in Fig. 5.1-19a. Both CL spectra consist of a blue peak centered at about 457 nm and a weak red peak centered at about 705 nm. However, the light blue luminescent exsolved albite has a much higher I_B/I_R ratio of about 20.3 than the dull blue luminescent exsolved K-rich feldspar which has a I_B/I_R ratio of about 4.9 (Table 5.1-2). The light blue luminescent exsolved Na-rich feldspar bands range in composition from $Ab_{92-96}Or_{1-3}An_{2-6}$, whereas the dull blue luminescent exsolved K-rich feldspar bands range from $Or_{66-72}Ab_{27-33}An_1$. (Table 5.1-2, Fig. 5.1-19b and Appendix 1). The compositions of both the

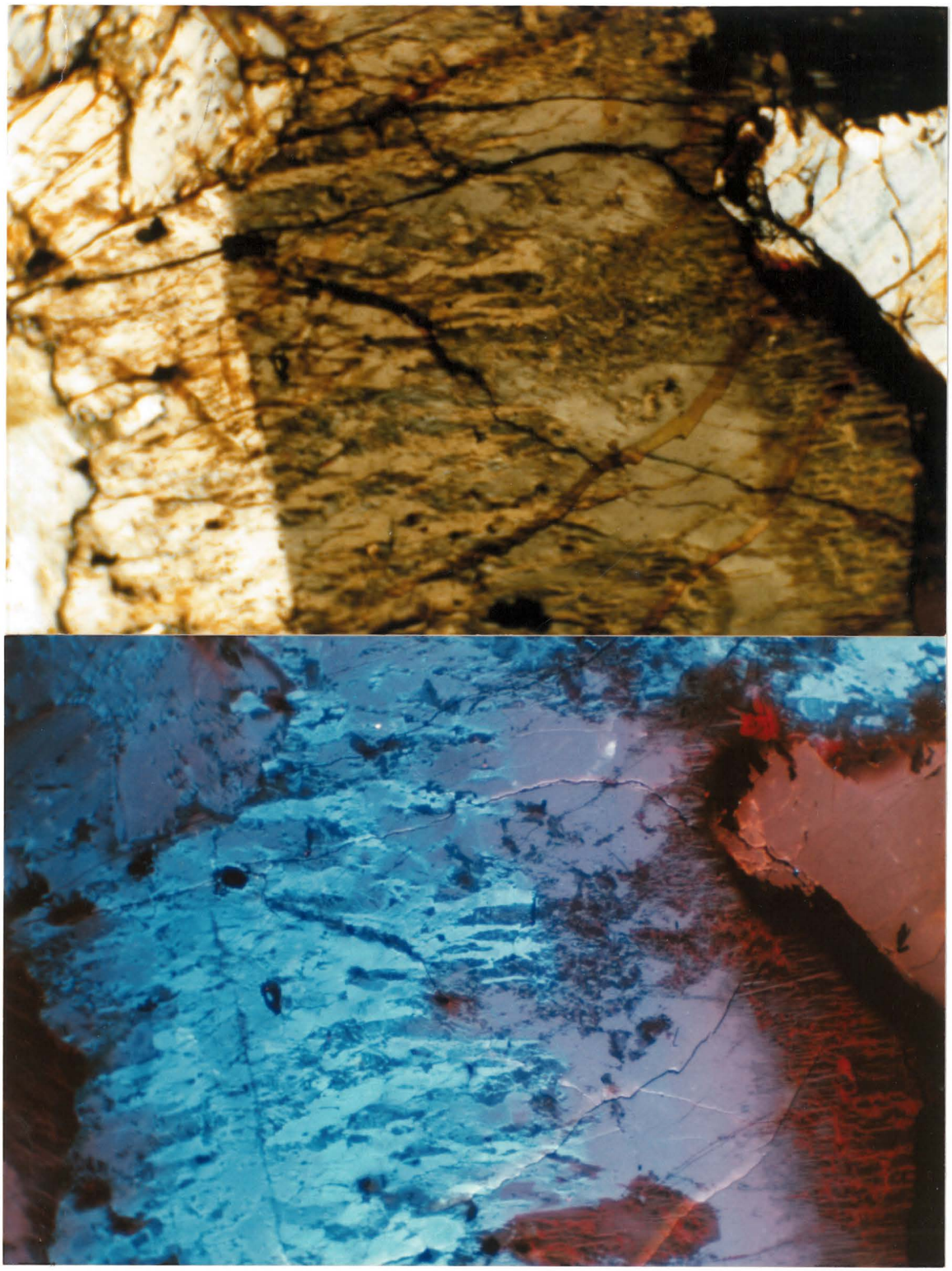

(a)

(b)

Fig. 5.1-18. Mantled feldspar in the upper series syenite (Sample C72), Center I. a. TrL. The irregular vein perthite is mantled by an intermediate optically homogeneous alkali feldspar mantle and deuteric coarsened antiperthitic rim. (Photographic conditions: 8s, ASA 400). b. CL. In the perthite core, the exsolved Na- and K-feldspars exhibit light blue and dull blue luminescence, respectively. The intermediate alkali feldspar mantle exhibits luminescence colours from light violet blue to light violet. In the deuteric coarsened antiperthitic rim, the secondary Na- and K-feldspars exhibit deep red and dark brown luminescence, respectively. The pink luminescent crystal is the apatite. Scale: 55 mm on photograph = 1 mm on thin section. (CL conditions: 10 kV, 0.8 Am. Photographic conditions: 30s, ASA 400).

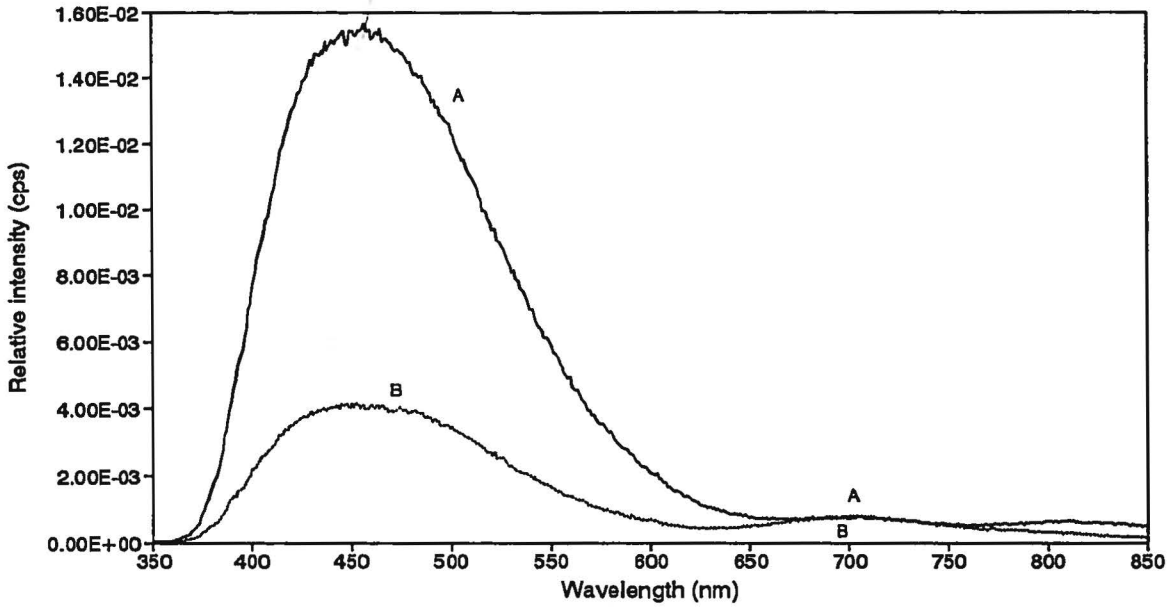

Fig. 5.1-19a. CL spectra of exsolved Na-rich and K-rich feldspars in the perthite core of the mantled feldspar crystal from the upper series of the layered ferroaugite syenites (Sample C72), Center I. Spectrum (A) is from the light blue luminescent exsolved Na-feldspar and Spectrum (B) is from the dull blue luminescent exsolved K-feldspar. CL conditions: 10 kV, 0.8 mA.

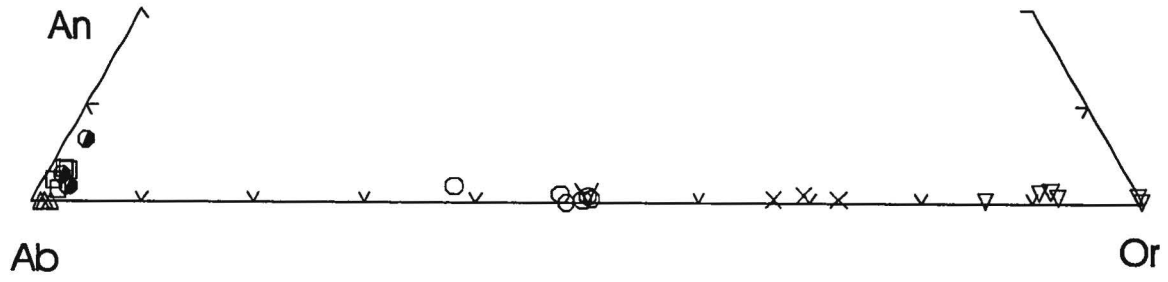

Fig. 5.1-19b. The compositions of the feldspars in the upper series of the layered ferroaugite syenites (Sample C72) plotted in the system Or-Ab-An.

The half-filled circles (O) are the light blue luminescent exsolved albite and the crosses (×) are the dull blue luminescent exsolved K-feldspars in the perthite core.

The open circles (O) are the light violet blue and light violet luminescent homogeneous alkali feldspars mantle.

The upper triangles are (▵) the deep red luminescent secondary albite and the down triangles (▿) are the dark grey and dark brown luminescent secondary K-feldspars in the antiperthite rim.

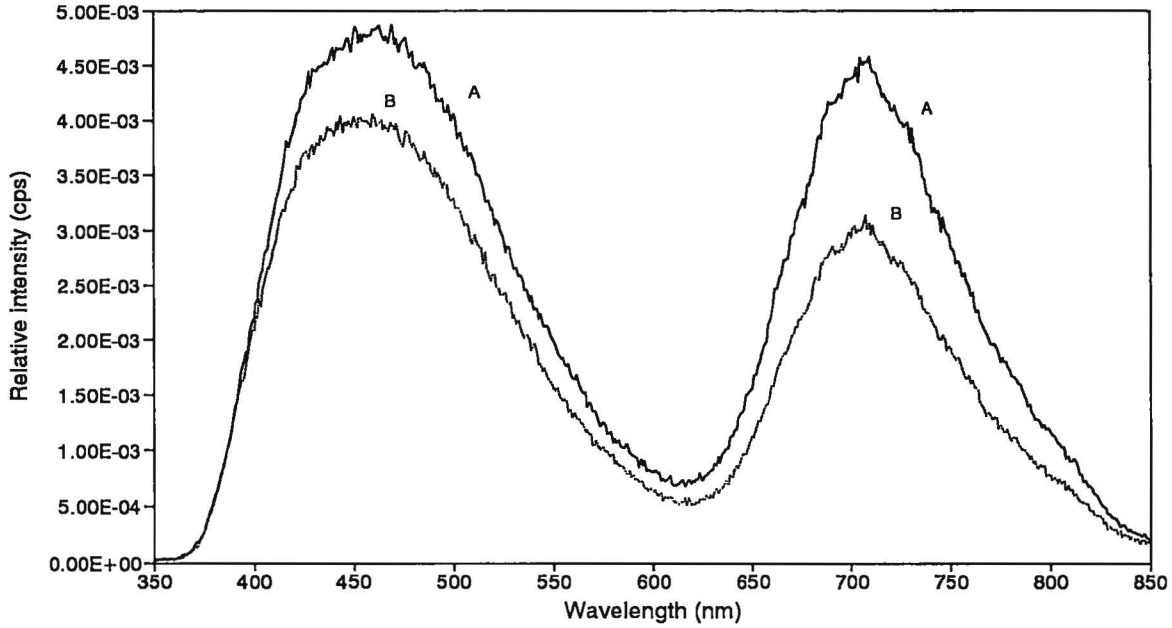

Fig. 5.1-20a. CL spectra of the intermediate homogeneous alkali feldspar mantle from the upper series of the layered ferroaugite syenites (Sample C72), Center I. The spectrum (A) is from the light bluish violet luminescent area, and the spectrum (B) is from the light violet blue luminescent area. CL conditions: 10 kV, 0.8 mA.

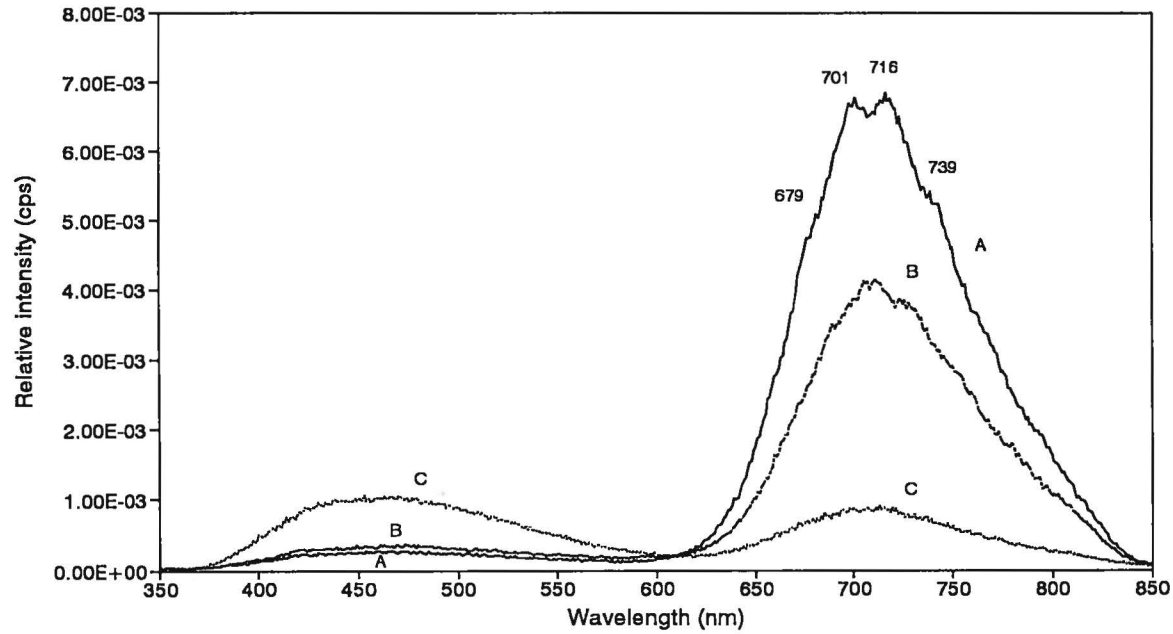

Fig. 5.1-20b. CL spectra of the secondary Na- and K-feldspars in the deuteric coarsened antiperthite rim of the mantled feldspar crystal from the upper series of the layered ferroaugite syenites (Sample C72), Center I. The spectrum (A) is from the deep red luminescent secondary albite. The spectrum (B) is from the brown luminescent secondary K-feldspar and spectrum (C) is from the grey luminescent secondary K-feldspar. CL conditions: 10 kV, 0.8 mA.

exsolved Na- and K-rich feldspars are similar to those exsolved Na- and K-rich feldspars in sample C65.

The intermediate mantles are commonly optically homogeneous alkali feldspar, or cryptoperthite with microbraid textures seen under SEM/BSE. Under CL, the cryptoperthitic mantle usually exhibits luminescent colours ranging from light violet blue to light bluish violet (Fig. 5.1-18a,b), and it grades into light violet along the contact with the deuteric coarsened feldspars rim. The CL spectra of the light violet and light violet blue luminescent cryptoperthitic mantles are shown in Fig. 5.1-20a. The spectra consist of blue peaks at about 460 nm and red peaks at about 707 nm. In both spectra, the intensity of the red peaks is nearly the same as that of the blue peaks with I_B/I_R ratios of about 1.1-1.3 (Table 5.1-2). These cryptoperthitic mantles range in composition from $Or_{37-50}Ab_{52-61}An_1$ (Table 5.1-2, Fig. 5.1-19b and Appendix 1), which is similar to the cryptoperthite patches in the irregular vein perthite in sample C65. The cryptoperthitic mantles contain about 0.43-1.45 mole % $KFeSi_3O_8$, which is higher than the $KFeSi_3O_8$ contents in the two exsolved feldspars in the core of the irregular vein perthite (about 0.27-0.53 mole % $KFeSi_3O_8$).

The deuteric coarsened antiperthitic rims consist of deep red luminescent secondary albite and grey or dark brown luminescent secondary K-feldspar (Fig. 5.1-18a,b). CL spectra of these secondary feldspars are shown in Fig. 5.1-20b. The deep red luminescent secondary albite consists of a very low blue peak centered at 466 nm and a very high red peak centered at 711 nm with

a I_B/I_R ratio about 0.04 (Table 5.1-2). A notable feature of this spectrum is that the red peak is split into four small peaks which are located at 679, 701, 716 and 739 nm. This energy splitting in the red-infrared region may reflect Fe^{3+} electron transitions in the feldspar crystal field. The grey luminescent secondary K-feldspar consists of a very weak blue peak at about 470 nm and a weak red peak centered at 711 nm with a I_B/I_R ratio of about 0.08 (Table 5.1-2). The dark brown luminescent secondary K-feldspar consists of a very low blue peak at centered 463 nm and a moderate red peak centered at 710 nm with a I_B/I_R ratio of about 1.3, and the splitting of the red peak also can be observed. The deep red luminescent secondary albite ranges in composition from $Ab_{98-99}Or_{1-2}$, whereas the dark grey and brown luminescent secondary K-feldspars range from $Or_{86-92}Ab_{7-14}An_1$ (Table 5.1-2, Fig 5.1-19b and Appendix 1). The deep red luminescent secondary albite contains about 1.54-2.41 mole % $KFeSi_3O_8$, and the dark grey and brown luminescent secondary K-feldspars contain about 1.10-1.46 mole % $KFeSi_3O_8$ (Appendix 1). The $KFeSi_3O_8$ contents in both secondary feldspars are higher than in the exsolved feldspars in the irregular vein perthite core and in cryptoperthitic mantles.

d. Homogeneous alkali feldspar mantled by a deuteric coarsened antiperthitic rim

In sample C68, most of the alkali feldspar crystals are optically homogeneous alkali feldspar and are commonly mantled by a deuteric coarsened antiperthitic rim (Fig. 5.1-21a). Under CL, the optically

homogeneous alkali feldspar exhibits light blue luminescence in the centre of the crystals (Fig. 5.1-21b). The CL colour usually grades into light violet blue in the intermediate mantle and light violet at the margins of the crystals. CL spectra from these different areas consist of blue peaks centered at about 450 nm and red peaks centered at about 698 nm (Fig. 5.1-22a). The energy level splitting in the red-infrared region also can be found in these spectra. With the change in luminescent colours from light blue through to light violet blue to light violet from the centre to the margins, the I_B/I_R ratios decrease from 6.0, 1.0 to 0.1, respectively (Table 5.1-2). The light blue luminescent core ranges in composition from $Or_{27-36}Ab_{63-72}An_{1-2}$, the light violet blue luminescent intermediate mantle ranges from $Or_{36-44}Ab_{55-63}An_1$ and the light violet luminescent margin ranges from $Or_{40-41}Ab_{59-60}An_1$ (Table 5.1-2, Fig. 5.1-23 and Appendix 1). As the luminescence colours grade from light blue through to light violet blue to violet from the centre to the margins, the $KFeSi_3O_8$ contents slightly increase from 0.47-0.6, 0.91-0.94 and 0.9-1.21 mole %, respectively. These optically homogeneous alkali feldspars have higher Ab contents than those cryptoperthitic patches and mantles in irregular vein perthite in samples C65 and C72.

In the deuteric coarsened antiperthitic rim, the deep red luminescent secondary albite ranges in composition from $Ab_{97-99}Or_{1-2}An_{<1}$, whereas the dull blue and brown luminescent secondary K-feldspars range from $Or_{84-92}Ab_{7-16}An_{1-2}$ (Table 5.1-2, Fig. 5.1-23 and Appendix 1). Both the secondary albite and K-feldspar contain high

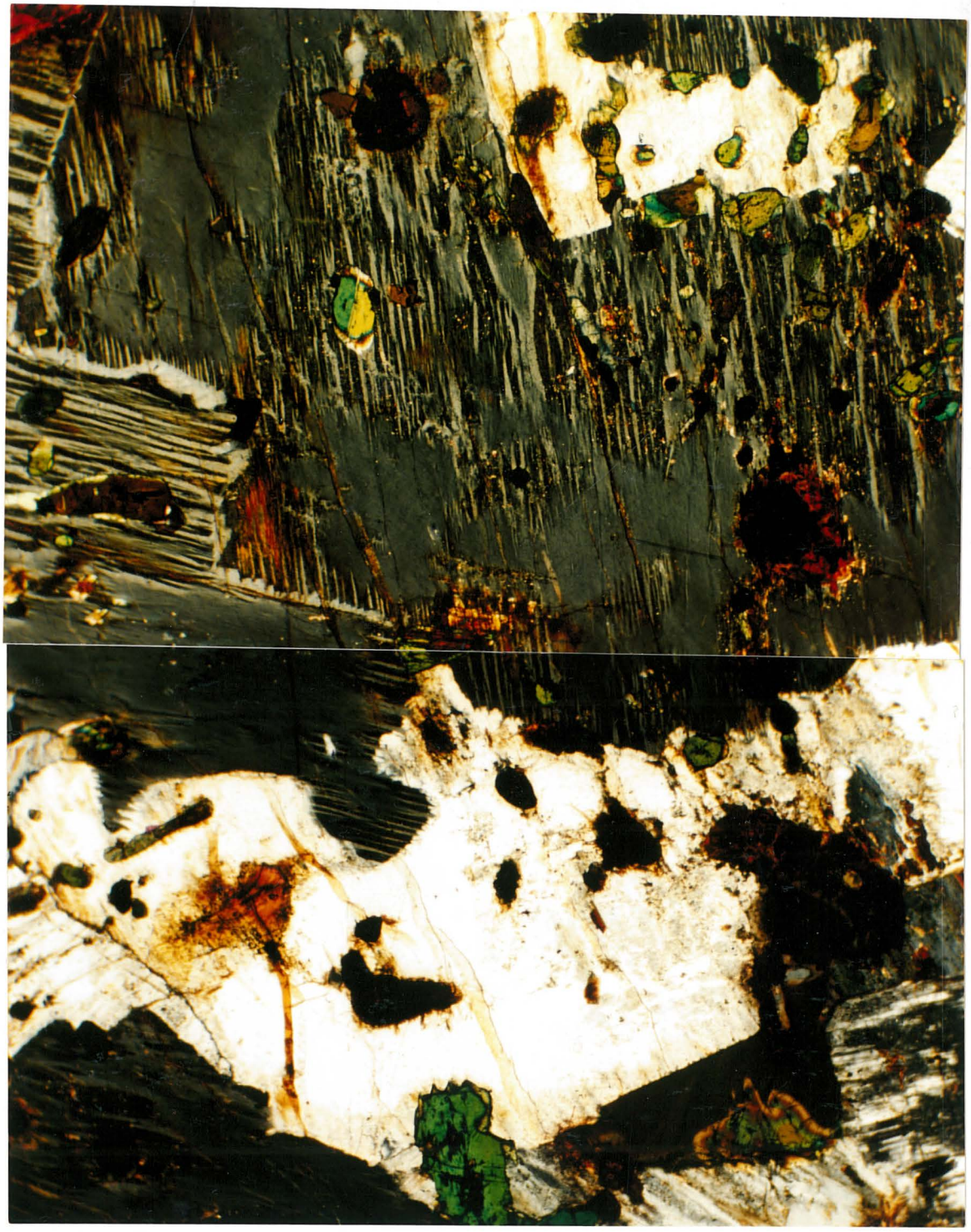

(a)

Fig. 5.1-21. Mantled feldspar in the upper series syenites (Sample C68), Center I. a. TrL. The optically homogeneous alkali feldspar crystals are mantled by a deuteric coarsened antiperthitic rim. (Photographic conditions: 17s, ASA 25).

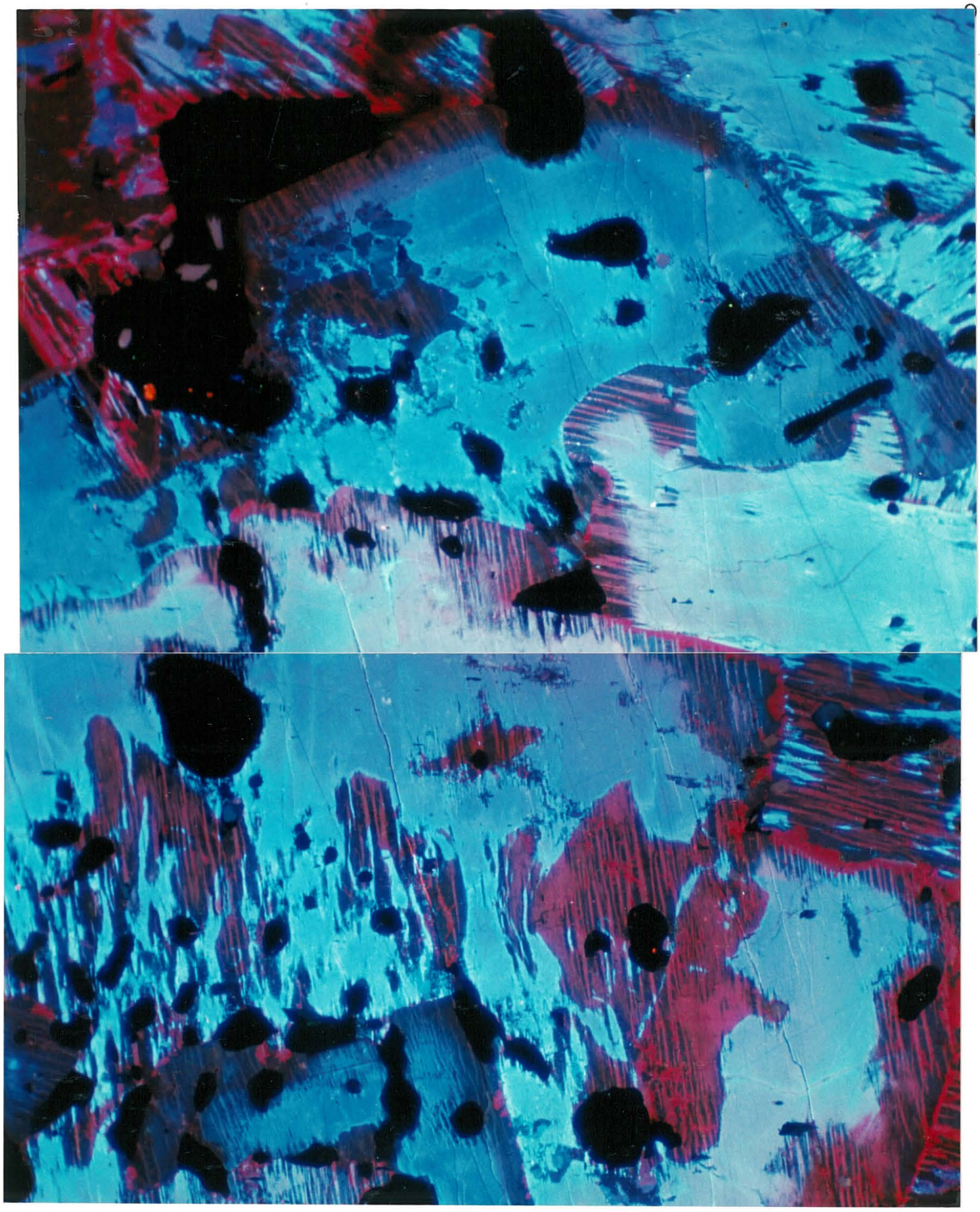

(b)

b. CL. The optically homogeneous alkali feldspar exhibits light blue luminescent in the centre, this grades to light violet blue luminescence in the intermediate areas and to light violet luminescence in the areas near the deuteric coarsened antiperthitic rim. In the antiperthitic rim, the secondary albite and K-feldspar show deep red and dark grey or brown luminescence, respectively. Scale: 55 mm on photograph = 1 mm on thin section. (CL conditions: 10 kV, 0.8 Am. Photographic conditions: 1m, ASA 400).

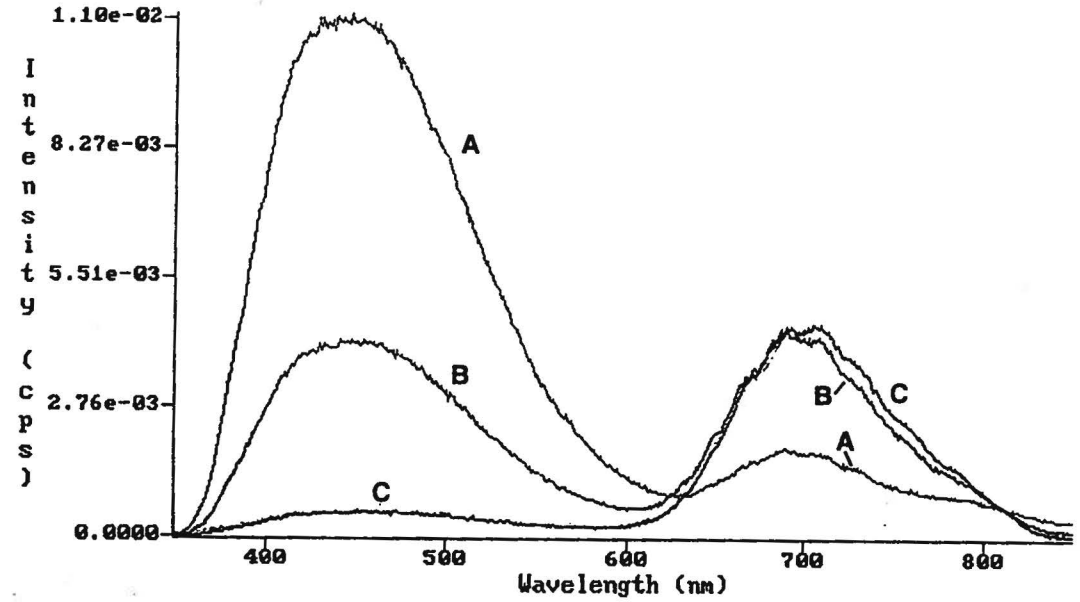

Fig. 5.1-22a. CL spectra of the optically homogeneous alkali feldspar core of the mantled feldspars crystals from the upper series of the layered ferroaugite syenites (Sample C68), Center I. The spectrum (A) is from the light blue luminescent in the centre of the homogeneous crystals, the spectrum (B) is from the light violet blue luminescent intermediate mantle of the crystals and the spectrum (C) is from the light violet luminescent margin of the crystals. CL conditions: 10 kV, 0.8 mA.

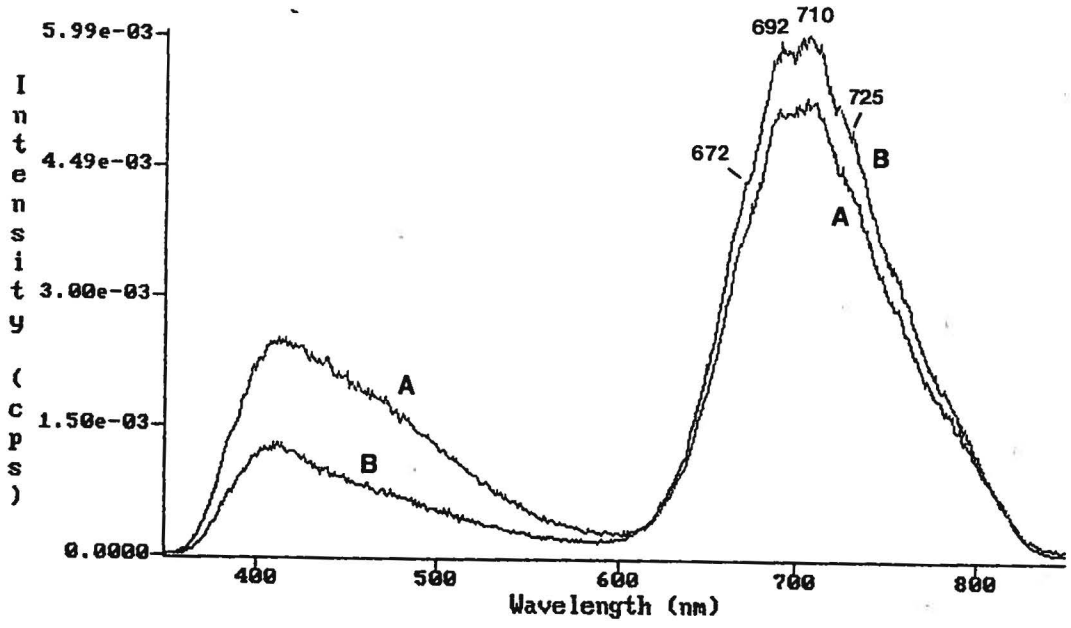

Fig. 5.1-22b. CL spectra of the albite twinned albite crystals in the upper series of the layered ferroaugite syenites (Sample C68), Center I. The spectrum (A) is from the violet luminescent areas in the albite crystal. The spectrum (B) is from the violet-red luminescent areas in the albite crystal. CL conditions: 10 kV, 0.8 mA.

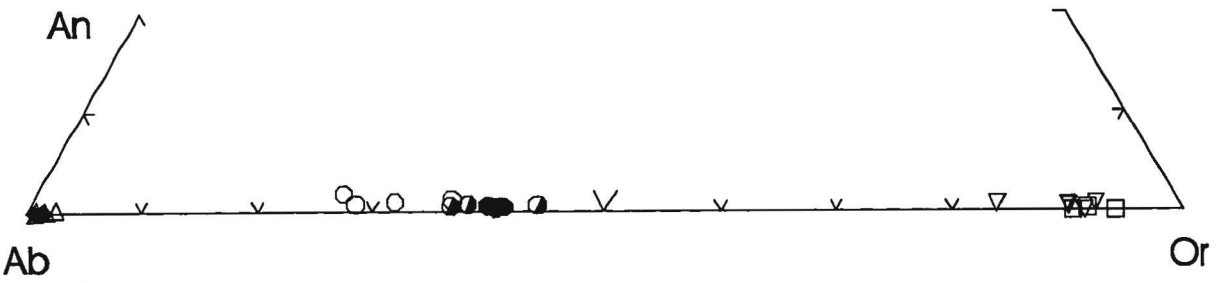

Fig. 5.1-23. The composition of the feldspars in the upper series of the layered ferroaugite syenites (Sample C68) plotted in the system Or-Ab-An.

The circles (○) are from the light blue luminescent core of the homogeneous alkali feldspar crystals, the half-filled circles (◐) are from the light violet blue luminescent intermediate mantle, and the filled circles (●) are from the light violet luminescent margin of the crystals.

The filled diamonds (♦) are the violet and red luminescent albite twinned albite.

The squares (□) are brown luminescent secondary K-feldspar within the albite crystal.

The upper triangles (▵) are the red and deep red luminescent secondary albite, and the down triangles (▿) are the dark grey and brown luminescent K-feldspars in the deuteric coarsened antiperthite rim.

$KFeSi_3O_8$ contents of about 1.67-2.69 and 2.57-4.75 mole %, respectively.

e. Albite twinned albite mantled by a deuteric coarsened antiperthitic rim

A few individual albite crystals are found in sample C68, the crystal is albite twinned with a clear appearance (Fig 5.1-24a). However, the albite crystal is partially altered by secondary K-feldspar which shows a turbid appearance near the centre of the crystal. The albite crystal is also mantled by a deuteric coarsened antiperthitic rim, as are most of the optically homogeneous alkali feldspar crystals. Under CL, the unaltered areas of the albite crystal exhibit luminescence colours from violet to violet-red, and

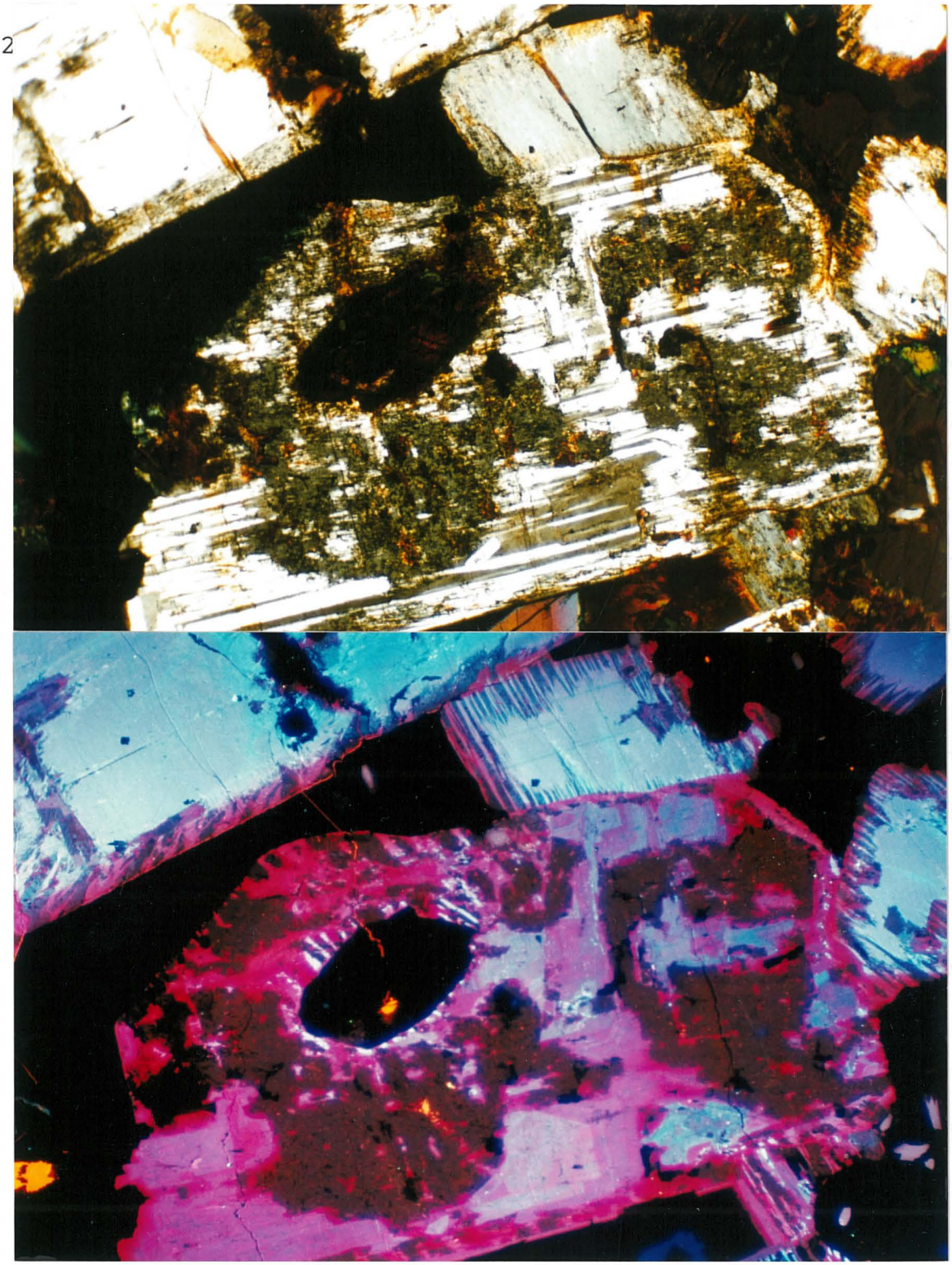

(a)

(b)

Fig. 5.1-24. Albite in the upper series syenite (Sample C68), Center I. a. TrL. The albite is mantled by a narrow deuteric coarsened antiperthitic rim, and replaced by the secondary K-feldspar in the core. (Photographic conditions: 30s, ASA 400). CL. The albite exhibits violet to violet-red luminescence, and the secondary K-feldspar exhibits brown luminescence. In the antiperthitic rim, the secondary Na- and K-feldspars show deep red and brown luminescence, respectively. Some light violet blue luminescent homogeneous alkali feldspar crystals are also mantled by the deuteric coarsened antiperthitic rim. Scale: 55 mm on photograph = 1 mm on thin section. (CL conditions: 10 kV, 0.8 Am. Photographic conditions: 4m, ASA 400).

shows some oscillatory zoning (Fig. 5.1-24b). The CL spectra from violet and violet-red albite are shown in Fig. 5.1-22b. The spectra consist of a low blue peak centered at 410-413 nm and high red peak centered at 700 nm with slight peak splitting at about 672, 692, 710 and 725 nm. The ratios of I_B/I_R are about 0.22-0.49 (Table 5.1-2, Fig. 5.1-22b). The violet and violet-red luminescent albite ranges in composition from $Ab_{98-99}Or_{1-2}$ and contains 1.53 to 2.55 mole % $KFeSi_3O_8$ (Table 5.1-2, Fig. 5.1-23 and Appendix 1).

The deuteric coarsened antiperthitic rim consists of red luminescent secondary albite and brown luminescent secondary K-feldspar (Fig. 5.1-24b). Both of the secondary feldspars have the same compositions as secondary feldspars in the deuteric coarsened antiperthitic rim of the optically homogeneous alkali feldspar crystals. Within the albite crystal, the turbid-looking secondary K-feldspar also exhibits brown luminescence with a composition of $Or_{90-94}Ab_{6-10}An_{<1}$ (Table 5.1-2, Fig. 5.1-23b and Appendix 1), which is similar to the secondary K-feldspar in the deuteric coarsened antiperthitic rim, but it contains relatively higher contents of $KFeSi_3O_8$ about 4.33-4.59 mole %.

5.1.4. Late-stage fluid-induced coarsening and replacement in the layered ferroaugite syenites

Late-stage fluid alteration is different between the lower series syenites and the upper series of syenites. In the lower series syenites, the late-stage fluids altered the homogeneous alkali feldspar crystals into two discrete secondary albite and K-feldspar

which occur mainly at the margins of the homogeneous alkali feldspar crystals or are randomly distributed within the crystals. In the upper series syenites, however, secondary feldspars are mainly deuteric coarsened feldspars which occur as an antiperthitic rim at the margins of the irregular vein perthite, patch perthite and the homogeneous alkali feldspar crystals.

a. Secondary feldspars in the lower series of the layered ferroaugite syenites

During late-stage fluid alteration, some of the homogeneous alkali feldspar crystals are replaced by secondary albite and K-feldspar at the margins in the lower series of the syenites. The secondary K-feldspar usually has a turbid, cloudy appearance, but the secondary albite is a clear, albite twinned crystal (Fig. 5.1-8a, -10a). Under CL, the secondary K-feldspar exhibits dull blue or purple luminescence with irregular outlines (Fig. 5.1-8b, -10b). The CL spectrum of the purple luminescent secondary K-feldspar consists of a narrow blue peak at 414 nm and two broad, weak red-infrared peaks centered at 702 and 804 nm with a I_B/I_R ratio of about 7.8 (Table 5.1-1 and Fig. 5.1-25b, spectrum A). In all of the analyzed samples, the purple luminescent secondary K-feldspars range in composition from $Or_{85-99}Ab_{0-14}An_{0-1}$ (Table 5.1-1), and the average value of $KFeSi_3O_8$ contents is about 0.38 mole %.

The secondary albite crystals exhibit various luminescence colours, such as light violet blue, violet and red, and some of them show oscillatory zoned textures (Fig. 5.1-8b, -10). In the

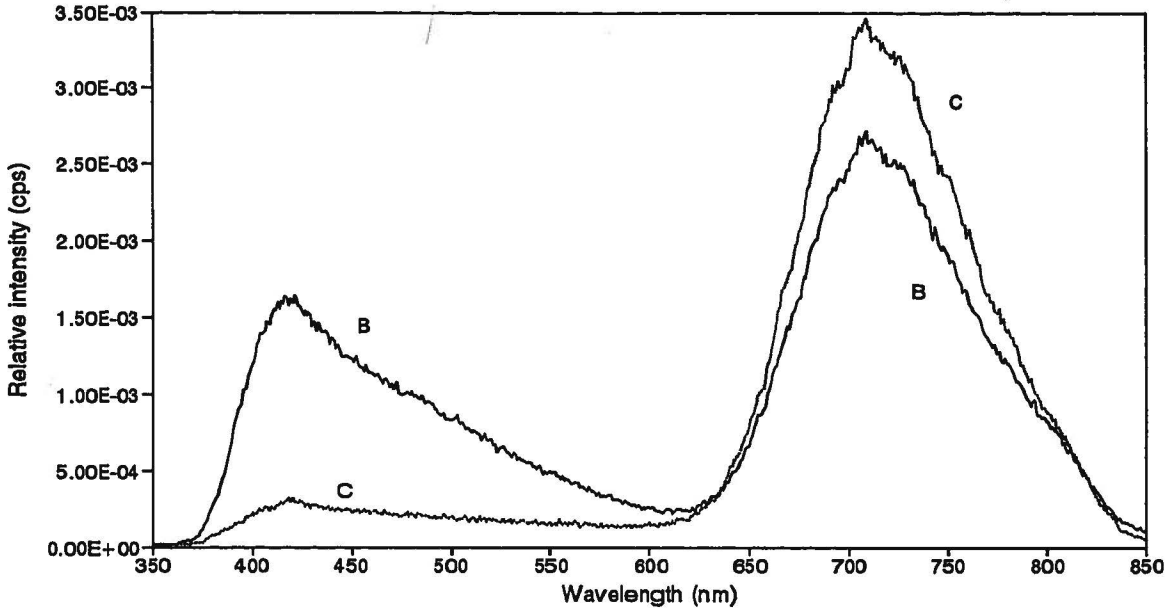

Fig. 5.1-25a. CL spectra of the secondary albites in the lower series of the layered ferroaugite syenites (Sample C55), Center I. Spectrum (B) is from the violet luminescent secondary albite. Spectrum (C) is from the deep red luminescent secondary albite. CL conditions: 10 kV, 0.8 mA.

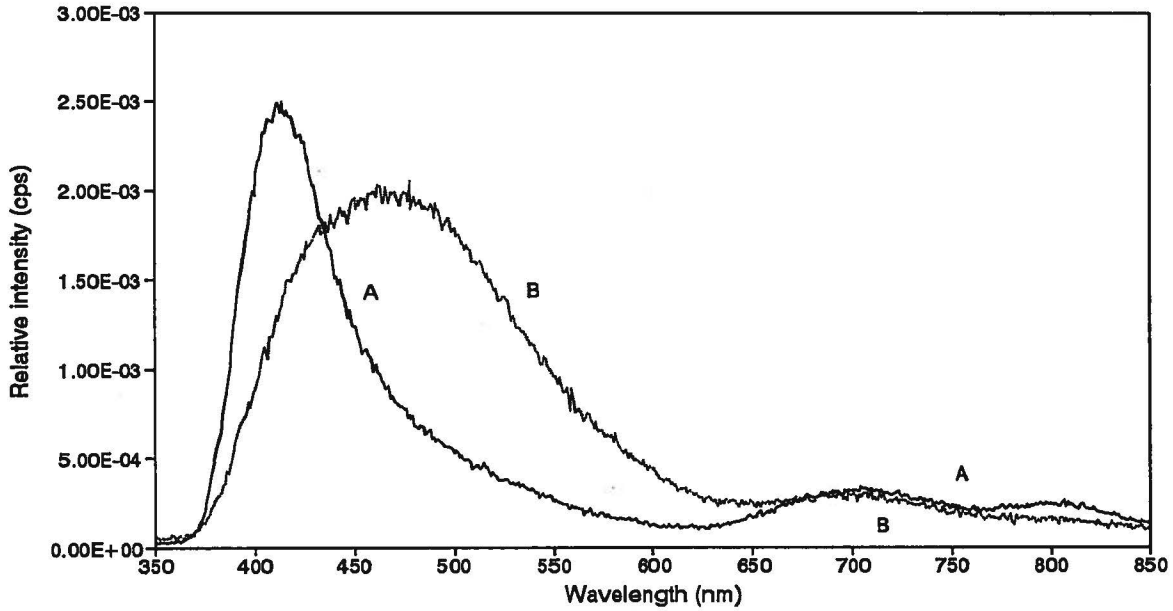

Fig. 5.1-25b. CL spectra of secondary K-feldspars in the layered ferroaugite syenites, Center I. Spectrum (A) is from the purple luminescent secondary K-feldspar which occurs at the margin of the homogeneous alkali feldspar crystal in sample C53. Spectrum (B) is from the greenish blue luminescent secondary K-feldspar which occurs in the centre of the irregular vein perthite crystal in sample C65. CL conditions: 10 kV, 0.8 mA.

interstices between the homogeneous alkali feldspar grains, the secondary albite crystals usually exhibit deep red luminescence and some of them are overgrown by a non luminescent secondary albite. The CL spectra of violet and deep red luminescent secondary albite crystals are shown in Fig. 5.1-25a. The spectra consist of blue peaks at about 420 nm and red peak centered at about 710 nm. As the luminescence colours change from violet to deep red, the I_B/I_R ratios decrease from about 0.6 to 0.1 (Fig. 5.1-25a, Table 5.1-2). The luminescence colour of the secondary albite sequence can be correlated with the replacement time. During the late-stage fluid-feldspar interactions, the earlier formed secondary albites usually exhibit dull blue or light violet blue luminescence, but the later formed is violet or deep red luminescence, and the latest formed secondary albite is non luminescent. The later formed albite has higher Ab contents than the earlier formed albites. In sample C55, e.g., the violet luminescent secondary albite ranges in composition from $Ab_{87-97}Or_{2-7}An_{1-6}$, the deep red luminescent secondary albite is from $Ab_{91-98}Or_{1-4}An_{1-5}$ and the non luminescent secondary albite is from $Ab_{97-98}Or_1An_{1-2}$ (Table 5.1-1, Appendix 1). In all analyzed samples, the secondary albites have end member compositions with a range in composition of $Ab_{87-98}Or_{1-10}An_{1-10}$ (Table 5.1-1, Appendix 1). For these secondary albites, the average value of $KFeSi_3O_8$ contents is about 0.48 mole %.

b. Secondary feldspars in the upper series of the layered ferroaugite syenites

As discussed above, most of the irregular vein perthite, patch perthite and homogeneous alkali feldspar crystals are mantled by an deuteric coarsened, antiperthitic rim in the upper series syenites. The antiperthitic rim consists of deep red luminescent secondary albite and dark grey, brown luminescent secondary K-feldspar. In all analyzed samples, the deep red luminescent secondary albites range in composition from $Or_{96-99}Ab_{1-3}An_{0-1}$, and the dark grey and brown luminescent secondary K-feldspars range in composition from $Or_{84-100}Ab_{6-16}An_{0-1}$ (Table 5.1-2, Appendix 1). The average value of $KFeSi_3O_8$ contents is about 2.58 mole % for the secondary albite and is about 1.90 mole % for the secondary K-feldspar.

However, some secondary K-feldspars occur in the centre of the irregular vein perthite and exhibit dull greenish blue luminescence (Fig. 5.1-14b). The CL spectrum consists of a broad blue peak centered at about 486 nm and a very weak red peak centered at about 704 nm with a I_B/I_R ratio of about 6.5 (Table 5.1-2, Fig. 5.1-25b spectrum B). The blue peak is shifted by about 20 nm to a longer wavelength as compared with the blue peaks in the spectra of the cryptoperthitic patches and the exsolved albite. This dull greenish blue luminescent secondary K-feldspar ranges in composition from $Or_{90-99}Ab_{4-9}An_1$ (Table 5.1-2, Appendix 1). These secondary K-feldspars have much lower $KFeSi_3O_8$ contents, with an average value of 0.23 mole %, than the brown luminescent secondary K-feldspars in the deuteric coarsened antiperthitic rim.

5.1.5. Thermal history of the alkali feldspars

Evolutions of the alkali feldspars in the layered ferroaugite syenites are shown in Fig. 5.1-26 for the lower series syenite, and in Fig. 5.1-27 for the upper series syenite. For the alkali feldspars in the lower series syenite, the path a-a′ on the incoherent solvus (SFS) indicates that the light blue to light violet blue luminescent alkali feldspar and the light violet blue luminescent alkali feldspar core ($Or_{32-56}Ab_{41-62}An_{1-8}$) may have crystallized at temperatures ≥700 °C (Fig. 5.1-26a). In comparison with the Or-Ab-An ternary system at 1 kbar (Fig. 5.1-4,-7b,-9,-11b), the homogeneous alkali feldspar crystallized during a temperature range from 900 to 750 °C.

The path b-b′ indicates that the light violet luminescent K-rich alkali feldspar rim ($Or_{50-59}Ab_{38-49}An_{1-3}$) may be formed at temperatures about 720-680 °C along the incoherent solvus (SFS) (Fig. 5.1-26a).

The path b-b′ and the point c on the coherent solvus (CS) indicate that the light violet luminescent exsolved K-rich feldspar ($Or_{58-60}Ab_{39-41}An_{1}$) and the light blue luminescent exsolved Na-rich feldspar ($Ab_{54-64}Or_{29-43}An_{3-7}$) in the incipient perthitic rim may have formed during cooling at temperatures about 620-580 °C and 650 °C, respectively during cooling (Fig. 5.1-26b).

The paths d-d′ and e-e′ on the incoherent solvus (SFS) indicate that the purple luminescent secondary K-feldspar ($Or_{85-99}Ab_{0-14}An_{0-1}$) and the violet to deep red luminescent secondary albite ($Ab_{87-98}Or_{1-7}An_{1-10}$) may have formed at temperatures about <450 °C and 620-<480 °C, respectively during late-stage fluid-feldspar interaction.

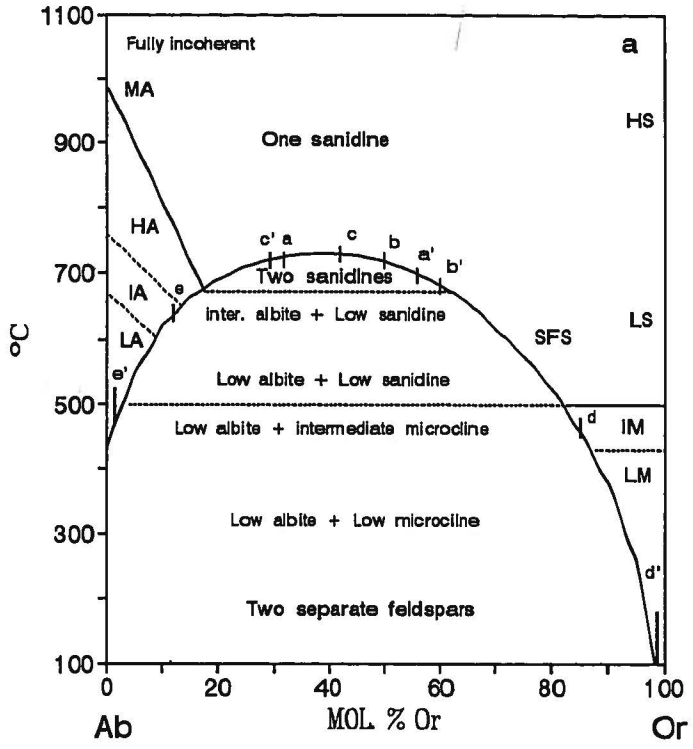

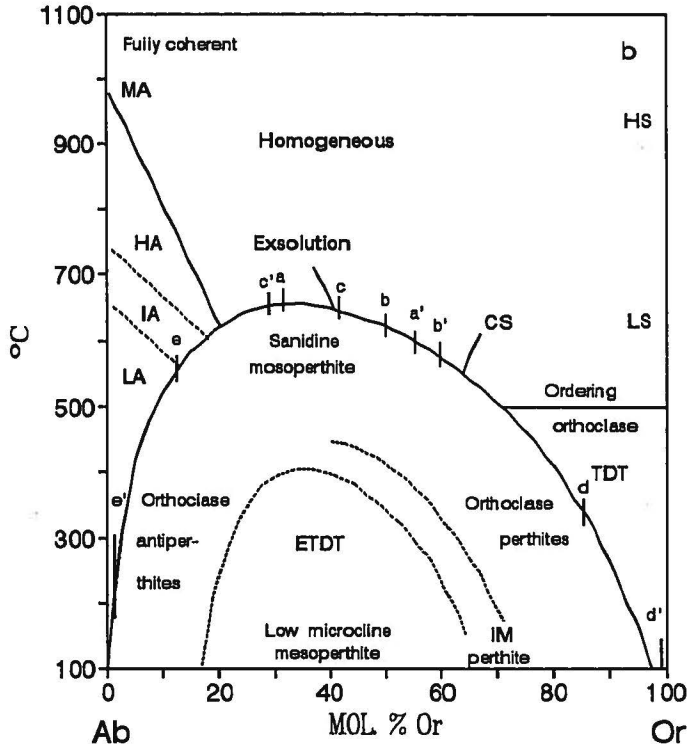

Fig. 5.1-26. The evolution of the alkali feldspars in the lower series of layered ferroaugite syenite from Center I are illustrated in the Or-Ab binary phase diagram.

The path a-a′ includes the optically homogeneous alkali feldspar and the optically homogeneous alkali feldspar core. The path b-b′ and c-c′ include the exsolved K-feldspar and Na-feldspar in the incipient perthititic rim and the K-rich alkali feldspar rims. The paths d-d′ and e-e′ include the secondary K-feldspar and the secondary albite.

Diagram (a) shows the phase relationships for An-free alkali feldspars under complete (incoherent) equilibrium and (b) shows different constrained equilibrium states as a function of bulk composition and T for completed coherent intergrowths (Brown and Parsons, 1989). SFS is the strain-free solvus and CS is the coherent solvus. TDT is the twin-domain microtexture and ETDT is the exsolution and the twin-domain microtexture. MA, HA, IA and LA are monoclinic, high, intermediate and low albite; IM and LM are intermediate and low microcline. IA and IM is the region of the rapid change in Y ordering.

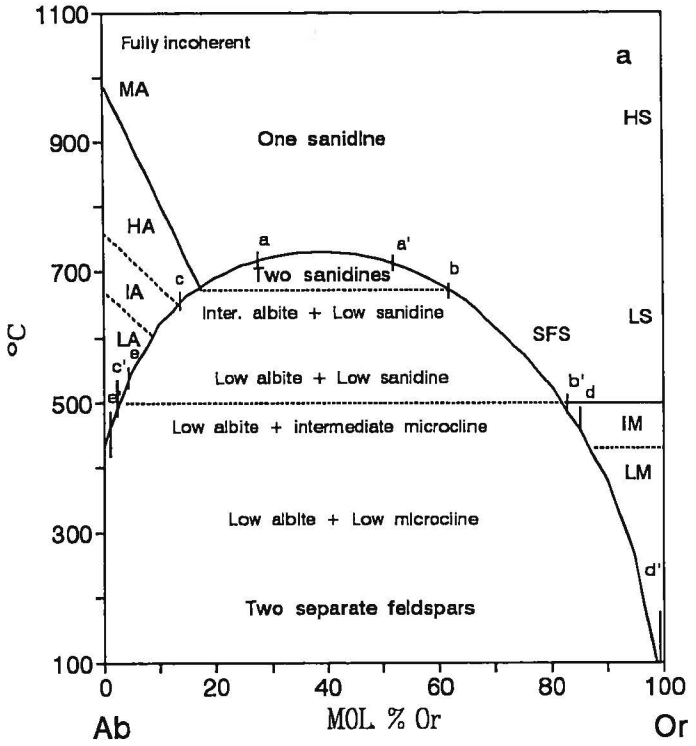

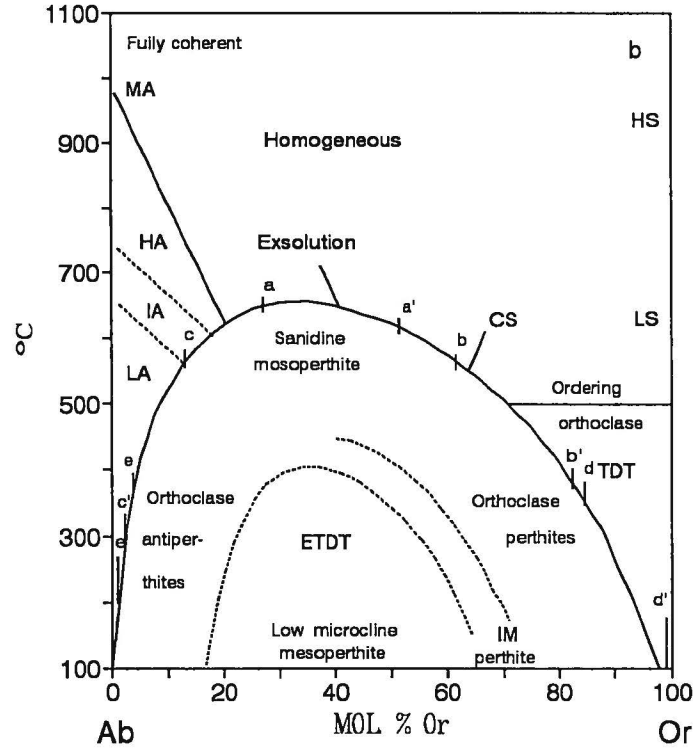

Fig. 5.1-27. The evolution of the alkali feldspars in the upper series of layered ferroaugite syenite from Center I are illustrated in the Or-Ab binary phase diagram.

The path a-a′ includes the optically homogeneous alkali feldspar cores, the crypto-perthitic patches in the core of the perthite, and homogeneous alkali feldspar mantles. The path b-b′ and c-c′ include the exsolved K-feldspar and Na-feldspar in the core of the perthite. The paths d-d′ and e-e′ include the secondary K-feldspar and the secondary Na-feldspar in the deuteric coarsened antiperthitic rim and the secondary K-feldspar in the fractures of the perthite core.

Diagram (a) shows the phase relationships for An-free alkali feldspars under complete (incoherent) equilibrium and (b) shows different constrained equilibrium states as a function of bulk composition and T for completed coherent intergrowths (Brown and Parsons, 1989). SFS is the strain-free solvus and CS is the coherent solvus. TDT is the twin-domain microtexture and ETDT is the exsolution and the twin-domain microtexture. MA, HA, IA and LA are monoclinic, high, intermediate and low albite; IM and LM are intermediate and low microcline. IA and IM is the region of the rapid change in Y ordering.

In comparison with the paths d-d′ and e-e′ on the coherent solvus (CS), the secondary K-feldspar and albite formed at <350 °C and <520 °C, respectively.

For the alkali feldspars in the upper series syenite, the path a-a′ on the incoherent solvus (SFS) indicates that the alkali feldspar with a composition of $Or_{27-52}Ab_{47-72}An_{1-3}$ crystallized at temperatures ≥700 °C (Fig. 5.1-27a). This compositional range includes the light blue to light violet luminescent homogeneous alkali feldspar core, the light greyish blue to light bluish violet luminescent cryptoperthitic patches in the perthite core; and the light violet blue to light violet luminescent homogeneous alkali feldspar mantles. In comparison with the Or-Ab-An ternary system at 1 kbar (Fig. 5.1-17,-19b,-23), the alkali feldspar crystallized at a temperature range from 825 to 750 °C. The microbraid texture of cryptoperthitic patches in the core and mantle of the perthite have developed at temperatures about 650-600 °C along the coherent solvus (CS) during cooling (Fig. 5.1-27b).

The paths b-b′ and c-c′ on the coherent solvus (CS) indicate that the dull blue luminescent exsolved K-feldspar ($Or_{61-82}Ab_{17-38}An_{1-3}$) and the light blue luminescent exsolved albite ($Ab_{87-97}Or_{1-10}An_{2-6}$) bands of the perthite formed at a temperature below 580 °C during cooling (Fig. 5.1-27b).

The paths d-d′ and e-e′ on the incoherent solvus (SFS) indicate that the grey to brown luminescent secondary K-feldspar ($Or_{84-100}Ab_{6-16}An_1$) and the deep red luminescent secondary albite ($Ab_{96-99}Or_{1-3}An_1$) in the deuteric coarsened antiperthitic rim formed at low

temperatures <460 and <540 °C (or <350 and <380 °C on the CS), respectively during late-stage fluid-feldspar interaction. Since the dull greenish blue luminescent secondary K-feldspar in the fractures of the perthite core (sample C65) has a composition of $Or_{90-99}Ab_{4-9}An_1$, it may have formed at <400 °C during late-stage fluid-feldspar interaction.

5.2. Feldspar crystals in the unlayered ferroaugite syenites

5.2.1. Introduction

Unlayered ferroaugite syenites are cumulates and generally have the same petrographic and mineralogical characteristics as the layered ferroaugite syenite unit. In the unlayered ferroaugite syenites, most of the feldspar crystals are optically homogeneous alkali feldspar and exhibit light violet blue luminescence under CL. Some feldspar crystals are incipient irregular vein perthite and also exhibit light violet blue luminescence. The optically homogeneous alkali feldspar crystals are usually mantled by a deuteric coarsened antiperthitic rim, which consists of deep red luminescent, untwinned, secondary albite and dark brown luminescent, secondary K-feldspar. However, some secondary albite patches, which occur between the homogeneous core and the antiperthitic rim, are albite twinned and exhibit purple luminescence.

5.2.2. Incipient irregular vein perthite

In the ferroaugite syenite (sample C188), the feldspar crystals are xenomorphic, incipient irregular vein perthite. Under transmitted light, the feldspar crystals show a weak irregular vein perthite texture core and relatively optically homogeneous margins (Fig. 5.2-1a). Under CL, the incipient irregular vein perthite core usually exhibits light violet blue luminescence with some light blue stripes, and the homogeneous rim exhibits light bluish violet luminescence (Fig. 5.2-1b). CL spectrum of the light violet blue

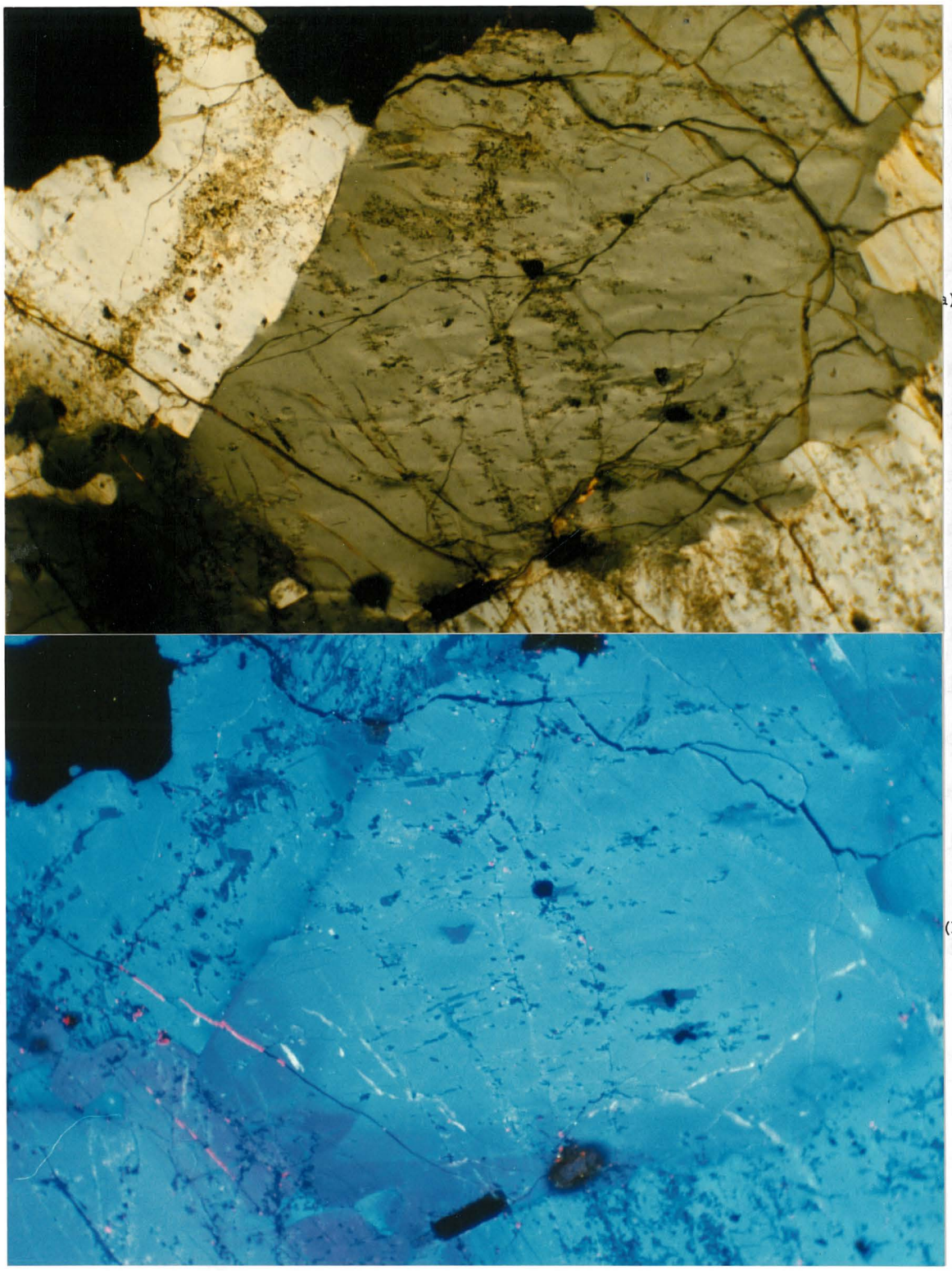

Fig. 5.2-1. Incipient irregular vein perthite in the unlayered ferroaugite syenite (Sample C188), Center I. a. TrL. The feldspar shows incipient irregular vein perthitic texture in the core, but the margins of the crystal is relatively optically homogeneous. (Photographic conditions: 8s, ASA 400). b. CL. The core exhibits light violet blue luminescence with some light blue luminescent stripes and the margins exhibit light bluish violet. Scale: 55 mm on photograph = 1 mm on thin section. (CL conditions: 10 kV, 0.8 Am. Photographic conditions: 15s, ASA 400).

luminescent alkali feldspar from the core consists of a high blue peak at 467 nm and a low red peak at 708 nm, and the ratio of I_B/I_R is about 3.1 (Fig 5.2-2a, spectrum A and Table 5.2-1). The light violet blue luminescent alkali feldspar core ranges in composition from $Or_{43-45}Ab_{50-51}An_{4-6}$ (Table 5.2-1, Fig 5.2-2b and Appendix 1).

5.2.3. Optically homogeneous alkali feldspar mantled with a deuteric coarsened antiperthitic rim

In sample C100, the alkali feldspar is brown, coarse-grained (≥ 3×7 mm) euhedral crystals which consist of an optically homogeneous core and a deuteric coarsened regular vein antiperthitic rim (Fig. 5.2-3a). The optically homogeneous alkali feldspar core usually has a clear appearance with embayed boundaries in contact with the antiperthitic rim, but the rim has a turbid-looking appearance with planar bounding crystal faces (Fig. 5.2-3a). Under CL, the optically homogeneous alkali feldspar cores usually exhibit light violet blue luminescence, and some of them contain a light violet luminescent oscillatory zone at the margins (Fig. 5.2-3b). The CL spectrum from the light violet blue luminescent homogeneous alkali feldspar core is shown in Fig. 5.2-4a. The spectrum consists of a low blue peak centered at 459 nm and a low red peak centered at 709 nm with a I_B/I_R ratio of about 0.8 (Fig 5.2-4a, spectrum A and Table 5.2-1). This light violet blue luminescent homogeneous alkali feldspar core has a higher I_B/I_R ratio than the light violet blue luminescent alkali feldspar homogeneous alkali feldspar core in the layered unit.

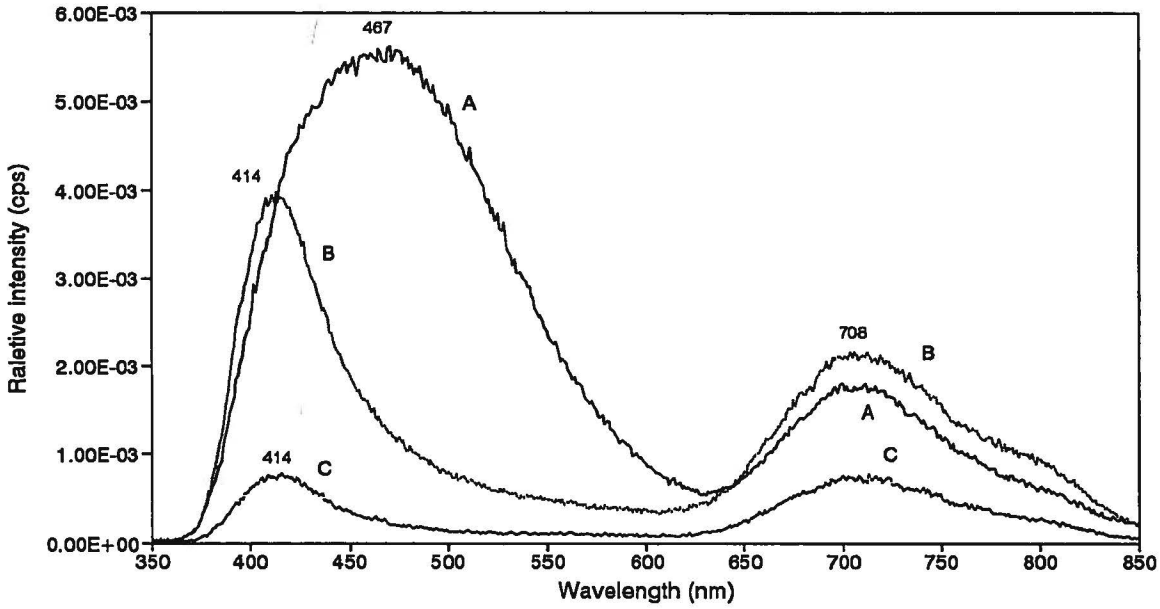

Fig. 5.2-2a. The CL spectra of the feldspars in the unlayered ferroaugite syenite (Sample C188), Center I. Spectrum (A) is from the light violet blue luminescent incipient irregular vein perthite. Spectrum (B) is from the purple luminescent secondary oligoclase, and the spectrum (C) is from the deep purple luminescent secondary albite at the margins of the incipient irregular vein perthite.

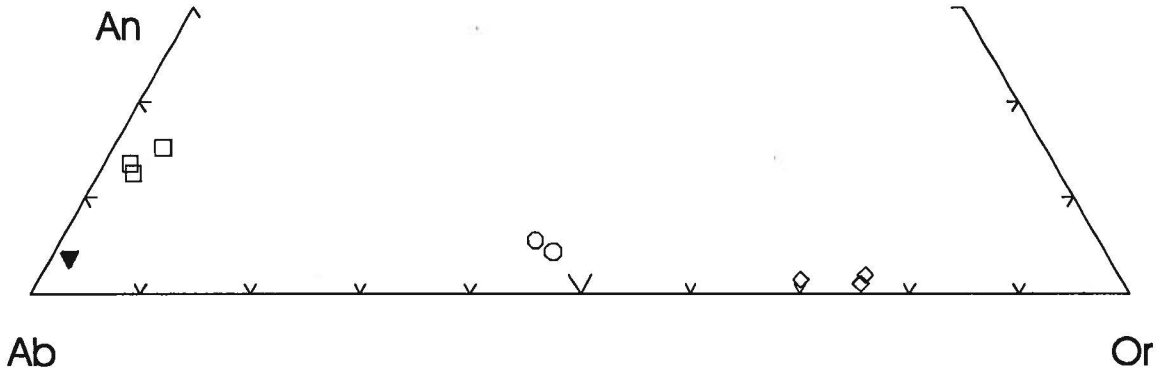

Fig. 5.2-2b. The compositions of the feldspars in the unlayered ferroaugite syenite (Sample C188) plotted in the system Or-Ab-An.

The circles (O) are the light violet blue luminescent incipient irregular vein perthite. The diamonds (◇) are the dull blue luminescent secondary K-feldspar. The squares (□) are the purple luminescent secondary oligoclase and the filled down triangles (▾) are the deep purple luminescent secondary albite at the margins of the incipient irregular vein perthite.

Table 5.2 - 1. Representative cathodoluminescence properties and compositions of feldspars in the unlayered ferroaugite syenites from Center I, Coldwell Complex, Ontario

Occurrence of feldspar	Sample No./ spectrum No.	Luminescence colour	Intensities (cps)					Compositions		
			Blue peak	(nm)	Red peak	(nm)	B/R ratio	Or	Ab	An
Incipient irregular vein perthite	C188/A	Light violet blue	5.47E-03	(467)	1.74E-03	(708)	3.14	43-45	50-51	4-6
Secondary K-rich feldspar	C188	Dull blue	N/A		A/N			67-75	23-29	1-2
Secondary oligoclase	C188/B	Purple	3.95E-03	(414)	2.07E-03	(708)	1.91	2-5	80-84	13-15
Secondary albite	C188/C	Deep purple	7.59E-04	(414)	7.52E-04	(708)	1.01	2	94	4
Microperthite, core	C100/A	Light violet blue	1.58E-03	(459)	1.94E-03	(709)	0.82	39-44	55-60	1
Microperthite, oscillatory zone, core	C100	Light violet	N/A		N/A			42-49	51-58	0-1
2nd. albite, antiperthite rim	C100/B	Red	1.43E-04		4.08E-03	(711)	0.04	1	99	
2nd. K-feldspar, antiperthite rim	C100	Brown	N/A		N/A			92-100	0-7	0-1
2nd. albite, between rim and core	C100/C	Purple	1.05E-03	(424)	1.12E-03	(709)	0.93	1-2	97-98	1-2
Homo. alkali feldspar, core	C305/A	Light violet blue	2.06E-03	(462)	3.81E-03	(711)	0.54	35-43	55-64	1-4
Homo. alkali feldspar host, mantle	C305/B	Light violet	7.10E-04	(466)	4.65E-03	(711)	0.15	42-58	42-57	1
Exsolved albite, mantle	C305	Dull red						1	98-99	0-1
Exsolved K-feldspar, mantle	C305	Blue	N/A		N/A			98-99		1-2
2nd. albite, antiperthite rim	C305/C	Red	5.43E-04		6.64E-03	(711)	0.08	1	98	1
2nd. K-feldspar, antiperthite rim	C305	Brown	N/A		N/A			97-99	0-2	1
Microperthite core, phenocryst	C101/A	Light blue	1.87E-03	(459)	1.54E-04	(708)	12.14	1-5	90-93	5-7
								79-88	11-20	1
Secondary K-rich feldspar, core	C101	Dull blue	N/A		N/A			53-67	31-45	1-2
Albite rim, phenocryst	C101/B	Light blue	2.85E-03	(454)	2.12E-04	(708)	13.43	1-4	80-94	3-9
Microperthite core, groundmass	C101/C	Light violet blue	1.33E-03	(456)	2.31E-03	(708)	0.58	35-40	60-64	1
Albite, antiperthite rim	C101	Red	N/A		N/A			1	99	
K-feldspar, antiperthite rim	C101	Dull blue, Brown	N/A		N/A			92-100	0-8	0-1

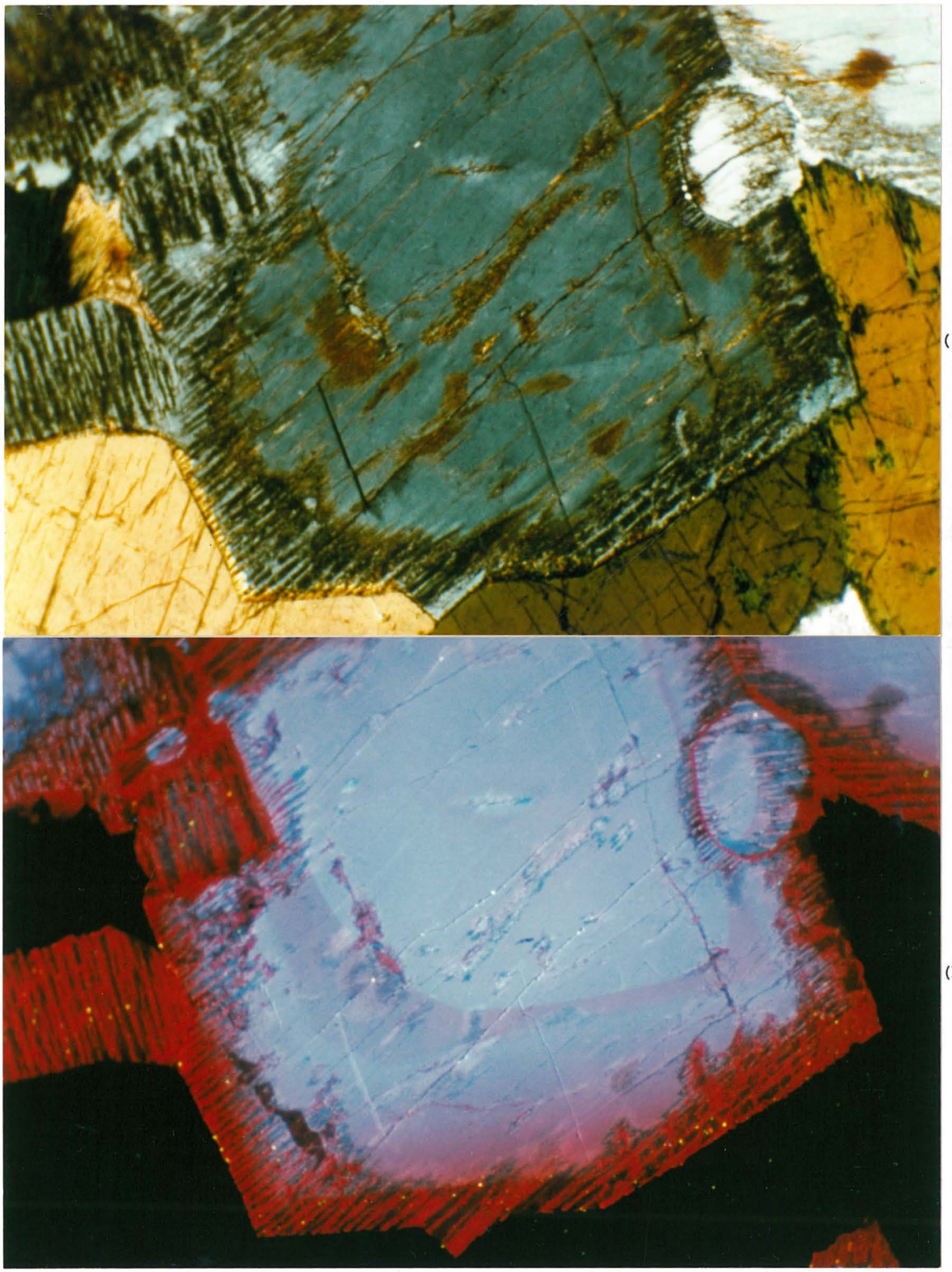

(a)

(b)

Fig. 5.2-3. Optically homogeneous alkali feldspar crystals are mantled by a deuteric coarsened antiperthitic rim in the unlayered ferroaugite syenite (Sample C100), Center I. a. TrL. The alkali feldspar crystals are mantled with an optically homogeneous core and antiperthitic rim. (Photographic conditions: 6s, ASA 400). b. CL. The optically homogeneous alkali feldspar core exhibits light violet blue luminescence and shows an oscillatory zone near the margins. In the deuteric coarsened antiperthitic rim, the secondary albite exhibits deep red luminescence and the secondary K-feldspar exhibits dark brown luminescence. Scale: 55 mm on photograph = 1 mm on thin section. (CL conditions: 10 kV, 0.8 Am. Photographic conditions: 1m, ASA 400).

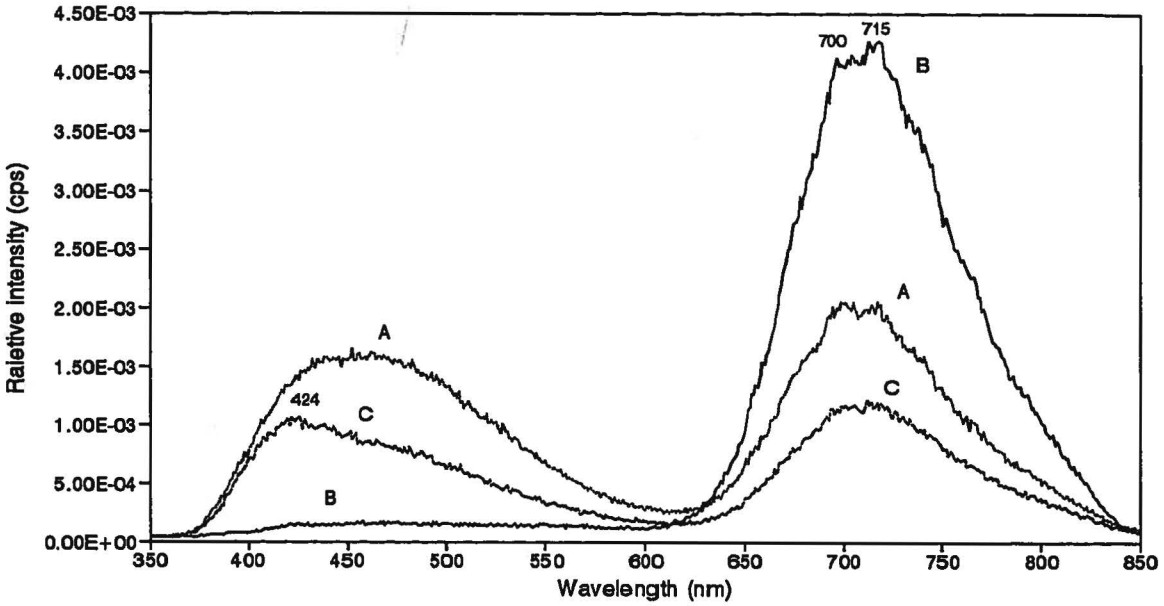

Fig. 5.2-4a. CL spectra of feldspars in the unlayered ferroaugite syenite (Sample C100), Center I. Spectrum (A) is from the light violet blue luminescent optically homogeneous alkali feldspar core. Spectrum (B) is from the red luminescent secondary albite in the deuteric coarsened antiperthitic rim. Spectrum (C) is from the purple luminescent secondary albite which occurs between the core and the antiperthitic rim. CL conditions: 10 kV, 0.8 Am.

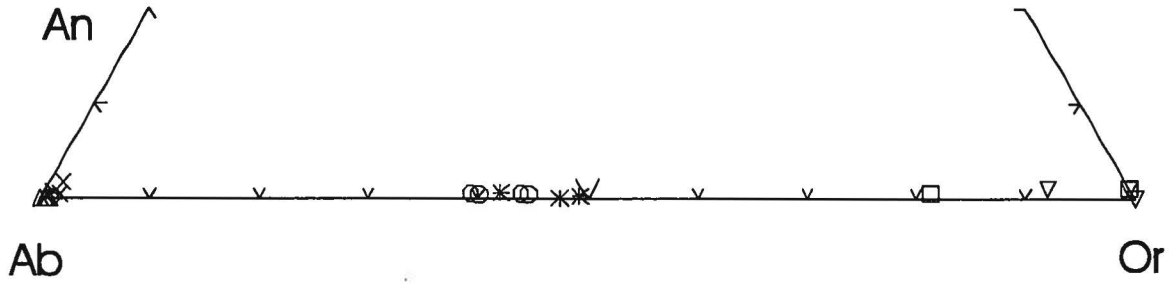

Fig. 5.2-4b. The compositions of the feldspars in the unlayered ferroaugite syenite (Sample C100) plotted in the system Or-Ab-An.

The circles (O) are the light violet blue luminescent optically homogeneous alkali feldspar core. The asterisks (*) are the light violet luminescent zone in the core. The upper triangles are (▵) the red luminescent secondary albite and the down triangles (▿) are the brown to dull blue luminescent secondary K-feldspar in the deuteric coarsened antiperthitic rim. The squares (□) are the dark blue luminescent secondary K-feldspar and the diamond (◇) is the light blue luminescent secondary albite in the fractures. The crosses (×) are the purple luminescent secondary albite which occurs between the core and the antiperthitic rim.

SEM/BSE images show that the optically homogeneous core is actually braid microperthite (Fig. 5.2-5a,b). The microbraid textures are well-developed in the areas near the antiperthitic rim and are poorly developed in the centre of the core (Fig. 5.2-5a). In comparison with the CL image in Fig. 5.2-3b, the poorly developed microperthite texture areas exhibit light violet blue luminescence, whereas the well-developed microperthite texture areas exhibit light violet luminescence. In the microperthite, the exsolved K-rich feldspar (light grey) is continuous lamellae with widths of less than 1 μm, whereas the exsolved Na-rich feldspar (dark grey) is lens-shaped lamellae with widths ranging from 1 to 2 μm. (Fig. 5.2-5b). The chemical diffusion between the exsolved K-rich feldspar and the exsolved Na-rich feldspar is not complete as indicated by some narrow grey bands (Na-rich feldspar) occurring within the light grey bands (K-rich feldspar).

The light violet blue luminescent microperthite core ranges in composition from $Or_{39-44}Ab_{55-60}An_1$ and contains 0.6-1.18 mole % $FeAlSi_3O_8$ (Table 5.2-1, Fig 5.2-4b and Appendix 1). The light violet luminescent oscillatory zone in the core ranges in composition from $Or_{42-49}Ab_{51-58}An_{0-1}$, and contains 1.02-1.4 mole % $KFeSi_3O_8$. The light violet luminescent oscillatory zone has higher contents of Or and $KFeSi_3O_8$ than the light violet blue luminescent microperthite core.

The deuteric coarsened antiperthitic rim consists of red luminescent secondary albite and brown luminescent secondary K-feldspar (Fig 5.2-3b). CL spectrum of the red luminescent secondary albite consists of a very high red peak centered at about 711 nm

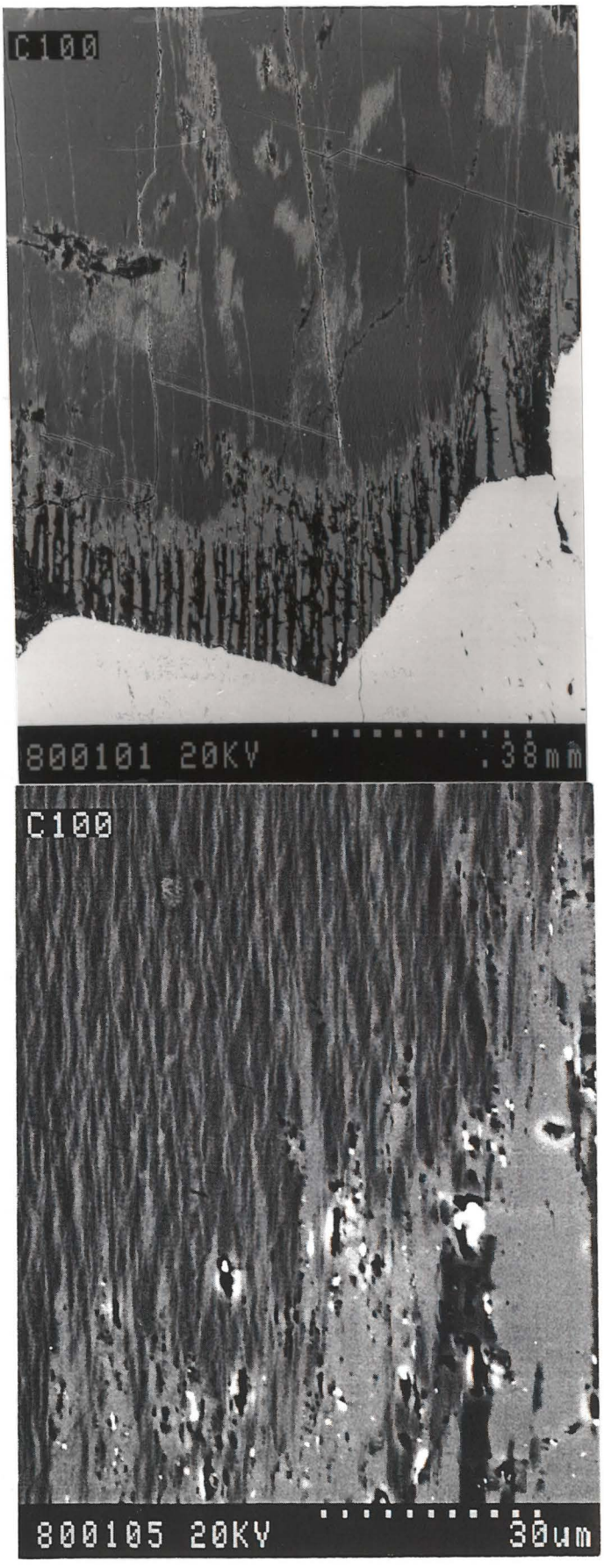

Fig. 5.2-5. SEM/BSE micro-photograph of the feldspar crystal in the unlayered ferro-augite syenites (Sample C100), Center I.

a. The feldspar crystal shows a braid microperthite core (grey) with a deuteric coarsened anti-perthite rim. The microbriad texture is well-developed in the areas near the antiperthitic rim and weakly developed in the centre of the core. In the antiperthitic rim, the dark grey areas are the secondary albite and the light grey areas are the secondary K-feldspar.

b. The braid microperthite textures in the areas near the antiperthitic rim. The image shows the detail of the intergrowths between the K-feldspar (light grey) and the albite (grey) lamellae. The white spots are Fe-bearing minerals and the black spots are micropores which are mainly distributed within the deuteric coarsened antiperthitic rim.

with a very low I_B/I_R ratio (0.04) (Fig. 5.2-4a). The red peak is split to form two peaks at 700 and 715 nm which is the same as the light violet blue luminescent microperthite core (Fig. 5.2-4a, spectrum B and Table 5.2-1). The red luminescent secondary albite ranges in composition from $Ab_{99-100}Or_{0-1}$ and contains 1.35-3.68 mole % $KFeSi_3O_8$, whereas the brown luminescent secondary K-feldspar ranges from $Or_{92-100}Ab_{0-7}An_{0-1}$ and contains 0.77-1.86 mole % $KFeSi_3O_8$ (Table 5.2-1, Fig. 5.2-4b and Appendix 1). Both of the secondary feldspars have end member compositions and contain higher $KFeSi_3O_8$ contents than the light violet luminescent microperthite core. These secondary feldspars in the deuteric coarsened antiperthitic rim have similar CL properties and compositions as those found in the layered ferroaugite syenites unit, thus the deuteric coarsening processes in the unlayered ferroaugite syenites is the same as in the layered unit.

However, the secondary albite which occurs in the areas between the microperthite core and the antiperthite rim is different from that in the layered syenites. This secondary albite is albite-twinned and exhibits purple luminescence (Fig. 5.2-6b). CL spectrum of the purple luminescent secondary albite consists of a blue peak at about 424 nm and a red peak at 709 nm with a I_B/I_R ratio of about 0.9 (Fig. 5.2-4a, spectrum C and Table 5.2-1). This purple luminescent secondary albite has end member compositions of $Ab_{97-98}Or_{1-2}An_{<1-2}$ which is similar to the red luminescent secondary albite in the antiperthite rim, but it contains relatively lower Fe contents (0-0.6 mole %, $KFeSi_3O_8$) than the red luminescent secondary

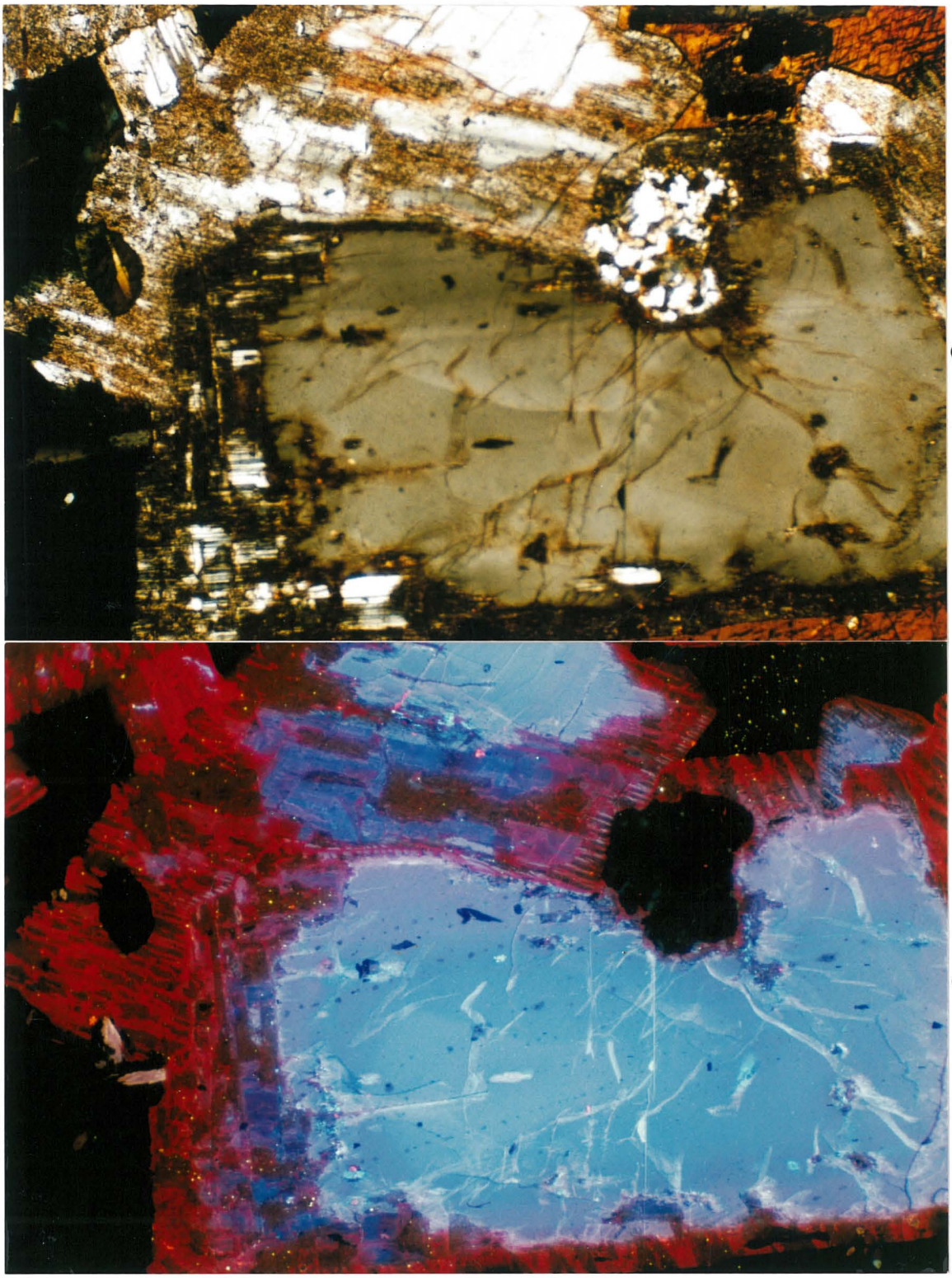

(a)

(b)

Fig. 5.2-6. Mantled feldspars in the unlayered ferroaugite syenite (Sample C100), Center I. a. TrL. The optically homogeneous alkali feldspar is mantled by a deuteric coarsened antiperthitic rim. Between the core and the rim, some secondary albite patches are albite twinned. (Photographic conditions: 15s, ASA 400). b. CL. The optically homogeneous alkali feldspar cores exhibit light violet blue luminescence. In the antiperthitic rim, the secondary albite exhibits deep red luminescence and the secondary K-feldspar exhibits brown luminescence. Between the core and the rim, the albite-twinned secondary albite exhibits purple luminescence. Scale: 55 mm on photograph = 1 mm on thin section. (CL conditions: 10 kV, 0.8 Am. Photographic conditions: 30s, ASA 400).

albite (Table 5.2-1, Fig. 5.2-4b and Appendix 1).

5.2.4. Optically homogeneous alkali feldspar mantled with an intermediate perthitic mantle and a deuteric coarsened antiperthitic rim

In samples C304 and C305, some of the alkali feldspar crystals are mantled with an optically homogeneous alkali feldspar core, an irregular, intermediate perthitic mantle and a deuteric coarsened antiperthitic rim (Fig. 5.2-7a,-8a). The optically homogeneous alkali feldspar core exhibits an uniform light violet blue luminescence (Fig. 5.2-7b, -8b). The CL spectrum from this core consists of a blue peak centered at 462 nm and a red peak centred at 711 nm with a I_B/I_R ratio of about 0.5 (Fig. 5.2-9a, spectrum A and Table 5.2-1). This light violet blue luminescent homogeneous alkali feldspar core ranges in composition from $Or_{35-43}Ab_{55-64}An_{1-4}$ and contains 0.50-0.99 mole % $KFeSi_3O_8$ (Table 5.2-1, Fig. 5.2-9b and Appendix 1). The CL properties and compositions of this optically homogeneous alkali feldspar core are similar to optically homogeneous alkali feldspars core in sample C100.

The intermediate mantle exhibits a heterogeneous light violet luminescence (Fig 5.2-7b, -8b). The CL spectrum from this mantle consists of a weak blue peak centered at 466 nm and a high red peak centered at 711 nm with a I_B/I_R ratio of about 0.2 (Fig 5.2-9a, spectrum B and Table 5.2-1). The intermediate mantle consists of optically homogeneous alkali feldspar host which is the same as the core, exsolved albite and K-feldspar blebs (Fig. 5.2-7a). The heterogeneous luminescence colours of the intermediate mantle is

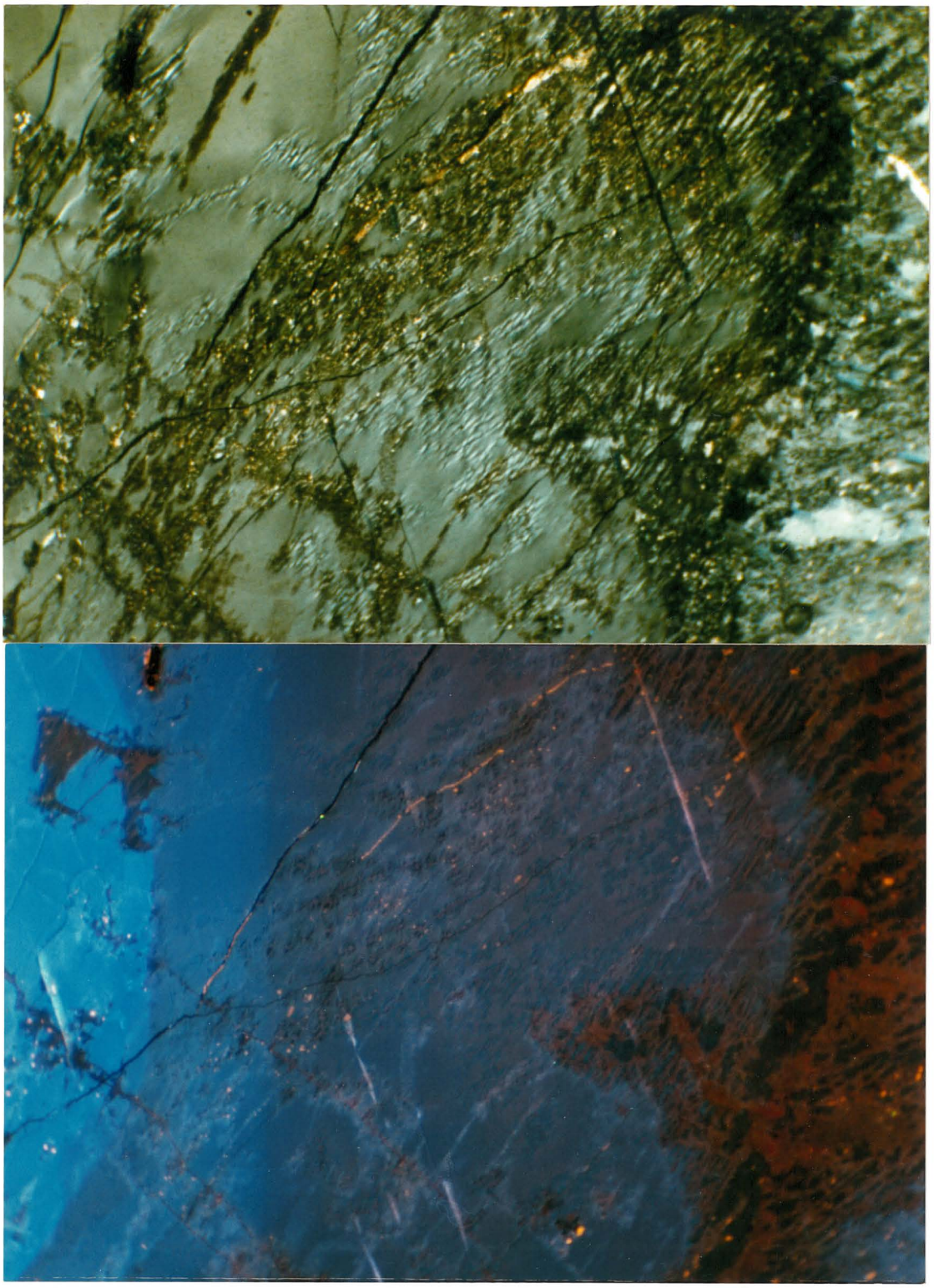

(a)

(b)

Fig. 5.2-7. Mantled feldspars in the unlayered syenite (Sample C305), Center I. a. TrL. The optically homogeneous alkali feldspar is mantled by an intermediate perthitic mantle and an anti-perthitic rim. There are many small blebs of microperthitic albite distributed within the mantle. (Photographic conditions: 0.5s, ASA 400). b. CL. The homogeneous alkali feldspar core exhibits light violet blue luminescence. The perthitic mantle exhibits light violet to violet luminescence. The albite blebs exhibit dull red luminescence and are surrounded by blue luminescent K-feldspar. In the deuteric coarsened antiperthitic rim, the secondary albite exhibits red luminescence and the secondary K-feldspar exhibits dark brown luminescence. Scale: 55 mm on photograph = 1 mm on thin section. (CL conditions: 10 kV, 0.8 Am. Photographic conditions: 1.2m, ASA 400).

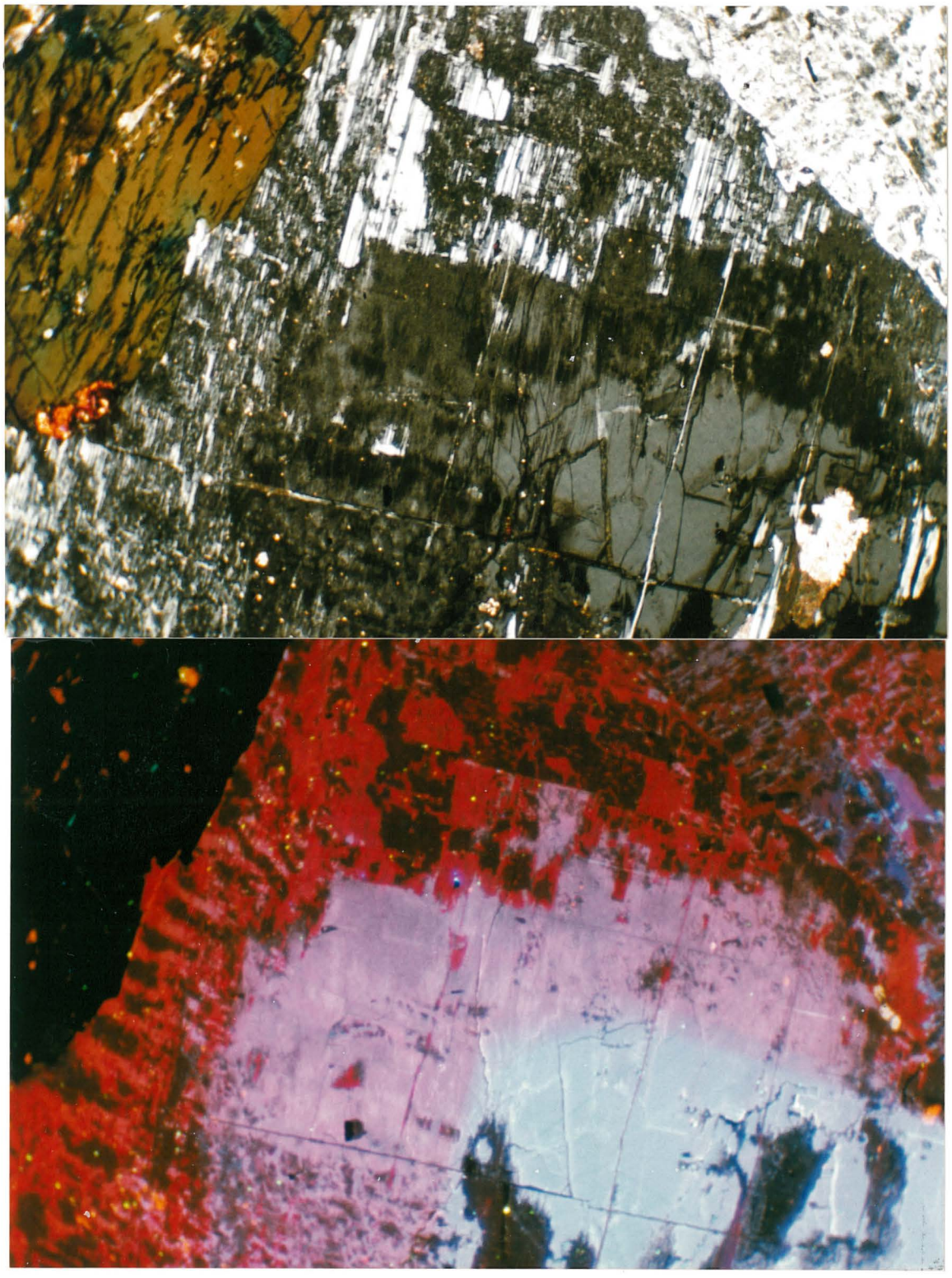

(a)

(b)

Fig. 5.2-8. Mantled feldspars in the unlayered syenite (Sample C305), Center I. a. TrL. The optically homogeneous alkali feldspar is mantled by an intermediate perthitic mantle and an antiperthitic rim. (Photographic conditions: 6s, ASA 400). b. CL. The homogeneous alkali feldspar core exhibits light violet blue luminescence. The perthitic mantle exhibits light violet to dull violet luminescence. Within the mantle, the light violet luminescent areas contain many micropores, whereas the dull violet luminescent areas contain many hematite grains. In the antiperthitic rim, the secondary albite exhibits red luminescence, whereas the secondary K-feldspar exhibits dark brown luminescence. Scale: 55 mm on photograph = 1 mm on thin section. (CL conditions: 10 kV, 0.8 Am. Photographic conditions: 1m, ASA 400).

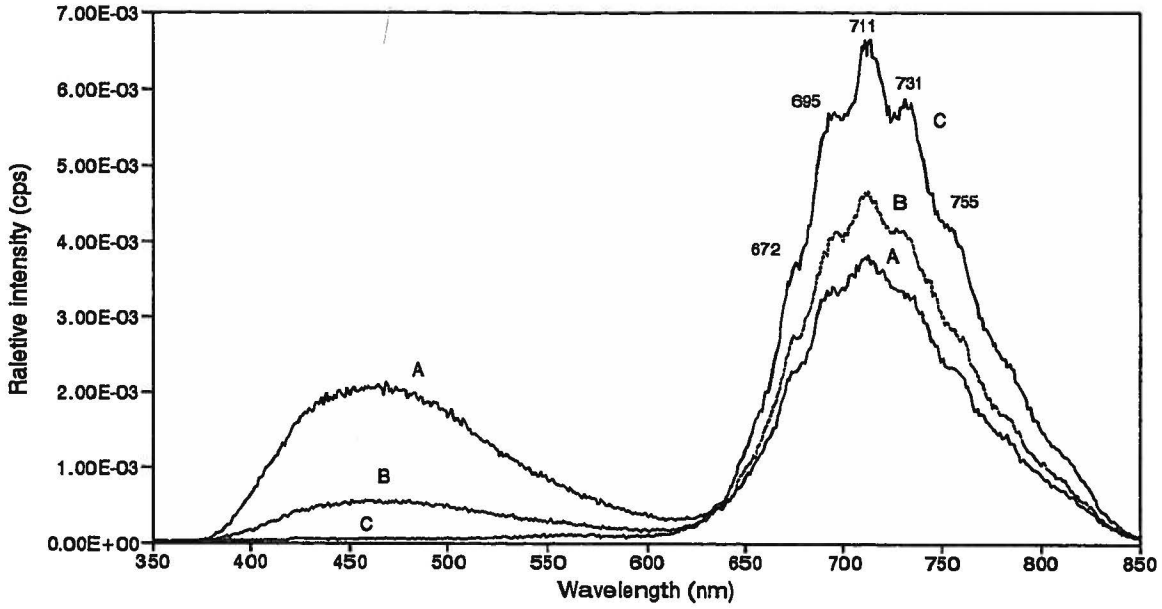

Fig. 5.2-9a. CL spectra of feldspars in the unlayered ferroaugite syenite (Sample C305), Center I. Spectrum (A) is from the light violet blue luminescent optically homogeneous alkali feldspar core. Spectrum (B) is from the light violet luminescent perthitic mantle. Spectrum (C) is from the red luminescent secondary albite in the deuteric coarsened antiperthitic rim. CL conditions: 10 kV, 0.8 Am.

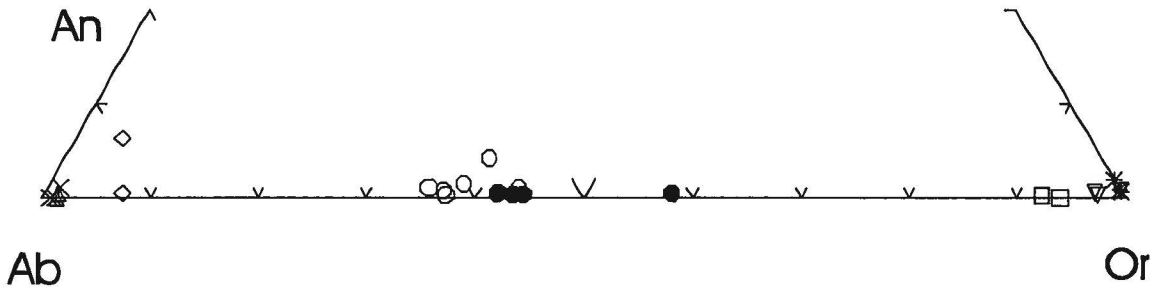

Fig. 5.2-9b. The compositions of the feldspars in the unlayered ferroaugite syenite (Sample C305) plotted in the system Or-Ab-An.

The circles (O) are the light violet blue luminescent optically homogeneous alkali feldspar core. The filled circles (•) are the light violet luminescent optically homogeneous alkali feldspar host in the mantle, and the crosses (×) are the dull red luminescent exsolved albite blebs in the mantle, whereas the asterisks (*) are the blue luminescent exsolved K-feldspar blebs in the mantle.

The upper triangles are (▵) the red luminescent secondary albite, and the down triangles (▿) are the brown to dull blue luminescent secondary K-feldspar in the deuteric coarsened antiperthitic rim. The squares (□) are the non luminescent secondary K-feldspar and the diamonds (◇) are the non luminescent secondary albite in the fracture.

caused by this irregularly formed microperthitic texture. Under CL, these exsolved albite and K-rich feldspar blebs exhibit dull red and blue luminescence, respectively, and the optically homogeneous alkali feldspar host exhibits luminescence colours ranging from bluish violet to violet blue (Fig 5.2-7b). The heterogeneous luminescence is also caused by hematitization which produces many small (±1μm) hematite grains and by micropores which are irregularly distributed within the mantle and show a turbid-looking appearance (Fig. 5.2-8a). Within the intermediate mantle (Fig. 5.2-8b), the hematite grains occur mainly in the dull violet luminescent areas, but the micropores occur mainly in the light violet luminescent areas. The bluish violet to violet luminescent, optically homogeneous alkali feldspar host ranges in composition from $Or_{42-58}Ab_{42-57}An_1$ and contains 2.11-5.97 mole % $KFeSi_3O_8$ (Table 5.2-1, Fig. 5.2-9b and Appendix 1), and it contains higher Or and Fe contents than the optically homogeneous alkali feldspar core. In the microperthitic areas, the dull red luminescent exsolved albite ranges in composition from $Ab_{98-99}Or_1An_{0-1}$ and contains 1.17-1.51 mole % $KFeSi_3O_8$, whereas the blue luminescent exsolved K-rich feldspar ranges from $Or_{98-99}An_{1-2}$ and contains 0.4-0.71 mole % $KFeSi_3O_8$.

In the deuteric coarsened antiperthitic rim, the secondary albite exhibits deep red luminescence, whereas the secondary K-feldspar exhibits brown luminescence (Fig 5.2-7b, -8b). The deep red luminescent secondary albite ranges in composition from $Ab_{98-99}Or_1An_{<1}$ and contains 1.26-1.32 mole % $KFeSi_3O_8$, whereas the brown luminescent secondary K-feldspar ranges from $Or_{97-99}Ab_{0-2}An_1$ and

contains 1.79-6.65 mole % $KFeSi_3O_8$ (Table 5.2-1, Fig 5.2-9b and Appendix 1). This deuteric coarsened antiperthitic rim is similar to those deuteric coarsened antiperthitic rims found in sample C100.

Fig. 5.2-9a shows that the blue peak intensity decreases from the optically homogeneous alkali feldspar core through to the intermediate perthitic mantle and to the secondary albite in the deuteric coarsened antiperthitic rim, whereas the red peak intensity gradually increases. The ratios of the I_B/I_R range from 0.5 through 0.2 to 0.1, respectively (Table 5.2-1). This changing peak intensity is the same as found in the C65 and C72 in the layered unit. The red peak splitting in these samples (C304 and C304) is much stronger than in the remainding samples, e.g., the red peak of the deep red luminescent secondary albite in the antiperthite rim is clearly split into five small peaks which are located at 672, 695, 711, 731 and 755 nm (Fig. 5.2-9a, spectrum C).

5.2.5. Microperthite mantled with an albite rim

Sample C101 is dark brown porphyritic-phaneritic syenite. Phenocrysts (≥ 3mm) in the sample are dark brown, Carlsbad twinned alkali feldspar crystals. The groundmass (≤ 1mm) mainly consists of fine-grained brown alkali feldspar, black amphibole and minor biotite. The feldspar phenocrysts are mantled with a microperthite core and an irregular albite rim (Fig. 5.2-10a). The phenocrysts core exhibits light blue luminescence with microbraid textures (Fig. 5.2-10b). The CL spectrum of the light blue luminescent

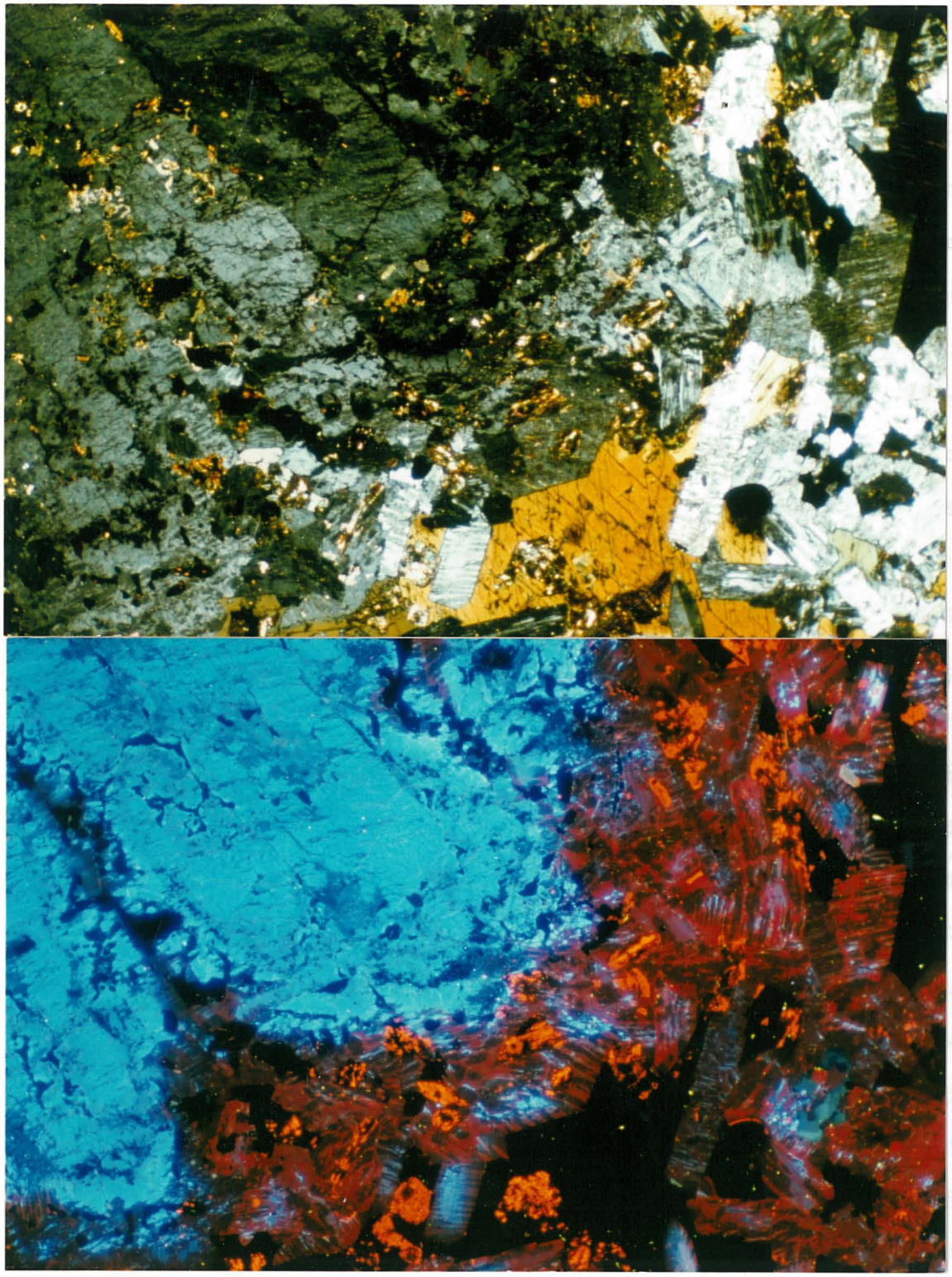

(a)

(b)

Fig. 5.2-10. Feldspars in the porphyritic-phaneritic syenite (Sample C101), Center I. a. TrL. The alkali feldspar phenocrysts are surrounded by the fine-grained antiperthite groundmass. (Photographic conditions: 3s, ASA 400). b. CL. The phenocrysts are mantled with a blue luminescent microperthitic core and a light blue luminescent albite rim. The rim is surrounded by fine-grained antiperthite which consists of red luminescent secondary albite and brown luminescent secondary K-feldspar. Some fine-grained feldspar crystals in the groundmass are mantled with a light violet blue microperthite core and an antiperthitic rim. Secondary K-feldspar exhibits dull blue luminescence which occurs in the core of the phenocrysts. The orange luminescent crystals are the calcite and the bluish grey luminescent crystals are the fluorite. Scale: 55 mm on photograph = 1 mm on thin section. (CL conditions: 10 kV, 0.8 Am. Photographic conditions: 30, ASA 400).

microperthite core consists of a high blue peak centered at 459 nm and a very weak red peak centered at 708 nm with a I_B/I_R ratio of about 12.1 (Fig. 5.2-11a, spectrum A and Table 5.2-1). Within the microperthite core, the exsolved albite (light blue luminescence bands) ranges in composition from $Ab_{90-93}Or_{1-5}An_{5-7}$, whereas the exsolved K-feldspar (dark blue luminescence bands) ranges from $Or_{79-88}Ab_{11-20}An_1$ (Table 5.2-1, Fig 5.2-11b and Appendix 1).

The albite rim of the feldspar phenocrysts exhibits light blue luminescence and it is partially replaced by fine-grained antiperthite and Fe-bearing minerals (non luminescence) (Fig 5.2-10b). The CL spectrum of the light blue albite rim consists of a very high blue peak centered at 454 nm and a very weak red centered at 708 nm, and the ratio of I_B/I_R is about 13.4 which is higher than in the core (Fig. 5.2-11a, spectrum B and Table 5.2-1). The light blue luminescent albite rim ranges in composition from $Ab_{80-94}Or_{1-4}An_{3-9}$ (Table 5.2-1, Fig 5.2-11b and Appendix 1).

The feldspar phenocrysts are surrounded by a fine-grained feldspar groundmass. Most of the groundmass is deuteric coarsened antiperthite which consists of red luminescent secondary albite and dull blue or brown luminescent secondary K-feldspar (Fig. 5.2-10b). However, some of the groundmass is mantled with a light violet blue luminescent core and a deuteric coarsened antiperthitic rim which consists of red luminescent secondary albite and brown luminescent secondary K-feldspar. The CL spectrum of the light violet blue luminescent core consists of a low blue peak centered at 456 nm and a high red peak centered at 708 nm with a I_B/I_R ratio of about 0.6

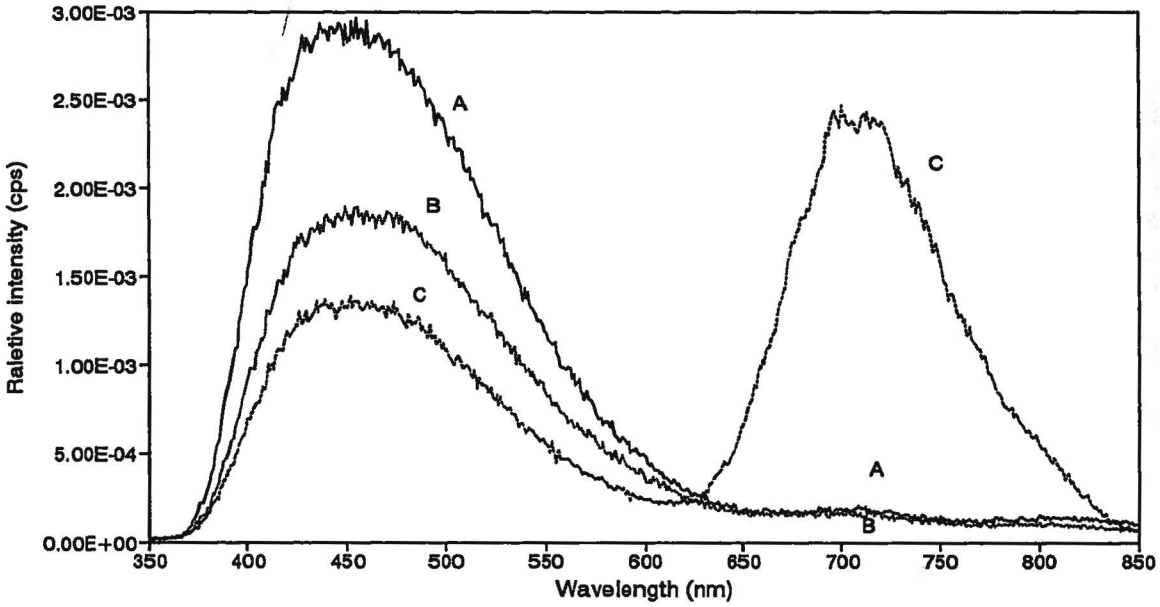

Fig. 5.2-11a. CL spectra of the feldspars in the unlayered ferroaugite syenite (Sample C101), Center I. Spectrum (A) is from the blue luminescent microperthite core of the feldspar phenocrysts. Spectrum (B) is from the light blue luminescent albite rim of the feldspar phenocrysts. Spectrum (C) is from the light violet blue luminescent microperthite core of the feldspar groundmass. CL conditions: 10 kV, 0.8 Am.

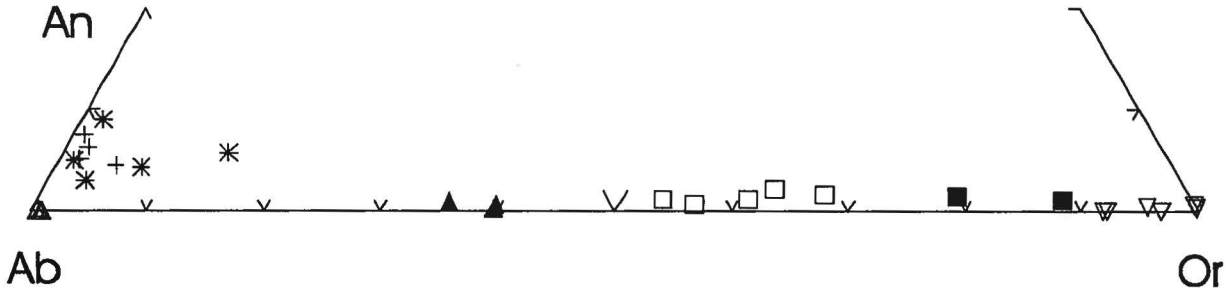

Fig. 5.2-11b. The compositions of the feldspars in the unlayered ferroaugite syenite (Sample C101) plotted in the system Or-Ab-An.

The crosses (+) are the light blue luminescent albite and the filled squares (■) are the dull blue luminescent K-feldspar in the microperthitic core of the feldspar phenocrysts. The asterisks (*) are the light blue luminescent albite rim of the feldspar phenocrysts. The squares (□) are the dull blue luminescent secondary K-rich feldspar in the centre of the microperthitic core of the feldspar phenocrysts.

The filled upper triangles (▲) are the light violet blue luminescent microperthite core of the feldspar groundmass.

The up-triangles (▲) are the red luminescent secondary albite and the down triangles (▼) are the dull blue to brown luminescent secondary K-feldspar in the deuteric coarsened antiperthitic rim and in the deuteric coarsened antiperthite of the groundmass.

(Fig. 5.2-11a, spectrum C and Table 5.2-1). SEM/BSE images show that the light violet blue luminescent core is microperthite with a tweed texture (Fig. 5.2-12a,b). Fig. 5.2-12a also shows that the secondary albite bands (dark grey) from the antiperthite rim extended into the microperthite core, whereas the secondary K-feldspar (grey) bands are embedded in the microperthite core. The micropores (black) and the Fe-minerals (white) are mainly distributed within the antiperthite rim.

The light violet blue luminescent microperthite core ranges in composition $Or_{35-40}Ab_{60-64}An_1$ and contains 0.57-0.73 mole % $KFeSi_3O_8$ (Table 5.2-1, Fig 5.2-11b and Appendix 1). For the antiperthite groundmass and the antiperthitic rim, the red luminescent secondary albite ranges in composition from $Ab_{99}Or_1$ and contains 0.99-2.10 mole % $KFeSi_3O_8$, whereas the dull blue or brown luminescent secondary K-feldspar ranges from $Or_{92-100}Ab_{0-8}An_{0-1}$ and contains 0.44-1.95 mole % $KFeSi_3O_8$. The Fe contents in both of the secondary albite and K-feldspar rim are higher than in the microperthite core.

5.2.6. Feldspar crystals mantled with a Na-feldspar core, an intermediate perthitic mantle and a deuteric coarsened antiperthitic rim

Some feldspar crystals have unusual textures in sample C302, the feldspar crystals are mantled with a Na-feldspar core, a perthitic intermediate mantle and a deuteric coarsened antiperthitic rim (Fig. 5.2-13a). The Na-feldspar cores are mainly optically homogeneous, but some of them are slightly exsolved into incipient

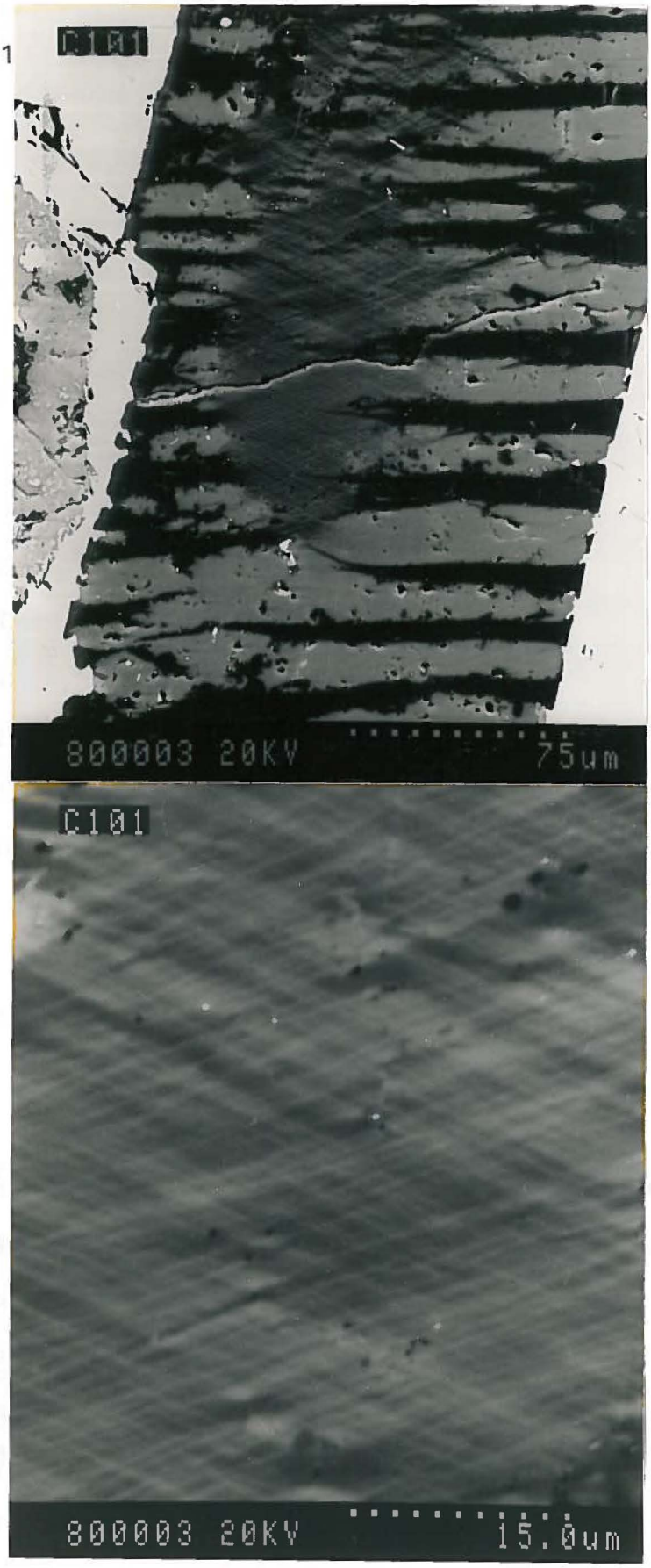

Fig. 5.2-12. SEM/BSE micrograph of the feldspar groundmass in the unlayered ferroaugite syenite (Sample C101), Center I. a. The fine-grained feldspar crystal (groundmass) is mantled with a microperthite core and an antiperthite rim. The microperthite core shows a tweed texture. The antiperthitic rim consists of secondary albite (dark grey) and secondary K-feldspar (light grey). The white spots are the Fe-bearing minerals and the black spots are the micropores which are mainly distributed within the rim. b. The tweed texture in the centre of the microperthite core consists of K-feldspar (light grey) and the albite (grey) lamellae.

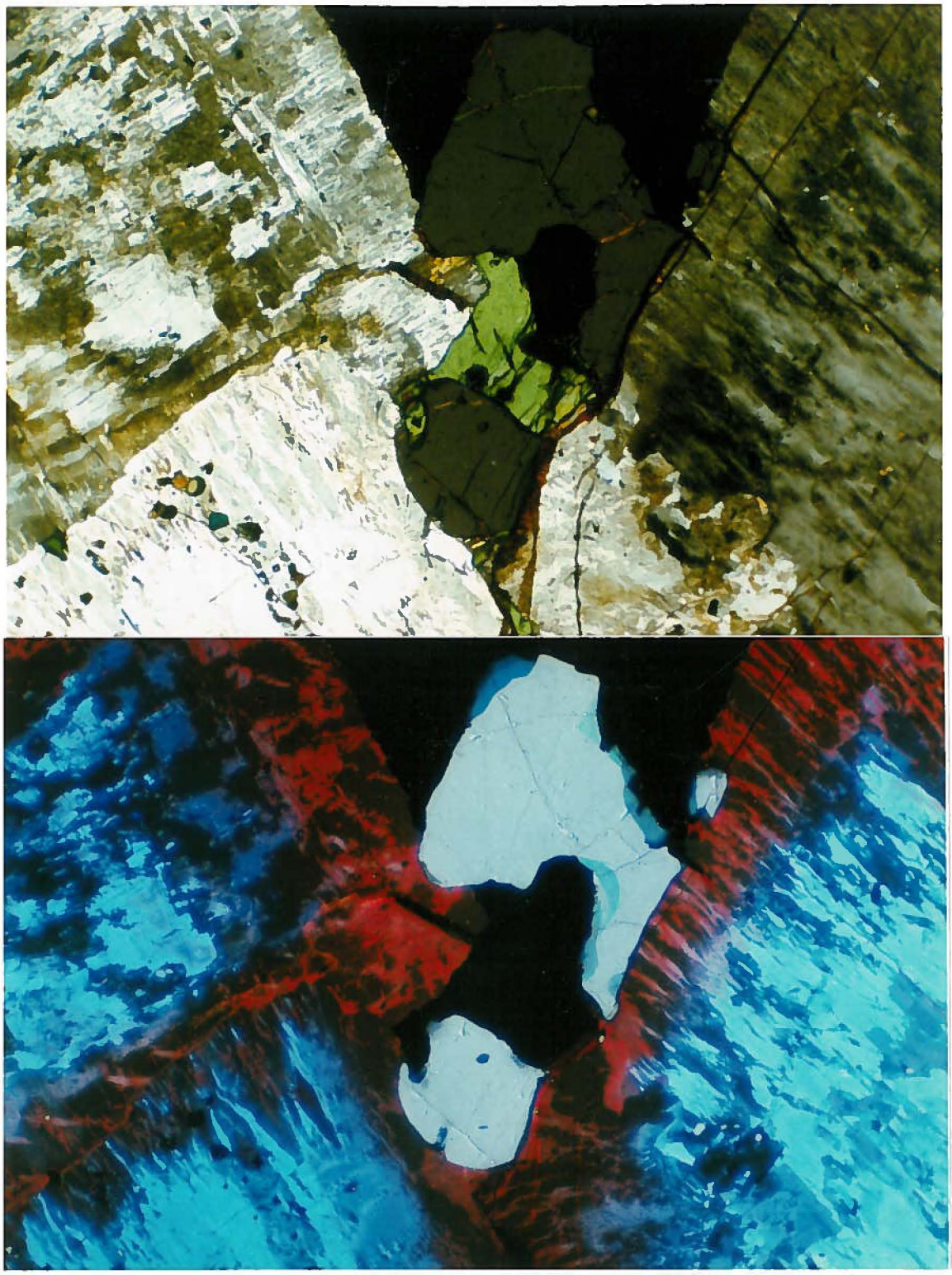

(a)

(b)

Fig. 5.2-13. Mantled feldspars in the recrystallized syenite (Sample C302), Center I. a. TrL. The feldspar is mantled with a Na-feldspar core, an intermediate perthitic mantle and an antiperthitic rim. There are many small grains of pyroxene and amphibole occurring in the areas between the core and the mantle. (Photographic conditions: 3s, ASA 400). b. CL. The Na-feldspar core exhibits light blue luminescence. In the perthitic mantle, the exsolved albite exhibits light blue luminescence and the exsolved K-feldspar exhibits dark blue luminescence. In the areas between the mantle and the rim, some secondary albite patches exhibit purple luminescence. Within the deuteric coarsened antiperthitic rim, the secondary albite exhibits deep red luminescence, whereas the secondary K-feldspar exhibits dark brown luminescence. The bluish grey luminescent grains are fluorite. Scale: 55 mm on photograph = 1 mm on thin section. (CL conditions: 10 kV, 0.8 Am. Photographic conditions: 30s, ASA 400).

perthite. There are many fine-grained pyroxene and amphibole mineral inclusions which occur in the area between the Na-feldspar core and the perthitic mantle. Under CL, the Na-feldspar cores exhibit light blue luminescence and range in composition from $Ab_{79-91}Or_{2-4}An_{6-18}$ (Fig. 5.2-13b, Fig. 5.2-14 and Appendix 1). The perthitic mantles consist of light violet blue luminescent microperthite patches, light blue luminescent exsolved albite and dull blue luminescent exsolved K-feldspar lamellae (Fig. 5.2-13b). The light violet blue luminescent microperthite ranges in composition from $Or_{48-53}Ab_{45-50}An_1$ (Fig. 5.2-14, Appendix 1). The light blue luminescent exsolved albite ranges in composition from $Ab_{93-96}Or_{1-3}An_{3-4}$, whereas the dull blue luminescent K-feldspar ranges from $Or_{81-93}Ab_{7-18}An_2$.

In the deuteric coarsened antiperthitic rim, the secondary albite exhibits purple, violet blue or deep red luminescence, whereas the secondary K-feldspar exhibits grey or brown luminescence (Fig. 5.2-13b). The compositions of these deuteric coarsened feldspars are near the end members; $Ab_{97-100}Or_{1-2}An_1$ for the secondary albite and $Or_{91-99}Ab_{3-8}An_1$ for the K-feldspar (Fig. 5.2-14, Appendix 1).

5.2.7. Late-stage fluid-induced coarsening and replacement in the unlayered ferroaugite syenites

a. Deuteric coarsened secondary feldspars

As discussed above, the deuteric coarsened feldspars usually form an antiperthitic rim surrounding the optically homogeneous alkali feldspar and the perthite. Within the deuteric coarsened antiperthitic rim, the secondary albite exhibits purple, violet

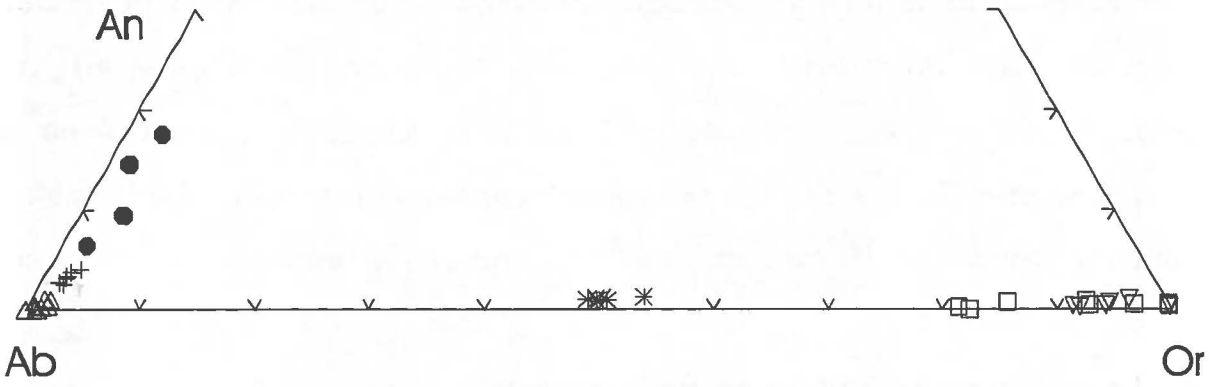

Fig. 5.2-14. The compositions of the feldspars in the unlayered ferroaugite syenite (Sample C302) plotted in the system Or-Ab-An.

The filled circles (•) are the light blue luminescent Na-feldspar core.

The crosses (+) are the light blue luminescent exsolved albite and the squares (□) are the dull blue luminescent exsolved K-feldspar, and the asterisks (*) are the light violet blue luminescent microperthite patches in the intermediate perthitic mantle.

The up-triangles are (▵) the purple, violet and red luminescent secondary albite and the down triangles (▿) are the grey, brown luminescent secondary K-feldspar in the deuteric coarsened antiperthitic rim.

blue or red luminescence, whereas the secondary K-feldspar exhibits grey, dull blue or brown luminescence. For all of the analyzed samples, the secondary albite ranges in composition from $Ab_{99-100}Or_{0-1}An_{0-<1}$, and contains about 1.89 mole % $KFeSi_3O_8$ (average value). Whereas the secondary K-feldspar ranges from $Or_{91-100}Ab_{0-8}An_{0-1}$ and contains about 1.74 mole % $KFeSi_3O_8$ (average value).

b. Secondary Na-feldspars replacement

In sample C188, the optically homogeneous alkali feldspar crystals are replaced by secondary Na-feldspar along their margins. The secondary Na-feldspar usually has a clear-looking appearance with irregularly-shaped outlines and albite twinning (Fig. 5.2-15a, -16a). Under CL, the secondary Na-feldspar exhibits purple or deep purple luminescence (Fig. 5.2-15b, -16b). The purple luminescent secondary Na-feldspar is oligoclase which is replaced by the deep purple luminescent secondary albite, and forms embayed boundaries with the purple luminescent secondary oligoclase (Fig. 5.2-16b).

CL spectra of the purple and deep purple luminescent secondary Na-feldspars are shown in Fig. 5.2-2a. Both of the spectra consist of a narrow blue peak centered at about 414 nm and broad red peak centered at about 708 nm. The I_B/I_R ratio is about 1.9 for the purple luminescent secondary oligoclase and is about 1.0 for the deep purple luminescent secondary albite (Table 5.2-1). The purple luminescent secondary oligoclase ranges in composition from $Ab_{80-84}Or_{2-5}An_{13-15}$ and contains 0.47-0.60 mole % $KFeSi_3O_8$, whereas the deep purple luminescent secondary albite has a composition of $Ab_{94}Or_2An_4$

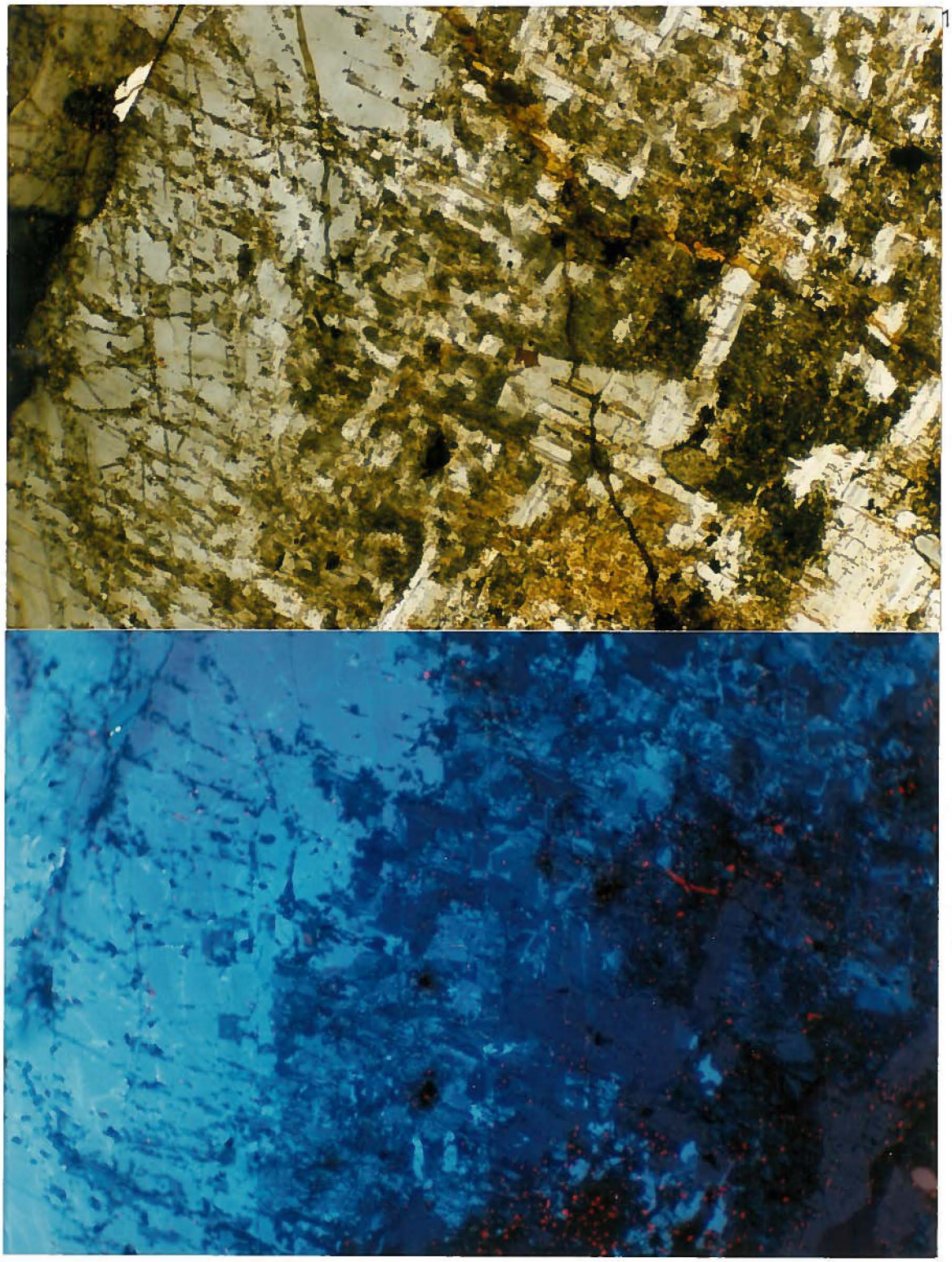

(a)

(b)

Fig. 5.2-15. Secondary feldspar replacement texture in the unlayered ferroaugite syenite (Sample C188), Center I. a. TrL. The optically homogeneous alkali feldspar is replaced by secondary albite (albite-twinned) and secondary K-feldspar (turbid-looking) at the margins. (Photographic conditions: 6s, ASA 400). b. CL. The optically homogeneous alkali feldspar exhibits light violet blue luminescence. The secondary albite exhibits purple luminescence, whereas the secondary K-feldspar exhibits dull blue luminescence. Scale: 55 mm on photograph = 1 mm on thin section. (CL conditions: 10 kV, 0.8 Am. Photographic conditions: 30s, ASA 400).

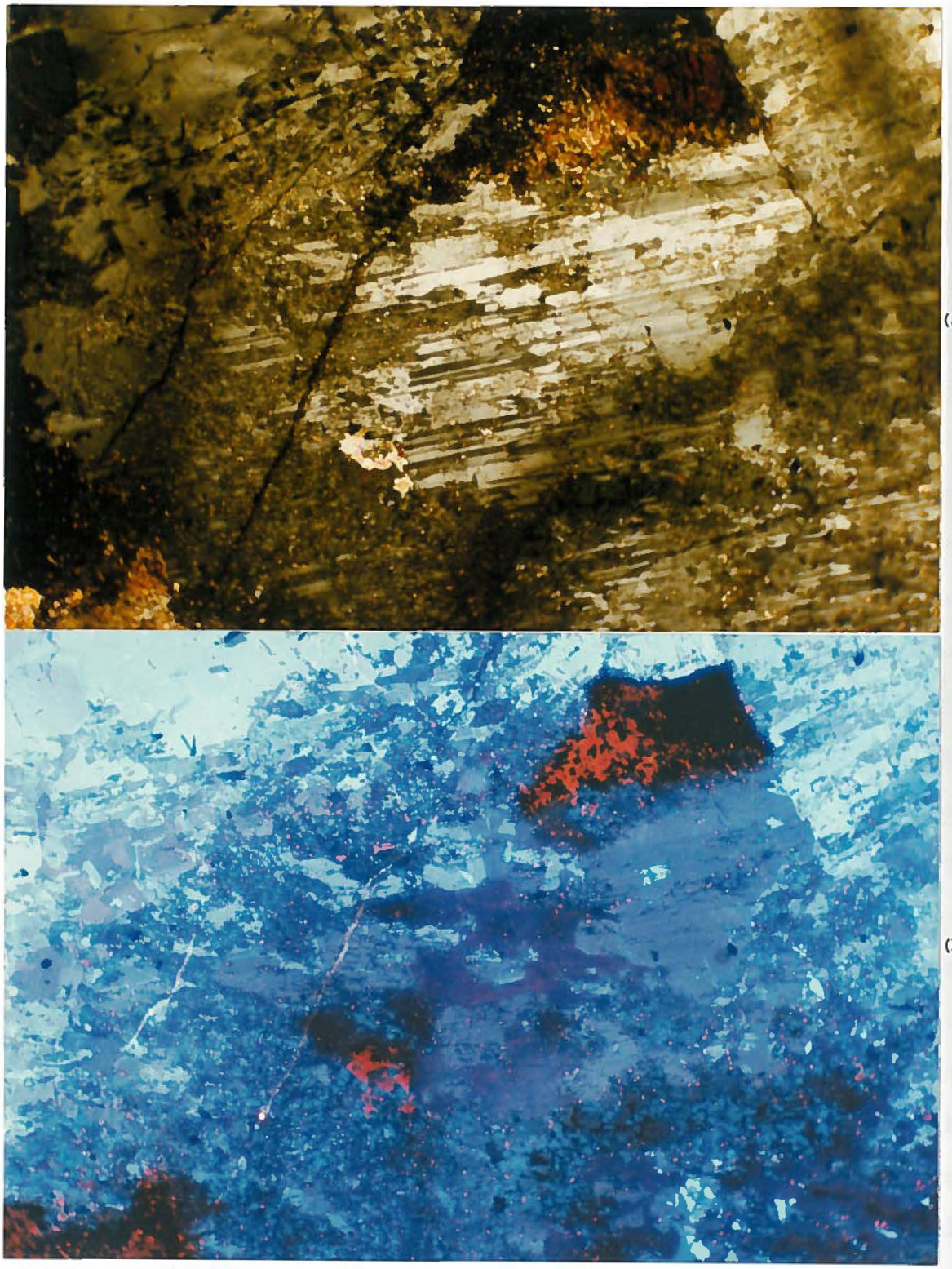

Fig. 5.2-16. Secondary feldspar replacement texture in the unlayered ferroaugite syenite (Sample C188), Center I. a. TrL. The optically homogeneous alkali feldspar is replaced by the albite-twinned secondary Na-feldspar at the margins. (Photographic conditions: 50s, ASA 400). b. CL. The purple luminescent areas are the secondary oligoclase, and the deep purple luminescent areas are the secondary albite. The light violet blue luminescent areas are the optically homogeneous alkali feldspar. Scale: 55 mm on photograph = 1 mm on thin section. (CL conditions: 10 kV, 0.8 Am. Photographic conditions: 30s, ASA 400).

and contains 0.39-0.52 mole % $KFeSi_3O_8$ (Table 5.2-1, Fig. 5.2-2b and Appendix 1). The I_B/I_R ratio and the An contents decrease, while the Ab contents increase from the earlier stage replacement of purple luminescent secondary oligoclase to the late-stage replacement of deep purple luminescent secondary albite.

The purple luminescent secondary albites also have been found in samples C100 and C302 (see section 5.2.3), but they usually occur in the areas between the core (optically homogeneous alkali feldspar core or albite core) and the deuteric coarsened antiperthitic rim. These purple luminescent secondary albites range in composition from $Ab_{97-98}Or_{1-2}An_{<1-2}$ and contain 0.25-0.67 mole % $KFeSi_3O_8$ (Appendix 1).

c. Secondary K-feldspar replacement

In sample C188, the optically homogeneous alkali feldspar crystals are also replaced by secondary K-rich feldspar with a turbid appearance (Fig. 5.2-15a, -16a). The secondary K-feldspar usually exhibits dark blue or dull blue luminescence and ranges in composition from $Or_{67-75}Ab_{23-29}An_{1-2}$ and contains 0.29-0.81 mole % $KFeSi_3O_8$ (Table 5.2-1, Fig. 5.2-2b and Appendix 1).

In sample C101, the microperthite core of the phenocryst is partially replaced by dull blue luminescent secondary K-rich feldspar which shows irregular outlines (Fig. 5.2-10b). The dull blue luminescent secondary K-rich feldspar ranges in composition from $Or_{53-67}Ab_{31-43}An_{1-2}$ and contains 0.35-0.53 mole % $KFeSi_3O_8$ (Table 5.2-1, Fig. 5.2-11b and Appendix 1). This secondary K-rich feldspar

contains many small (≤ 1μm) grains of an Fe-bearing mineral, pyrite, calcite and quartz, which may be observed only under high magnification in SEM/BSE images.

5.2.8. Thermal history of the feldspars

Evolution of the alkali feldspars in the unlayered ferroaugite syenites is shown in Fig. 5.2-17. The path a-a′ on the incoherent solvus (SFS) indicates that the alkali feldspar with a composition of $Or_{35-49}Ab_{51-64}$ may have crystallized at temperatures ≥720 °C, and exsolved during cooling into the braid and tweed microperthite at temperatures about 650-620 °C along the coherent solvus (CS) during cooling. This compositional range includes the light violet blue luminescent incipient irregular vein perthite; the light violet blue luminescent, optically homogeneous alkali feldspar core and the microperthitic core of the mantled feldspar crystals; and the light violet blue luminescent microperthite core of the mantled feldspar groundmass. In comparison with the Or-Ab-An ternary system at 1kbar (5.2-2b,-4b,-9b,-11b,-14), the alkali feldspar crystallized at a temperature range from 825 to 750 °C.

The paths b-b′ and c-c′ on the coherent solvus (CS) indicate that the dull blue luminescent exsolved K-feldspar ($Or_{79-93}Ab_{7-20}An_{1-2}$) and the light blue luminescent exsolved albite ($Ab_{90-96}Or_{1-5}An_{3-7}$) bands in the mantle of the perthite and in the core of the phenocrysts formed during cooling at temperatures below 420 °C and 520 °C, respectively (Fig. 5.1-17a).

The path d-d′ on the incoherent solvus (SFS) indicates that the

light blue luminescent albite rim ($Ab_{80-94}Or_{1-4}An_{3-9}$) of the phenocrysts may have formed at a temperature range from 680-600 °C along the incoherent solvus (SFS) (Fig. 5.1-17b).

Since the secondary albite ($Ab_{99-100}Or_{0-1}An_{0-<1}$) and K-feldspar ($Or_{91-100}Ab_{0-8}An_{0-1}$) in the deuteric coarsened antiperthitic rim have end member compositions, they formed at a very low temperature below 350 °C on the SFS (or <300 on the CS), which is indicated by the path e-b′ for the secondary K-feldspar.

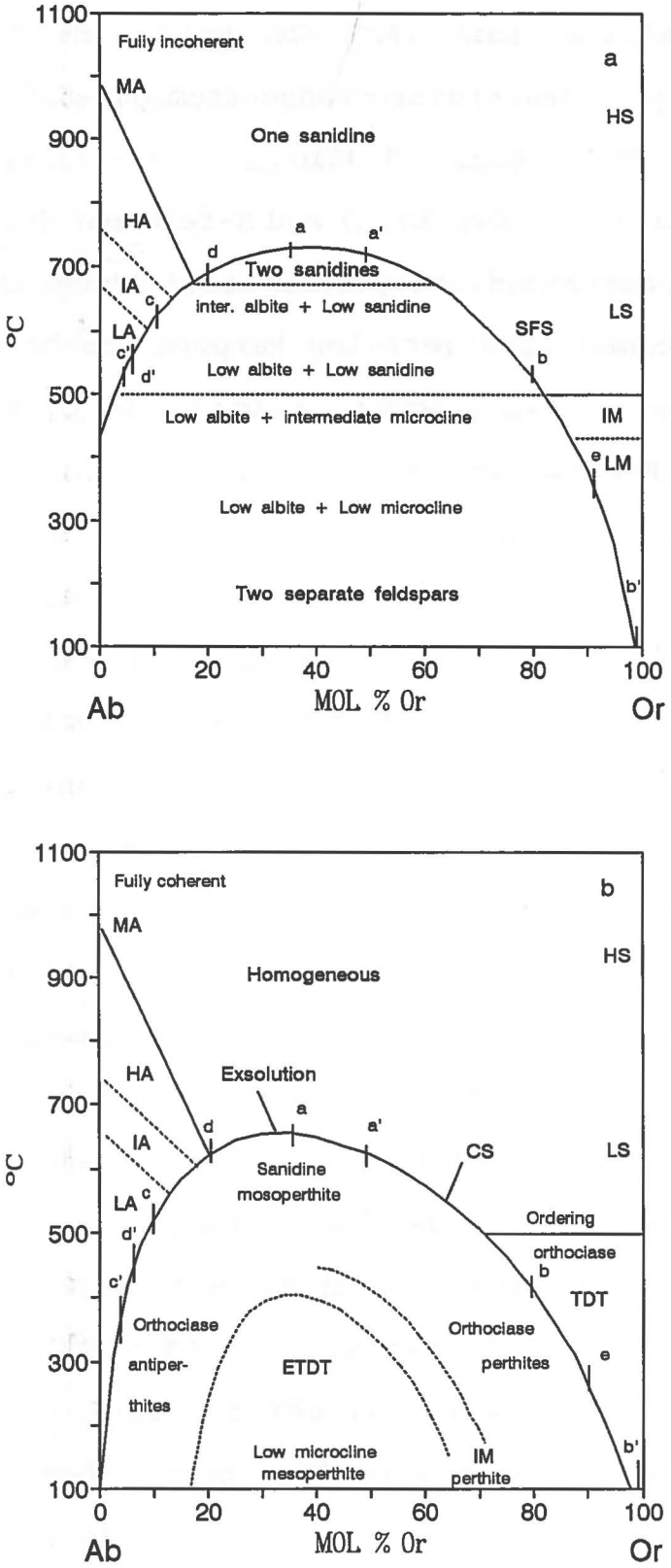

Fig. 5.2-17. The evolution of the alkali feldspars in the unlayered ferroaugite syenite from Center I is illustrated in the Or-Ab binary phase diagram.

The path a-a′ includes the incipient irregular vein perthite; the optically homogeneous alkali feldspar core and the microperthitic core of the mantled alkali feldspar; and the microperthite core of the mantled feldspar groundmass. The path b-b′ and c-c′ include the exsolved K-feldspar and exsolved albite in the mantle of the perthite and in the core of the feldspar phenocrysts. The path d-d′ indicates the albite rim of the phenocrysts. The path e-b′ indicates the deuteric coarsened secondary albite.

Diagram (a) shows the phase relationships for An-free alkali feldspars under complete (incoherent) equilibrium and (b) shows different constrained equilibrium states as a function of bulk composition and T for completed coherent intergrowths (Brown and Parsons, 1989). SFS is the strain-free solvus and CS is the coherent solvus. TDT is the twin-domain microtexture and ETDT is the exsolution and the twin-domain microtexture. MA, HA, IA and LA are monoclinic, high, intermediate and low albite; IM and LM are intermediate and low microcline. IA and IM is the region of the rapid change in Y ordering.

CHAPTER 6

CATHODOLUMINESCENCE PROPERTIES AND COMPOSITIONS OF THE FELDSPARS IN NEPHELINE SYENITES FROM CENTER II

6.1. Feldspars in the layered syenites from Pic Island

6.1.1. Introduction

The layered syenites in Center II consist of light grey coloured miaskitic nepheline syenites, and dark grey coloured amphibole nepheline syenites. The igneous layering in the syenites is caused by rhythmic accumulations of mafic minerals, namely; Fe-rich olivine, calcic clinopyroxene, calcic amphibole, magnetite and apatite. The felsic minerals, dominately feldspar, are essentially intercumulus phases. The layering in the syenites is well developed at Pic Island, and is poorly developed in the Redsucker Cove area (Mitchell and Platt, 1982).

In thin section, the alkali feldspars in both the amphibole nepheline syenite and the miaskitic nepheline syenites occur as idiomorphic to hypidiomorphic homogeneous crystals (Fig. 6.1-1a). Perthitic intergrowths and twinning are not well developed. Microcline twinning has not been observed in thin sections. There are secondary Na- and K-feldspars which occur at the margins of the alkali feldspar. These secondary feldspars commonly have a clouded appearance (Fig. 6.1-1a, -2a) which is due to a late-stage fluid alteration. Albite-twinned secondary Na-feldspar and deuterically coarsened perthite or antiperthite have not been observed in thin sections.

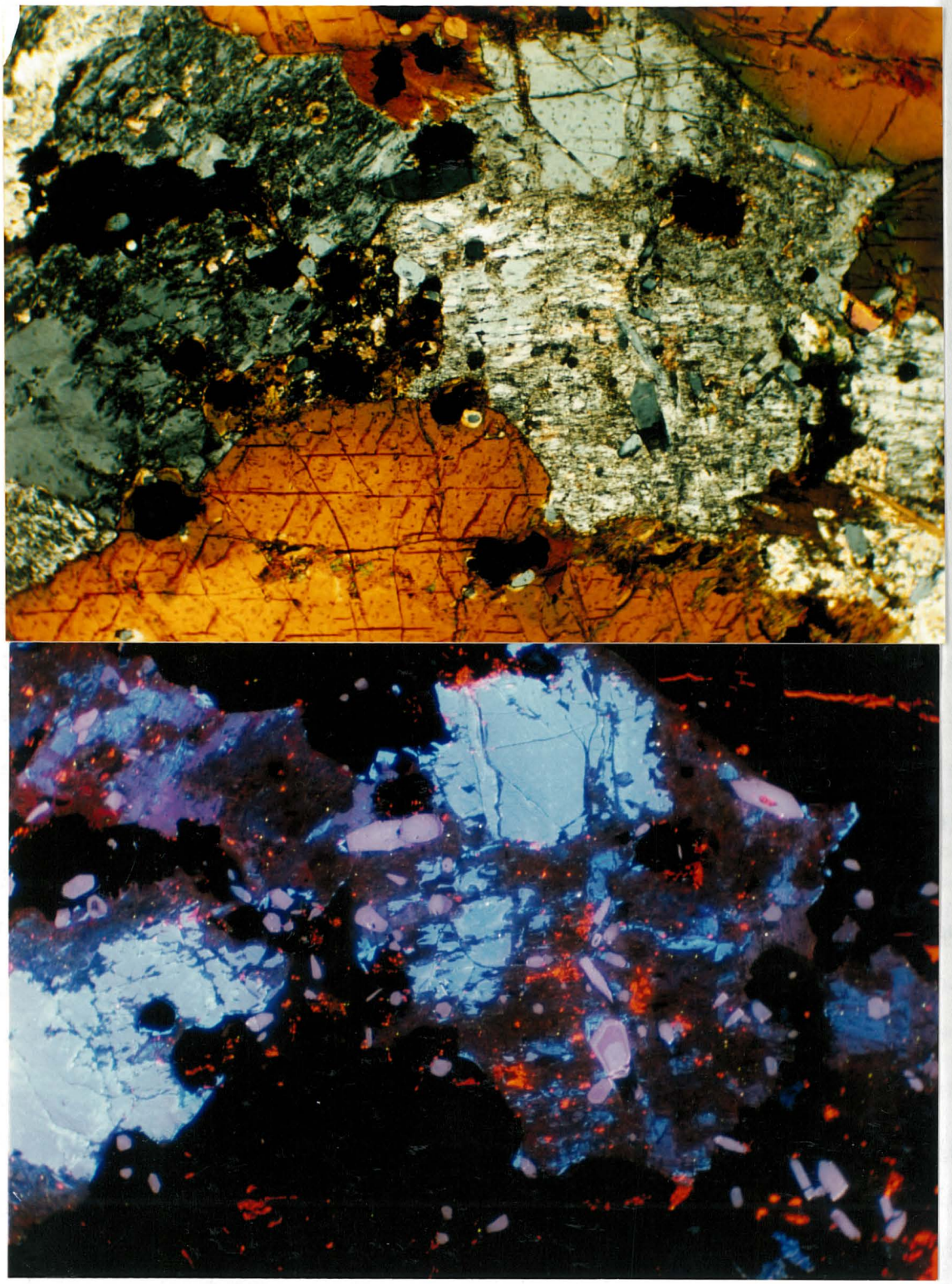

Fig. 6.1-1. Homogeneous alkali feldspar in the layered amphibole nepheline syenite (sample C623) from Center II, Pic Island. a: TrL (Photographic conditions: 15 s, ASA 25). b: CL. the light violet blue luminescent areas are the homogeneous alkali feldspars. The light violet luminescent areas are the secondary Na-feldspars and the dull blue or dark brown luminescent areas are the secondary K-feldspars. There are many small grains of pink-luminescing apatite which are zoned and orange-luminescing calcite. Scale: 55 mm on photograph = 1 mm on thin section. (CL conditions: 10 kV, 0.8 mA. Photographic conditions: 2 min, ASA 400).

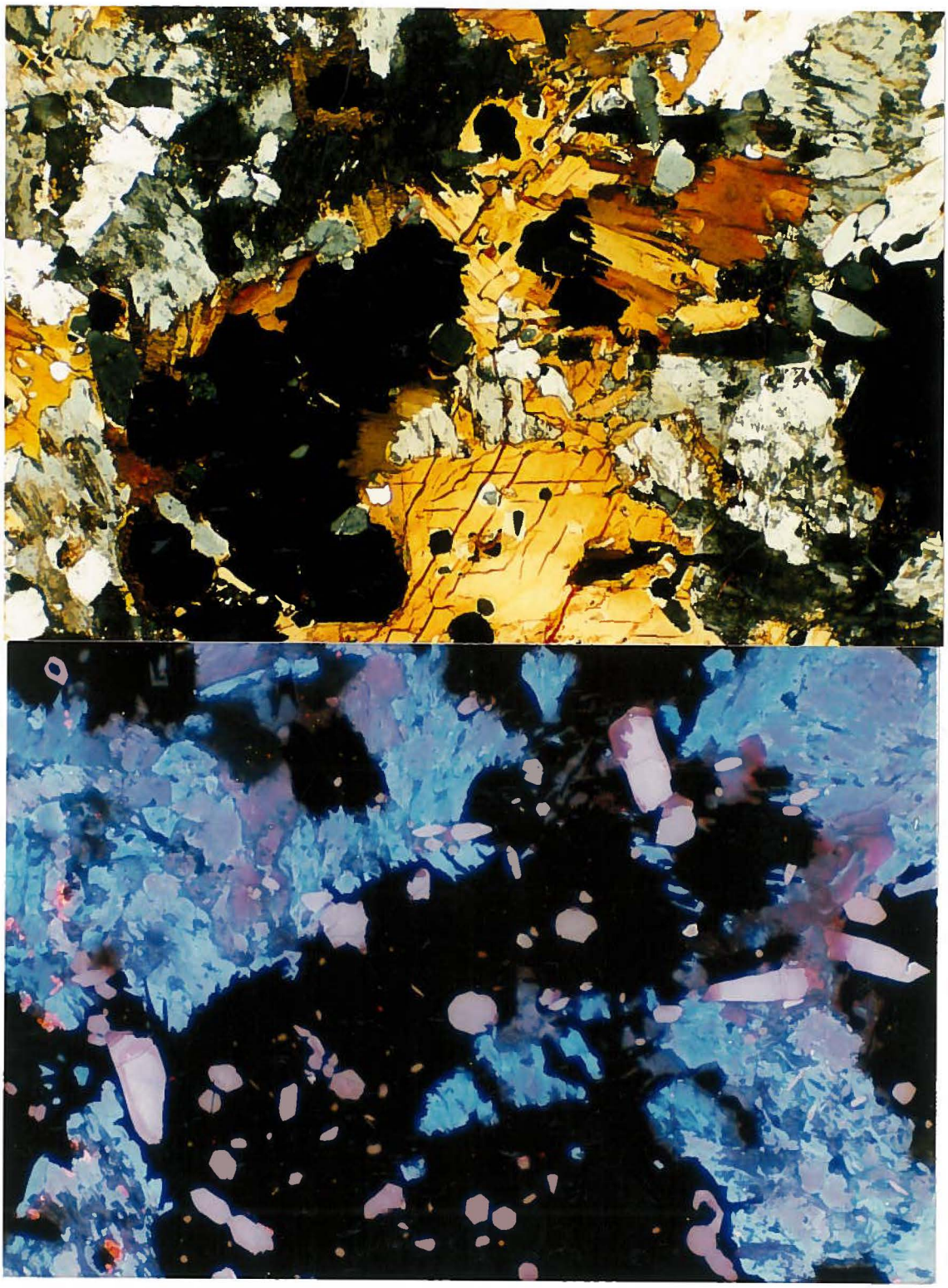

Fig. 6.1-2. Feldspars in the layered amphibole nepheline syenite (sample C629) from Center II, Pic Island. a: TrL (Photographic conditions: 20 s, ASA 25). b: CL. The light violet blue luminescent areas are the homogeneous alkali feldspar. The light blue luminescent areas are the Na-rich feldspars. The light violet luminescent areas are the K-rich feldspars. The dull blue luminescent areas are the secondary K-feldspars. There are many grains of pink-luminescing apatite which are zoned. Scale: 55 mm on photograph = 1 mm on thin section. (CL: conditions: 10 kV, 0.8 mA. Photographic conditions: 2 min, ASA 400).

In the miaskitic nepheline syenites, plagioclase mainly occurs as rhomb-shaped homogeneous crystals. Some of the crystals are slightly zoned as they show an optically distinct rim (Fig. 6.1-3).

Under CL, the luminescence colour of the alkali feldspars differs slightly from the plagioclase, the alkali feldspars commonly reveal light violet blue luminescence and the plagioclase commonly reveals light greyish blue luminescence. The secondary Na-feldspars commonly reveal light violet luminescence, and the secondary K-feldspars commonly reveal dull blue luminescence.

6.1.2. Alkali feldspar in the amphibole nepheline syenite

In the amphibole nepheline syenite, the alkali feldspar exhibits a homogeneous light violet blue luminescence (Fig. 6.1-1b, -2b). The CL spectrum consists of a blue peak at 453 (or 457) nm and a red peak at 705 (or 710) nm (Fig. 6.1-4, spectrum A; Fig. 6.1-5, spectrum A). The blue peak intensity is always higher than the red peak intensity, and the ratios of I_B/I_R are about 2.5 to 4.1 (Table 6.1-1).

These homogeneous alkali feldspars have compositions of Or_{39-50} $Ab_{45-56}An_{2-6}$ (Table 6.1-1, Fig. 6.1-7 and Appendix 2). There is only a small variation in the Or content (about 10 %) in these three samples. SEM/BSE images confirm that the homogeneous alkali feldspar is a truly unexsolved phase (Fig. 6.1-9a,b).

At the margins of most homogeneous alkali feldspar grains, the luminescence colours gradually change from light violet blue to light blue (Fig. 6.1-2b). The blue peak intensity of this light

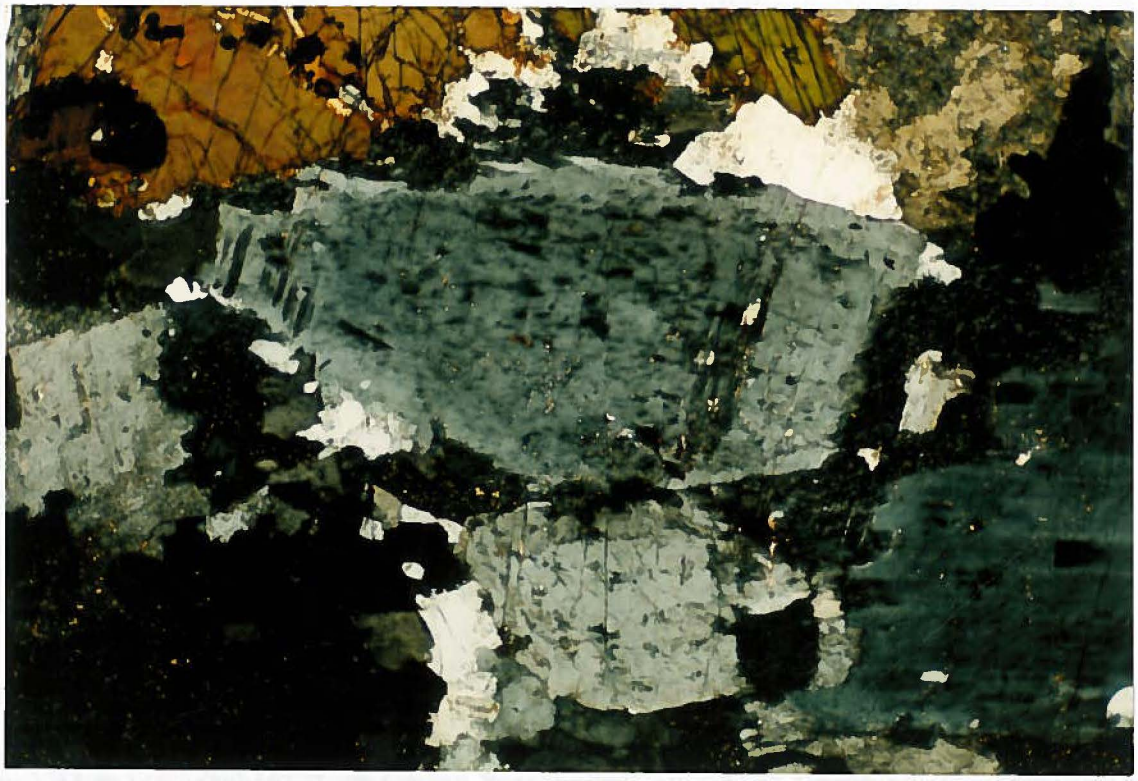

Fig. 6.1-3. TrL. Rhomb-shaped oligoclase crystals in the layered miaskitic nepheline syenite (sample C626) from Center II, Pic Island. Generally, they are homogeneous, although some of them are slightly zoned with an optically distinct rim. Scale: 55 mm on photograph = 1 mm on thin section. Photographic conditions: 8 s, ASA 25.

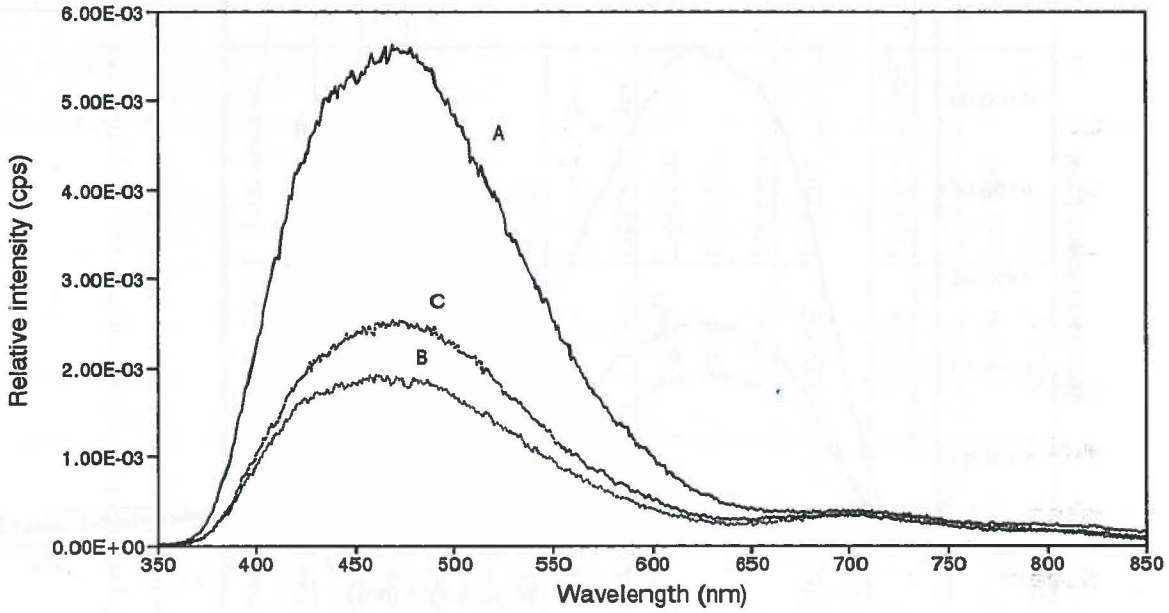

Fig 6.1-4. CL spectra of the alkali feldspars in the amphibole nepheline syenite (sample C623) from Center II, Pic Island. (A) is from a light violet blue luminescing homogeneous alkali feldspar. (B) is from a dull blue luminescing secondary K-feldspar, and (C) is from a light violet luminescing sceondary Na-feldspar. CL conditions: 10 kV, 0.8 mA.

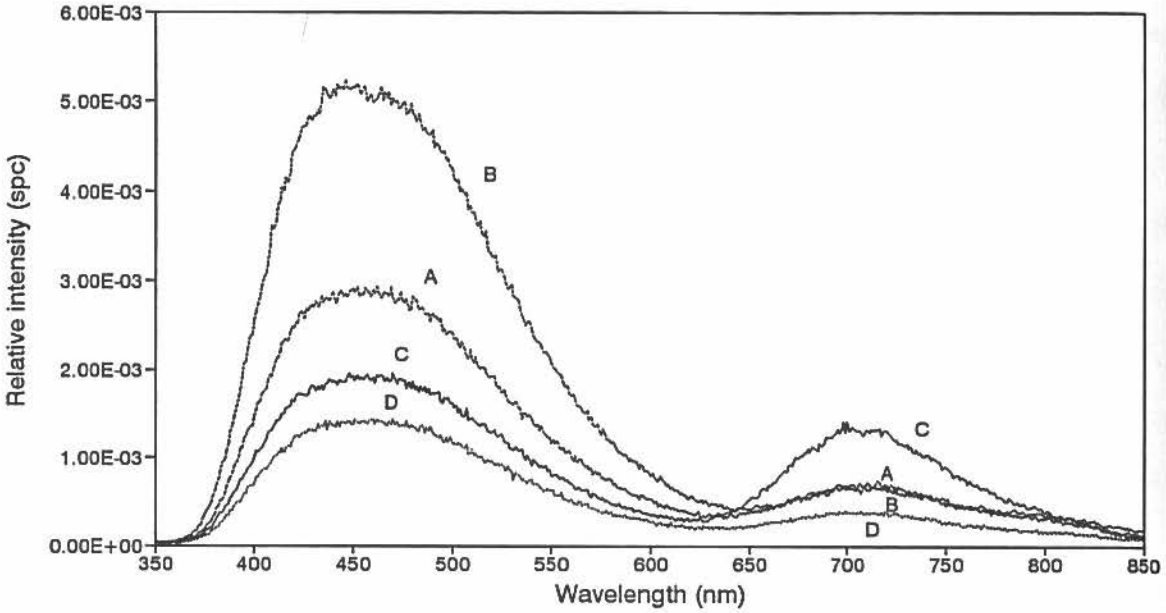

Fig. 6.1-5. CL spectra of feldspars in the amphibole nepheline syenite (sample C629) from II, Pic Island. (A) is from a light blue luminescent homogeneous alkali feldspar. (B) is from a light blue luminescent Na-rich feldspar. (C) is from a light violet luminescent K-rich feldspar. (D) is from a dull blue luminescent secondary K-feldspar which is formed during late-stage fluid alteration. CL conditions: 10kV, 0.8 Am.

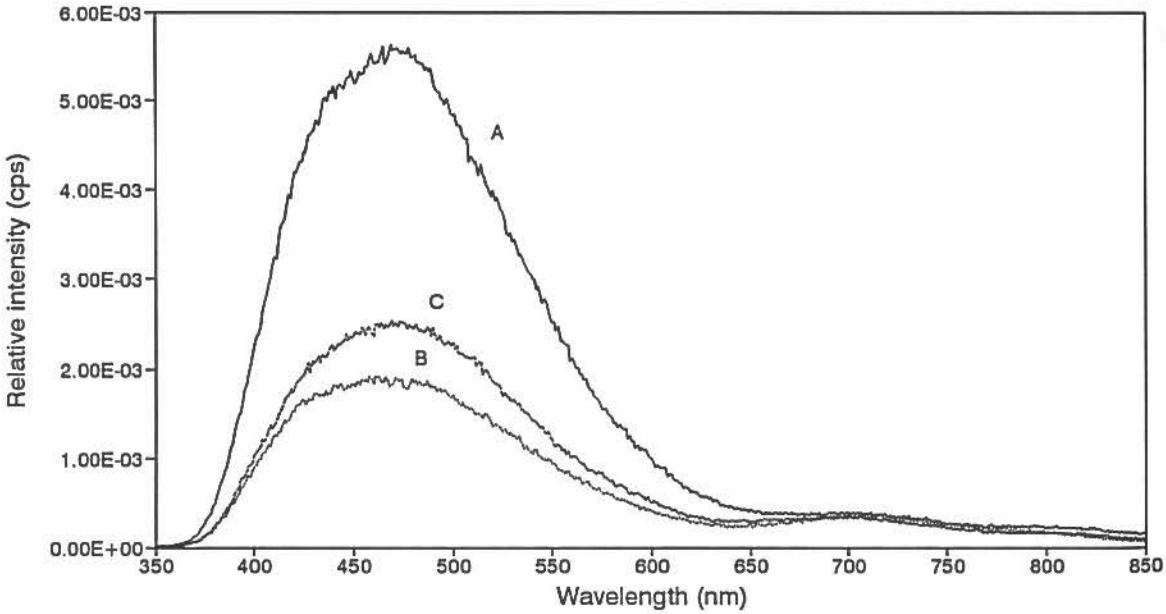

Fig. 6.1-6. CL spectra of feldspars in the miaskitic nepheline syenite (sample C626) from Center II, Pic Island. (A) is from a light greyish blue luminescent oligoclase core. (B) and (C) is from a grey and greyish blue luminescent secondary K-feldspar rim respectively. These rims are formed during late-stage fluid alteration. CL conditions: 10 kV, 0.8 Am.

Table 6.1-1. Representative cathodoluminescence properties and compositions of feldspars in the layered amphibole nepheline syenite and miaskitic nepheline syenite from Center II, Pic Island, Coldwell Complex, Ontario

Occurrence of feldspar	Sample No./ spectrum No.	Luminescence colour	Intensities (cps)					Compositions		
			Blue peak	(nm)	Red peak	(nm)	B/R ratio	Or	Ab	An
Amphibole nepheline syenite:										
Homogeneous alkali feldspar	C623/A	Light violet blue	2.61E-03	(453)	1.03E-03	(705)	2.52	45-50	48-52	2-3
Secondary K-feldspar	C623/B	Dull blue	1.20E-03	(453)	2.47E-04	(708)	4.86	87-97	2-12	1
Secondary Na-feldspar	C623/C	Light violet	4.94E-04	(423)	7.40E-04	(708)	0.67	1-2	90-95	4-9
Secondary Na-feldspar	C623	Non CL	N/A		N/A			1-2	95-98	1-4
Homogeneous alkali feldspar	C629/A	Light violet blue	2.88E-03	(457)	7.11E-04	(710)	4.05	41-48	48-55	3-4
Homogeneous alkali feldspar	C630	Light violet blue	N/A		N/A			39-50	45-56	5-6
Na-rich feldspar	C629/B	Light blue	5.00E-03	(457)	6.92E-04	(710)	7.23	1-3	85-89	10-12
Na-rich feldspar	C630	Light blue	N/A		N/A			1-3	84-89	9-15
K-rich feldspar	C629/C	Light violet	1.91E-03	(458)	1.24E-03	(708)	1.54	61-66	33-37	1-2
Secondary K-feldspar.	C629/D	Dull blue	1.40E-03	(458)	4.00E-04	(707)	3.51			
Miaskitic nepheline syenite:										
Oligoclase, core	C626/A	Light greyish blue	5.54E-03	(468)	4.05E-04	(699)	13.67	1-6	73-77	19-22
Homogeneous alkali feldspar	C226	Light violet blue	N/A		N/A			56-70	28-42	2
Secondary K-feldspar, rim	C626/B	Dull blue	1.87E-03	(465)	3.64E-04	(708)	5.13			
Secondary K-feldspar, rim	C626/C	Grey	2.51E-03	(471)	3.51E-04	(705)	7.16	62-81	17-35	1-3

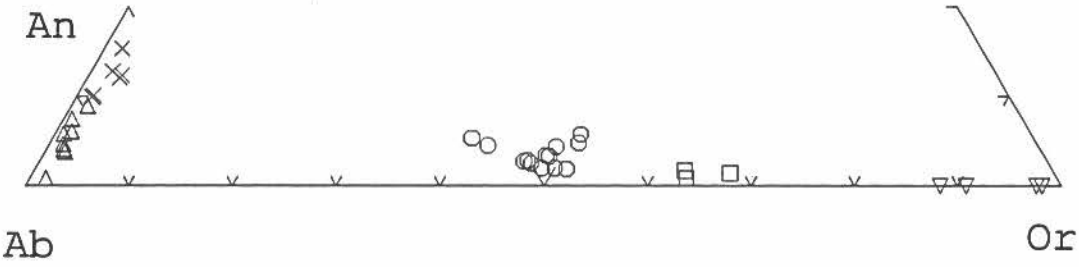

Fig. 6.1-7. The compositions of the feldspars in the layered amphibole nepheline syenite (samples C623, C629, C630) plotted in the system Or-Ab-An. The circles (○) are the light violet blue luminescent homogeneous alkali feldspars. The squares (□) are the light violet luminescent K-rich feldspars, and the crosses (×) are the light blue luminescent Na-rich feldspars. The up-triangles (△) are the lihgt violet luminescent secondary Na-feldspars and the down-triangles (▽) are dull blue or dark brown luminescent secondary K-feldspars.

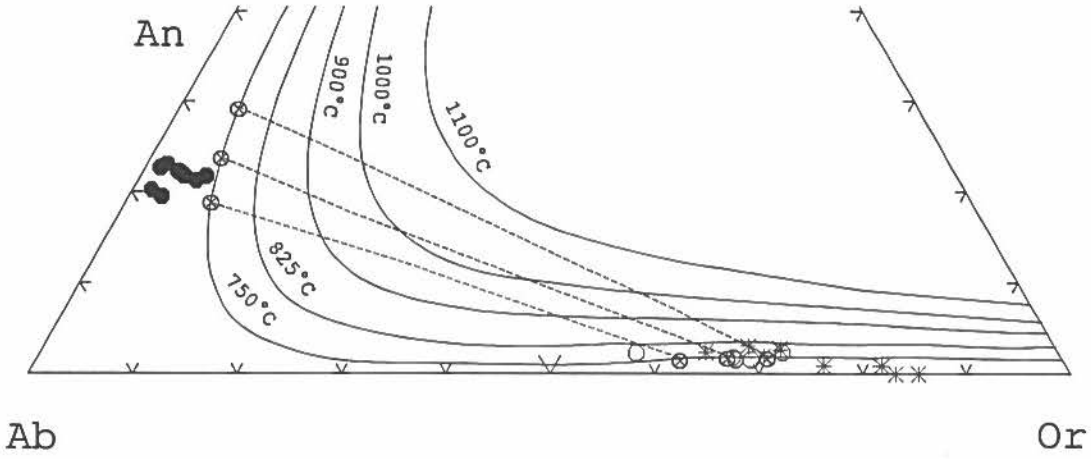

Fig. 6.1-8. The compositions of the feldspars in the layered miaskitic nepheline syenites (samples C624, C626) plotted in the system Or-Ab-An. The filled circles (●) are the light greyish blue luminescent homogeneous oligoclase. The asterisks (*) are the greyish blue or grey luminescent secondary K-feldspar which occur as patches within the oligoclase or as rims around the oligoclase margins. The open circles (○) are light violet blue luminescent homogeneous alkali feldspars.

The isotherms and the two feldspars pairs are from Fuhrman and Lindsley (1988).

Fig. 6.1-9. SEM/BSE micrograph of the feldspars in the layered amphibole nepheline syenite (sample C623). a. The alkali feldspar is homogeneous and replaced by the secondary Na-feldspar and K-feldspar in the margins. b. The detail of the replacement texture in the alkali feldspar. The light grey areas are the secondary K-feldspars and the black areas are the secondary Na-feldspars. The intermediate grey areas are homogeneous alkali feldspar.

blue luminescing margins (Fig. 6.1-5, spectrum B) is higher than that of the light violet blue centre (Fig. 6.1-5, spectrum A), whereas the red peak intensity is very low and the same as that of the homogeneous alkali feldspar centre. Thus, light blue luminescing margins have a higher I_B/I_R ratio (7.2) than the homogeneous alkali feldspar centre (2.5-4.1) (Table 6.1-1). The light blue luminescing margins are Na-rich feldspars which range in composition from $Ab_{84-89}An_{9-15}Or_{1-3}$ (Table 6.1-1, Fig. 6.1-7 and Appendix 2).

K-rich feldspars occur as individual grains at the margins of homogeneous alkali feldspar grains and show light violet luminescence (Fig 6.1-2b). These light violet blue luminescing K-rich feldspars have a relatively lower intensity of the blue peak, and a relatively higher intensity of the red peak than the homogeneous alkali feldspar (Fig 6.1-5 spectrum C). The ratio of I_B/I_R is about 1.5 and range in composition is from $Or_{61-66}Ab_{33-37}An_{1-2}$ (Table 6.1-1, Fig. 6.1-7 and Appendix 2).

6.1.3. Plagioclase and alkali feldspar in the miaskitic nepheline syenite

In the miaskitic nepheline syenite, the plagioclase exhibits a homogeneous light greyish blue luminescence colour (Fig 6.1-10b), which is similar to that of the light violet blue luminescent homogeneous alkali feldspar and the light blue luminescent Na-rich feldspar. However, the CL spectrum of the plagioclase is different in that it only shows an intense blue peak centred at 468 nm which

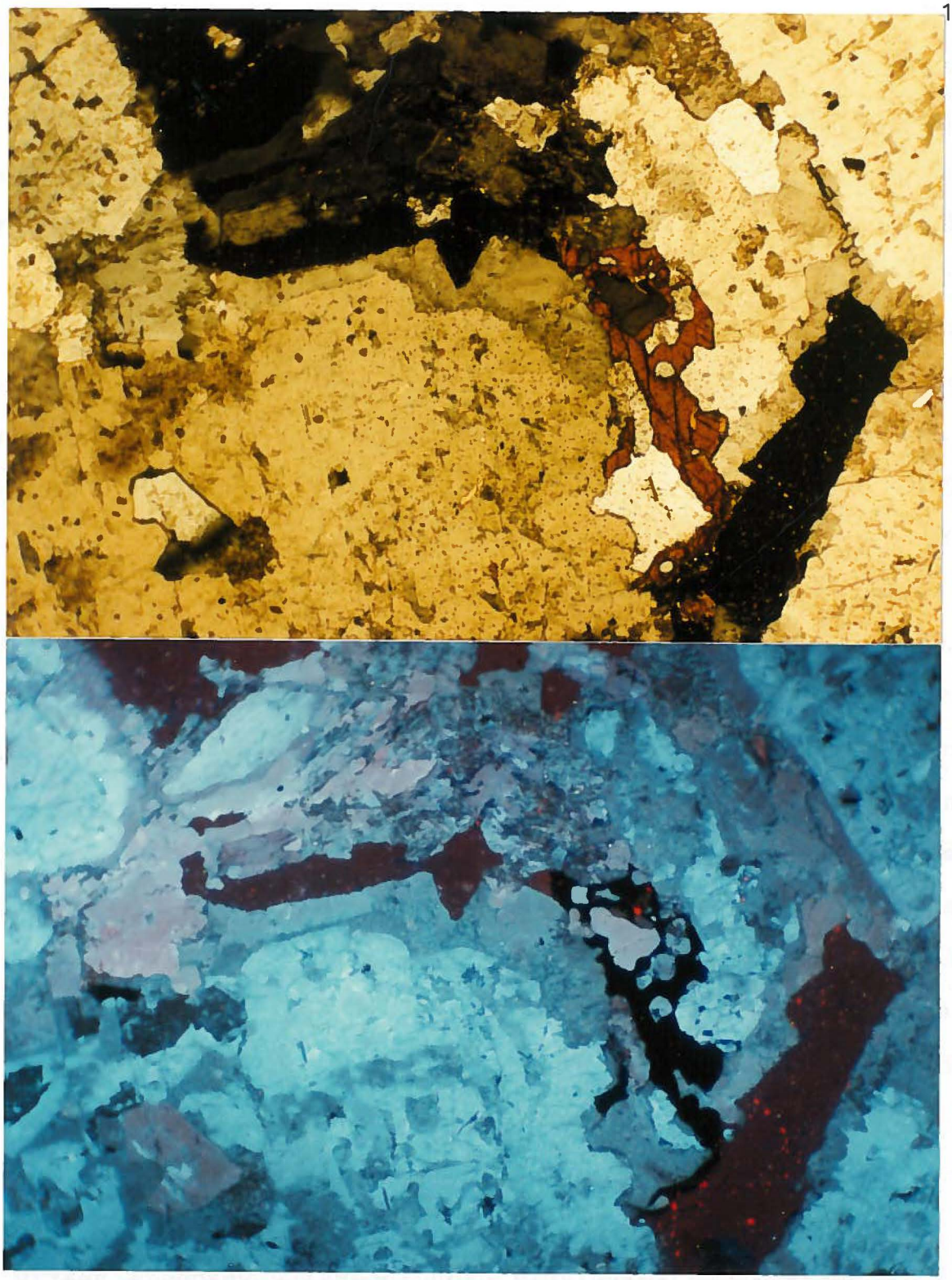

Fig. 6.1-10. Oligoclase crystals in the layered miaskitic nepheline syenite (sample C626) from Center II, Pic Island. a: TrL (Photographic conditions: 8 s, ASA 400). b: CL. The oligoclase shows a light greyish blue homogeneous luminescence. The greyish blue and grey luminescent rims and patches are the K-feldspars which replace the oligoclase during a late-stage fluid-feldspar interaction. The alkali feldspar shows a light violet blue luminescence. Scale: 55 mm on photograph = 1 mm on thin section. (CL conditions 10 kV, 0.8 mA. Photographic conditions: 30 s, ASA 400).

has shifted to a longer wavelength region by about 10 nm compared to both the alkali feldspar and Na-rich feldspar (Fig 6.1-6, spectrum A). The plagioclase has a very high I_B/I_R ratio of about 13.7. The plagioclase is oligoclase, as it ranges in composition from $An_{19-22}Ab_{73-79}Or_{1-6}$ (Table 6.1-1, Fig. 6.1-8 and Appendix 2).

The homogeneous alkali feldspar exhibits a light violet blue luminescenec and range in composition is from $Or_{56-70}Ab_{28-42}An_2$ (Table 6.1-1, Fig. 6.1-8 and Appendix 2). The orthoclase content of this alkali feldspar is higher (17-20 %) than that of the homogeneous alkali feldspar in the amphibole nepheline syenite.

6.1.4. Secondary feldspars replacement

In the amphibole nepheline syenite, the clouded margins of the homogeneous alkali feldspar crystals have completely broken down into discrete crystals of Na-feldspar and K-feldspar as a consequence of late stage fluid deuteric alteration. The secondary Na-feldspar exhibits a variety of luminescent colours ranging from light violet blue to light violet. Some Na-feldspar has no luminescence, and the secondary K-feldspar commonly shows a dull blue or dark brown luminescence (Fig. 6.1-1b, -2b).

For the light violet luminescing secondary Na-feldspar, the blue peak (Fig. 6.1-4, spectrum C) has a relatively lower intensity than that of the homogeneous alkali feldspar (Fig. 6.1-4, spectrum A). The red peak has a relatively high intensity which is nearly the same as that of the homogeneous alkali feldspar. This secondary Na-feldspar has a ratio of I_B/I_R about 0.67 (Table 6.1-1). For the dull

blue luminescing secondary K-feldspar, the blue peaks and the red peaks have lower intensities than those of the homogeneous alkali feldspar (Fig. 6.1-4, spectrum B; 6.1-6, spectrum D). The ratios of I_B/I_R of this secondary K-feldspars are from 3.51 to 4.86 (Table 6.1-1).

BSE images (Fig. 6.1-9a,b) show that the homogeneous alkali feldspar has been replaced by the secondary Na-feldspar and K-feldspar at crystal margins during late stage deuteric alteration. The secondary Na-feldspar and K-feldspar have a distinct boundary which indicates that cation diffusion (by an alkali-cation exchange reaction) is nearly complete during the alteration. Figure 6.1-9b also shows some fine cross-cutting replacement textures within the homogeneous alkali feldspar crystal where the replacement mineral is dominated by K-feldspar in association with a large amount of micropores.

The secondary Na-feldspar ranges in composition from $Ab_{90-98}Or_{1-2}An_{4-9}$, whereas the secondary K-feldspar ranges from $Or_{87-97}Ab_{2-12}An_1$ (Table 6.1-1, Fig. 6.1-7 and Appendix 2).

In the miaskitic nepheline syenite, a late-stage deuteric fluid alteration occurs along the margins of the oligoclase crystals to form a replacement rim, or occurs within the oligoclase crystals to form some small patches. The CL shows that the replacement rim or patches have a greyish blue or grey luminescence (Fig. 6.1-10b). Although these secondary feldspars have nearly the same CL spectral profile as the oligoclase, the ratios of I_B/I_R (5.1-7.2) are relatively lower than for the oligoclase (13.7) (Fig. 6.1-6,

spectra B,C, Table 6.1-1).

Analysis shows these greyish blue or grey luminescent rims and patches are K-rich feldspars which have a range in composition of $Or_{62-81}Ab_{17-35}An_{1-2}$ (Table 6.1-1). Compared with those normal secondary K-feldspars which occur at the margins of the alkali feldspar, these greyish blue or grey luminescent secondary K-feldspars have higher An contents and the blue peak positions are shifted by about 10 nm to a longer wavelength (Table 6.1-1).

6.1.5. Thermal history of the feldspars

a. Thermal history of the feldspars in the layered miaskitic nepheline syenite

Since the oligoclase coexists with homogeneous alkali feldspar in the layered miaskitic nepheline syenite (Fig 6.1-10), the two-feldspar thermometer can be used to estimate the crystallization temperatures in the Or-Ab-An ternary system (Fuhrman and Lindsley 1988). Figure 6.1-8 shows that compositional data of the oligoclase from the layered miaskitic nepheline syenite are distributed below the 750 °C isotherm, whereas the homogeneous alkali feldspar are mainly distributed between 750 °C and 825 °C isotherms. However, the oligoclase in the layered miaskitic nepheline syenite is slightly lower in An content compared with the plagioclase in the calculated model (Fuhrman and Lindsley, 1988). Equilibrium between alkali feldspar and oligoclase may not have occurred in the layered miaskitic nepheline syenite.

In the Or-Ab binary system (Fig. 6.1-11), the light violet blue

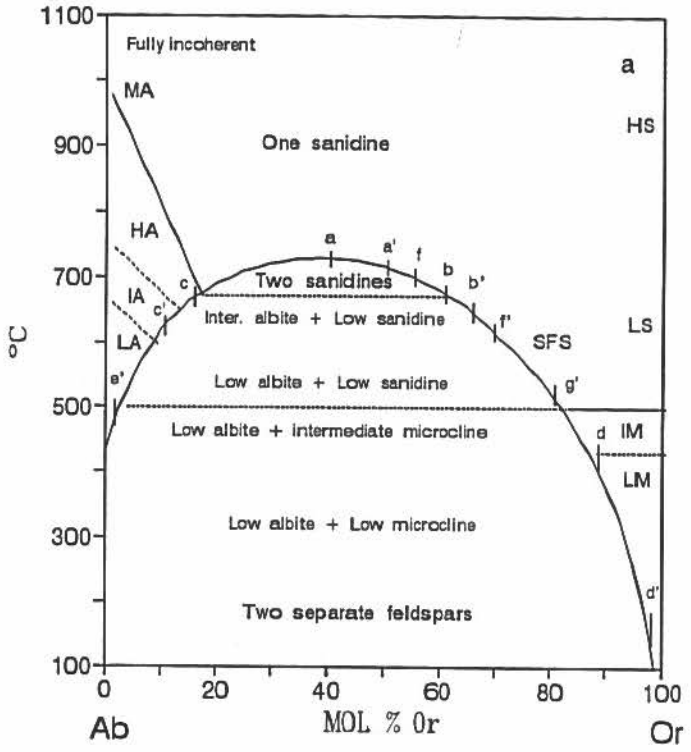

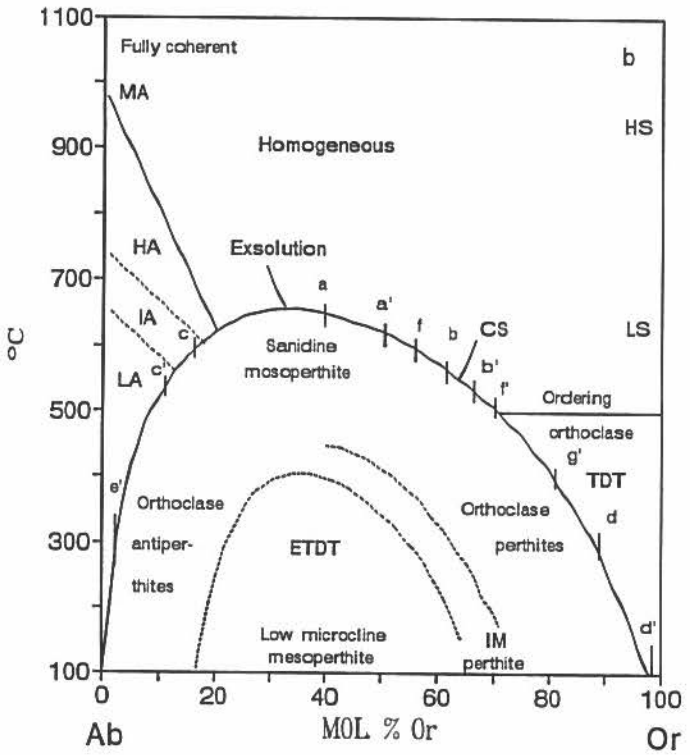

Fig. 6.1-11. The evolutions of the alkali feldspars in the layered amphibole nepheline syenite and miaskitic nepheline syenite from Center II, Pic Island are illustrated in the Or-Ab binary phase diagram.

For the layered amphibole nepheline syenite, the path a-a′ is the homogeneous alkali feldspar. The path b-b′ and c-c′ is K-rich feldspar and Na-rich feldspar respectively. The path d-d′ and c′-e′ is the secondary K-feldspar and Na-feldspar respectively.

For the miaskitic nepheline syenite, the path f-f′ is the homogeneous alkali feldspar. The path b′-g′ the secondary K-feldspar.

Diagram (a) shows the phase relationships for An-free alkali feldspars under complete (incoherent) equilibrium and (b) shows different constrained equilibrium states as a function of bulk composition and T for completed coherent intergrowths (Brown and Parsons, 1989). SFS is the strain-free solvus and CS is the coherent solvus. TDT is the twin-domain micro-texture and ETDT is the exsolution and the twin-domain microtexture. MA, HA, IA and LA are monoclinic, high, intermediate and low albite; IM and LM are intermediate and low microcline. IA and IM is the region of the rapid change in Y ordering.

luminescent homogeneous alkali feldspar ($Or_{56-70}Ab_{28-42}An_2$) may have crystallized at temperatures about 620-700 C° on the incoherent solvus (SFS) (path f-f′).

The greyish blue or grey luminescent secondary K-feldspar ($Or_{62-81}Ab_{17-35}An_{1-2}$) may have replace the oligoclase at a temperature range about 500-650 C° during an early fluid-feldspar interaction (path b′-g′ on the SFS).

b. Thermal history of the alkali feldspars in the amphibole nepheline syenite

In the Or-Ab binary system (Fig. 6.1-11), the light violet blue luminescent homogeneous alkali feldspar may have crystallized at temperatures ≤710 °C on the incoherent solvus (SFS) (path a-a′). The light blue luminescent oligoclase ($Ab_{84-89}Or_{1-3}An_{9-15}$) and the light violet luminescent K-rich feldspar ($Or_{61-66}Ab_{33-37}An_{1-2}$) bands in the perthite may have exsolved during cooling at temperatures about 550-500 °C and 600-550 C° under the fully coherent solvus (CS), respectively (paths b-b′ and c-c′).

The deuteric alteration may have occurred at very low temperatures. According to the composition of the secondary K-feldspars ($Or_{87-97}Ab_{2-12}An_1$), the deuteric alteration may have occurred at temperatures about <350 °C on SFS (or <300 on CS) during a late-stage fluid-feldspar interaction.

6.2. Feldspar crystals in the Neys Park syenites

6.2.1. Introduction

Neys park syenites of Center II consist of perthitic nepheline syenite and miaskitic nepheline syenite (plagioclase-bearing, homogeneous alkali feldspar syenite).

The perthitic nepheline syenites (Samples C97, C109, C111, C112, C1538b, C1863, C3118a, C3118b, C3118c, C3118d, N1A, N2A, N3A, N3B and N3C) occur as light grey, fine-grained or coarse-grained rocks and mainly consist of alkali feldspars, amphibole, magnetite, and apatite. These syenites usually contain some white to brick-red irregular pegmatitic patches which consist of nepheline, K-feldspar, albite, hydromuscovite, natrolite and thomsonite.

The miaskitic nepheline syenite (Sample C114) occurs as a greenish grey coarse-grained rock which consists of optically homogeneous alkali feldspar, plagioclase, amphibole, pyroxene, nepheline, sodalite and apatite. The plagioclase usually occurs at the core of the homogeneous alkali feldspar crystals.

6.2.2. Alkali feldspars in the perthitic nepheline syenites

In thin sections, the alkali feldspar occurs as fine-grained, granular, hypidiomorphic crystals (groundmass) or as coarse-grained, turbid, idiomorphic crystals (phenocrysts). The fine-grained feldspar crystals are mostly regular to irregular vein perthites and some of them are Carlsbad twinned (Fig. 6.2-1a,2a). However, some perthite grains show cross-hatched twinned microcline in the margins (Fig. 6.2-1a), and some contain unexsolved alkali

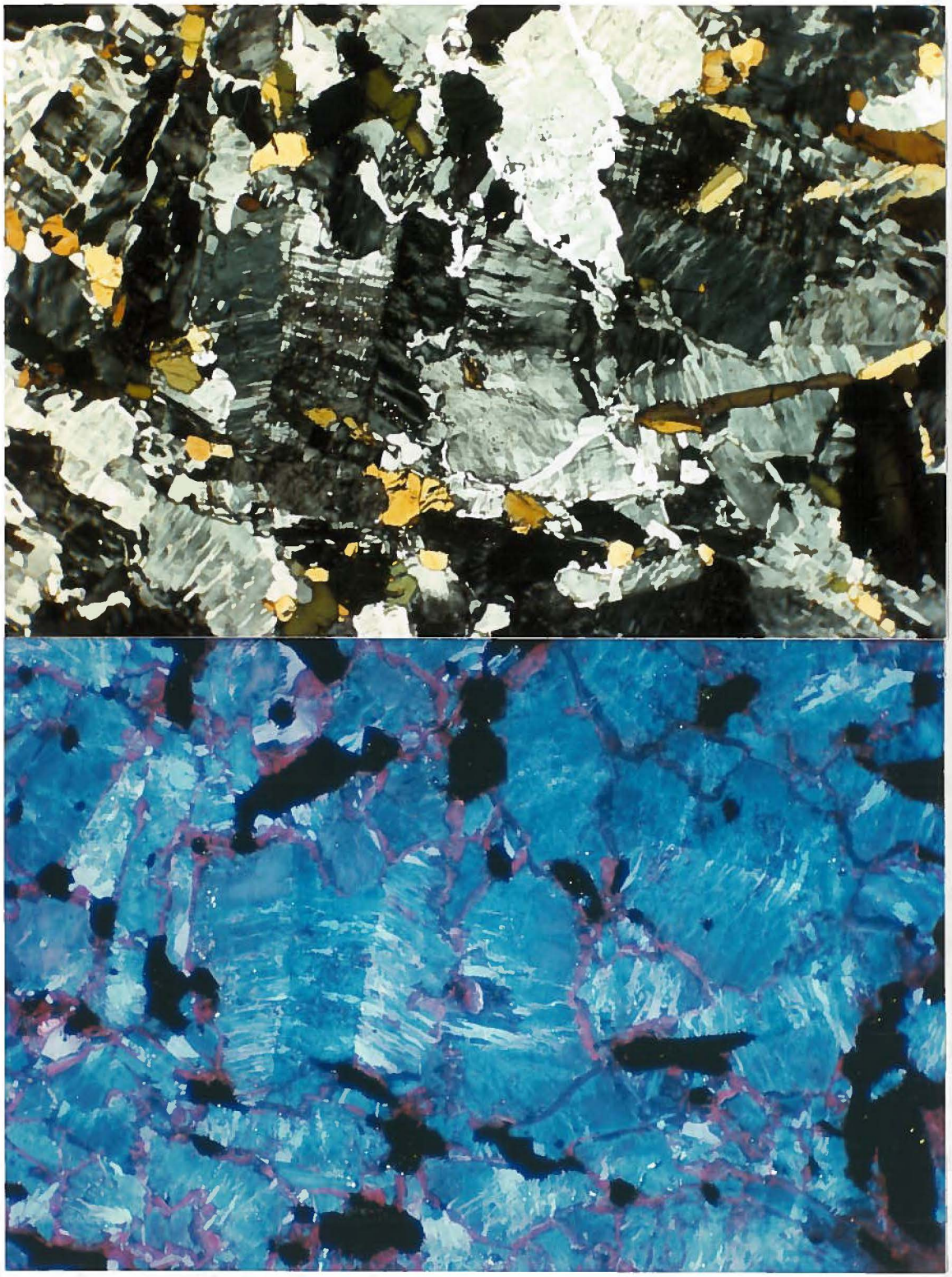

Fig 6.2-1. Fine-grained feldspars in the perthitic nepheline syenite (Sample N3B) from Center II, Neys Park. a. TrL. The feldspar crystals are Carlsbad twinned perthite and some the crystals show cross-hatched microcline twinnig in the margins. The secondary albite occurs as clear crystals surrounding the perthite grains. (Photographic conditions: 8 s, ASA 25) b. CL. The light blue luminescent bands are the exsolved Na-feldspar and the dull blue luminescent areas are the host K-feldspar. The dull red luminescent areas are the secondary albite. The microcline commonly shows a violet blue luminescence. Scale: 55 mm on photograph = 1 mm on thin section. (CL conditions: 10 kV, 0.8 Am. Photographic conditions: 2 min, ASA 400.)

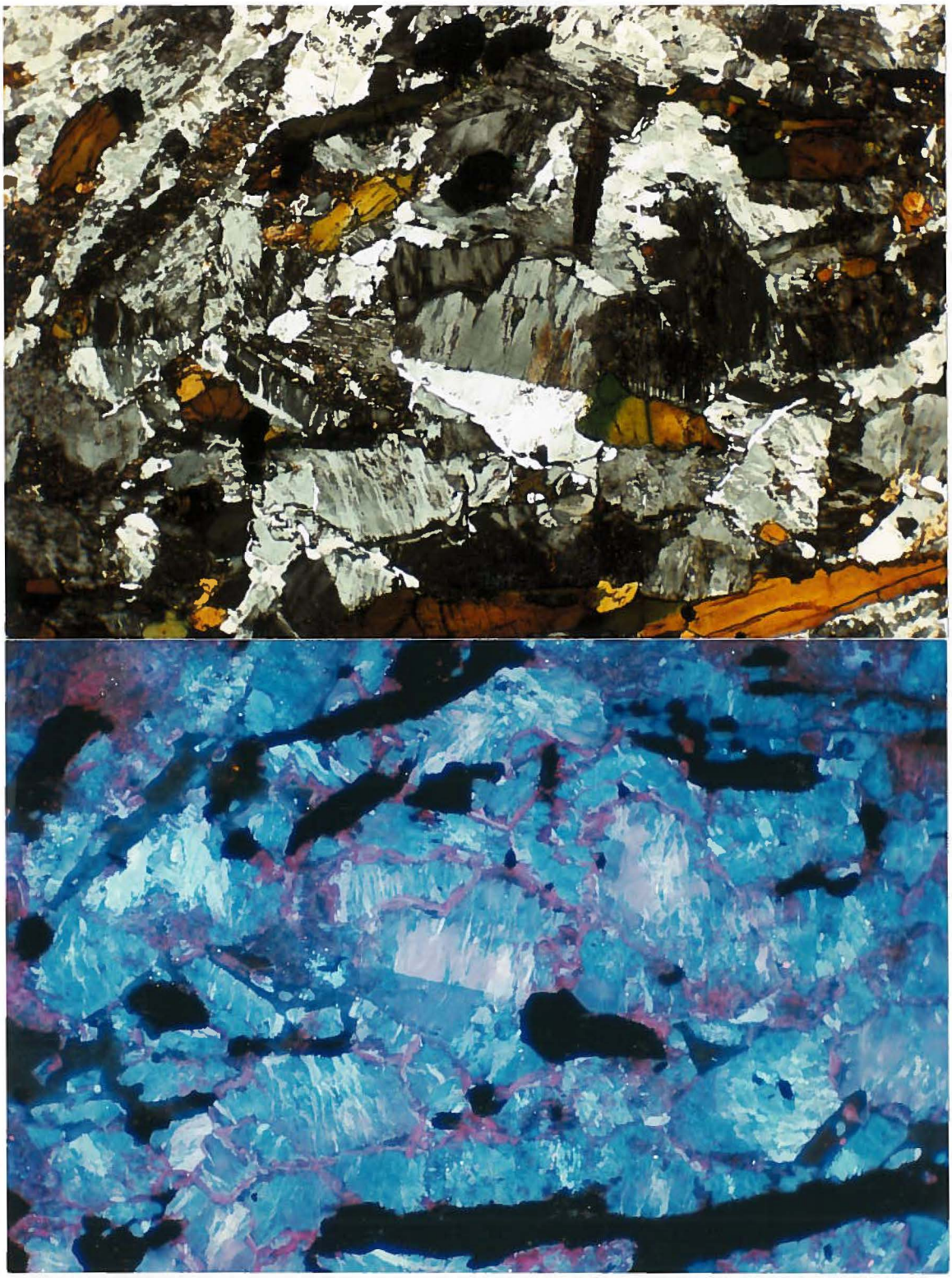

Fig. 6.2-2. Fine-grained feldspars in the perthitic nepheline syenite (Sample N3C) from Center II, Neys Park. a. TrL. Unexsolved alkali feldspar occurs in the centre of the perthite. The secondary albite occurs as a clear crystal surrounding the perthite grains. (Photographic conditions: 12 s, ASA 25) b. CL. CL reveals that the unexsolved alkali feldspar has a light violet or light violet blue luminescence. The light blue luminescent areas are the exsolved Na-feldspar and the dull blue luminescent areas are the host K-feldspar. The dull red luminescent veins are secondary albite. Scale: 55 mm on photograph = 1 mm on thin section. (CL conditions: 10 kV, 0.8 Am. Photographic conditions: 1.5 min, ASA 400.)

feldspar at their centres (Fig. 6.2-2a). There are only a few individual microcline grains found in the samples. These fine-grained perthite grains (groundmass) are usually surrounded by optically untwinned secondary albite. The coarse-grained feldspar crystals (phenocrysts) are either irregular vein perthite (Fig. 6.2-3a) or patch perthite (Fig. 6.2-4a), and some of them show deuteric unmixed patch antiperthite in the margins (Fig. 6.2-5a).

a. Exsolved Na-feldspar and host K-feldspar in the perthite

Under CL, in both the fine- and coarse-grained perthite the exsolved Na-feldspar exhibits a light blue luminescence, whereas the host K-feldspar exhibits a dull blue luminescent (Fig. 6.2-1b,-2b,-3b,-4b,-5b). For the Carlsbad twinned perthite, two individuals of a twin usually exhibit different luminescence colours. One side of the twin usually shows a lighter luminescence colour than the other side of the twin (Fig. 6.2-1b).

The CL spectra show that the light blue luminescent exsolved Na-feldspars have a high intensity blue peak and a high intensity red peak (Fig. 6.2-6, spectrum B and Fig. 6.2-7, spectrum A), the ratios of I_B/I_R range from 1.41 to 2.06 (Table 6.2-1). The dull blue luminescent host K-feldspars have a much lower luminescent intensity than the Na-feldspars, and show a low blue peak and a weak red peak (Fig. 6.2-6, spectrum C and Fig. 6.2-7, spectrum B), the ratios of I_B/I_R are from 2.11 to 2.43 (Table 6.2-1).

The exsolved Na-feldspars range in composition from $Ab_{95-99}Or_{1-2}An_{1-4}$, whereas the host K-feldspars range in composition from

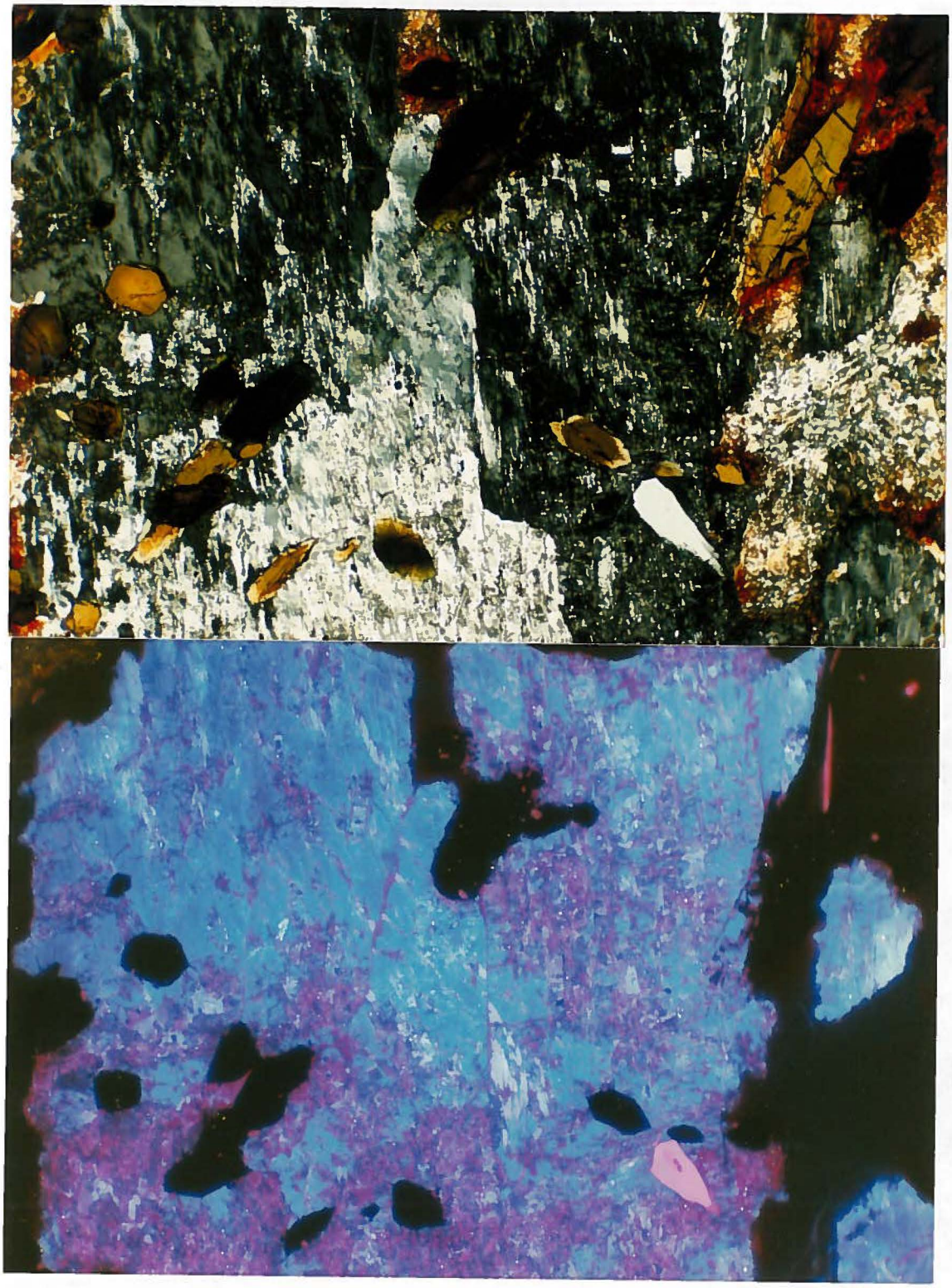

Fig. 6.2-3. Coarse-grained feldspars in the perthitic nepheline syenite (Sample C97) from Center II, Neys Park. a. TrL. The feldspar crystals are the irregular vein perthite. (Photographic conditions: 8 s, ASA 25) b. CL. The light blue luminescent areas are exsolved Na-feldspar and the blue luminescent areas are the host K-feldspar. The light violet luminescent areas are the secondary Na-feldspars and the dull blue luminescent areas are the secondary K-feldspars. Scale: 55 mm on photograph = 1 mm on thin section. (CL conditions: 10 kV, 0.8 Am. Photographic conditions: 1.8 min, ASA 400.)

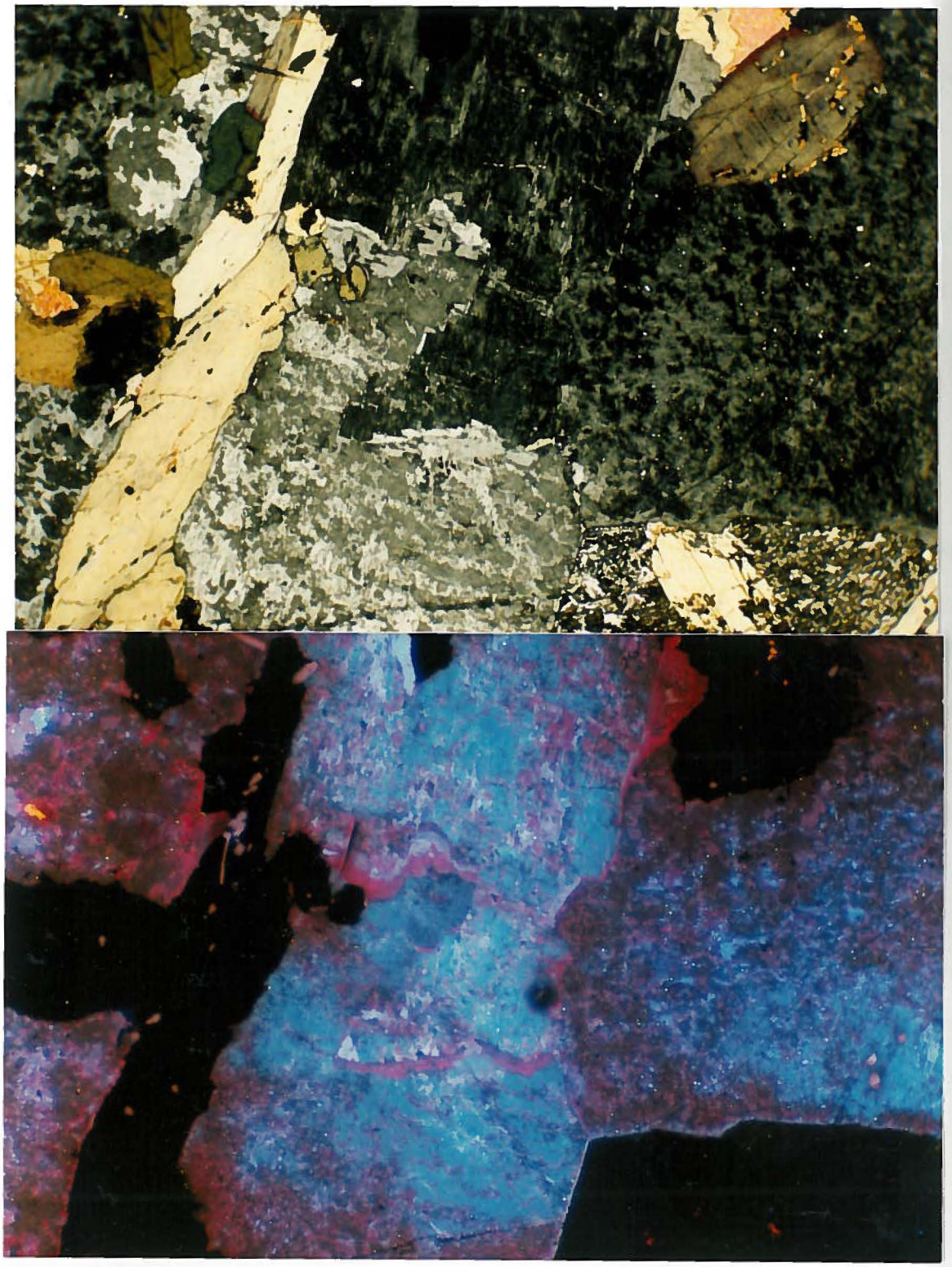

Fig. 6.2-4. Coarse-grained feldspar in the perthitic nepheline syenite (Sample N3B) from Center II, Neys Park. a. TrL. The feldspar crystals are the patch perthite. (Photographic conditions: 8 s, ASA 25) b. CL. The light blue luminescent areas are the exsolved Na-feldspar and the blue luminescent areas are the K-feldspar. The dull red luminescent areas are secondary Na-feldspar and the dull blue to brown luminescent areas are the secondary K-feldspar. The dull red and deep red luminescent irregular veins are the secondary albite. Scale: 55 mm on photograph = 1 mm on thin section. (CL conditions: 10 kV, 0.8 Am. Photographic conditions: 2 min, ASA 400.)

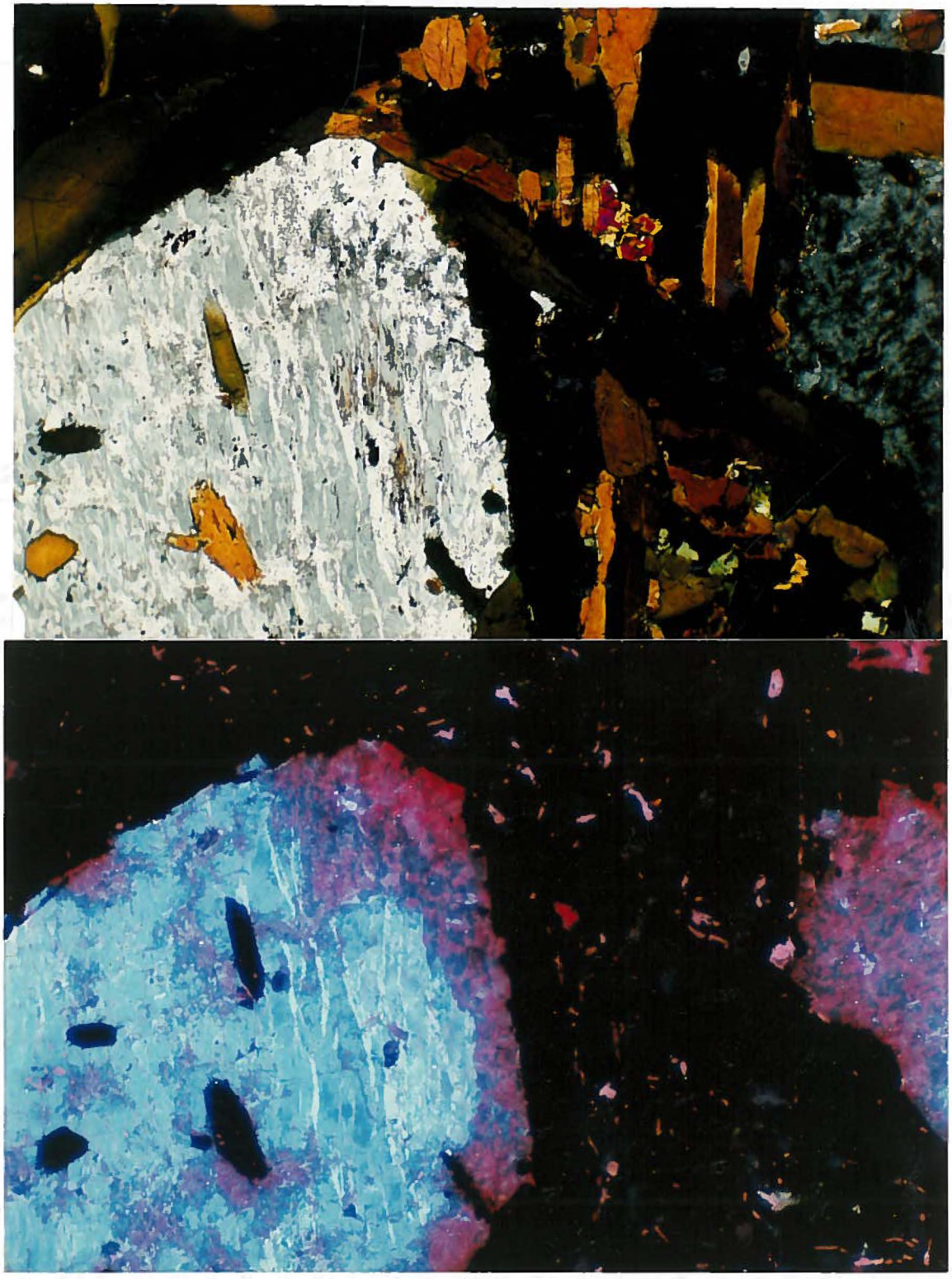

Fig. 6.2-5. Coarse-grained feldspar in the perthitic nepheline syenite (Sample N1A) from Center II, Neys Park. a. TrL. The feldspar crystals are irregular vein perthite with an irregular patch antiperthite rims. (Photographic conditions: 8 s, ASA 25) b. CL. The light blue luminescent bands are the Na-feldspar and the blue luminescent areas are the K-feldspar. In the antiperthite, the secondary Na-feldspars show dull violet to deep red luminescence and the secondary K-feldspars show dull blue luminescence. Scale: 55 mm on photograph = 1 mm on thin section. (CL conditions: 10 kV, 0.8 Am. Photographic conditions: 1.5 min, ASA 400.)

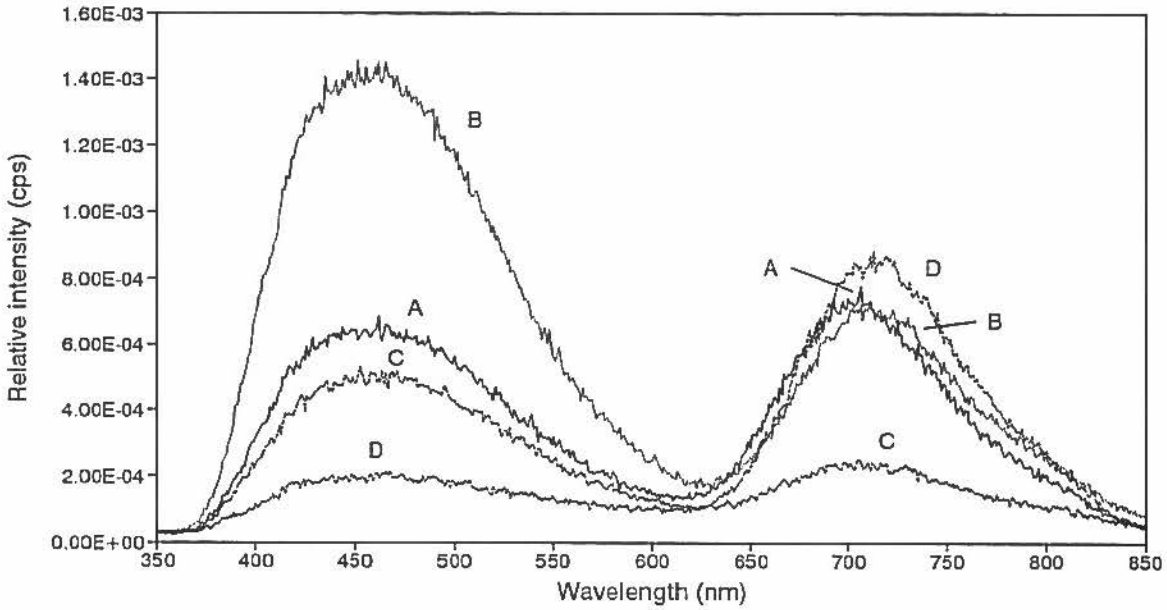

Fig 6.2-6. CL spectra of fine-grained feldspars in the perthitic nepheline syenite (Sample N3C) from Center II, Pic Island. (A) is from a light violet blue luminescent unexsolved alkali feldspar. (B) is from a light blue luminescent exsolved Na-feldspar and (C) is from a light violet blue luminescent host K-feldspar. (D) is from a dull red luminescent secondary albite. CL conditions: 10 kV, 0.8 mA.

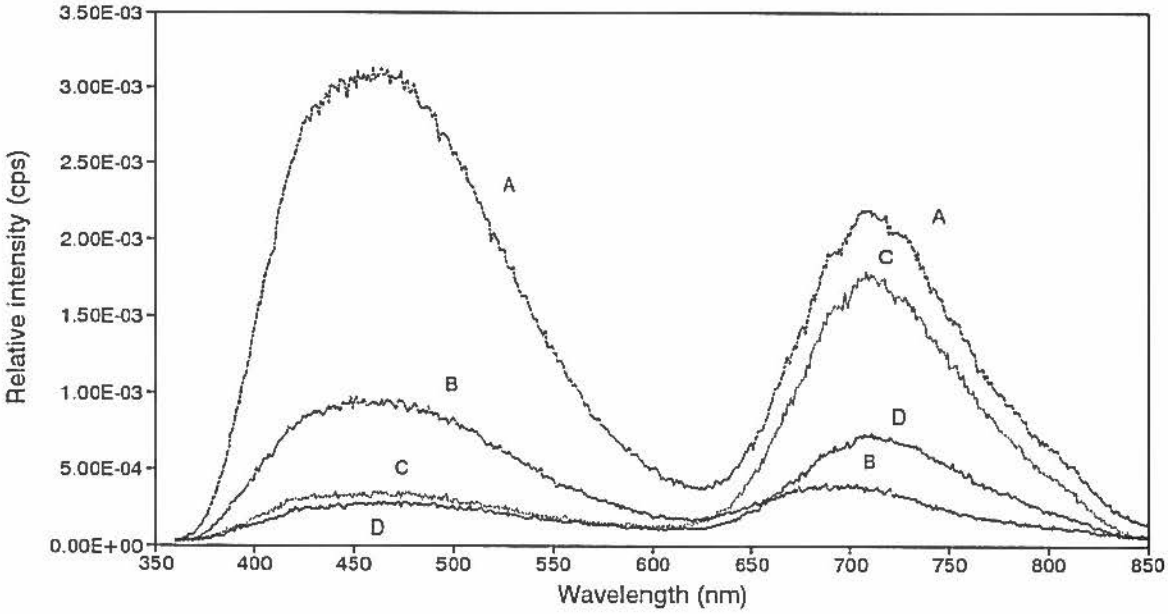

Fig 6.2-7. CL spectra of coarse-grained feldspars in the perthitic nepheline syenite (Sample N3B) from Center II, Pic Island. (A) is from a light blue luminescent Na-feldspar and (B) is from a light violet blue luminescent K-feldspar. (C) is from a dull red luminescent secondary Na-feldspar and (D) is from a brown luminescent secondary K-feldspar. CL conditions: 10 kV, 0.8 mA.

Table 6.2-1. Representative cathodoluminescence properties and compositions of feldspars in perthitic nepheline syenite and miaskitic nepheline syenite from Center II, Neys Park, Coldwell Complex, Ontario

Occurrence of feldspar	Sample No./ spectrum No.	Luminescence colour	Intensities (cps)					Compositions		
			Blue peak	(nm)	Red peak	(nm)	B/R ratio	Or	Ab	An
Perthitic Nepheline Syenite:										
Unexsolved alkali feldspar	N3C/A	Light violet blue	6.52E-04	(461)	7.27E-04	(704)	0.90	73-75	24-26	1
Exsolved Na-feldspar	N3C/B	Light blue	1.46E-03	(456)	7.09E-04	(716)	2.06	1-2	97-99	1-2
Host K-feldspar	N3C/C	Light violet blue	5.28E-04	(461)	2.50E-04	(711)	2.11	86-92	7-13	1
Secondary albite, margins	N3C/D	Dull red	1.95E-04	(461)	8.76E-04	(716)	0.22	1	97-99	1-2
Exsolved Na-feldspar	N3B/A	light blue	3.09E-03	(461)	2.18E-03	(708)	1.41	1	95-99	1-4
Host K-feldspar	N3B/B	Light violet blue	9.37E-04	(461)	3.85E-04	(697)	2.43	84-93	6-15	1
Secondary Na-feldspar	N3B/C	Dull red	3.58E-04	(461)	1.79E-03	(710)	0.20	1	97-98	1-2
Secondary K-feldspar	N3B/D	Brown	2.83E-04	(459)	7.46E-04	(701)	0.38	97-100	0-3	0-1
Exsolved Na-feldspar	N2A/A	Light blue	1.71E-03	(463)	8.58E-04	(713)	1.99	2	96-97	1-2
Host K-feldspar	N2A/B	Dull blue	3.67E-04	(470)	1.54E-04	(708)	2.38	88-89	11	1
Microcline	N2A/C	Dull blue	2.81E-04	(470)	9.43E-05	(704)	2.98	93-96	3-6	1
Secondary albite, margins	N2A/D	Dull red	1.35E-04		4.75E-04	(713)	0.28	1-2	97-98	1
Miaskitic Nepheline Syenite:										
Oligoclase, core	C114/A	Dull bluish grey	3.28E-03	(465)	1.74E-04	(800)	18.83	1-2	73-76	22-26
Alkali feldspar, rim	C114/B	Light blue	5.92E-03	(470)	3.88E-04	(694)	15.29	38-48	49-57	3-6
Alkali feldspar, margins	C114/C	Dull violet	2.22E-03	(465)	3.44E-04	(707)	6.44	52-65	33-45	2-3
2nd alkali feldspar, core	C114/D	Dull violet	1.61E-03	(464)	4.55E-04	(701)	3.53	48-50	46-49	3-4
Relict plagioclase, core	C114/E	Dull blue	6.65E-04	(466)	1.72E-04	(800)	3.87	1-2	87	11-13
Gabbro:										
Plagioclase	C107/A	Light blue	1.39E-03	(462)	1.77E-04	(799)	7.88	1-2	45-51	47-54
2nd K-feldspar, margins	N/A	Light violet blue	N/A		N/A			69-90	10-29	1-2

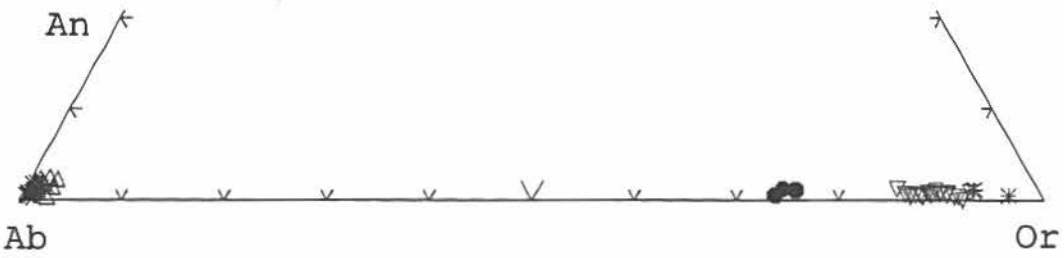

Fig. 6.2-8a. The compositions of feldspars in the perthitic nepheline syenite (Samples N3C,N2A,C3118A,C3118D,C97,C109,C111,C1863) plotted in the system Or-Ab-An. The filled circles (•) are the light violet blue luminescent unexsolved alkali feldspars. The asterisks (*) are the light violet blue luminescent microclines. The up-triangles (▵) are the light blue luminescent exsolved Na-feldspars and the down-triangles (▿) are the light violet blue luminescent K-feldspars. The crosses (×) are the dull red luminescent secondary albite.

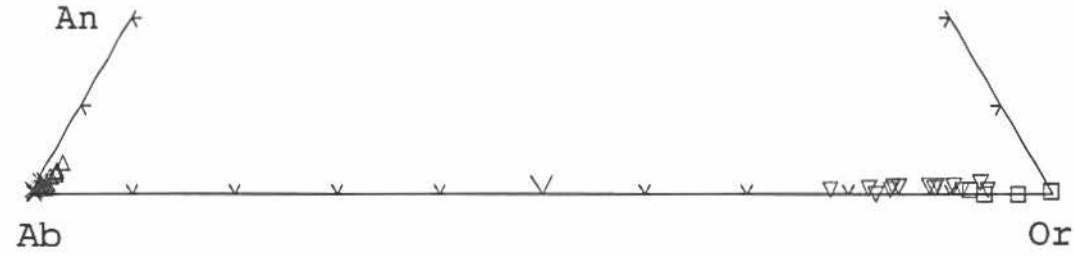

Fig. 6.2-8b. The compositions of feldspars in the perthitic nepheline syenites (Samples N1A, N3B) plotted in the system Or-Ab-An. The up-triangles (▵) are the light blue luminescent Na-feldspars and the down-triangles (▿) are the light violet blue luminescent K-feldspars. The crosses (×) are the dull red and deep red luminescent secondary Na-feldspar, the squares(□) are the dull blue and brown luminescent secondary K-feldspars in the antiperthite rim.

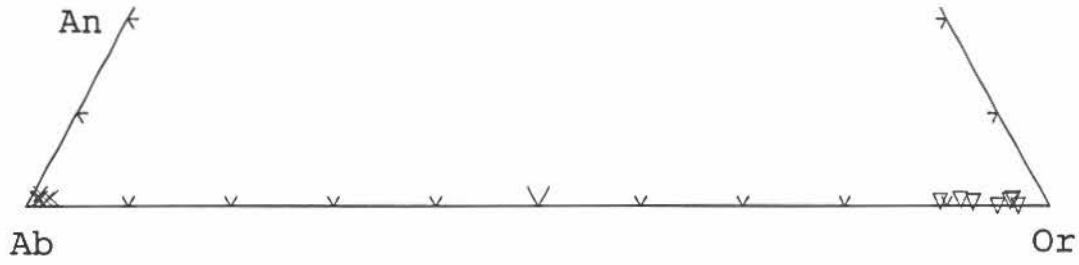

Fig 6.2-8c. The compositions of feldspars in the brick-red irregular pegmatitic patches from the perthitic nepheline syenites (Samples N3A) plotted in the system Or-Ab-An. The (▿) are the dull blue luminescent K-feldspars. The crosses (×) are the dull red luminescent secondary albite.

$Or_{84-93}Ab_{6-15}An_1$ (Table 6.2-1, Fig. 6.2-8a, 8b and Appendix 2).

b. Unexsolved alkali feldspar in the perthite

The unexsolved alkali feldspar is rarely observed at the centre of the fine-grained perthite crystals (Fig. 6.2-2a). The CL shows that the unexsolved alkali feldspar has an uniform light violet or light violet blue luminescence (Fig. 6.2-2b). The CL spectrum shows that the intensity of the blue peak is nearly the same as height as the red peak (Fig. 6.2-6, spectrum A), and the ratio of I_B/I_R is about 0.9 (Table 6.2-1). The variation in the luminescence colour between the two individuals of a Carlsbad twin (e.g., one side of the twin has a light violet luminescence and other side of the twin has a light violet blue luminescence) are due to the crystal orientation (Fig. 6.2-2b). This unexsolved alkali feldspar has an uniform composition of $Or_{73-75}Ab_{24-26}An_1$ (Table 6.2-1, Fig. 6.2-8a and Appendix 2).

c. Microcline twinning in the perthite

The microcline twinned feldspars are characterized by cross-hatched twinning in thin section. These feldspars mostly occur in the margins of the perthite (Fig. 6.2-1a), and some individual grains are rarely found in the areas adjacent to the perthite grains (Fig. 6.2-9a). The microcline usually has a uniform dull blue luminescence colour which is the same as that of the host K-feldspar (Fig. 6.2-1b,9b). The CL spectrum of the microcline twinned phase also has the same profile as that of the host

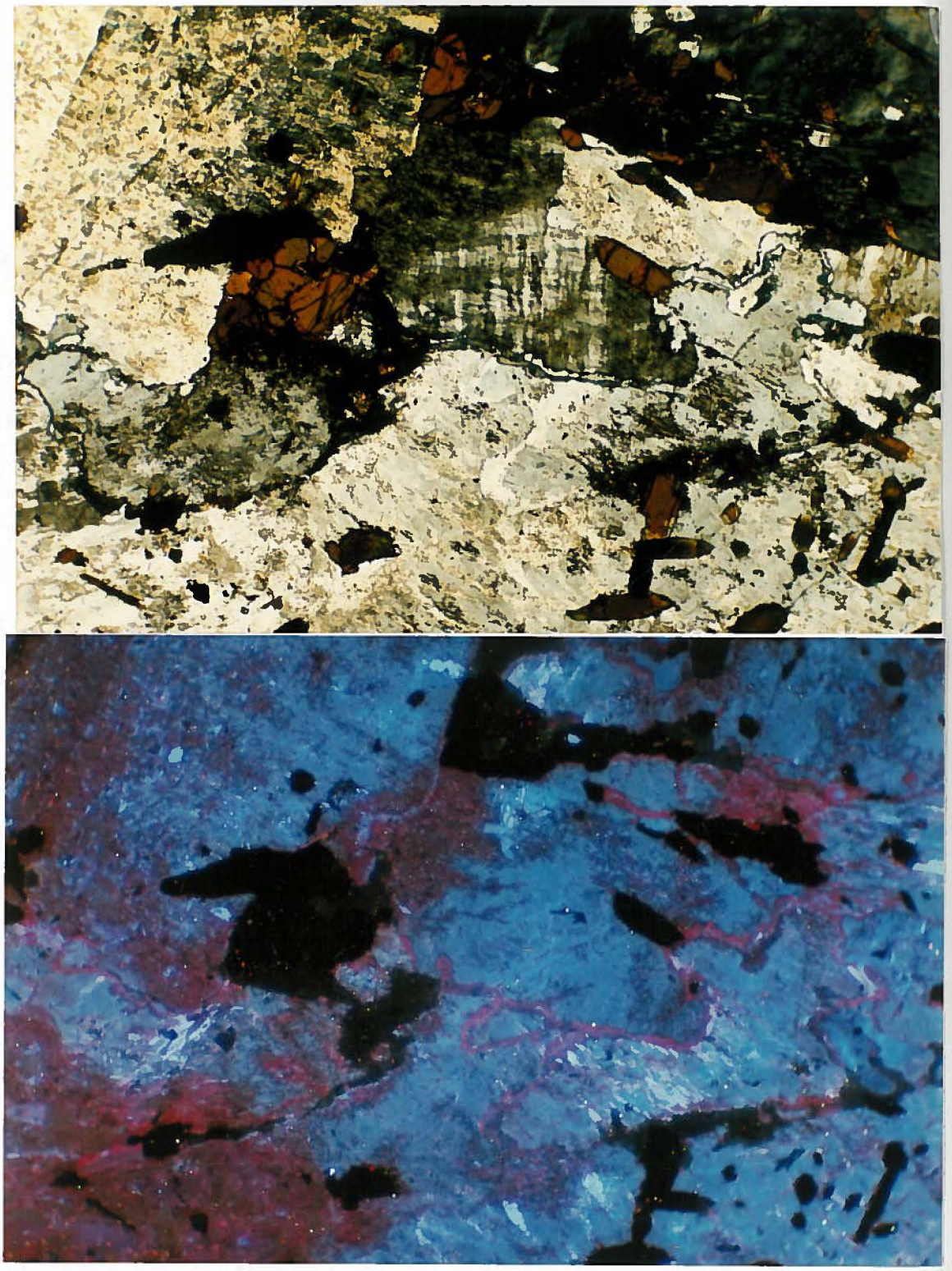

Fig. 6.2-9. Microcline in the perthitic nepheline syenite (Sample N2A) from Center II, Neys Park. a. TrL. The microcline grain shows cross-hatched pattern and is surround by the secondary albite. The rest of the feldspar grains are perthite. (Photographic conditions: 8 s, ASA 25) b. CL. The light blue luminescent bands are the exsolved Na-feldspar and the dull blue luminescent areas are the exsolved K-feldspar. The microcline also shows a dull blue luminescence. The secondary albite shows a dull red luminescence and the secondary K-feldspar shows a brown luminescence. Scale: 55 mm on photograph = 1 mm on thin section. (CL conditions: 10 kV, 0.8 Am. Photographic conditions: 2.5 min, ASA 400.)

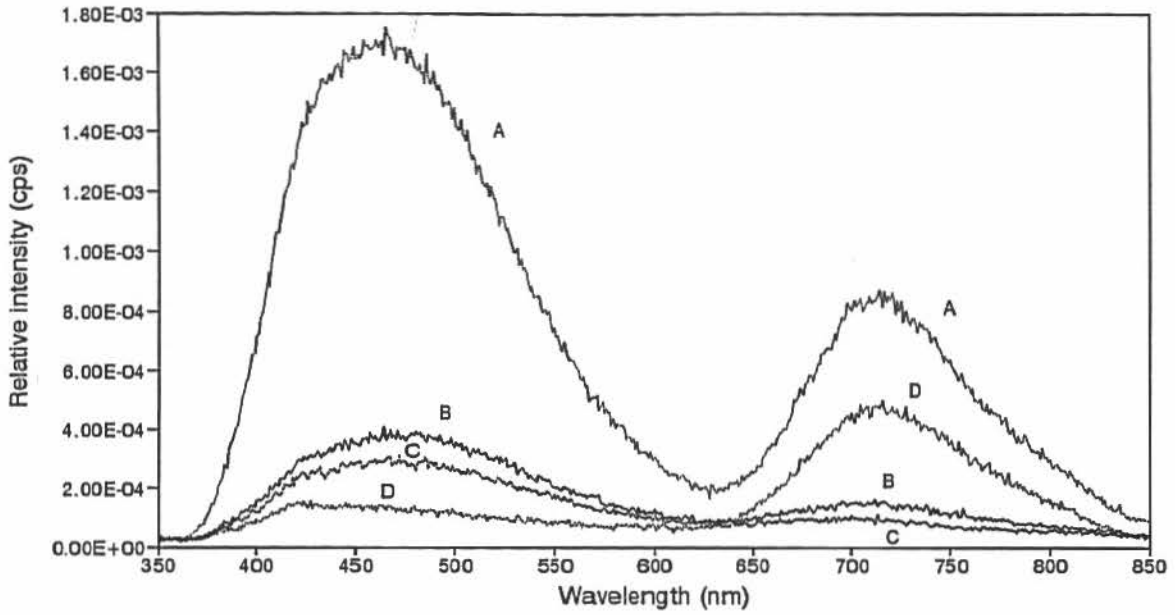

Fig. 6.2-10. CL spectra of feldspars in the perthitic nepheline syenite (Sample N2A) from Center II, Pic Island. (A) is from a light blue luminescent exsolved Na-feldspar and (B) is from a dull blue luminescent exsolved K-feldspar. (C) is from a dull blue luminescent microcline. (D) is from a dull red luminescent secondary albite. CL conditions: 10 kV, 0.8 mA.

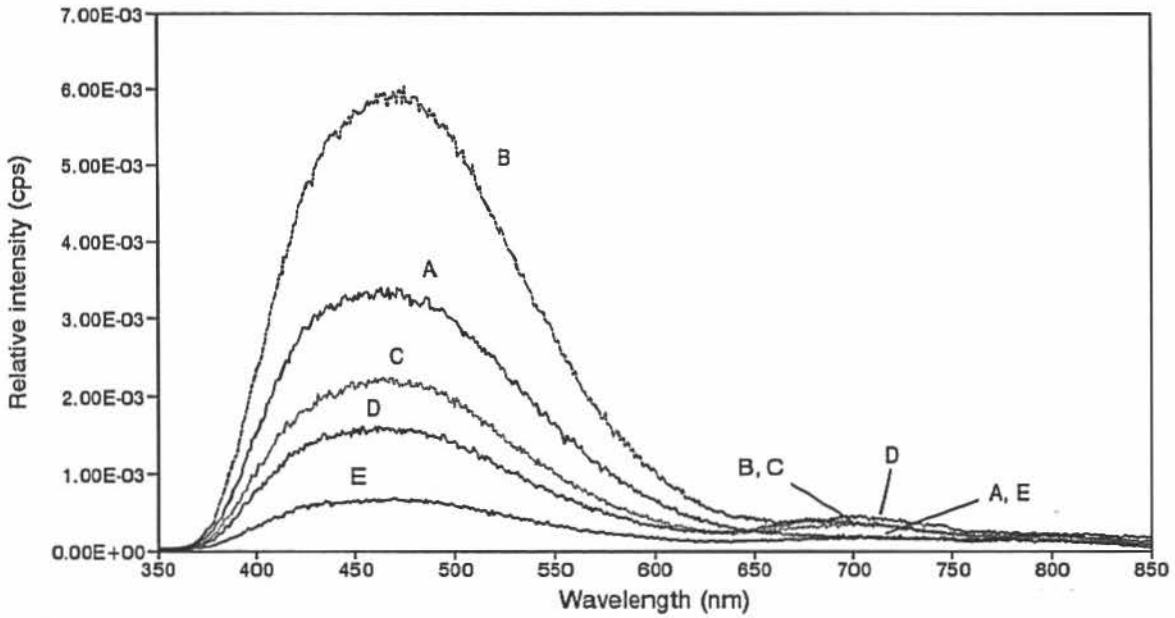

Fig. 6.2-11. CL spectra of feldspars in the miaskitic nepheline syenite (Sample C114) from Center II, Pic Island. (A) is from the dull bluish grey luminescent oligoclase core. (B) is from the light blue luminescent alkali feldspar rim. (C) is from the dull violet luminescent alkali feldspar which occurs in the margins of the rim. (D) is from a dull violet luminescent secondary alkali feldspar which occurs in the oligoclase core. (E) is from a dull blue luminescent relict oligoclase which occurs in the core. CL conditions: 10 kV, 0.8 mA.

K-feldspar (Fig. 6.2-10, spectrum c and b). However, the total luminescence intensity is slightly lower than the host K-feldspar.

The microcline twinned phases are potassic-rich feldspar which have a narrow range in composition from $Or_{93-96}\,Ab_{3-6}\,An_{1}$ (Table 6.2-1, Fig. 6.2-8a and Appendix 2). The orthoclase content of this microcline is slightly higher than that of the exsolved K-feldspar. As the microcline phase usually occurs in the margins of the perthite and has end member compositions, the microcline may be a later phase formed at a relatively low temperature.

d. Feldspars in the pegmatitic patches

Feldspars usually occur as euhedral crystals to subhedral in the pegmatitic patches from the perthitic nepheline syenite. Most of the K-feldspars are replaced by secondary albite, and are also strongly hematitized or sericitized by a late-stage fluid. The Na-feldspars are relatively fresher than the K-feldspars and are albite twinned (Fig. 6.2-12a).

The K-feldspar exhibits a weak, heterogeneous dull blue luminescence (Fig. 6.2-12b), whereas the Na-feldspar reveals dull red luminescence under CL. The heterogeneous luminescent colour of the K-feldspar is due to sericitization and hematitization during the late-stage fluid alteration. The luminescent intensity of the K-feldspar is much weaker than for the host K-feldspar which occurs outside of the pegmatitic patches.

The K-feldspar ranges in composition from $Or_{89-97}Ab_{3-10}An_{<1}$, whereas the Na-feldspar ranges from $Ab_{97-99}Or_{2-1}An_{1}$ (Fig. 6.2-8c, Appendix 2).

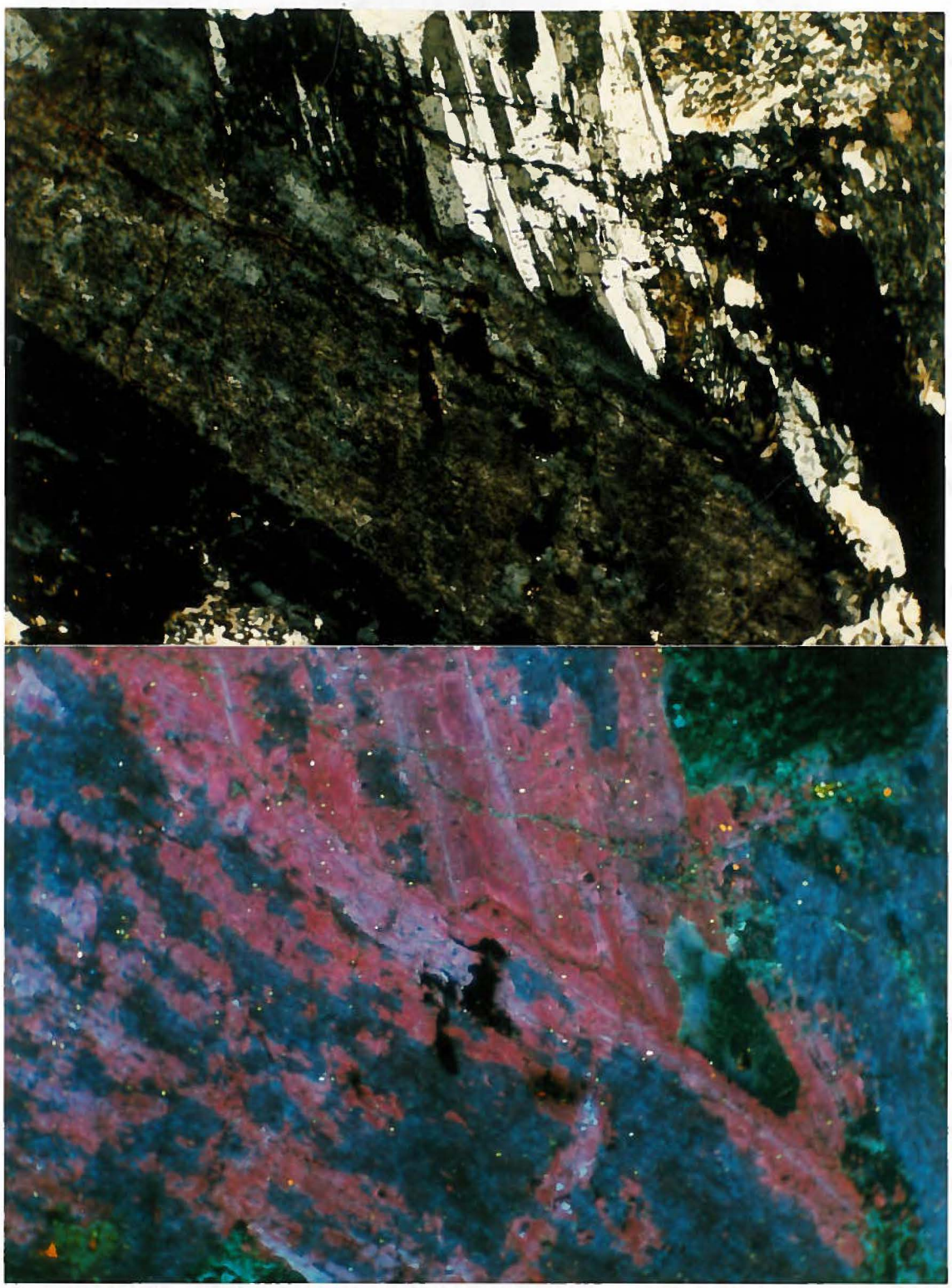

Fig. 6.2-12. Feldspars occur inside the pegmatitic patch within the perthitic nepheline syenite (Sample N3A) from Center II, Neys Park. a. TrL. The K-feldspar is replaced by secondary albite and strongly altered by hematitization and sericitization (Photographic conditions: 1.5 s, ASA 25) b. CL. The K-feldspar shows a dull blue luminescence, and the secondary albite shows a dull red luminescence. The dull green luminescent areas are thomsonite. Scale: 55 mm on photograph = 1 mm on thin section. (CL conditions: 10 kV, 0.8 Am. Photographic conditions: 4 min, ASA 1000.)

The Or content in the K-feldspar is slightly richer than the host K-feldspar in the perthite which occurs outside of the pegmatitic patches (Fig. 6.2-8a, 8b).

6.2.3. Feldspars in the miaskitic nepheline syenite

Most feldspar crystals in the miaskitic nepheline syenite consist of a plagioclase core and an alkali feldspar mantle (Fig. 6.2-13a, 14a). Some fine-grained alkali feldspar crystals are unzoned and are Carlsbad twinned.

In the zoned feldspar crystals, the cores are usually twinned by albite law and the rims are optically homogenous (Fig. 6.2-14a). CL reveals that the plagioclase cores have uniform bluish grey luminescence (Fig. 6.2-13b, 14b). The CL spectrum consists of a high blue peak at 470 nm and a very weak red peak at 800 nm (Fig. 6.2-11, spectrum A), and the ratio of I_B/I_R is about 18.8 (Table 6.2-1).

Under CL, the optically homogeneous alkali feldspar rims reveal light blue luminescence near the core, and dull bluish violet luminescent towards the margins (Fig. 6.2-13b, 14b). These light blue luminescent alkali feldspar internal rims have higher luminescent intensities than the plagioclase cores. The CL spectrum consists of a high blue peak at 470 nm and a weak red peak at 694 nm (Fig. 6.2-11, spectrum B), and the ratio of I_B/I_R is about 15.3 (Table 6.2-1). The dull bluish violet luminescent margins of the rims were affected by late-stage fluid-feldspar interaction as described in section 6.2.5.

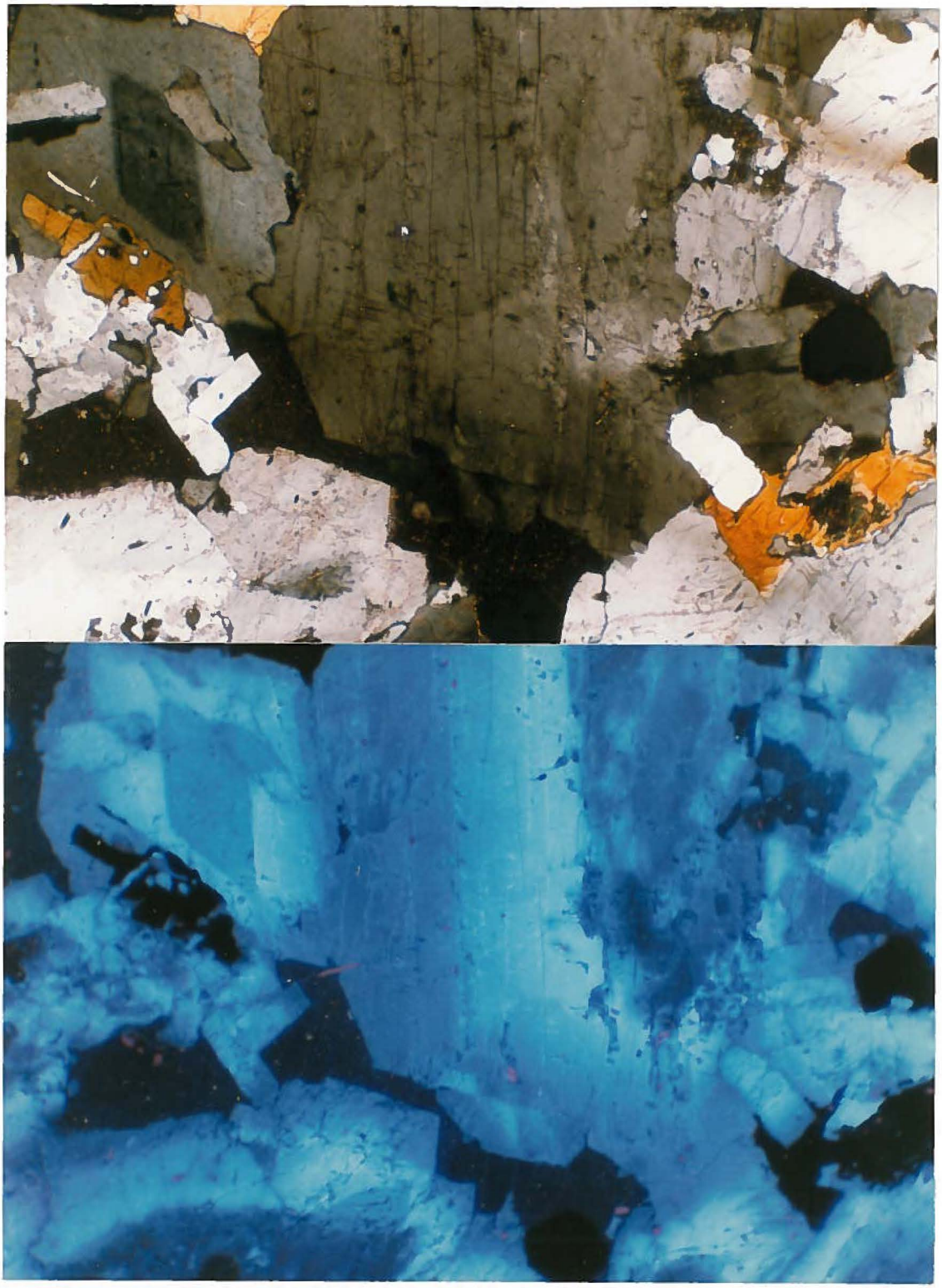

Fig. 6.2-13. Zoned feldspars in the miaskitic nepheline syenite (Sample C114) from Center II, Neys Park. a. TrL. The feldspar crystals are mantled with a rhombic oligoclase core and a homogeneous alkali feldspar rim (Photographic conditions: 4 s, ASA 400) b. CL. The bluish grey luminescent rhombic core is an oligoclase. The light blue luminescent rim is alkali feldspar. The margins of the rim reveals a dull violet luminescence which is the alkali feldspar with a higher Or content than the rim. In some cores, the irregular shaped dull violet luminescent areas are the secondary alkali feldspar, and dull blue luminescent areas are the relict oligoclase which remains a rhombic shape. Scale: 55 mm on photograph = 1 mm on thin section. (CL conditions: 10 kV, 0.8 Am. Photographic conditions: 25 s, ASA 400.)

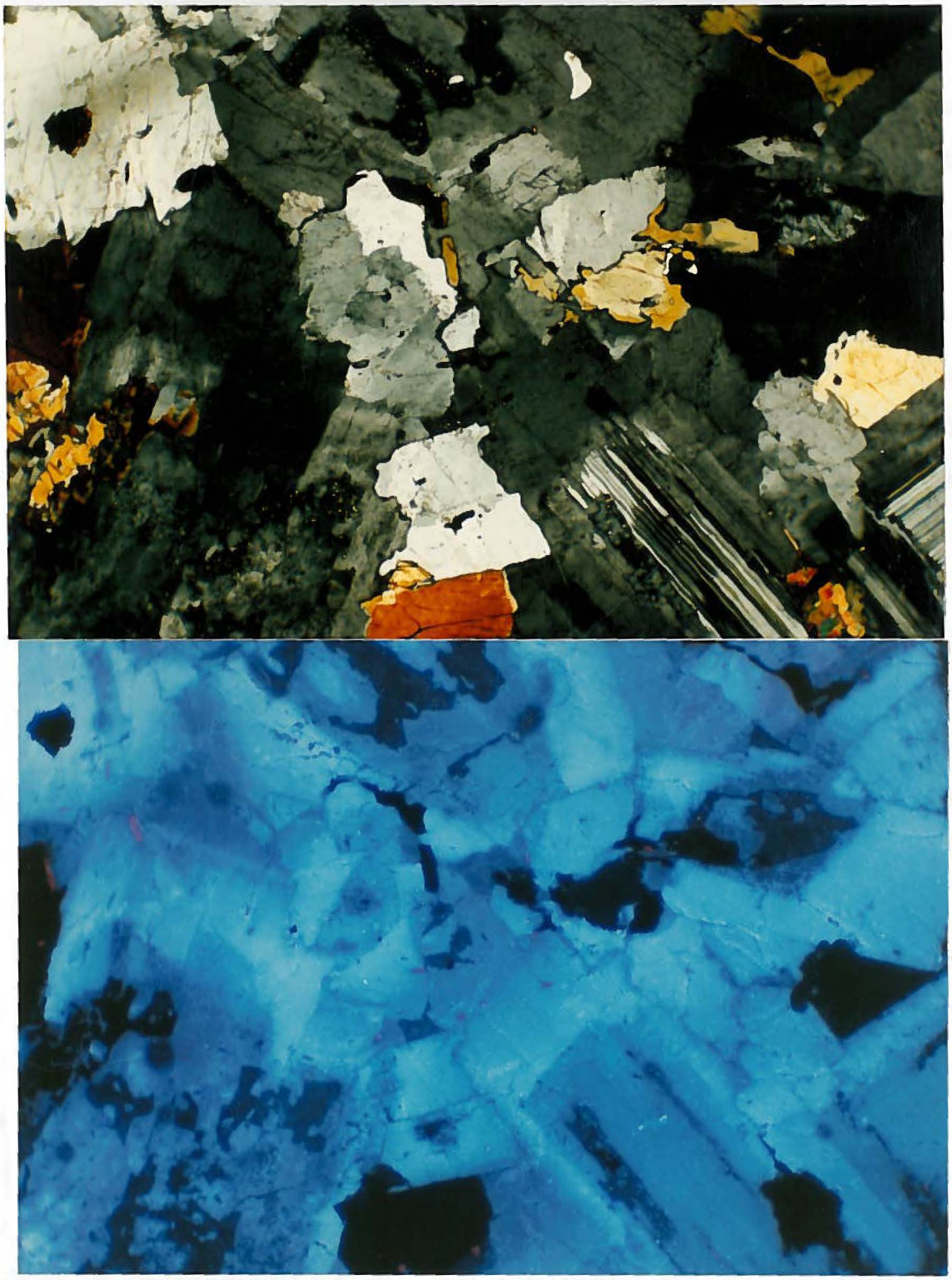

Fig. 6.2-14. Feldspars in the miaskitic nepheline syenite (Sample C114) from Center II, Neys Park. a. TrL. Most feldspar crystals are mantled with an albite twinned oligoclase core and a homogeneous alkali feldspar rim. Some fine-grained feldspar crystals are Carlsbad twinned homogeneous alkali feldspar. (Photographic conditions: 8 s, ASA 25) b. CL. The oligoclase cores show dull bluish grey luminescence. The alkali feldspar rims show light blue luminescence. The dull violet luminescent areas in the margins of the rim are the secondary alkali feldspars. In the core, the irregular shaped dull violet and dull blue luminescent areas are the secondary alkali feldspar and the relict oligoclase respectively. Scale: 55 mm on photograph = 1 mm on thin section. (CL conditions: 10 kV, 0.8 Am. Photographic conditions: 25 s, ASA 400.)

The compositional data show that the dull bluish grey luminescent cores are oligoclase which have a narrow range in compositions of $Ab_{73-76}An_{22-26}Or_{1-2}$. The light blue luminescent alkali feldspar mantles have a range in composition from $Or_{38-48}Ab_{49-57}An_{3-6}$ (Table 6.2-1, Fig. 6.2-15a and Appendix 2).

6.2.4. Plagioclase in Neys Park gabbro

The plagioclase in the gabbro from Neys Park area occurs as idiomorphic crystals which are Carlsbad and albite twinned (Fig. 6.2-16a). This plagioclase usually shows a uniform light blue luminescence under CL (Fig. 6.2-16b). The CL spectrum of this plagioclase consists of a high intensity blue peak at 462 nm and a very weak red peak at 800 nm (Fig. 6.2-17). The CL spectrum has a similar profile to that of the oligoclase core in the miaskitic nepheline syenite. However, the ratio of I_B/I_R of the plagioclase (7.9) is lower than that of the oligoclase core (18.8) (Table 6.2-1).

This plagioclase has a range in composition from $An_{47-54}Ab_{44-51}Or_{1-2}$ (Table 6.2-1, Fig. 6.2-15b and Appendix 2), i.e. between andesine and labradorite. The anorthite contents in this plagioclase have a very small variation of only about 7 %. Since the plagioclase has an uniform luminescent colour and a very narrow composition range, the plagioclase crystals may have crystallized under equilibrium conditions.

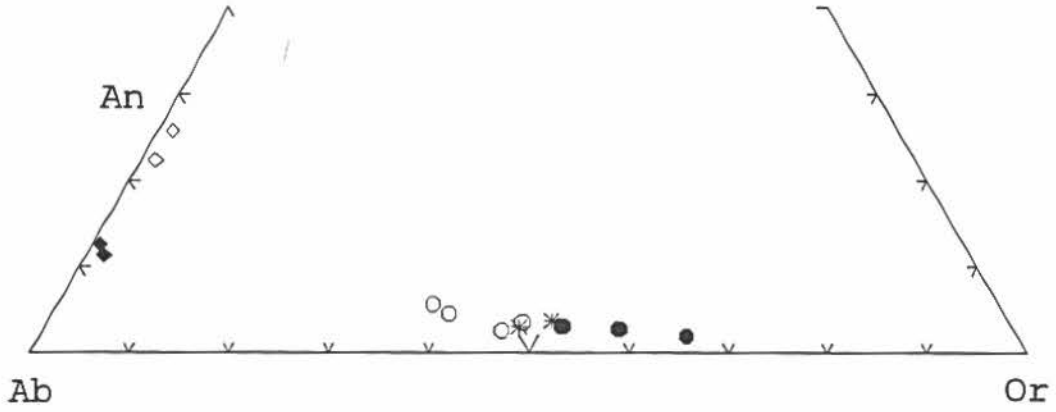

Fig. 6.1-15a. The compositions of feldspars in the miaskitic nepheline syenite (Samples C114) plotted in the system Or-Ab-An. The open diamonds (◇) are the dull bluish grey luminescent oligoclase cores. The open circles (○) are the light blue luminescent alkali feldspar rims.

The filled circles (●) are the dull bluish violet secondary alkali feldspar in the margins of the rims and the asterisks (*) are dull violet luminescent secondary alkali feldspars in the cores. The filled diamonds (◆) are the dull blue luminescent relict oligoclases in the cores.

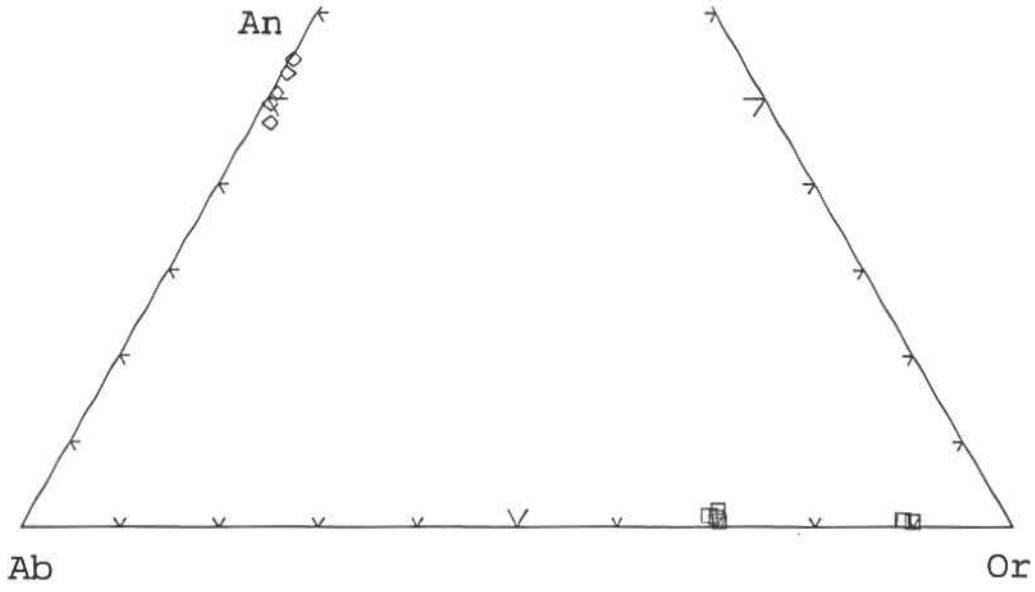

Fig. 6.2-15b. The compositions of feldspars in the gabbro (Samples C107) plotted in the system Or-Ab-An. The open diamonds (◇) are the light blue luminescent andesines and the open squares (□) are the secondary K-feldspars occurring in the margins.

Fig. 6.2-16. Plagioclase in the gabbro (Sample C107) from Center II, Neys Park. a. TrL. The plagioclase crystals are albite and Carlsbad twinned. (Photographic conditions: 1 s, ASA 400) b. CL. The plagioclase crystals show a light blue luminescence. The violet luminescent crystals are the apatite and the orange luminescent spots are the calcite. Scale: 55 mm on photograph = 1 mm on thin section. (CL conditions: 10 kV, 0.8 Am. Photographic conditions: 30 s, ASA 400.)

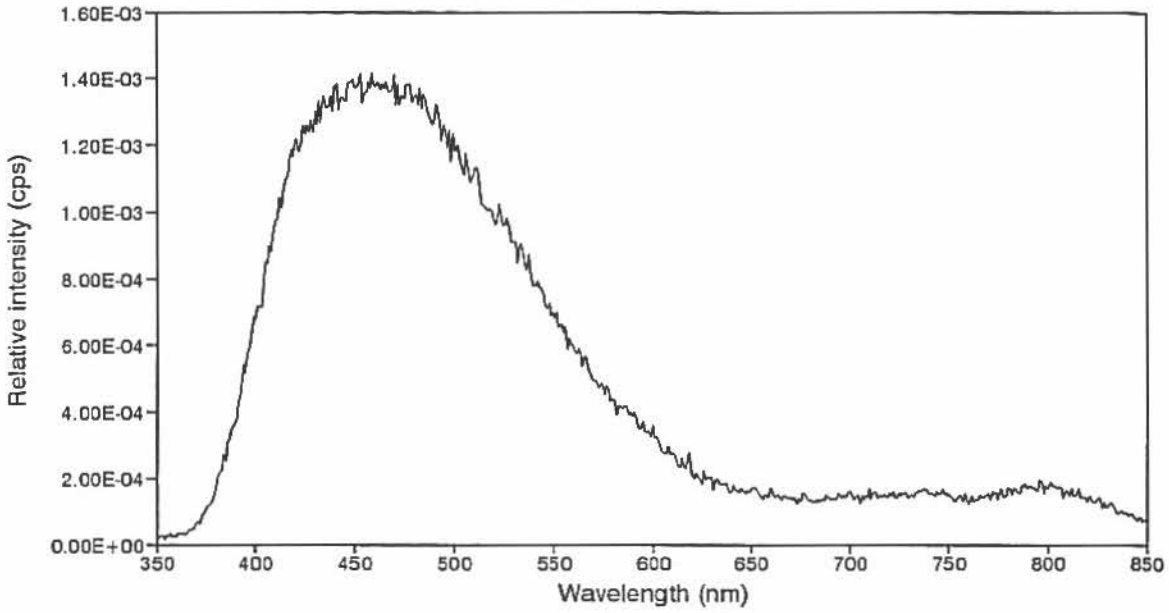

Fig. 6.2-17. CL spectrum of a light blue luminescent plagioclase (andesine-labradorite) in the gabbro (Sample C107) from Center II, Pic Island. CL conditions: 10 kV, 0.8 mA.

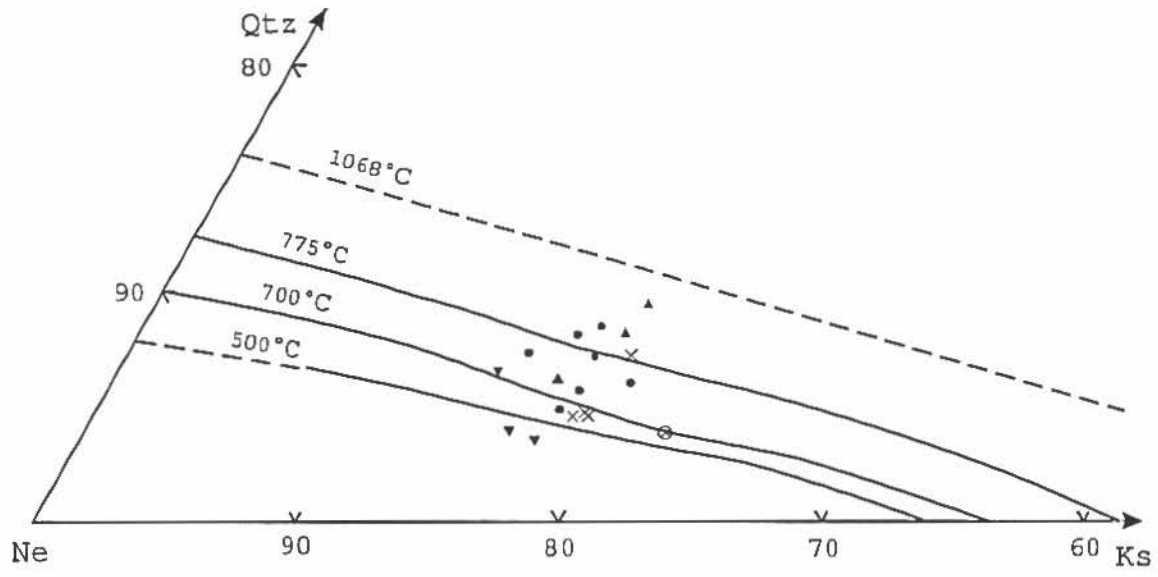

Fig. 6.2-18. Composition of nepheline plotted in part of the $NaAlSiO_4$-$KalSiO_4$-SiO_2 system. The filled up-triangles (▲) are the nephelines from inside pegmatitic patches in the perthitic nepheline syenite (N3A). The filled down-triangles (▼) are the secondary nephelines from the miaskitic nepheline syenite (C114). The crosses (×) are the nephelines from the late pegmatitic syenite (C472).

The filled circles (•) are the nepheline data from Mitchell and Platt (1982). The crossed circle (⊗) is the ideal composition of the Morozewicz's nepheline. Isotherms of the limits solid solutions are from Hamilton (1961).

6.2.5. Late-stage fluid-induced coarsening and replacement in the nepheline syenites and the gabbro

a. Deuteric coarsening in the perthitic nepheline syenite

Deuteric coarsening in the perthitic nepheline syenite only associates with the coarse-grained perthitic phenocrysts and forms secondary patch antiperthite along the margins of the phenocrysts (Fig. 6.2-3a, 4a, 5a). In this secondary patch antiperthite, the secondary Na-feldspar exhibits a dull red luminescence, whereas thesecondary K-feldspar has a dull blue or brown luminescence (Fig. 6.2-4b, 5b). For the dull red luminescent secondary Na-feldspar, the CL spectrum consists of a high red peak at 710 nm and a weak blue peak at 461 nm (Fig. 6.2-7, Spectrum C), and the ratio of I_B/I_R is about 0.2 (Table 6.2-1). For the brown luminescent secondary K-feldspar, the CL spectrum consists of a weak red peak at 701 nm and a very weak blue peak at 459 nm (Fig. 6.2-7, Spectrum D), and ratio of I_B/I_R is about 0.4 (Table 6.2-1). The brown luminescent K-feldspar has a much lower luminescence intensity than the dull red luminescent secondary Na-feldspar. The secondary Na-feldspar has a range in composition of $Ab_{97-98}Or_1An_{1-2}$, whereas the secondary K-feldspar has a range of $Or_{97-100}Ab_{0-3}An_{0-1}$ (Table 6.2-1, Fig. 6.2-8b and Appendix 2).

b. Secondary albite

Secondary albite is clear, untwinned crystals which occur as interlocking grains occupying the interstices between the fine-

grained perthite groundmass (Fig. 6.2-1a, 2a), and the coarse-grained perthite phenocrysts (Fig. 6.2-4a). This secondary albite exhibits a dull red or deep red luminescence (Fig. 6.2-1b, 2b, 4b). The CL spectrum consists of a red peak at 716 nm and a blue peak at 461 nm, the intensity of the red peak is higher than that of the blue peak (Fig 6.2-6, spectrum D), and the ratio of I_B/I_R is about 0.2 (Table 6.2-1). This dull red luminescent secondary albite has a range in composition of $Ab_{97-99}An_{1-2}Or_1$ (Table 6.2-1, Fig 6.2-8a and Appendix 2).

c. Late-stage replacement in the miaskitic nepheline syenite

The late-stage replacement in the miaskitic nepheline syenite is different from the deuteric coarsening in the perthitic nepheline syenite. It usually produces: (1) secondary K-rich feldspar in the margins of the alkali feldspar rim, and (2) replacement of oligoclase with secondary K-rich feldspar and nepheline in the cores.

As noted in section 6.2.3., from the alkali feldspar internal rim towards the outer edge of the rim, the CL colour changes from light blue to dull violet luminescence as a result of late-stage fluid-feldspar interaction (Fig. 6.2-13b, 14b). The CL spectrum of this dull violet outer rim consists of a blue peak at 465 nm and a weak red peak at 707 nm, and has a lower I_B/I_R ratio (6.4) than the light blue luminescent internal rims (Table 6.2-1 and Fig. 6.2-11, Spectrum C). This dull violet luminescent outer rim has a range in composition of $Or_{52-65}Ab_{33-45}An_{2-3}$, and has higher Or contents than the

light blue luminescent internal rims (Table 6.2-1).

The oligoclase cores are commonly replaced by nepheline (Fig. 6.2-19a). Contemporaneously, the oligoclase may be also altered to secondary K-rich feldspar showing a dull violet luminescence (Fig. 6.2-19b) with a very low blue peak at 464 nm and a weak red peak at 701 nm, and the ratio of I_B/I_R is about 3.53 (Table 6.2-1 and Fig. 6.2-11, Spectrum D). This secondary K-rich feldspar has a range in composition of $Or_{48-50}Ab_{46-49}An_{3-4}$ (Table 6.2-1, Fig 6.2-15a and Appendix 2).

The oligoclase core is typically not completely altered to secondary K-rich feldspar. Figure 6.2-19b shows that dull blue luminescent irregular spots within the dull violet luminescent secondary K-rich feldspar are relict oligoclase. The relict oligoclase has a very low luminescence intensity, and the CL spectrum consists of a blue peak at 466 nm and a weak red peak at 800 nm, and the ratio of I_B/I_R is about 3.87 (Fig. 6.2-11, Spectrum D and Table 6.2-1). This relict oligoclase has a range in composition of $Ab_{87}An_{11-13}Or_{1-2}$ which has higher Ab and lower An contents compared with the unaltered oligoclase cores ($Ab_{73-76}An_{22-26}$ Or_{1-2}) (Table 6.2-1, Fig 6.2-15a and Appendix 2).

d. Late-stage replacement in the gabbro

The plagioclase (andesine-labradorite) crystals in the gabbro are relatively fresher than the oligoclase in the miaskitic nepheline syenites. During late-stage fluid-feldspar interaction, the plagioclase crystals are replaced by nepheline (dark grey CL color)

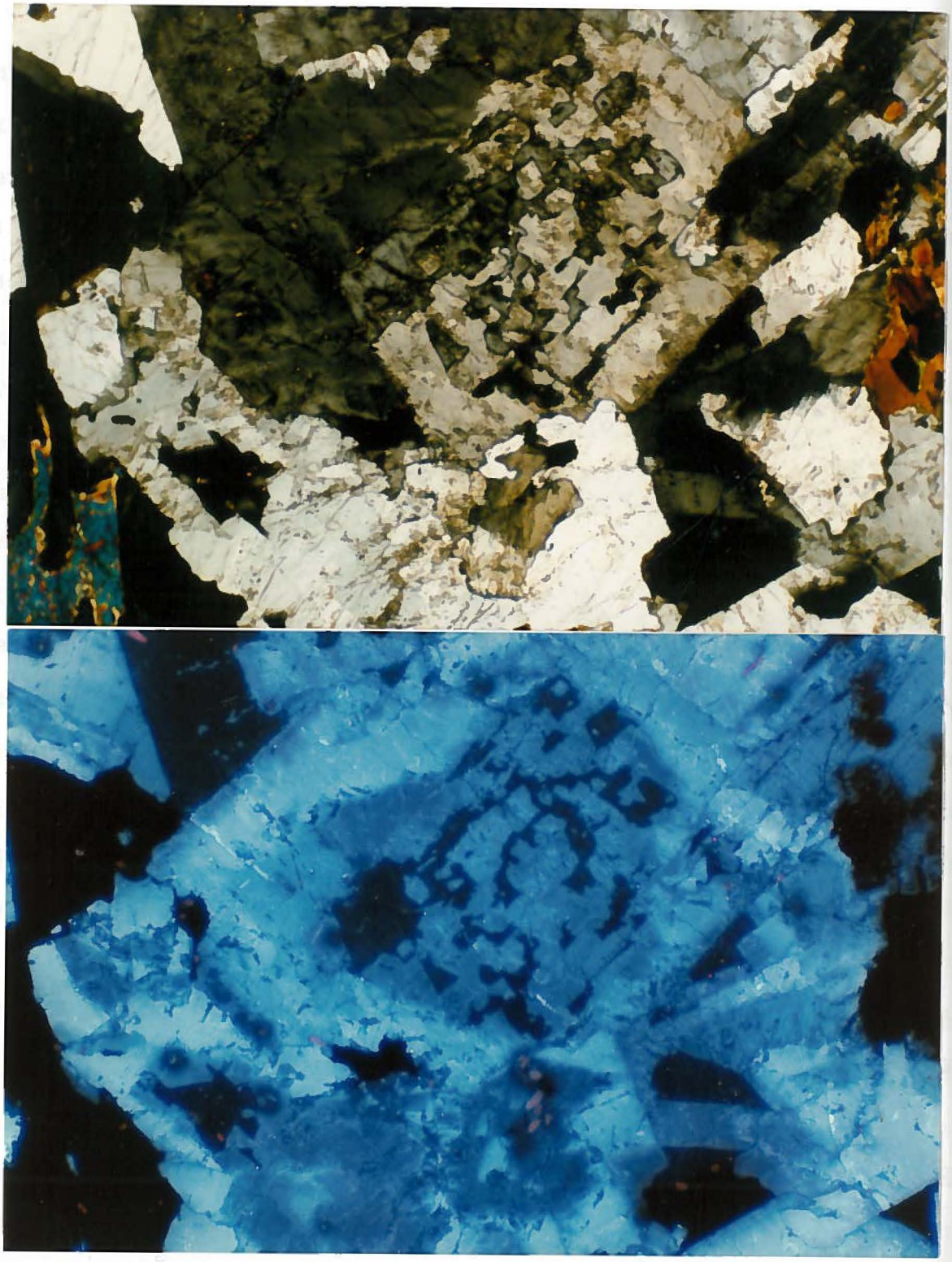

Fig. 6.2-19. K-rich alkali feldspar and nepheline replace oligoclase core in the miaskitic nepheline syenite (Sample C114) from Center II, Neys Park. a. TrL. The oligoclase core is replaced by nepheline. (photographic conditions: 1 s, ASA 400) b. CL. The bluish grey luminescent oligoclase core is replaced by the dull violet luminescent secondary K-rich alkali feldspar and the dark blue luminescent nepheline. The dull blue luminescent irregular spots within the dull violet luminescent secondary K-rich alkali feldspar is the relict oligoclase. Scale: 55 mm on photograph = 1 mm on thin section. (CL conditions: 10 kV, 0.8 Am. Photographic conditions: 30 s, ASA 400.)

and altered to secondary K-rich feldspar (dull violet CL colour) along the margins (Fig. 6.2-20b). The secondary K-rich feldspar has a compositional range of $Or_{69-90}Ab_{10-29}An_{1-2}$ (Table 6.2-1).

Nepheline-plagioclase intergrowths have been described by a number of authors. Henderson and Gibb (1972) reported plagioclase-nepheline intergrowths in a syenite from the Marangudzi complex, Rhodesia (Zimbabwe). They concluded that the intergrowths are formed by resorption of the plagioclase by the magmatic melt and simultaneous replacement by nepheline.

Rao and Murthy (1974) optically observed nepheline-plagioclase intergrowths in the nepheline syenites from the Eastern Ghat province of India. They concluded that the nepheline is the product of K-feldspar replacement of the plagioclase in a silica deficient environment. The process presumably involves an alkali exchange metasomatic reaction as follows:

$$3(NaAlSi_3O_8) + (CaAlSi_2O_8) + 2K^+ \rightarrow 2(KAlSi_3O_8) + (NaAlSi_3O_8) + 2(NaAlSiO_4) + Ca^{2+}$$

Plagioclase — Alkali feldspar — Nepheline

Mitchell and Platt (1978) studied the nepheline-plagioclase intergrowths within the feldspar-porphyry xenoliths in the host-rock of recrystallized nepheline syenites from Center II, Mink Creek and Redsucker Cove areas. They proposed that intergrowths were formed by Na-K metasomatism of plagioclase at high temperatures. The source of the metasomatic fluids is thought to be the host nepheline syenite.

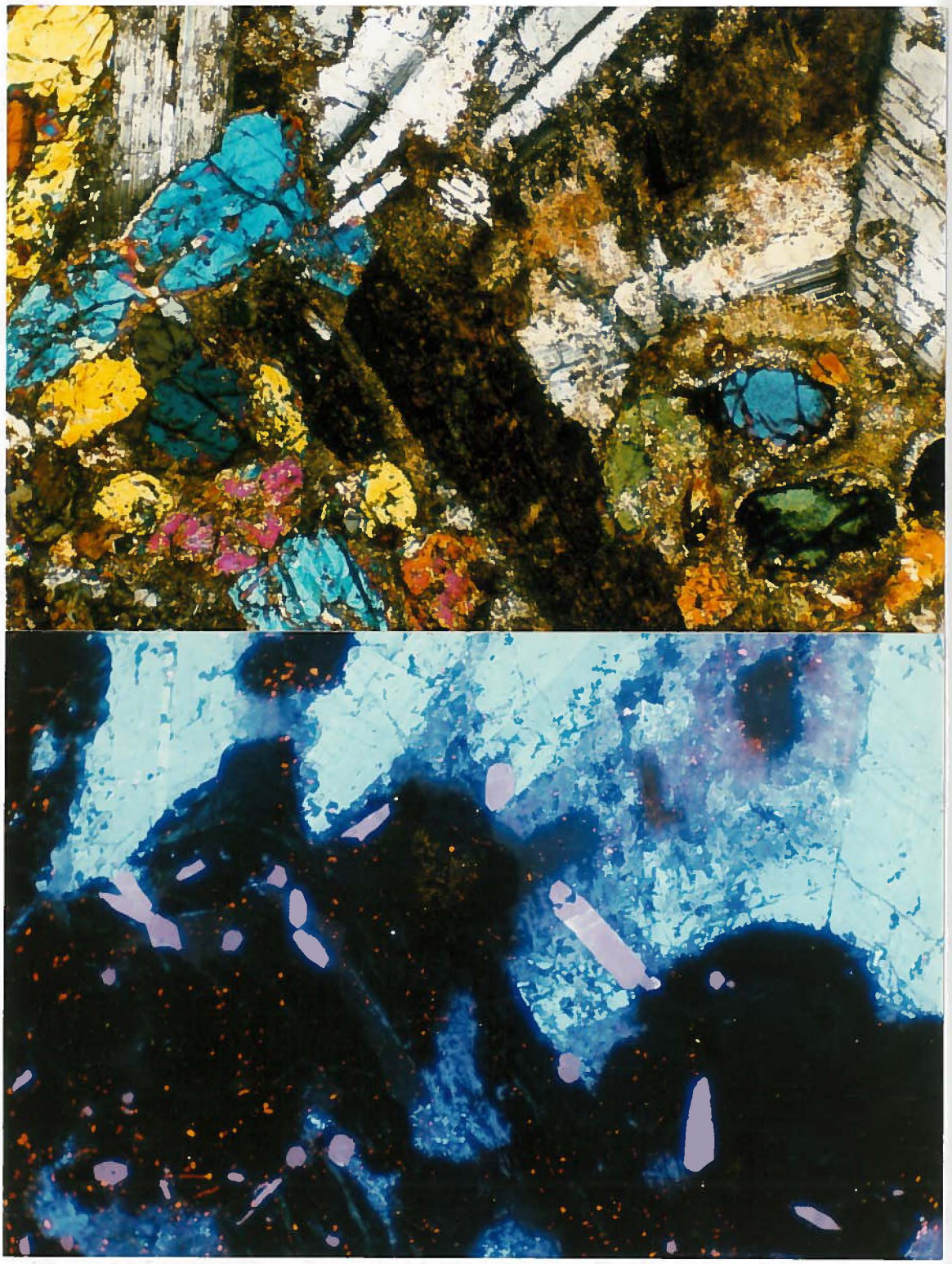

Fig. 6.2-20. K-rich feldspar and nepheline replacing plagioclase in gabbro (Sample C107) from Center II, Neys Park. a. TrL. The plagioclase crystals are albite and Carlsbad twinned. (Photographic conditions: 2 s, ASA 400) b. CL. The light blue luminescent plagioclase crystals are replaced by the dark blue luminescent nepheline and the dull violet luminescent secondary K-rich alkali feldspar along the crystals margins. The violet luminescent crystals are the apatite and the orange luminescent spots are the calcites. Scale: 55 mm on photograph = 1 mm on thin section. (CL conditions: 10 kV, 0.8 Am. Photographic conditions: 1.5 min, ASA 400.)

The present studies suggest that the nepheline and secondary K-rich alkali feldspar replacement of the oligoclase core in the miaskitic nepheline syenite may involve a K-rich, late-stage magmatic fluid which reacts with the oligoclase to produce the secondary alkali feldspar and nepheline.

The late-stage fluid alteration in the gabbro may follow the same process as in the miaskitic nepheline syenites. The K-rich metasomatic fluids react with the plagioclase to form nepheline and secondary K-rich alkali feldspar.

6.2.6. Nepheline geothermometry

As the nepheline coexists with the K-feldspar, the crystallization temperature of the nepheline can be estimated by using the limits of nepheline solid solution in the $NaAlSiO_4$-$KAlSiO_4$-SiO_2-H_2O system (Hamilton 1961).

The nepheline geothermometer indicates that the nepheline coexisting with K-feldspar which occurs inside the patches has an equilibrium temperature range of 725-875 °C (Fig. 6.2-18). This temperature range is in the upper part of the equilibrium temperature range determined by Mitchell and Platt (1982). The nepheline which occurs in the miaskitic syenite coexisting with the secondary K-feldspar has a relatively low equilibrium temperature range of <500-700°C. This temperature range is located at the lower part of the equilibrium temperature range determined by Mitchell and Platt. The nepheline which occurs in late pegmatitic syenite has a temperature range of 600-775 °C, and has a composition near

the ideal Morozewicz's nepheline (Fig. 6.2-18).

It has long been recognized that the composition of nepheline in igneous rocks is related to the composition of the magmas from which they crystallized and the crystallization temperature of the nepheline (Hamilton and MacKenzie, 1965; Powell and Powell, 1977; Edgar, 1984). Plutonic nephelines have compositions in the Morozewicz-Buerger convergence field from $Ne_{74.0}Ks_{22.1}Q_{3.9}$ to $Ne_{72.9}Ks_{27.1}$ (Tilley, 1954). With increasing temperature, the limits of nepheline solid solution increase with respect to both SiO_2 and $KAlSiO_4$ (Hamilton, 1960). The compositions of the nepheline in the syenites from Neys Park, all lie outside the Morozewicz-Buerger field and are similar to nephelines found in the syenites from Pic Island and Mink Creek-Redsucker Cove areas (Mitchell and Platt, 1982).

Mitchell and Platt (1982) suggested that the nepheline equilibrium temperatures in the syenites are consistent with prolonged re-equilibration at high temperatures during a recrystallization event, followed by relatively rapid cooling to prevent low temperature equilibration of nepheline to compositions within the Morozewicz-Buerger field.

6.2.7. Thermal history of the alkali feldspars

Evolution of the alkali feldspars in perthitic nepheline syenite, miaskitic nepheline syenite and gabbro are shown in Fig. 6.2-21 and Fig. 6.2-22.

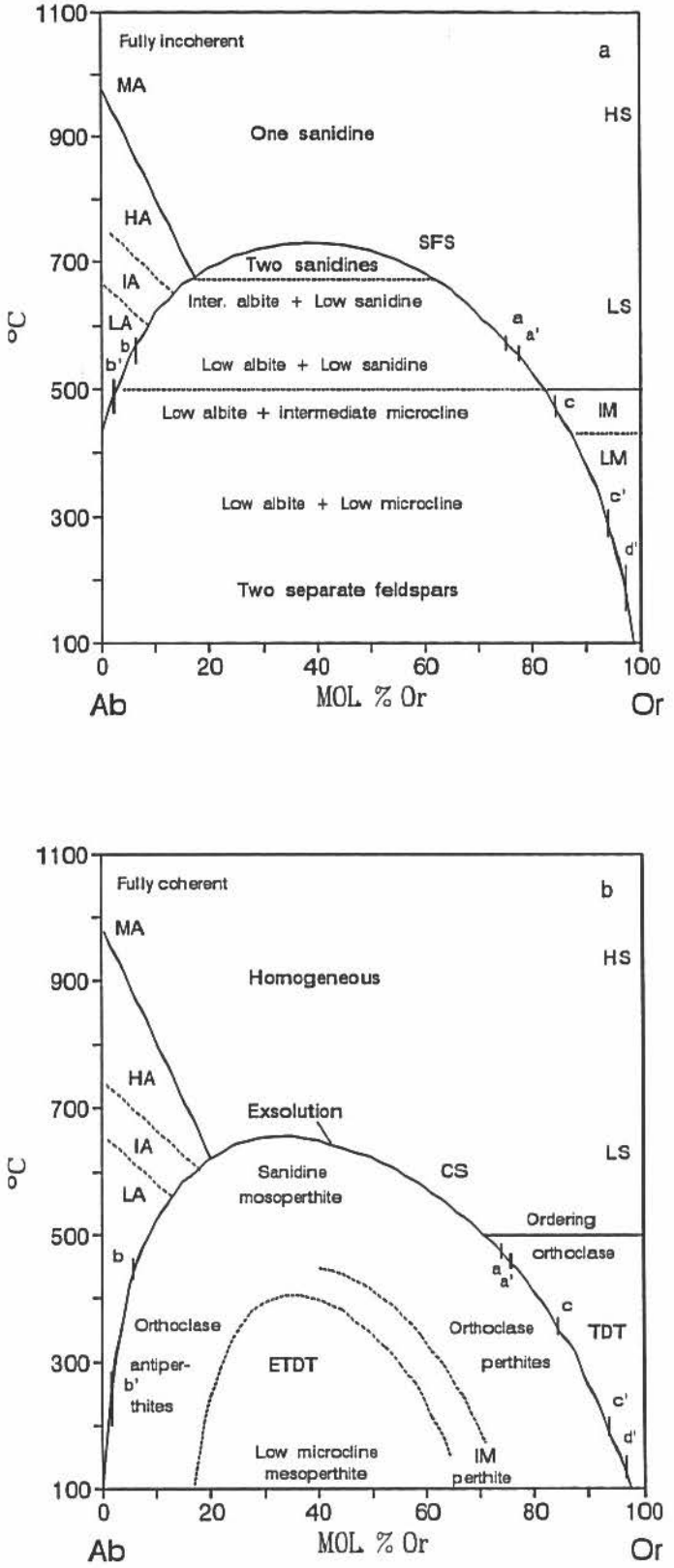

Fig. 6.2-21. The evolution of the alkali feldspars in the perthitic nepheline syenite from Center II, Neys Park are illustrated in the Or-Ab binary phase diagram. The path a-a′ is the unexsolved alkali feldspar at the centre of the fine-grained perthite. The path b-b′ and c-c′ is the exsolved Na-feldspar and K-feldspar respectively. The path c-d′ is the microcline in the fine-grained perthite margins.

Diagram (a) shows the phase relationships for An-free alkali feldspars under complete (incoherent) equilibrium and (b) shows different constrained equilibrium states as a function of bulk composition and T for completed coherent intergrowths (Brown and Parsons, 1989). SFS is the strain-free solvus and CS is the coherent solvus. TDT is the twin-domain microtexture and ETDT is the exsolution and the twin-domain microtexture. MA, HA, IA and LA are monoclinic, high, intermediate and low albite; IM and LM are intermediate and low microcline. IA and IM is the region of the rapid change in Y ordering.

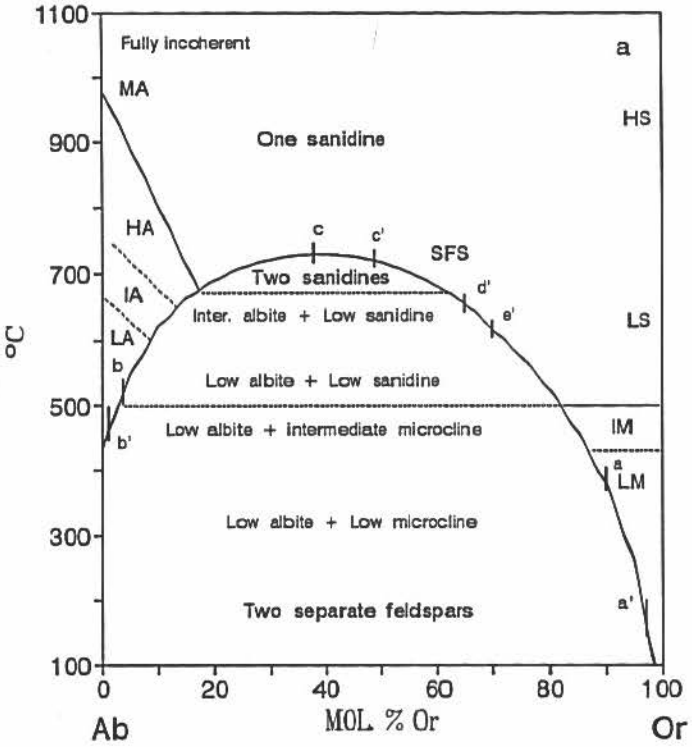

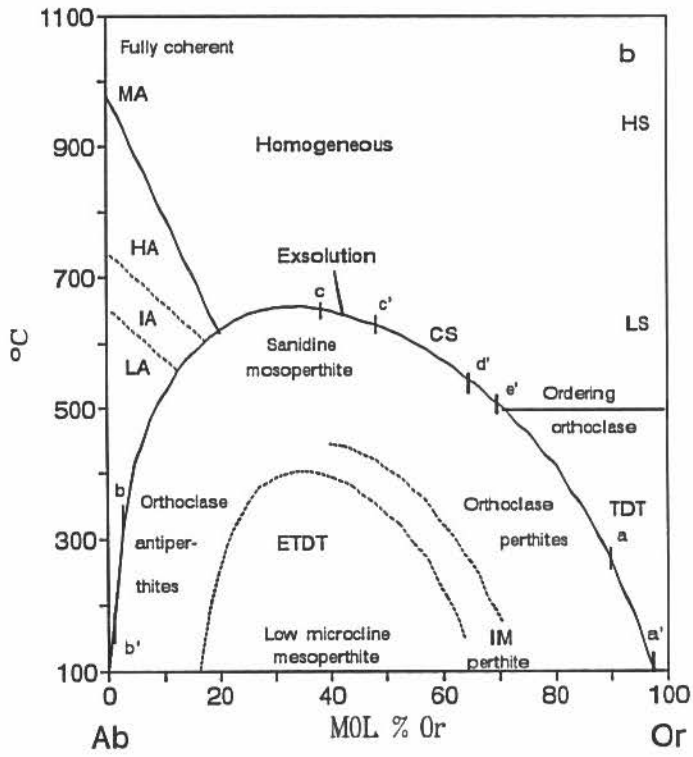

Figure 6.2-22. The evolution of the alkali feldspars in the perthitic nepheline syenite, miaskitic nepheline syenite and in the gabbro from Center II, Neys Park are illustrated in the Or-Ab binary phase diagram.

The path a-a′ is the K-feldspar and b-b′ is Na-feldspar inside the brick-red irregular pegmatitic patches from the perthitic nepheline syenite.

The path c-c′ is the alkali feldspar rim of the oligoclase-alkali feldspar mantled crystals from the miaskitic nepheline syenite. The path c-d′ is the secondary K-rich alkali feldspars in the outer edge of the alkali feldspar rim and in the oligoclase core.

The path e′-a is the secondary K-rich alkali feldspar in the margins of the plagioclase from the gabbro.

Diagram (a) shows the phase relationships for An-free alkali feldspars under complete (incoherent) equilibrium and (b) shows different constrained equilibrium states as a function of bulk composition and T for completed coherent intergrowths (Brown and Parsons, 1989). SFS, CS, TDT, ETDT, MA, HA, IA, LA, HS, LS, IM and LM as in Fig. 6.2-21.

a. Unexsolved alkali feldspar, perthite and microcline in the perthitic nepheline syenite

In the perthitic nepheline syenite, the light violet blue luminescent unexsolved alkali feldspars ($Or_{73-75}Ab_{24-26}An_1$) in the centre of the fine-grained perthite may have formed at temperatures about 575-450 °C between the incoherent (SFS) and the coherent solvus (CS) (Fig. 6.2-21a,b, path a-a′).

The perthite ($Ab_{95-99}Or_{1-2}An_{1-4}$ for the exsolved albite and $Or_{84-93}Ab_{6-15}An_1$ for the host K-feldspar) texture formed during cooling at a temperature below 450 °C under the coherent solvus (Fig. 6.2-21b, paths b-b′ and c-c′).

Along the margins of the perthite, the host K-feldspar may be converted into cross-hatched microcline ($Or_{93-96}Ab_{3-6}An_1$) at a temperature below 300 °C (Fig. 6.2-21, path c′-d′). However, the process which formed of microcline is not very clear, it may be involved with late-stage fluid-feldspar interaction.

b. Two feldspars in the pegmatitic patches from perthitic nepheline syenite

Since no perthitic texture was observed in the pegmatitic patches, the crystallization of K-feldspar and albite may be only considered under the incoherent solvus to produce two unmixed feldspars. The crystallization temperatures of the K-feldspar ($Or_{89-97}Ab_{3-10}An_{<1}$) range from 550 to 500 °C, whereas the albite ($Ab_{97-99}Or_{2-1}An_1$) range from 475 to 300 °C (Fig. 6.2-22a, path a-a′ and b-b′).

c. Secondary feldspars in the perthitic nepheline syenite

Since the secondary antiperthite, perthite ($Ab_{97-98}Or_1An_{2-1}$ and $Or_{97-100}Ab_{0-3}An_{0-1}$) and the secondary albite ($Ab_{97-99}Or_1An_{1-2}$) have end member compositions, they may have formed at a low temperature below 300 °C during late-stage fluid alteration.

d. Alkali feldspar and secondary K-rich feldspar in the miaskitic nepheline syenite

In the miaskitic nepheline syenite, the light blue luminescent alkali feldspar rim ($Ab_{38-48}Or_{49-57}An_{3-6}$) of the oligoclase-alkali feldspar mantled crystals may have crystallized at temperatures ≤725 °C on the incoherent solvus which produce a homogeneous texture (Fig. 6.2-22a,b, path c-c′).

The secondary K-rich feldspar in the outer edge of the alkali feldspar rim and in the oligoclase core may have formed at temperatures about 700-500 °C between both SFS and CS solvus (Fig. 6.2-22a,b, path c′-d′). This temperature range agrees with the secondary K-rich feldspar - nepheline equilibrium temperatures which were determined by the nepheline geothemometer (Fig. 6.2-18).

The secondary K-rich feldspar in the margins of the plagioclase from the gabbro has a wide temperature range from 300-600 °C between both SFS and CS (Fig. 6.2-22a,b, path e′-a).

6.3. Recrystallized nepheline syenites in Center II

The recrystallized nepheline syenites are fine-grained, grey to dark grey rocks which commonly have allotriomorphic granoblastic and porphyroblastic textures. These syenites are mainly distributed in the Redsucker Core-Mink Creek and Pic Island area (Mitchell and Platt, 1982). Feldspars in these nepheline syenites have been recrystallized and consist of alkali feldspar, plagioclase relicts and alkali feldspar neoblasts. Under CL, these feldspars reveal distinct recrystallization textures which are discussed in the following sections.

6.3.1. Feldspars in mosaic granuloblastic nepheline syenite

The mosaic granuloblastic nepheline syenite (Sample C587) is recrystallized and is characterized by well-developed curved triple junctions between felsic and mafic minerals. This recrystallized texture is also described by Mitchell and Platt (1982). When the recrystallization occurred, the original larger grains of felsic minerals developed subgrains and complex serrated boundaries. Grain boundary bulging leads to consumption of larger grains to form smaller neoblast grains. Increasing recrystallization leads to development of a mosaic granuloblastic texture with well-developed triple junctions between crystals with curved boundaries.

The CL properties and compositions characteristic of these feldspars are described in the following sections.

a. Alkali feldspar relicts and neoblasts

Alkali feldspars in the mosaic granuloblastic nepheline syenite show relict magmatic fabrics and metamorphic textures, which are represented by the subhedral alkali feldspar noeblasts replace the lath-shaped alkali feldspar relicts (Fig. 6.3-1a). This replacement usually occurs along the margins of the alkali feldspar relict.

The alkali feldspar relicts and neoblasts are usually difficult to distinguish using a conventional polarizing microscope, but with CL, they reveal clearly distinct luminesecnce colours. The alkali feldspar relict crystals commonly show light blue luminescent colour (Fig. 6.3-1b) with an intensense blue peak at 458 nm, and a low intensity red peak at about 700 nm (Fig. 6.3-2a, spectrum A). The ratio of the I_B/I_R is about 3.67 (Table 6.3-1).

Most alkali feldspar neoblast crystals exhibit light violet blue luminescent colour, and some are slightly zoned with a light violet luminescent core and a light violet blue luminescent rim (Fig. 6.3-1b). The CL spectrum from the core of the neoblast shows that the luminescence intensity of the blue peak and the red peak are nearly the same with the ratio of I_B/I_R is about 1.15 (Fig. 6.3-2b, spectrum A and Table 6.3-1). The CL spectrum from the rim of the neoblasts show that the blue peak is slightly higher than the red peak, and the ratio of I_B/I_R is about 1.41 (Fig. 6.3-2b, spectrum B and Table 6.3-1).

The light blue luminescent alkali feldspar relicts contain 1.27-3.60 wt% Na_2O and 10.02-13.58 wt% K_2O, whereas the light violet blue luminescent alkali feldspar neoblasts contain 2.72-4.98 wt% Na_2O

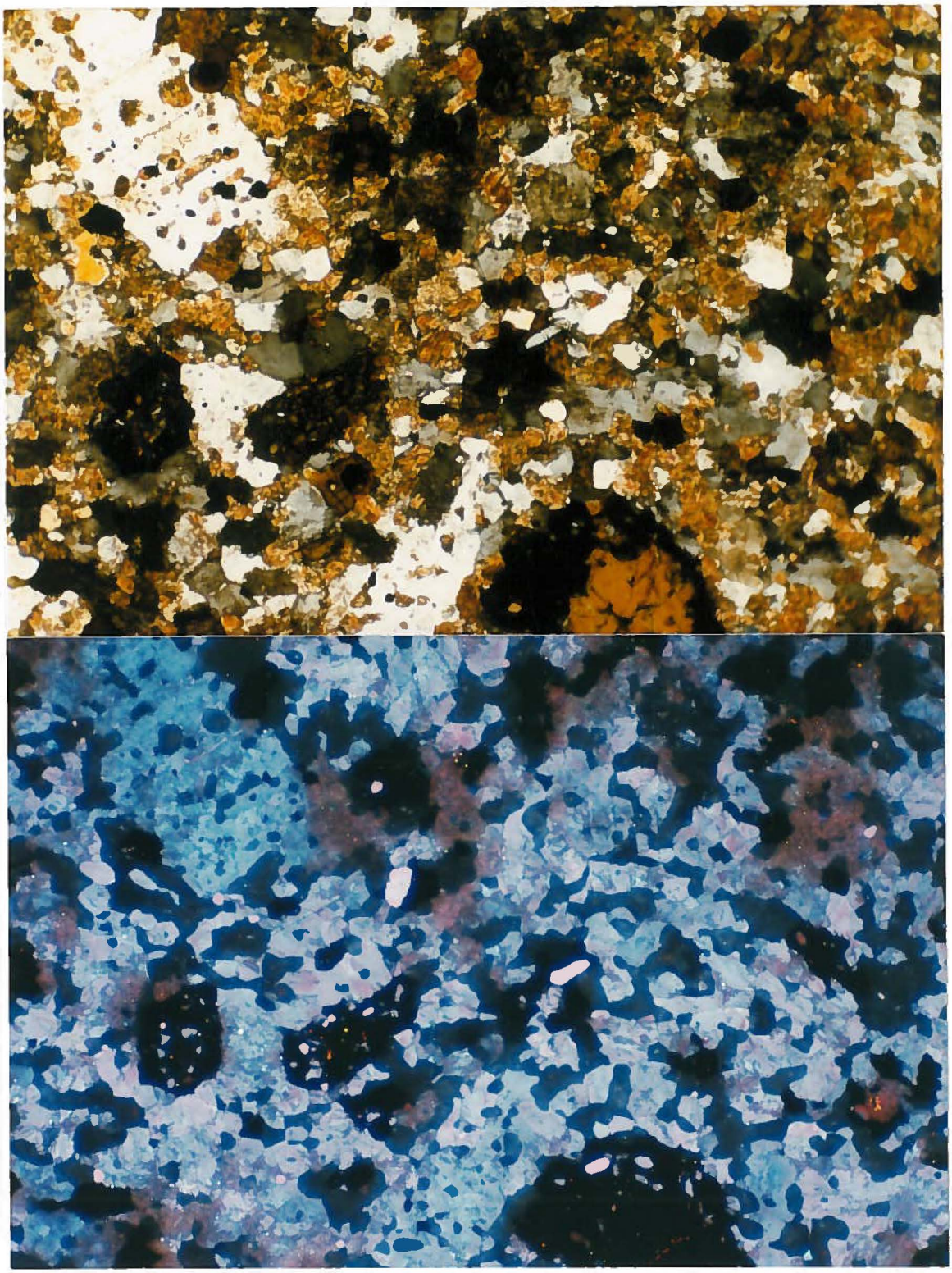

Fig 6.3-1. Alkali feldspar in mosaic granuloblastic nepheline syenite (Sample C587) from Center II, Coldwell Complex, Ontario. a: The lath-shaped alkali feldspar relicts are corroded by the fine-grained, subhedral alkali feldspar neoblasts. TrL (Photographic conditions: 3s, ASA 400). b: CL. The light blue luminescent lath-shaped crystals are the alkali feldspar relicts. The light violet blue luminescent subhedral grains are neoblasts and some of neoblasts are zoned. The pink luminescent fine grains are apatite. Scale: 55 mm on photograph = 1 mm on thin section. (CL conditions: 10 kV, 0.8 mA. Photographic conditions: 3 min, ASA 400).

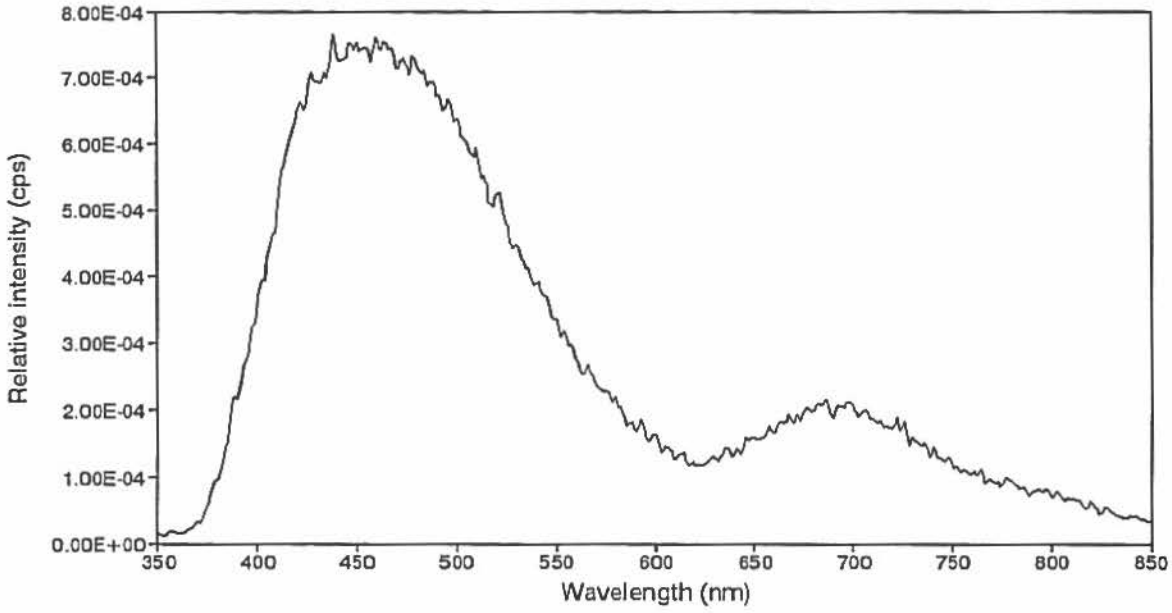

Fig. 6.3-2a. CL spectrum of a light blue luminescent relict alkali feldspar in the mosaic granuloblastic nepheline syenite (Sample C587) from Center II, Coldwell Complex Ontario. CL conditions: 10 kV, 0.8 mA.

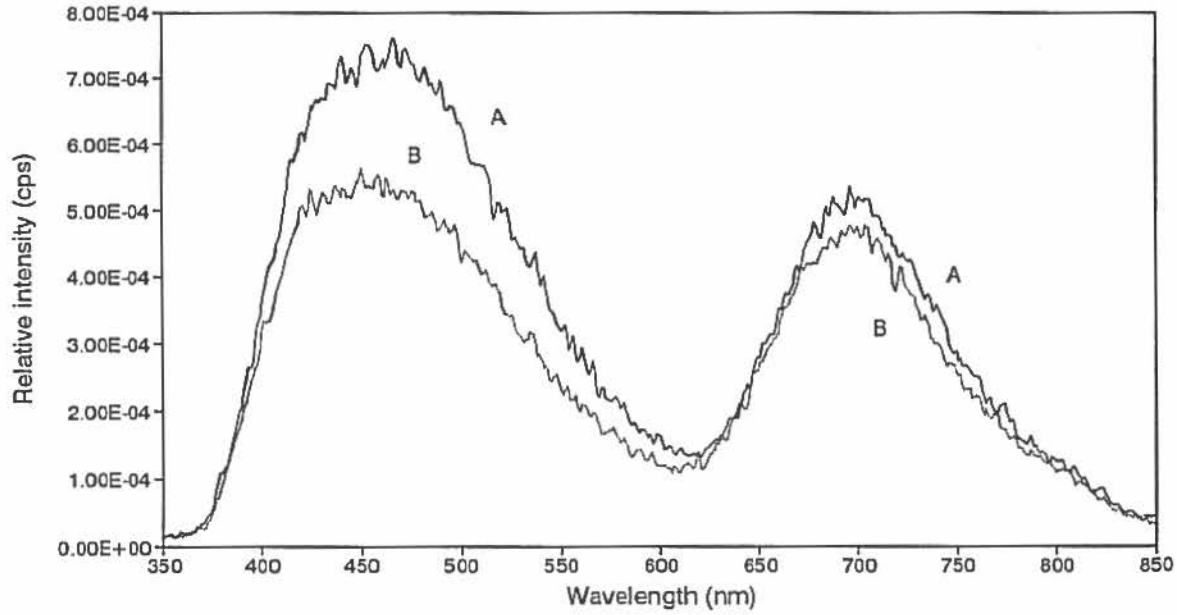

Fig. 6.3-2b. CL spectra of feldspar neoblast in the mosaic granuloblastic nepheline syenite (Sample C587) from Center II, Coldwell Complex, Ontario. (A) is from the light violet luminescent alkali feldspar neoblast core. (B) is from the light violet blue luminescent alkali feldspar neoblast rim. CL conditions: 10 kV, 0.8 mA.

Table 6.3-1. Representative cathodoluminescence properties and compositions of feldspars in recrystallized nepheline syenite from Center II, Coldwell Complex, Ontario

Occurrence of feldspar	Sample No./ spectrum No.	Luminescence colour	Intensities (cps)					Compositions		
			Blue peak	(nm)	Red peak	(nm)	B/R ratio	Or	Ab	An
Mosaic Nepheline Syenite:										
Relict alkali feldspar	C587/A	Light blue	7.56E-04	(461)	2.06E-04	(693)	3.67	64-85	13-35	1-2
Neoblast alkali feldspar, core	C587/B	Light violet	5.35E-04	(455)	4.66E-04	(698)	1.15	57	42	1
Neoblast alkali feldspar, rim	C587/C	Light violet blue	7.27E-04	(463)	5.16E-04	(698)	1.41	62	36	2
Neoblast alkali feldspar	C587	Light violet blue	N/A		N/A			52-71	27-47	1-2
Relict plagioclase	C587	Non CL						1	21-29	70-79
Secondary albite	C587	Dull red	N/A		N/A			1	95-99	1-5
Porphyroblastic Nepheline Syenite:										
Alkali feldspar, core	C571/A	Light blue	1.99E-03	(461)	4.86E-04	(706)	4.10	53-55	40-42	3-5
Alkali feldspar, core	C571/B	Light violet	1.37E-03	(461)	9.50E-04	(700)	1.45	62-69	30-37	1
Alkali feldspar, rim	C571/C	Light violet blue	2.51E-03	(458)	1.08E-03	(700)	2.33	51-60	36-45	2-4
Alkali feldspar, groundmass	C571/D	Light violet blue	1.75E-03	(458)	3.91E-04	(700)	4.47	45-62	35-51	3-5
Albite, core	C267/A	Bright light blue	4.02E-03	(460)	2.94E-04	(704)	13.67	5-7	84-88	7-9
Alkali feldspar, core	C267/B	Light violet blue	1.36E-03	(460)	6.99E-04	(704)	1.95	40-46	52-57	3-4
2nd alkali feldspar, core	C267	Dull blue	N/A		N/A			52-61	33-46	1-5
Alkali feldspar, mantle	C267	Dull blue	N/A		N/A			69-75	25-30	1
Alkali feldspar, inner rim	C267/C	Dull blue	1.40E-03	(460)	1.77E-04	(695)	7.94	52-54	46-47	1
Alkali feldspar, middle rim	C267/D	Light violet blue	1.05E-03	(460)	2.42E-04	(795)	4.32	43-47	51-55	1-3
Alkali feldspar, outer rim	C267/E	Light violet	8.03E-04	(460)	2.91E-04	(795)	2.76	63-66	33-37	1
Plagioclase, core	C572/A	Blue	7.55E-04	(466)	4.28E-04	(707)	1.76	1-2	48-58	42-49
Plagioclase, rim	C572/B	Light violet	3.71E-04	(458)	4.80E-04	(715)	0.77	1-6	66-73	25-33

Table 6.3-1 continued

Porphyroblastic Nepheline Syenite:

Occurrence of feldspar	Sample No./ spectrum No.	Luminescence colour	Intensities (cps)					Compositions		
			Blue peak	(nm)	Red peak	(nm)	B/R ratio	Or	Ab	An
Alkali feldspar, core	C677/A	Light violet blue	4.36E-03	(468)	1.94E-03	(705)	2.24	28-37	59-69	3-4
Alkali feldspar, core	C677	Light violet blue	N/A		N/A			33-43	55-63	1-4
Albite, core	C677/B	Light blue	7.28E-03	(466)	1.35E-03	(705)	5.38	2-5	89-93	4-7
K-feldspar, mantle	C677	Dull blue	N/A		N/A			65-66	33-34	1
Alkali feldspar, inner rim	C677/C	Light violet blue	3.40E-03	(468)	6.37E-04	(700)	5.34	41-56	43-58	1
Alkali feldspar, mid rim	C677/D	Light blue violet	2.06E-03	(474)	5.98E-04	(689)	3.44	39-52	48-60	1-2
Alkali feldspar, outer rim	C677/E	Light violet	1.80E-03	(473)	9.43E-04	(699)	1.91	49-66	34-50	1
2nd K-feldspar, fracture	C677/F	Dull blue	3.00E-03	(473)	8.59E-04	(700)	3.49	83-97	2-16	1

and 8.5-10.82 wt% K_2O (Appendix 2). The alkali feldspar relicts are slightly enriched in K_2O with a compositional range of $Or_{64-85}Ab_{13-35}An_{1-2}$, while the alkali feldspar neoblasts are slightly poorer in K_2O with a compositional range of $Or_{52-71}Ab_{27-47}An_{1-2}$ (Table 6.3-1, Fig 6.3-3a and Appendix 2).

For zoned alkali feldspar neoblasts, the light violet luminescent core has a composition of $Or_{57}Ab_{42}An_1$ and the light violet blue luminescent rim has composition of $Or_{62}Ab_{36}An_2$ (Table 6.3-1). The albite content slightly decreases from the core to the rim.

b. Plagioclase relicts

A few hypidiomorphic plagioclase relicts are found in thin section. The plagioclase relicts have no luminescence and are corroded and surrounded by dull red luminescent albitized feldspar ($Ab_{95-99}Or_1An_{1-5}$) grains in the form of a corona structure. This occurs as a patch in the background of the light violet blue luminescent alkali feldspar. The plagioclase relicts (bytownite) have a range in composition of $An_{70-79}Ab_{21-29}Or_1$ (Table 6.3-1, Fig 6.3-3a and Appendix 2).

6.3.2. Feldspars in porphyroblastic syenites

The porphyroblastic syenites (Samples C571, C572, C573, C267 and C677) are characterized by unusual zoned poikiloblastic textures in the amphibole and alkali feldspar porphyroblasts. The zoned poikiloblastic textures of the feldspars are a result of recrystallization. In transmitted light, the alkali feldspar

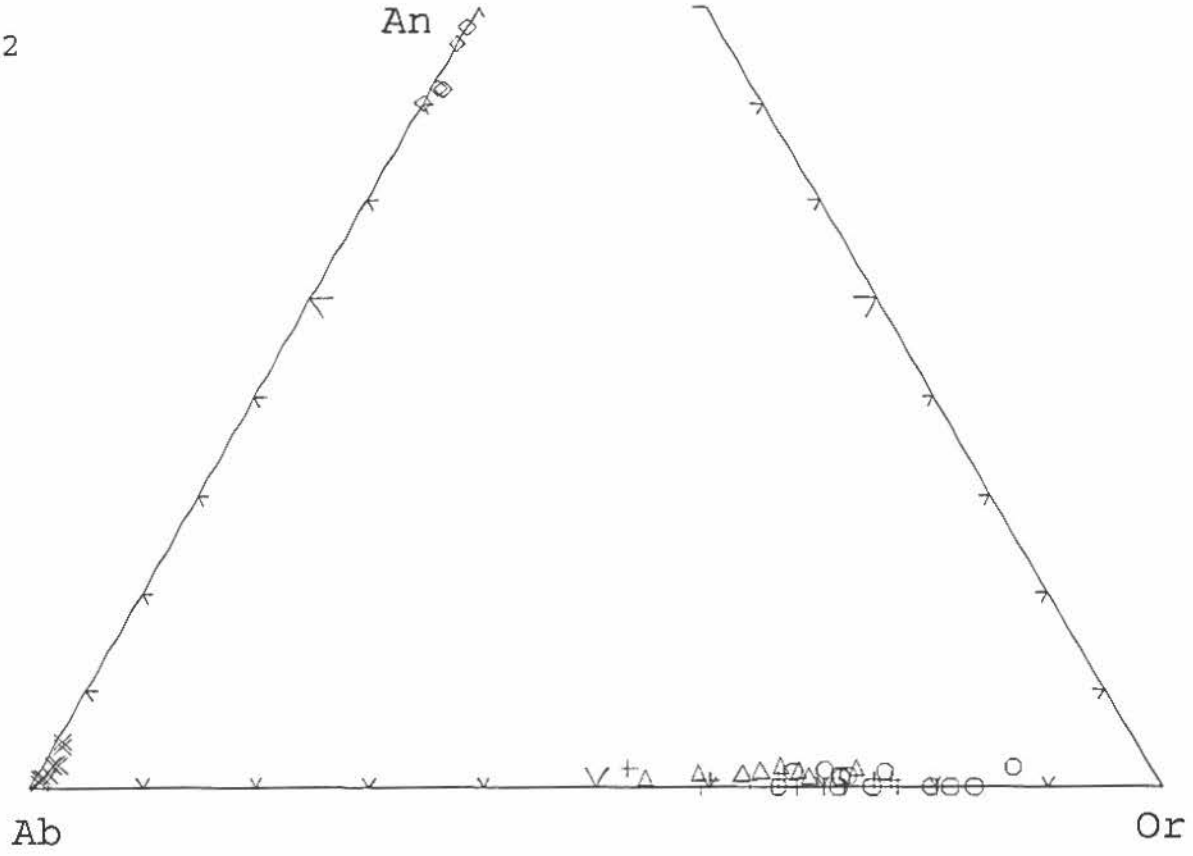

Fig. 6.3-3a. The compositions of feldspars in the mosaic granuloblastic nepheline syenite (Sample C587) plotted in the system Or-Ab-An. The open circles (○) are the light blue luminescent alkali feldspar relicts. The up-triangles (△) are the light violet blue luminescent alkali feldspar neoblasts. The crosses (+) are the alkali feldspar relicts and neoblasts (undivided). The open diamonds (◇) are the plagioclase relicts. The crosses (×) are the dull red luminescent secondary albite.

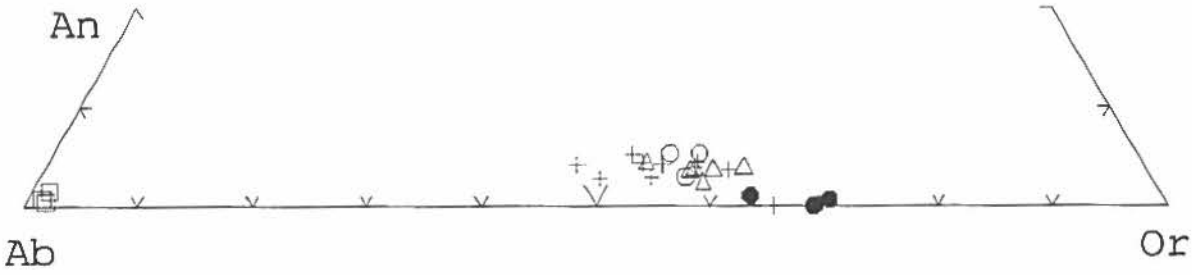

Fig. 6.3-3b. The compositions of alkali feldspar in porphyroblastic nepheline syenite (Sample C571) plotted in the system Or-Ab-An. The filled circles (●) are light violet luminescent alkali feldspar cores and the open circles (○) are light blue luminescent alkali feldspar cores. The up-triangles (△) are the light violet blue luminescent alkali feldspar rims. The crosses (+) are the light violet blue luminescent alkali feldspar groundmass. The squares (□) are the dull blue luminescent secondary Na-K-feldspar in the core.

porphyroblasts commonly show a recrystallized rim and a relict feldspar core (Fig. 6.3-4a). The recrystallized rims are corroded and include many small inclusions of amphibole and sericitized nephline. The groundmass of the porphyroblastic syenites has the same texture as the mosaic granuloblastic syenites.

a. Alkali feldspar porphyroblast

Cores of the alkali feldspar porphyroblast

Usually the cores of the alkali feldspar porphyroblasts are relict feldspars. These relicts exhibit a variety of luminescent colours in each porphyroblastic grain within a thin section. The range of luminescent colours varies from light blue to light violet. Generally, the light blue luminescent feldspar cores are richer in albite content than the light violet luminescent feldspar cores.

The porphyroblastic feldspar crystals (Samples C571, C572) from Redsucker Cove area have light blue to light violet luminescent cores (Fig. 6.3-4,-5,-6). The CL spectrum of the light blue luminescent core consists of a high blue peak at 461 nm and a low red peak at 706 nm with a ratio of I_B/I_R of about 4.10 (Fig. 6.3-7a, spectrum A and Table 6.3-1). The light violet luminescent core has a relatively lower blue peak, and a relatively higher red peak than the light blue luminescent core. The ratio of I_B/I_R is about 1.45 (Fig. 6.3-7a, spectrum B; Table 6.3-1). The light blue luminescent cores have the composition of $Or_{43-49}Ab_{46-49}An_{5-7}$, and the light violet luminescent cores have the composition of $Or_{53-55}Ab_{40-42}An_{3-5}$

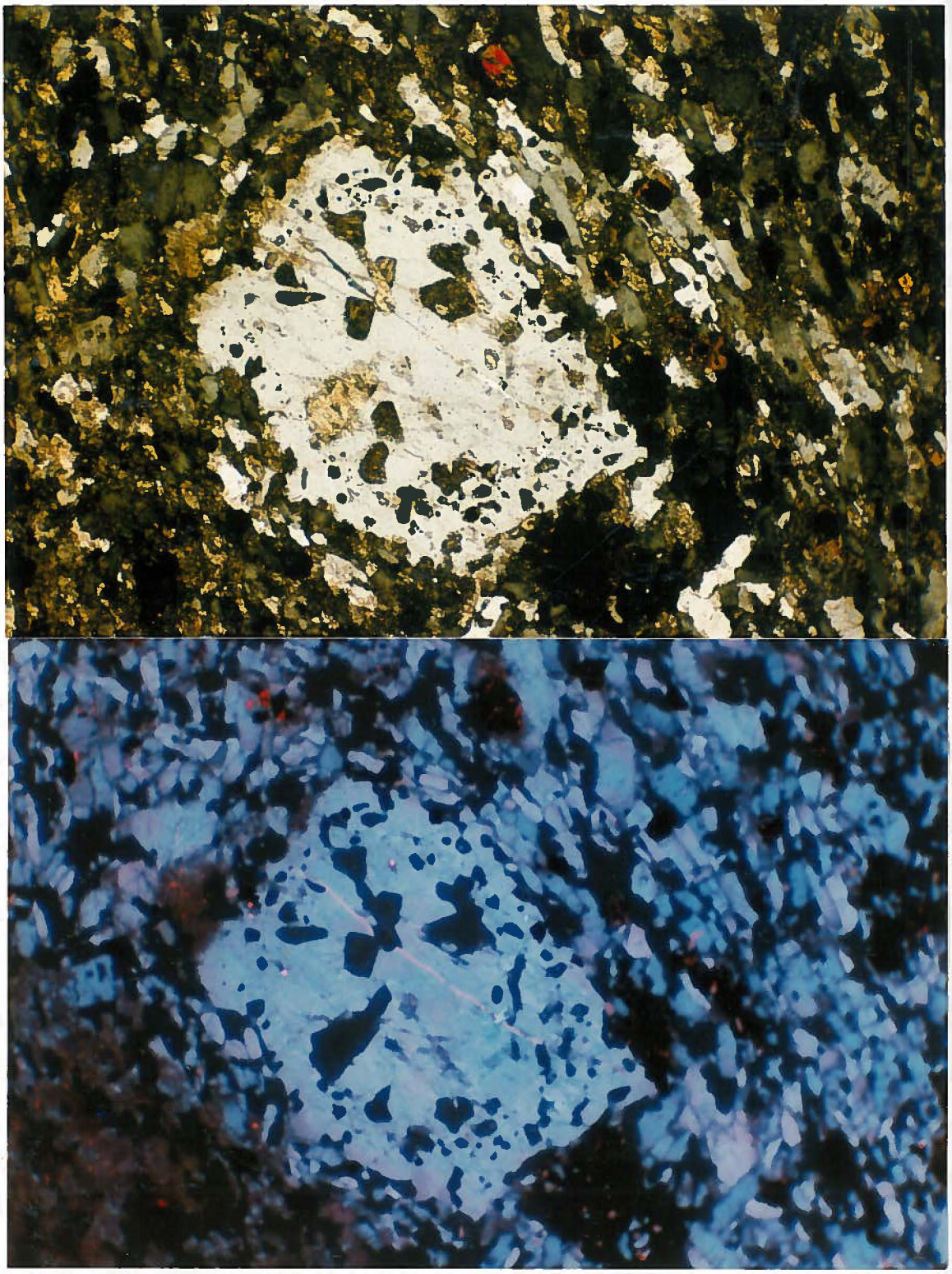

Fig. 6.3-4. Alkali feldspar in the porphyroblastic nepheline syenite (Sample C571) from Center II, Redsucker Cove, Coldwell Complex. a. TrL. The feldspar porphyroblast has an alkali feldspar relict core and a recrystallized rim which included many small grains of sericitized nepheline. (Photographic conditions: 8 s, ASA 400) b. CL. The porphyroblast feldspar reveals light violet blue luminescence. The groundmass of the feldspar reveals dull blue or light violet blue luminescence. Scale: 55 mm on photograph = 1 mm on thin section. (CL conditions: 10 kV, 0.8 Am. Photographic conditions: 1.8 min, ASA 400).

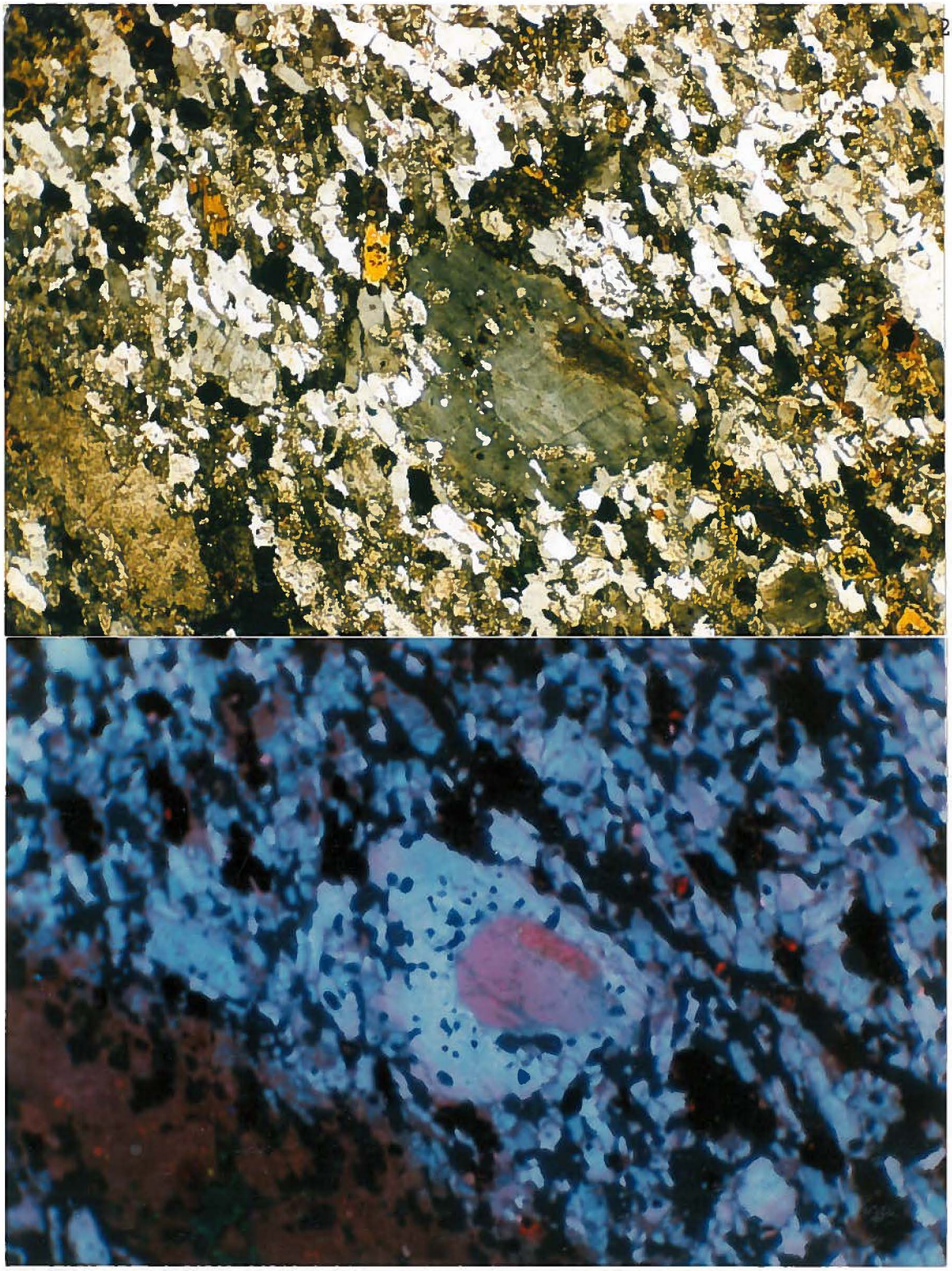

Fig. 6.3-5. Alkali feldspar in the porphyroblastic nepheline syenite (Sample C571) from Center II, Redsucker Cove, Coldwell Complex. a. TrL. The feldspar porphyroblast has an alkali feldspar relict core and a recrystallized rim which has included many small grains of the sericitized nepheline. (Photographic conditions: 8 s, ASA 400) b. CL. The relict core reveals light violet luminescence and the recrystallized rim reveals light violet blue luminescence. The groundmass of the feldspar reveals dull blue or light violet blue luminescence. Scale: 55 mm on photograph = 1 mm on thin section. (CL conditions: 10 kV, 0.8 Am. Photographic conditions: 1.8 min, ASA 400).

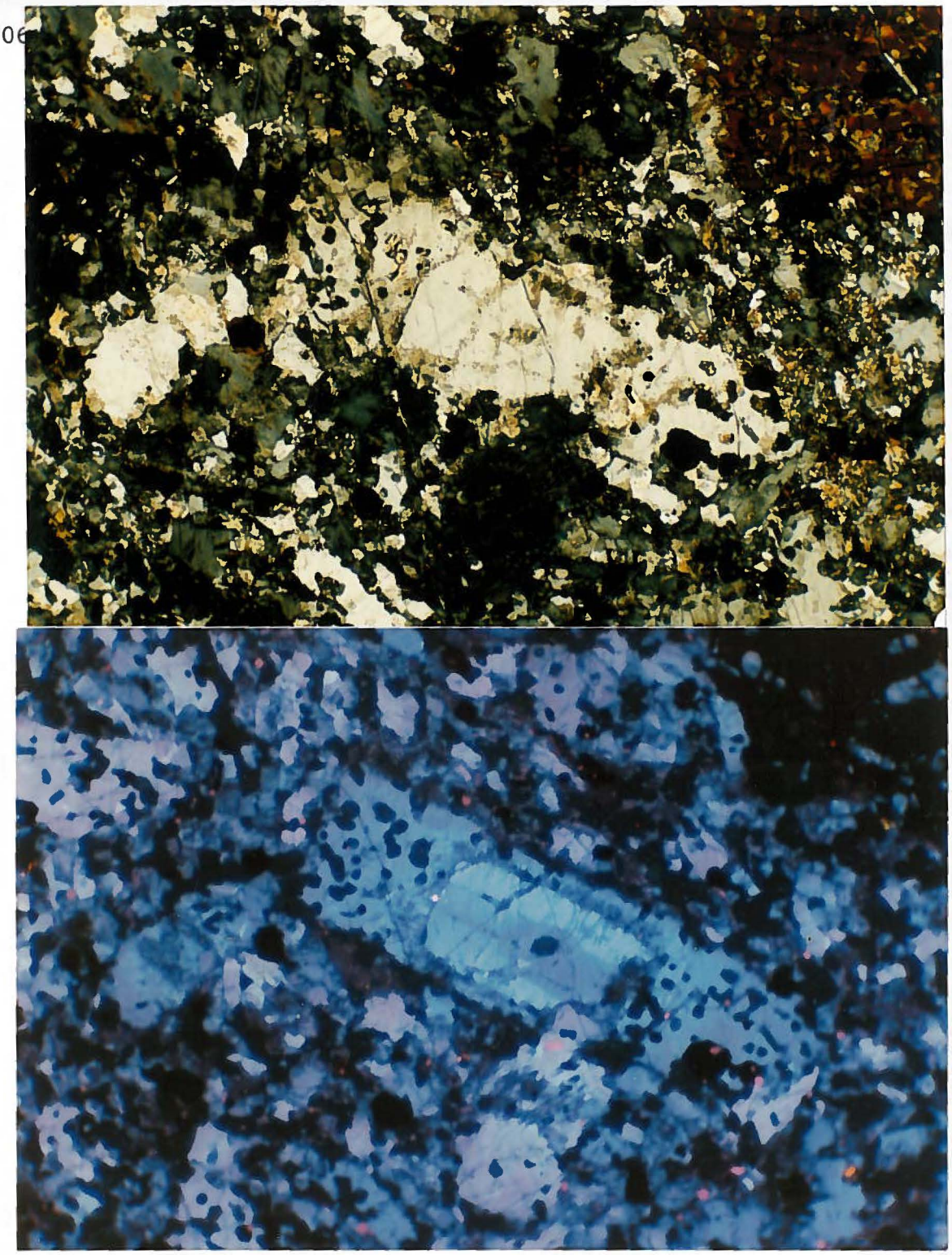

Fig. 6.3-6. Alkali feldspar in the porphyroblastic nepheline syenite (Sample C572) from Center II, Redsucker Cove, Coldwell Complex. a. TrL. The feldspar porphyroblast has an alkali feldspar relict core and a narrow mantle with K-feldspar and oligoclase intergrowths, and a recrystallized alkali feldspar rim. (Photographic conditions: 8 s, ASA 25) b. CL. The relict core reveals light blue luminescence and the centre of the core reveals light violet blue luminescence. The mantle reveals dull blue luminescence and the rim reveals light violet blue luminescence. The groundmass of the feldspar reveals dull blue or light violet blue luminescence. Scale: 55 mm on photograph = 1 mm on thin section. (CL conditions: 10 kV, 0.8 Am. Photographic conditions: 1.2 min, ASA 400).

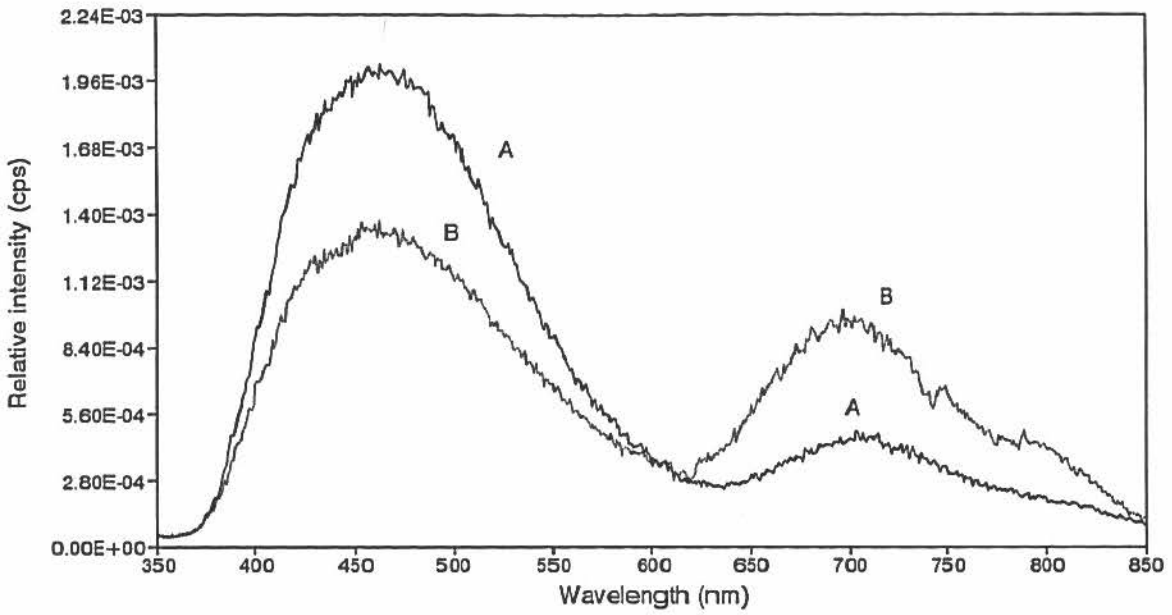

Fig. 6.3-7a. CL spectra of the feldspar relict core of the porphyroblast in the porphyroblastic nepheline syenite (Sample C571) from Center II, Redsucker Cove, Coldwell Complex Ontario. (A) is from a light blue luminescent alkali feldspar relict core. (B) is from a light violet luminescent alkali feldspar relict core. CL conditions: 10 kV, 0.8 mA.

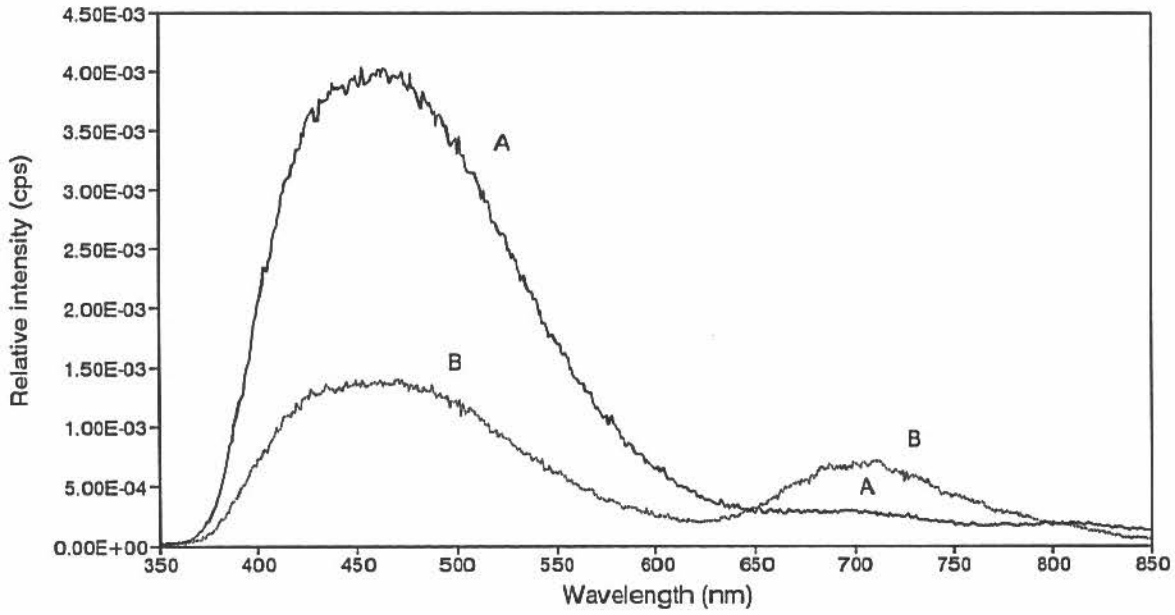

Fig. 6.3-7b. CL spectra of feldspar relict core of a porphyroblast in the porphyroblastic nepheline syenite (Sample C267) from Center II, Pic Island, Coldwell Complex, Ontario. (A) is from very bright light blue luminescent albite relict core. (B) is from the light violet blue luminescent alkali feldspar relict core. CL conditions: 10 kV, 0.8 mA.

(Table 6.3-1, Fig. 6.3-3b,-8a and Appendix 2).

The porphyroblastic feldspar crystals from Pic Island (Sample C267) contain very bright light blue luminescent cores (Fig. 6.3-9b) and some light violet blue luminescent cores (Fig. 6.3-10b). The CL spectrum of the very bright, light blue luminescent core consists of a very high blue peak at 460 nm and a very weak red peak at 704 nm, and the ratio of I_B/I_R is about 13.67 (Fig. 6.3-7b, spectrum A; Table 6.3-1). The light violet blue luminescent core consists of a low blue peak at 460 nm and a high red peak at 704 nm, the ratio of I_B/I_R is about 1.95 (Fig. 6.3-7b, spectrum B; Table 6.3-1). The very bright, light blue luminescent core is an albite with a composition of Ab_{84-88} Or_{5-7} An_{7-9}, and the light violet blue luminescent core is an alkali feldspar with a composition of Or_{40-46} $Ab_{52-57}An_{3-4}$ (Table 6.3-1, Fig 6.3-8b and Appendix 2). This alkali feldspar core has a similar composition and luminecent colour as the cores from the Redsucker Cove area.

The porphyroblastic feldspar crystals (Sample C677) from the western margin of Center II shows an alkali feldspar relict core with no twinning in transmitted light (Fig. 6.3-11a). Under the CL, the centre of the core reveals a homogeneous light violet blue luminescent which is unexsolved alkali feldspar, and the margins of the core shows a perthite texture (Fig. 6.3-11b). The perthite texture consists of light violet blue luminescent Na-rich feldspar stripes and alternating with light bluish violet K-rich feldspar stripes. Very bright, light blue luminescent albite occurs along the edges of the core.

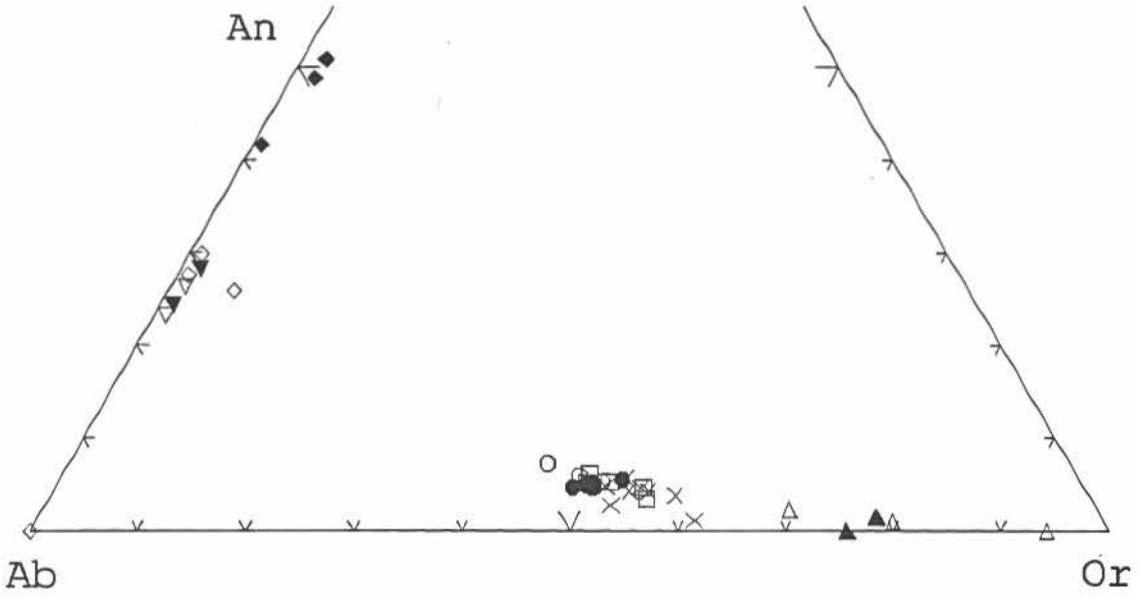

Fig. 6.3-8a. The compositions of feldspars in the porphyroblastic nepheline syenite (Sample C572) from Center II, Redsucker Cove, Coldwell Complex plotted in the system Or-Ab-An. For the alkali feldspar porphyroblast, the open circles (○) are the light blue luminescent alkali feldspar relict cores and the filled circles (•) are the light violet blue luminescent alkali feldspar in the centre of the core. The up-triangles (▵) are the dull blue luminescent K-feldspar and the down-triangles (▿) are the light blue luminescent oligoclase in the mantle. The squares (□) are the light blue luminescent recrystallized alkali feldspar rims.

For the plagioclase relicts, the filled diamonds (♦) are the blue luminescent andesine cores and the open diamonds (◇) are the light violet luminescent oligoclase rims.

The crosses (×) are the light violet blue luminescent alkali feldspar groundmass and filled up-triangles (▴) are the dull blue luminescent secondary K-feldspar and filled down-triangles (▾) are light blue luminescent secondary oligoclase in the margins of the alkali feldspar groundmass.

Fig. 6.3-8b. The compositions of feldspars in the porphyroblastic nepheline syenite (Sample C267) from Center II, Pic Island, Coldwell Complex plotted in the system Or-Ab-An. The filled circles (•) are the light blue luminescent albite relict core and the open circles (○) are light violet blue luminescent alkali feldspar relict core. The open diamonds (◇) are the secondary alkali feldspar in the core.

The up-triangles (▵) are the dull blue luminescent K-feldspar and the down-triangles (▿) are light blue luminescent Na-feldspar in the mantle.

The asterisks (*) are the light violet luminescent recrystallized alkali feldspar rim (undivided). The filled squares (■) are the dull blue luminescent recrystallized alkali feldspar inner rim and half-filled squares (◫) are the light violet blue luminescent recrystallized alkali feldspar intermediate rim and open squares (□) are the light violet luminescent recrystallized alkali feldspar outer rim.

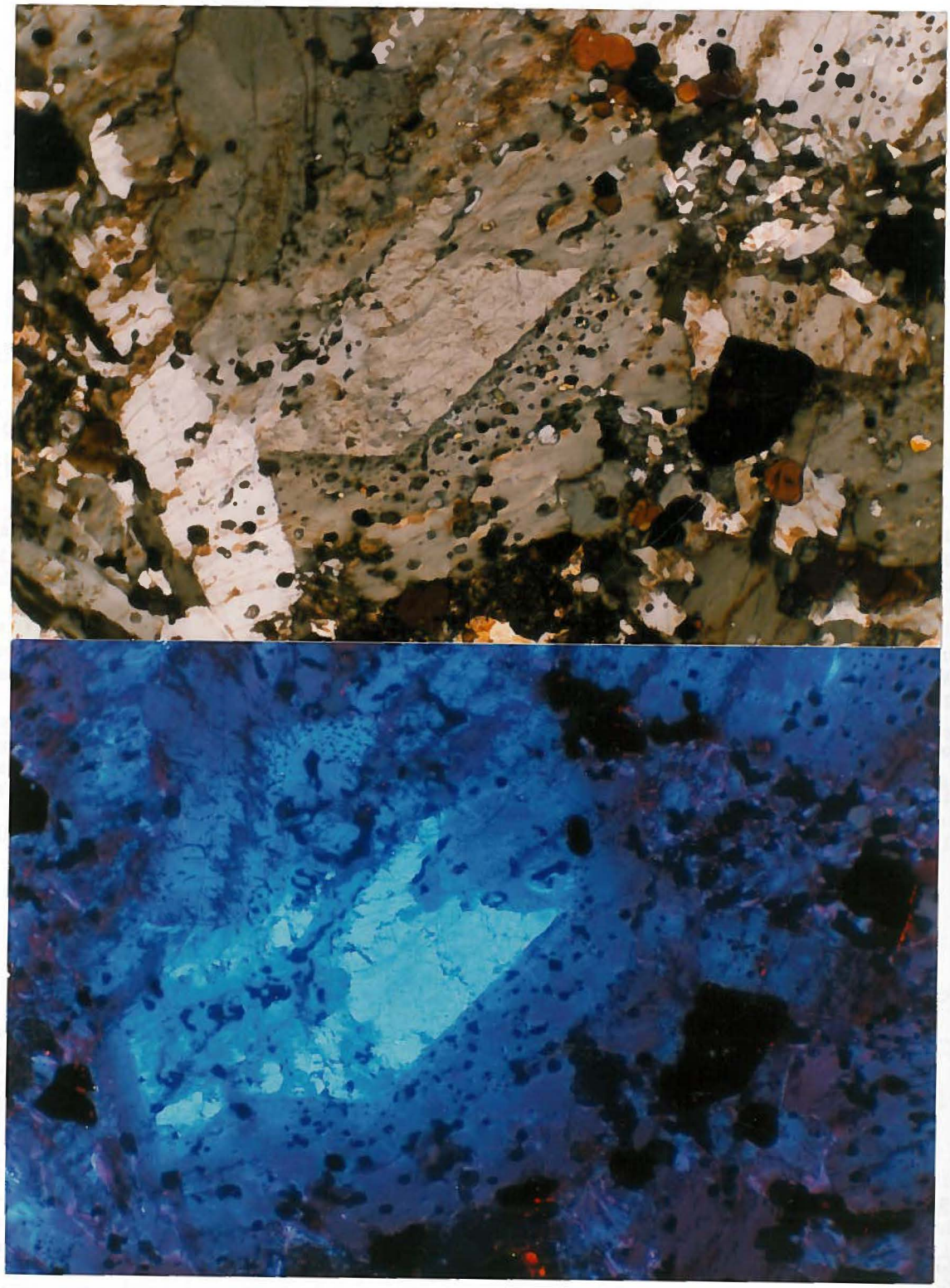

Fig. 6.3-9. Alkali feldspar in the porphyroblastic nepheline syenite (Sample C267) from Center II, Pic Island, Coldwell Complex. a. TrL. The feldspar porphyroblast has an albite relict core and a K-feldspar narrow mantle and a recrystallized alkali feldspar rim. (Photographic conditions: 3 s, ASA 400) b. CL. The albite relict core reveals a very bright light blue luminescence. The mantle reveals dull blue luminescence and the rim reveals light violet blue luminescence. The groundmass of the feldspar reveals light violet blue or light violet luminescence. Scale: 55 mm on photograph = 1 mm on thin section. (CL conditions: 10 kV, 0.8 Am. Photographic conditions: 1.8 min, ASA 400).

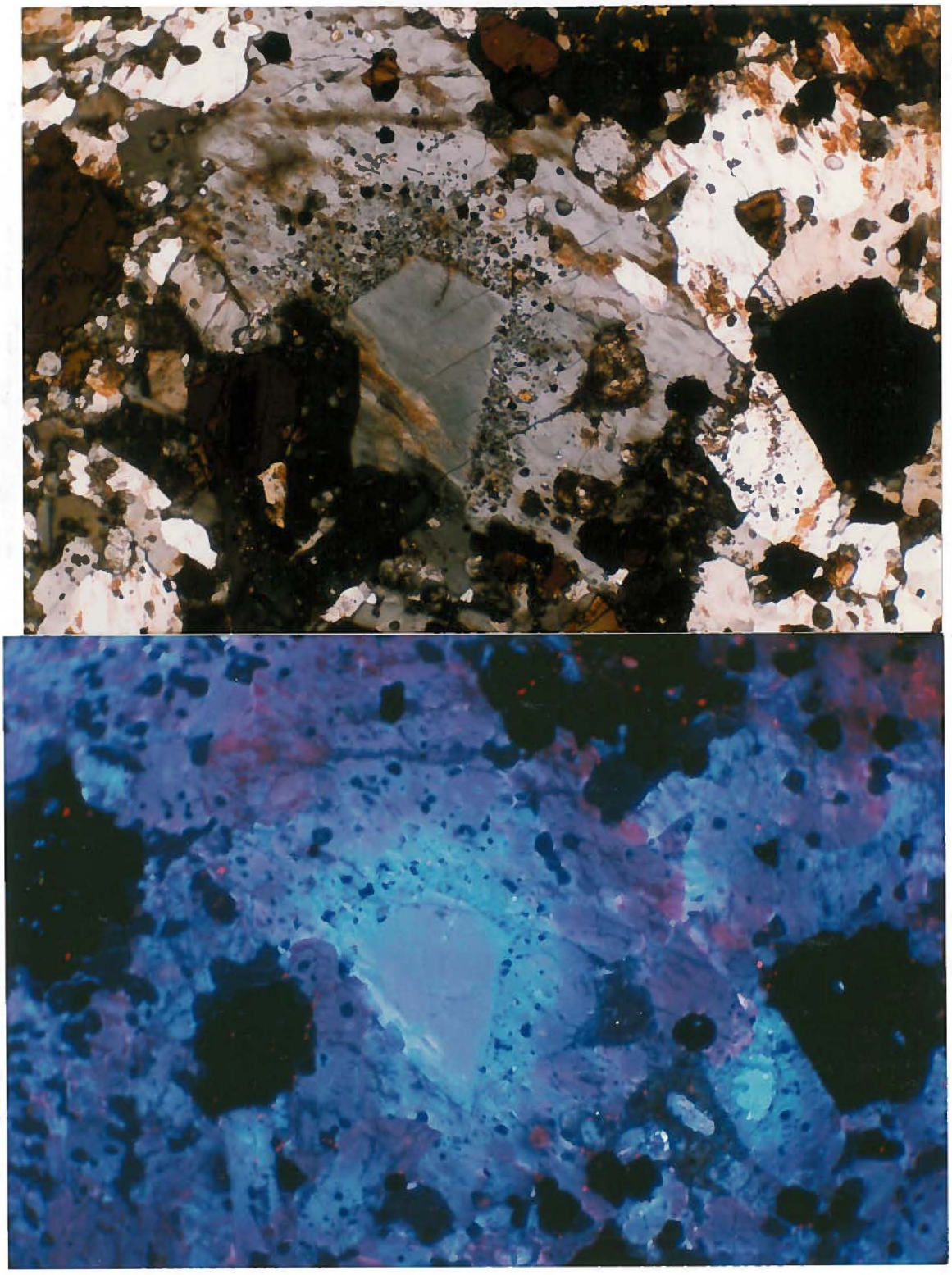

Fig. 6.3-10. Alkali feldspar in the porphyroblastic nepheline syenite (Sample C267) from Center II, Pic Island, Coldwell Complex. a. TrL. The feldspar porphyroblast has an alkali relict core and a narrow mantle with K-feldspar and Na-feldspar intergrowths, and a recrystallized alkali feldspar rim. (Photographic conditions: 3 s, ASA 400) b. CL. The relict core reveals light violet blue luminescence. The mantle reveals dull blue luminescence. The inner rim reveals dull blue luminescence and the intermediate rim reveals light violet blue luminescence and the outer rim reveals light violet luminescence. The groundmass of the feldspar reveals light violet blue or light violet luminescence. Scale: 55 mm on photograph = 1 mm on thin section. (CL conditions: 10 kV, 0.8 Am. Photographic conditions: 2 min, ASA 400).

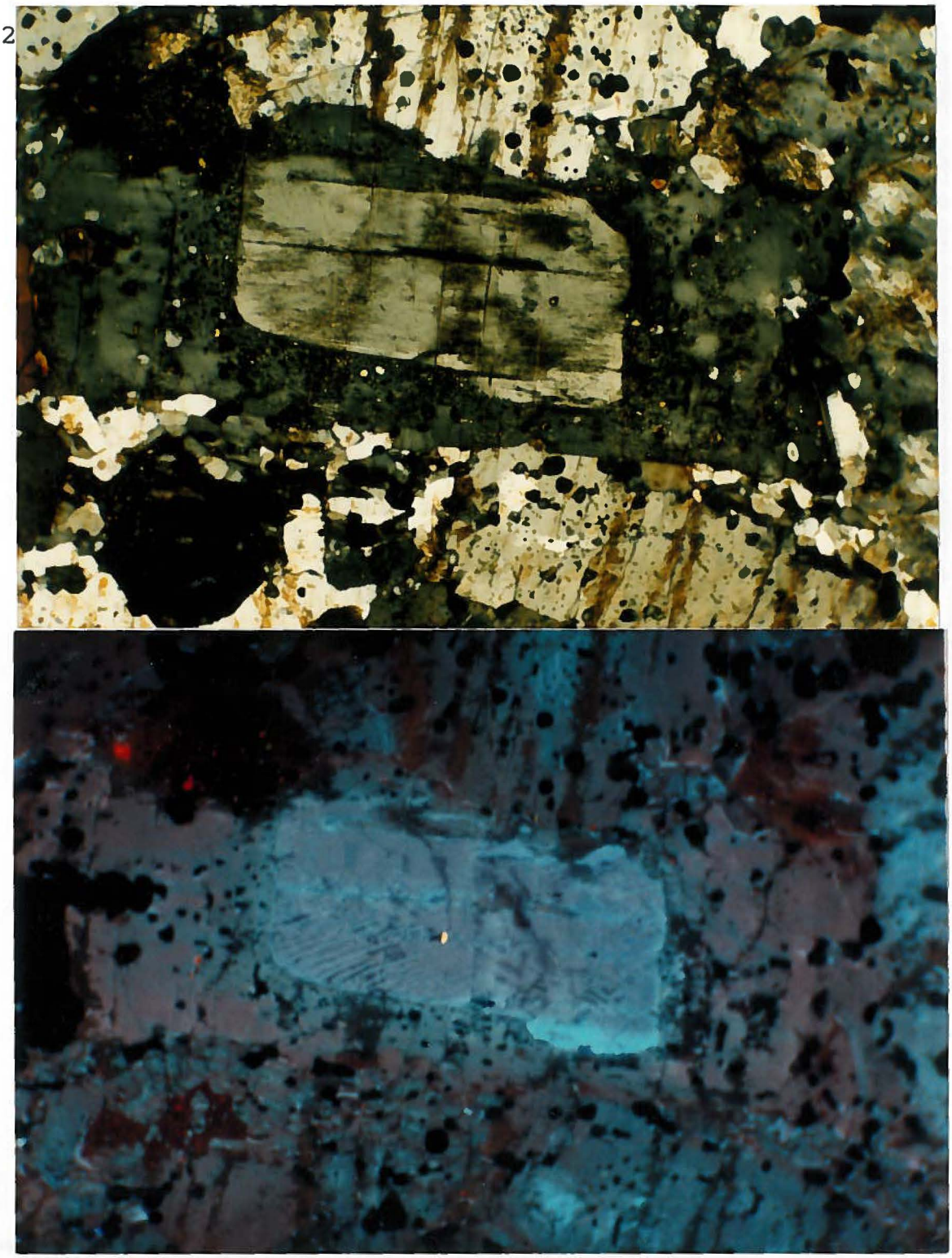

Fig. 6.3-11. Alkali feldspar in the porphyroblastic nepheline syenite (Sample C677) from the western margin of Center II, Coldwell Complex. a. TrL. The feldspar porphyroblast has an alkali feldspar relict core and a recrystallized rim. (Photographic conditions: 8 s, ASA 25) b. CL. In the relict core, the homogeneous light violet blue luminescent areas are the unexsolved alkali feldspar, and the light violet blue luminescent stripes are the Na-rich feldspar and the light bluish violet stripes are the K-rich feldspar. The recrystallized alkali feldspar rim reveals a dull blue luminescence in the inner rim and a light violet in the outer rim. Scale: 55 mm on photograph = 1 mm on thin section. (CL conditions: 10 kV, 0.8 Am. Photographic conditions: 3 min, ASA 400).

The CL spectrum of the light violet blue unexsolved alkali feldspar in the relict core, consists of a blue peak at 468 nm and a red peak at 705 nm, the ratio of I_B/I_R is about 2.24 (Fig. 6.3-12, spectrum A and Table 6.3-1). The CL spectrum of the very bright, light blue luminescent albite consists of a high blue peak at 466 nm and a low red peak at 705 nm, the ratio of I_B/I_R is about 5.38 (Fig. 6.3-12, spectrum B and Table 6.3-1). The light violet blue luminescent relict core has a range in composition of $Or_{28-37}Ab_{59-69}An_{3-4}$ (Fig. 6.3-13). The light violet blue luminescent Na-rich feldspar stripes of the perthite exsolution have a range in composition of $Ab_{89-93}Or_{2-5}An_{4-7}$, whereas the light bluish violet luminescent K-rich feldspar stripes have a range in composition of $Or_{33-43}Ab_{55-63}An_{1-4}$ (Table 6.3-1, Fig 6.3-13 and Appendix 2).

Mantles of the alkali feldspar porphyroblast The porphyroblastic feldspar crystals usually have a very narrow dull blue luminescent zone around the relict cores (Fig 6.3-6b, -9b, -11b). Because this zone is very narrow, CL spectra could not be obtained. Most of the dull blue luminescent zone is a K-rich feldspar with a composition of $Or_{65-75}Ab_{25-34}An_1$ (Table 6.3-1, Fig. 6.3-8b, -13 and Appendix 2). This K-rich feldspar is commonly hematitized. Generally, the hematite is very fine grained with a grain size of about 1-2 microns. Some mantles are intergrowths of K-rich feldspar ($Or_{68-94}Ab_{6-30}An_{1-2}$) with albite ($Ab_{87-90}Or_{10-5}An_{3-5}$) or oligoclase ($Ab_{73-77}An_{22-25}Or_1$) (Fig. 6.3-8b, -8b and Appendix 2). Hematitization in the albite and the oligoclase is much less than in the K-rich feldspar.

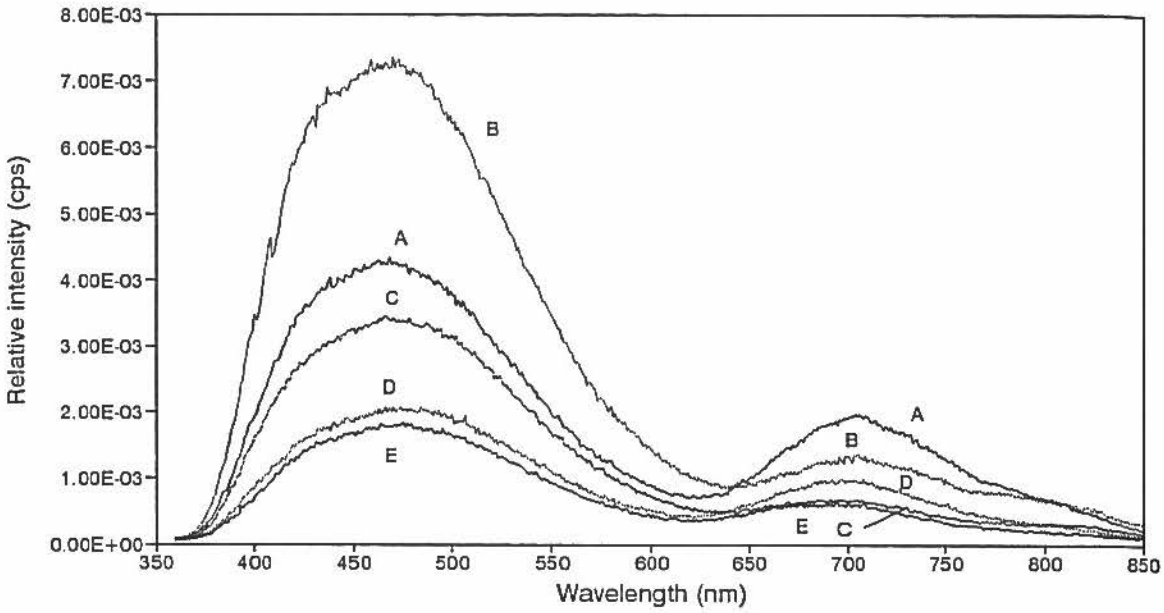

Fig. 6.3-12. CL spectra of alkali feldspar of a porphyroblast in the porphyroblastic nepheline syenite (Sample C677) from the western margin of Center II, Coldwell Complex Ontario. (A) is from the light violet blue luminescent relict core. (B) is from the light blue luminescent albite along the edges of the core. (C) is from the dull blue luminescent inner rim. (D) is from the light violet blue luminescent intermediate rim. (E) is from the light violet luminescent outer rim. CL conditions: 10 kV, 0.8 mA.

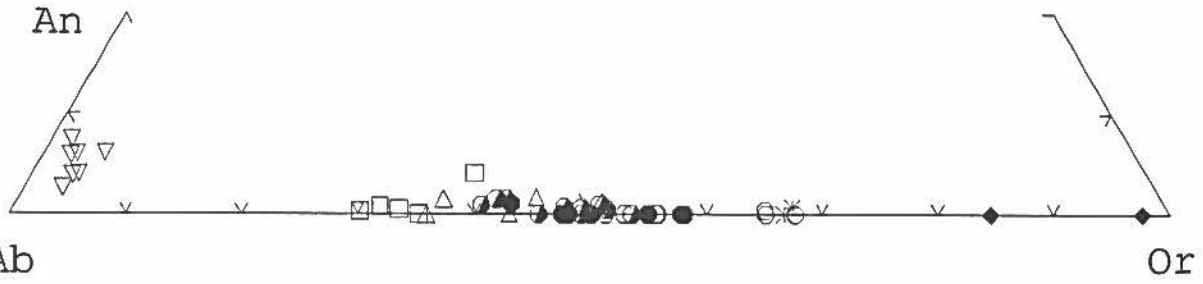

Fig. 6.3-13. The compositions of alkali feldspar in the porphyroblastic nepheline syenite (Sample C677) from the western margin Center II, Coldwell Complex plotted in the system Or-Ab-An. The squares (□) are the light violet blue luminescent alkali feldspar core. The up-triangles (▵) are the light bluish violet luminescent K-rich feldspar stripes and the down-triangles (▿) are the light violet blue luminescent Na-rich feldspar stripes in the core which form the polysynthetic twinning texture. The asterisks (*) are the dull blue luminescent K-feldspar mantle.

The open circles (○) are the dull blue luminescent recrystallized alkali feldspar inner rim and the half-filled circles (◐) are the light violet blue luminescent recrystallized alkali feldspar intermediate rim. The filled circles (•) are the light violet luminescent recrystallized alkali feldspar outer rim.

The filled diamonds (◆) are the dull blue luminescent secondary K-feldspar in the fracture.

Recrystallized rims of the alkali feldspar porphyroblast In the recrystallized alkali feldspar rims near the mantle, many small euhedral to subhedral grains of the sericitized nepheline, amphibole and magnetite occur as inclusions (Fig. 6.3-9, -10). These minerals inclusions are formed during the early stages of recrystallization.

The recrystallized alkali feldspar rims generally reveal a dull blue, light violet blue and light violet luminescence from the inner rims through to the intermediate areas of the rim to the outer rims respectively (Fig. 6.3-5b, -6b, -9b, -10b, -11b). The CL spectra analyses show that this luminescence trend is due to the gradual decrease in the blue peak intensity and the increase in the red peak intensity (Fig. 6.3-14a and Table 6.3-1). For example, the CL spectra of the sample C267 shows that the blue peaks gradually decrease and the red peaks gradually increase from the dull blue luminescent inner rim through to the light violet blue luminescent intermediate rim to the light violet luminescent outer rim. The ratios of I_B/I_R decreased from 7.94, 4.32 to 2.76, respectively.

All of the recrystallized rims are unexsolved alkali feldspar which range in composition from $Or_{45-65}Ab_{34-53}An_{1-2}$ for all of analyzed samples (Table 6.3-1, Fig. 6.3-3b, -8a, -8b, -13 and Appendix 2), and have a more uniform composition than those of the cores. However, there is a small fluctuation in composition occurring within the recrystallized rim. For example, from the dull blue luminescent inner rim through to the light violet blue luminescent intermediate rim to the light violet luminescent outer rim,

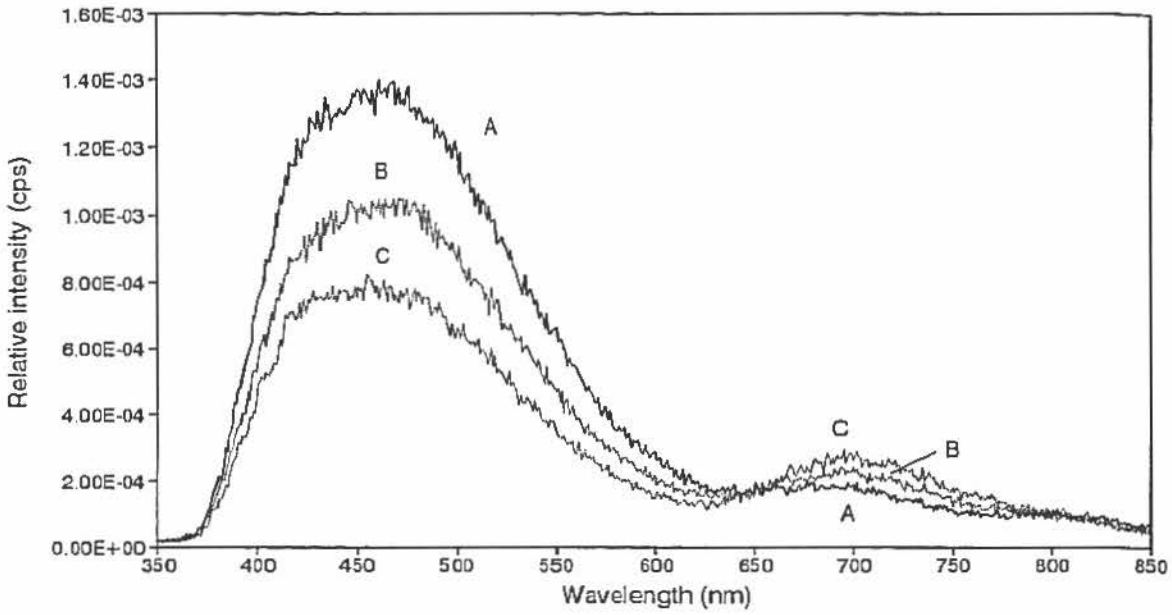

Fig. 6.3-14a. CL spectra of the recrystallized alkali feldspar rim of the porphyroblast in the porphyroblastic nepheline syenite (Sample C267) from Center II, Pic Island, Coldwell Complex Ontario. (A) is from the dull blue luminescent inner rim. (B) is from the light violet blue luminescent intermediate rim. (C) is from the light violet luminescent outer rim. CL conditions: 10 kV, 0.8 mA.

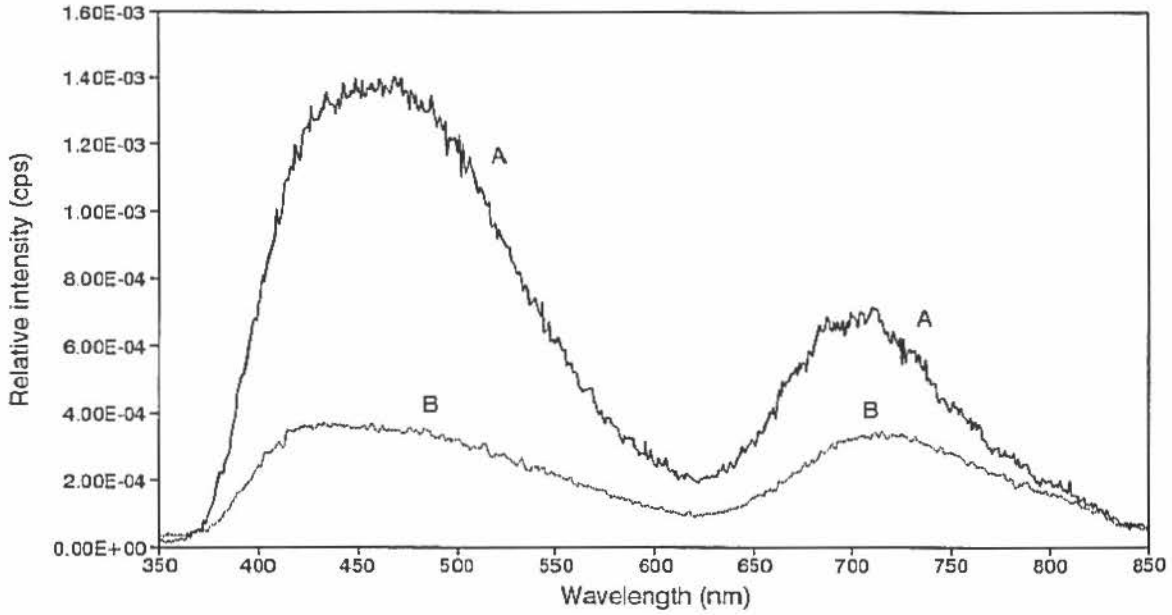

Fig. 6.3-14b. CL spectra of a plagioclase relict in the porphyroblastic nepheline syenite (Sample C572) from Center II, Pic Island, Coldwell Complex, Ontario. (A) is from the blue luminescent andesine core. (B) is from the light violet luminescent oligoclase rim. CL conditions: 10 kV, 0.8 mA.

the corresponding change in compositions is from ($Or_{52-54}Ab_{46-47}An_1$) to ($Or_{42-47}Ab_{51-53}An_{1-3}$) to ($Or_{63-66}Ab_{32-37}An_1$) respectively (Table 6.3-1, Fig. 6.3-8b). Note that the recrystallized feldspar rims ($Or_{48-60}Ab_{36-47}Ab_{2-6}$) in the Pic Island area are slightly richer in Or and An contents than the recrystallized rims ($Or_{43-66}Ab_{33-55}Ab_{1-3}$) in the Redsucker Cove area (Appendix 2).

b. Plagioclase porphyroblast

There are only a few idiomorphic plagioclase relict clusters which occur in the groundmass of the porphyroblastic syenites (Fig. 6.3-15a). In transmitted light, the plagioclase is colourless and contains no inclusions. The plagioclase is Carlsbad twinned, but apparently lacks albite polysynthetic twinning.

The CL reveals that plagioclase relicts are actually albite twinned, and are zoned with small, blue luminescent colour cores and larger, light violet luminescent rims (Fig. 6.3-15b). For the light blue luminescent core, the CL spectrum shows that the blue peak is twice as high as the red peak, and the ratio of I_B/I_R is about 1.76 (Table 6.3-1 and Fig. 6.3-14b). For the light violet luminescent rim, the CL spectrum shows that the blue peak is nearly equal high to the red peak, and the ratio of I_B/I_R is about 0.77. The total luminescence intensity of the plagioclase is much lower than of the alkali feldspar.

The blue luminescent core is andesine with a composition of $An_{42-49}Ab_{48-58}Or_{1-2}$ and the light violet luminescent rim is oligoclase with a composition of $An_{25-33}Ab_{66-73}Or_{1-6}$ (Table 6.3-1, Fig. 6.3-8a and

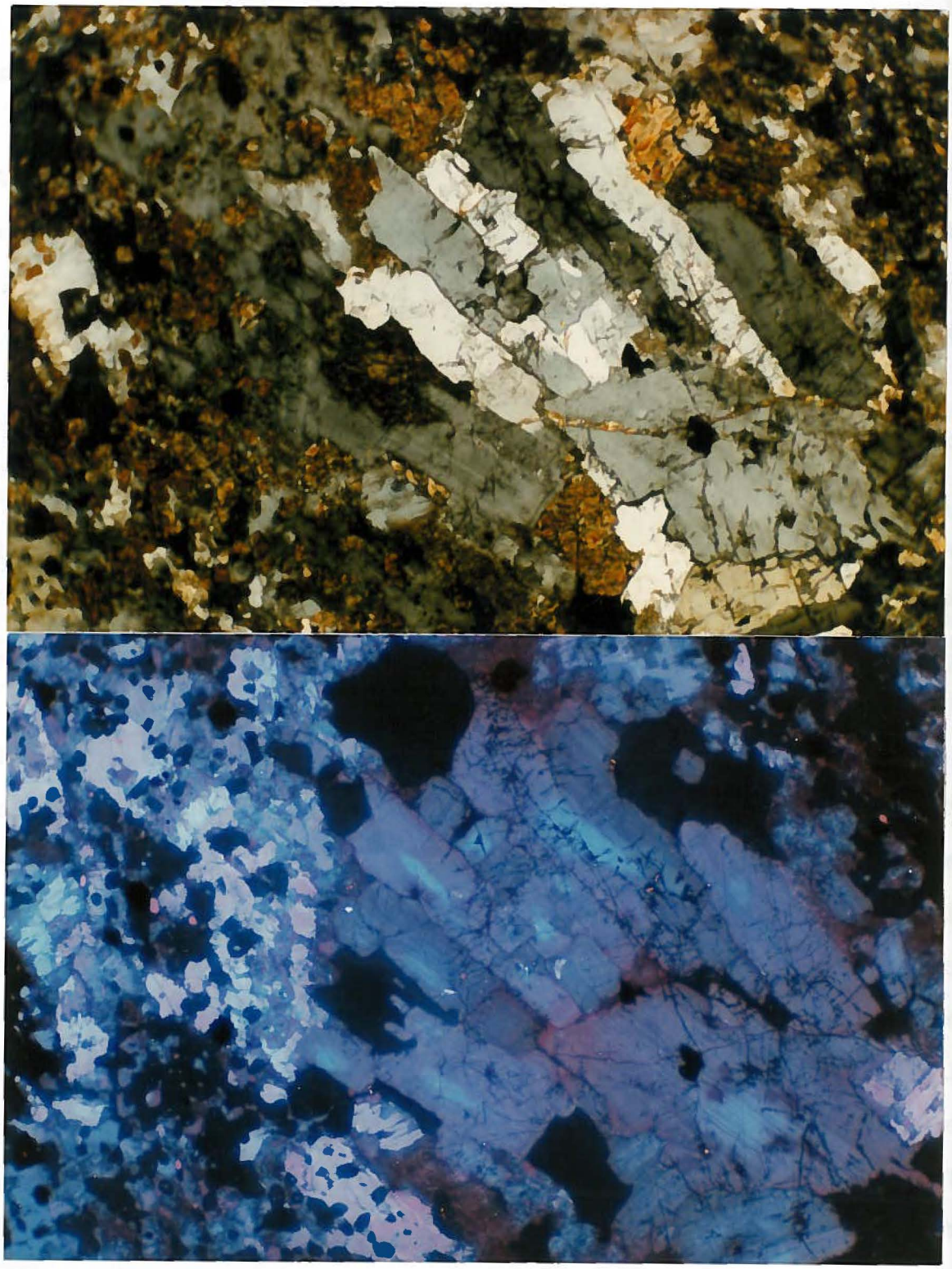

Fig. 6.3-15. Plagioclase relicts in the porphyroblastic nepheline syenite (Sample C572) from Center II, Redsucker Cove, Coldwell Complex. a. TrL. Plagioclase relicts contain no inclusions and are Carlsbad twinned, but apparently lack albite polysynthetic twinning. (Photographic conditions: 2 s, ASA 400) b. CL. The plagioclase relicts exhibit blue luminescent cores and light violet blue luminescent rims, and some of them are albite twinned. The groundmass of the alkali feldspar exhibits dull blue or light violet blue luminescence. Scale: 55 mm on photograph = 1 mm on thin section. (CL conditions: 10 kV, 0.8 Am. Photographic conditions: 2 min, ASA 400).

Appendix 2). The plagioclase relicts exhibit an increase in albite and orthoclase content from the core to the rim while the anorthite content decreases from the core to the rim.

c. Alkali feldspar groundmass

The groundmass feldspars in the porphyroblastic nepheline syenite from Redsucker Cove exhibit luminescence colours ranging from light blue to light violet blue (Fig. 6.3-4b,-5b,-6b), with a compositional range from $Or_{45-62}Ab_{39-51}An_{1-5}$ (Table 6.3-1, Fig. 6.3-3b, -8a and Appendix 2). The range in composition is slightly larger than in the recrystallized rim because the groundmass feldspars, as in the mosaic granuloblastic syenites, may represent both the relict and the neoblast feldspars. The groundmass of the porphyroblastic syenite is enriched in albite ($Or_{45-62}Ab_{39-51}$) compared with that of the mosaic granuloblastic syenite. The groundmass of the mosaic granuloblastic is enriched in orthoclase content (Or_{64-85} Ab_{13-35} for the relicts and $Or_{52-71}Ab_{27-47}$ for the neoblasts) and is more evolved. Mitchell and Platt (1982) found that more evolved syenites are enriched in potassium.

6.3.3. Evolution of recrystallization

Mitchell and Platt (1982) suggested that the deformation and recrystallization in center II " must have occurred at temperatures which were high enough to promote rapid diffusion and to allow extensive grain boundary migration and bulge nucleation from subgrains ". The textural evidence of this process was discussed in

detail by Mitchell and Platt (1982).

The CL and SEM/EDS studies of recrystallization in these nepheline syenites from Center II provide additional textural and chemical evidence which is described in the above sections.

The process of initial recrystallization may involve a potassium rich metasomatic fluid which reacted with the initial feldspars (alkali feldspars and plagioclase relicts) and crystallized in the margin of the core to form the potassic mantle. The alteration caused a re-distribution of the K and Na contents between the metasomatic fluid and the metamorphic minerals. The evidence of this process is clearly shown in Fig. 6.3-9b. A potassic metasomatic fluid reacted with an initial albite core (light blue luminescent) to produce a secondary alkali feldspar (dull blue luminescent) with a composition of $Or_{52-61}Ab_{33-46}An_{1-5}$ (Fig. 6.3-8b and Appendix 2). The secondary alkali feldspar occurs in smaller fractures within the albite core. Contemporaneously, the potassic fluid crystallized on the margin of the core to form the mantle with a composition of $Or_{69-75}Ab_{25-30}An_{1}$ (Table 6.3-1, Fig. 6.3-8b and Appendix 2) which has less Na and more K content than the secondary alkali feldspar.

After the mantles were formed, the K contents were depleted in the metasomatic fluid. Thus the recrystallized rims ($Or_{45-65}Ab_{34-53}An_{1-2}$) were formed under Na-rich conditions in comparison with the mantles.

CHAPTER 7

CATHODOLUMINESCENCE PROPERTIES AND COMPOSITIONS OF THE FELDSPARS IN SYENITES FROM CENTER III

7.1. Feldspars in Magnesio-hornblende Syenite

7.1.1. Introduction

The magnesio-hornblende syenite (samples C180 and C2123), mainly consist of homogeneous K-feldspar and zoned plagioclase (oligoclase -labradorite). The K-feldspar grains are Carlsbad twinned, euhedral or subhedral crystals. The plagioclase grains are Carlsbad and albite twinned, subhedral crystals. Some of the plagioclase crystals are mantled as there are different extinction angles between the centre and the margin of the crystal. The plagioclase crystals have been commonly altered to fine-grained sericite in the core during late-stage hydrothermal alteration. Under CL, the K-feldspar crystals commonly exhibit a homogeneous light blue or blue luminescence, whereas the plagioclase crystals exhibit light greenish blue luminescence in the core and light violet blue in the rim. Secondary plagioclases (albite and oligoclase) exhibit dull violet luminescence or have no luminescence.

7.1.2. K-feldspar

Under CL, the K-feldspar crystals commonly exhibit homogeneous light blue luminescence (sample C2123) (Fig. 7.1-1b) or blue luminescence (sample C180) (Fig. 7.1-2b,-3b). For both the blue and the light blue luminescent K-feldspar, the CL spectra consist of a

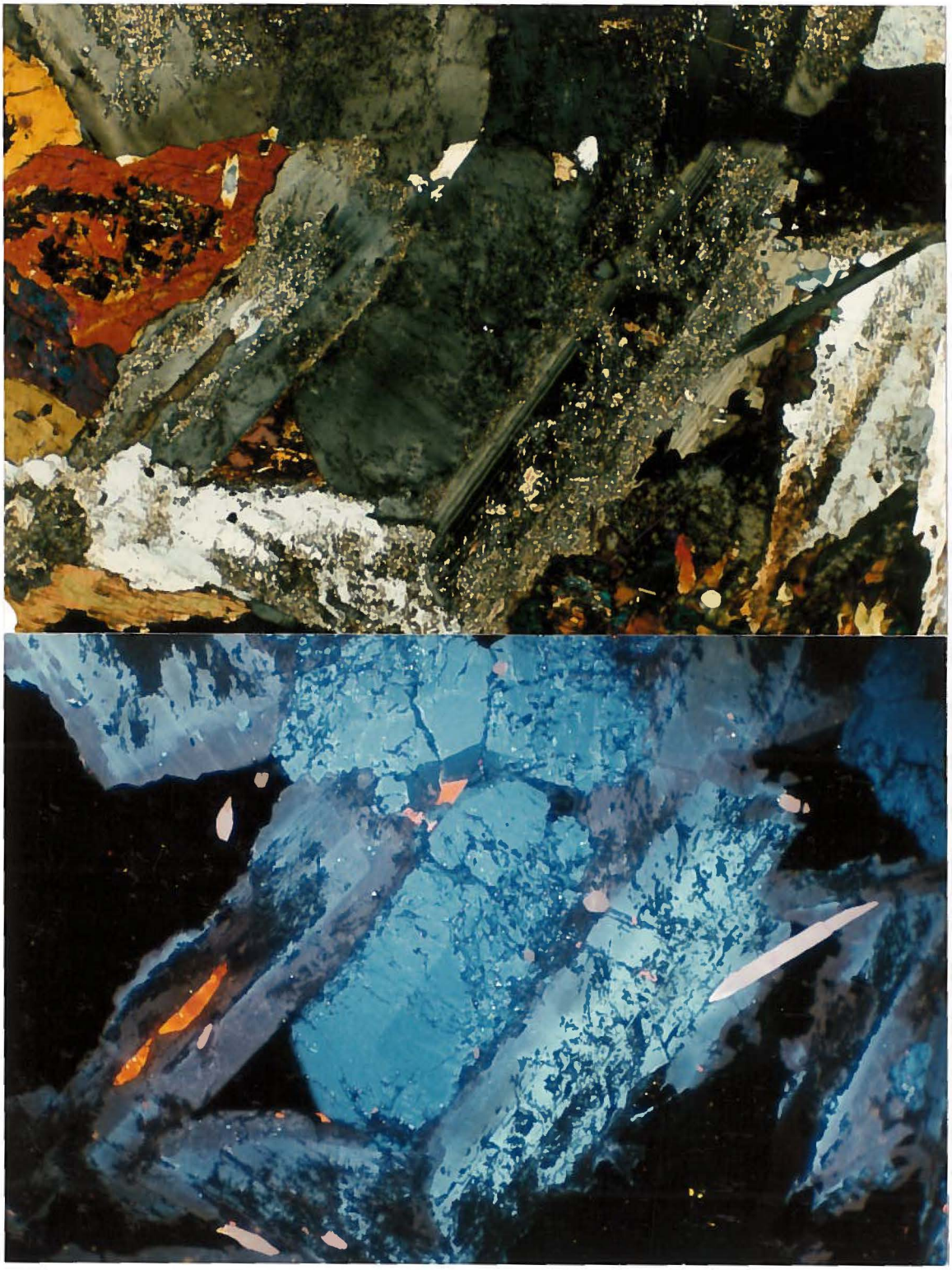

Fig. 7.1-1. K-feldspar and plagioclase in the magnesio-hornblende syenite (Sample C2123) from Center III, Coldwell Complex. a. TrL. (Photographic conditions: 2 s, ASA 400) b. CL. The K-feldspar is Carlsbad twinned and exhibits light blue luminescence. The plagioclase is albite or Carlsbad twinned, light greenish blue luminescent labradorite core with a light violet blue oligoclase rim. The pink luminescent crystals are the apatite and the orange luminescent crystals are the calcite. Scale: 35 mm on photograph = 1 mm on thin section. (CL conditions: 10 kV, 0.8 Am. Photographic conditions: 30 s, ASA 400.)

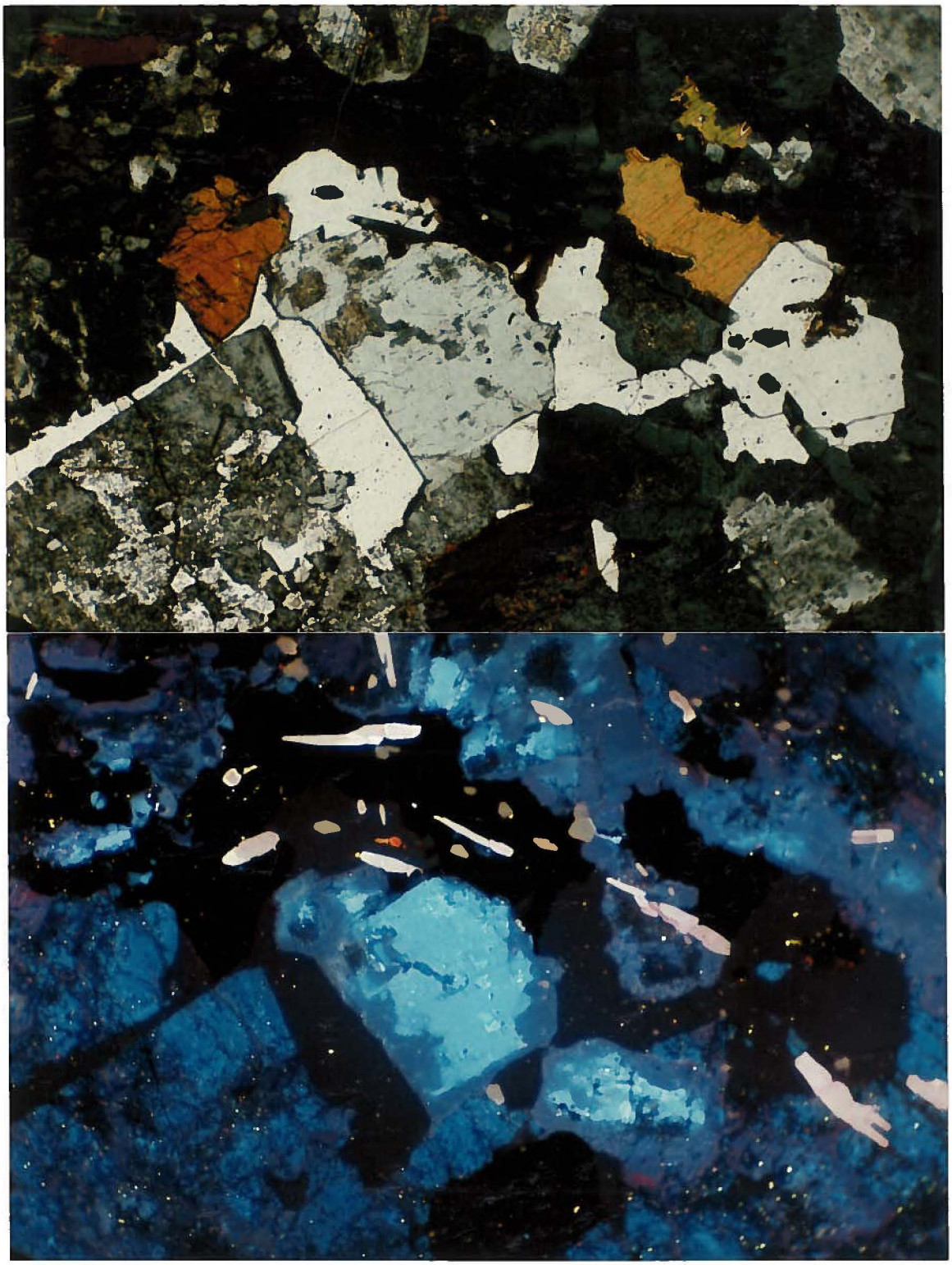

Fig. 7.1-2. K-feldspar and plagioclase in the magnesio-hornblende syenite (Sample C180) from Center III, Coldwell Complex. a. TrL. (Photographic conditions: 1 s, ASA 400) b. CL. The K-feldspar exhibits blue luminescence. The plagioclase exhibits a light greenish blue luminescent oligoclase core surrounded by a dull violet luminescent secondary oligoclase with the light blue luminescent K-rich feldspar inclusions in the core. The pink and dull pink luminescent crystals are the apatite. Scale: 55 mm on photograph = 1 mm on thin section. (CL conditions: 10 kV, 0.8 Am. Photographic conditions: 30 s, ASA 400.)

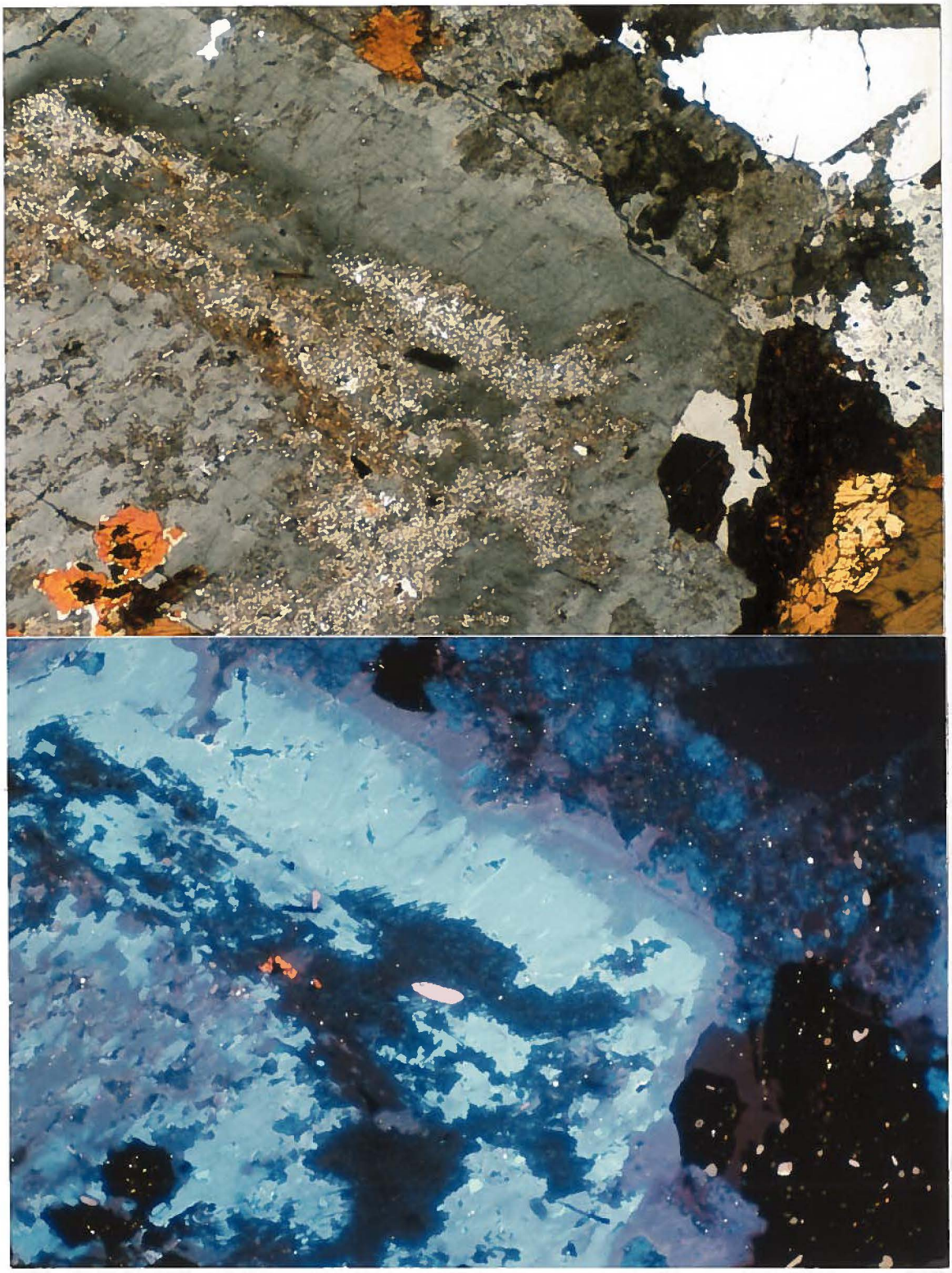

Fig. 7.1-3. K-feldspar and plagioclase in the magnesio-hornblende syenite (Sample C180) from Center III, Coldwell Complex. a. TrL. (Photographic conditions: 2 s, ASA 400) b. CL. The K-feldspar exhibits blue luminescence. The plagioclase exhibits a light greenish blue luminescent oligoclase core and a light violet blue luminescent oligoclase rim. The dull violet luminescent areas are secondary oligoclase. Scale: 35 mm on photograph = 1 mm on thin section. (CL conditions: 10 kV, 0.8 Am. Photographic conditions: 30 s, ASA 400.)

high intensity blue peak centered at 463 nm, and a low intensity red peak centered at 698 nm and a very weak peak centered in the infrared region at about 815 nm (Fig. 7.1-4a, spectrum A; Fig. 7.1-4b, spectrum A and Table 7.1-1). The ratio of I_B/I_R is about 6.0 for the blue luminescent K-feldspar, and is about 14.7 for the light blue luminescent K-feldspar.

The blue luminescent K-feldspar ranges in composition from $Or_{86-89}Ab_{10-14}An_{0-1}$ (Table 7.1-1, Fig. 7.1-5a, -5b and Appendix 3), and the light blue luminescent K-feldspar ranges from $Or_{75-86}Ab_{13-24}An_1$. The Or content is slightly higher in the blue luminescent K-feldspar than in the light blue luminescent K-feldspar.

7.1.3. Plagioclase

Under CL, plagioclase crystals reveal a clearly zoned texture with a light greenish blue luminescent core and a light violet blue luminescent rim (Fig. 7.1-1b,-3b). In sample C180, the CL spectra of the light greenish core consists of a broad blue peak centered at 463 nm and a broad red peak centered at 714 nm with a ratio of I_B/I_R about 6.7 (Fig. 7.1-4a, spectrum B and Table 7.1-1). In sample C2123, the light greenish core consists of a broad blue peak centered at 480 nm and a broad red peak centered at 720 nm with a ratio of I_B/I_R about 11.7 (Fig. 7.1-4b, spectrum B and Table 7.1-1). The blue peak from these light greenish luminescent cores is broader than the blue peak from the blue luminescent K-feldspar, and the blue peak positions of the light greenish luminescent cores shift to a longer wavelength by about 17 nm compared with the blue

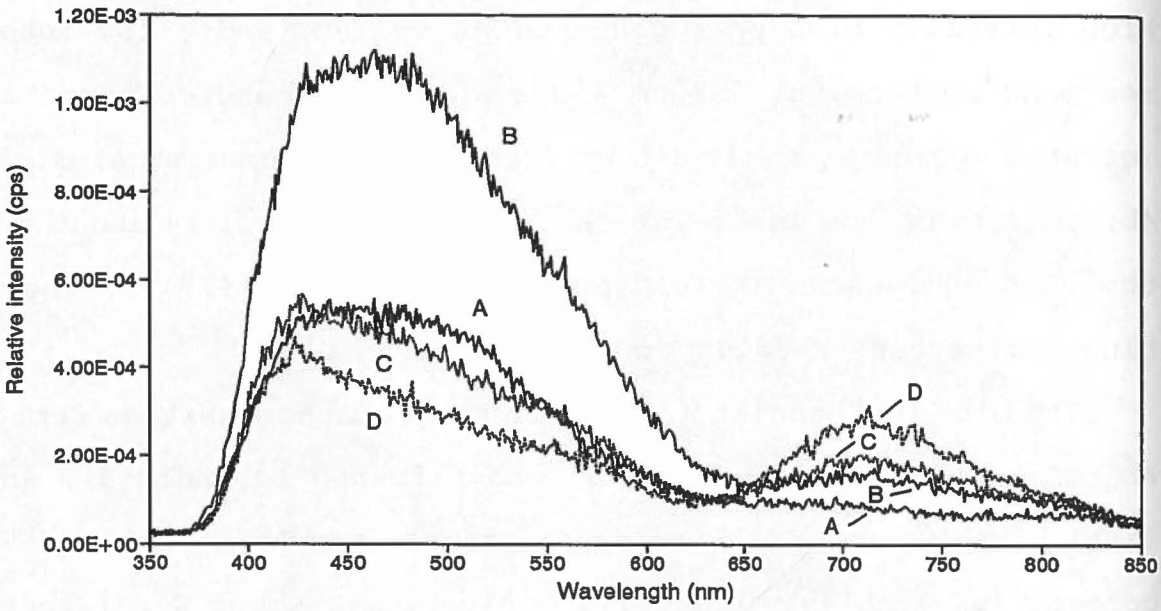

Fig. 7.1-4a. CL spectra of the feldspars in magnesio-hornblende syenite (Sample C180) from Center III, Coldwell Complex, Ontario. (A) is from the blue luminescent K-feldspar. (B) is from the light greenish blue luminescent oligoclase core. (C) is from the light violet blue luminescent oligoclase rim. (D) is from the dull violet luminescent secondary oligoclase in the margins of the K-feldspar and oligoclase. CL conditions: 10 kV, 0.8 mA.

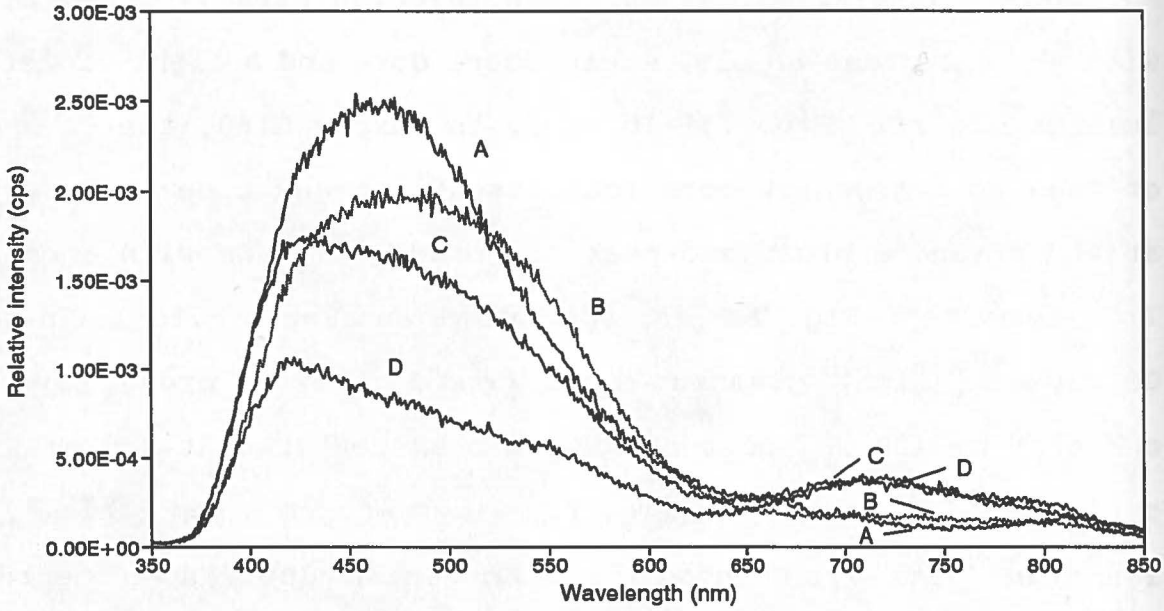

Fig. 7.1-4b. CL spectra of the feldspars in the magnesio-hornblende syenite (Sample C2123) from Center III, Coldwell Complex, Ontario. (A) is from the blue luminescent K-feldspar. (B) is from the light greenish blue luminescent labradorite core. (C) is from the light violet blue luminescent oligoclase rim. (D) is from the dull violet luminescent secondary oligoclase in the margins of the plagioclase. CL conditions: 10 kV, 0.8 mA.

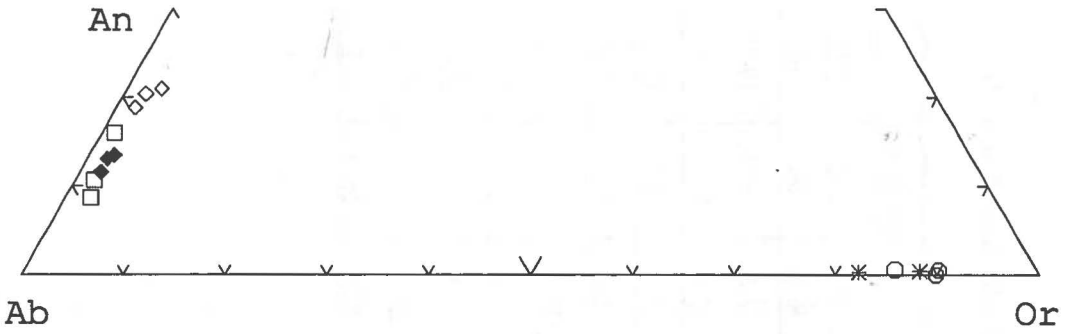

Fig. 7.1-5a. The compositions of feldspars in the magnesio-hornblende syenite (Sample C180) from Center III, Coldwell Complex plotted in the system Or-Ab-An. The open circles (O) are the blue luminescent K-feldspar. The open diamonds (◇) are the light greenish blue luminescent oligoclase core and the filled diamonds (◆) are the light violet blue luminescent oligoclase rim. The asterisks (*) are the light blue luminescent K-feldspar spots in the core.

The squares (□) are the dull violet luminescent secondary oligoclase in the margins of the K-feldspar and oligoclase.

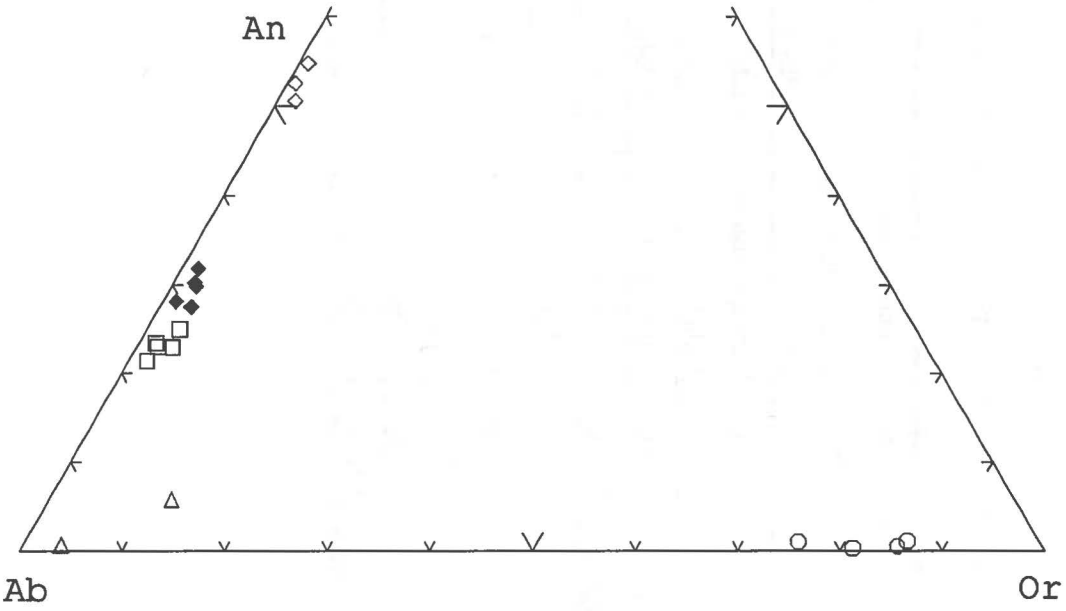

Fig. 7.1-5b. The compositions of feldspars in the magnesio-hornblende syenite (Sample C2123) from Center III, Coldwell Complex plotted in the system Or-Ab-An. The open circles (O) are the blue luminescent K-feldspar. The open diamonds (◇) are the light greenish blue luminescent labradorite core and the filled diamonds (◆) are the light violet blue luminescent oligoclase rim.

The squares (□) are the dull violet luminescent secondary oligoclase in the margins of the K-feldspar and the oligoclase. The up-triangles (△) are the non-luminescent Na-feldspar in the interstices of the K-feldspar.

Table 7.1-1. Representative cathodoluminescence properties and compositions of feldspars in magnesio-hornblende syenite from Center III, Coldwell Complex, Ontario

Occurrence of feldspar	Sample No./ spectrum No.	Luminescence colour	Intensities (cps)					Compositions		
			Blue peak	(nm)	Red peak	(nm)	B/R ratio	Or	Ab	An
K-feldspar	C180/A	Blue	5.57E-04	(463)	9.30E-05	(698)	5.98	86-89	10-14	0-1
Oligoclase, core	C180/B	Light greenish blue	1.12E-03	(463)	1.66E-04	(714)	6.74	2-3	76-79	19-21
K-feldspar spots, core	C180	Light blue	N/A		N/A			82-88	12-18	<1
Oligoclase, rim	C180/C	Light violet blue	5.25E-04	(426)	1.96E-04	(711)	2.68	2-3	84-86	12-13
Secondary Oligoclase, margin	C180/D	Dull violet	4.70E-04	(423)	3.15E-04	(713)	1.49	1-2	83-89	9-16
K-feldspar	C2123/A	Light blue	2.46E-03	(464)	1.80E-04	(700)	13.69	75-86	13-24	1
Labradorite, core	C2123/B	Light greenish blue	1.97E-03	(480)	1.66E-04	(720)	11.91	1-2	44-48	51-55
Oligoclase-andesine, rim	C2123/C	Light violet blue	1.73E-03	(425)	3.87E-04	(718)	4.49	1-3	67-71	28-32
Secondary Oligoclase, margin	C2123/D	Dull violet	1.02E-03	(421)	3.62E-04	(718)	2.82	2-4	72-77	21-25
Secondary Na-feldspar	C2123	Non CL						4-12	82-96	1-6

peak positions of the blue luminescent K-feldspar.

For the light violet blue luminescent rims, the CL spectra consist of a blue peak at about 425 nm and a broad red peak between 711 and 718 nm (Fig. 7.1-4a, spectrum C; Fig. 7.1-4b, spectrum C and Table 7.1-1). The ratios of I_B/I_R are between 2.7 and 4.5. In these CL spectra, the right side (longer wavelength) of the blue peak usually has a lesser slope than that of the blue luminescent K-feldspar. This may indicate that the right side of the blue peak from these light violet blue luminescent rims probably overlaps with an unresolved green peak at about 550 nm.

For the sample C180, the light greenish blue luminescent core is oligoclase with compositions of $Ab_{76-79}An_{19-21}Or_{2-3}$ (Table 7.1-1, Fig. 7.1-5a and Appendix 3), and the light violet blue rim is also oligoclase with compositions of $Ab_{84-86}An_{12-13}Or_{2-3}$. For the sample C2123, the light greenish blue luminescent core is labradorite with compositions of $An_{51-55}Ab_{44-48}Or_{1-2}$ (Table 7.1-1, Fig. 7.1-5b and Appendix 3), but the light violet blue luminescent rim is the oligoclase-andesine with compositions of $Ab_{67-71}An_{28-32}Or_{1-3}$. In both samples, the rim has a higher Ab content than the core.

In the oligoclase core (sample C180), CL reveals some small, bright, light blue luminescent inclusions, these inclusions are the K-rich feldspar with compositions of $Or_{82-88}Ab_{12-18}An_{<1}$ (Table 7.1-1 and Appendix 3). These light blue luminescent inclusions contain higher Ba content (2.29-3.1 wt.% BaO) than the blue luminescent K-feldspar (0.45-0.79 wt.% BaO) (Table 7.1-1 and Appendix 3).

7.1.4. Late-stage, fluid-induced replacement (Secondary plagioclase)

During late-stage fluid-feldspar interaction, the plagioclase and the K-feldspar crystals are replaced by a secondary plagioclase. Under CL, the secondary plagioclase exhibits dull violet luminescence and occurs as irregular rims replacing the zoned plagioclase, as irregular patches replacing plagioclase in the cores, or as irregular veins cross cutting the K-feldspar grains (Fig. 7.1-1b, -2b, -3b). The CL spectra of the dull violet luminescent plagioclase consists of a blue peak centered at about 423 (or 421) nm and a red peak centered at about 713 (718) nm (Table 7.1-1 and Fig. 7.1-4a, spectrum D and Fig. 7.1-4b. spectrum D). Generally, these CL spectra are identical to that of the spectra from the light violet blue luminescent rims, but they have low ratios of I_B/I_R which lie between 1.5 and 2.8 (Table 7.1-1).

Some secondary feldspars occur in the sericitized oligoclase or labradorite core, and have no luminescence (Fig. 7.1-1b and Fig. 7.1-2b).

The dull violet luminescent secondary plagioclase is oligoclase with compositions of $Ab_{83-89}An_{9-16}Or_{1-2}$ for sample C180, and compositions of $Ab_{72-77}An_{21-25}Or_{2-4}$ for sample C2123 (Table 7.1-1, Fig. 7.1-4a,-4b and Appendix 3). The non luminescent secondary feldspars are the albite with compositions of $Ab_{82-96}An_{1-6}Or_{4-12}$.

7.1.5. Thermal history of the feldspars

The thermal history of the plagioclase and optically homogeneous

alkali feldspar in the magnesio-hornblende syenite is shown in Fig. 7.1-6a,b. In Fig. 7.1-6a, the path a-a′ indicates that the plagioclase may have fractionally crystallized at a temperature range from 900 to 750. However, the initial crystallization temperature of the plagioclase may be higher than 850 °C, because most the light greenish blue luminescent plagioclase core has been replaced by the secondary plagioclase in the centre areas.

In the Fig. 7.1-6b, the path b-b′ on incoherent solvus (SFS) indicates that the light blue luminescent alkali feldspar crystals with a composition of $Or_{75-86}Ab_{13-24}$ may have crystallized at a temperature range from 580-450 °C, which is much lower than the temperature range of the plagioclase crystallization.

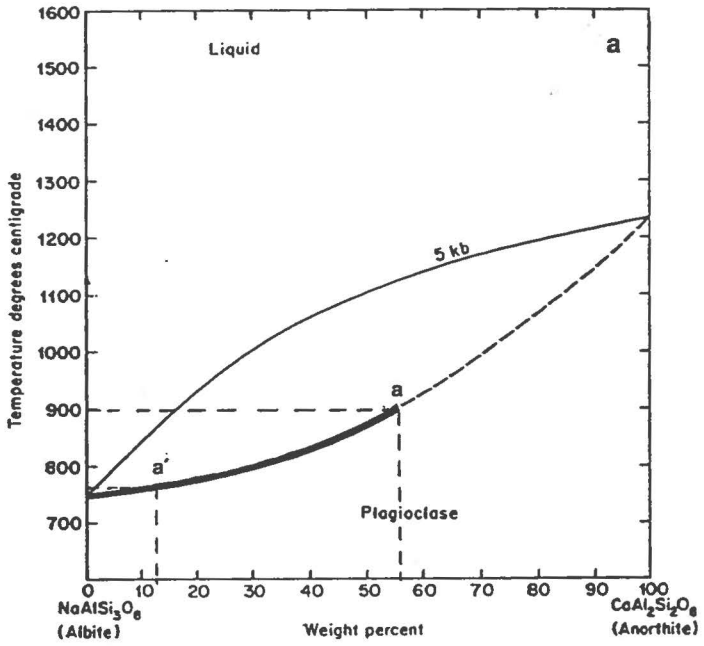

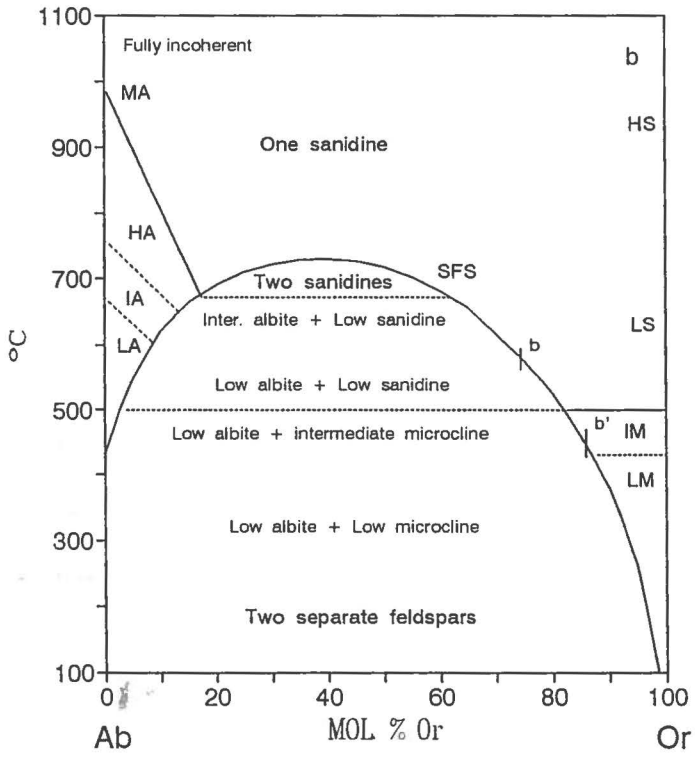

Fig. 7.1.1-6. The evolutions of the plagioclase and the optically homogeneous alkali feldspar in the magnesio-hornblende syenite from Center III are illustrated in the Ab-An and Or-Ab binary phase diagrams.

The path a-a′ in diagram (a) shows the zoned plagioclase crystals have fractionally crystallized at a temperature range from 750-850 °C.

The path b-b′ in diagram (b) shows the optically homogeneous alkali feldspar has crystallized at a temperature range from 450-580 °C along the incoherent solvus (SFS). The diagram (b) shows the phase relationships for An-free alkali feldspars under complete (incoherent) equilibrium. SFS is the strain-free solvus. MA, HA, IA and LA are monoclinic, high, intermediate and low albite; IM and LM are intermediate and low microcline. IA and IM is the region of the rapid change in Y ordering (Brown and Parsons, 1989).

7.2. Feldspars in Ferro-edenite Syenite

7.2.1. Introduction

In ferro-edenite syenite, feldspars mainly consist of mantled alkali feldspar and irregular vein antiperthite. The mantled feldspar crystals usually consist of an unexsolved alkali feldspar or microperthite core and a deuteric coarsened antiperthite rim. The cores usually exhibit light blue or light violet blue luminescence with an composition intermediate between Ab-Or end members. In the deuteric coarsened antiperthite rims, Na-feldspar usually exhibits a dull red or deep red luminescence, whereas K-feldspar is a dull blue or brown luminescent. The Na- and K-feldspar have compositions close to end member compositions. The irregular vein antiperthite crystals have the same luminescence properties and compositions as the deuteric coarsened antiperthitic rims of the mantled feldspar crystals.

Some secondary feldspars in the microperthitic cores are K-feldspars which exhibit dull blue luminescence. However, most secondary feldspars occurring in the edges of the deuteric coarsened antiperthitic rim are albites, which usually exhibit purple or dull red luminescence. The secondary feldspars usually have compositions near their end members, but the secondary albite has higher a An content (2-5 mole%) than the deuteric coarsened Na-feldspar (0-1 mole%) in the antiperthite rims of the mantled feldspar crystals.

7.2.2. Mantled feldspars

In the ferro-edenite syenite, mantled feldspar crystals exhibit a great variety in zonation textures. These mantled feldspars include:

(a) An unexsolved alkali feldspar core and a deuteric coarsened perthitic rim.

(b) A braid microperthitic core and a deuteric coarsened antiperthitic rim.

(c) An albite core and a deuteric coarsened antiperthitic rim.

(d) A braid microperthitic core, intermediate albite mantle and albite rim.

(e) An oscillatory zoned alkali feldspar core and a deuteric coarsened antiperthitic rim.

Textures (b) and (e) are the most commonly. CL characteristics and compositions of the mantled feldspar crystals are described in the following sections.

a. Mantled feldspar with an unexsolved core and a deuteric coarsened perthitic rim

In sample C2124, the feldspar crystals are usually mantled with an unexsolved alkali feldspar core and a turbid deuteric coarsened perthitic rim (Fig. 7.2-1a). The unexsolved core exhibits a homogeneous light violet blue luminescence (Fig. 7.2-1b). CL spectrum of this core consists of a blue peak centered at 466 nm and a high red peak centered at 708 nm with a ratio of I_B/I_R about 0.9 (Fig. 7.2-2, spectrum A and Table 7.2-1).

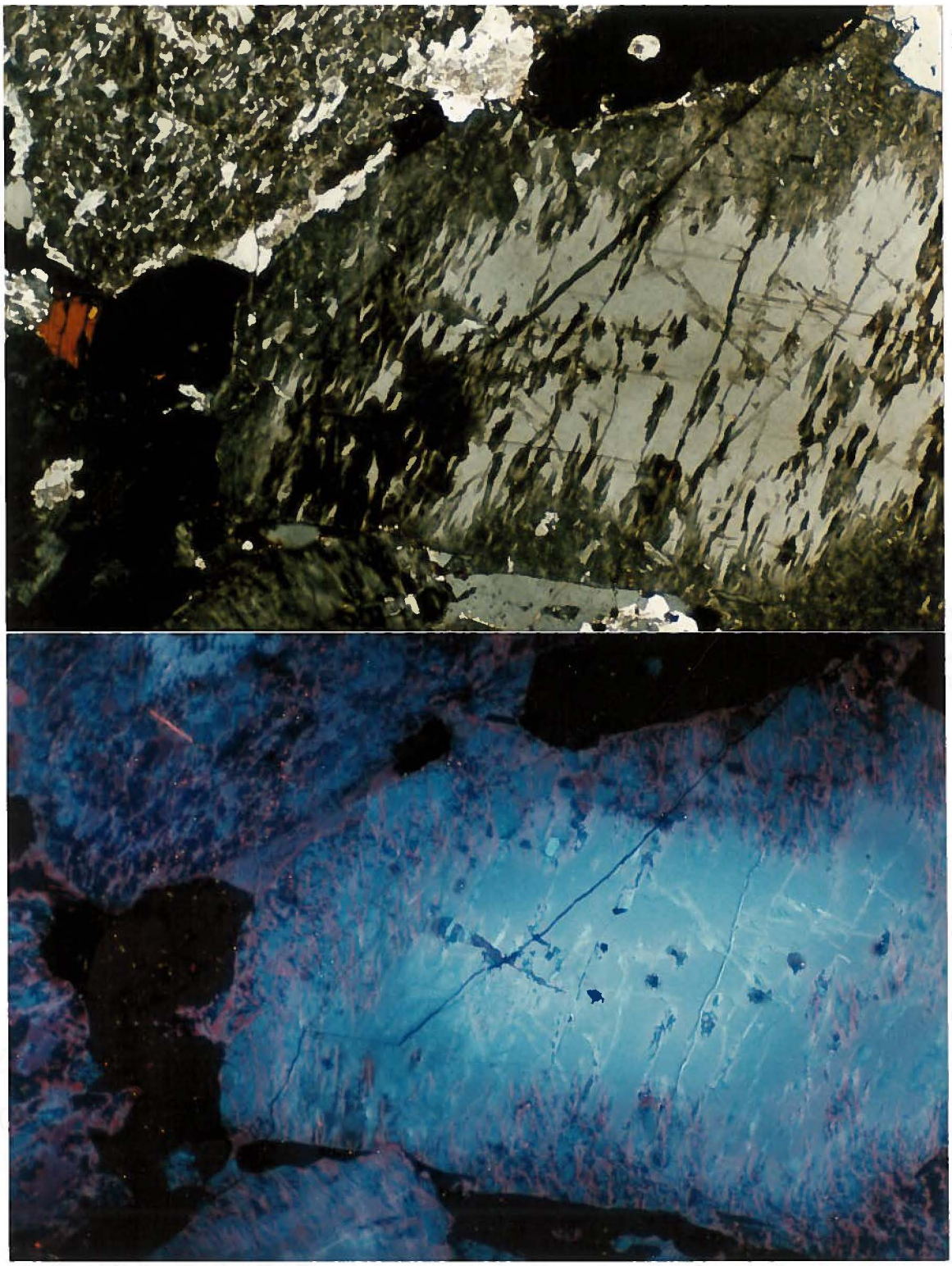

Fig. 7.2-1. Mantled feldspar crystal in ferro-edenite syenite (Sample C2124) from Center III, Coldwell Complex. a. TrL. The feldspar crystal is mantled with an unexsolved alkali feldspar core and a deuteric coarsened perthitic rim. (Photographic conditions: 2 s, ASA 400). b. CL. The unexsolved alkali feldspar core exhibits a light violet blue luminescence. In the deuteric coarsened perthitic rim, exsolved Na-feldspar exhibits dull violet luminescence, whereas K-feldspar host exhibits dull blue luminescence. Secondary albite occurs in the interstices between the mantled feldspar grains and exhibits dull red luminescence. Scale: 50 mm on photograph = 1 mm on thin section. (CL conditions: 10 kV, 0.8 Am. Photographic conditions: 1 nim, ASA 400).

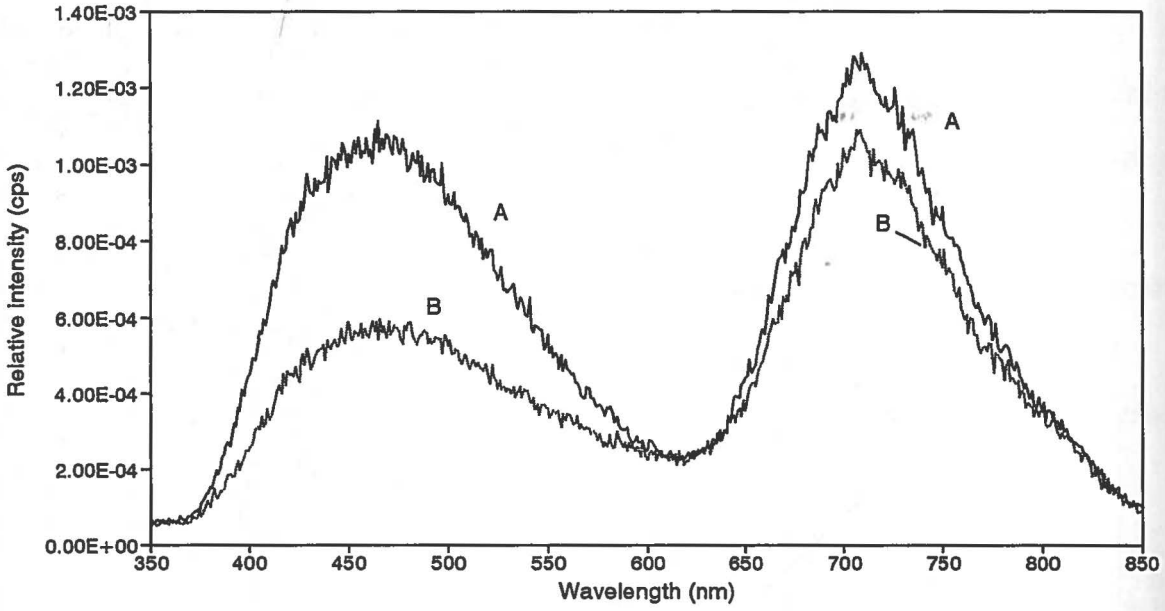

Fig. 7.2-2. CL spectra of mantled feldspar in ferro-edenite syenite (Sample C2124) from Center III, Coldwell Complex, Ontario. (A) is from the light violet blue luminescent unexsolved alkali feldspar core. (B) is from the dull violet luminescent exsolved Na-feldspar in the deuteric coarsened perthitic rim. CL conditions: 10 kV, 0.8 mA.

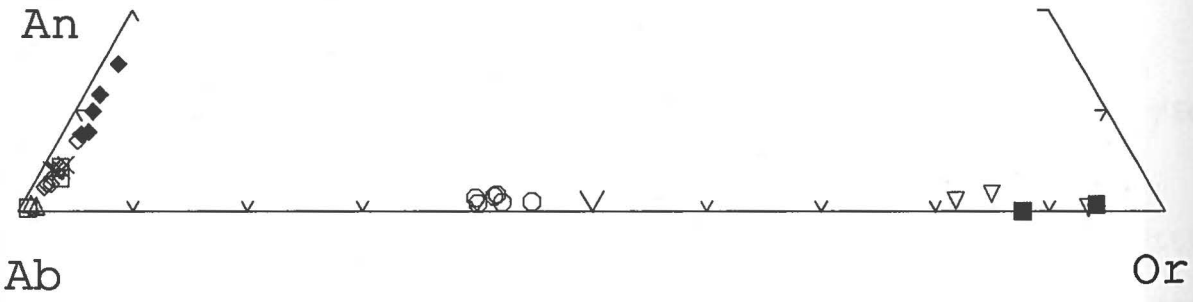

Fig. 7.2-3. The compositions of the feldspars in the ferro-edenite syenite (C2124) from Center III plotted in the system Or-Ab-An.

For the mantled feldspar crystals, the circles (○) are the light violet blue luminescent unexsolved alkali feldspar in the core. The up-triangles (▵) are the dull violet red luminescent exsolved albite and the down-triangles (▿) are the dull blue luminescent K-feldspar host in the deuteric coarsened perthitic rim. The crosses (×) are the dull red luminescent secondary albite in the interstices between feldspar grains.

For the xenolith, the filled diamonds (◆) and diamonds (◇) are the light blue luminescent plagioclase in the core and at the margins of the xenolith, respectively. The squares (□) are the dull red luminescent albite and the filled squares (■) are the dull blue luminescent K-feldspar of the perhtite at the margins of the plagioclase.

Table 7.2-1. Representative cathodoluminescence properties and compositions of feldspars in ferro-edenite syenite from Center III, Coldwell Complex, Ontario

Occurrence of feldspar	Sample No./ spectrum No.	Luminescence colour	Intensities (cps)					Compositions		
			Blue peak	(nm)	Red peak	(nm)	B/R ratio	Or	Ab	An
Homo. alkali feldspar, core	C2124/A	Light violet blue	1.06E-03	(466)	1.25E-03	(708)	0.85	39-44	55-59	1-2
Exsolved albite, perthitic rim	C2124/B	Dull violet	5.93E-04	(473)	1.09E-03	(708)	0.54	1	98-99	1
K-feldspar host, perthitic rim	C2124	Dull blue	N/A		N/A			81-93	6-18	1-2
Secondary albite, interstitial	C2124/D	Dull red	N/A		N/A			1-2	94-95	4-5
Plagioclase, xenolith	C2124/C	Light blue	2.80E-03	(465)	1.83E-03	(709)	1.53	1-2	84-96	2-15
Albite, perthite, xenolith	C2124	Dull red	N/A		N/A			1-2	94-99	0-4
K-feldspar, perthite, xenolith	C2124	Dull blue	N/A		N/A			88-94	6-12	0-1
Microperthite, core	C294/A	Light blue	2.98E-03	(463)	7.13E-04	(706)	4.17	49-71	28-49	1-2
Secondary K-feldspar, core	C294/B	Dull blue	7.45E-04	(459)	6.85E-04	(706)	1.09	90-99	0-9	1
Albite, mantle	C294	Light blue	N/A		N/A			1-4	92-97	1-6
Albite, rim	C294/C	Light violet blue	3.85E-03	(461)	2.86E-03	(707)	1.35	1-3	95-98	1-3
Albite, antiperthite rim	C294/D	Deep red	3.33E-04	(466)	2.30E-03	(708)	0.14	1-2	98-99	0-1
K-feldspar, antiperthite rim	C294	Brown	N/A		N/A			86-100	0-13	0-1
2nd.-albite, antiperthite rim	C294	Purple	N/A		N/A			1-2	95-98	1-4
Albite host, antiperthite	C2224/A	Blue-L. violet blue	1.10E-03	(459)	1.05E-03	(709)	1.05	2-7	91-97	1-2
Exsolved K-feldspar, anti.	C2224/B	Dull blue	7.88E-04	(466)	9.79E-04	(708)	0.81	88-90	9-11	1
Secondary albite	C2224	Dull red	N/A		N/A			1	96-97	2-3

Within the deuteric coarsened perthitic rim, K-feldspar host exhibits dull blue luminescence and exsolved albites exhibit dull violet luminescence (Fig. 7.2-1b). CL spectrum of the dull violet luminescent albite consists of a low blue peak centered at 473 nm and a high red peak centered at 708 nm with a ratio of I_B/I_R about 0.5 (Fig. 7.2-2, spectrum B and Table 7.2-1).

The light violet blue luminescent unexsolved alkali feldspar core ranges in composition from $Or_{39-44}Ab_{55-59}An_{1-2}$ (Table 7.2-1, Fig. 7.2-3 and Appendix 3). In the deuteric coarsened perthitic rim, the dull blue luminescent K-feldspar host ranges in composition from Or_{81-93} $Ab_{6-18}An_{0-2}$ and the dull violet exsolved albite from $Ab_{98-99}Or_1An_1$.

b. Mantled feldspar with a braid microperthite core and a deuteric coarsened antiperthitic rim

In the ferro-edenite syenite, some mantled feldspar crystals (samples C2232, C294, C2068 and C2223) consist of a braid microperthitic core and a turbid, deuteric coarsened antiperthitic rim. The braid microperthitic cores usually exhibit light blue luminescence under CL (Fig. 7.2-4b). The braid microperthitic texture only can be observed under high magnification using SEM/BSE. Within the deuteric coarsened antiperthitic rim, albite host exhibits deep red luminescence whereas K-feldspar is dark brown luminescent.

The light blue luminescent braid microperthitic cores usually have intermediate compositions in the Ab-Or system and range in composition from $Or_{26-38}Ab_{59-71}An_{2-3}$ (Fig. 7.2-5 and Appendix 3).

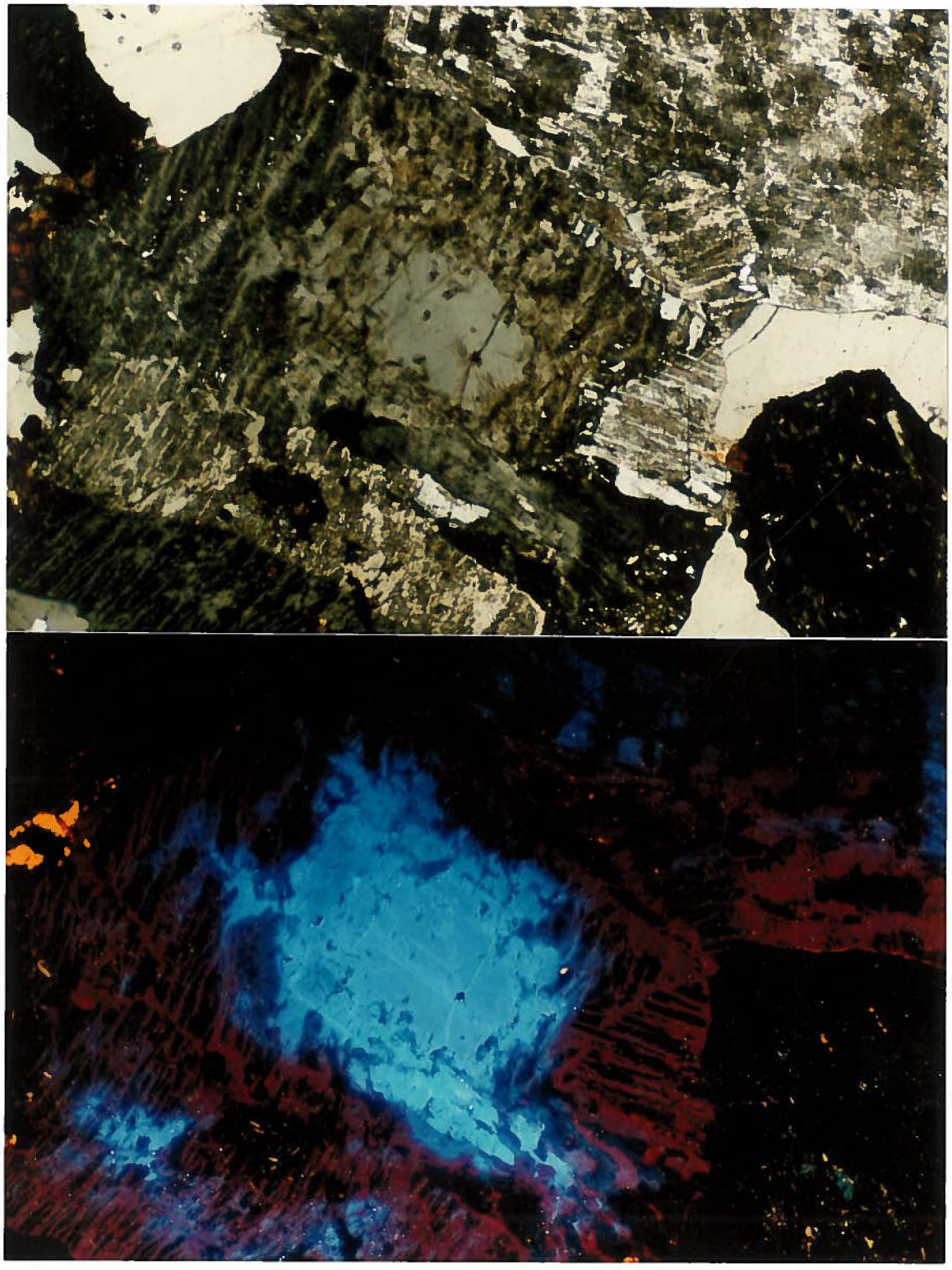

Fig. 7.2-4. Mantled feldspar crystal in ferro-edenite syenite (Sample C2232) from Center III, Coldwell Complex. a. TrL. The feldspar crystal is mantled with a microperthite core and a deuteric coarsened antiperthitic rim, or is mantled with an albite twinned Na-feldspar core and a deuteric coarsened antiperthitic rim. (Photographic conditions: 2 s, ASA 400). b. CL. The microperthite and the albite core exhibits a light violet blue luminescence. In the deuteric coarsened antiperthitic rim, the Na-feldspar exhibits deep red luminescence and the K-feldspar exhibits dark brown luminescence. The secondary albite exhibits purple luminescence. Scale: 50 mm on photograph = 1 mm on thin section. (CL conditions: 10 kV, 0.8 Am. Photographic conditions: 1 nim, ASA 400).

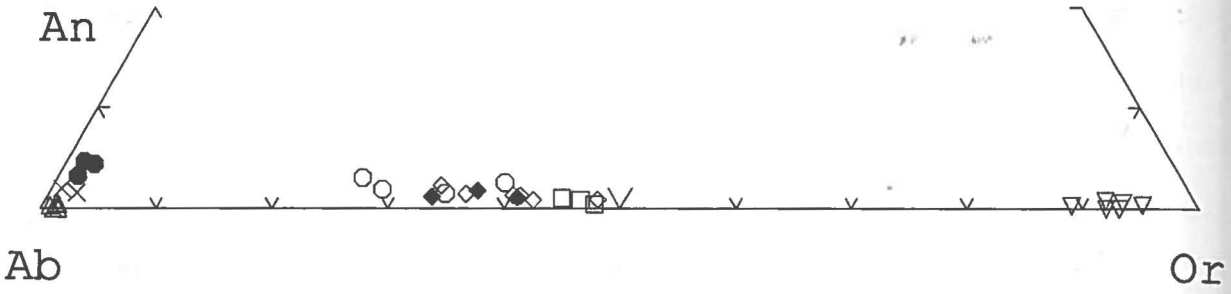

Fig. 7.2-5. The compositions of the feldspars in the ferro-edenite syenite (C2232) from Center III plotted in the system Or-Ab-An.

For the mantled feldspar crystals, the circles (∘) are the light blue luminescent microperthitic cores and the filled circles (•) are the light blue luminescent albite cores.

For the oscillatory zoned core, the squares (□) are the light bluish violet luminescent microperthite at centre of the core, and the diamonds (◇) the are light violet blue luminescent microperthite at margins of the core and the filled diamonds (◆) are the light blue luminescent microperthite at margins of the near deuteric coarsened antiperthitic rim.

For the deuteric coarsened antiperthitic rim, the up-triangles (▵) are the red luminescent albite and the down-triangles (▿) are the dark brown luminescent K-feldspar. The crosses (×) are the purple luminescent secondary albite.

However, in the deuteric coarsened antiperthitic rim, the deep red luminescent albite host ranges in composition from $Ab_{98-99}Or_{1-2}An_{0-1}$, whereas the dark brown luminescent exsolved K-feldspar is from $Or_{89-95}Ab_{5-11}An_{0-1}$.

c. Mantled feldspar with an albite core and a deuteric coarsened antiperthitic rim

In sample C2232, a feldspar crystal is mantled with an albite-twinned core and a deuteric antiperthitic rim (Fig. 7.2-4a). The albite core exhibits a light blue luminescence which similar to that of the braid microperthitic core. However, the light blue luminescent albite-twinned core ranges in composition from Ab_{90-95} $Or_{2-3}An_{3-8}$ (Fig. 7.2-5 and Appendix 3). The deuteric coarsened antiperthitic rim has the same luminescence characteristics and compositions as those of the antiperthitic rim of the braid microperthitic core (see above).

d. Mantled feldspar with a braid microperthite core, intermediate albite mantle and albite rim

In sample C294, some feldspar crystals are mantled with a braid microperthitic core, a narrow intermediate albite mantle and albite rim. In transmitted light, the core shows an unusual brown colour (Fig. 7.2-6a), it may be due to hematitization during late-stage hydrothermal alteration. Under CL, the core exhibits light blue luminescence (Fig. 7.2-6b). CL spectrum of this light blue luminescent core consists of a high blue peak centered at 463 nm

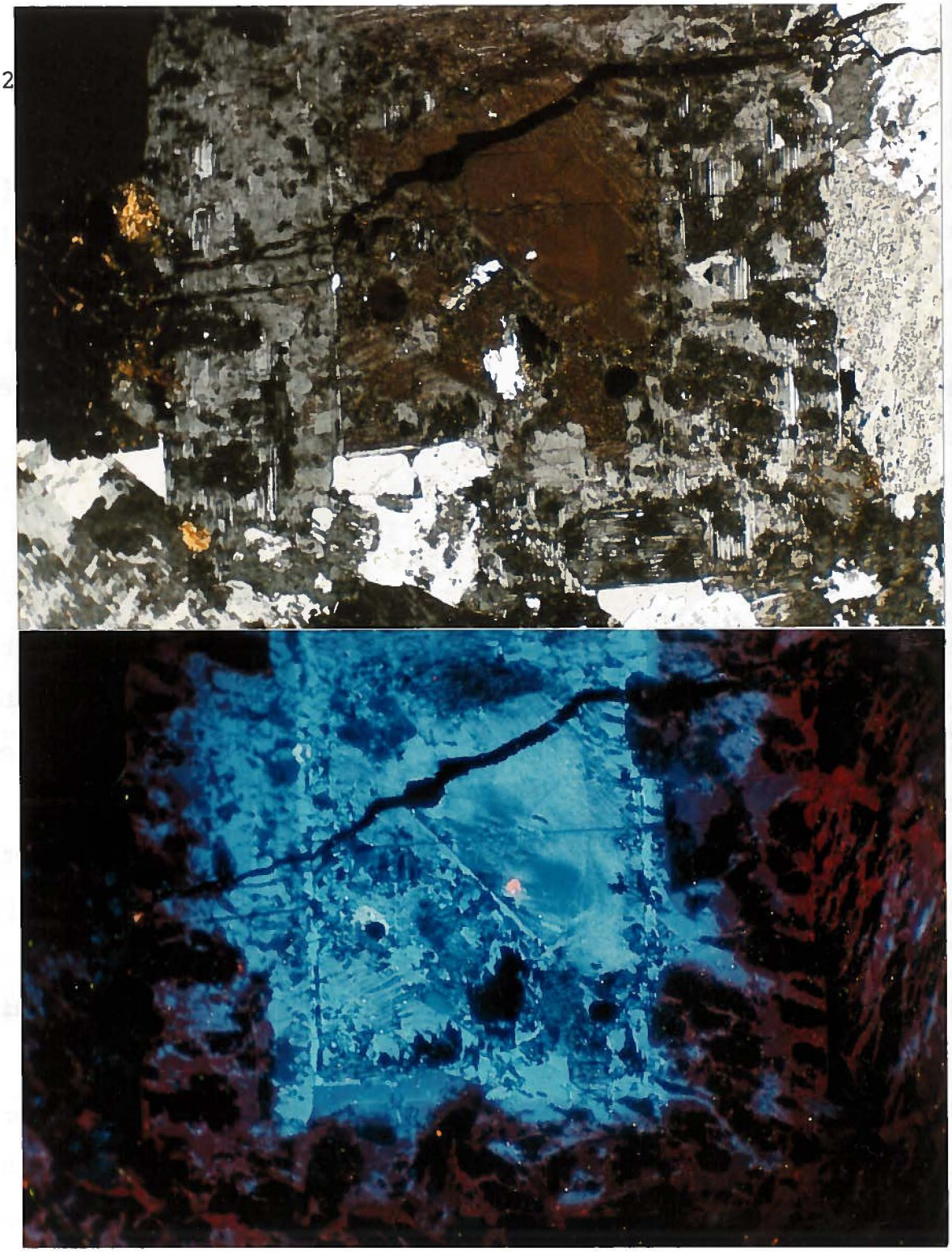

Fig. 7.2-6. Mantled feldspar crystal in ferro-edenite syenite (Sample C294) from Center III, Coldwell Complex. a. TrL. The feldspar crystal is mantled with a microperthite core, intermediate albite mantle and albite rim. The albite rim is surrounded by deuteric coarsened antiperthite. Secondary Na-feldspar is albite twinned. (Photographic conditions: 2s, ASA 400). b. CL. The microperthite core exhibits a light blue luminescence, the intermediate albite mantle exhibits bright, light blue luminescence and the albite rim exhibits light violet blue luminescence. Secondary K-feldspar exhibits dull blue luminescence in the core. In deuteric coarsened antiperthitic rim, the Na-feldspar exhibits deep red luminescence and K-feldspar exhibits dark brown luminescence. The secondary albite exhibits purple luminescence. Scale: 35 mm on photograph = 1 mm on thin section. (CL conditions: 10 kV, 0.8 Am. Photographic conditions: 30s, ASA 400).

and a very low red peak centered at 706 nm with a ratio of I_B/I_R about 4.2 (Fig. 7.2-7a, spectrum A and Table 7.2-1). The light blue luminescent core ranges in composition from $Or_{49-71}Ab_{28-49}An_{1-2}$ (Table 7.2-1, Fig. 7.2-7b and Appendix 3) and contains mole% $KFeSi_3O_8$ from 0.9 to 4.3. This core also contains many very small hematite grains (< 1 μm) and micropores which are only visible in SEM/BSE.

The albite intermediate mantle exhibits bright, light blue luminescence (Fig. 7.2-6b) and ranges in composition from $Ab_{92-97}Or_{1-4}$ An_{1-6} (Table 7.2-1, Fig. 7.2-7b and Appendix 3).

In the rim, the albite exhibits light violet blue luminescence (Fig. 7.2-6b). CL spectrum of this light violet blue luminescent albite consists of a high blue peak centered at 461 nm and low red peak centered at 707 nm with a ratio of I_B/I_R about 1.4 (Fig. 7.2-7a spectrum B and Table 7.2-1). This light violet blue luminescent albite rim ranges in composition from $Ab_{95-98}Or_{1-3}An_{1-3}$ (Table 7.2-1, Fig. 7.2-7b and Appendix 3).

The light violet luminescent albite rim is surrounded by deuteric coarsened antiperthite at the margins. Within the antiperthite, the albite host exhibits deep red luminescence, whereas the exsolved K-feldspar is dark brown luminescent (Fig. 7.2-6b). CL spectrum of the deep red luminescent albite host consists of a very low blue peak centered at 466 nm and a very high red peak centered at 708 nm, and the ratio of I_B/I_R is about 0.1 (Fig. 7.2-7a, spectrum C and Table 7.2-1). The deep red luminescent albite ranges in composition from $Ab_{98-99}Or_{1-2}An_{0-1}$ and the dark brown luminescent K-feldspar ranges in composition from $Or_{90-100}Ab_{0-10}An_{0-1}$ (Fig. 7.2-7b and Appendix 3).

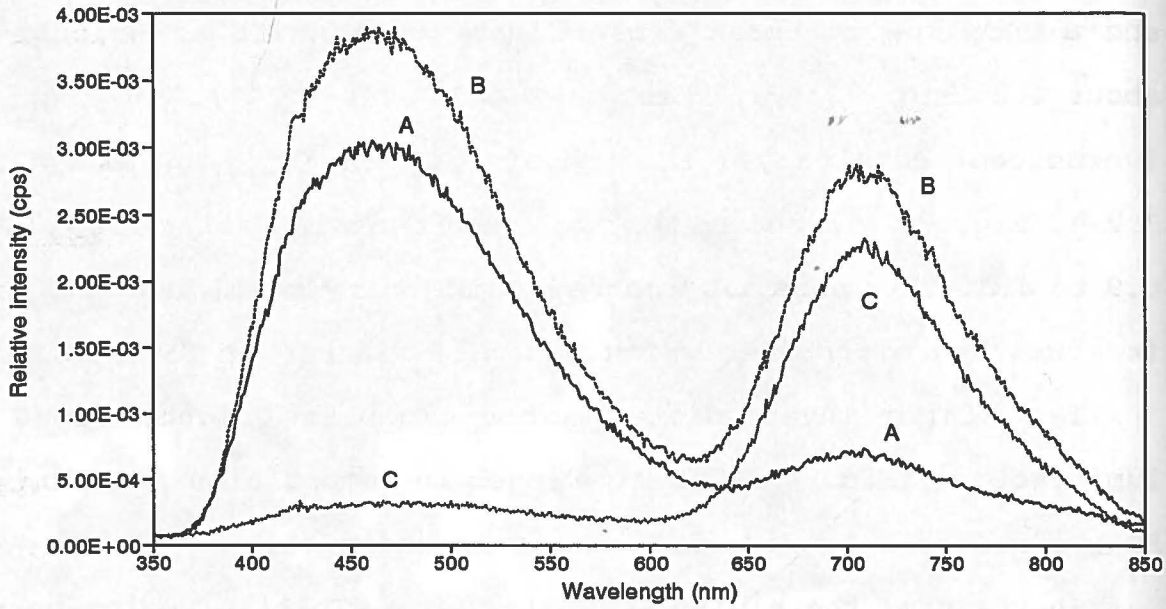

Fig. 7.2-7a. CL spectra of feldspars in ferro-edenite syenite (Sample C294) from Center III, Coldwell Complex, Ontario. (A) is from the light blue luminescent microperthite in the core of the mantled feldspar. (B) is from the light blue luminescent albite rim. (C) is from the deep red albite in the deuteric coarsened antiperthitic rim. CL conditions: 10 kV, 0.8 mA.

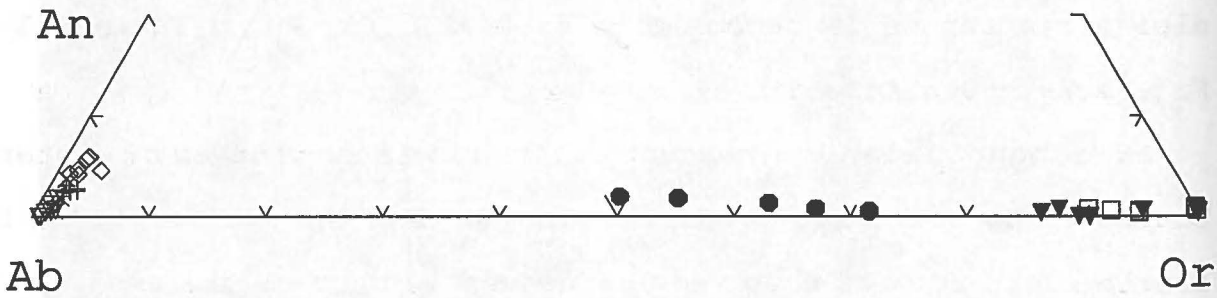

Fig. 7.2-7b. The compositions of the feldspar crystals in the ferro-edenite syenite (C294) from Center III plotted in the system Or-Ab-An.

The filled circles (•) are the light blue luminescent microperthitic core. The diamonds (◇) are the light blue luminescent intermediate albite mantle. The crosses (+) are the light violet blue luminescent albite rim.

The down-triangles (▾) are the dull red to deep red luminescent albite and the filled down-triangles (▾) are the dull blue to dark brown luminescent K-feldspar in the deuteric coarsened antiperthitic rim and in the antiperthite.

The squares (□) are the dull blue luminescent secondary K-feldspar in the microperthitic core. The crosses (×) are the purple luminescent secondary albite in the antiperthitic rim.

e. Mantled feldspar with an oscillatory zoned alkali feldspar core and a deuteric coarsened antiperthitic rim

In samples C2025, C2232, C182, C322 and C2068, some feldspar crystals are mantled with an oscillatory zoned alkali feldspar core and a deuteric coarsened antiperthitic rim. The oscillatory zones are usually represented by alternating bluish violet luminescing zones and light violet blue luminescent zones (Fig. 7.2-8b, -9b, -10b). The oscillatory cores with the most zones are perthites or incipient perthites consisting of exsolved K-feldspars, Na-feldspars and microperthitic patches (Fig. 7.2-8b, 9b). Commonly, the exsolved K-feldspars exhibit dull blue luminescence; the exsolved Na-feldspars exhibit light violet blue to violet luminescence; and the microperthitic patches exhibit bluish violet to light violet luminescence. The microperthitic patches usually have intermediate compositions.

For example in sample C182, in the centre of the oscillatory zoned core, the bluish violet luminescent microperthite patches range in composition from $Or_{21-35}Ab_{64-78}An_{1}$ (Fig. 7.2-9b, Fig. 7.2-11a and Appendix 3). At the margins of the oscillatory zoned core, the light violet luminescent microperthitic patches range in composition from $Or_{38-48}Ab_{51-61}An_{1}$ (Fig. 7.2-11a and Appendix 3). The Or contents increase from the centre of the core to the margins of the core. In the deuteric coarsened antiperthitic rim, the albite host exhibits deep red luminescence and ranges in composition from $Ab_{97-99}Or_{1-2}An_{0-1}$, whereas the exsolved K-feldspar is dull blue or dark brown luminescent with compositions of $Or_{87-96}Ab_{4-12}An_{0-1}$ (Fig. 7.2-11a

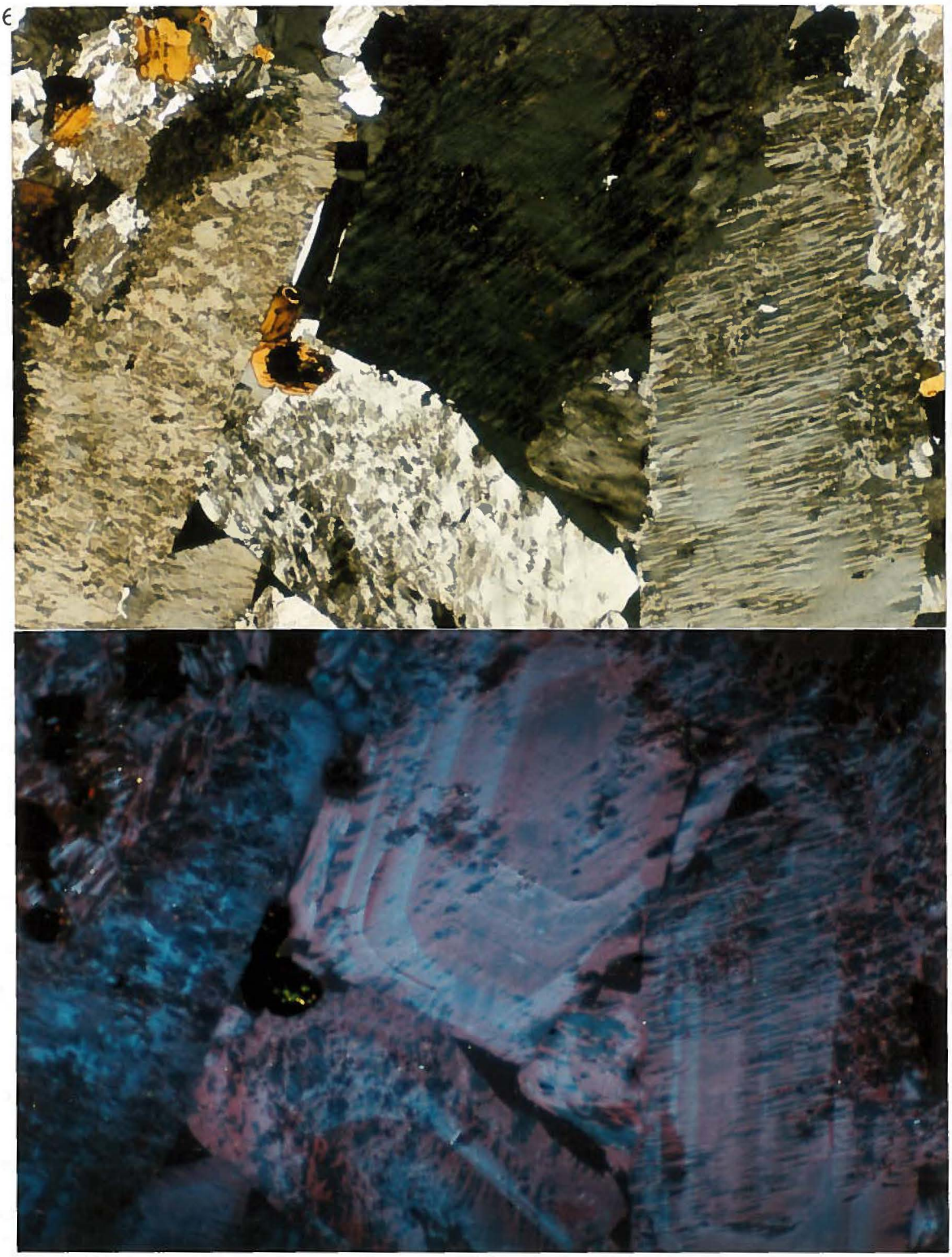

Fig. 7.2-8. Oscillatory zoned alkali feldspar crystals in ferro-edenite syenite (Sample C2068) from Center III, Coldwell Complex. a. TrL. Feldspar crystals are irregular vein antiperthite and contain some microperthite patches. (Photographic conditions: 2 s, ASA 400). b. CL. The feldspar crystals exhibit oscillatory zoning under CL. CL also reveals that the exsolved Na-feldspar exhibits light blue to light violet blue luminescence and the exsolved K-feldspar exhibits dull blue luminescence. Scale: 35 mm on photograph = 1 mm on thin section. (CL conditions: 10 kV, 0.8 Am. Photographic conditions: 1 nim, ASA 400).

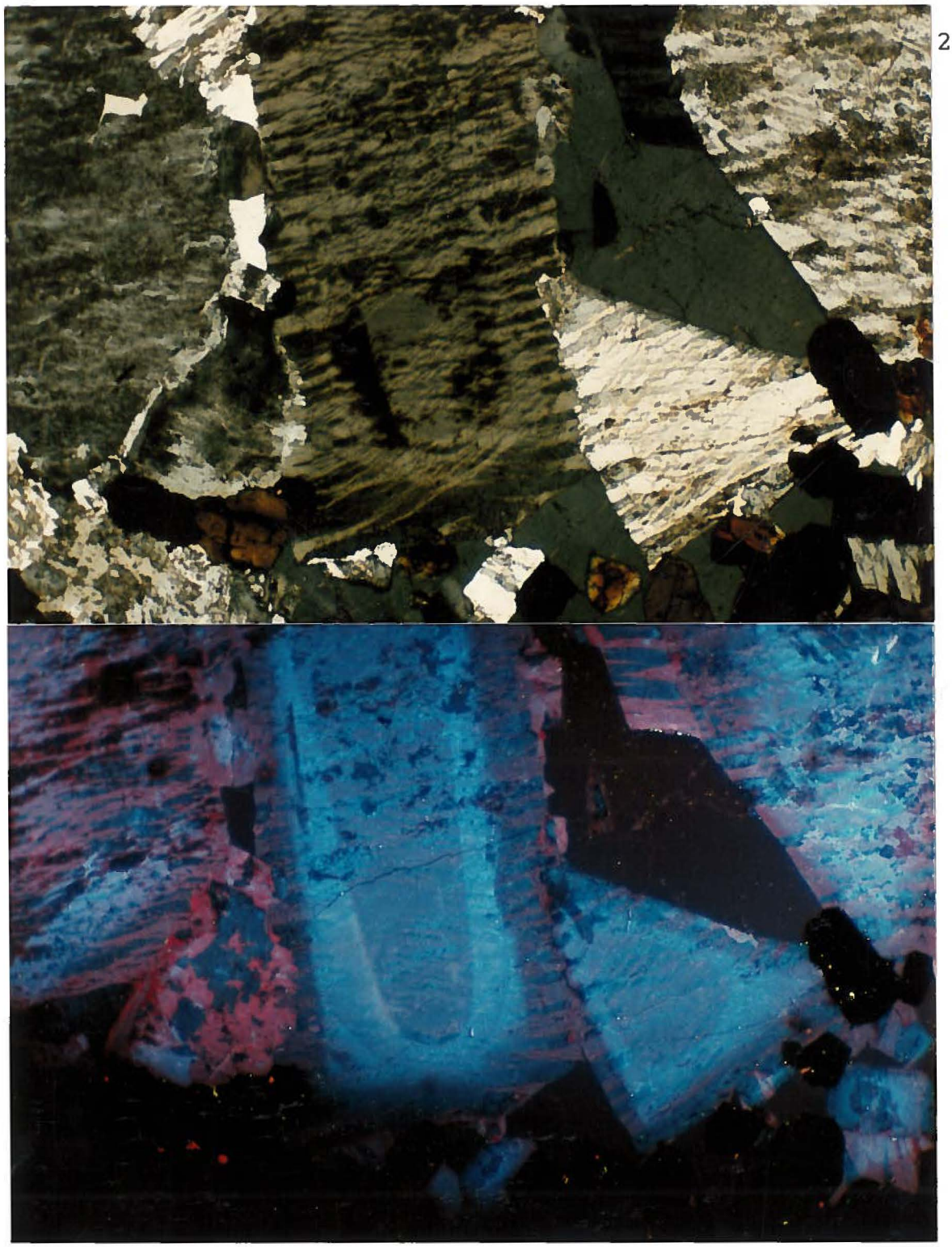

Fig. 7.2-9. Oscillatory zoned alkali feldspar crystals in ferro-edenite syenite (Sample C182) from Center III, Coldwell Complex. a. TrL. The feldspar crystals are irregular vein antiperthite and contain some microperthite patches. (Photographic conditions: 2 s, ASA 400). b. CL. The feldspar crystals are mantled with an oscillatory zoned core and a deuteric coarsened antiperthite rim. In the oscillatory zoned core, the microperthite patches exhibit light violet blue to bluish violet luminescence, the exsolved Na-feldspar exhibits light blue to light violet blue luminescence, and the exsolved K-feldspar exhibits dull blue luminescence. Scale: 50 mm on photograph = 1 mm on thin section. (CL conditions: 10 kV, 0.8 Am. Photographic conditions: 1 nim, ASA 400).

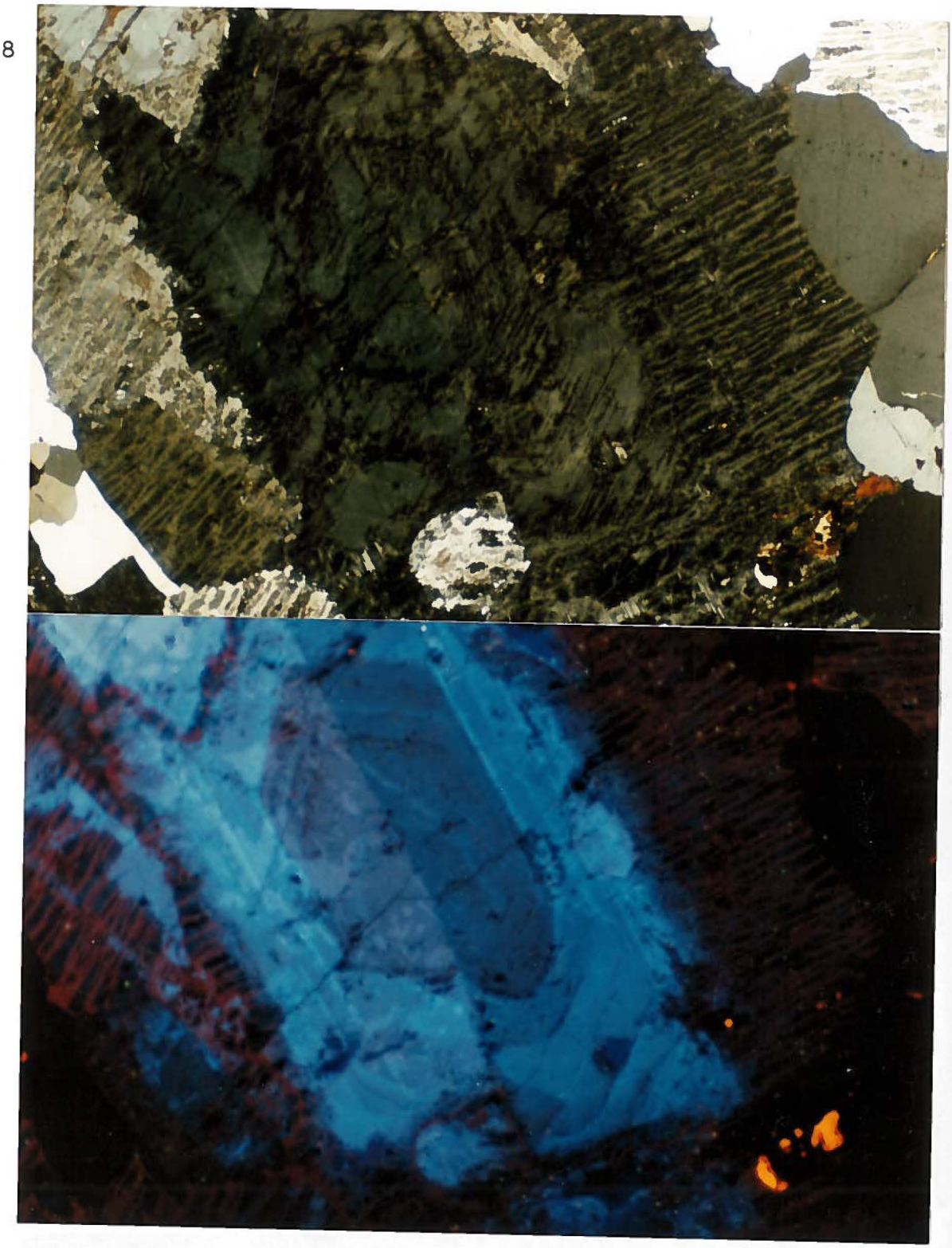

Fig. 7.2-10. Oscillatory zoned alkali feldspar in ferro-edenite syenite (Sample C2232) from Center III, Coldwell Complex. a. TrL. The feldspar is mantled with a microperthitic core and a deuteric coarsened antiperthitic rim. (Photographic conditions: 2 s, ASA 400). b. CL. In the oscillatory core, the microperthite exhibits light bluish violet luminescence in the centre of the core and exhibits light blue to light violet blue luminescent zoning in the margins of the core. In the deuteric coarsened antiperthitic rim, the exsolved Na-feldspar exhibits deep red luminescence and the exsolved K-feldspar exhibits dull blue to dark brown luminescence. Scale: 35 mm on photograph = 1 mm on thin section. (CL conditions: 10 kV, 0.8 Am. Photographic conditions: 1 nim, ASA 400).

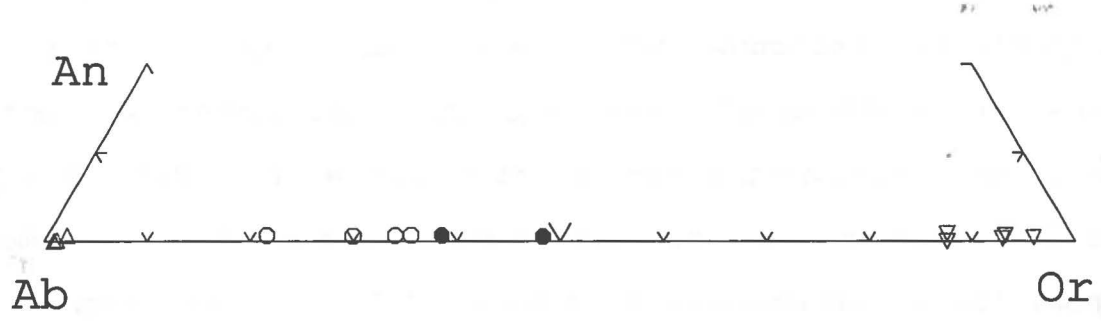

Fig. 7.2-11a. The compositions of the mantled feldspar in the ferro-edenite syenite (C182) from Center III plotted in the system Or-Ab-An.

The open circles (O) are the light violet blue luminescent microperthite in the centre of the oscillatory zoned core, and the filled circles (•) are the light violet luminescent microperthite in the margins of the oscillatory core. The up-triangles (▵) are the dull red luminescent albite host and the down-triangles (▿) are the dull blue luminescent exsolved K-feldspar in the deuteric coarsened antiperthite rim.

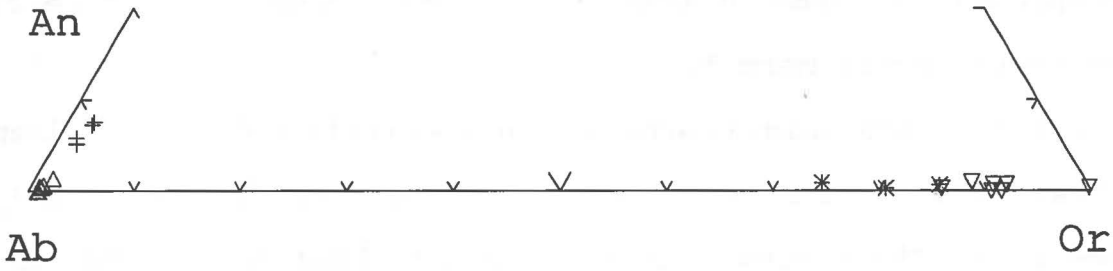

Fig. 7.2-11b. The compositions of the feldspars in the ferro-edenite syenite (C2025) from Center III plotted in the system Or-Ab-An.

The crosses (+) are the light blue luminescent exsolved albite and the asterisks are dull blue luminescent K-feldspar in the perthite core. The up-triangles (▵) are the dull red luminescent albite host and the down-triangles (▿) are the dull blue luminescent exsolved K-feldspar in the deuteric coarsened antiperthite rim and in oscillatory zoned antiperthite.

and Appendix 3).

However, some of the oscillatory zoned cores only contain braid microperthite, and show light bluish violet luminescent zones at the centre of the oscillatory core and light violet to light blue luminescent zones at the margins of the core (Fig. 7.2-10b). These oscillatory zoned cores are alkali feldspars and have intermediate compositions. For example in sample C2232, in the centre of the oscillatory zoned core, the light bluish violet luminescent microperthite ranges in composition from $Or_{44-48}Ab_{52-55}An_{1}$ (Fig. 7.2-10b, Fig. 7.2-5 and Appendix 3). In the margins of the oscillatory zoned core, the microperthite exhibits light violet blue to light blue luminescence zoning and ranges in composition from $Or_{36-48}Ab_{51-64}An_{1-2}$ in the areas near the centre core, and from $Or_{33-41}Ab_{58-66}An_{1-2}$ in the areas near the deuteric coarsened antiperthitic rim (Fig. 7.2-5 and Appendix 3). The Or contents decrease from the centre of the core to the outer margins.

For the deuteric coarsened antiperthitic rim, the deep red luminescent albite host ranges in composition from $Ab_{98-99}Or_{1-2}An_{0-1}$, whereas the dark brown luminescent exsolved K-feldspar is from $Or_{89-95}Ab_{5-11}An_{0-1}$ (Fig. 7.2-5 and Appendix 3), which are the same as that the antiperthitic rim of the braid microperthitic core (see above section b).

7.2.3. Irregular vein antiperthite

In the ferro-edenite syenite (sample C2224), some feldspar crystals show an irregular vein antiperthite texture and no

deuteric coarsened rim (Fig. 7.2-12a). Under CL, the Na-feldspar host usually exhibits light violet blue or dull violet blue luminescence, whereas the exsolved K-feldspar exhibits dull blue (greyish) luminescence (Fig. 7.2-12b). Some feldspar crystals are slightly zoned with a dull violet blue core and a blue or light violet blue rim. CL spectrum of the light violet blue luminescent Na-feldspar host consists of a blue peak centered at 459 nm and a red peak centered at 709 nm. The blue peak intensity is nearly the same as the red peak and the ratio of I_B/I_R is about 1.1 (Fig. 7.2-13a, spectrum A and Table 7.2-1). CL spectrum of the dull blue luminescent exsolved K-feldspar consists of a blue peak centered at 466 nm and a red peak centered at 708 nm. The blue peak intensity is slightly lower than the red peak and the ratio of I_B/I_R is about 0.8 (Fig. 7.2-13a, spectrum B and Table 7.2-1).

The blue or light violet blue luminescent albite host ranges in composition from $Ab_{91-97}Or_{2-7}An_{1-2}$, whereas the dull blue luminescent exsolved K-feldspar is from $Or_{88-90}Ab_{9-11}An_1$ (Table 7.2-1, Fig. 7.2-13b and Appendix 3). These antiperthites may be slightly effected by late-stage fluid alteration because no red luminescent deuteric coarsened rim has been observed, and dull red luminescent secondary albite replaced the albite host merely in some areas within individual antiperthite grains or formed a narrow rim in some feldspar groundmass (see section 7.2.7).

However, irregular vein antiperthites in most of the samples (C182, C294, C322, C371, C2025 and C2223) are strongly affected by the late-stage fluid-feldspar interaction. Under CL, within these

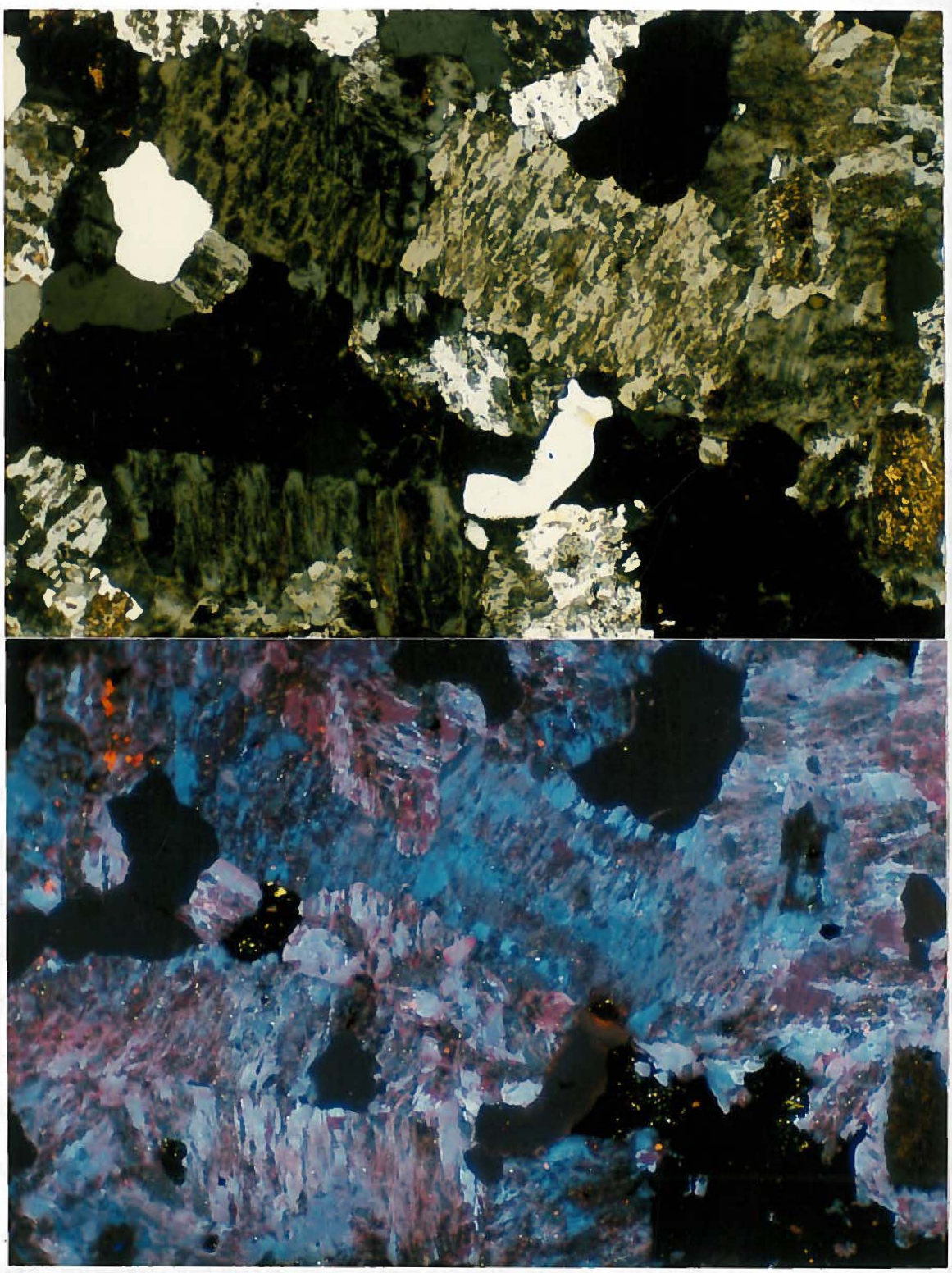

Fig. 7.2-12. Feldspar crystals in ferro-edenite syenite (Sample C2224) from Center III, Coldwell Complex. a. TrL. Feldspar crystals are irregular vein antiperthite. (Photographic conditions: 2 s, ASA 400). b. CL. In the antiperthite, the Na-feldspar host exhibits blue or light violet blue luminescence, and the exsolved K-feldspar exhibits dull blue luminescence. The secondary albite exhibits dull red luminescence. Scale: 50 mm on photograph = 1 mm on thin section. (CL conditions: 10 kV, 0.8 Am. Photographic conditions: 1 nim, ASA 400).

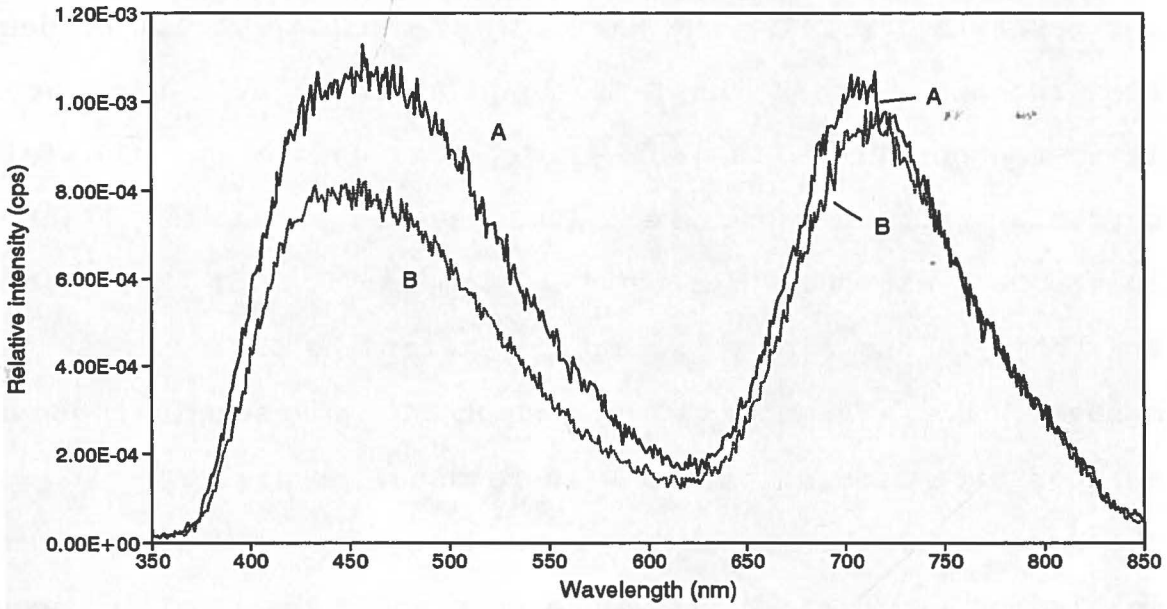

Fig. 7.2-13a. CL spectra of antiperthite in the ferro-edenite syenite (Sample C2224) from Center III, Coldwell Complex, Ontario. (A) is from the light violet blue luminescent Na-feldspar host. (B) is from the dull blue luminescent exsolved K-feldspar. CL conditions: 10 kV, 0.8 mA.

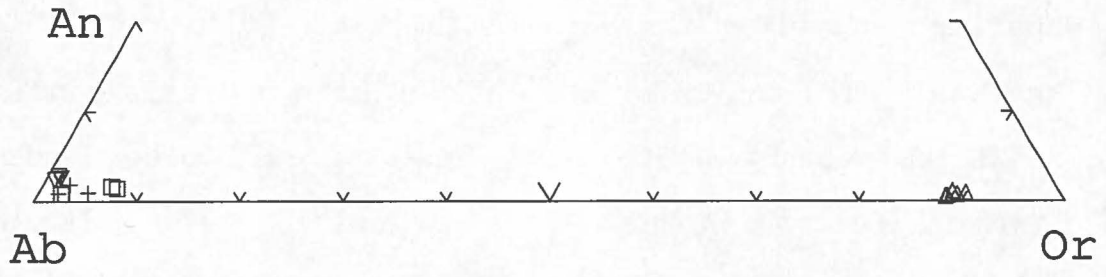

Fig. 7.2-13b. The compositions of the antiperthite in the ferro-edenite syenite (C2224) from Center III plotted in the system Or-Ab-An.

The crosses (+) are the blue luminescent albite host and the squares (□) are the light violet blue luminescent albite host. The up-triangles (▵) are the dull blue luminescent exsolved K-feldspar. The down-triangles (▿) are the dull red luminescent secondary albite.

antiperthite crystals, the Na-feldspar exhibits violet or deep red luminescence whereas the K-feldspar exhibits dull blue or brown luminescence (Fig. 7.2-14b, -15b, -16b). Although, the feldspar crystals contain some red luminescent zones or light blue luminescent microperthite patches. Compositions of the Na-feldspar and the K-feldspar in these antiperthites are usually near the end members, i.e., similar to the deuteric coarsened feldspars in antiperthite rims of the mantled feldspar crystals.

For example in sample C371, the irregular vein antiperthite is mantled by a violet luminescence core and a deep red luminescence rim (Fig. 7.2-14b). The core consists of a light violet luminescent albite host with composition of $Ab_{99-100}Or_{0-1}An_{<1}$ and a dull blue luminescent exsolved K-feldspar with composition of $Or_{83-92}Ab_{8-16}An_{0-1}$ (Fig. 7.2-17a and Appendix 3). The rim consists of deep red luminescent albite host with composition of $Ab_{99-100}Or_{0-1}An_{<1}$ and brown luminescent exsolved K-feldspar with composition of $Or_{86-95}Ab_{5-13}An_{0-1}$ (Fig. 7.2-17a and Appendix 3). The Or contents in the exsolved K-feldspar increase from the core to the rim.

In sample C182 and C294, the antiperthite crystals consist of a dull red luminescent Na-feldspar host, a dull blue luminescent exsolved K-feldspar and light violet blue luminescent microperthitic patches (Fig 7.2-15b, -16b). The dull red luminescent albite host ranges in composition from $Ab_{97-99}Or_{1}An_{1-2}$, whereas the dull blue luminescent exsolved K-feldspar ranges in composition from $Or_{86-95}Ab_{5-13}An_{<1}$ (Fig. 7.2-7b,-11a and Appendix 3). These antiperthite crystals have the same luminescence properties

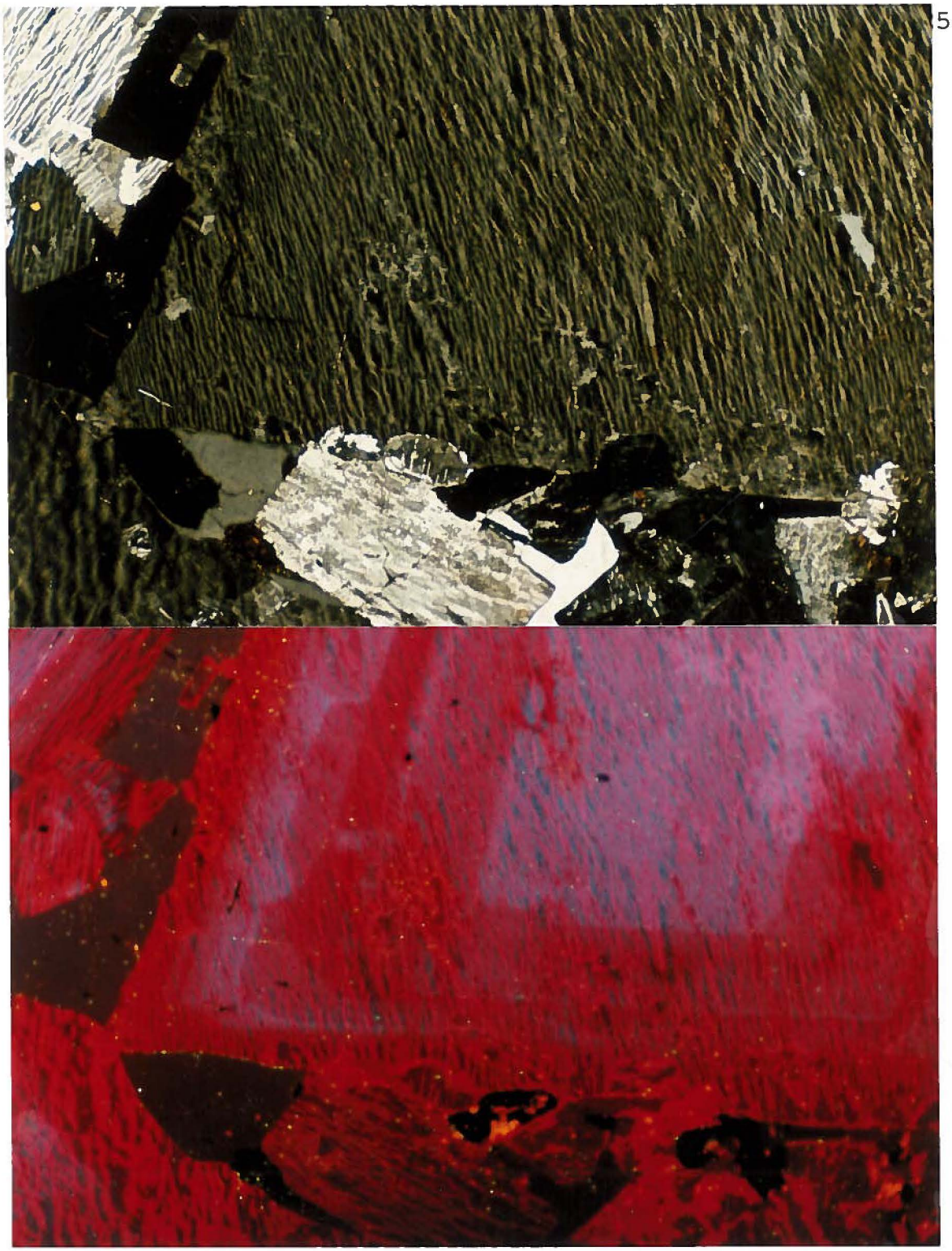

Fig. 7.2-14. Irregular vein antiperthite in the ferro-edenite syenite (Sample C371) from Center III, Coldwell Complex. a. TrL. (Photographic conditions: 2s, ASA 400). b. CL. The antiperthite is zoned with a light violet luminescent core and a deep red luminescent rim. In the core, the Na-feldspar host exhibits light violet luminescence and the exsolved K-feldspar exhibits dull blue luminescence. In the rim, the Na-feldspar host exhibits deep red luminescence and the exsolved K-feldspar exhibits brown luminescence. Scale: 50 mm on photograph = 1 mm on thin section. (CL conditions: 10 kV, 0.8 Am. Photographic conditions: 4 min, ASA 400).

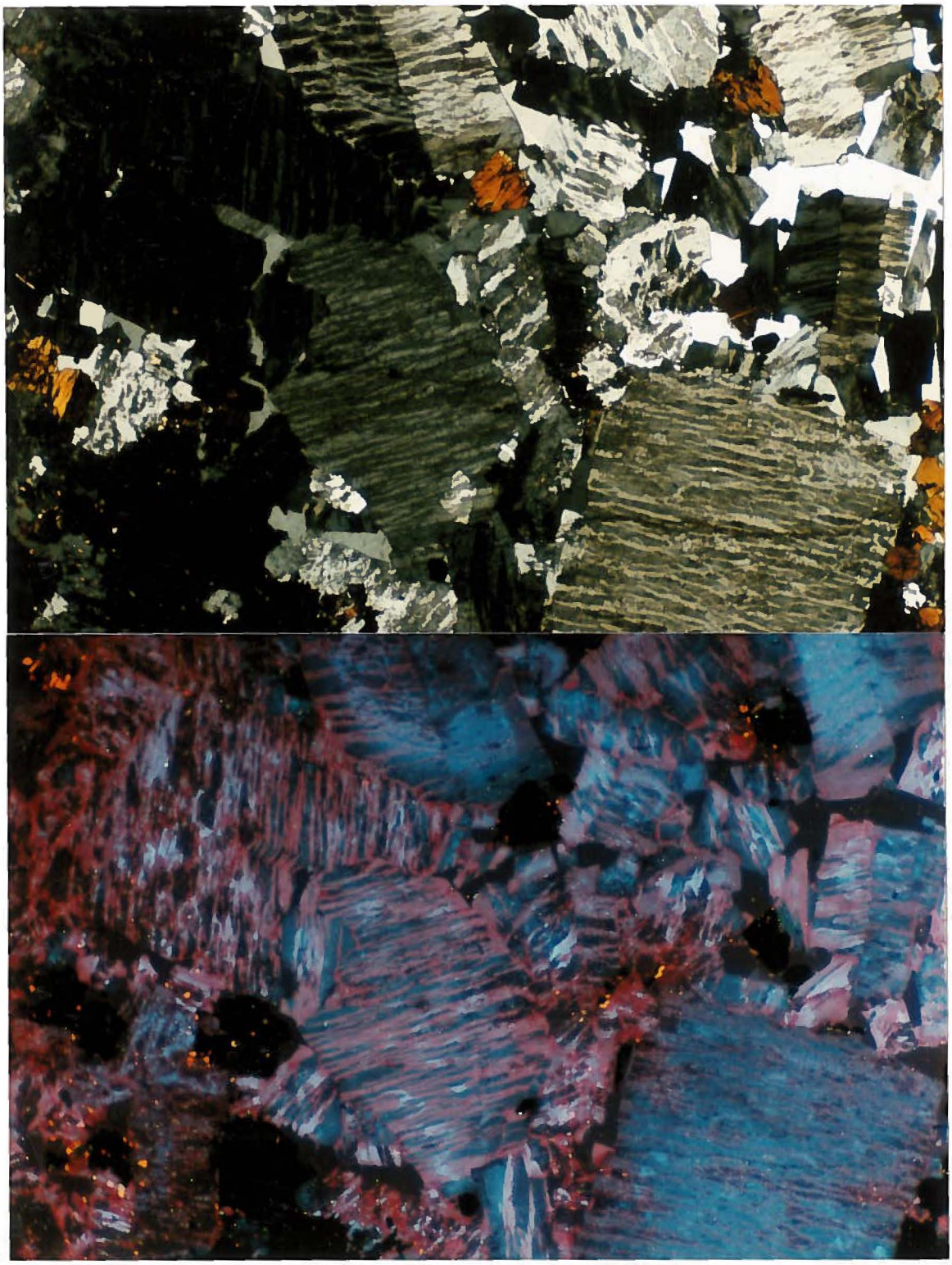

Fig. 7.2-15. Irregular vein antiperthite in the ferro-edenite syenite (Sample C182) from Center III, Coldwell Complex. a. TrL. (Photographic conditions: 2s, ASA 400). b. CL. In the antiperthite, the microperthite patches exhibit light violet blue luminescence, the Na-feldspar host exhibits dull red luminescence and the exsolved K-feldspar exhibits dull blue luminescence. Scale: 50 mm on photograph = 1 mm on thin section. (CL conditions: 10 kV, 0.8 Am. Photographic conditions: 1 min, ASA 400).

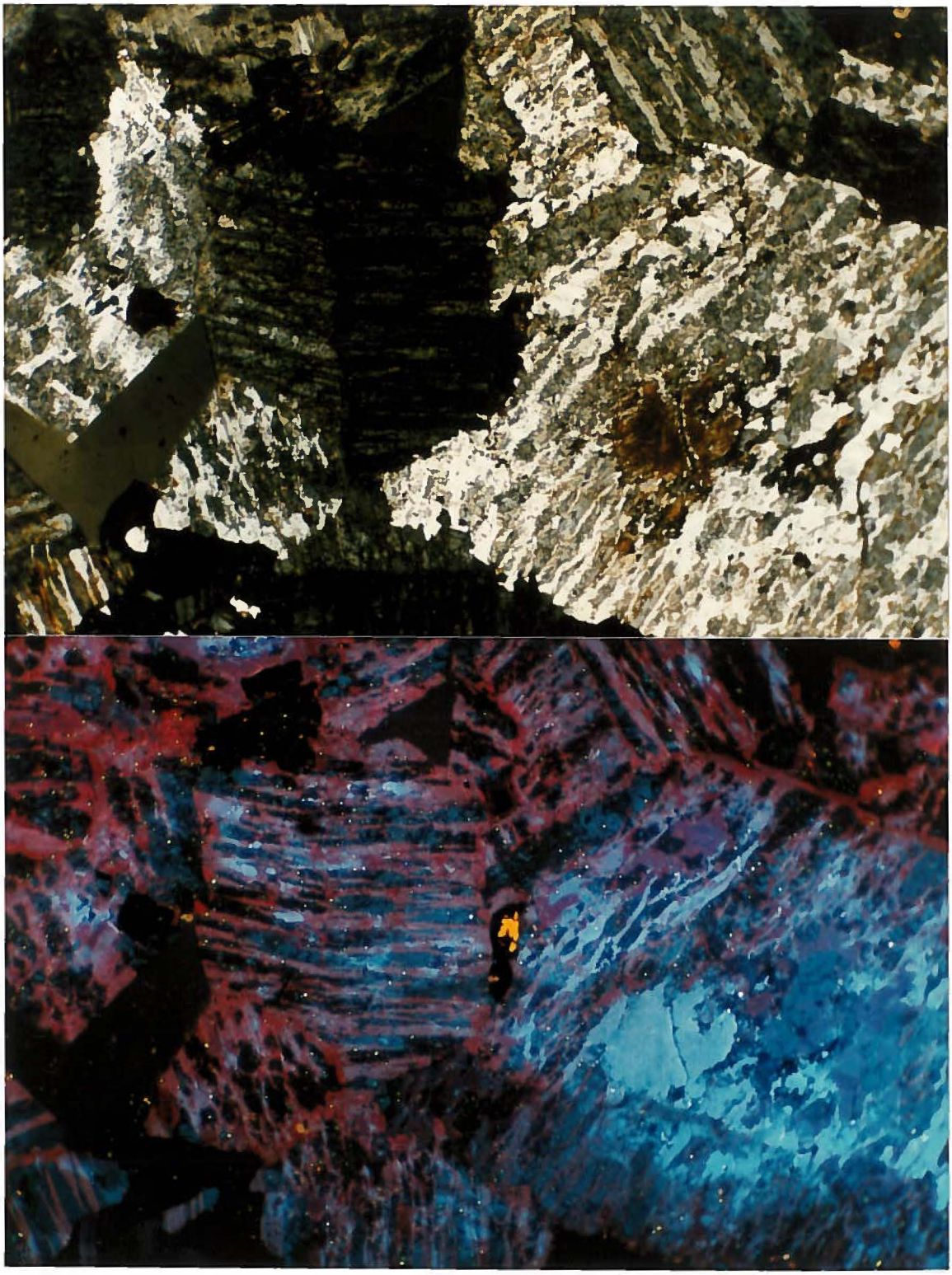

Fig. 7.2-16. Irregular vein antiperthite in the ferro-edenite syenite (Sample C294) from Center III, Coldwell Complex. a. TrL. (Photographic conditions: 1s, ASA 400). b. CL. In the antiperthite, the microperthite patches exhibit light violet blue luminescence, the Na-feldspar host exhibits dull red luminescence and the exsolved K-feldspar exhibits dull blue luminescence. Scale: 50 mm on photograph = 1 mm on thin section. (CL conditions: 10 kV, 0.8 Am. Photographic conditions: 1 min, ASA 400).

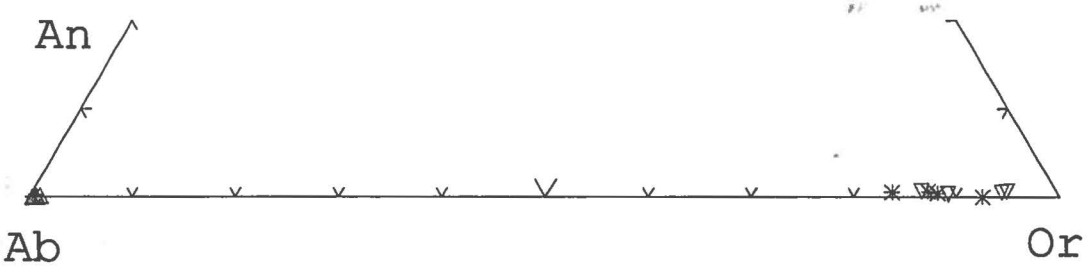

Fig. 7.2-17a. The compositions of the feldspars in the ferro-edenite syenite (C371) from Center III plotted in the system Or-Ab-An.

The crosses (+) are the light violet luminescent albite host and the asterisks (*) are the dull blue luminescent exsolved K-feldspar in the core of antiperthite. The up-triangles (▵) are the deep red luminescent albite host and the down-triangles (▿) are the brown luminescent exsolved K-feldspar in the rim of the antiperthite.

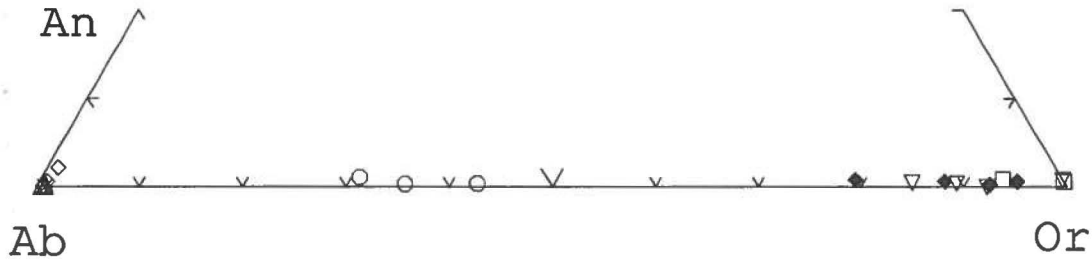

Fig. 7.2-17b. The compositions of the feldspars in the ferro-edenite syenite (C322) from Center III plotted in the system Or-Ab-An.

For mantled feldspar crystals, the diamonds (◇) are the light blue luminescent albite host and the filled diamonds (◆) are the dull blue luminescent exsolved K-feldspar in antiperthite core. The open circles (○) are the light violet blue luminescent microperthite in intermediate mantle. The up-triangles (▵) are the red luminescent albite host and the down-triangles (▿) are the brown luminescent exsolved K-feldspar in deuteric coarsened antiperthitic rim.

For feldspar inclusions in biotite, the squares (□) and the cross (+) are the dark brown luminescent K-feldspar and albite, respectively.

and compositions as the deuteric coarsened feldspars in the antiperthitic rim of the mantled feldspar crystals.

7.2.4. Feldspar-quartz-biotite intergrowths

Feldspar-quartz-biotite intergrowth texture is observed in sample C322. The texture consists of some small, lens-shaped feldspar and quartz grains included in a biotite crystal parallel to the basal cleavage (Fig. 7.2-18a). Most of the feldspar grains are perthite and under CL, they and quartz grains exhibit dark brown luminescence (Fig. 7.2-18b). The dark brown luminescent perthite consists of K-feldspar with composition of $Or_{93-99}Ab_{0-6}An_1$ and albite with a composition of $Ab_{99}Or_1$ (Fig. 7.2-17b and Appendix 3).

7.2.5. Graphic intergrowth

Graphic intergrowth texture is observed in sample C2135 with angular cuneiform quartz interconnected within feldspar crystals (Fig, 7.2-19a). The feldspar crystals have diverse textures which consist of perthite, mesoperthite, antiperthite and albite-twinned Na-feldspar, within a single thin section. Under CL, the K-feldspar exhibits dull blue luminescence whereas the Na-feldspar exhibits dull violet or violet luminescence (Fig. 7.2-19b). Deuteric coarsened antiperthitic rims and secondary feldspars are not observed, implying that late-stage fluid induced alteration did not occur in this sample.

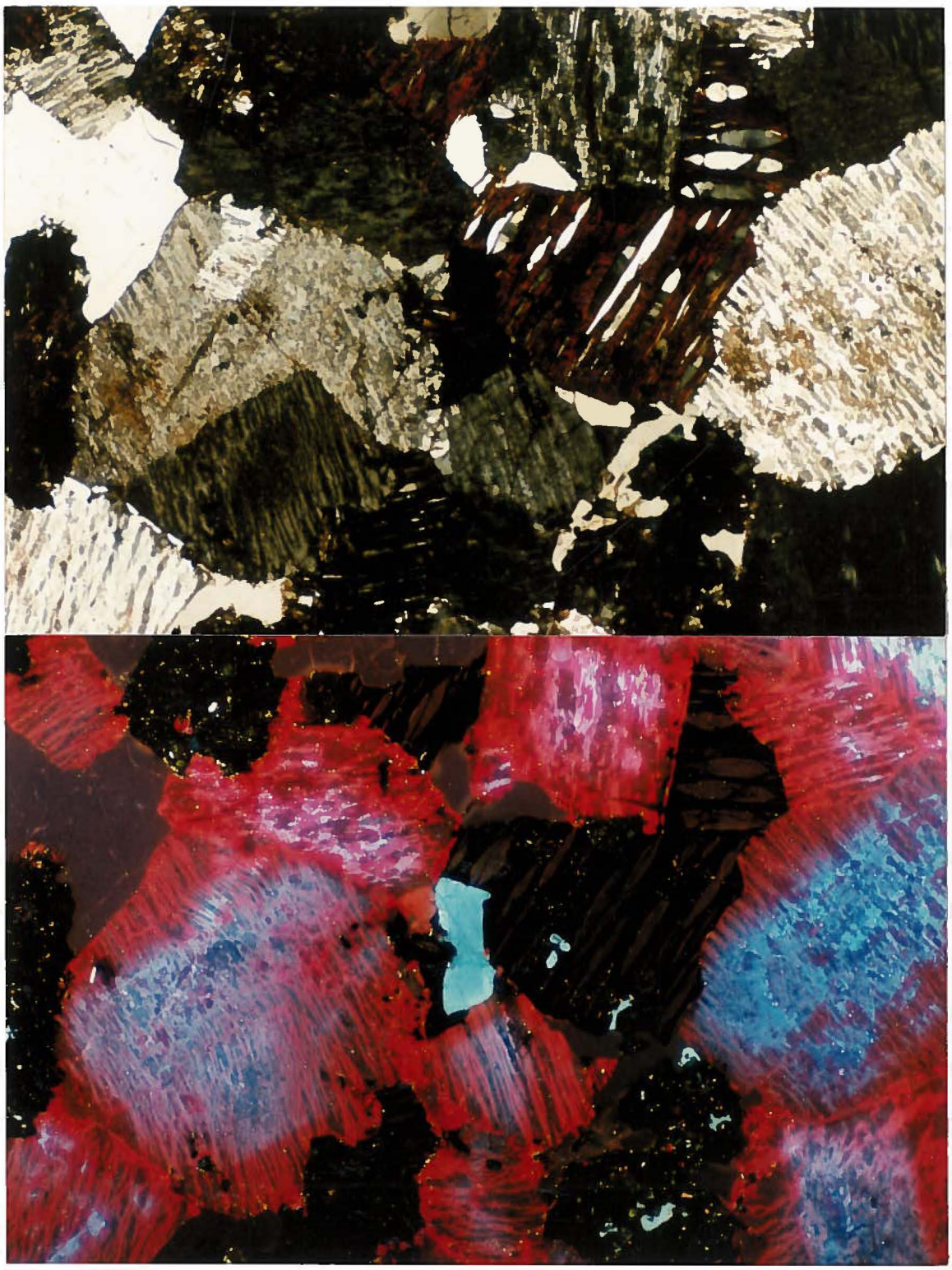

Fig. 7.2-18. Secondary feldspars intergrowths with biotite and quartz texture in the ferro-edenite syenite (Sample C322) from Center III, Coldwell Complex. a. TrL. The lens-shaped feldspars and quartz grains are included in biotite parallel to the basal cleavage. Most of the feldspar inclusions are perthite. (Photographic conditions: 2s, ASA 400). b. CL. Within the biotite grains, the feldspars exhibit dark brown luminescence and the quartz also exhibits dark brown luminescence. Light blue luminescent crystals in centre of picture are fluorite. Scale: 50 mm on photograph = 1 mm on thin section. (CL conditions: 10 kV, 0.8 Am. Photographic conditions: 1 min, ASA 400).

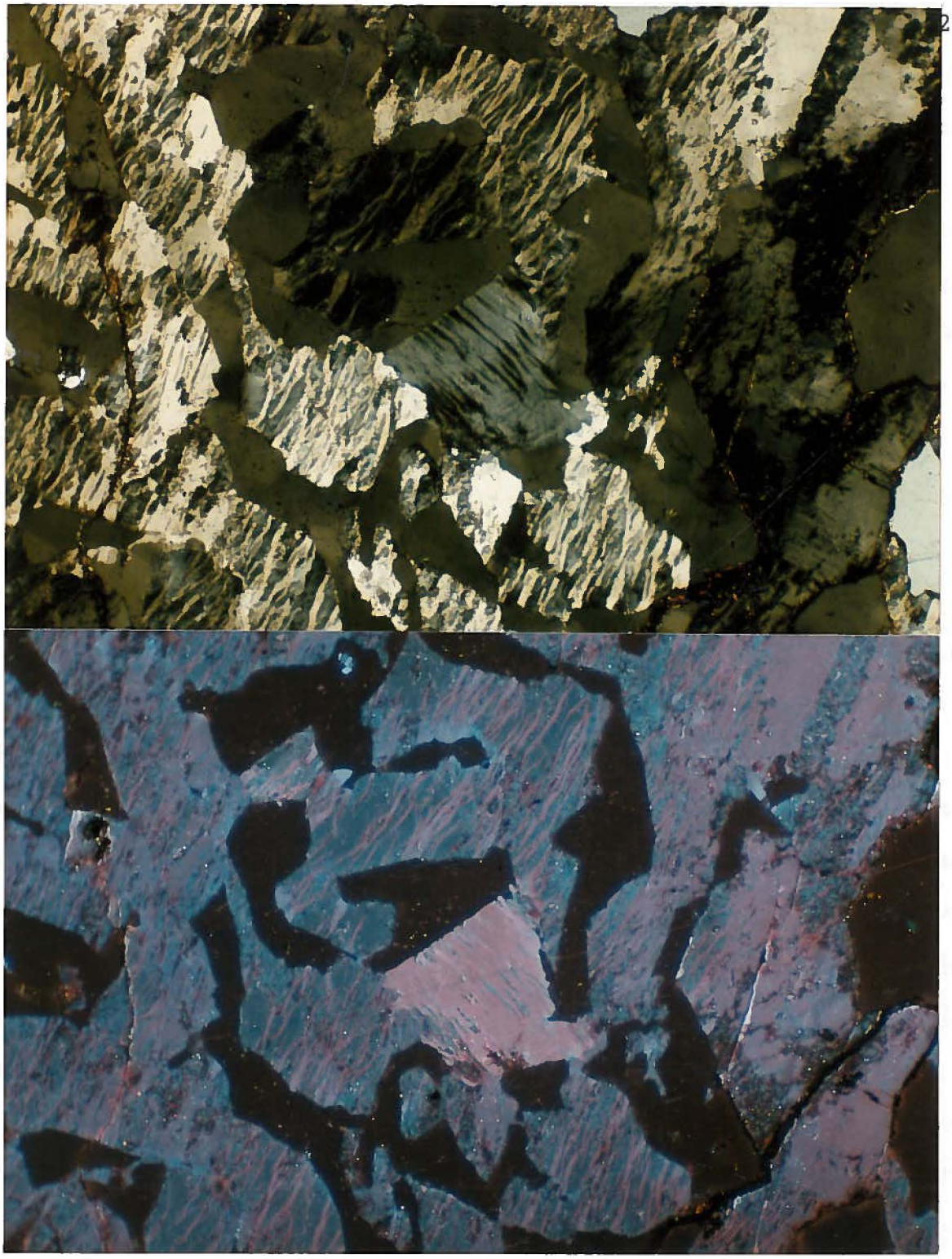

Fig. 7.2-19. Graphic intergrowth texture in the ferro-edenite syenite (Sample C2135) from Center III, Coldwell Complex. a. TrL. Feldspars intergrown with angular cuneiform quartz. The feldspar crystals have diverse textures which consist of perthite, mesoperthite, antiperthite and albite-twinned Na-feldspar. (Photographic conditions: 1.5s, ASA 400). b. CL. The exsolved K-feldspar exhibits dull blue luminescence and the exsolved Na-feldspar exhibits dull violet or violet luminescence. Scale: 50 mm on photograph = 1 mm on thin section. (CL conditions: 10 kV, 0.8 Am. Photographic conditions: 1 min, ASA 400).

7.2.6. Late-stage fluid induced coarsening and replacement

a. Deuteric coarsened perthite and antiperthite

As discussed above, deuteric coarsened feldspars form the perthitic rims of the unexsolved alkali feldspar cores, and form antiperthitic rims on most mantled feldspar crystals as a consequence of late-stage fluid-feldspar interaction. For all analyzed antiperthitic rims, the deuteric coarsened albites range in composition from $Ab_{97-100}Or_{0-2}An_{0-1}$ and the deuteric coarsened K-feldspars range in composition from $Or_{85-100}Ab_{0-15}An_{0-1}$ (Fig. 7.2-2b, -5,-7b,-11a,-11b,-13b,-17a,-17b and Appendix 3).

b. Secondary feldspars

1). Secondary K-feldspar

Secondary K-feldspars usually occur in the small fractures, or as irregular patches replacing the microperthite in the core of mantled feldspar crystals (samples C294 and C2232). The secondary K-feldspars commonly contain many very small (few μm) hematite grains and micropores which are only visible in SEM/BES. The secondary K-feldspars usually exhibit dull blue luminescence (Fig. 7.2-4b, -6b). The dull blue luminescent secondary K-feldspar ranges in composition from $Or_{90-99}Ab_{0-9}An_{1}$ (Fig. 7.2-5,-7b and Appendix 3).

2). Secondary albite

Secondary albites usually occur in the interstices between perthite or antiperthite grains, or occur as irregular veins cutting the deuteric coarsened perthitic or antiperthitic rims.

These secondary albites usually exhibit dull red, or purple luminescence. In sample C2124, dull red luminescent secondary albite ranges in composition from $Ab_{94-95}Or_{1-2}An_{4-5}$ (Fig. 7.2-1b, Fig. 7.2-2b and Appendix 3). In sample C2224, the dull red luminescent secondary albite ranges in composition from $Ab_{96-97}Or_{1}An_{2-3}$ (Fig. 7.2-12b, Fig. 7.2-13b and Appendix 3). In samples C2232 and C294, secondary albites exhibit purple luminescent, some are albite twinned (C294), and range in composition from $Ab_{95-98}Or_{1-2}An_{1-4}$ (Fig. 7.2-4b,-6b, Fig. 7.2-5b,-7b and Appendix 3). In generally, the secondary albite has higher An contents (1-5 mole%) than the deuteric coarsened albite (0-1 mole%) in the antiperthitic rims of mantled feldspar crystals.

7.2.7. Plagioclase in a xenolith of metasomatized basalt

In a xenolith of metasomatized basalt (sample C2124), the plagioclase crystals usually exhibit light blue luminescence (Fig. 7.2-20b). In the areas near the contact with the ferro-edenite syenite, some of the plagioclase crystals are replaced along the rim by secondary perthitic feldspars. CL spectrum of the light blue luminescent plagioclase consists of a high blue peak centered at 465 nm and a red peak centered at 709 nm with a ratio of I_B/I_R about 1.5 (Fig. 7.2-21 and Table 7.2-1). In the areas further way from contact with the ferro-edenite syenite, the plagioclase ranges in composition from $Ab_{84-91}An_{8-15}Or_{1-2}$ (Fig. 7.2-2b and Appendix 3). However, in the areas near the contact, the plagioclase ranges in composition from $Ab_{91-96}An_{3-7}Or_{1-2}$ (Fig. 7.2-2b and Appendix 3). The Ab

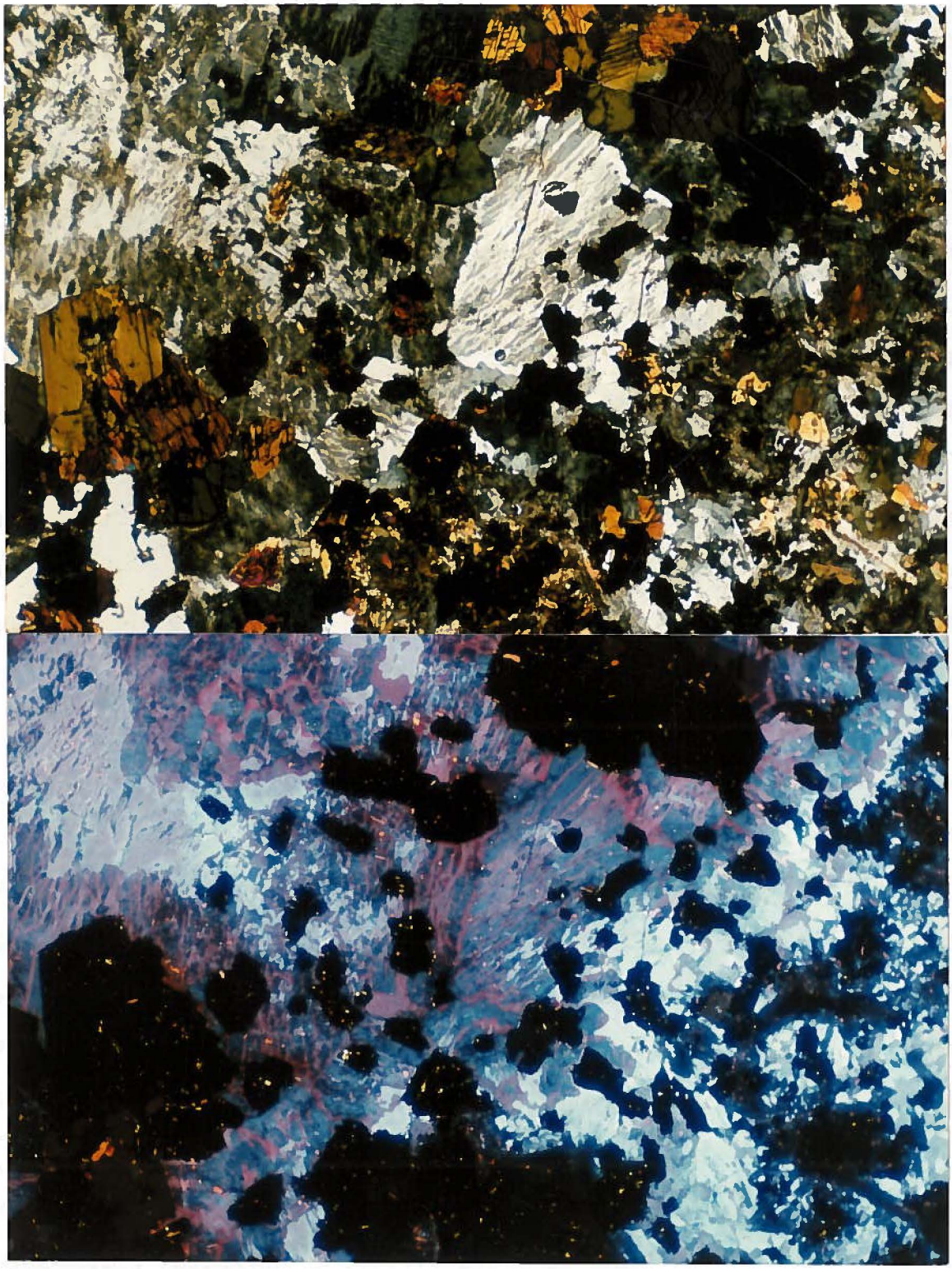

Fig. 7.2-20. Plagioclase and perthite in xenolith in the ferro-edenite syenite (Sample C2124) from Center III, Coldwell Complex. a. TrL. (Photographic conditions: 2s, ASA 400). b. CL. Plagioclase grains exhibit light blue luminescence and are replaced by perhtite along the xenolith margins. In the perthite, the K-feldspar exhibits dull blue luminescence and the albite exhibits dull violet luminescence. Scale: 35 mm on photograph = 1 mm on thin section. (CL conditions: 10 kV, 0.8 Am. Photographic conditions: 1 min, ASA 400).

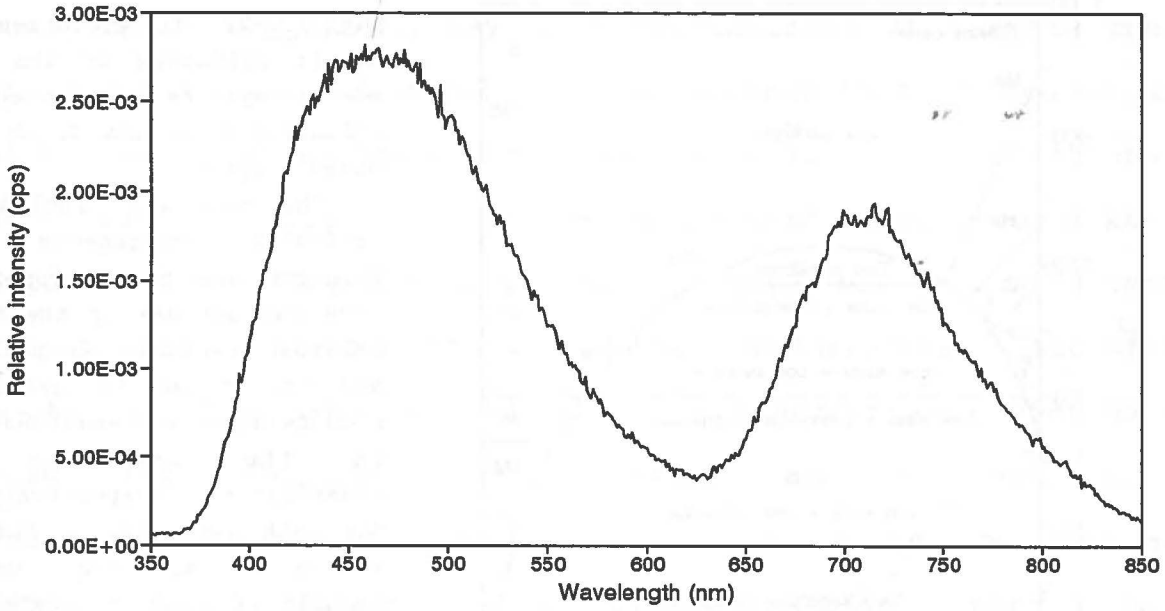

Fig. 7.2-21. CL spectrum of the light blue luminescent plagioclase in xenolith (Sample C2124) from Center III, Coldwell Complex, Ontario. CL conditions: 10 kV, 0.8 mA.

contents in the plagioclase increase as the distance from the contact decreases.

At the margins of the xenolith, the plagioclase is replaced by perthite which forms an irregular rim surrounding plagioclase crystals (Fig. 7.2-20b). In the perthite, the K-feldspar exhibits dull blue luminescence with composition of $Or_{88-94}Ab_{6-12}An_{0-1}$ and the albite exhibits dull violet luminescence with composition of Ab_{94-99} $Or_{1-2}An_{0-4}$. (Fig. 7.2-2b and Appendix 3).

7.2.8. Thermal history of the feldspars

The thermal history of the alkali feldspars in the ferro-edenite syenite is shown in Fig. 7.2-22. The path a-a′ on the incoherent solvus (SFS) indicates that the alkali feldspar crystals with a

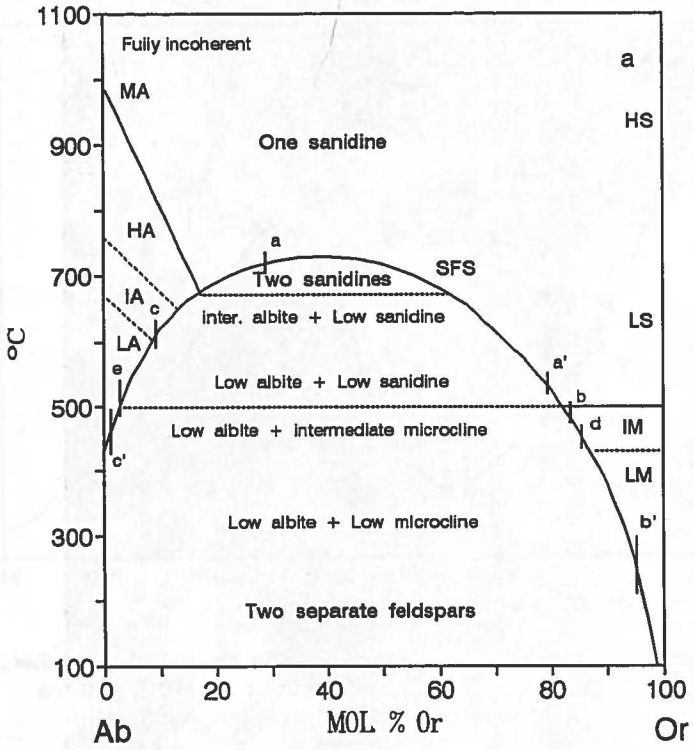

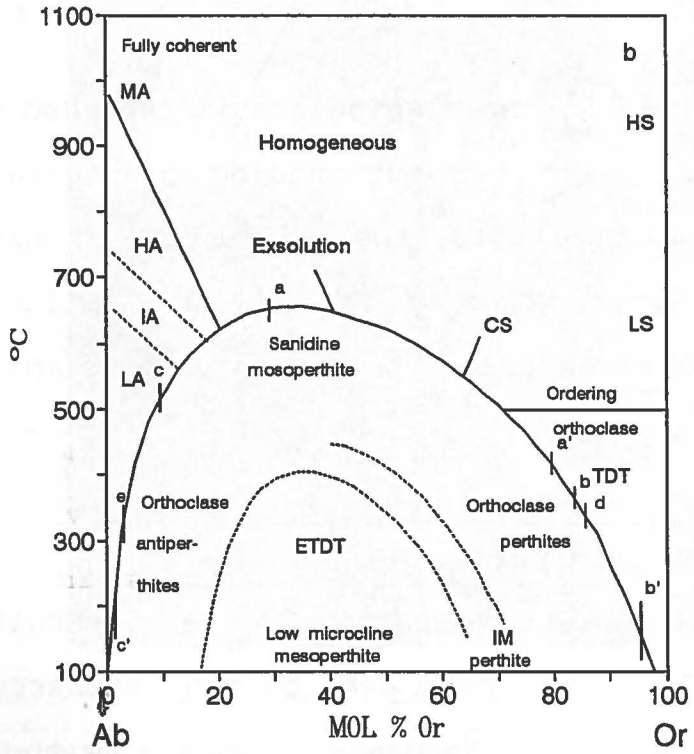

Fig. 7.2-22. The evolution of the alkali feldspars in the ferro-edenite syenite from Center III is illustrated in the Or-Ab binary phase diagram.

The path a-a′ includes the optically homogeneous alkali feldspar and the microperthitic core and patches in the mantled feldspar crystals. The paths b-b′ and c-c′ include the exsolved K-rich feldspar and exsolved albite in the irregular vein anperthitite, respectively, and the path c-c′ also includes the albite core, mantle and rim in the mantled feldspar crystals. The points d and e indicate that the secondary K-feldspar and albite in the deuteric coarsened antiperthitic rim are formed at temperatures bellow 350 °C.

Diagram (a) shows the phase relationships for An-free alkali feldspars under complete (incoherent) equilibrium and (b) shows different constrained equilibrium states as a function of bulk composition and T for completed coherent intergrowths (Brown and Parsons, 1989). SFS is the strain-free solvus and CS is the coherent solvus. TDT is the twin-domain microtexture and ETDT is the exsolution and the twin-domain microtexture. MA, HA, IA and LA are monoclinic, high, intermediate and low albite; IM and LM are intermediate and low microcline. IA and IM is the region of the rapid change in Y ordering.

composition of $Or_{21-71}Ab_{28-78}$ may have crystallized at temperatures about ≥725-520 °C, and developed the microperthite textures at about 650-420 °C along the coherent solvus (CS). This compositional range includes the light violet blue luminescent homogeneous alkali feldspar core ($Or_{39-44}Ab_{55-59}$); the light blue luminescent microperthitic core ($Or_{49-71}Ab_{28-49}$) and the braid microperthitic core ($Or_{26-38}Ab_{59-71}$); the light bluish violet luminescent microperthite core and margin ($Or_{44-48}Ab_{52-55}$ and $Or_{33-41}Ab_{58-66}$); and the bluish violet luminescent microperthite patches ($Or_{21-48}Ab_{51-78}$) in the mantled feldspar crystals. In comparison with the Or-Ab-An ternary system at 1 Kbar, the alkali feldspar crystallized at about 750 °C.

The path c-c′ on the incoherent solvus (SFS) indicates that the light blue luminescent albite core in sample C2232 and the light blue luminescent intermediate mantle and rim in sample C294, all with compositions of $Ab_{90-98}Or_{1-4}$, formed at a relatively low temperature range from 600-450 °C.

The paths b-b′ and c-c′ on the coherent solvus (CS) indicate that the exsolved K-feldspar with a composition of $Or_{83-95}Ab_{5-16}$ and the exsolved albite with composition of $Ab_{91-100}Or_{0-7}$ formed during cooling at temperatures below 370 °C and 520 °C, respectively. These compositional ranges include the dull violet blue, dull blue and brown luminescent exsolved K-feldspar; and the blue, light violet blue, violet and deep red luminescent exsolved albite in the irregular vein antiperthite.

Since the secondary albite and K-feldspar in the deuteric coarsened antiperthitic rim have end member compositions, they

formed at very low temperatures about <350 °C below the points e and d.

7.3. Feldspars in Contaminated Ferro-edenite Syenite

7.3.1. Introduction

In the contaminated ferro-edenite syenite, the feldspar phenocrysts mainly consist of zoned plagioclase, K-feldspar, perthite and antiperthite. Groundmass feldspars mainly consist of K-feldspar, perthite, antiperthite and secondary Na-feldspar.

The plagioclase crystals are commonly mantled with an oligoclase-andesine core and an albite rim. Under CL, the oligoclase-andesine cores exhibit light greenish blue luminescence, whereas the albite rims exhibit light blue to light violet blue luminescence. The cores are usually replaced by dull blue luminescent secondary Na- and K-feldspars. The plagioclase phenocrysts are usually surrounded by a blue to dull blue luminescent, K-rich feldspar groundmass.

Most perthite phenocrysts are Carlsbad twinned and exhibit an irregular vein texture. Some of them are mantled with an incipient perthitic core and a deuteric coarsened perthitic rim. Under CL, the exsolved Na-feldspar exhibits light blue luminescence, whereas the K-feldspar host exhibits light violet blue luminescence. Some unexsolved feldspar occurs in the centre of the perthitic core and exhibits variable luminescence colours from light blue to light violet. These perthite phenocrysts usually associate with the blue luminescent perthite groundmass or the dull blue luminescent K-feldspar groundmass.

The antiperthite phenocrysts are Carlsbad twinned and usually exhibit a regular vein texture. Under CL, the exsolved K-feldspar exhibits dull blue luminescence whereas the Na-feldspar host

exhibits red luminescence. Some of the antiperthite crystals are mantled with a braid microperthite core or mantle. This braid microperthite exhibits light blue luminescence. The antiperthite phenocrysts are usually associated with the dull red luminescent antiperthite groundmass.

Secondary feldspars in this contaminated ferro-edenite syenite are mainly deuteric coarsening feldspars and the secondary Na-feldspar.

7.3.2. Plagioclase phenocrysts

The plagioclase phenocrysts (in samples C2036, C2029) are usually mantled with light greenish blue luminescent cores and light blue to light violet blue luminescent rims (Fig. 7.3-1b, -2b). For example, in sample C2036, the CL spectrum of the light greenish blue luminescent core consists of a very high, broad blue peak centered at about 473 nm and a very weak peak centered at about 815 nm (Table 7.3-1 and Fig. 7.3-3a, spectrum A). Since no red peak occurs at about 700 nm, the light greenish blue core has a very high I_B/I_R ratio of about 33.7.

The CL spectrum of the light blue luminescent inner rim consists of a high blue peak centered at about 453 nm, a weak red peak centered at about 707 nm and a very weak infrared peak at about 800 nm (Table 7.3-1 and Fig. 7.3-3a, spectrum B), the ratio of I_B/I_R is about 3.0. The CL spectrum of the light violet blue luminescent outer rim consists of a low blue peak centered at about 460 nm, a very weak red peak centered at about 700 nm and a very weak

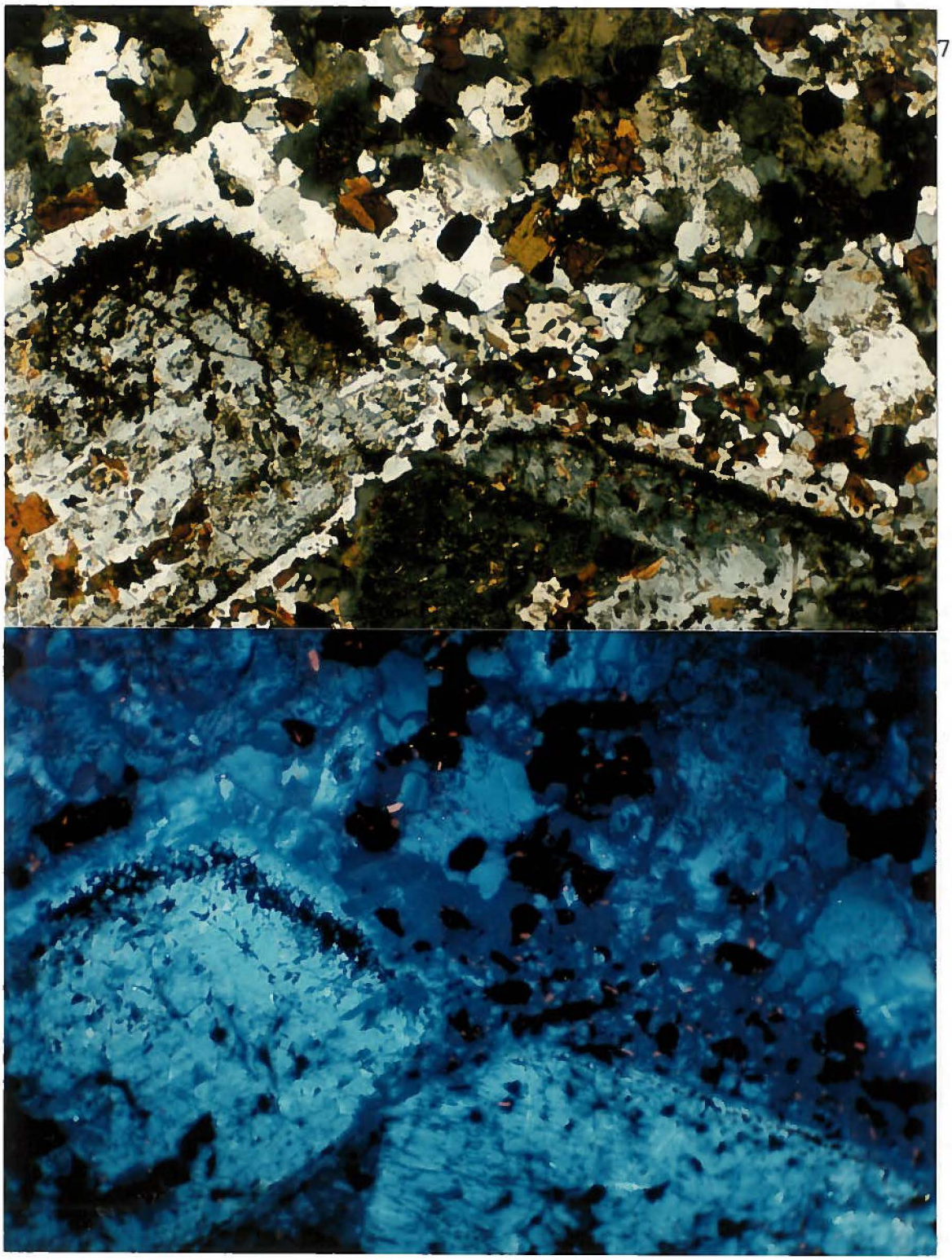

Fig. 7.3-1. Plagioclase phenocryst and K-feldspar groundmass in contaminated ferro-edenite syenite (Sample C2036) from Center III, Coldwell Complex. a. TrL. (Photographic conditions: 2 s, ASA 400) b. CL. The plagioclase phenocrysts are mantled with a light greenish blue luminescent oligoclase-andesine core and a light blue to light violet blue albite rim. The K-feldspar grains in groundmass are slightly mantled with blue luminescent cores and dull blue luminescent rims. The dull violet luminescent areas which surround the K-feldspar in the groundmass are the secondary K-feldspar. Scale: 50 mm on photograph = 1 mm on thin section. (CL conditions: 10 kV, 0.8 Am. Photographic conditions: 8 s, ASA 400).

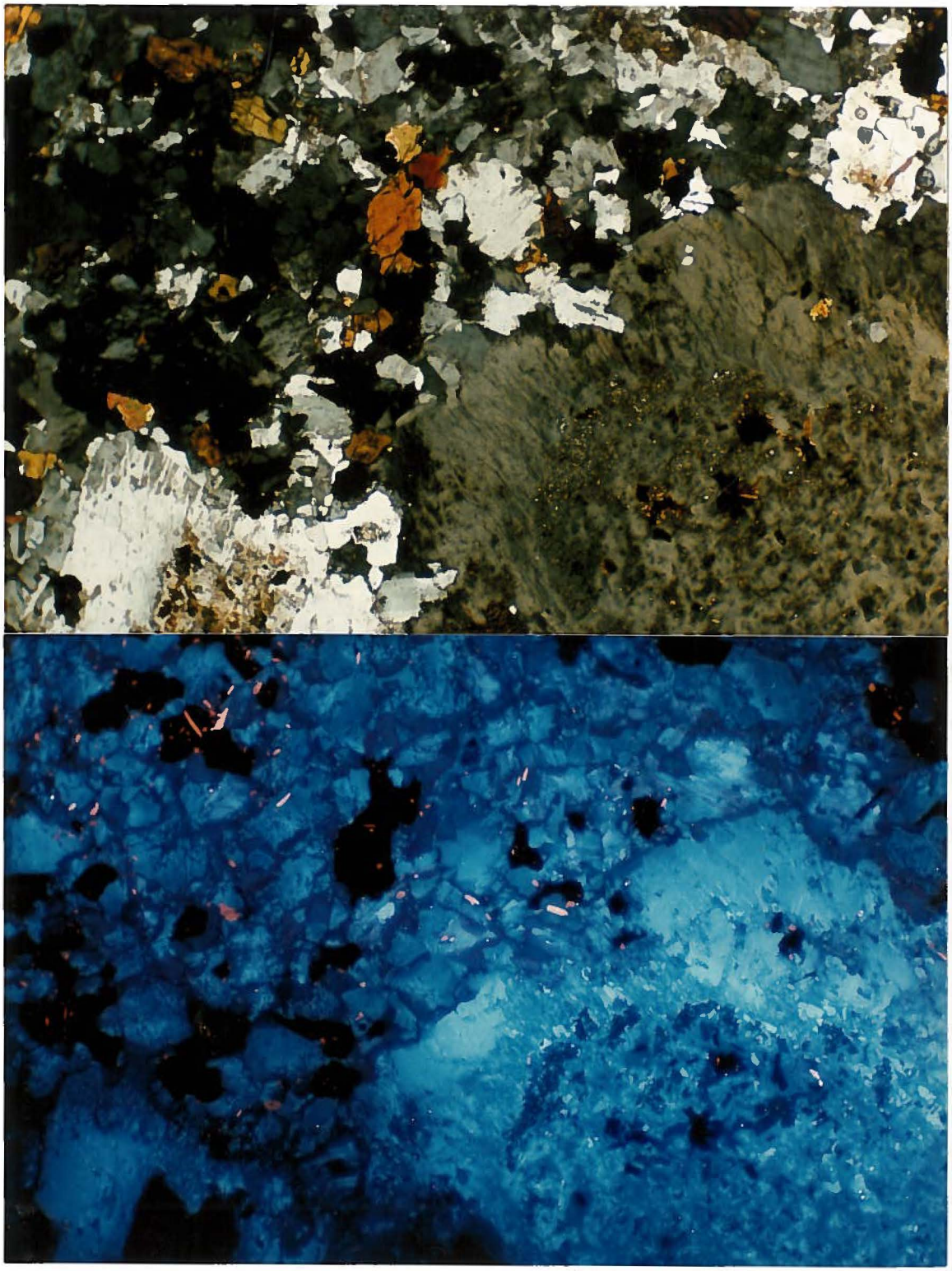

Fig. 7.3-2. Plagioclase phenocrysts and K-feldspar groundmass in contaminated ferro-edenite syenite (Sample C2036) from Center III, Coldwell Complex. a. TrL. (Photographic conditions: 1 s, ASA 400) b. CL. The core of the plagioclase phenocryst is replaced by dull blue luminescent secondary Na- and K-feldspar, and the light blue luminescent albite rim is replaced by dull blue luminescent secondary K-feldspar. The K-feldspar grains in the groundmass are slightly mantled with blue luminescent cores and dull blue luminescent rims. The dull violet luminescent areas which surround the K-feldspar grains in the groundmass are the secondary Na-feldspar. Scale: 50 mm on photograph = 1 mm on thin section. (CL conditions: 10 kV, 0.8 Am. Photographic conditions: 15 s, ASA 400).

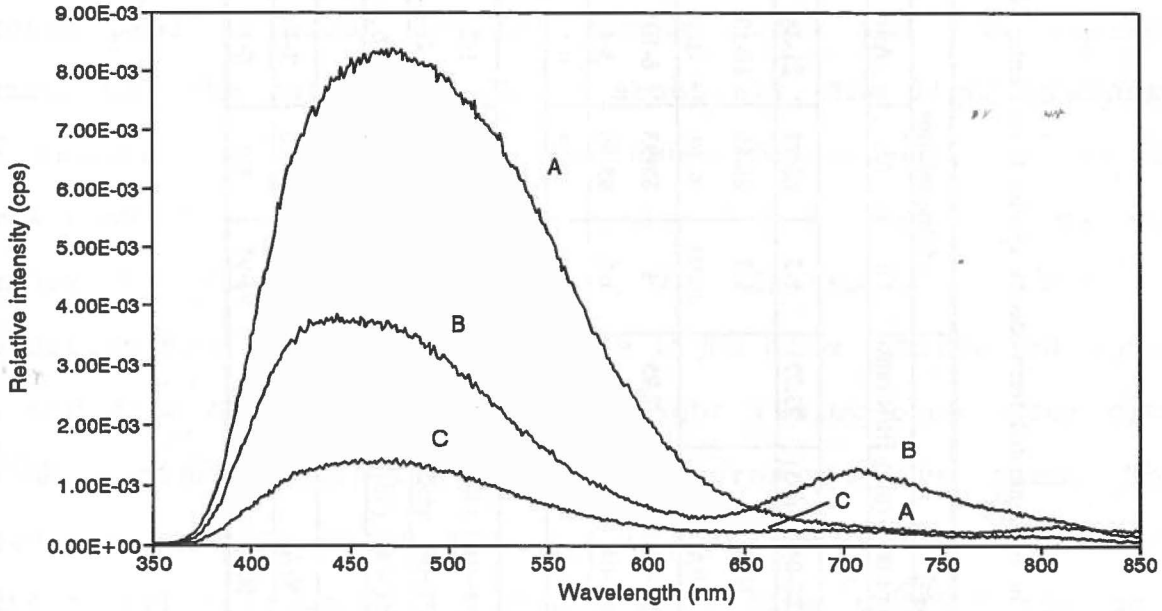

Fig. 7.3-3a. CL spectra of the feldspar phenocryst in the contaminated ferro-edenite syenite (Sample C2036) from Center III, Coldwell Complex, Ontario. (A) is from the light greenish blue luminescent oligoclase-andesine core. (B) is from the light blue luminescent Na-feldspar in the inner rim. (C) is from the light violet blue luminescent Na-feldspar in the outer rim. CL conditions: 10 kV, 0.8 mA.

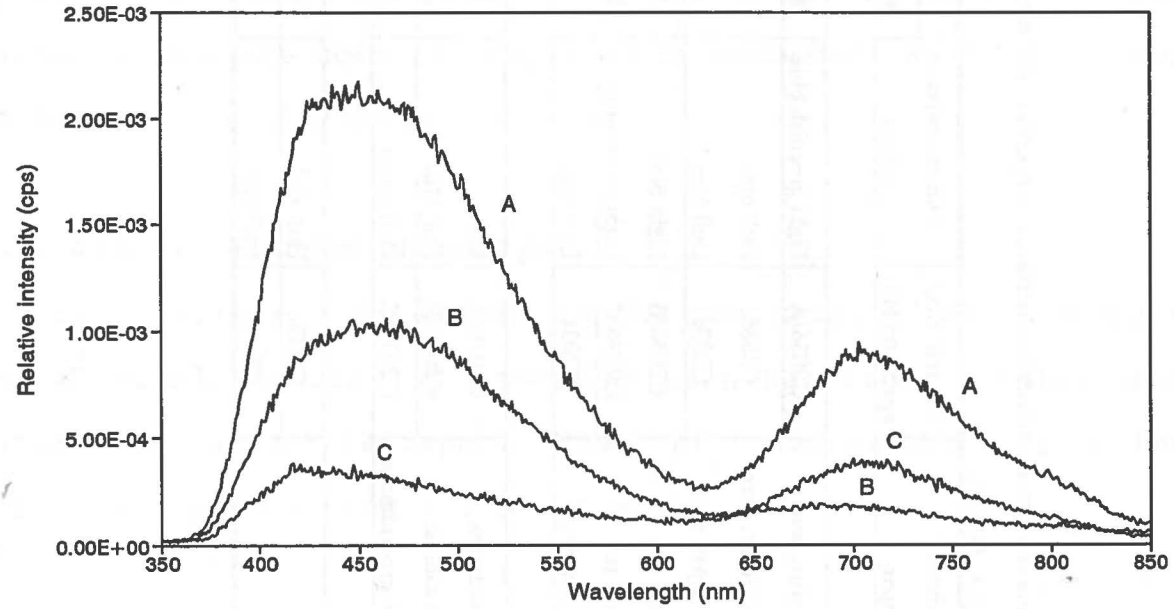

Fig. 7.3-3b. CL spectra of the feldspar groundmass in the contaminated ferro-edenite syenite (Sample C2036) from Center III, Coldwell Complex, Ontario. (A) is from the violet blue luminescent K-feldspar and (B) is from the dull blue luminescent K-feldspar. (C) is from the dull violet luminescent secondary Na-feldspar. CL conditions: 10 kV, 0.8 mA.

Table 7.3-1. Representative cathodoluminescence properties and compositions of feldspars in contaminated ferro-edenite syenite from Center II Coldwell Complex, Ontario

Occurrence of feldspar	Sample No./ spectrum No.	Luminescence colour	Intensities (cps)					Compositions		
			Blue peak	(nm)	Red peak	(nm)	B/R ratio	Or	Ab	An
Phenocryst:										
Oligoclase-andesine, core	C2036/A	Light greenish blue	8.34E-03	(473)	2.47E-04	(695)	33.77	1-2	62-77	21-38
Secondary Na-feldspar, core	C2036	Dull blue	N/A		N/A			1-2	86-88	10-13
Secondary K-feldspar, core	C2036	Dull blue	N/A		N/A			79-93	6-20	1
Na-feldspar, inner rim	C2036/B	Light blue	3.74E-03	(453)	1.27E-03	(707)	2.95	1	89-93	6-10
Na-feldspar, outer rim	C2036/C	Light violet blue	1.41E-03	(460)	2.30E-04	(700)	6.13	1-2	95-96	3-4
2nd K-feldspar, inner rim	C2036	Dull blue	N/A		N/A			75-83	16-25	0-1
Groundmass:										
K-feldspar, groundmass	C2036/A	Blue	2.09E-03	(452)	8.94E-04	(707)	2.33	79-83	15-20	1-2
K-feldspar, groundmass	C2036/B	Dull blue	1.01E-03	(460)	1.87E-04	(695)	5.39	91	8	1
2nd Na-feldspar, groundmass	C2036/C	Dull violet	3.11E-04	(457)	3.85E-04	(707)	0.81	1	94-98	1-5
Aplitic dike:										
Na-feldspar	C2036	Dull violet	N/A		N/A			1-2	94-96	3-4
K-feldspar	C2036	Dull blue	N/A		N/A			91-95	4-9	0-1

infrared peak at about 809 nm, (Table 7.3-1 and Fig. 7.3-3a, spectrum C), the ratio of I_B/I_R is about 6.1. The light greenish blue luminescent cores are oligoclase-andesine which range in composition from $Ab_{62-77}An_{21-38}Or_{1-2}$ (Table 7.3-1, Fig. 7.3-4a and Appendix 3). Whereas the rims are the albites which range in composition from $Ab_{89-93}An_{6-10}Or_1$ for the light blue luminescent inner rim, and from $Ab_{95-96}An_{3-4}Or_{1-2}$ for the light violet blue outer rim. The Ab contents increase from the cores to the rims. The oligoclase-andesine cores are usually replaced by secondary Na-feldspar and K-feldspar and the albite rims usually are only replaced by K-feldspar.

In sample C2065 (Fig. 7.3-5b), the light greenish blue luminescent plagioclase crystals are andesines which range in composition from $Ab_{52-65}An_{33-45}Or_{1-2}$ (Fig. 7.3-4c and Appendix 3). These andesine grains are commonly replaced by secondary Na-feldspar and K-feldspar along the margins.

7.3.3. Alkali feldspar phenocrysts

Alkali feldspar phenocrysts in the contaminated ferro-edenite syenite, mainly consist of irregular vein perthite, regular vein antiperthite and K-feldspar. Most of the perthite and the antiperthite grains show a zoned texture.

a. Irregular vein perthite

Most the irregular vein perthite phenocrysts (sample C2063) are mantled with an incipient perthitic core and a deuteric coarsened

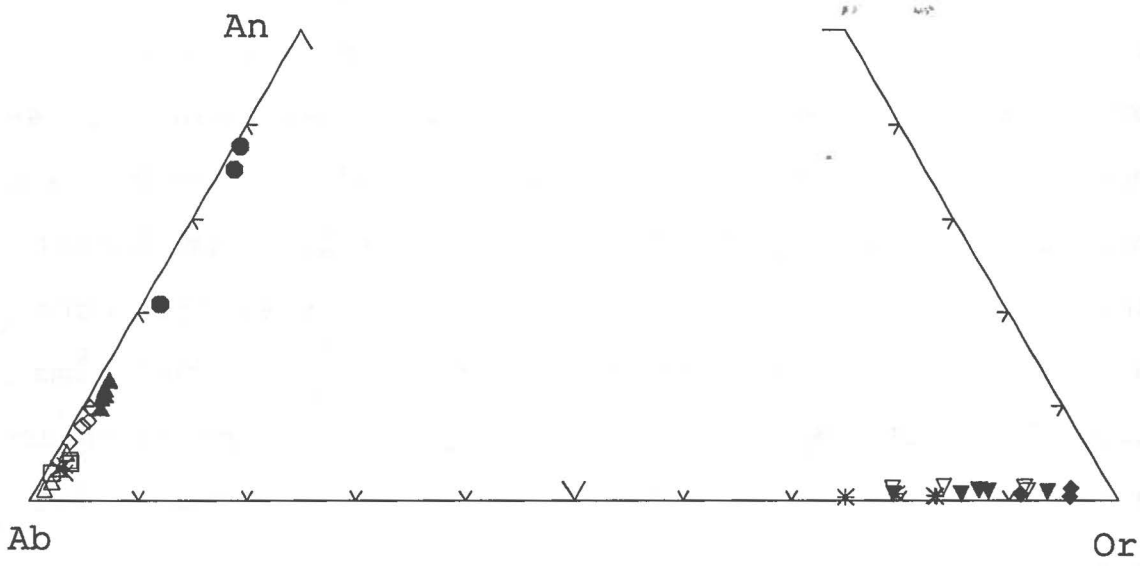

Fig. 7.3-4a. Compositions of the feldspars in the contaminated ferro-edenite syenite (C2036) from Center III plotted in the system Or-Ab-An.

The filled circles (•) are the light greenish blue luminescent oligoclase-andesine core, and the diamonds (◇) are the light blue luminescent Na-feldspar inner rim and the crosses (×) are the light violet blue luminescent Na-feldspar outer rim of the plagioclas phenocrysts.

The filled up-triangles (▲) and the filled down-triangles (▼) are the dull blue luminescent secondary Na-feldspar and K-feldspar in the core of the plagioclas phenocrysts, respectively. The asterisks (∗) are the dull blue luminescent secondary K-feldspar in the inner rim of the plagioclase phenocrysts.

The open down-triangles (▽) are the violet blue to dull blue luminescent K-feldspar groundmass and the open up-triangles (△) are the dull violet luminescent secondary Na-feldspar in the K-feldspar groundmass.

The squares (□) are the dull violet luminescent Na-feldspar and the filled diamonds (◆) are the dull blue luminescent K-feldspar in the aplitic dike.

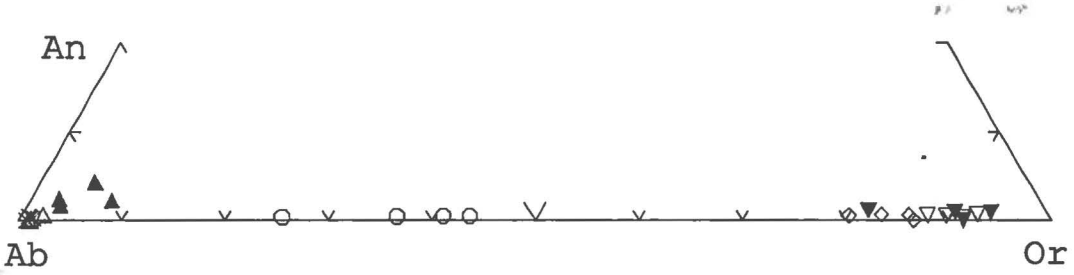

Fig. 7.3-4b. The compositions of the feldspars in the contaminated ferro-edenite syenite (C2176) from Center III plotted in the system Or-Ab-An.

The filled up-triangles (▲) are the light blue luminescent exsolved Na-feldspar and the filled down-triangles (▼) are the light violet blue luminescent K-feldspar host in the perthite phenocryst.

The circles (O) are the light violet blue luminescent braided microperthite core or mantle of the antiperthite phenocryst. The down-triangles (▽) are the dull blue luminescent exsolved K-feldspar and the up-triangles (△) are the red luminescent Na-feldspar host in the antiperthite phenocrysts.

The diamonds (◇) are the dull blue luminescent secondary K-feldspar and the crosses (×) are the dull red luminescent secondary Na-feldspar in the groundmass.

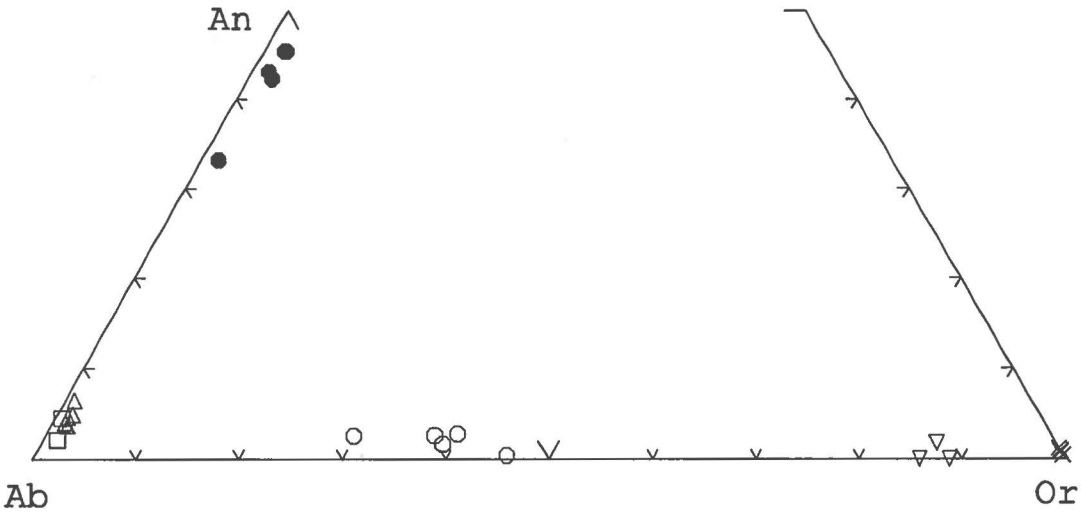

Fig. 7.3-4c. The compositions of the feldspars in the contaminated ferro-edenite syenite (C2063 and C2065) from Center III plotted in the system Or-Ab-An.

For the sample C2065, the filled circles (•) are the light greenish blue luminescent andesine phenocrysts. The down-triangles (▽) are the dull blue luminescent K-feldspar. The crosses (×) are the non-luminescent secondary K-feldspar in the core of the andesine. The up-triangles (△) are the light violet, dull blue luminescent secondary Na-feldspar in the groundmass.

For the sample C2063, the circles (◦) are the light blue to light violet blue luminescent unexsolved alkali feldspar in the centre of the incipient perthitic core of the irregular vein perthite phenocryst. The squares (□) are the light blue luminescent deuteric coarsening secondary Na-feldspar in the perthitic rim of the irregular vein perthite phenocryst.

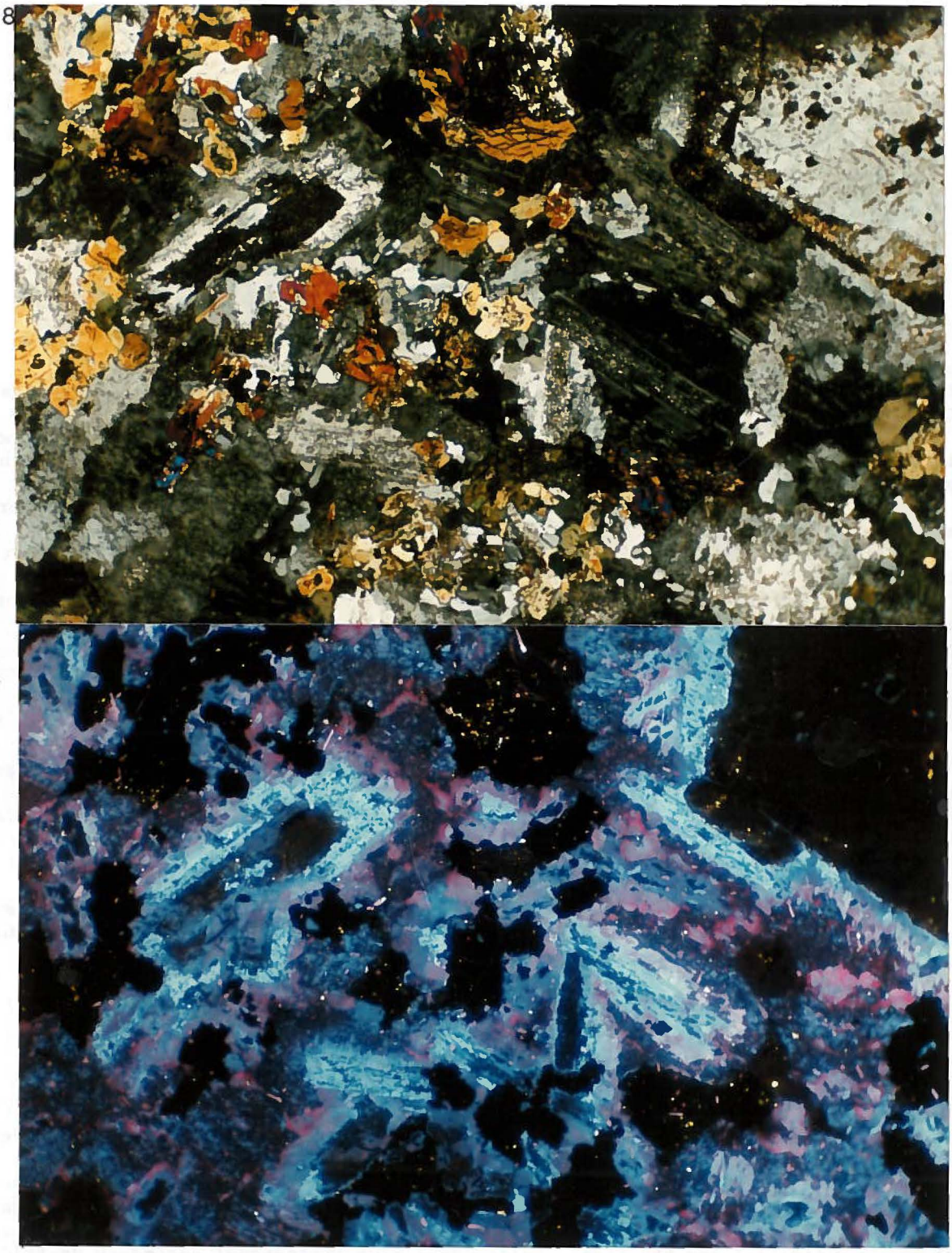

Fig. 7.3-5. Feldspars in the contaminated ferro-edenite syenite (Sample C2065) from Center III, Coldwell Complex. a. TrL. (Photographic conditions: 2 s, ASA 400) b. CL. The andesine phenocrysts exhibit light greenish blue luminescence some of which are replaced by non luminescent secondary K-feldspar in the core. The unaltered K-feldspar grains exhibit dull blue luminescence. The andesine phenocrysts are also replaced by dull violet or dull blue luminescent secondary Na-feldspar and dull blue luminescent secondary K-feldspar along the margins. Scale: 50 mm on photograph = 1 mm on thin section. (CL conditions: 10 kV, 0.8 Am. Photographic conditions: 45 s, ASA 400).

perthitic rim (Fig. 7.3-6 and Fig. 7.3-7), or are mantled with an incipient perthitic core, a braid microperthite mantle and a deuteric coarsened perthitic rim (Fig. 7.3-8). The incipient perthitic cores usually contain unexsolved alkali feldspars in the centre of the core. However, some of the perthite phenocrysts (sample C2176) are unzoned and only show an irregular vein perthite texture (Fig. 7.3-9).

In the centre of the incipient perthite cores (sample C2063), the unexsolved alkali feldspars exhibit variable luminescence colours from light blue (Fig. 7.3-6b) through to light violet blue (Fig. 7.3-8b) to light violet (Fig. 7.3-7b). The light blue luminescent unexsolved alkali feldspar ranges in composition from Or_{30-40} Ab_{57-68} An_3 and the light violet blue luminescent unexsolved alkali feldspar ranges in composition from $Or_{40-46}Ab_{54-59}An_{1-2}$ (Fig. 7.3-4c and Appendix 3). However, the CL image can not distinguish very well the exsolved Na-feldspar from the exsolved K-feldspar from the unexsolved alkali feldspar host. The unexsolved alkali feldspar gradually changes in composition to Na-feldspar or K-feldspar.

In sample C2176, for the irregular vein perthite phenocrysts, the exsolved Na-feldspar exhibits light blue luminescence and ranges in composition from $Ab_{90-95}Or_{3-8}An_{2-4}$ (Fig. 7.3-9b and Appendix 3). The K-feldspar host exhibits light violet blue luminescence and ranges in composition from $Or_{82-94}Ab_{5-17}An_1$.

b. Regular vein antiperthite

In sample C2176, some alkali feldspar phenocrysts are regular

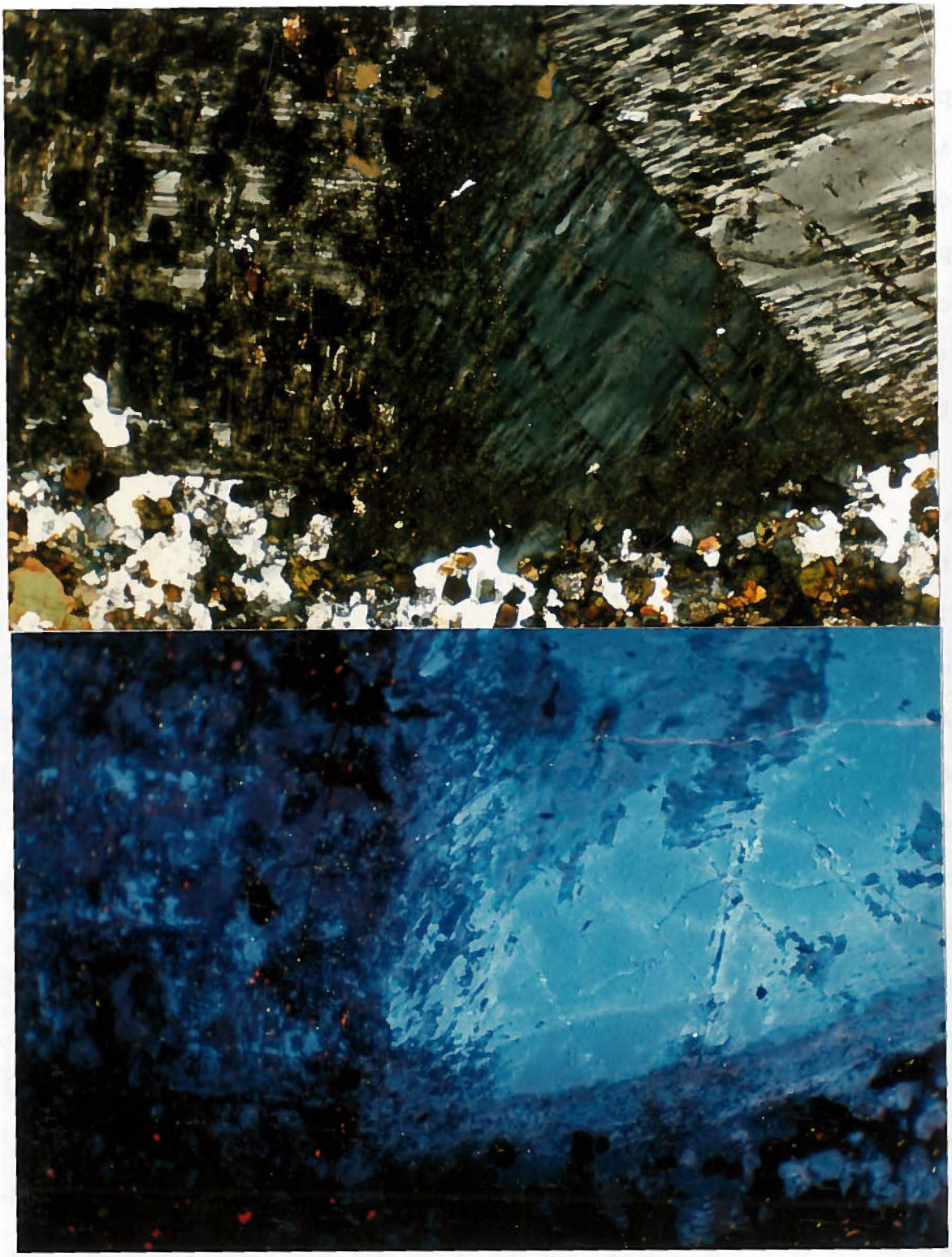

Fig. 7.3-6. An irregular vein perthite phenocryst in the contaminated ferro-edenite syenite (Sample C2063) from Center III, Coldwell Complex. a. TrL. The perthite phenocryst is mantled with a incipient perthitic core and a deuteric coarsening perthitic rim. The incipient perthitic core contains some unexsolved alkali feldspar in the centre. (Photographic conditions: 3 s, ASA 400). b. CL. The incipient perthitic core exhibits a light blue luminescence. In the deuteric coarsening perthitic rim, the secondary Na-feldspar exhibits light blue to light violet blue luminescence, whereas the secondary K-feldspar exhibits dull blue luminescence. Scale: 50 mm on photograph = 1 mm on thin section. (CL conditions: 10 kV, 0.8 Am. Photographic conditions: 15 s, ASA 400).

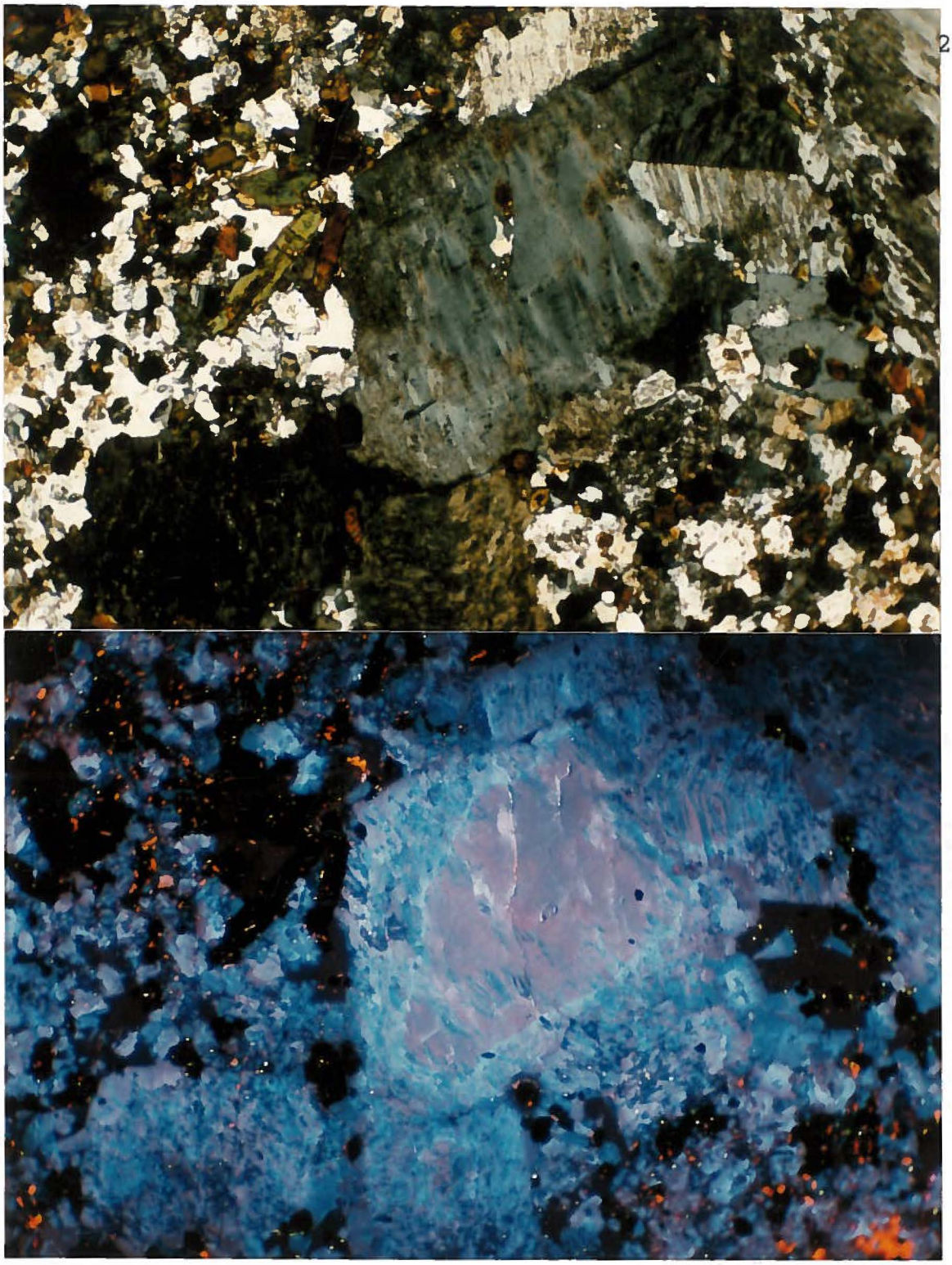

Fig. 7.3-7. An irregular vein perthite phenocryst in the contaminated ferro-edenite syenite (Sample C2063) from Center III, Coldwell Complex. a. TrL. The perthite phenocryst is mantled with an incipient perthitic core and a deuteric coarsening perthitic rim. The incipient perthitic core contains some unexsolved alkali feldspar in the centre. (Photographic conditions: 2 s, ASA 400). b. CL. The incipient perthitic core exhibits light violet luminescence. In the deuteric coarsening perthitic rim, the secondary Na-feldspar exhibits light blue to light violet blue luminescence, whereas the secondary K-feldspar exhibits dull blue luminescence. Scale: 50 mm on photograph = 1 mm on thin section. (CL conditions: 10 kV, 0.8 Am. Photographic conditions: 30 s, ASA 400).

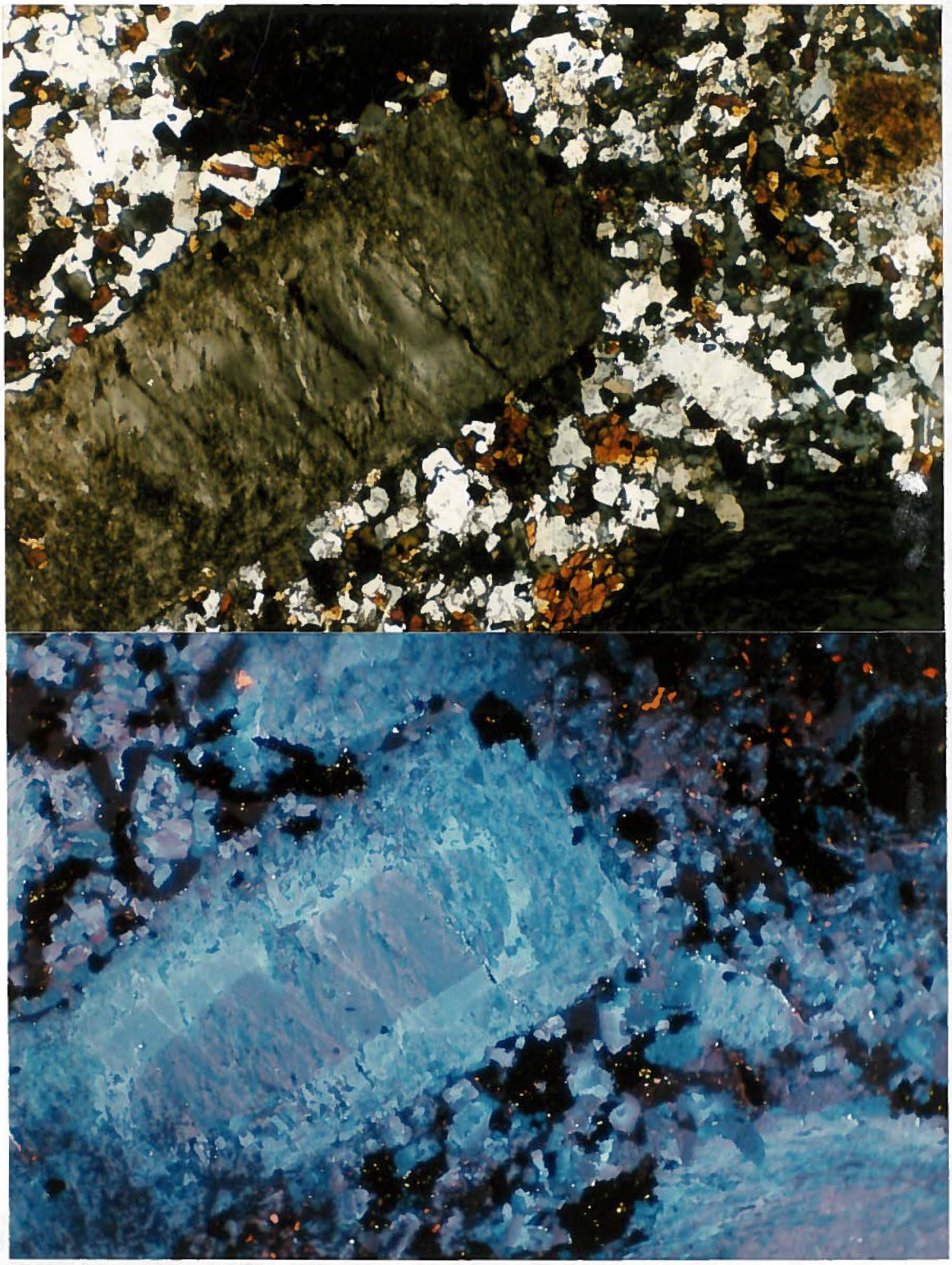

Fig. 7.3-8. An irregular vein perthite phenocrysts in the contaminated ferro-edenite syenite (Sample C2063) from Center III, Coldwell Complex.

a. TrL. The perthite phenocryst is mantled with an incipient perthitic core and a deuteric coarsening perthitic rim. The incipient perthitic core contains some unexsolved alkali feldspar in the centre of the core. (Photographic conditions: 2 s, ASA 400).

b. CL. The phenocryst reveals an incipient perthitic core with bluish luminescence and a mantle with light violet blue luminescence and a deuteric coarsening perthitic rim. In the core, the unexsolved alkali feldspar exhibits bluish violet luminescence and the exsolved Na-feldspar exhibit light violet luminescence, whereas the exsolved K-feldspar exhibits blue luminescence. The homogeneous light violet blue luminescent mantle is the braid microperthite which was examined by SEM/BSE. In the deuteric coarsening perthitic rim, the Na-feldspar exhibits light blue to light violet blue luminescence and the K-feldspar exhibits dull blue luminescence.

The feldspar grains in the groundmass are usually mantled with a dull violet core and a light violet mantle and dull violet rim, and are coarsened with dark blue luminescent secondary K-feldspar and dull violet luminescent secondary Na-feldspar along the margins. Scale: 50 mm on photograph = 1 mm on thin section. (CL conditions: 10 kV, 0.8 Am. Photographic conditions: 30 s, ASA 400).

Fig. 7.3-9. An irregular vein perthite and regular vein antiperthite phenocrysts in the contaminated ferro-edenite syenite (Sample C2176) from Center III, Coldwell Complex.

a. TrL. The phenocrysts are irregular vein perthite (Photographic conditions: 2 s, ASA 400).

b. CL. In the perthite phenocrysts, the exsolved Na-feldspar exhibits light blue luminescence and the K-feldspar host exhibits light violet blue luminescence. These perthite phenocrysts are usually associated with fine-grained perthite groundmass which has the same luminescence characteristics as the perthite phenocrysts (CL conditions: 10 kV, 0.8 Am. Photographic conditions: 1 min, ASA 400).

c. TrL. The phenocrysts are regular vein antiperthite. (Photographic conditions: 1 s, ASA 400).

d. CL. In the antiperthite phenocrysts, the exsolved K-feldspar exhibits dull blue luminescence, whereas the Na-feldspar host exhibits red luminescence. Some of these antiperthite phenocrysts contain a light violet blue luminescent core or mantle, or some braid microperthite patches. These antiperthite phenocrysts are usually associated with a fine-grained antiperthite groundmass which has the same luminescence characteristics as the antiperthite phenocrysts (CL conditions: 10 kV, 0.8 Am. Photographic conditions: 1.5 min, ASA 400).

In the groundmass, as the perthites gradually change to antiperthites from the blue luminescent areas to the red luminescent areas, the luminescence colour of the surrounding secondary albite gradually changes from dull violet to deep red. Scale: 50 mm on photograph = 1 mm on thin section.

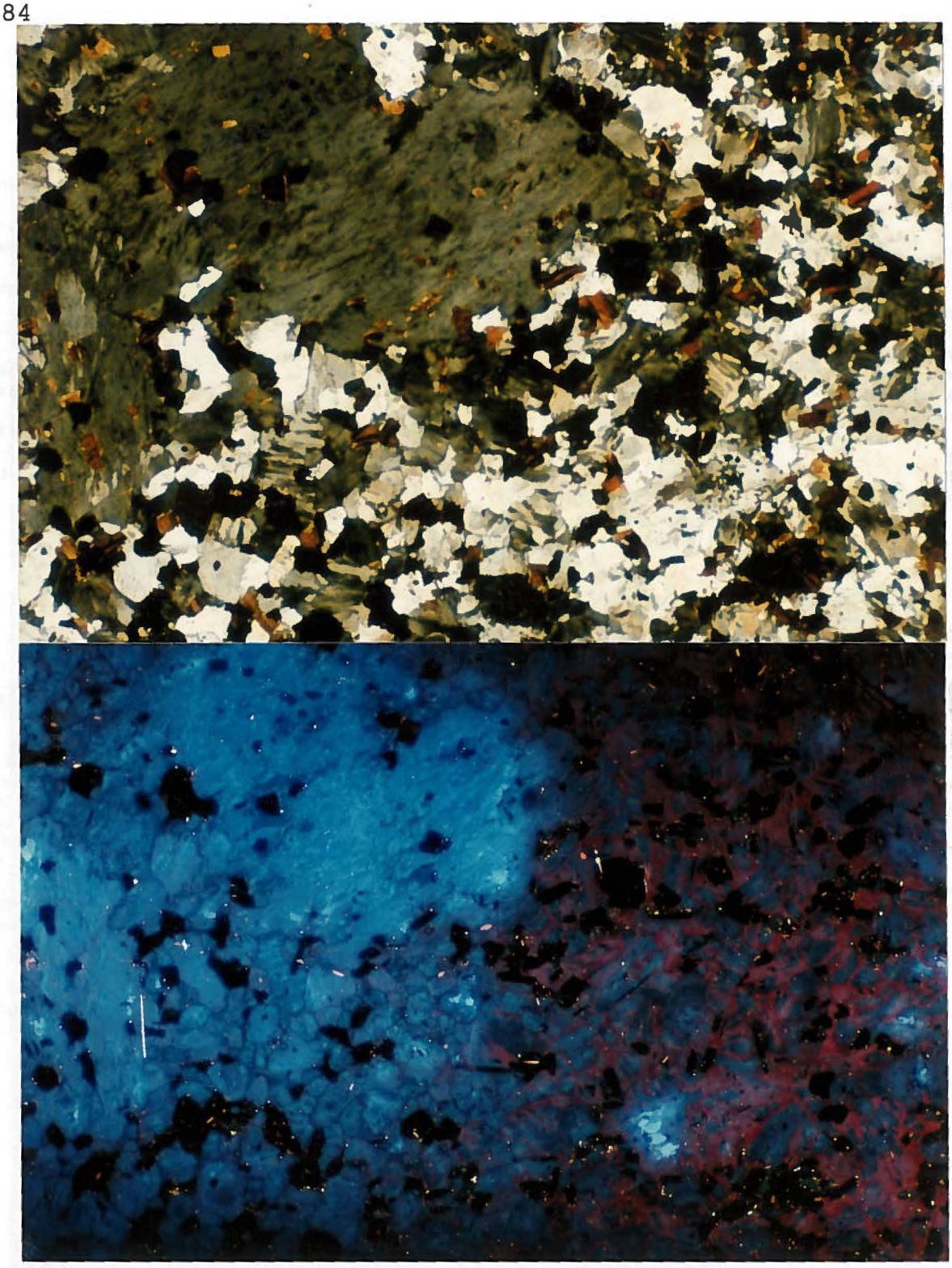

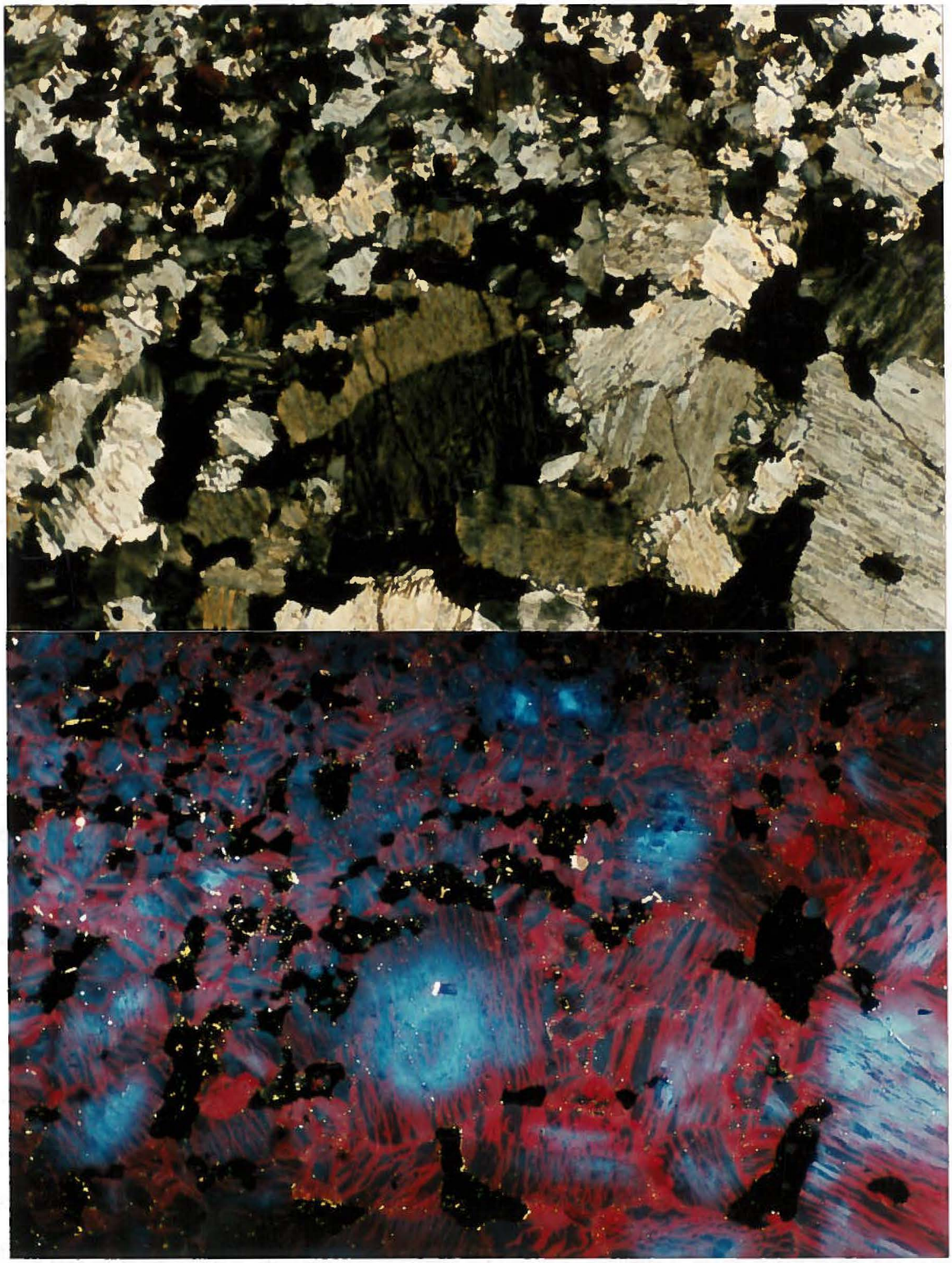

vein antiperthite. Under CL, the exsolved K-feldspar exhibits dull blue luminescence and ranges in composition from $Or_{88-92}Ab_{7-12}An_{<1}$ (Fig. 7.3-9d, Fig. 7.3-4b and Appendix 3). The albite host exhibits red luminescence and ranges in composition from $Ab_{97-99}Or_{1-2}An_{<1}$. Some of these antiperthite grains are mantled irregularly with a light blue to light violet blue luminescent core or mantle, and others only contain some light violet blue luminescent patches (Fig. 7.3-9d). A SEM/BSE image reveals that the light blue luminescent areas are braid microperthite and range in composition from $Or_{25-43}Ab_{56-74}An_{<1}$ (Fig. 7.3-4b and Appendix 3). The formation of these antiperthites may be related to late-stage fluid alteration, the evidence from adjacent feldspars groundmass will be given in the next section.

c. K-feldspar

Carlsbad twinned K-feldspar phenocrysts are observed in the sample C2065, but most of the crystals are strongly sericitized during late-stage hydrothermal alteration. Some unaltered K-feldspar grains exhibit dull blue luminescence and range in composition from $Or_{86-89}Ab_{11-14}An_{0-2}$ (Fig. 7.3-5b, Fig. 7.3-4c and Appendix 3).

7.3.4. Groundmass of feldspars

Feldspars grains in the groundmass of the contaminated ferro-edenite syenite are mostly K-feldspar, although some are mantled K-feldspar or perthite.

Under CL, the K-feldspar grains in the groundmass (sample c2036) are slightly mantled with a blue luminescent core and a dull blue luminescent rim (Fig. 7.3-2b). The CL spectrum of the blue luminescent core consists of a high intensity blue peak centered at 452 nm and a low intensity red peak centered at 707 nm and the ratio of I_B/I_R is about 2.3 (Table 7.3-1 and Fig. 7.3-3b, spectrum A). The dull blue luminescent rim consists of a low intensity blue peak centered at 460 nm and a low intensity red peak centered at 695 nm and the ratio of I_B/I_R is about 5.4. The blue luminescent cores range in composition from $Or_{79-83}Ab_{15-20}An_{1-2}$ (Table 7.3-1, Fig. 7.3-4a and Appendix 3), whereas the dull blue luminescent rims range in composition from Or_{91} Ab_8 An_1. However, in the sample C2063, K-feldspar crystals in the groundmass are usually mantled with a dull violet luminescent core, a light blue luminescent mantle and a light violet rim (Fig. 7.3-8b).

There are two different types of feldspars in the groundmass from sample C2176 (Fig. 7.3-9b and Fig. 7.3-9d). The CL picture Fig. 7.3-9d is taken just to the right of Fig. 7.3-9b. Fig. 7.3-9b and Fig. 7.3-d show the groundmass between the irregular vein perthite phenocrysts (blue luminescent areas) and the regular vein antiperthite phenocrysts (red luminescent areas). In the blue luminescent areas, the feldspar grains in the groundmass are fine-grained perthite, which consist of the light blue luminescent exsolved Na-feldspar and the light violet blue luminescent K-feldspar host. In the red luminescence areas, the feldspars in the groundmass are fine-grained antiperthite, and composed of dull blue

luminescent exsolved K-feldspar and dull red luminescent Na-feldspar host. From the blue luminescent areas to the red luminescent areas, the blue luminescent perthite grains gradually change into the red luminescent antiperthite grains. This evidence may indicate that the antiperthite grains in the groundmass and the regular vein antiperthite phenocrysts (red luminescence) developed from perthite grains in the groundmass and irregular vein perthite phenocrysts (blue luminescence) during a late-stage fluid-feldspar interaction.

7.3.5. Late-stage fluid-induced replacement and deuteric coarsening

a. Secondary feldspars within plagioclase crystals

In the sample C2036, the oligoclase-andesine cores of the plagioclase crystals are usually replaced by dull blue luminescent secondary Na- and K-feldspar (Fig. 7.3-2b, 10b). The albite rims of the phenocrysts are only replaced by irregular veins of dull blue luminescent secondary K-feldspar cross cutting the albite rim. The dull blue luminescent secondary Na-feldspar ranges in composition from $Ab_{86-88}An_{10-13}Or_{1-2}$, whereas the secondary K-feldspar ranges in composition from $Or_{75-93}Ab_{6-25}An_{0-1}$ (Table 7.3-1, Fig. 7.3-4a and Appendix 3).

In sample C2065, the cores of the andesine are usually replaced by the secondary K-feldspar which has no luminescence (Fig. 7.3-5b). The secondary K-feldspar has a range in composition of Or_{99-100} An_{0-1} (Fig. 7.3-4c and Appendix 3). This secondary K-feldspar has a higher Or content and a lower An content than the other secondary

K-feldspar in Center III.

b. Deuteric coarsening secondary feldspars

As noted above, the deuteric coarsened feldspars form turbid perthitic rims surrounding incipient perthitic cores. The albite ($Ab_{95-97}Or_1An_{2-5}$) in the deuteric coarsened rim exhibits light blue to light violet blue luminescence (Fig. 7.3-6b,-7b,-8b), whereas the K-feldspar usually exhibits dull blue luminescence. With progressive coarsening, the albite exhibits dull violet luminescence, and the K-feldspar exhibits dark blue luminescence. Both of the feldspars occur as two separated grains along the exterior edge of the perthitic rim or along the margins of the K-feldspar in the groundmass.

c. Secondary albite in the groundmass

During late-stage fluid-feldspar interaction, secondary albite formed as interlocking grains occupying the interstices between the K-feldspar, the perthite or the antiperthite grains in the groundmass. Secondary albite usually exhibits dull violet luminescence in the areas which are less affected by late-stage fluids, but it exhibits deep red luminescence in the areas which are strongly affected by the late-stage fluids.

For example, in sample C2036, the secondary albite occurs as interlocking grains surrounding the K-feldspar grains in the groundmass and exhibits dull violet luminescence (Fig. 7.3-2b,-9b). The CL spectrum consists of a very low blue peak at about 457 nm

and a red peak at 707 nm with a ratio of I_B/I_R about 0.8 (Fig. 7.3-3b, spectrum C and Table 7.3-1). This dull violet luminescent secondary albite ranges in composition from $Ab_{94-98}Or_1An_{1-5}$ (Table 7.3-1, Fig. 7.3-4a and Appendix 3)

In the sample C2176, secondary albite occurs as a narrow interlocking grains surrounding the perthite grains in the groundmass. The secondary albite exhibits dull violet luminescence in the blue luminescent areas (Fig. 7.3-9b), and exhibits deep red luminescence in the red luminescent areas (Fig. 7.3-9b,-9d).

In the sample C2065, secondary albite occurs as groundmass surrounding the andesine and K-feldspar phenocrysts, and the secondary albite replaces the andesine along its margins (Fig. 7.3-5a). This secondary albite exhibits light violet blue to light violet or dull blue luminescence (Fig. 7.3-5b). The light violet luminescent secondary albite ranges in composition from $Ab_{94-95}Or_{1-2}An_{4-5}$, and the dull blue luminescent albite ranges in composition from $Ab_{93-95}Or_1An_{4-7}$ (Fig. 7.3-4c and appendix 3).

7.3.6. Feldspars in aplitic dike

The contaminated ferro-edenite syenite is cut by a late-stage aplitic dike (Fig. 7.3-10a). The aplitic dike mainly consists of Na-feldspar, K-feldspar, quartz and minor biotite. Under CL, the albite exhibits dull violet luminescence and ranges in composition from $Ab_{94-96}Or_{1-2}An_{3-4}$ (Fig. 7.3-10b, Table 7.3-1, Fig. 7.3-4a and Appendix 3). The K-feldspar exhibits dull blue luminescence and ranges in composition from $Or_{91-95}Ab_{4-9}An_{0-1}$.

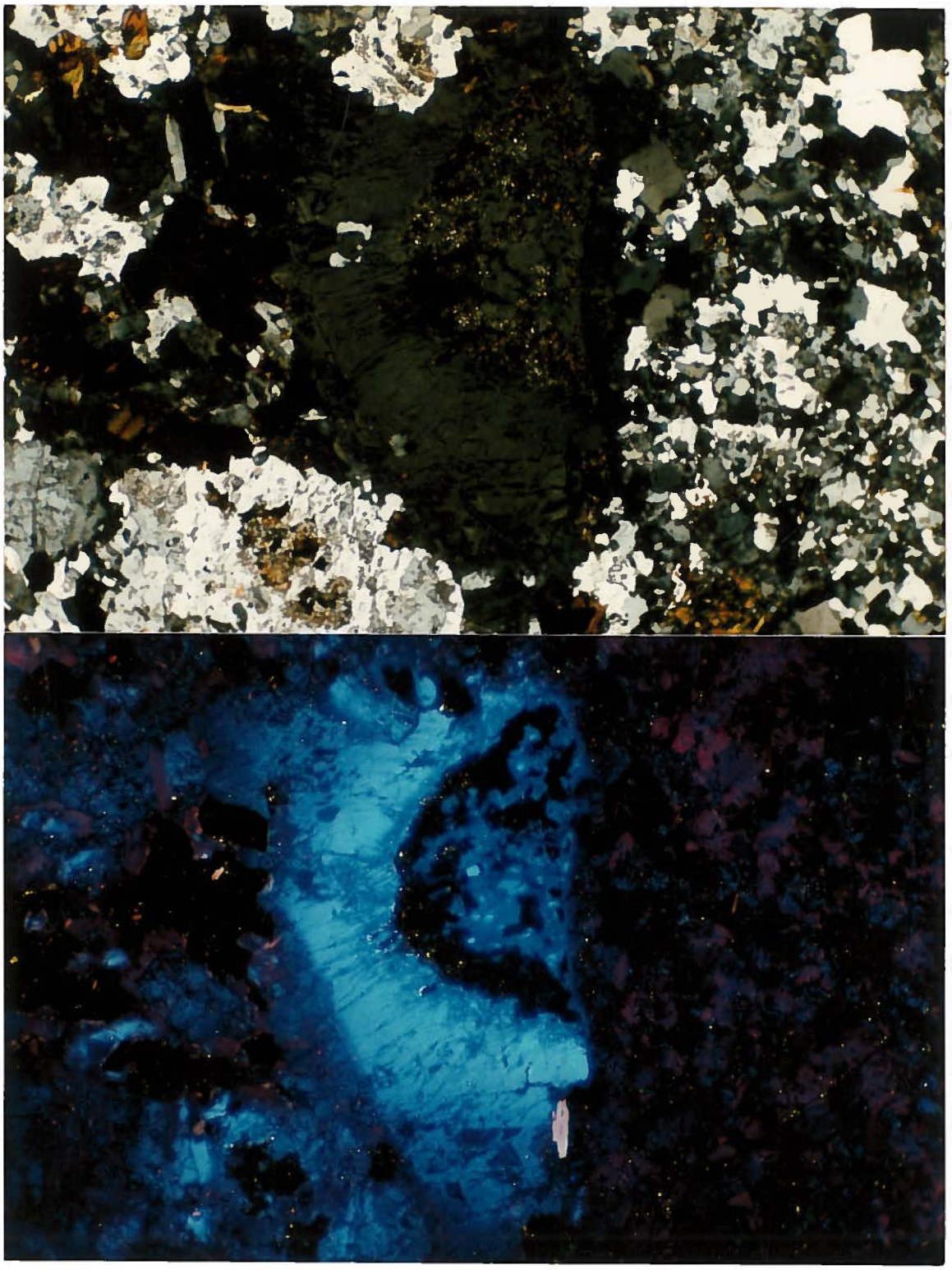

Fig. 7.3-10. Feldspars in the aplitic dike in the contaminated ferro-edenite syenite (Sample C2036) from Center III, Coldwell Complex. a. TrL. (Photographic conditions: 1.5 s, ASA 400) b. CL. In the aplitic dike, on the right hand side, the Na-feldspar exhibits dull violet luminescence and the K-feldspar exhibits dull blue luminescence. In the contaminated ferro-edenite syenite, on the left hand side, the plagioclase phenocryst core is replaced by dull blue luminescent secondary Na- and K-feldspar, and the light blue luminescent albite rim is replaced by dull blue luminescent secondary K-feldspar. The K-feldspar grains in the groundmass exhibit blue to dull blue luminescence. The secondary Na-feldspar exhibits dull violet luminescence. Scale: 50 mm on photograph = 1 mm on thin section. (CL conditions: 10 kV, 0.8 Am. Photographic conditions: 30 s, ASA 400).

7.3.7. Thermal history of the feldspars

The thermal history of the plagioclase in the contaminated ferro-edenite syenite is shown in Fig. 7.3-11. The path a-a′ indicates that the plagioclase may have fractionally crystallized at a temperature range from 850 to 750 °C. However, the initial crystallization temperature of the plagioclase phenocrysts may be higher than 850 °C, because most the cores of the plagioclase phenocrysts have been replaced by the secondary Na- and K-feldspar.

The evolution of the alkali feldspars in the contaminated ferro-edenite syenite is shown in Fig. 7.3-12. The path a-a′ on the incoherent solvus (SFS) indicates that the alkali feldspar phenocrysts with a composition of $Or_{25-46}Ab_{54-74}$ may have crystallized at temperatures ≥700 °C. This compositional range includes the light blue to light violet blue luminescent unexsolved alkali feldspar patches ($Or_{30-46}Ab_{54-59}$) in the centre of the irregular vein perthite phenocrysts; and the light blue luminescent braid microperthite patches ($Or_{25-43}Ab_{56-74}$) in the core and the mantle of the regular vein antiperthite phenocrysts. The microperthite textures may have formed during cooling at temperatures 650-620 °C on the coherent solvus (CS).

The paths b-b′ and c-c′ on the coherent solvus (CS) indicate that the exsolved K-feldspar with composition of $Or_{82-94}Ab_{5-17}$ and exsolved albite with composition of $Ab_{90-99}Or_{1-8}$ formed during cooling at temperatures below 400 °C and 520 °C, respectively. These compositional ranges include the light violet blue, dull blue luminescent exsolved K-feldspar; and light blue, light violet blue

and red luminescent exsolved albite in the irregular vein perthite and regular vein antiperthite phenocrysts.

The path e-d′ on the incoherent solvus (SFS) indicates that the K-feldspar phenocrysts may have crystallized at temperatures about 440-360 °C. The path d-d′ on the incoherent solvus (SFS) indicates that the mantled K-feldspar with a composition of $Or_{79-91}Ab_{8-20}$ in the groundmass may have formed at temperatures about 530-350 °C.

Since the secondary albite and K-feldspar in the deuteric coarsened antiperthitic rim have end member compositions, they formed at a very low temperature below 350 °C.

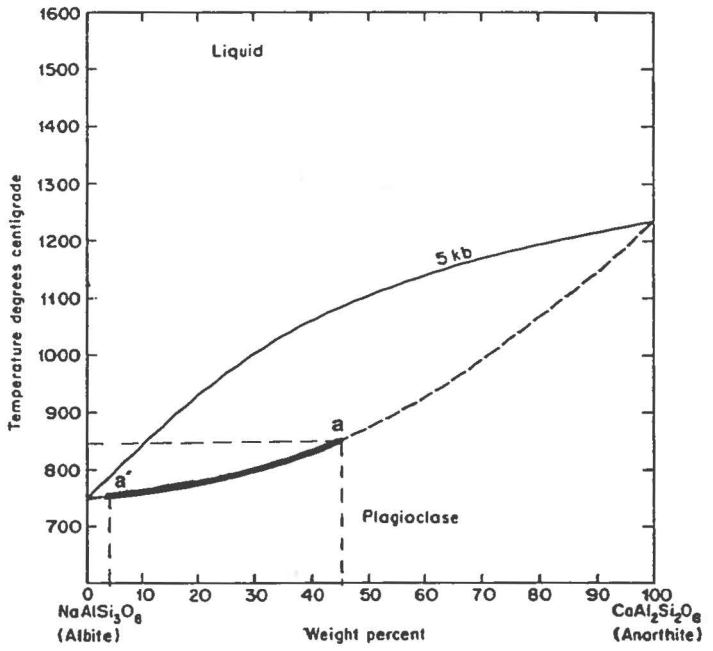

Fig. 7.3-11. The evolution of the plagioclase phenocrysts in the contaminated ferro-edenite syenite from Center III is illustrated in the Ab-An binary phase diagram. The path a-a′ shows the zoned plagioclase phenocrysts have crystallized fractionally at a temperature range from 750-850 °C. The Ab-An system is at P_{H_2O} of 5 kb (From Ehlers, 1972).

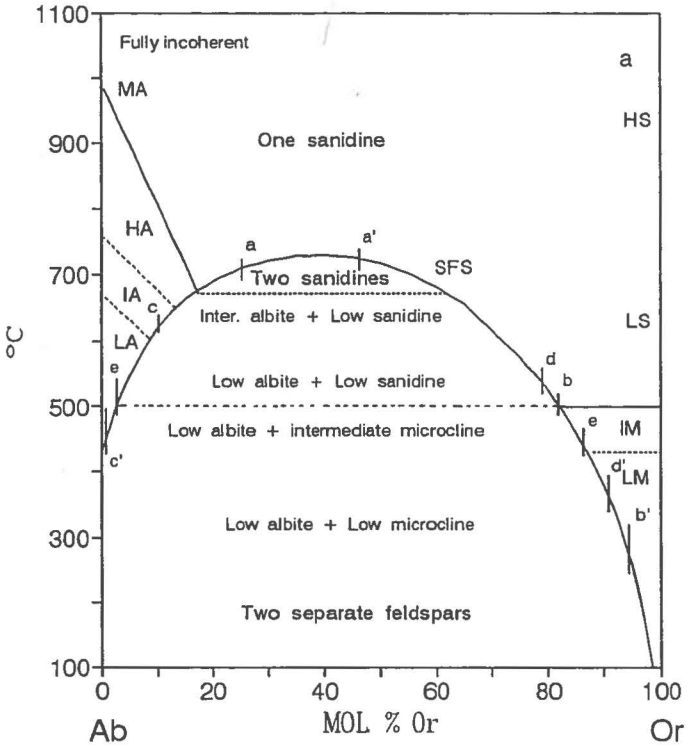

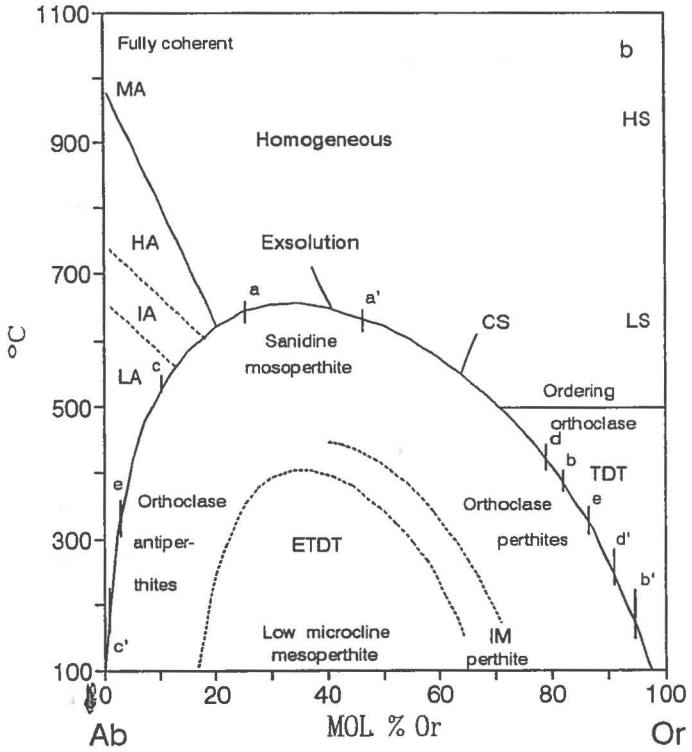

Fig. 7.3-12. The evolution of the alkali feldspars in the contaminated ferro-edenite syenite from Center III is illustrated in the Or-Ab binary phase diagram.

The path a-a′ includes the unexsolved alkali feldspar and the braid microperthite patches in the core and the mantle of the regular and irregular vein antiperthite pheno-crysts. The paths b-b′ and c-c′ include the exsolved K-feldspar and the exsolved albite in the regular and irregular vein anperthitite pheno-crysts. The path e-d′ is the K-feldspar phenocryst and the path d-d′ is the mantled K-feldspar in the groundmass.

Diagram (a) shows the phase relationships for An-free alkali feldspars under complete (incoherent) equilibrium and (b) shows different constrained equilibrium states as a function of bulk composition and T for completed coherent intergrowths (Brown and Parsons, 1989). SFS is the strain-free solvus and CS is the coherent solvus. TDT is the twin-domain microtexture and ETDT is the exsolution and the twin-domain microtexture. MA, HA, IA and LA are monoclinic, high, intermediate and low albite; IM and LM are intermediate and low microcline. IA and IM is the region of the rapid change in Y ordering.

7.4. Feldspars in Quartz Syenite

7.4.1. Introduction

Quartz syenites contain homogeneous alkali feldspar, incipient perthite, mantled feldspar and irregular vein antiperthite. The homogeneous alkali feldspar and the incipient perthite are subhedral, Carlsbad twinned crystals which exhibit light blue to blue luminescence under CL. The mantled feldspar crystals commonly consist of an albite core and a deuteric coarsened antiperthitic rim. The albite core usually exhibits light blue luminescence. Within the deuteric coarsened antiperthitic rim, the albite host usually exhibits dull red to deep red luminescence and the exsolved K-feldspar exhibits dull blue to dark blue luminescence. The irregular vein antiperthite commonly are euhedral, Carlsbad twinned crystals, some of which reveal oscillatory zones under CL. These oscillatory zoned antiperthite crystals commonly consist of a dull red luminescent core, a violet luminescent mantle and a dull red to deep red luminescent rim. Within these zones, the albite host usually exhibits violet to deep red luminescence and the exsolved K-feldspar exhibits dull blue to dark blue luminescence. In the unzoned irregular vein antiperthite, the albite host exhibits deep red luminescence whereas the exsolved K-feldspar exhibits dull red luminescence.

Secondary K-feldspar exhibits dull blue luminescence and only occurs in the albite core. Secondary albite usually exhibits deep red luminescence and occupies the interstices between antiperthite grains.

In a xenolith of Center I syenite, the feldspar crystals are

irregular vein perthite and the K-feldspar host exhibits blue luminescence and exsolved albite exhibits light blue luminescence.

7.4.2. Homogeneous alkali feldspar

The feldspar crystals in some of the quartz syenites (samples C2001, C2060 and C2087) contain Carlsbad twinned homogeneous alkali feldspar and incipient perthite. The margins of the homogeneous alkali feldspar crystals are usually exsolved incipient perthite (Fig. 7.4-1a). Under CL, most of these homogeneous alkali feldspar and the incipient perthites exhibit a homogeneous light blue or blue luminescence, and some are mantled with a light violet blue luminescent irregular rim (Fig. 7.4-1b). The blue luminescent homogeneous alkali feldspar core consists of a high blue peak centered at 450 nm and a low red peak centered at 708 nm with a ratio of I_B/I_R about 3.5 (Fig. 7.4-2a, spectrum A and Table 7.4-1). Whereas, the light violet luminescent alkali feldspar rim consists of relatively lower blue peak (450 nm) and red peak (703 nm) intensities than the blue luminescent alkali feldspar, and has a ratio of I_B/I_R about 7.4 (Fig. 7.4-2a, spectrum B and Table 7.4-1).

The blue luminescent alkali feldspar core ranges in composition from $Or_{26-47}Ab_{52-71}An_{1-3}$, whereas the light violet blue luminescent alkali feldspar rim has a composition of $Or_{15}Ab_{83}An_2$ (Fig. 7.4-3a and Appendix 3). The Ab content increases from the core to the rim.

7.4.3. Mantled feldspar with albite core and antiperthitic rim

In the quartz syenite (samples C173, C330, C369, C367, C2136 and C2154), some of the feldspar crystals are mantled and consist of an

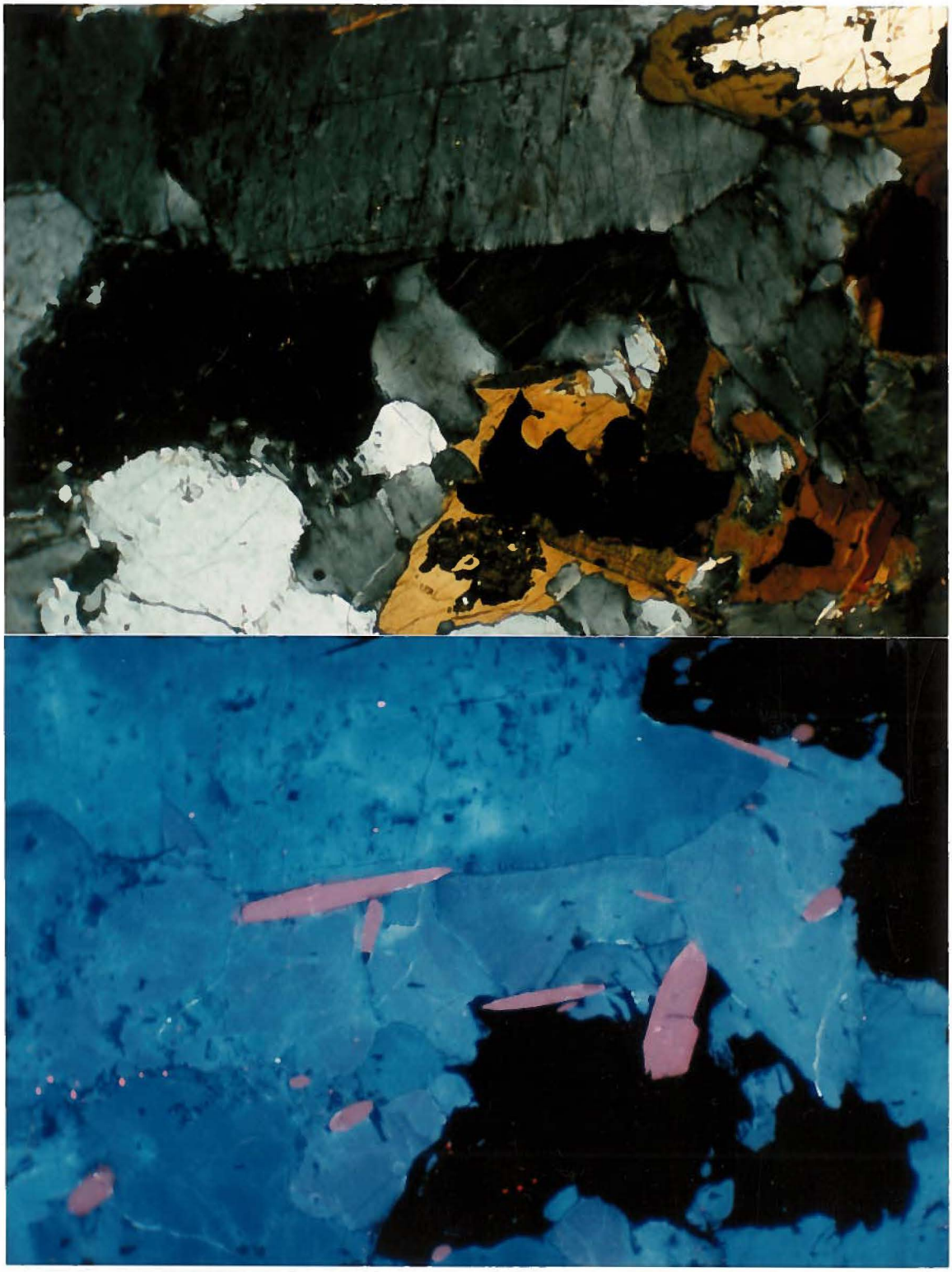

Fig. 7.4-1. Homogeneous alkali feldspar in quartz syenite (Sample C2087) from Center III, Coldwell Complex. a. TrL. Homogeneous alkali feldspar some of which show incipient perthitic rims along the margins (Photographic conditions: 1 s, ASA 400) b. CL. The homogeneous alkali feldspar exhibits blue luminescence, and exhibits light violet blue luminescence at the margins. The pink luminescent crystals are the apatite. Scale: 55 mm on photograph = 1 mm on thin section. (CL conditions: 10 kV, 0.8 Am. Photographic conditions: 10 s, ASA 400.)

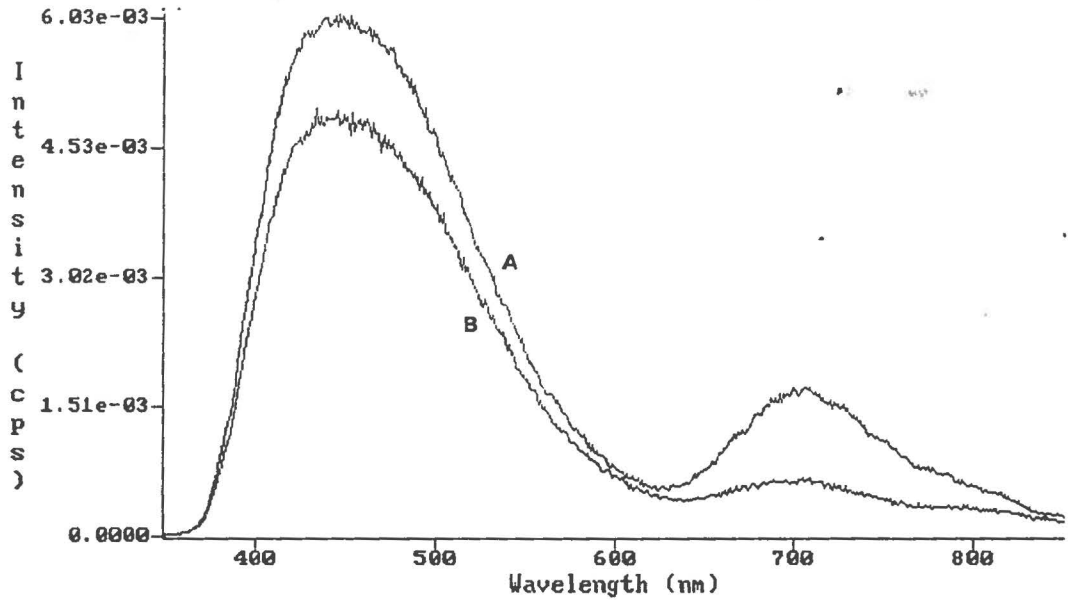

Fig. 7.4-2a. CL spectra of homogeneous alkali feldspar in quartz syenite (Sample C2087) from Center III, Coldwell Complex, Ontario. (A) is from the blue luminescent homogeneous alkali feldspar core. (B) is from the light violet blue luminescent alkali feldspar rim. CL conditions: 10 kV, 0.8 mA.

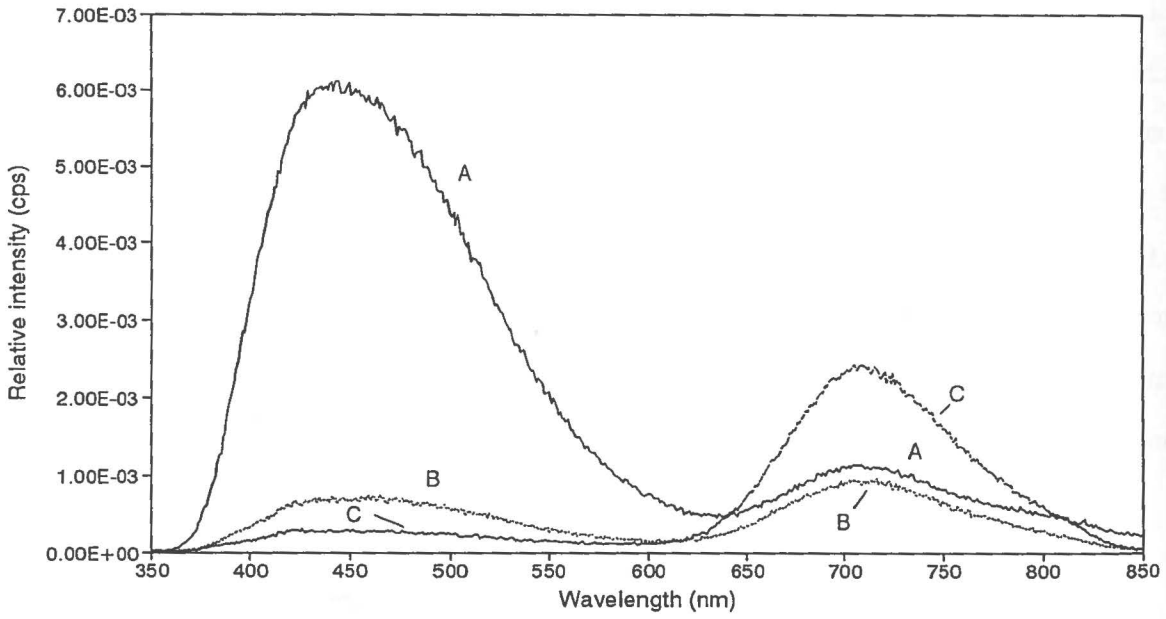

Fig. 7.4-2b. CL spectra of mantled feldspar in the quartz syenite (Sample CC173) from Center III, Coldwell Complex, Ontario. (A) is from the light blue luminescent albite core. (B) is from the dull blue luminescent K-feldspar and (C) is from the dull red luminescent albite in the deuteric coarsened antiperthitic rim. CL conditions: 10 kV, 0.8 mA.

Table 7.4-1. Representative cathodoluminescence properties and compositions of feldspars in quartz syenite from Center III, Coldwell Complex, Ontario

Occurrence of feldspar	Sample No./ spectrum No.	Luminescence colour	Intensities (cps)					Compositions		
			Blue peak	(nm)	Red peak	(nm)	B/R ratio	Or	Ab	An
Homo. alkali feldspar, core	C2087/A	Blue	6.03E-03	(450)	1.72E-03	(703)	3.50	26-47	52-71	1-3
Homo. alkali feldspar, rim	C2087/B	Light violet blue	4.88E-03	(450)	6.60E-04	(709)	7.39	15	83	2
Albite, core	C173/A	Light blue	6.01E-03	(449)	1.15E-03	(708)	5.22	1	93-94	5-6
K-feldspar, antiperthitic rim	C173/B	Dull blue	7.31E-04	(449)	8.95E-04	(708)	0.82	1	99	
Albite, antiperthitic rim	C173/C	Dull red	2.62E-04	(449)	2.45E-03	(708)	0.11	91-96	4-9	0-1
Secondary albite	C173	Deep red	N/A		N/A			1-2	98-99	
Albite, core	C330/A	Light blue	5.74E-03	(449)	1.31E-03	(711)	4.38	1-9	91-99	0-2
Secondary K-feldspar, core	C330	Dull blue	N/A		N/A			90-94	6-9	0-1
K-feldspar, antiperthite rim	C330	Red	N/A		N/A			1	99	
Albite, antiperthitic rim	C330	Dark blue	N/A		N/A			91-92	7-9	0-1
Albite, antiperthite	C2092/A	Deep red	2.52E-04		8.83E-03	(711)	0.03	0-2	98-99	
K-feldspar, antiperthite	C2092	Dull red	N/A		N/A			89-96	3-9	0-2
Secondary albite	C2092/B	Deep red	1.68E-04		8.41E-03	(711)	0.02	0-1	99-100	0-1
Albite, perthite in xenolith	C2092	Light blue	N/A		N/A			1-2	97-99	1
K-feldspar, perthite in xenolith	C2092	Dull blue	N/A		N/A			84-99	0-15	0-1

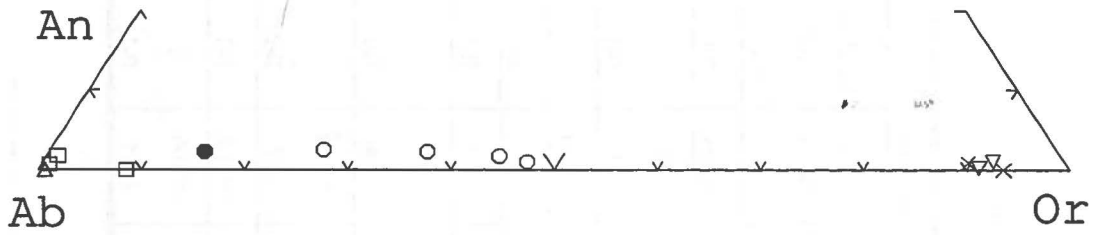

Fig. 7.4-3a. The compositions of the feldspars in the quartz syenite (C2087 and C330) from Center III plotted in the system Or-Ab-An.

For sample C2087, the open circles (○) are the blue luminescent homogeneous alkali feldspar in the core and the filled circle (●) is the light violet blue luminescent Na-rich feldspar in the margins.

For sample C330, the open squares (□) are the light blue luminescent albite core. The up-triangle (▵) is the red luminescent albite and the down-triangles (▿) are the dark blue luminescent K-feldspar in the deuteric coarsened antiperthitic rim. The crosses (×) are the dull blue luminescent secondary K-feldspar in the albite core.

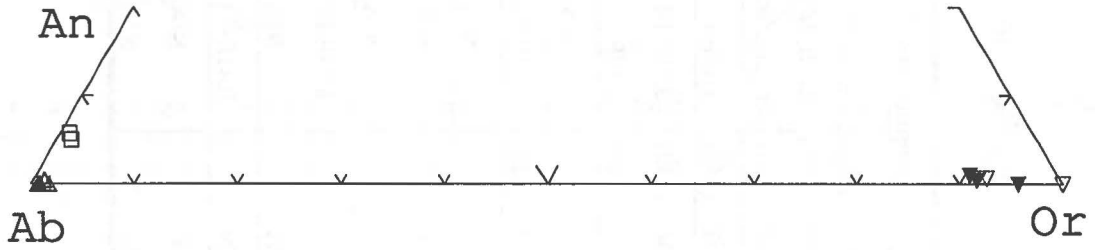

Fig. 7.4-3b. The compositions of the feldspars in the quartz syenite (C173 and C369) from Center III plotted in the system Or-Ab-An.

For sample C173, the open squares (□) are the light blue luminescent albite core. The filled up-triangles (▲) are the dull red luminescent albite host and the filled down-triangles (▼) are the dull blue luminescent exsolved K-feldspar in the oscillatory zoned antiperthite. The crosses (+) are the deep red luminescent secondary albite in the interstices between the antiperthite grains.

For sample C369, the up-triangles (▵) are the red, violet and dull red luminescent albite host and the down-triangles (▿) are the dark blue and dull blue luminescent exsolved K-feldspar in the oscillatory zoned antiperthite.

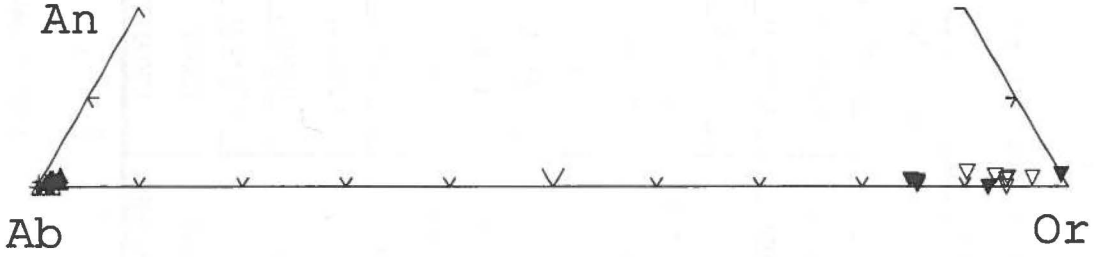

Fig. 7.4-3c. The compositions of the feldspars in the quartz syenite (C2092) from Center III plotted in the system Or-Ab-An.

The up-triangles (▵) are the deep red luminescent albite host and the down-triangles (▿) are the dull red luminescent exsolved K-feldspar in the antiperthite. The crosses (+) are the deep red luminescent secondary albite in the interstices between the antiperthite grains.

The filled down-triangles (▼) are the blue luminescent K-feldspar host and the filled up-triangles (▲) are the light blue luminescent exsolved albite in the perthite in the xenolith.

albite core and a deuteric coarsened antiperthitic rim. Under CL, the albite core usually exhibits light blue luminescence (Fig. 7.4-4b, -5b). CL spectrum of the light blue luminescent albite core consists of a high blue peak centered at 449 nm and a low red peak centered at 708 nm (Fig. 7.4-2b, spectrum A). The ratio of I_B/I_R is about 5.2 in sample C173 and 4.4 in sample C330 (Table 7.4-1). The light blue luminescent albite core ranges in composition from $Ab_{93-94}Or_1An_{5-6}$ in sample C173 and from $Ab_{91-99}Or_{1-9}An_{0-2}$ in sample C330 (Table 7.4-1, Fig. 7.4-3a,b and Appendix 3).

Within the deuteric coarsened antiperthitic rim, the albite exhibits dull red luminescence whereas the K-feldspar exhibits dull blue luminescence (Fig. 7.4-4b, -5b). CL spectrum of the dull red luminescent albite consists of a very low blue peak centered at 449 nm and a high red peak centered at 708 nm with a ratio of I_B/I_R about 0.1 (Fig. 7.4-2b, spectrum C and Table 7.4-1). The dull blue luminescent exsolved K-feldspar consists of a low intensity blue peak centered at 449 nm and a low intensity red peak centered at 708 nm with a ratio of I_B/I_R about 0.8 (Fig. 7.4-2b, spectrum B and Table 7.4-1). The dull red luminescent albite ranges in composition from $Ab_{91-96}Or_{4-9}An_{0-1}$ whereas the dull blue luminescent K-feldspar ranges from Or_{99} Ab_1 (Table 7.4-1 and Appendix 3).

7.4.4. Oscillatory zoned antiperthite

Oscillatory zoned antiperthite crystals are also observed in the quartz syenites (samples C173, C330, C367, C369 and C2136). The oscillatory zoned antiperthite crystal are commonly mantled with a

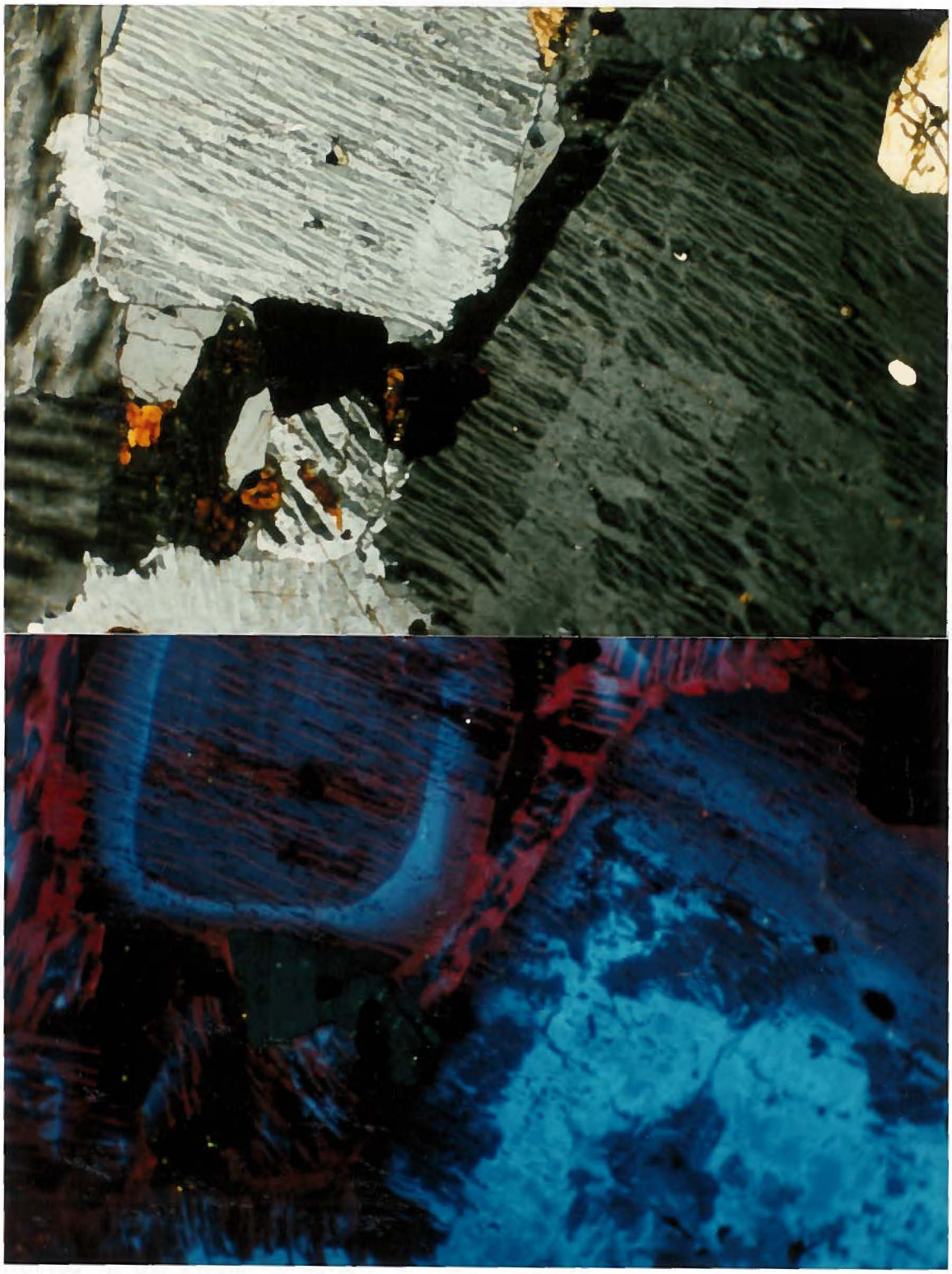

Fig. 7.4-4. Mantled feldspar crystals in quartz syenite (Sample C173) from Center III, Coldwell Complex. a. TrL. The mentled feldspar crystal (on the right) has an albite core and a deuteric coarsened antiperthitic rim. (Photographic conditions: 1 s, ASA 400) b. CL. The albite core exhibits light blue luminescence. In the deuteric coarsened antiperthitic rim, the albite host exhibits dull red luminescence and the exsolved K-feldspar exhibits dull blue luminescence. Another antiperthite crystal (on the left) is mantled with an oscillatory zoned antiperthitic core and a deuteric coarsened antiperthitic rim. Scale: 55 mm on photograph = 1 mm on thin section. (CL conditions: 10 kV, 0.8 Am. Photographic conditions: 30 s, ASA 400.)

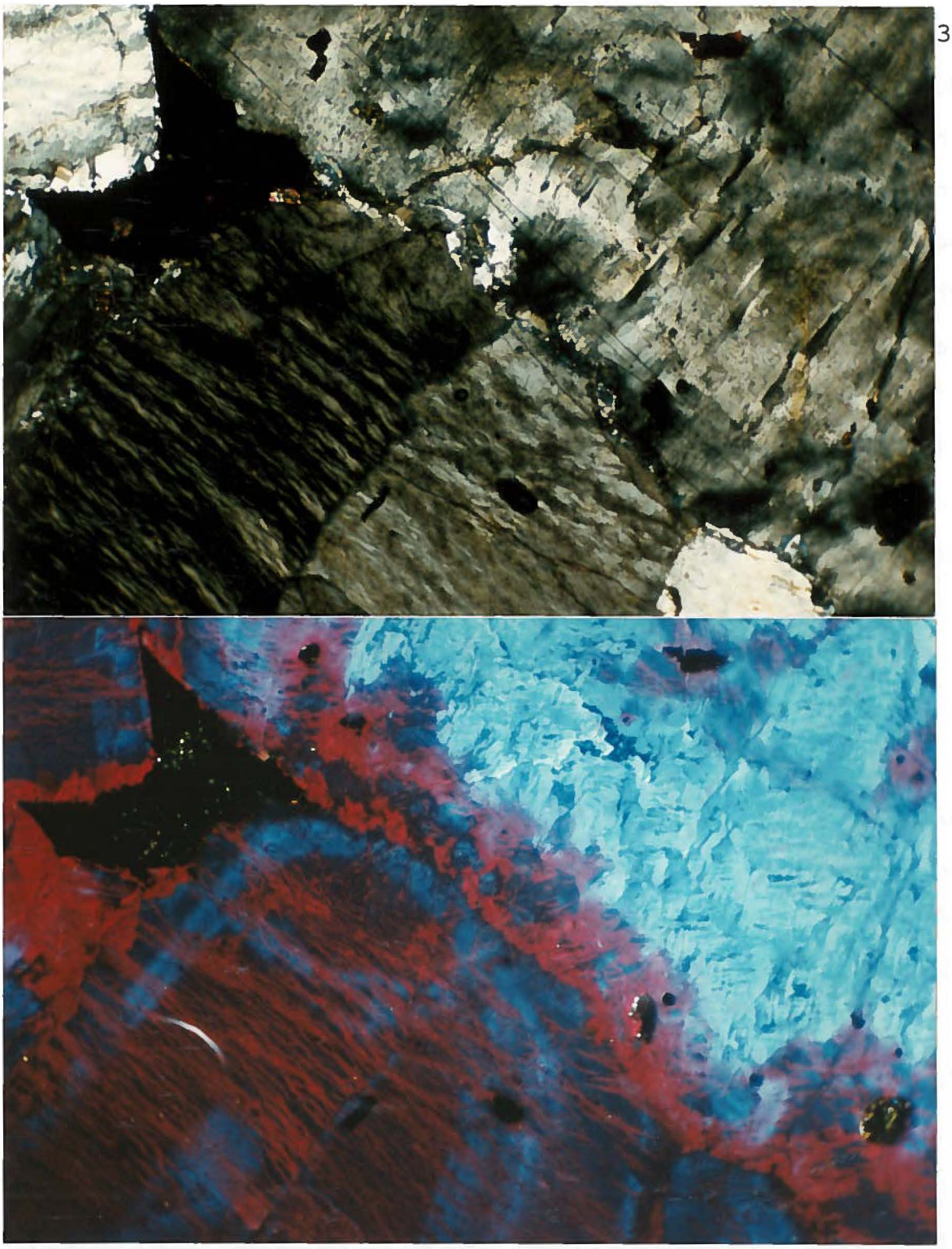

Fig. 7.4-5. Mantled feldspar crystals in quartz syenite (Sample C330) from Center III, Coldwell Complex. a. TrL. (Photographic conditions: 1 s, ASA 400) b. CL. The feldspar crystals are mantled with a light blue luminescent albite core, or an oscillatory zoned antiperthitic core and a deuteric coarsened antiperthitic rim. Within the antiperthitic core or the rim, the albite host exhibits red luminescence and the exsolved K-feldspar exhibits dull blue luminescence. Secondary K-feldspar occurs in the albite core and exhibits dull blue luminescence. Secondary albite occurs in the interstices and exhibits deep red luminescence. Scale: 55 mm on photograph = 1 mm on thin section. (CL conditions: 10 kV, 0.8 Am. Photographic conditions: 15 s, ASA 400.)

dull red luminescent antiperthite core, a violet luminescent antiperthite mantle and a dull red to deep red luminescent antiperthite rim (Fig. 7.4-4, -6). In most samples, between the mantle and the rim, there is a narrow light blue luminescent zone. The luminescence colours of the albite host and the exsolved K-feldspar are variable between these different zones.

For example, in sample C369, within the antiperthitic core, the albite host exhibits a dull red luminescence and the exsolved K-feldspar exhibits a dark blue luminescence (Fig 7.4-6b). However, within the violet luminescent mantle, the albite host exhibits violet luminescence and the exsolved K-feldspar exhibits dull blue luminescence. Within the dull red to red luminescent rim, the albite host exhibits dull red to red luminescence and the exsolved K-feldspar exhibits dark blue luminescence. The albite host and the exsolved K-feldspar in these different zones have similar near end member compositions, i.e, the albite host ranges in composition from $Ab_{98}Or_{1-2}An_{0-1}$, whereas the exsolved K-feldspar is from Or_{91-100} $Ab_{0-8}An_{0-1}$ (Appendix 3).

7.4.5. Irregular vein antiperthite

A typical antiperthite crystal in quartz syenite (sample C2092) from Center III is shown in Fig. 7.4-7a. The antiperthite has an irregular vein texture and both the albite host and the exsolved K-feldspar contain many small grains of hematite. Under CL, the albite host exhibits deep red luminescence, whereas the exsolved K-feldspar exhibits dull red luminescence (Fig. 7.4-7b). The CL

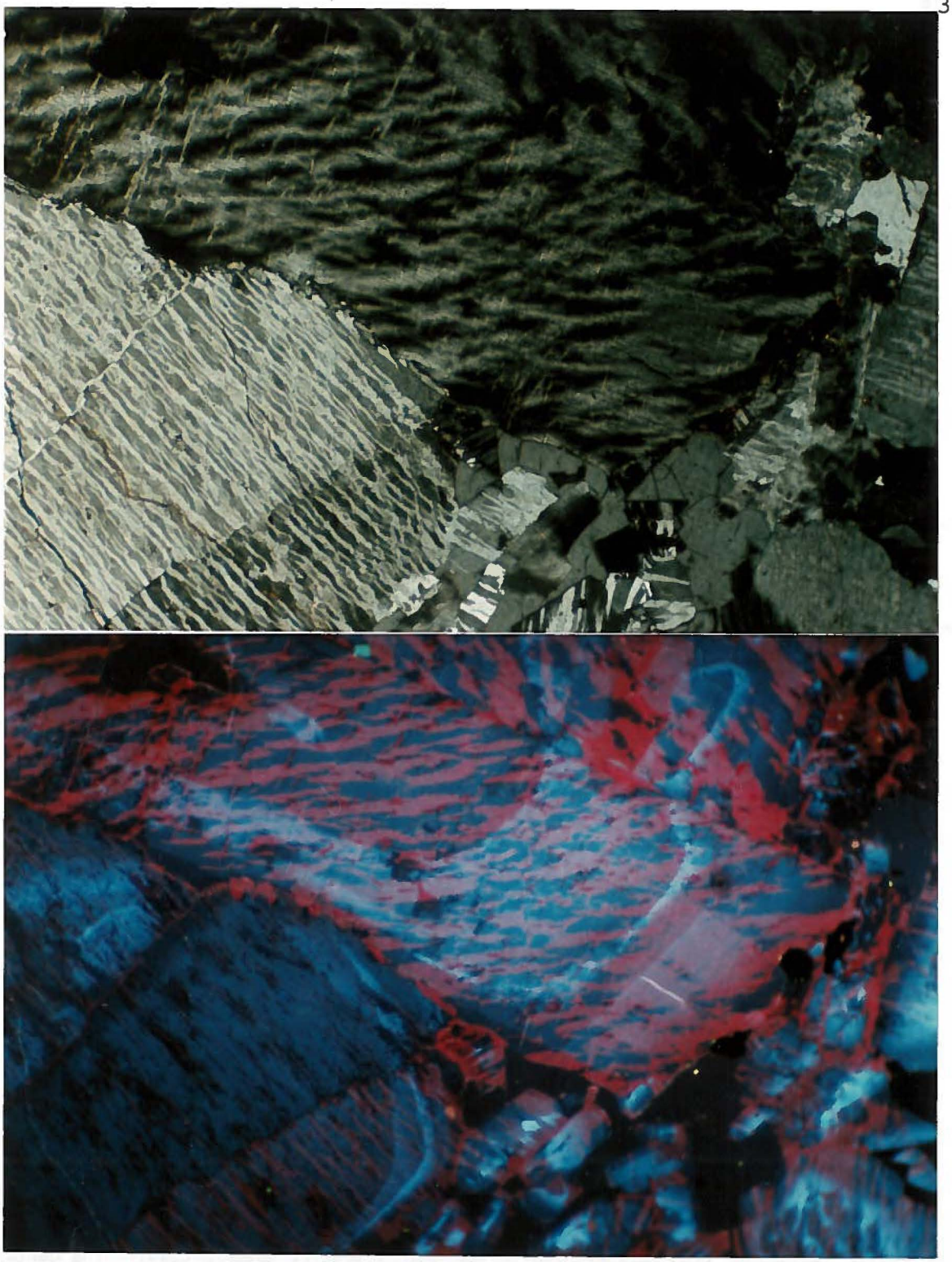

Fig. 7.4-6. Oscillatory zoned antiperthite in the quartz syenite (Sample C369) from Center III, Coldwell Complex. a. TrL. (Photographic conditions: 1 s, ASA 400) b. CL. The antiperthite crystals are mantled with a red luminescence core, a violet luminescence mantle and dull red luminescence rim. The albite host exhibits light violet blue, violet dull red or red luminescence and the exsolved K-feldspar exhibits dull blue or dark blue luminescence. Scale: 55 mm on photograph = 1 mm on thin section. (CL conditions: 10 kV, 0.8 Am. Photographic conditions: 1 min, ASA 400.)

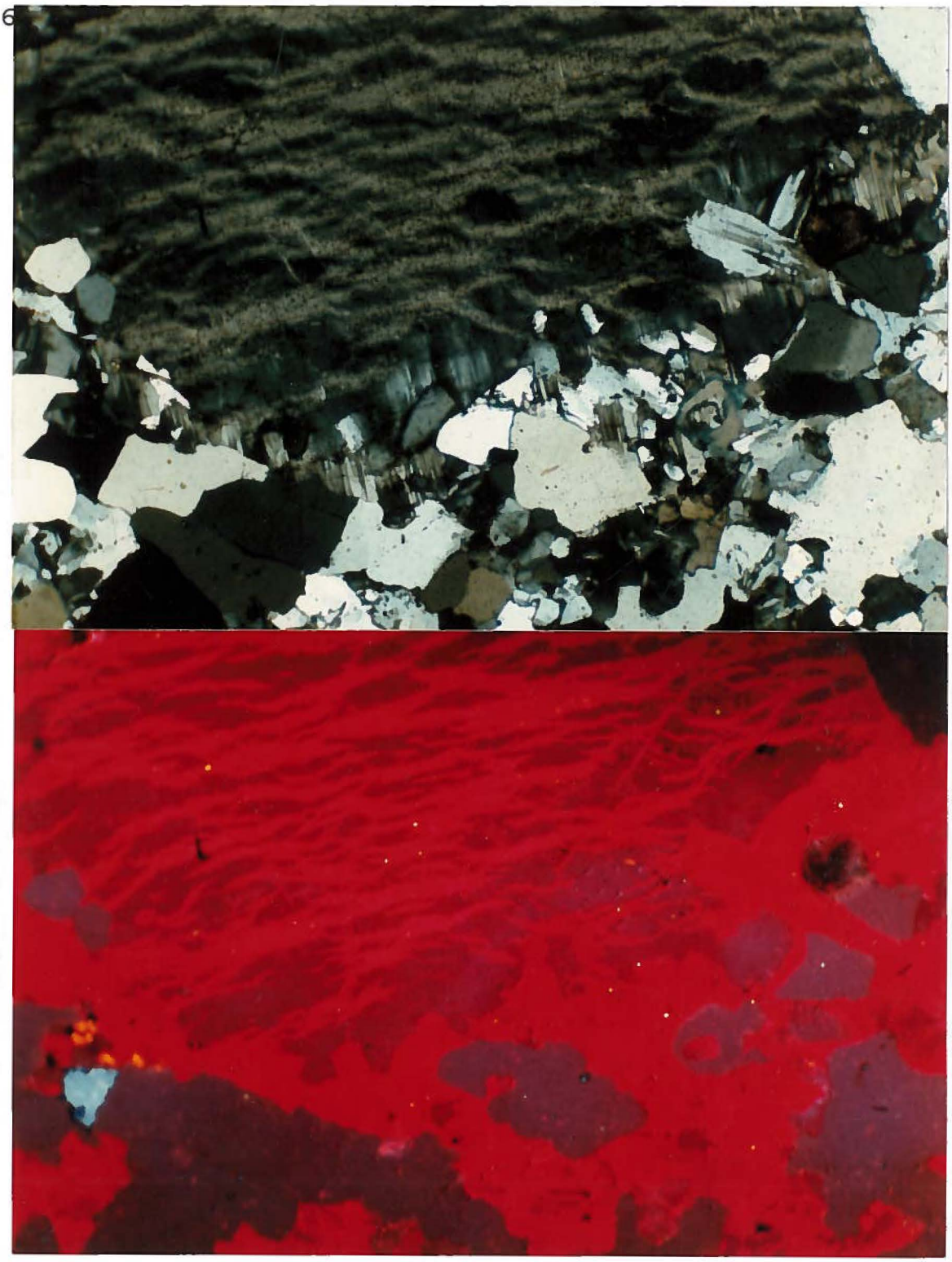

Fig. 7.4-7. Irregular vein antiperthite in the quartz syenite (Sample C2092) from Center III, Coldwell Complex. a. TrL. The coarse-grained feldspar is an irregular vein antiperthite crystal and the many small-grained feldspars are the secondary albite (Photographic conditions: 4 s, ASA 400) b. CL. Within the antiperthite, the albite host exhibits deep red luminescence and the exsolved K-feldspar exhibits dull red luminescence. The secondary albite exhibits deep red luminescence. Scale: 55 mm on photograph = 1 mm on thin section. (CL conditions: 10 kV, 0.8 Am. Photographic conditions: 2 min, ASA 400.)

spectrum of the deep red luminescent albite host only contains a high intensity red peak centered at about 711 nm with a ratio of I_B/I_R about 0.03 (Fig. 7.4-8, spectrum A and Table 7.4-1).

The deep red luminescent albite host ranges in composition from Ab_{98-99} Or_{0-2}, whereas the dull red luminescent K-feldspar ranges from $Or_{89-96}Ab_{3-9}An_{0-2}$ (Fig. 7.4-3c, Table 7.4-1 and Appendix 3). Both the albite host and exsolved K-feldspar contain high Fe contents, i.e., the albite host contains 1.5-4 mole% $KFeSi_3O_8$ and the exsolved K-feldspar contains 1.7-3.1 mole% $KFeSi_3O_8$ (Appendix 3). The high Fe contents may be due to the presence of small hematite inclusions.

7.4.6. Late stage fluid induced deuteric coarsening and replacement in the quartz syenites

a. Deuteric coarsened antiperthitic rim

As described above, the deuteric coarsened feldspars usually form as an antiperthitic rim surrounding the albite core during late-stage fluids-feldspar interaction (Fig. 7.4-4a, -5a). The albite usually exhibits dull red to deep red luminescence and the K-feldspar exhibits dull blue to dark blue luminescence (Fig. 7.4-4b, -5b). Both the deuteric coarsened albite and K-feldspar have compositions near their end members.

b. Secondary K-feldspar and secondary Na-feldspar

In quartz syenite, the secondary K-feldspar usually occurs as irregular vein or patches replacing the albite in the core of mantled feldspars (sample C330). The secondary K-feldspar exhibits

dull blue luminescence (Fig. 7.4-5b) and ranges in composition from $Or_{90-94}Ab_{6-9}An_{0-1}$ (Table 7.4-1 and Appendix 3).

Secondary albite usually occurs as interlocking grains occupying the interstices between the antiperthite grains. Most of the secondary albite grains are untwinned crystals (Fig. 7.4-4a,-5a). However, some secondary albite grains are albite twinned (Fig. 7.4-7a). Both twinned and twin-free secondary albite usually exhibit deep red luminescence (Fig. 7.4-4b,-5b,-7b) and have compositions near those of the end member. In sample C173, e.g., the twin-free, deep red luminescent secondary albite (Fig. 7.4-4b) ranges in composition from $Ab_{98-99}Or_{1-2}$ (Table 7.4-1, Fig. 7.4-3b and Appendix 3). In sample C2092, the albite-twinned, deep red luminescent secondary albite (Fig. 7.4-7) shows only a high red peak centered at about 711 nm in the CL spectrum with a I_B/I_R ratio about 0.02 (Fig. 7.4-8, spectrum B and Table 7.4-1). The ablite-twinned, deep red luminescent secondary albite ranges in composition from Ab_{99-100} $Or_{0-1}An_{0-1}$ (Table 7.4-1 and Appendix 3).

7.4.7. Perthite in a xenolith of Center I syenite

Feldspar crystals in the xenolith of Center I syenite (sample C2092) are irregular vein perthite. Within the perthite, the K-feldspar host exhibits blue luminescence and the exsolved albite exhibits light blue luminescence. The K-feldspar host ranges in composition from $Or_{84-99}Ab_{0-15}An_{0-1}$, whereas the exsolved albite ranges from $Ab_{97-99}Or_{1-2}An_1$ (Fig. 7.4-3c and Appendix 3). Both the K-feldspar host and the exsolved Na-feldspar contain very low Fe contents,

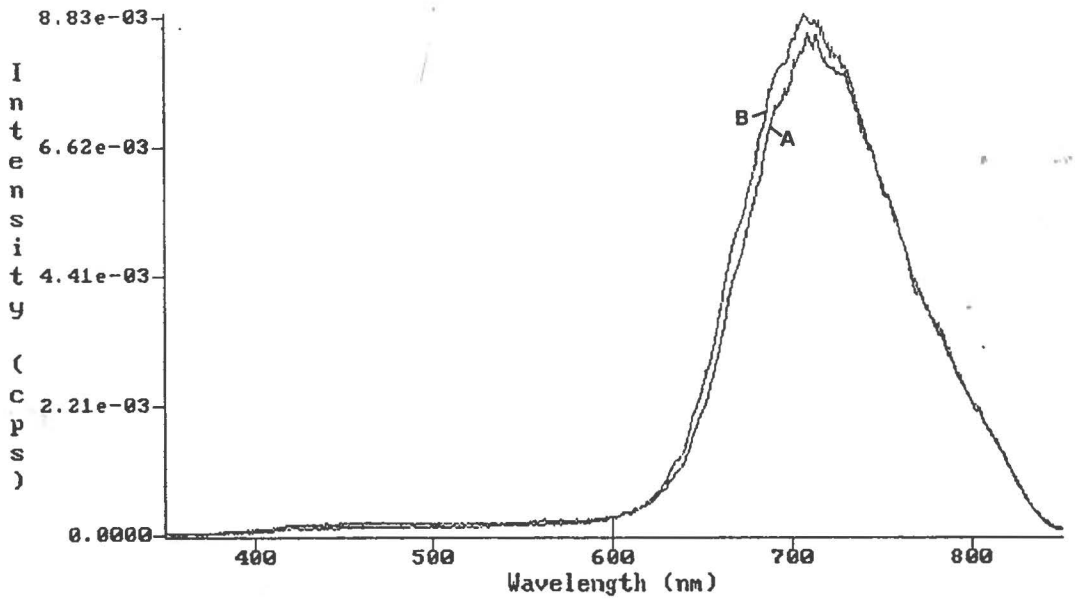

Fig. 7.4-8. CL spectra of feldspars in quartz syenite (Sample C2092) from Center III, Coldwell Complex, Ontario. (A) is from the deep red luminescent albite host of the irregular vein antiperthite. (B) is from the deep red luminescent albite-twinned secondary albite. CL conditions: 10 kV, 0.8 mA.

i.e., 0-0.6 mole% ($KFeSi_3O_8$) in the K-feldspar host and 0-0.7 mole% ($KFeSi_3O_8$) in the exsolved albite (Appendix 3).

7.4.8. Thermal history of the feldspars

The thermal history of the alkali feldspars in the quartz syenite is shown in Fig. 7.4-9. The path a-a′ on the incoherent solvus (SFS) indicates that the blue luminescent homogeneous alkali feldspar core ($Or_{26-47}Ab_{52-71}$) may have crystallized at temperatures ≥700 °C, and the point b indicates that the light violet blue luminescent homogeneous alkali feldspar rim ($Or_{15}Ab_{83}$) may have crystallized at temperatures about 660 °C.

The path c-c′ on the incoherent solvus (SFS) indicates that the light blue luminescent albite core ($Ab_{91-99}Or_{1-9}$) formed at temperatures about 600-450 °C.

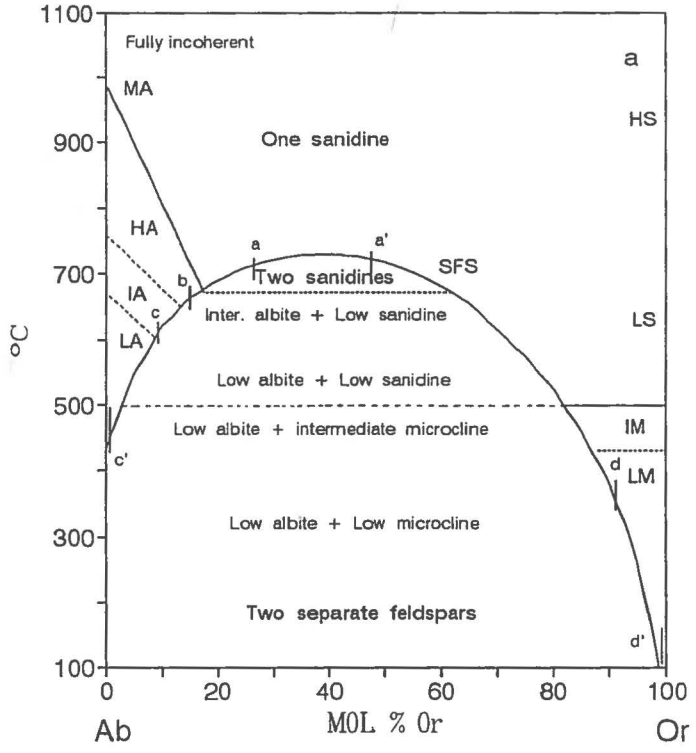

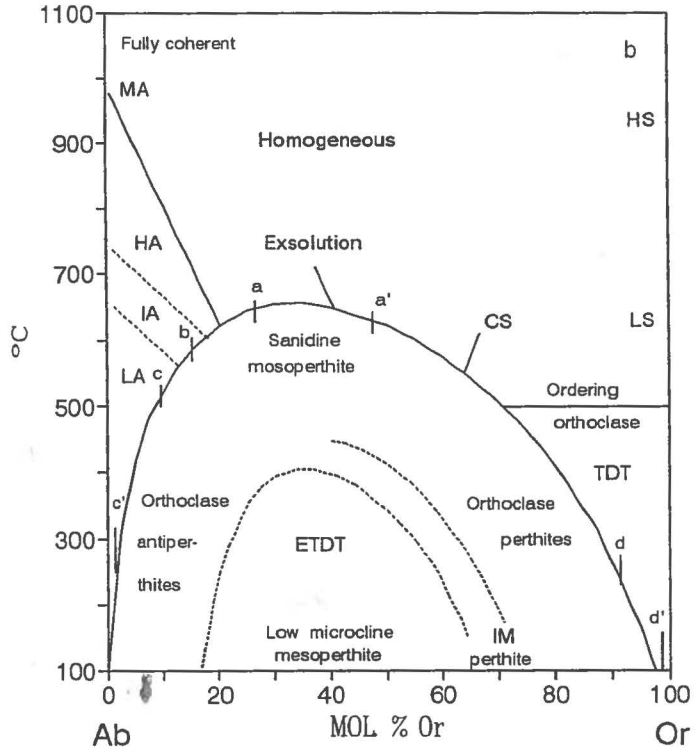

Fig. 7.4-9. The evolution of the alkali feldspars in the quartz syenite from Center III is illustrated in the Or-Ab binary phase diagram.

The path a-a′ and point b indicate the core and the rim of the optically homogeneous alkali feldspar, respec-tively. The path c-c′ indicates the albite core of the mantled feldspar crystals. The path d-d′ and e-e′ include the exsolved K-feldspar and albite in the oscillatory zoned and irregular vein antiperthite, and the secondary K-feldspar and albite in the deuteric coarsened antiperthite rim.

Diagram (a) shows the phase rela-tionships for An-free alkali feldspars under complete (incoherent) equili-brium and (b) shows different cons-trained equilibrium states as a func-tion of bulk composition and T for completed coherent intergrowths (Brown and Parsons, 1989). SFS is the strain-free solvus and CS is the coherent solvus. TDT is the twin-domain microtexture and ETDT is the exsolu-tion and the twin-domain microtexture. MA, HA, IA and LA are monoclinic, high, intermediate and low albite; IM and LM are intermediate and low microcline. IA and IM is the region of the rapid change in Y ordering.

The paths d-d′ and e-e′ indicate that the exsolved K-feldspar ($Or_{91-100}Ab_{0-9}$) and albite ($Ab_{98-99}Or_{0-2}$) in the oscillatory zoned and unzoned irregular vein antiperthite, and the dueteric coarsened K-feldspar ($Or_{99}Ab_{1}$) and albite ($Ab_{91-96}Or_{4-9}$) may have formed at temperatures about 350 °C.

CHAPTER 8

REVIEW OF LUMINESCENCE CENTERS IN APATITES

8.1. Introduction

Apatite, $Ca_{10}(PO_4)_6(F,Cl,OH)_2$ is a hexagonal mineral with a space group $P6_3/m$ (Beevers and McIntyre, 1946). Ca^{2+} ions occupy two symmetrically distinct sites, Ca_I and Ca_{II} sites, which are located near the centre of the [001] hexad (Fig. 8-1a). The Ca_I site (point symmetry 3; multiplicity=4) is coordinated with nine oxygen atoms and are bonded to tetrahedral PO_4 groups to form composite chains parallel to c-axis, whereas the Ca_{II} site (point symmetry m; multiplicity=6) bonds to six oxygen atoms and one column anion (F,Cl,OH). The column anion lies on the sixfold screw axis (Beevers and McIntyre, 1946; Hughes et al., 1989, 1991a).

In natural apatite crystals, the Ca^{2+} ion can be substituted by Na, K, Sr, Mg, Ba, Pb, Mn^{2+}, Sn, Y and REE^{3+}, and the PO_4 group can be substituted by SiO_4, SO_4 and CO_3. Since the divalent Ca ions exist in two distinct Ca_I and Ca_{II} sites in the apatite structure, the site occupancy and charge balance for the trivalent REE ions and divalent elements (Sr^{2+} and Mn^{2+}) substituting for Ca^{2+} in apatite structures have been studied by many authors (Roeder et al., 1987 Hogarth, 1988; Binder and Troll, 1989; Hughes et al., 1991a, 1991b; Liu and Comodi, 1993; Rakovan and Reeder, 1994).

Site occupancy of REE has been studied by Hughes et al. (1991a). The results of four light REE-enriched apatite structure refinements indicated that the REE^{3+} ions can occupy both the Ca_I

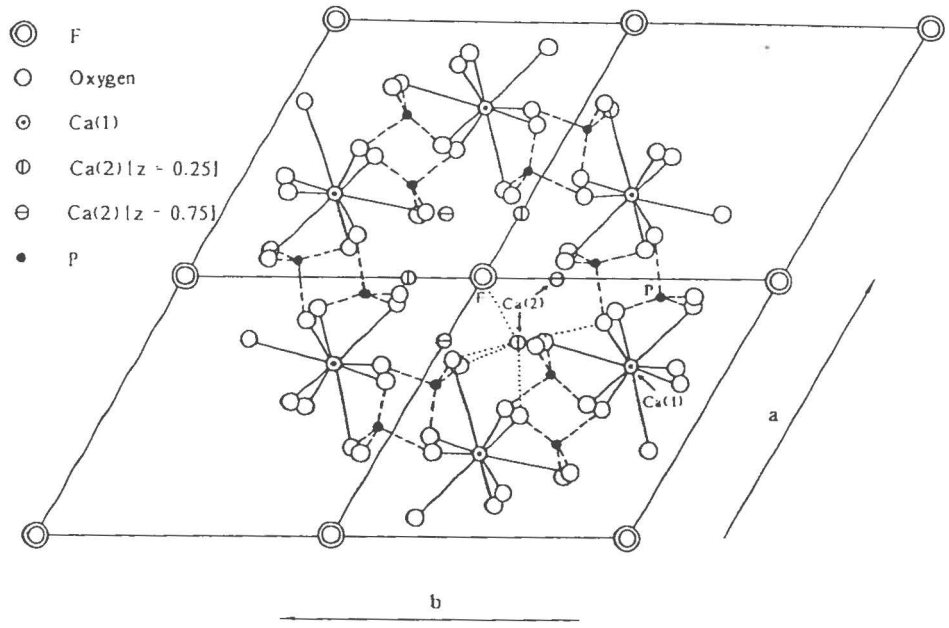

Fig. 8-1a. A portion of four unit cells of the fluorapatite, $Ca_5(PO_4)_3F$, structure projected on the (001) plane (from Hughes et al., 1989). The solid and dotted lines indicate Ca^{2+} in Ca_I and Ca_{II} sites, respectively.

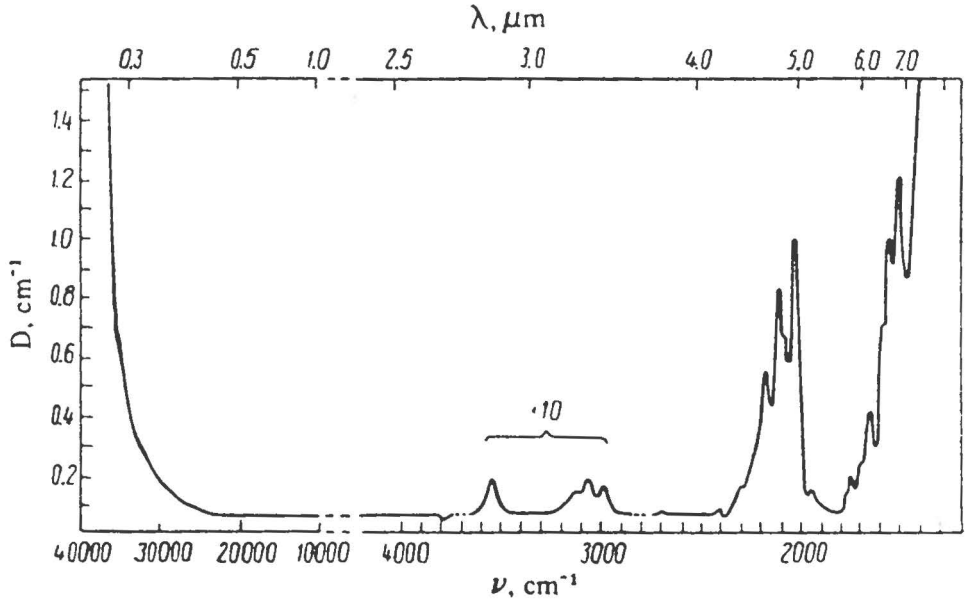

Fig. 8-1b. Absorption spectrum of a non-activated fluorapatite crystal, specimen thickness 0.2 mm (from Morozov et al., 1970).

and Ca_{II} sites, but they largely prefer the Ca_{II} site with $REE_{Ca_I}/REE_{Ca_{II}}$ ratios from 1.76 to 3.00. Hughes et al. (1991a) calculated the bond valence requirements for substituent REEs in the apatite structure and suggested that La, Ce and Pr would preferentially substitute at the Ca_{II} site, whereas Pm and Sm substitute at the Ca_I site and Nd^{3+} substitutes at both the Ca_I and Ca_{II} sites. Structural ordering of Sr and Mn in apatite crystals have also been studied by Hughes et al. (1991b), the results of two Sr-enriched apatite crystals structure refinements indicated that the Sr^{2+} ion is ordered almost completely into the Ca_{II} site. The results of two Mn-enriched apatites indicated that the Mn^{2+} ion occupies both the Ca_I and Ca_{II} sites, but prefers the Ca_I site.

The REE^{3+} ions substituting for the Ca^{2+} ion in the apatite structure require a coupled substitution to maintain charge balance. Roeder et al. (1987) found that the total number of REE ions in apatite is generally proportional to the total number of Na + Si ions. Thus, they suggested that charge balance is maintained by the following schemes $REE^{3+} + Si^{4+} \rightleftharpoons Ca^{2+} + P^{5+}$ and $REE^{3+} + Na \rightleftharpoons 2Ca^{2+}$. The degree of alkalinity or silica saturation of the crystallization environment may control the amount of Na or Si substituting for the REE^{3+} ions in the apatite structure. Rønsbo (1989) found that the same coupled substitutions occur in apatites from alkaline rocks in the Ilìmaussaq intrusion, South Greenland. Rønsbo (1989) also found that the substitution of $REE^{3+} + Si^{4+} \rightleftharpoons Ca^{2+} + P^{5+}$ in the apatites is predominantly found in a nonperalkaline or slightly peralkaline environment, i.e., in augite syenite and

sodalite foyaite. Whereas, the substitution $REE^{3+} + Na \rightleftharpoons 2Ca^{2+}$ in the apatites is predominantly found in the highly peralkaline environment, i.e., in quartz-bearing peralkaline pegmatite.

Hughes et al. (1991) reported that the contents of Na + Si atoms per unit cell versus the refined total REE atoms per unit cell in the apatite crystals have a linear correlation. They suggested that the apatite charge balance is only maintained by a combination of the $REE^{3+} + Si^{4+} \rightleftharpoons Ca^{2+} + P^{5+}$ and $REE^{3+} + Na \rightleftharpoons 2Ca^{2+}$ substitutions and not by any other mechanisms such as vacancies in the structure. Liu and Comodi (1993) found a clear direct relationship between the sums of REE + S and Si + Na in 24 apatite samples from carbonatite and other alkaline rocks, they confirmed that the apatite charge balance is mainly maintained by the above heterovalent substitutions. However, they suggested that the charge balance also involves a substitution of $SO_4^{2-} + Si_4^{4-} \rightleftarrows 2PO_4^{3-}$ in most of the apatites, except in four Si-, CO_3-rich apatite samples from carbonatite. These four apatites may also involve a substitution of $(SO_4^{2-}, CO_3^{2-}, CO_3OH^{2-}) + Si_4^{4-} \rightleftarrows 2PO_4^{3-}$, and the excess of negative charge could be balanced through LREE entry in the apatite lattice.

Based on an investigation of absorption and luminescence spectra of REE-activated fluorapatite, Morozov et al. (1970) concluded that the trivalent REE ions mainly substitute for Ca^{2+} in the lower symmetry Ca_{II} site with the charge compensated by O^{2-} replacing F^- or rarely by the formation of vacancies at the Ca_{II} site to form a basic activator center. However, a small amount of the trivalent REE ions may also substitute for Ca^{2+} in the higher symmetry Ca_I

site to form an other type of activator center (see section 8.7.).

8.2. Luminescence of apatites

Pure apatite crystals exhibit no luminescence, such as the synthetic hydroxyapatite, fluorapatite and chlorapatite without the addition of any activator ions (Mariano, 1989; Morozov et al., 1970). In the absorption spectrum, fluorapatite crystals are transparent, i.e., no absorption bands are observed in a wide wavelength region from about 300 to 2800 nm and the absorption edge occurs at about 300 nm (Fig. 8-1b). However, in the infrared region from 2800 to 6000 nm, absorption bands are observed. These absorption bands are mainly caused by vibrations of the $[PO_4]$ tetrahedra, and the hydroxyl group which isomorphously replaces fluorine ions. Therefore, the wide transparent wavelength range in spectrum of non-activated apatite crystals is convenient for the study of luminescence spectra of REE-activated apatites in the visible and infrared regions.

Natural apatites in petrogenetically different rocks exhibit diverse luminescence colours. Smith and Stenstrom (1965) found that apatites in basaltic rocks exhibit yellowish luminescence and are mantled by a narrow brownish luminescent rim; In alkaline plutonic rocks from Greenland, apatite exhibits lavender luminescence; In microcline perthite in Precambrian rocks from Finland, apatite exhibits yellowish luminescence; In pegmatites, apatite exhibits green luminescence. Smith and Stenstrom (1965) presumed that the different luminescence colours of apatites were related to chemical

composition variations.

Natural apatites are known to concentrate rare earth elements and other ions, such as Mn^{2+} and Sr^{2+}. The presence of some as activator ions, such as Ce^{3+}, Sm^{3+}, Dy^{3+}, Eu^{2+}, Sm^{2+} and Mn^{2+} in apatite crystals have been demonstrated by early Russian work from luminescence spectra (Marfunin, 1979). The above authors concluded that the blue and violet luminescence in apatite is due to Ce^{3+} and Eu^{2+} emission; and various hues of pink, violet-pink and yellow-pink luminescence are due to Sm^{3+} and Dy^{3+} emission; the yellow luminescence is due to Mn^{2+}. However, Marfunin (1979) indicated that the identification of the impurities in apatite crystals according to their luminescence colours is qualitative. A complete set of the activator ions can not be identified because some emission lines and bands may overlap each other in the visible region and extend over the IR (Sm^{2+}) and UV (Ce^{3+}) regions.

Luminescence spectra can provide qualitative identification of activator ions in apatite host, since the emission lines in the luminescence spectra are characteristic of the activator ions. For REE-bearing apatite hosts, the luminescence lines (or peaks) are produced by two types of electron transitions, i.e., f-f and f-d, of the REE^{2+} or REE^{3+} activator ions within their inner shells. The characteristic of luminescence spectra of activator ions in apatite crystals are reviewed in the following sections.

8.3. Mn^{2+} activation

The Mn^{2+} activator ion in apatite emits a yellow luminescence

colour (Mariano, 1978; Marfunin, 1979). Mariano (1988) illustrated that an apatite which contains 240 ppmw Mn in a pegmatite from Palermo, New Hampshire exhibits yellow luminescence. Its CL spectrum consists of a broad band at about 565 nm (Fig. 8-2a) which is similar to the spectrum of Mn^{2+}-activated synthetic fluorapatite doped with 1.09 wt% Mn (Fig. 8-2b). However, in many natural and synthetic Mn^{2+}-activated apatites, the peak positions of Mn^{2+} emission vary from 562 to 580 nm (Mariano, 1978, 1988; Roeder et al., 1987). Mariano (1988) suggested that the peak positions shifting in this wavelength region are due to variations of configuration of the atomic species around the Mn^{2+} ion in the apatites.

8.4. Sm^{3+} activation

Mariano (1978, 1988, 1989) attributed Sm^{3+} activator ions in apatite crystals to the emission of narrow bands at about 560, 600, 645 and 710 nm (Fig. 8-3a). The relative luminescence intensities of the bands always decrease from 600, 645 to 710 nm. Marfunin (1979) showed a luminescence spectrum of Sm^{3+}-activated apatite between 540 and 660 nm region which consists of three groups of narrow lines distributed in about 545-560, 585-605 and 635-655 nm, regions corresponding to the electronic transitions from the lowest excited level $^4G_{5/2}$ to ground multiplets of $^6H_{5/2}$, $^6H_{7/2}$ and $^6H_{9/2}$ levels, respectively (Fig. 8-3b). A photoluminescence (PL) spectrum of synthetic Sm-doped fluorapatite crystals was given by Morozov et al. (1970). The Sm-doped fluorapatite crystal was excited by a

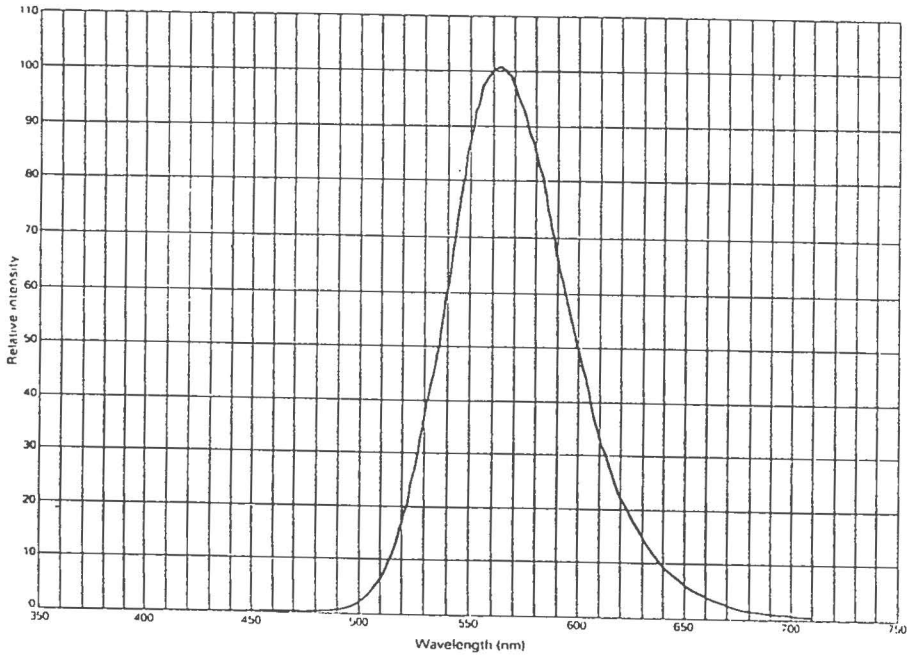

Fig. 8-2a. Mn^{2+}-activated pegmatite apatite from Palermo, New Hampshire. The apatite contains 240 ppmw Mn and exhibits yellow luminescence with a broad emission peak centered at 565 nm. CL conditions: 13 kV, 0.1 mA (from Mariano, 1988).

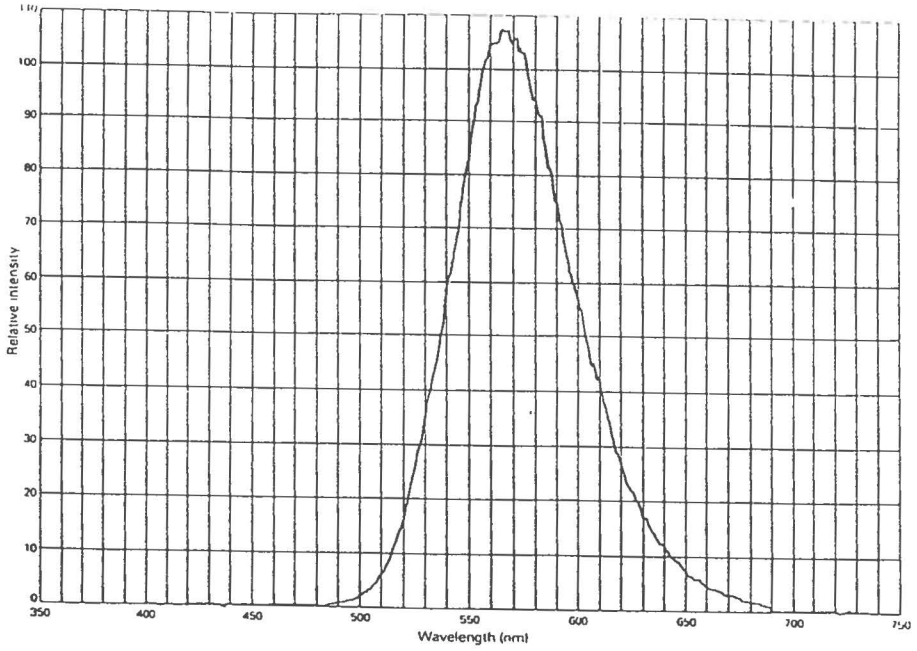

Fig. 8-2b. Synthetic Mn^{2+}-activated fluorapatite with 1.09 wt% Mn. The sample exhibits yellow luminescence with a broad emission peak centered at 565 nm. CL conditions: 7 kV, 0.15 mA (from Mariano, 1988).

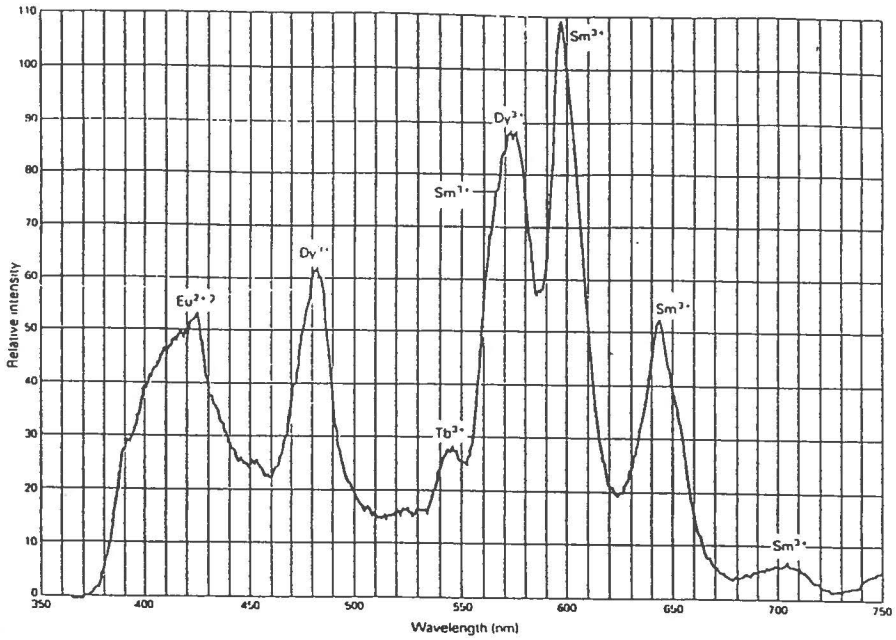

Fig. 8-3a. Apatite from Mineville, New York. The apatite contains 500 ppmw Sm, 50 ppwm Eu, 70 ppmw Tb and 440 ppmw Dy and exhibits violet luminescence. CL conditions: 17 kV, 0.15 mA (from Mariano, 1988).

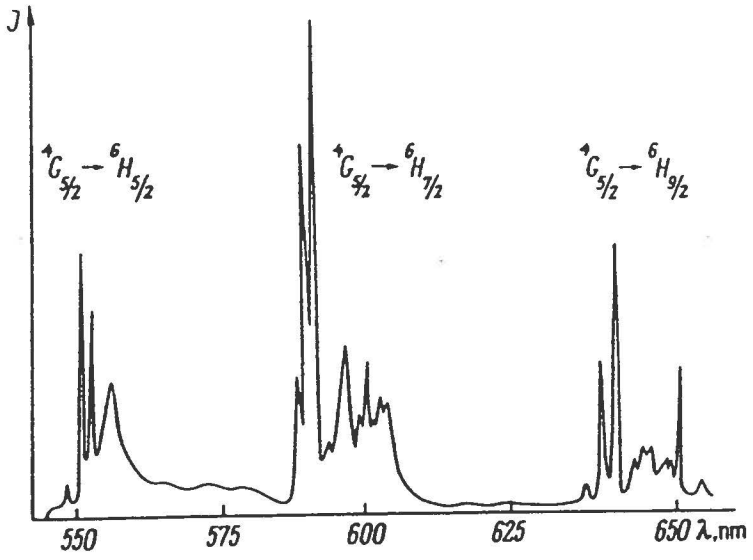

Fig. 8-3b. Luminescence spectrum of Sm^{3+} in apatite (from Marfunin, 1979).

mercury lamp to produce a number luminescence lines due to Sm^{3+} ion in the red-orange (between about 560 and 750 nm) and infrared regions (between about 900 and 1000 nm) (Fig. 8-4), which correspond to transitions from the lowest excited level $^4G_{5/2}$ to ground multiplets ^6H_j and ^6F_j . The lowest excited level $^4G_{5/2}$ is separated from the highest ground level $^6F_{11/2}$ by an energy interval of about 7500 cm^{-1}, which is the same as in Sm^{3+}-activated $LaCl_3$ and CaF_2 crystals (Dieke and Crosswhite, 1963; Marfunin, 1979).

8.5. Dy^{3+} activation

In natural REE-activated apatites, the CL emission bands which occur at about 480 and 575 nm are attributed to Dy^{3+} ions activation (Fig. 8-3a) (Mariano, 1978, 1988, 1989). Morozov et al. (1970) showed a luminescence (PL) spectrum of Dy-doped fluorapatite between 400 and 900 nm (Fig. 8-4). The spectrum consists of five groups of lines in wavelengths of about 470-500, 570-600, 650-700, 750-800 and 850 nm regions corresponding to the electronic transitions of Dy^{3+} ion from lowest exciting level $^4F_{9/2}$ to ground multiplet of ^6H_j (levels $^6H_{15/2}$, $^6H_{13/2}$ and $^6H_{11/2}$) and to multiplet ^6F_j. The groups of lines in the 470-500 and 570-600 nm regions (corresponding to transitions of $^4F_{9/2}\rightarrow{}^6H_{15/2}$ and $^4F_{9/2}\rightarrow{}^6H_{13/2}$) have higher luminescence intensities than other groups of lines.

8.6. Tb^{3+} activation

In CL spectra of natural apatites, a narrow band occurring at about 545 nm is attributed to Tb^{3+} ion emission (Fig. 8-3a)

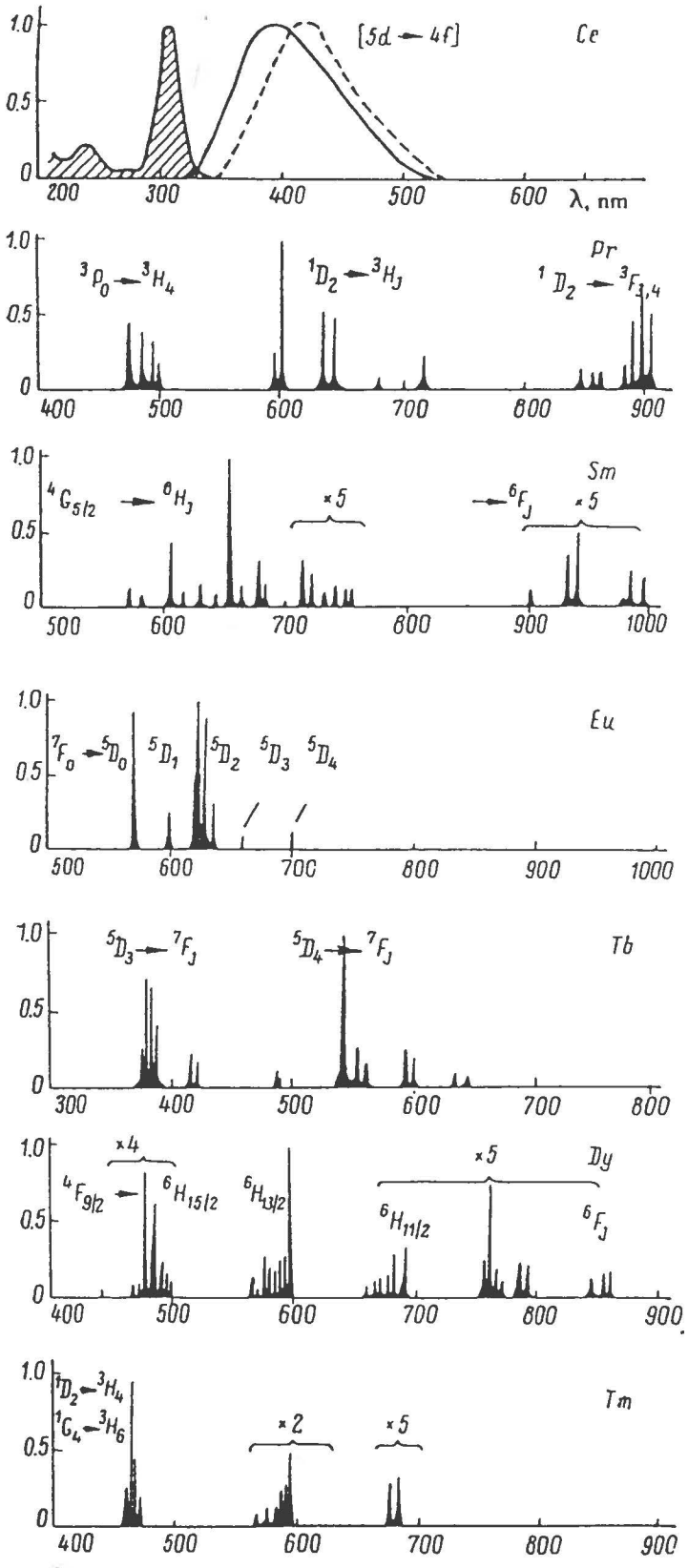

Fig. 8-4. Luminescence spectra (PL) of REE^{3+}-doped fluorapatite crystals (from Morozov et al., 1970).

(Mariano, 1978, 1988). However, this narrow emission band is not observed in most natural apatites (Mariano, 1978; Roeder et al., 1987). This has been explained by the Tb^{3+} emission band being masked by the strongest emission bands of Mn^{2+}, Sm^{3+} and Dy^{3+} in the wavelength region of about 560-600 nm (Roeder et al., 1987). However, if the Mn content is low in apatite, the Tb^{3+} emission band can be resolved from the Dy^{3+} and Sm^{3+} bands. Tb^{3+} ions may have a high efficiency for luminescence even though the concentration of Tb in natural apatites is very low. Mariano (1988) reported that two apatites from Mineville, New York and Kiglapait Intrusion, Labrador, contain 70 and 38.4 ppmw Tb, respectively. In both cases, the apatite showed a well resolved emission band occurring at about 545 nm. In a subsequent paper, Mariano (1989) illustrated a CL spectrum of supergene apatite which contains a well-resolved, high intensity Tb^{3+} emission band at 544 nm (Fig. 8-5a). The apatite was from botryoidal laterite crusts of a carbonatite from Mt. Weld, Western Australia. Mariano (1989) suggested under such strong oxidizing conditions as occur in laterites, Mn occurs in a higher valence state, therefore Mn^{2+} does not occur as activator ion in the apatite.

Luminescence spectra (PL) of Tb^{3+}-doped synthetic apatite have been given by Morozov et al. (1970). The spectrum consists of two groups of lines in the near ultraviolet (about 370-420 nm) and visible (about 480-650 nm) regions corresponding to the electron transitions of Tb^{3+} ion from two excited states $^5D_3$ and $^5D_4$ to ground multiplet ^7F_j (Fig. 8-4). The states $^5D_3$ and $^5D_4$ are separated by a

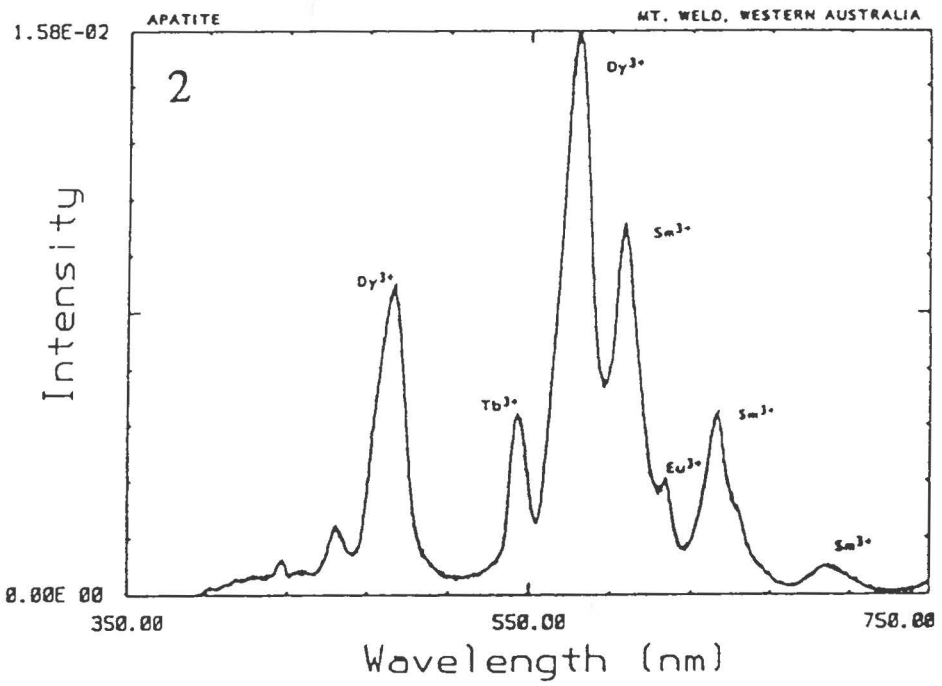

Fig. 8-5a. CL spectrum of the supergene apatite, $Ca_5(PO_4, CO_3)_3F$, in botryoidal laterite crusts of carbonatite from Mt. Weld, Western Australia. The spectrum contains a well-resolved Tb^{3+} emission band at 544 nm. CL conditions: 5 kV, 0.4 mA (from Mariano, 1989).

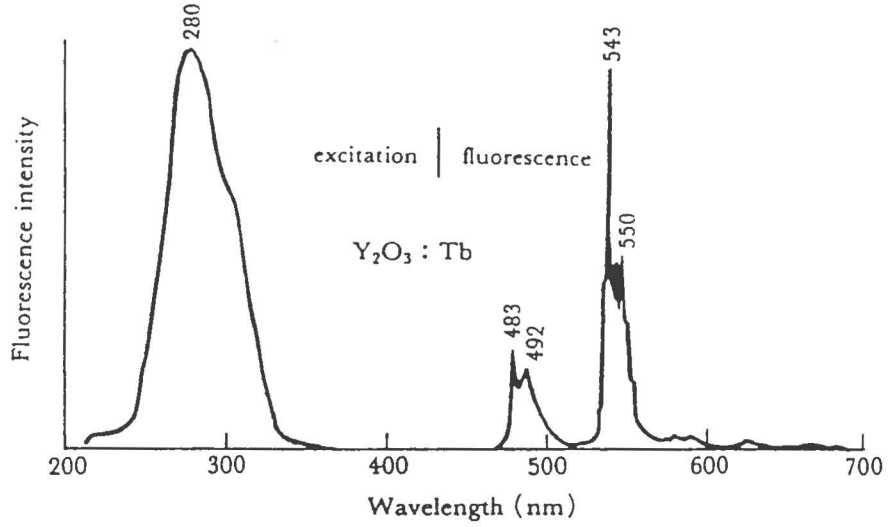

Fig. 8-5b. Luminescence and excitation spectra of Tb^{3+}-doped Y_2O_3 (0.001 mole Tb) crystals. The luminescence spectrum of Tb^{3+} consists of a series of groups of lines in the region near 483, 543, 583, 623 and 666 nm (from Ozawa, 1990).

wide energy gap of about 5600 cm^{-1} which is the same as found in Tb-doped $LaCl_3$ and CaF_2 crystals (Dieke and Crosswhite, 1963; Marfunin, 1979). Morozov et al. (1970) also noted that the luminescence spectra of Tb^{3+}-fluorapatite crystals are polarized. In industrial phosphors studies (Ozawa, 1990), the CL spectrum of green luminescent Tb-activated Y_2O_3 (doped with 0.001 mole Tb) consists of five groups of lines in the wavelength about 483, 543, 583, 623 and 666 nm in visible regions (Fig. 8-5b). These emission groups of lines have been assigned to the electronic transitions from the lowest excited state $^5D_4$ of Tb^{3+} ion to the multiplet ground state $^7F_{6-3}$. However, the luminescence lines of the transitions from the $^5D_3$ state are not detected in Y_2O_3. The intensities of the groups at the 623 and 666 nm are very low, but the group at the 543 nm has the highest luminescent intensity than other groups and has the same wavelength as the Tb^{3+} emission band in the luminescence spectra of natural apatites. For the natural apatites, therefore, the Tb^{3+} emission band at about 545 nm can be assigned to electronic transitions from the lowest excited state $^5D_4$ to the ground state of level $^7H_5$.

8.7. Eu^{2+} and Eu^{3+} activations

CL spectra of Eu-activated apatites may contain two types of activator ions: Eu^{2+} and Eu^{3+}. Luminescence spectra of Eu^{2+} and Eu^{3+} activations are quite different. Although both ions are associated with the same type of f-f transition, the Eu^{2+} ion produces a broad emission band in the blue region and the Eu^{3+} ion produces a series

of narrow peaks in the red region of CL spectrum (Marfunin, 1978). CL spectrum of apatite in carbonatite from Llallagua, Bolivia is a typical example showing Eu^{2+} and Eu^{3+} ion activations (Mariano and Ring, 1975; Roeder et al., 1987; Mariano, 1988, 1989). The apatite contains 0.146 wt% Eu_2O_3 and the CL spectrum consists of a broad peak centered at about 450 nm and four weak or narrow peaks at about 585, 613, 645 and 690, superposed on a broad Mn^{2+} peak (Fig. 8-6a). The broad peak at about 450 nm was attributed to Eu^{2+} activation, whereas the peaks in the longer wavelengths were attributed to Eu^{3+} activation.

In a synthetic Eu-doped apatite ($Ca_{4.95}Eu_{0.05}(PO_4)_3F_{0.95}Cl_{0.05}$), the Eu^{2+} activator ions produce a broad emission band at 460 nm (Fig 8-6b), whereas the Eu^{3+} activator ions emit a number of narrow peaks at 590, 615 and 695 nm (Mariano and Ring, 1975; Mariano 1988). The emission peak at 615 nm has a higher luminescence intensity than other Eu^{3+} activator ion emission peaks. Roeder et al. (1987) also illustrated a CL spectrum of Eu-doped apatite which was synthesized at low oxygen fugacity. As a result, the broad emission peak of Eu^{2+} activation at 450 nm is higher than the emission peaks of Eu^{3+} in the red region. The peak positions of Eu^{2+} and Eu^{3+} in synthetic Eu-doped apatites are nearly the same as those found in the Llallagua apatite. In most CL spectra of natural apatites, the broad blue peaks which occur at wavelengths about 400-420 nm have been tentatively assigned as Eu^{2+} activation (Mariano and Ring, 1975; Roeder et al., 1987). However, these peak positions are simply not the same as the Eu^{2+} peak position found in the synthetic Eu-doped

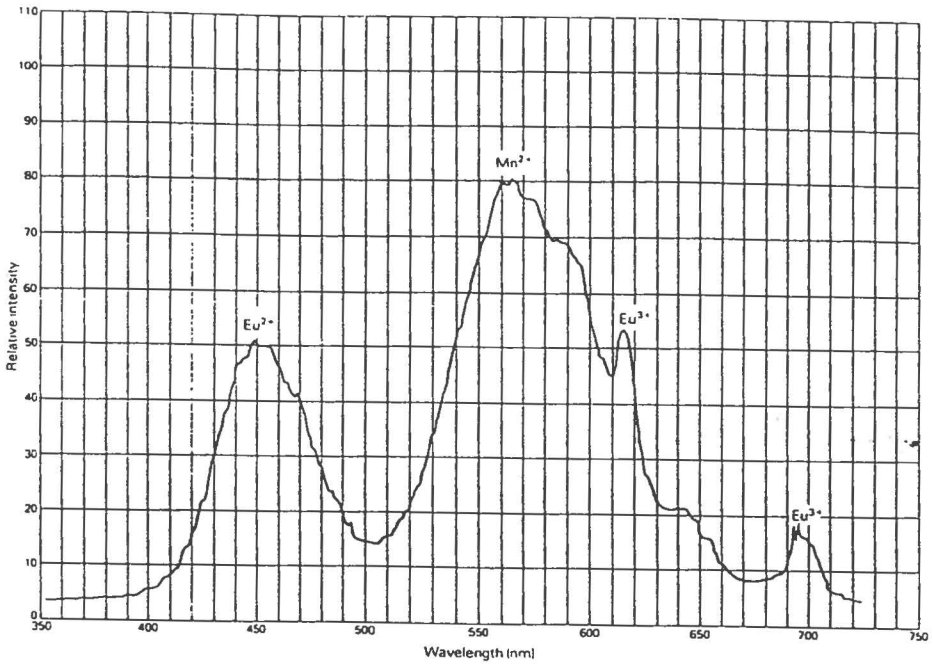

Fig. 8-6a. CL spectrum of Eu^{2+}, Eu^{3+} and Mn^{2+}-activated apatite from Llallagua, Bolivia. The apatite exhibits blue luminescence with some yellow luminescent areas. The Eu^{2+} emits a broad band centered at 450 nm and the Eu^{3+} emits a number narrow bands superposing on the broad Mn^{2+} band.

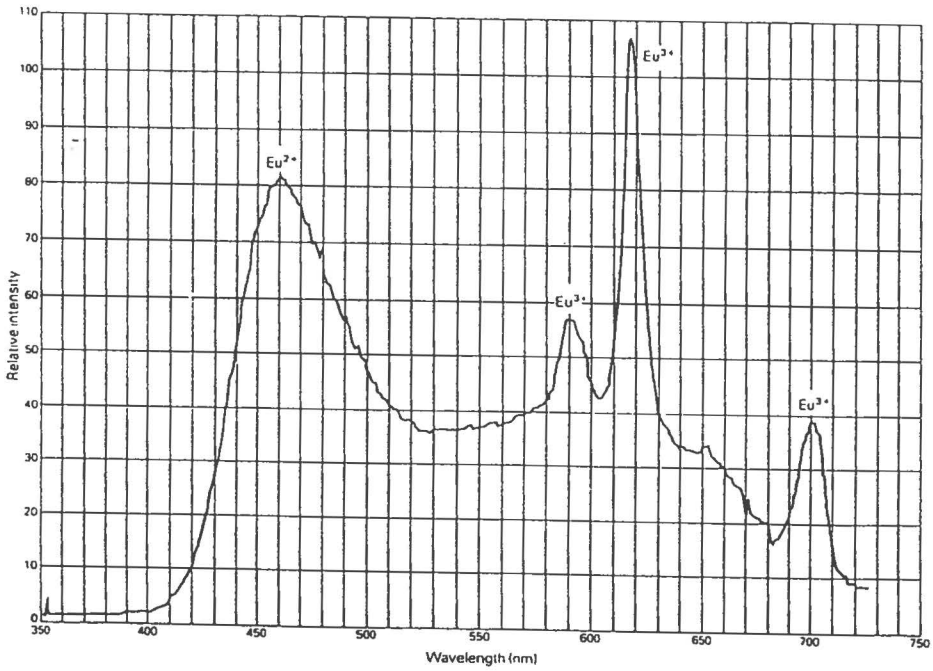

Fig. 8-6b. CL spectrum of synthetic apatite ($Ca_{4.95}Eu_{0.05}(PO_4)_3F_{0.95}Cl_{0.05}$). The synthetic apatite exhibits violet luminescence and shows the characteristic emission from both Eu^{2+} and Eu^{3+}. CL conditions: 6 kV, 0.6 mA (from Mariano, 1988).

apatites. Although the emission peak in the 400-420 nm range has been assigned to Eu^{2+} activation by these authors, they also noted that peaks in this region may be produced by several different luminescence centers, such as strontium substitution in carbonatite apatites (Mariano and Ring, 1975); some other unknown activator such as Ce^{3+} and crystal defect centers in apatite (Roeder et al., 1987); and a structural defect produced by anomalous amounts of total REE substituting for Ca^{2+} in the structure of carbonatite apatite (Mariano, 1988).

Morozov et al. (1970) reported that the synthetic Eu^{3+}-activated fluorapatite crystals emit a quite intense red-orange luminescence. Eu^{3+} activator ions produce five groups of luminescence lines in the regions of about 572-582, 598-599, 625-635, 655 and 700 nm corresponding to transitions of $^7D_0 \rightarrow {}^5F_{0,1,2,3,4}$ (Fig. 8-4). Morozov et al. (1970) also noted that the line spectrum of the Eu^{3+} ion was observed on a continuous background emission in most of Eu^{3+}-activated fluorapatite crystals. The continuous background emission is produced by the host material (fluorapatite crystal) itself. Luminescence of the Eu^{3+} ion is strongly polarized and some of the luminescence lines are practically completely polarized. Morozov et al. (1970) suggested that Eu^{3+} activator ions in the fluorapatite crystals probably occupy two sites Ca_I and Ca_{II}. In the region of the transitions between the two non-degenerate terms $^5D_0$ and $^7F_0$, the luminescence spectrum from a phase parallel to the c-axis shows two weak lines at 577 and 579 nm, whereas the luminescence spectrum from a phase perpendicular the c-axis shows at least three lines at

572, 577 and 583 nm with different elementary emitter (572 nm - circular electric oscillator, 577 nm - circular magnetic, 582 nm - linear magnetic oscillator). This obviously suggests a difference in the multiplicity of the activator ions. The line at 572 nm was observed at all temperatures down to helium temperature. Thus it was interpreted as a pure electron transition from $^5D_0$ to $^7F_0$ in the basic type of activator. Since this line has a high luminescence intensity, the activator center may occur in a low local symmetry crystalline field (Ca_{II} site) because the Ca_{II} site has a higher density than the Ca_I site at a section parallel to the basal plane. Also the polarization of the transition $^5D_0 \rightarrow {}^7F_0$ indicates that the presence of luminescence centers in the basal plane are different from those in the prismatic plane. The centers in the basal plane may be formed by a replacement of low-symmetry calcium sites (Ca_{II}) with Eu^{3+} activator ions. Morozov et al. (1970) assumed that a number of relatively weak lines observed in several groups of luminescence lines ($^5D_0$-$^7F_{0,1,2}$) belong to activator centers with a higher local symmetry (Ca_I site), for which the prohibition of electrical dipole transitions is more strictly fulfilled.

8.8. Pr^{3+} activation

Morozov et al. (1970) reported that the luminescence spectra (PL) of synthetic Pr-doped fluorapatite consists of three groups of lines in the blue (about 450-500 nm), red (about 600-710 nm) and infrared (about 850-910 nm) regions (Fig. 8-4). The group of lines in the blue region correspond to the transitions Pr^{3+} ion between

energy levels of $^3P_0$ and $^3H_4$, whereas the group of lines in the red region correspond to the transitions between $^1D_2$ and ^3H_J, and the group of lines in infrared region correspond to the transitions between $^1D_2$ and $^3F_{3,4}$. Since Pr^{3+} ion has an even number of electrons in its configuration, transitions in uniaxial fluorapatite crystals are strongly polarized.

8.9. Ce^{3+} activation

Absorption and luminescence (PL) spectra of synthetic Ce^{3+}-activated fluorapatite crystals were reported by Morozov et al. (1970). The absorption spectrum consists of two broad excitation bands at 240 and 310 nm (Fig 8-4). These two excitation bands correspond to the transitions from ground state of configuration $^4f_1$ ($^2F_{5/2}$) to states of configuration $^5d_1$ and is split by a crystal field. A similar splitting is observed in the Ce-doped CaF_2 crystals (Morozov et al., 1970). However, the luminescence spectrum shows only a broad emission peak in the blue region with variable peak positions between 395 and 420 nm. In comparison, the emission peak positions of Ce-doped CaF_2 crystals are shifted to a longer wavelength. In Ce-doped fluorapatite crystals, two emission bands which correspond to transitions from the excited state to two levels of the ground multiplets $^2F_{5/2}$ and $^2F_{7/2}$ are absent. The shift in peak positions and the absence of two emission bands in the luminescence spectra cannot be explained by Morozov et al. (1970).

8.10. Ho^{3+} and Er^{3+} activations

Ho^{3+}-activated fluorapatite crystals emit a number of high intensities lines in the infrared region near 2000 nm (Morozov et al., 1970). These lines were assigned to transitions from level $^5I_7$ to ground level $^5I_8$. However, luminescence spectra of Ho^{3+}-activated fluorapatite crystals do not exhibit the green luminescence, seen in most other hosts (e.g., $LaCL_3$, CaF_2), corresponding to a resonant transition from level $^5S_2$ to the ground level $^5I_8$ (Dieke and Crosswhite, 1963; Marfunin, 1979).

Er^{3+} ions in fluorapatite crystals have a similar behaviour to Ho^{3+} ions. Er^{3+} ions emit a number of high intensity lines in the infrared region near 1500 nm, caused by resonance transitions from $^4I_{13/2}$ to $^4I_{15/2}$. The Er^{3+} ions spectra also does not exhibit the green luminescence characteristic of most other hosts (e.g., $LaCL_3$, CaF_2), corresponding to transitions from level $^4S_{3/2}$ to the ground level $^4I_{15/2}$ (Dieke and Crosswhite, 1963; Marfunin, 1979). Morozov et al. (1970) attributed the absence of luminescence lines in the green region and intensify of lines in infrared region that are related to fast non-radiative (multiphonon) transitions (or relaxation) in the high energy levels ($^5S_2$ of Ho^{3+}, $^4S_{3/2}$ of Er^{3+}), and to a localization of the remaining excitation energy on the lowest radiative levels ($^5I_7$ of Ho^{3+}, $^4I_{13/2}$ of Er^{3+}).

8.11. Gd^{3+}, Tm^{3+}, Nd^{3+} and Yb^{3+} activations

Luminescence spectra of gadolinium, thulium, neodymium and ytterbium in synthetic fluorapatite crystals are also reported by

Morozov et al. (1970). In luminescence spectrum (spark phosphoroscope) of Gd-doped fluorapatite crystals, the emissions of the Gd^{3+} activator ion are completely located in the ultraviolet region and consist of five narrow lines between 310 and 315 nm, corresponding to transitions from the lowest excited level $^6P_{7/2}$ to ground state of level $^8S_{7/2}$.

Luminescence spectra of Tm-doped fluorapatite crystals consist of a high intensity group of lines in the blue region (centered at about 460 nm) and two weak groups of lines in the orange-red region (centered at about 580 and 670 nm) (Fig. 8-4). The spectrum is characteristic of Tm^{3+} ions and reflects superposition of transitions between two pairs of levels: $^1D_2 \rightarrow {}^3H_4$ and $^1G_4 \rightarrow {}^3H_6$. Luminescence spectra of the Tm-doped fluorapatite crystals are strongly polarized. In industrial phosphor studies (Ozawa, 1991), Y2O3:Tm (0.001 mole) crystals also emit a blue luminescence and the CL spectrum consists of a group of lines around 453 nm assigned to the transition $^1D_2 \rightarrow {}^3F_4$.

Luminescence spectra of trivalent neodymium and ytterbium in fluorapatite crystals are entirely in the infrared regions. The luminescence spectra of Nd^{3+} ions consist of four groups of lines at 900, 1060, 1300 and 1800 nm corresponding to transitions from level $^4F_{3/2}$ to ground multiplet ^4I_J. The luminescence spectra of Yb^{3+} ions consist of two groups of lines in 960 and 1040 nm regions corresponding to transitions from $^3F_{5/2}$ to ground level $^2F_{7/2}$.

8.12. Sr^{2+} activation

Hayward and Jones (1991) reported that the apatite phenocrysts commonly contain 0.4-1.2 wt% SrO in carbonatite from Qasiarsuk, South Greenland. The apatite phenocrysts are usually mantled with blue luminescent oscillatory zoned cores and violet luminescent rims. Some of the cores show a dark blue luminescent zone adjacent to the violet rims. Strontium usually decreases from the centre of the blue luminescent core to its margin and is usually slightly lower in the dark blue luminescent zones compared with the cores. The Sr contents have a wide variation in the violet luminescent rims, they are either higher or lower than the cores. However, no luminescence spectra of the apatite were presented.

In a wolgiditic lamproite (Australia), Sr-bearing apatite crystals usually are mantled, and have light purple luminescent cores and purple-yellow to dull purple luminescent oscillatory zoned rims. CL spectra of these apatite crystals usually consist of a broad peak at about 420 nm with the highest intensity and a number of narrow peaks at about 470, 570, 590, 640 and 800 nm with relatively low intensities (Fig. 8-7). The apatite usually contains about 2-4 wt% SrO, but the REE concentrations in the apatites are usually under the detection limits of the SEM/EDS. Thus the broad peak at 420 nm is probably due to Sr activation.

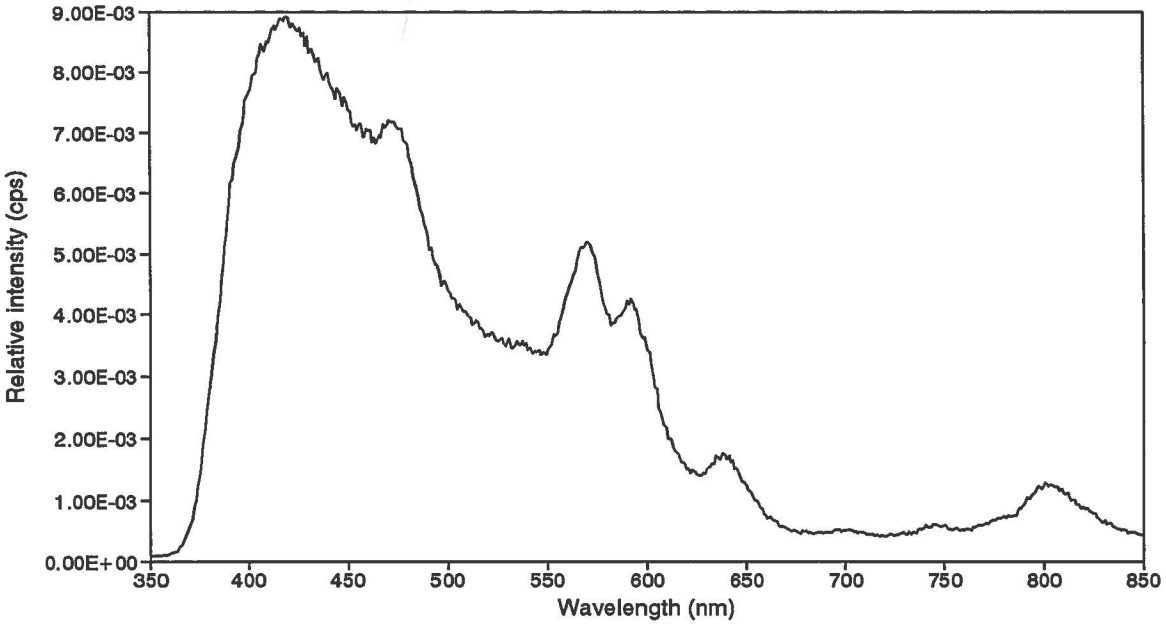

Fig. 8-7. CL spectrum of Sr-bearing apatite in wolgiditic lamproite. The emission peak at about 420 nm is probably due to Sr activation.

CHAPTER 9

THE LUMINESCENCE SPECTRA OF THE REE-ACTIVATED APATITES

9.1. Introduction

Apatite crystals are particularly suitable as hosts for rare-earth elements (REE). Previous investigations of apatite CL are by Mariano (1978) and Roeder et al. (1987). To understand the energy level structures of rare earth ions in the apatite crystal field, and to interpret the CL spectra of natural occurring apatites, eleven REE (La, Ce, Pr, Nd, Sm, Eu, Gd, Dy, Er, Yb, and Lu) -doped apatites were investigated by CL. The synthetic REE-apatites containing Ce, Pr, Sm, Eu, Dy, Er emit characteristic luminescence lines or peaks under electron beam irradiation. The other (La, Nd, Gd, Yb, and Lu) synthetic apatites have no luminescence in the visible or near infrared region.

The synthetic REE-apatites were grown by Dr. M. Fleet at the University of Western Ontario and were analyzed by Dr. R.H. Mitchell by using electron microprobe. Compositions of these synthetic REE-apatites are given in Table 9-1. The luminescence spectra have no energy correction. All were acquired using the same electron beam current and voltage (0.8 Am and 8 kV). The luminescence properties of individual rare earth doped apatites are discussed in the following sections.

9.2. Sm-apatite

Under electron beam irradiation, the apatite:Sm (1,900 ppm)

Table 9-1. The compositions (wt%) of REEs doped apatites.

Sample No.	AP19	AP23,36	AP37	AP24	AP38	AP21	AP22	AP25	AP26	AP2
REE	La	Ce	Pr	Nd	Sm	Eu	Gd	Er	Yb	Lu
CL Colour	Non	Light Blu	Brick Red	Non	Orange red	Light Blu	Non	Light Blu	Non	Non
Analyses	3	7	1	2	1	3	4	2	3	1
CaO	54.57	54.84	53.90	54.60	54.16	54.43	54.20	54.38	54.50	54.53
P2O5	41.47	42.02	41.39	41.62	41.69	41.27	42.39	42.09	43.02	42.21
Na2O	0.11	0.15	0.12	0.13	0.10	0.11	0.12	0.14	0.12	0.05
RE2O3	0.18	0.27	n.d.	0.23	0.19	0.14	0.14	n.d.	0.03	n.d.
SiO2	0.10	0.12	0.15	0.13	0.08	0.10	0.12	0.11	0.10	0.09
F	3.33	3.23	4.09	2.96	4.02	2.99	3.34	3.18	3.02	3.03
Total	99.76	100.63	99.65	99.67	100.24	99.03	100.31	99.88	100.79	99.91
O-F	1.40	1.36	1.72	1.25	1.69	1.26	1.41	1.34	1.27	1.28
Total	98.36	99.27	97.93	98.42	98.55	97.78	98.90	98.54	99.51	98.63
	NUMBERS OF IONS THE BASIS OF 26 (O, F)									
P	6.009	6.032	5.984	6.036	5.999	6.026	6.079	6.066	6.127	6.081
Ca	10.007	9.963	9.863	10.021	9.863	10.057	9.837	9.920	9.823	9.943
Na	0.037	0.050	0.040	0.043	0.033	0.037	0.039	0.045	0.039	0.016
Si	0.017	0.020	0.026	0.022	0.014	0.017	0.020	0.018	0.017	0.015
RE	0.011	0.017		0.014	0.011	0.008	0.008		0.001	
F	1.802	1.732	2.209	1.604	2.161	1.629	1.789	1.712	1.607	1.631
P site	6.026	6.052	6.010	6.058	6.012	6.043	6.099	6.084	6.144	6.097
Ca site	10.055	10.030	9.903	10.078	9.907	10.102	9.884	9.964	9.863	9.959

1. The concentration could be lower than 300 ppm for those zero amounts of HREE in the apatites.

2. P site = P + Si; Ca site = Ca + Na + RE.

synthetic samples show orange red luminescence colour. The luminescence spectrum of the apatite:Sm (Fig. 9-1a) consists of four groups bands in the wavelength regions near 558, 594, 639 and 701 nm using size 5 mm entrance and exit slits for the spectrophotometer.

When the entrance and exit slits are changed to a smaller size (0.25 mm), and all optical lenses are removed, each luminescence band in the spectrum can be resolved into a number of narrower lines (Fig. 9-1b, -1c).

The luminescence band at 558 nm (using 5 mm slits) consists of three low intensity peaks which are at wavelengths of about 564, 566, and 571 nm. The most intense band of apatite:Sm peaking at 594 nm (using 5 mm slits) can be separated into three lines which are located at 599, 607, and 617 nm. The band at 639 nm can be separated into two individual lines : 645 and 655 nm. The weak band near the infrared region, 701 nm (using 5 mm slits), consists of two very weak peaks at 706 and 712 nm.

The first three groups of luminescence lines for Sm in the crystal field of apatite are generally in agreement with the Sm^{3+}-activation in oxidized REE-phosphors reported by Ozawa (1990). Who simply assigned that electronic transitions of the Sm^{3+} are from a lower emitting level $^4G_{5/2}$ to $^6H_{5/2}$, $^6H_{7/2}$, $^6H_{9/2}$. However, the Sm^{3+} in the apatite crystal field has a unique, higher intensity line at the wavelength 599 nm than in the REE-phosphors, and the latter commonly have higher intensities in the wavelength 608 nm.

Sm^{3+} has five $4f$ electrons configuration and has 73 multiplets

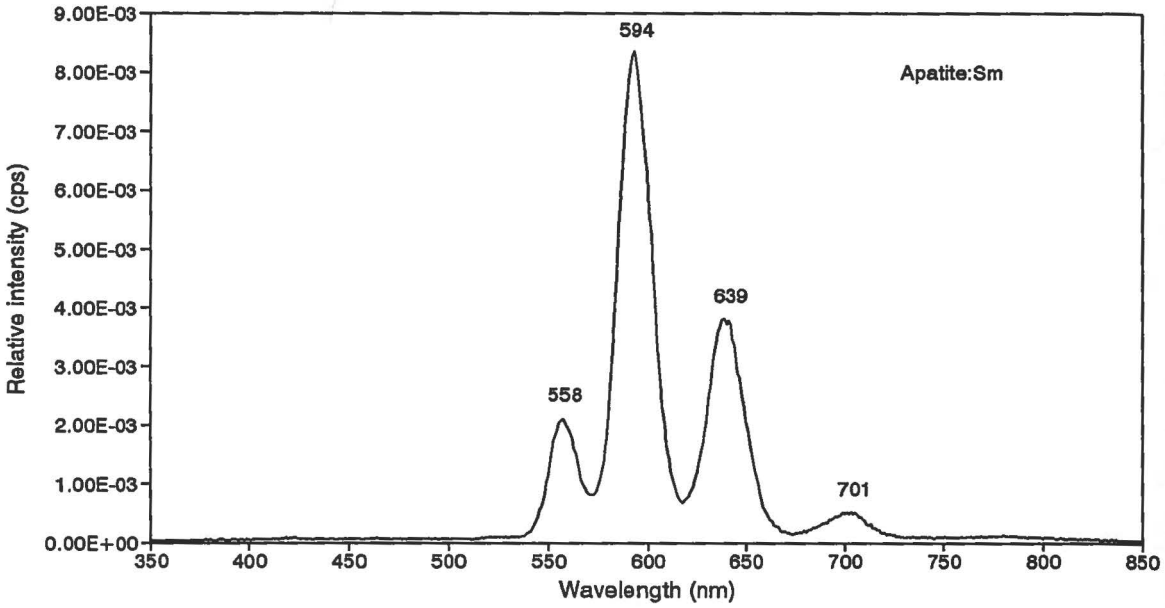

Fig. 9-1a. CL spectrum of a Sm-doped apatite obtained by using 5 mm entrance and exit slits. CL conditions: 8 keV, 0.8 Am, magnification 10×10.

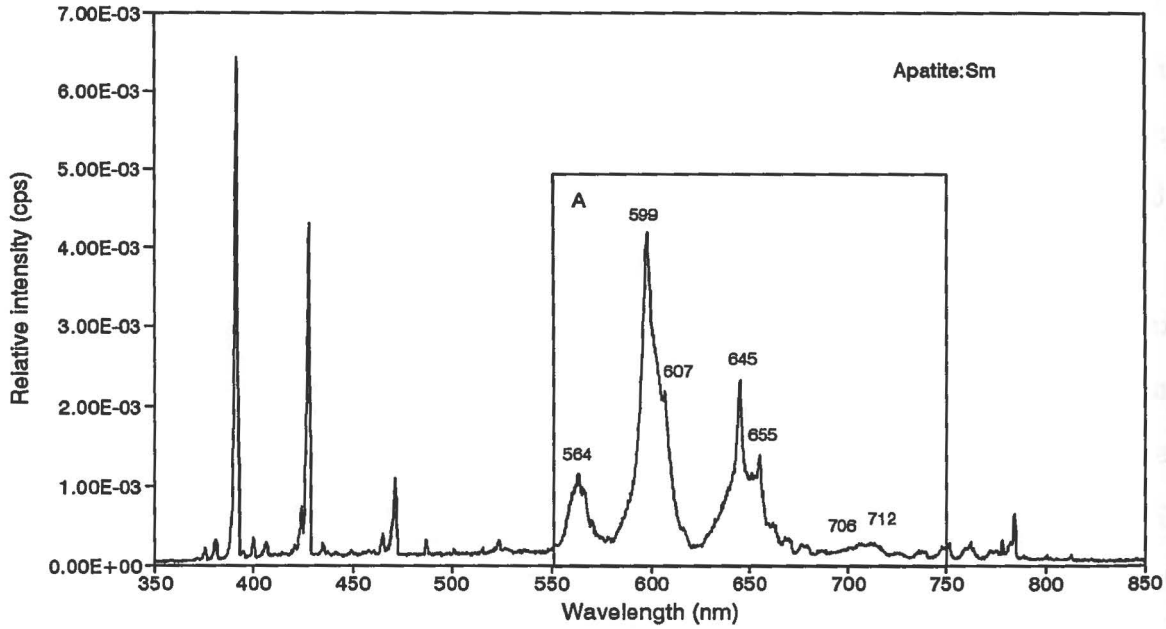

Fig. 9-1b. CL spectrum of a Sm-doped apatite obtained by using 0.25 mm entrance and exit slits. CL conditions: 8 keV, 0.8 Am. The emission lines which are the Cathode-ray tube output occur in region between 375 and 525 nm, and about 780 nm (see section 1.3.4.).

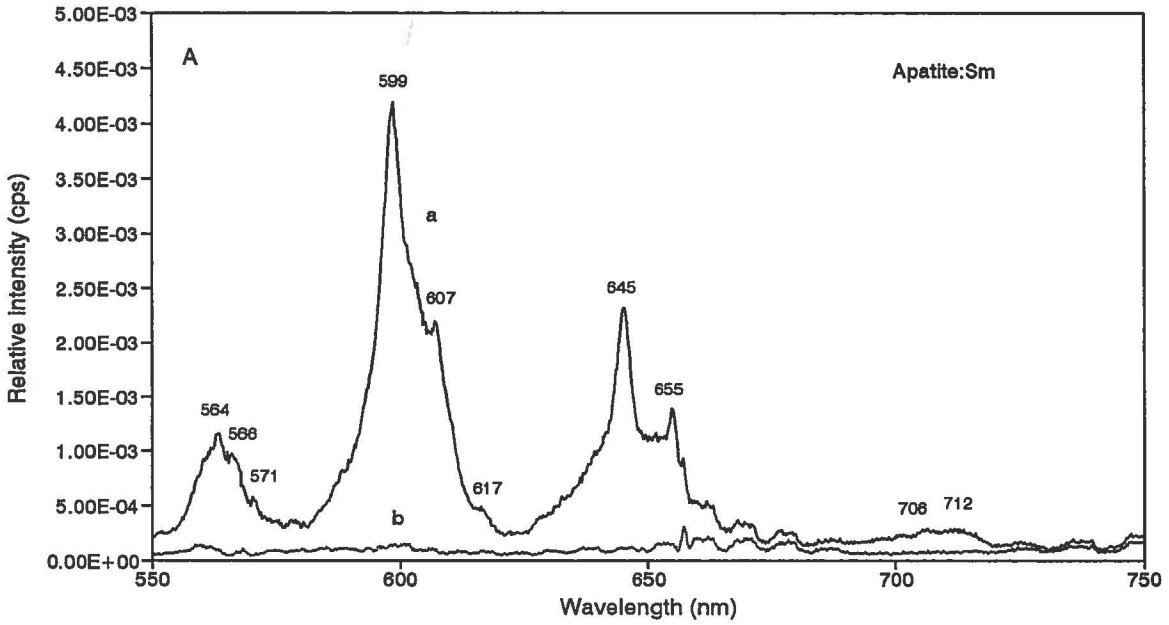

Fig. 9-1c. Spectrum (a) is the Sm-doped apatite CL spectrum. Spectrum (b) is a background spectrum of the Cathode-ray tube output. The spectra are obtained between 550 and 750 nm by using 0.25 mm entrance and exit slits. CL conditions: 8 keV, 0.8 Am.

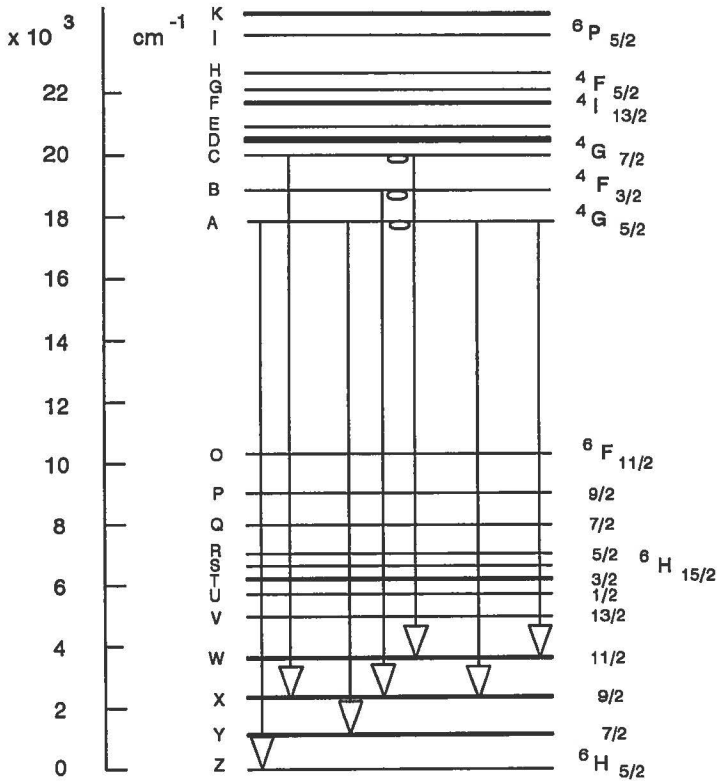

Fig. 9-1d. Sm^{3+} ion transitions in the apatite crystal field. The energy levels of Sm^{3+} are observed in $LaCl_3$ crystal and the pendant half-circles indicate fluorescing levels (after Wybourne, 1962; Magno and Dieke, 1962).

which produce 198 energy levels through spin-orbit interaction (Axe and Dieke, 1962; Wybourne, 1962). In this $4f^5$ configuration, the ^6H multiplet is the lowest energy level which consists of six states and the $^6H_{5/2}$ is the ground of this level. The detailed measurement of the absorption and fluorescence spectra of that trivalent samarium in hexagonal $LaCl_3$ (D_6 symmetry) crystal have been made by Magno and Dieke (1962). Those measurements have given a considerable amount of information on the energy levels below 30,000 cm^{-1} (up 330 nm) of the $4f^5$ configuration. To compare with these energy levels of Sm^{3+} in the $LaCl_3$ crystal (see table II in Magno and Dieke, 1962), the energy levels of Sm^{3+} in the apatite can be identified as belong the ^6H multiplets and the energy level scheme show in Fig. 9-1d. The first group of Sm:apatite luminescence lines which are located at 564 and 566 nm can be assigned as electronic transitions from $^4G_{5/2}$ to ground state $^6H_{5/2}$, and from $^4G_{7/2}$ to $^6H_{9/2}$ respectively. The second group of luminescence lines which are located at 599, 607 and 617 nm can be assigned as the electronic transitions from $^4G_{5/2}$, $^4H_{5/2}$ and $^4G_{7/2}$ states to $^6H_{7/2}$, $^6H_{9/2}$ and $^6H_{11/2}$ respectively. The third and fourth group lines (645, 706 and 712 nm) can be assigned as the electronic transitions from $^4G_{5/2}$ to $^6H_{9/2}$ and $^6H_{11/2}$ respectively. There are two luminescence lines at 571 and 655 nm which have not been found in the Sm^{3+} crystal field of the $LaCl_3$. Thus these energy levels cannot be interpreted.

The observed energy levels of Sm^{3+} in the apatite crystal field are also nearly the same as the 12 spin-orbit states of Sm^{3+} in LaF_3

(see table I in Rast et al. 1967). Table 9-2 shows that wavelength positions of the luminescence lines for Sm^{3+} in the apatite are comparable with the fluorescence spectrum of Sm^{3+} in LaF_3. The Sm^{3+}

Table 9-2. Comparison between CL spectrum of Sm3+ in apatite and fluorescence spectrum of Sm3+ in LaF3.

Apatite	LaF3				
CL (nm)	Air (A)	Vacuum (cm)	Intensity	Terminal	Level
	5598.7	17856.3	s	0	
	5614.0	17808.0	m	48	6H5/2
564	5635.0	17741.0	w	115	
566					
571 (?)					
	5931.0	16855.9	s	1000	
	5946.4	16812.2	m	1044	6H7/2
599	5996.8	16670.9	m	1185	
607	6031.0	16576.0	m	1280	
617					
	6389.4	15646.6	s	2210	
	6403.7	15611.7	m	2245	
654	6444.1	15513.8	w	2343	6H9/2
	6472.0	15446.9	w	2409	
	6499.0	15383.0	w	2473	
655 (?)					
	6972.0	14339.0	m	3517	
	6996.5	14289.0	m	3567	
	7036.0	14209.0	m	3647	6H11/2
	7047.0	14186.0	m	3670	
706	7075.0	14130.0	m	3726	
712	7108.0	14065.0	m	3791	
	7761.0	12881.0	w	4975	
	7804.0	12810.0	w	5046	6H13/2
	7848.0	12739.0	w	5117	
	7872.0	12700.0	w	5156	

The data of fluorescence spectrum of Sm3+ in LaF3 are selected from Rast et al. (1967).

in LaF_3 is either a bimolecular hexagonal cell having a space-group symmetry of $P6_3/mmc$ (D_{6h}^4) with the lanthanum ions having D_{3h} site symmetry, or it belongs to the trigonal system with a probable space-group symmetry of P3c1 (D_{3d}^4) and a unit cell containing six molecules. The lanthanum ions being in C_2 sites (Rast et al. 1967). These symmetries are very similar as the apatite which has a space-group symmetry is $P6_3/m$. Thus the structure of energy level (f^5) configurations are nearly same in the both crystals.

9.3. Dy-apatite

Apatite:Dy (about 1000 ppm) has a light cream-yellow luminescence colour. The luminescence spectrum of apatite:Dy consists of four bands which occur at the wavelengths 475, 570, 657 and 746 nm when 5 mm slits are employed (Fig. 9-2a).

When the slits are changed to 0.25 mm, the band at 475 nm (using 5 mm slits) is resolved into four Dy luminescing peaks which are located at wavelength 457, 476, 481 and 484 nm, and with other two cathode-ray tube output peaks which are located at 465 and 471 nm (Fig. 9-2b, -2c).

The peaks at the wavelength 570 nm (using 5 mm slits) are poorly resolved by using 0.25 mm slits. There are three Dy luminescing peaks which occur at wavelengths 575, 578 and 595 nm. The left shoulder of that the high intensity peak centred at 575 nm, probably, masks some luminescence peaks in the region between 570 and 573 nm. The peak at 560 nm is the cathode-ray tube output peak (Fig. 9-2b, -2d).

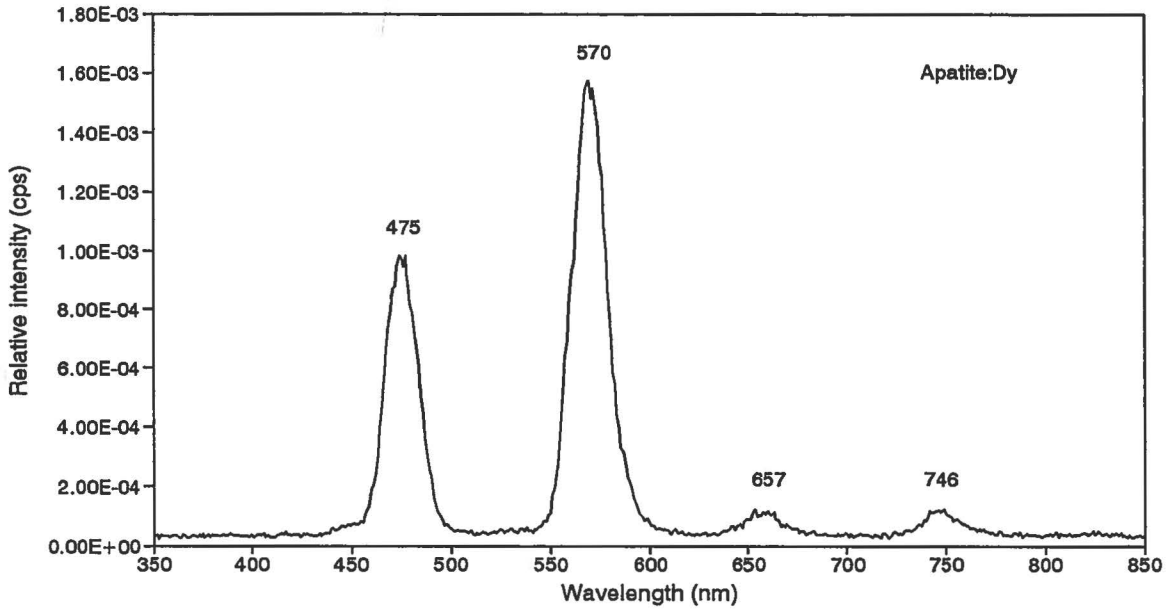

Fig. 9-2a. CL spectrum of a Dy-doped apatite obtained by using 5 mm entrance and exit slits. CL conditions: 8 keV, 0.8 Am, magnification 10×10.

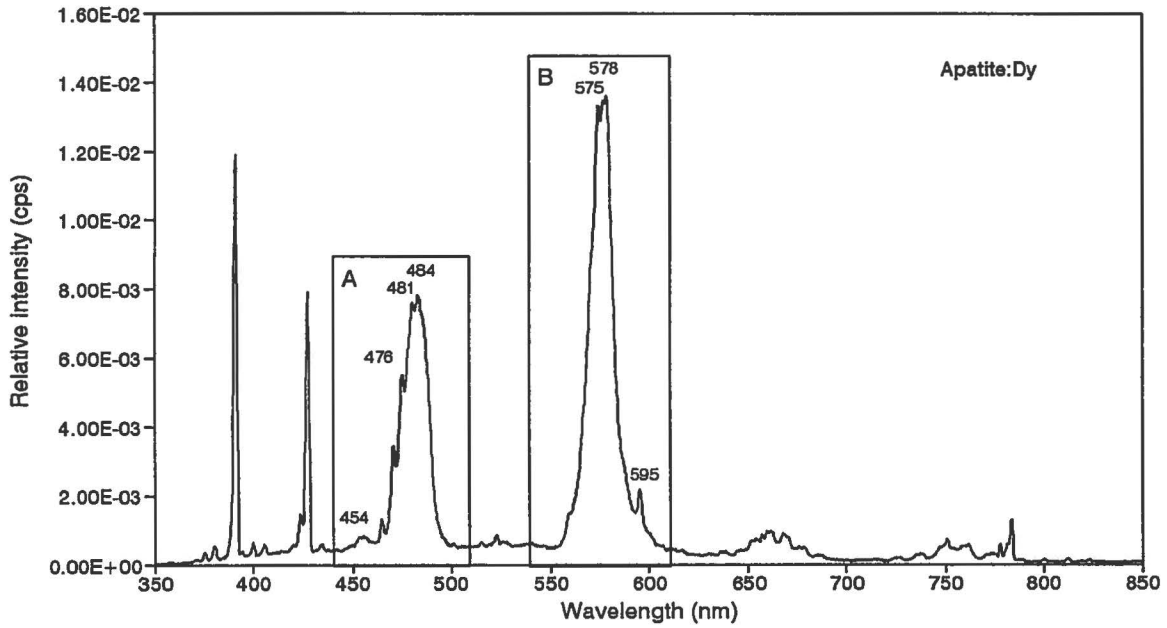

Fig. 9-2b. CL spectrum of a Dy-doped apatite obtained by using 0.25 mm entrance and exit slits. CL conditions: 8 keV, 0.8 Am. The narrow emission lines which are the Cathode-ray tube output occur in a region between 375 and 450 nm, and at about 780 nm (see section 1.3.4.).

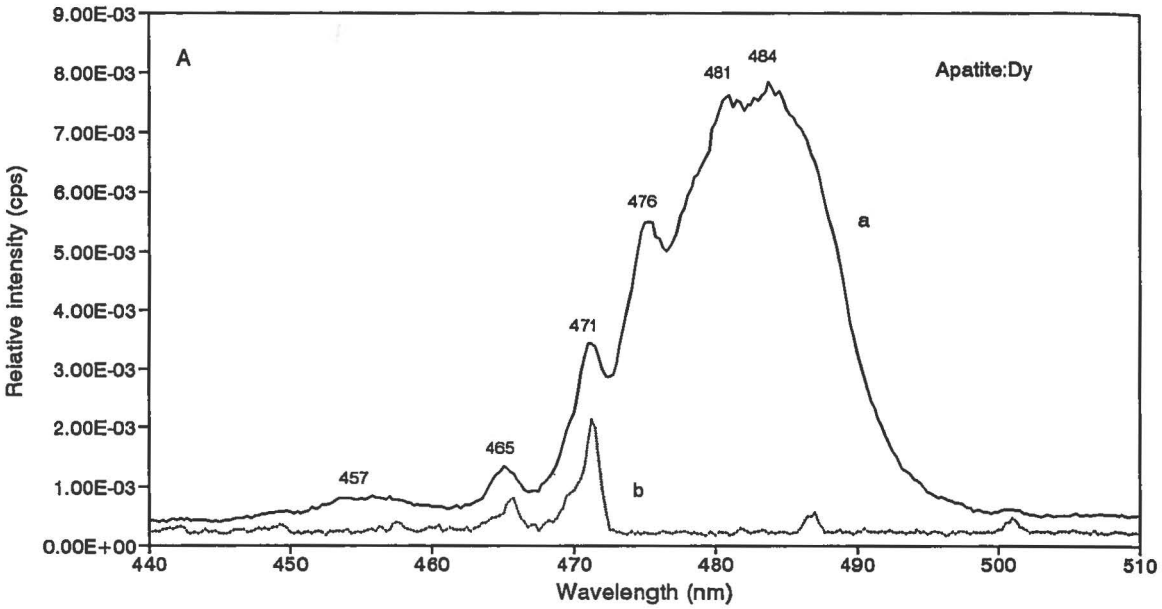

Fig. 9-2c. Spectrum (a) is a Dy-doped apatite CL spectrum. Spectrum (b) is the background spectrum of the Cathode-ray tube output. The spectra are obtained between 440 and 510 nm by using 0.25 mm entrance and exit slits. CL conditions: 8 keV, 0.8 Am.

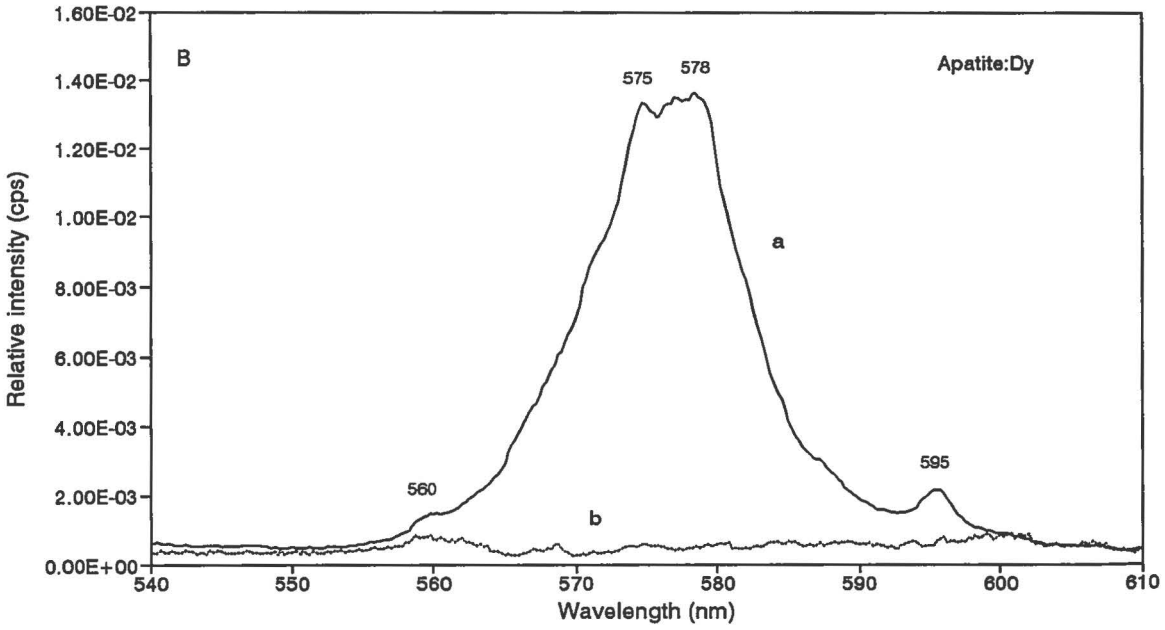

Fig. 9-2d. Spectrum (a) is a Dy-doped apatite CL spectrum. Spectrum (b) is the background spectrum of the Cathode-ray tube output. The spectra are obtained between 540 and 610 nm by using 0.25 mm entrance and exit slits. CL conditions: 8 keV, 0.8 Am.

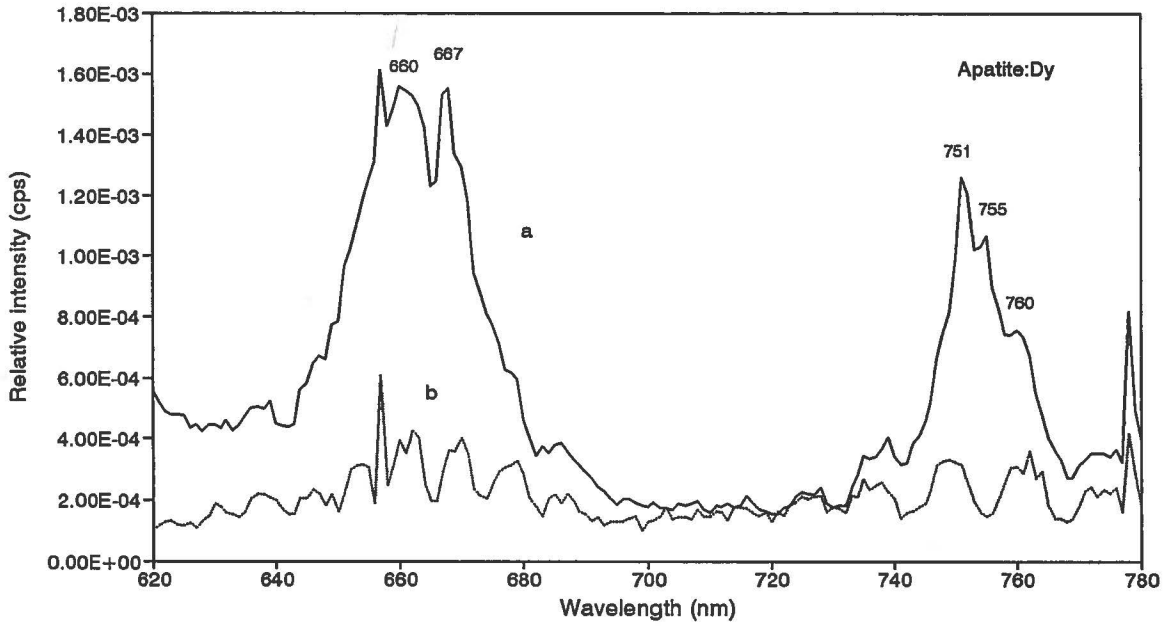

Fig. 9-2e. Spectrum (a) is a Dy-doped apatite CL spectrum. Spectrum (b) is a background spectrum of the Cathode-ray tube output. The spectra are obtained between 620 and 780 nm by using 0.25 mm entrance and exit slits. CL conditions: 8 keV, 0.8 Am.

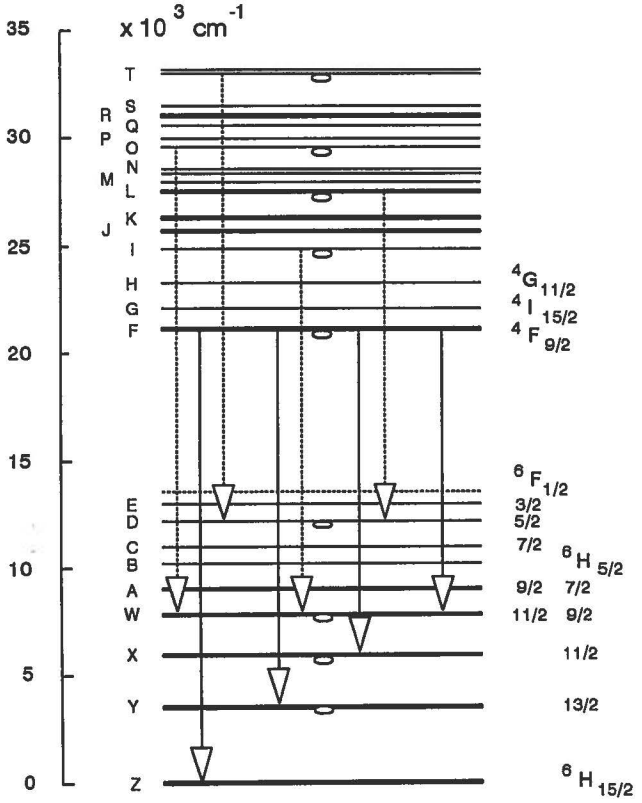

Fig. 9-2f. Dy^{3+} ion transitions in the apatite crystal field. The energy levels of Dy^{3+} are observed in $LaCl_3$ crystal and the pendant half-circles indicate fluorescing levels (after Crosswhite and Dieke, 1961; Wybourne, 1962; Crosswhite and Moos, 1967).

In the red to infrared regions, the area for the two low intensity bands in the 657 and 746 nm (using 5 mm slits), most of the apatite:Dy luminescence peaks overlap with the cathode-ray tube output peaks. However, some of the Dy luminescence peaks can be identified by contrast with the relatively intensities of the cathode-ray background peaks. Figure 9-2e shows that the peaks located at 660, 667, 751, 755 and 760 nm, obviously, are enhanced by Dy luminescence.

These Dy luminescence peaks in the apatite are characteristic luminescence peaks of Dy^{3+} in the crystal field. They can be compared with the optical fluorescence or luminescence lines of Dy^{3+} in many of the dysprosium-doped phosphors, such as in $LaCl_3$ (Crosswhite and Dieke, 1961), LaF_3 (Fry, 1968), $CaWO_4$ (Wortman and Sanders, 1971) and REE-oxides (Ozawa, 1990).

The Dy^{3+} ion belongs to the configuration of $4f^9$ and it has 198 energy levels producing by this $4f$ configuration. According to Hund's rules the ^6H multiplet is the lowest energy level in that configuration, and it is split by spin-orbit interaction into an inverted multiplet which consists of six states. The $^6H_{15/2}$ level is the ground state of this energy level. A detailed investigation of Dy^{3+} energy levels in $LaCl_3$ crystal had been made by Crosswhite and Dieke (1961). They obtained about 200 fluorescence lines of Dy^{3+} from the ultraviolet to the infrared region, and identified most of the electronic levels and electronic energy levels splitting in the crystal field. The fluorescence spectrum from 450 to 1100 nm in the LaF_3 has been observed by Fry et al. (1968), and the energy levels

Table 9-3. Comparison between CL spectrum of Dy3+ in apatite and fluorescence spectrum of Dy3+ in LaF3.

Apatite CL (nm)	LaF3 Air (A)	Vacuum (cm)	Intensity	Observed Stark levels (cm)	Energy level
(457)					
	4747.4	21058.3	2	0	
	4750.9	21042.8	10	17	
476	4762.7	20990.6	7	69	
	4775.2	20935.2	8	124	6H15/2
	4788.9	20875.8	6	184	
	4794.6	20851.0	7	208	
481	4817.3	20752.7	7	307	
(484)					
	5694.1	17557.2	10	3502	
	5700.5	17537.5	2	3522	
	5718.2	17483.2	10	3576	
	5732.0	17441.1	3	3618	6H13/2
	5735.8	17429.5	6	3630	
575	5740.7	17414.6	9	3645	
	5757.4	17364.1	3	3695	
(578)					
	6587.0	15177.2	4	5882	
600	6598.8	15150.1	10	5909	
	6605.7	15134.3	3	5925	6H11/2
	6614.2	15114.8	1	5945	
	6628.5	15082.2	1	5977	
	6649.1	15035.5	2	6024	
(667)					
	7446.2	13426.0	2	7633	
	7464.0	13394.0	4	7665	
	7498.6	13332.2	2	7727	
751	7516.2	13300.9	10	7758	
	7541.6	13256.1	4	7803	6H9/2,
	7547.4	13245.9	3	7813	6F11/2
	7563.6	13217.6	2	7842	
	7589.8	13172.0	1	7887	
	7615.9	13126.8	1	7933	
	7666.4	13040.3	1	8019	
	7699.6	12984.1	1	8075	

The data of fluorescence spectrum of Dy3+ in LaF3 are selected from Fry et al. (1968).

for Dy^{3+} have been calculated including the interactions of all the

multiplets of the $4f^9$ configuration. To compare with these Dy^{3+} fluorescence lines, the energy levels of Dy^{3+} in the apatite crystal field can be identified and show in the Figure 9-2f and Table 9-3. The luminescence peaks at 476 and 481 nm can be assigned as electronic transition from $^4F_{9/2}$ to the ground state $^6H_{15/2}$, and the peaks at 575, 660 and 751 nm can be assigned as electronic transitions from $^4F_{9/2}$ (or$^6F_{11/2}$) to $^6H_{13/2}$, $^6H_{11/2}$ and $^6H_{13/2}$ respectively.

These peaks (457, 484, 578 and 667nm) are wide and diffuse, they are the emission from higher Stark components of the electronic levels I, T, O and L (Fig. 9-2f). These energy levels have high stability which are indicated by a relatively large gap between themselves and the next lower level (Crosswite and Dieke, 1961).

9.4. Eu-apatite

Synthetic apatite:Eu commonly shows a very bright, light blue luminescence colour under electron beam irradiation. Some of the apatite:Eu grains show light violet-blue luminescence colour. After prolonged electron beam irradiation, those light violet-blue luminescing apatite:Eu gradually loose their violet colour, and change to light blue colour.

Luminescence spectra of apatite:Eu (using 5 nm slits) consist of three narrow luminescence bands with wavelengths of 587, 612 and 694 nm, and a very broad peak centred at 450 nm (Fig. 9-3a). The intensity of the broad peak at 450 nm is inversely proportional to the length of time of the electron beam irradiation.

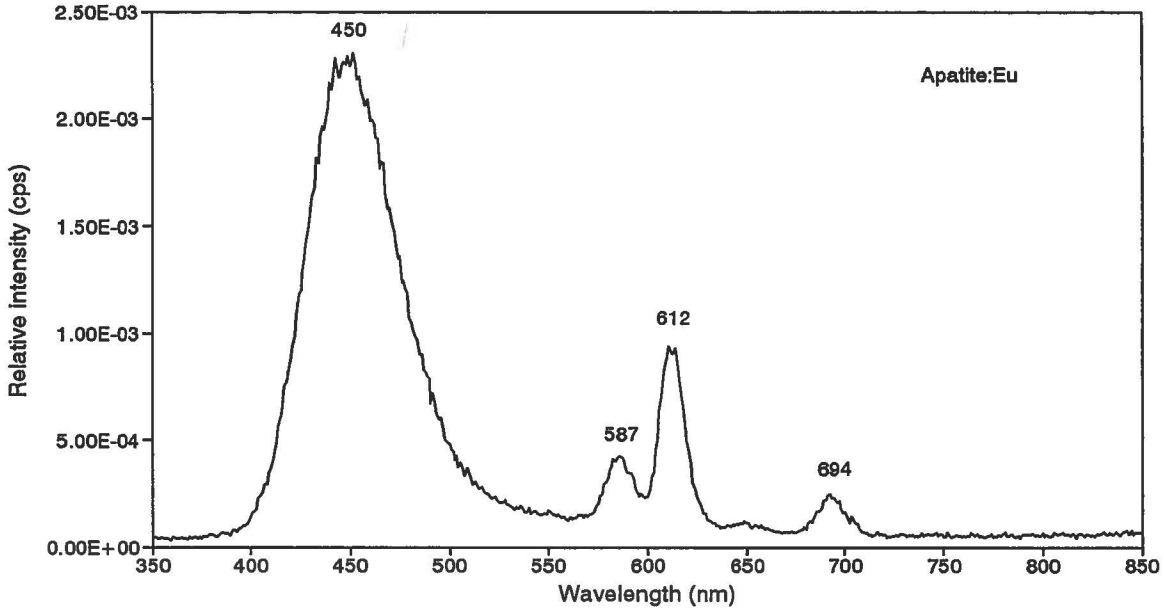

Fig. 9-3a. CL spectrum of a Eu-doped apatite obtained by using 5 mm entrance and exit slits. CL conditions: 8 keV, 0.8 Am, magnification 10×10.

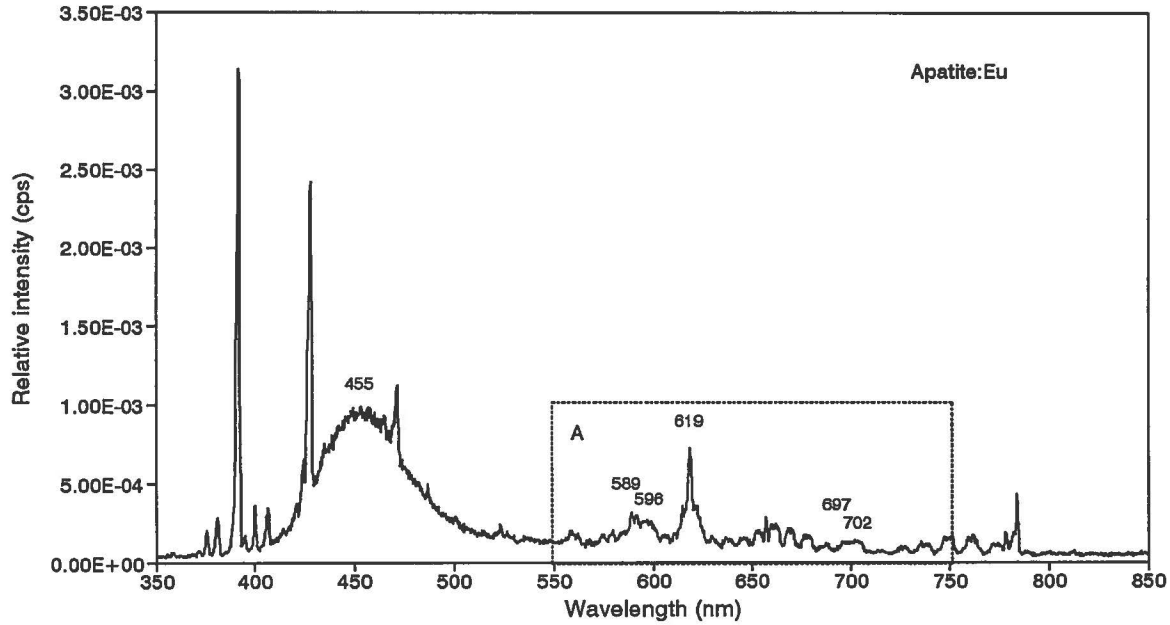

Fig. 9-3b. CL spectrum of a Eu-doped apatite obtained by using 0.25 mm entrance and exit slits. CL conditions: 8 keV, 0.8 Am. The narrow emission lines which are the Cathode-ray tube output occur in a region between 375 and 525 nm, and at about 780 nm (see section 1.3.4.).

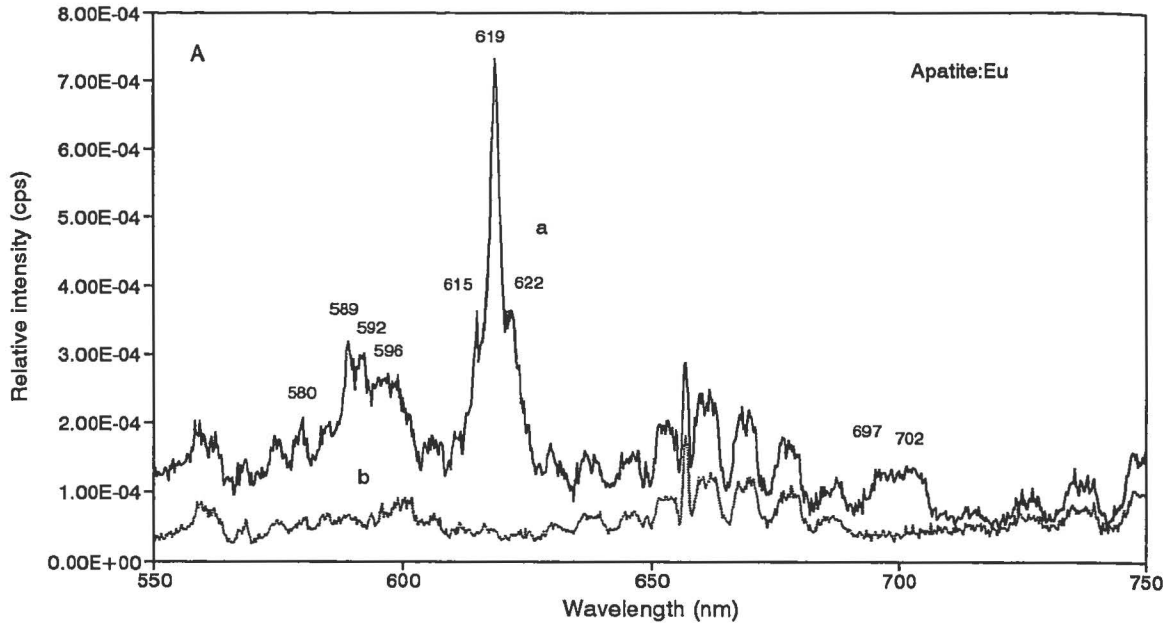

Fig. 9-3c. Spectrum (a) is a Eu-doped apatite CL spectrum. Spectrum (b) is a background spectrum of the Cathode-ray tube output. The spectra are obtained between 550 and 750 nm by using 0.25 mm entrance and exit slits. CL conditions: 8 keV, 0.8 Am.

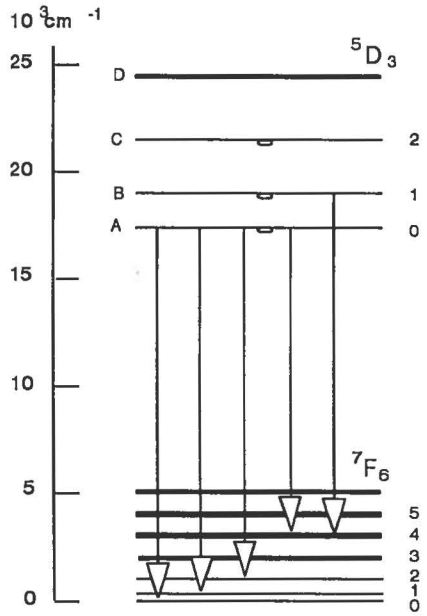

Fig. 9-3d. Eu^{3+} ion transitions in the apatite crystal field. The part of 4*f* shell energy levels of the Eu^{3+} are observed in $LaCl_3$ crystal and the pendant half-circle indicate the fluorescing levels (Dieke et al. 1963; Nieuwpoort et al. 1967).

When the 0.25 mm slits are employed, the most intense single band at 612 nm (using 5 mm slits) can be resolved into three individual lines located at 615, 619 and 622 nm, and the band at 587 nm (using 5 mm slits) can be resolved into three individual small lines which occur at 589, 592 and 596 nm (Fig. 9-3b, -3c). The band at 694 nm (using 5 mm slits) consists of two weak peaks with centres at 697 and 702 nm. However, many small and weak lines are overlapped by the cathode-ray tube output lines which can not be resolved at this time.

These luminescence lines of apatite:Eu are in generally agreement with the Eu^{3+} emission lines in many europium-doped oxides and salts, such as in $LaCl_3$ (DeShazer and Dieke, 1963), EuF_3 (Caspers and Rast, 1967), YVO_4 (Brecher et al., 1967), REE oxide phosphors (Ropp, 1964; Ozawa, 1990) and other materials (Van Uitert and Johnson, 1964). The Eu^{3+} ion belongs to the $4f^6$ configuration and has 119 multiplets which yield 295 energy states through spin-orbit interaction. In this configuration, the Eu^{3+} has three lowest excited states ^5D_j (j=0,1,2) and the ground multiplet ^7F_j (j=0,1,2,$\cdots$,6) has seven spin-orbit states.

Compared with the observed energy levels in $LaCl_3$ and in EuF_3, the luminescence lines of Eu^{3+} in apatite can be identified as shown in Figure 9-3d. The weak line at 580 nm can be assigned to transition from the lowest excited state $^5D_0$ to the ground state $^7F_0$. The luminescence lines from 589 nm to 596 nm can be assigned to transition $^5D_0 \rightarrow {}^7F_1$. The luminescence lines from 615 nm to 619 nm are generally assigned to transition $^5D_0 \rightarrow {}^7F_2$, and the peaks at 697

and 702 nm can be assigned to transition $^5D_0 \rightarrow {}^7F_4$. The lines at about 622 nm are assigned to transition $^5D_1 \rightarrow {}^7F_4$ (Brecher et al. 1967).

The $^7F_2$ level (state) consists of four sublevels, three nondegenerate (A_1, B_1, B_2) and one degenerate (E). The B_2 and E levels are an electric dipole, and have been identified by Brecher et al. (1967) as the $^5D_0 \rightarrow {}^7F_2$ emission of Eu^{3+} in YVO_4. This electric dipole shows a polarized component along the c axis at 6155.2 Å and a perpendicular component at 6193.8 Å. The other two sublevels of the $^7F_2$ are optically forbidden. In our experiment, most of the apatite:Eu grains in the thin section are oriented parallel to the c axis, and the spectra are obtained with the emitted light propagated near perpendicular to the c axis. Thus, the spectra reveal most of the nondegenerate transitions which show a higher intensity at the 619 nm line than at the 615 nm line.

The strong continuous luminescence in the wavelength about 450 nm (using 5 mm slits) can not be resolved by using 0.25 mm slits (Fig. 9-3b). Considering that the luminescence intensity of this band exhibits a time decay property, the excitation band is probably related to a perturbed level of the activator (Ropp, 1964), or related to $Eu^{2+} \rightarrow Eu^{3+}$ charge transfer interactions (DeShazer and Dieke, 1963; Ozawa, 1990).

9.5. Pr-apatite

Apatite:Pr shows brick red luminescence colour under electron beam irradiation. The luminescence spectrum of the apatite:Pr is

shown in Figure 9-4a (using 5 mm slits). There is a weak peak which is located in the lower wavelength region at about 485 nm. The most intense luminescence bands of the apatite:Pr are located at 592 and 615 nm, and the latter probably masks small peaks in the wavelength about 637 nm. When the 0.25 mm slits are employed, the intense band at 592 nm is shifted to 599 nm. The rest of bands are very weak and overlap with the Cathode-ray tube output lines. Separation of these lines in the luminescence spectra is extremely difficult at this time.

These apatite:Pr luminescence spectra are generally in agreement with those that have been found previously from Pr^{3+} in $LaCl_3$ (Sayer et al., 1955; Sayer and Freed, 1955; Dieke and Sarup, 1958; Sarup and Crozier, 1965) and in LaF_3 (Gravely, 1970). Pr^{3+} in the apatite crystal field is mainly involves the transitions from two lowest levels ^3H and ^3F to upper levels $^3P_{0,1}$ and $^1D_2$ in the $4f^2$ configuration (Fig. 9-4b). The transitions from the lowest lying ground level $^3H_4$ to upper energy levels of $^3P_0$, $^3P_1$ are indicated by the weak luminescence peak at about 487 nm, and to another upper energy level of $^1D_2$ is indicated by the intense luminescence line at 599 nm. The very weak peak at about 522 nm can be assigned to the transition from the lower level $^3H_5$ to the upper level $^3P_1$, and the peaks at 615 and 637 nm can be assigned to the transitions from the lower levels $^3H_6$ and $^3F_2$ to the upper level $^3P_0$ respectively.

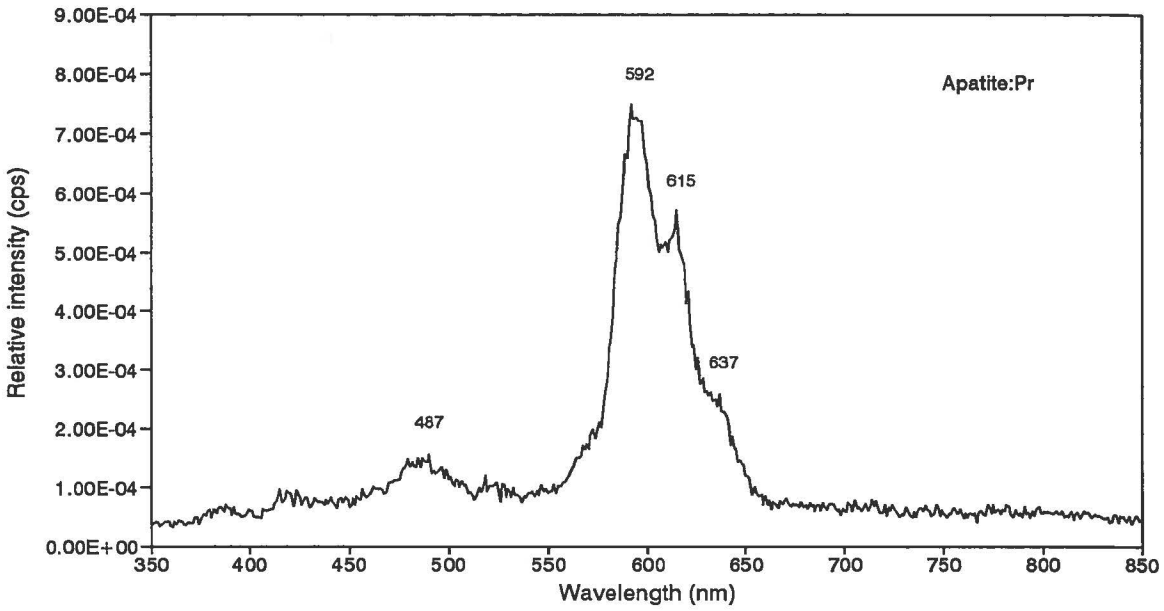

Fig. 9-4a. Spectrum (a) is a Pr-doped apatite CL spectrum. The spectra are obtained by using 5 mm entrance and exit slits. CL conditions: 8 keV, 0.8

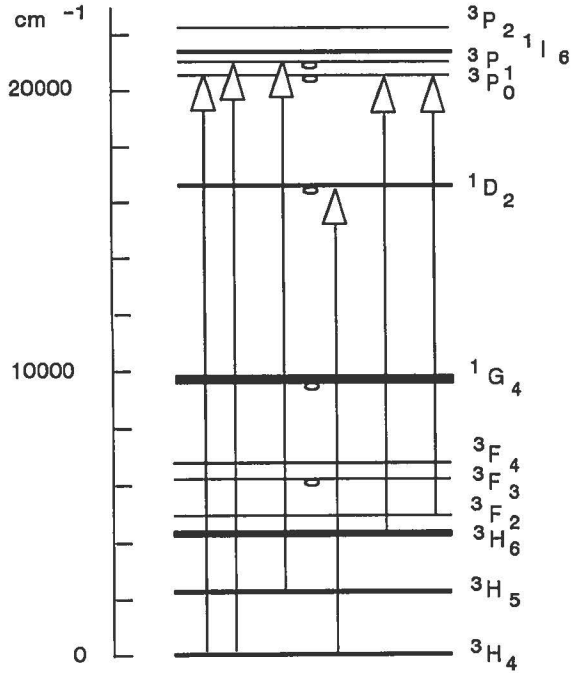

Fig 9-4b. Pr^{3+} ion transitions from lower states ^3H and ^3F to upper states $^3P_{0,1}$ and $^1D_2$ in the apatite crystal field. The Pr^{3+} ion energy levels are observed in $PrCl_3$, and fluorescence is observed from the levels marked with a half-circle (Sayer et al., 1955; Dieke et al., 1958, 1963).

9.6. Ce-apatite

Apatite:Ce reveals light blue luminescence colour. The CL spectrum consists of a continuous luminescence peak centred at 440 nm and with two weak peaks at 593 and 637 nm in the visible region (Fig. 9-5). The energy level difference between that two peaks is about 0.14 eV (1200 cm^{-1}).

The fluorescence of Ce^{3+}-actived compounds have been reported by many authors in earlier years (Freed, 1931; Lang, 1936; Weber and Bierig, 1964; Blass and Bril, 1967; Laud et al., 1971). However, no complete crystal field analysis has been attempted. The Ce^{3+} ion usually emit a broad band and with two peaks in the long-wavelength near ultraviolet region. Since the $4f^1$ configuration of the Ce^{3+} ion has a doublet ground state ($^2F_{5/2}$ and $^2F_{7/2}$) and with a separation of about 0.28 eV (2 200 cm^{-1}) in the different crystals, such as chloride, ethylsulfate and CaF_2.

However, a smaller separation of 0.18 eV between energy levels $^2F_{5/2}$ and $^2F_{7/2}$ in the SrS phosphors was reported by Keller (1958) who shown that the Ce^{3+} emitted two peaks. One is located at 494 nm (2.51 eV) and another is located at 532 nm (2.33 eV), which are assigned as the electronic transitions from the both excited state ($^2D_{3/2}$, $^2D_{5/2}$) to $^2F_{5/2}$ and $^2F_{7/2}$. Keller (1958) suggested that the difference of the separation of the ground state may be due to the change in spin orbit interactions in the crystal field.

Blasse and Bril (1967) investigated a number of compounds of the Ce^{3+}-activated phosphors. They found that the positions of the Ce^{3+} of the emission peaks are dependent upon host lattices. Usually,

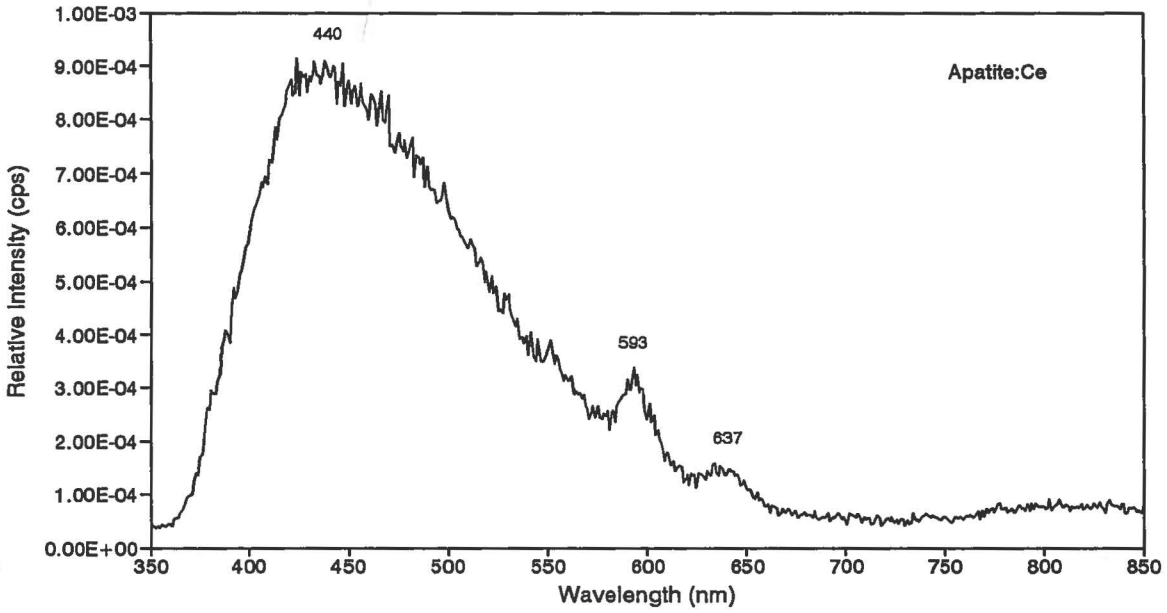

Fig. 9-5. CL spectrum of a Ce-doped apatite obtained by using 5 mm entrance and exit slits. CL conditions: 8 keV, 0.8 Am, magnification 10×10.

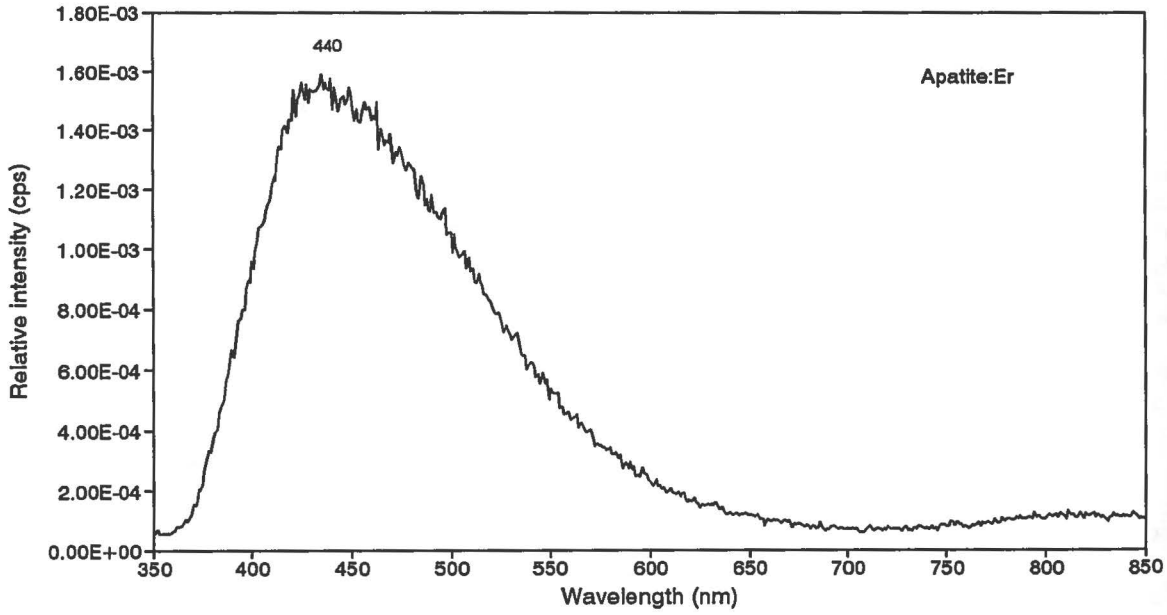

Fig. 9-6. CL spectrum of a Er-doped apatite obtained by using 5 mm entrance and exit slits. CL conditions: 8 keV, 0.8 Am, magnification 10×10.

the fluorescence emission peaks are in the near ultraviolet region for most oxide host lattices. However, if the lowest 5*d* level crystal field splitting and the lower symmetrical splitting are large, the Ce^{3+} emission can be expected in the visible region.

9.7. Er-apatite

Apatite:Er shows light blue luminescence colour. The spectrum of apatite:Er only shows a very broad peak centred at about 440 nm (Fig. 9-6) which is from continuous background excitation (Varsanyi and Dieke, 1962). The luminescence lines of Er^{3+} may not be observed without using suitable filters because the Er^{3+} lines are not sufficiently separated from this continuous background below 500 nm region.

However the excitation states of Er^{3+} also depend on the host crystals. In calcium tungstate ($CaWO_4$), e.g., groups of Er^{3+} fluorescence lines are near 410, 543 and 654 nm (Van Uitert and Soden, 1960; Van Uitert and Johnson, 1966), but in the $ErCl_3$ (Hexagonal), a number of strong groups of emission lines are prominently near 557, 640 and 844 nm (Dieke and Singh, 1961; Varsanyi and Dieke, 1962). Thus apatite:Er may not produce a particular luminescence line of Er^{3+} in visible region.

CHAPTER 10

CATHODOLUMINESCENCE PROPERTIES AND COMPOSITIONS OF THE APATITES IN COLDWELL ALKALINE COMPLEX

10.1. Introduction

Cathodoluminescence spectra of natural apatites from different rock types (e.g., carbonatite, syenite and lamproite) always consist of nine luminescence peaks, which are located at wavelengths about 450, 480, 540, 570, 590, 640, 700, 750 and 800 nm (Fig. 10.1-1). Luminescence spectra of apatites are usually obtained by conventional CL equipment, such as the Luminoscope, and have a poor line resolutions. Thus, the fine structure of the line spectra of REE-activated ions (e.g., Ce^{3+}, Pr^{3+}, Sm^{3+}, Eu^{3+}, Tb^{3+}, Dy^{3+} and Er^{3+}) and other activators (e.g., Mn^{2+} and Sr^{2+}) in apatite hosts cannot be resolved in such low resolution spectra (see Chapter 1 and Chapter 9). In comparison with the CL spectra of synthetic REE-activated apatites (Fig. 10.1-2), every luminescence peaks in the CL spectra of natural apatites can be produced by emission of several REE-activated ions, and the peak cannot be simply identified which a single activator as was suggested by Mariano (1978, 1988, 1989).

For convenience, the nine luminescence peaks of apatite are named as peak 1... peak 9 in order from the blue to the infrared region. Luminescence peak 1 occurs at a wavelength of about 450 nm and is a broad peak due to Eu^{2+} emission, it may overlap with some broad peaks which are produced by Ce^{3+}, Er^{3+} and Sr^{2+} emission at about 420

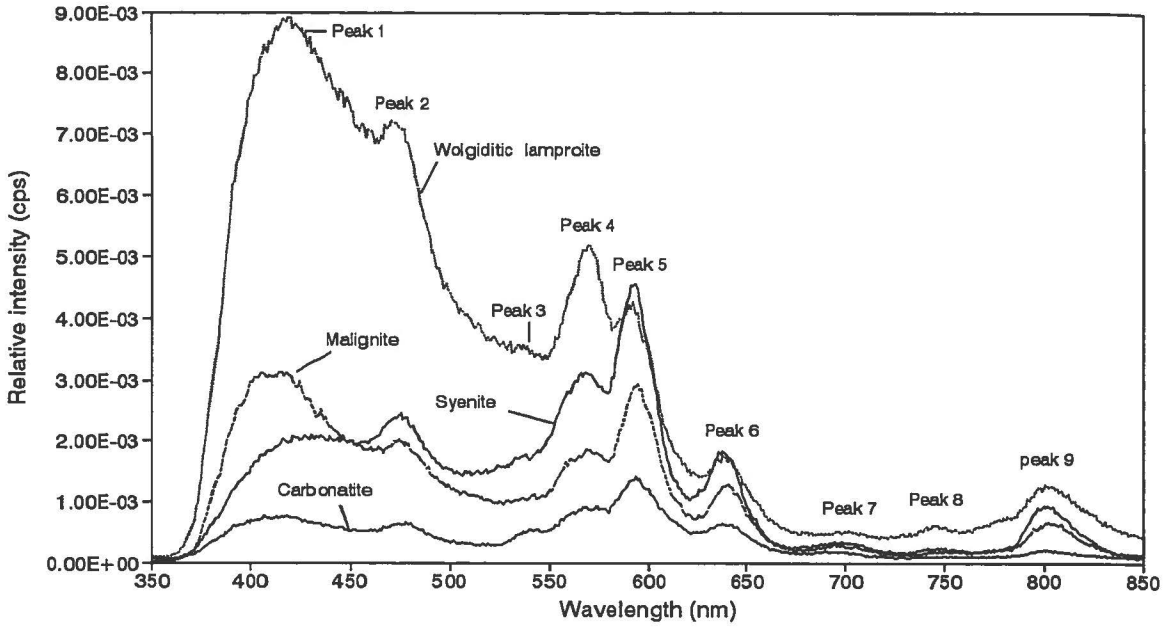

Fig. 10.1-1. CL spectra of apatites from different alkalic rocks. In syenite (Coldwell Complex, Ontario), malignite (Poohbah Lake Complex, Ontario), wolgiditic lamproite (Australia) and carbonatite (Prairie Lake Complex, Ontario), CL spectra of apatites always consist of nine luminescence peaks which are located at wavelengths of about 450, 540, 570, 590, 640 700, 750 and 800 nm. CL conditions: 10 kV, 0.8 mA.

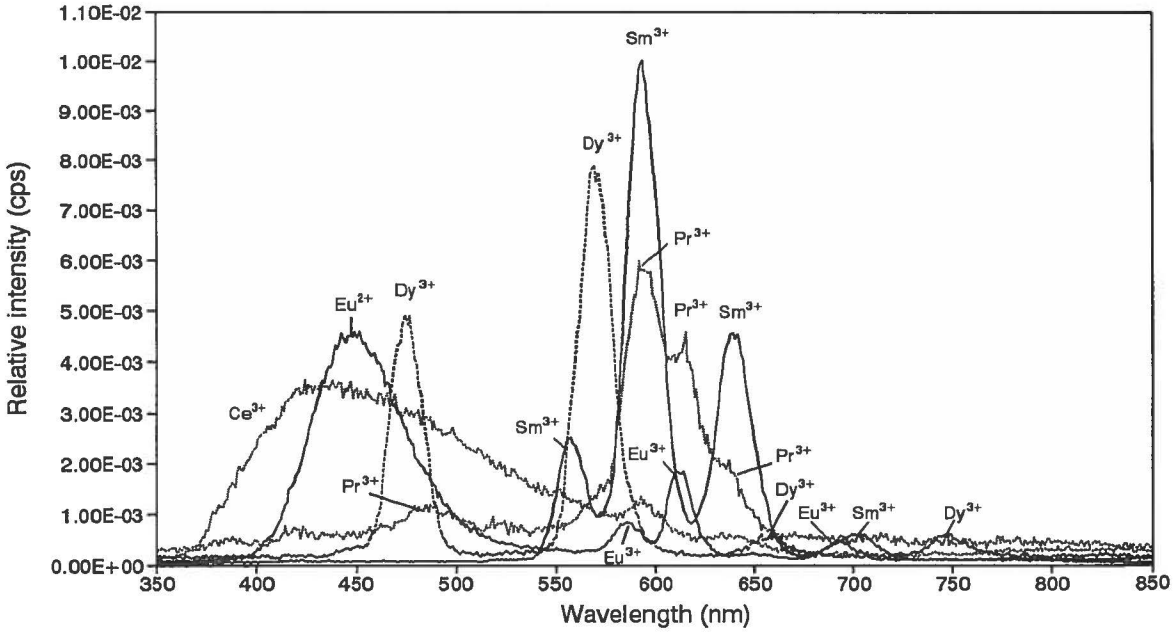

Fig. 10.1-2. CL spectra of REE (Ce, Pr, Eu, Sm and Dy) -doped apatites. CL conditions: 10 kV, 0.8 mA.

nm in the apatite crystal field. Luminescence peak 2 at about 480 nm is dominated by Dy^{3+} emission, but it may overlap with Pr^{3+} and Tb^{3+} emission. Luminescence peak 3 at about 540 nm is due to Tb^{3+} emission, but may overlap with Mn^{2+} emission if the Tb^{3+} peak is superposed on a high intensity background. Luminescence peak 4 at about 570 nm is due to Dy^{3+} emission, but the left shoulder of the peak may mask Sm^{3+} emission at about 558 nm. Luminescence peak 5 at about 590 nm is dominated by Sm^{3+} and Pr^{3+} emission, but may overlap with Ce^{3+} emission. The left shoulder of peak may mask an Eu^{3+} emission at about 587 nm and the right shoulder may mask Eu^{3+} and Pr^{3+} emissions at about 612 nm and 615 nm, respectively. Luminescence peak 6 at about 640 nm is due to Sm^{3+}, Pr^{3+} and Ce^{3+} emission, but the right shoulder of the peak may mask Eu^{3+} and Dy^{3+} emission at about 650 nm and 657 nm, respectively. Luminescence peak 7 at about 700 nm is due to Eu^{3+} and Sm^{3+} emission. Luminescence peak 8 at about 750 nm is due to Dy^{3+} emission. The causes of luminescence peak 9 at about 800 nm are unknown.

10.2. Apatite crystals in Center I

10.2.1. Apatite crystals in the layered ferroaugite syenites

In the layered ferroaugite syenites from Center I, the apatite crystals are usually euhedral, colourless, short prismatic or tabular crystals. In the basal level of the lower series of layered syenite, some apatite crystals have a long prismatic habit. In the lower series of layered syenite, CL reveals that most apatite crystals are zoned with a small, brownish pink luminescent core and

a broad, pink or light pink rim. However, in the basal level of the lower series, most apatite crystals are unzoned and exhibit uniform pink luminescence. In the syenites which are strongly affected by late-stage fluids, pink or brownish pink zoned apatite crystals are mantled by a distinctly yellow luminescent rim. In the upper series of layered syenite, most apatite crystals exhibit brownish pink luminescence. However, apatite crystals may be zoned; with a brownish pink core and a light pink rim; a light pink core and a brownish pink rim; a pink core with a brownish pink intermediate mantle and a light pink rim.

a. Pink luminescent apatite crystals

In the basal level of the lower series syenite (sample C35), apatite crystals exhibit pink luminescence (Fig. 5.1-2b). The CL spectrum (Fig. 10.2-1) shows that the intensities of luminescence peak 4 and peak 5 are higher than peak 1, 2 and 6, which may indicate that the concentrations of Sm^{3+}, Dy^{3+} and Pr^{3+} activators are higher than those of the Eu^{2+}, Ce^{3+} and Er^{3+} activators. SEM/EDS analyses show that the pink apatite contains 0.08-0.32 atoms per formula unit (apfu) of total REE (0.01-0.05 apfu La, 0.04-0.13 apfu Ce, n.d.-0.08 apfu Pr and 0.004-0.07 apfu Nd) with 0.06-0.21 apfu of Si (Appendix 4-1).

b. Apatite crystals mantled with a brownish pink luminescent core and a light pink luminescent rim

In the lower series syenite (samples C40, C47 and C58), most

apatite crystals are mantled with a small, brownish pink luminescent core and a broad, pink or light pink rim (Fig. 5.1-5b, -6b, -10b). CL spectra of these zoned apatite grains are represented in Fig. 10.2-2. The brownish pink core (spectrum A) has a relatively lower intensity than the light pink rim (spectrum B). In the spectrum of the brownish pink core, peak 1 and peak 2 has nearly the same luminescence intensity as peak 4 and peak 5. However, in the spectrum of the light pink luminescent apatite rim, peak 1 and peak 2 has a much lower luminescence intensity than peak 4 and peak 5. By comparing these two spectra at nearly the same intensity level of peak 1 (multiply the spectrum A by 2.6) (Fig. 10.2-2), the spectrum of the light pink luminescent apatite rim has relatively higher intensities of the peak 4, 5 and 6 than the spectrum of the brownish pink luminescent apatite core. This may indicate that the brownish pink luminescent core has a relatively higher ratio of Eu^{2+} (or Ce^{3+}) activator to Sm^{3+} and Pr^{3+} (or Dy^{3+}) activators than the pink rim. In contrast, the light pink luminescent rim has a relatively higher ratio of Sm^{3+} and Pr^{3+} (or Dy^{3+}) activators to Eu^{2+} (or Ce^{3+}) activator than the brownish pink luminescent core.

SEM/EDS analyses show the brownish pink cores contain 0.49-0.57 apfu total REE (0.08-0.12 apfu La, 0.25-0.30 apfu Ce, n.d.-0.05 apfu Pr and 0.12-0.16 apfu Nd) with 0.42-0.52 apfu Si (Appendix 4-1), whereas the light pink luminescent rims contain 0.10-0.24 apfu total REE (n.d.-0.07 apfu La, 0.06-0.17 apfu Ce, n.d.-0.05 apfu Pr and n.d.-0.05 apfu Nd) with 0.08-0.17 apfu Si. The contents of

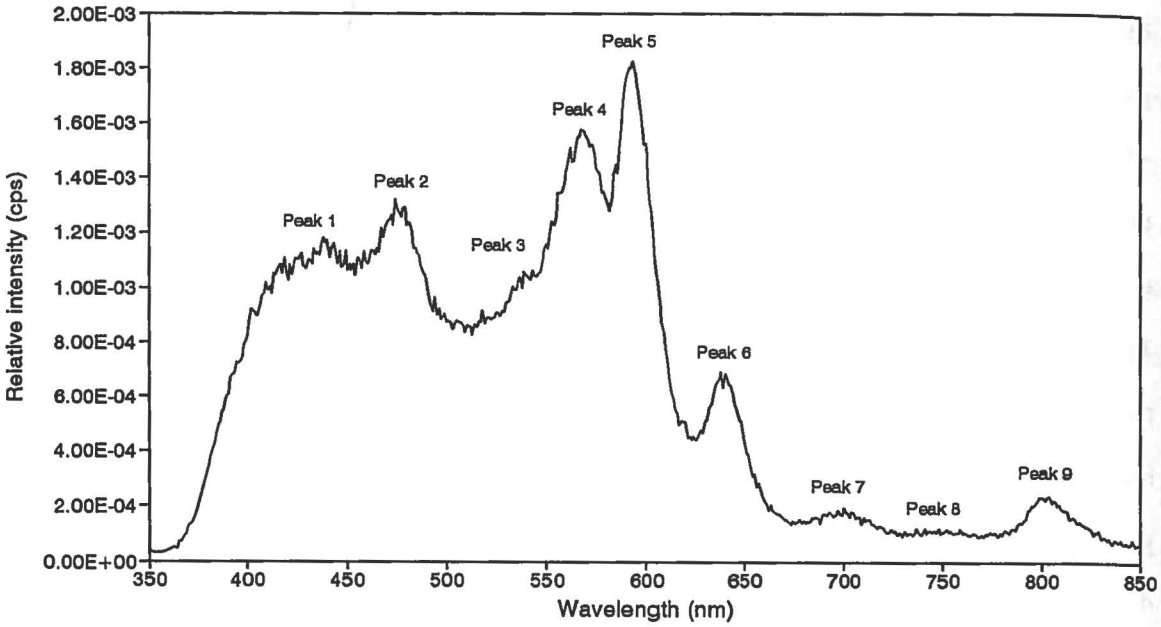

Fig. 10.2-1. CL spectrum of pink luminescent apatite in the layered ferroaugite syenite (C35), Center I. CL conditions: 10 kV, 0.8 mA.

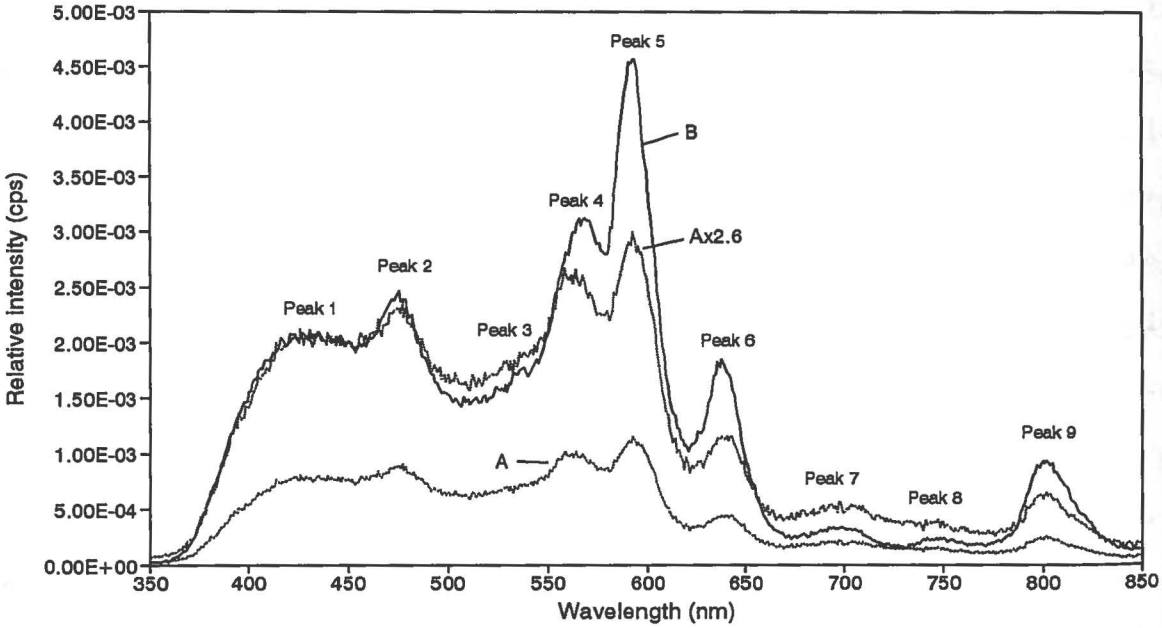

Fig. 10.2-2. CL spectrum of a mantled apatite crystal in the layered ferroaugite syenite (C47), Center I. Spectrum (A) is from the brownish pink luminescent core. Spectrum (B) is from the light pink luminescent rim. CL conditions: 10 kV, 0.8 mA.

total REE (La, Ce, Pr and Nd) and Si in the brownish pink luminescent core are higher than in the light pink luminescent rim.

In the upper series syenite (samples C65, C68 and C72), most apatite crystals exhibit brownish pink luminescence. Some crystals are mantled with a brownish pink core and a light pink rim. The CL spectra from the brownish pink cores and from light pink rims are similar to those of mantled apatite crystals in the lower series syenite. The brownish pink luminescent cores contain 0.25-0.51 apfu of total REE (0.06-0.11 apfu, 0.13-0.24 apfu, n.d.-0.05 apfu and 0.06-0.12 apfu Nd) with 0.21-0.45 apfu of Si, whereas the light pink rims contain 0.08-0.30 apfu total REE (n.d.-0.05 apfu La, 0.05-0.14 apfu Ce, n.d.-0.05 apfu Pr and n.d.-0.07 apfu Nd) (Appendix 4-1). The contents of total REE and Si in the brownish pink core are higher than that in the light pink rim. The results of SEM/EDS analyses are similar to the mantled apatite crystals in the lower series syenite.

b. Apatite crystals mantled with a pink luminescent core, a brownish pink luminescent intermediate mantle and a yellow luminescent rim

In sample C58, some apatite crystals are mantled with a pink luminescent core, a brownish pink intermediate mantle and a yellow rim. However, some of the crystals are zoned with a brownish pink core and a yellow rim, and the brownish pink core crystallized at the same time as the brownish pink mantle of the mantled crystals mentioned above. These apatite crystals usually are subhedral

crystals with an irregular boundary between the brownish pink intermediate mantle and the yellow rim. These apatite crystals are surrounded by alkali feldspar which is almost completely replaced by secondary albite and K-feldspar during late-stage fluid-feldspar interaction.

The CL spectra of the pink luminescent core (spectrum A), the brownish pink intermediate mantle (spectrum B) and the yellow rim (spectrum C) are shown in Fig. 10.2-3a. The luminescent intensity of the pink core is higher than of the brownish pink mantle with a nearly similar spectral profile. By comparing these two spectra at nearly the same intensity level of peak 1 (spectrum B × 1.4) (Fig. 10.2-3b), the brownish pink luminescent apatite mantle has higher intensities for peak 5 and 6 than the pink luminescent core, this may indicate that the pink luminescent core has a relatively higher ratio of Eu^{2+} (or Ce^{3+}) activators to Sm^{3+} and Pr^{3+} activators than the brownish pink mantle. Whereas the brownish mantle has a relatively higher ratio of Sm^{3+} and Pr^{3+} activators to Eu^{2+} (or Ce^{3+}) activators than the pink core. In comparison with the spectra of the pink core and the brownish pink mantle, the spectrum from the yellow rim has relatively higher intensities for peak 2, 4; and peak 3 is well resolved from left shoulder of the peak 4 (Fig. 10-3a, spectrum C). These features of the CL spectrum indicate that the yellow rim probably contains higher concentrations of Dy^{3+} and Tb^{3+} activators than the pink core and the brownish pink mantle.

SEM/EDS analyses show that the pink cores contain 0.12-0.13 apfu total REE (0.02-0.04 apfu La, 0.06-0.07 apfu Ce and 0.03-0.04 apfu

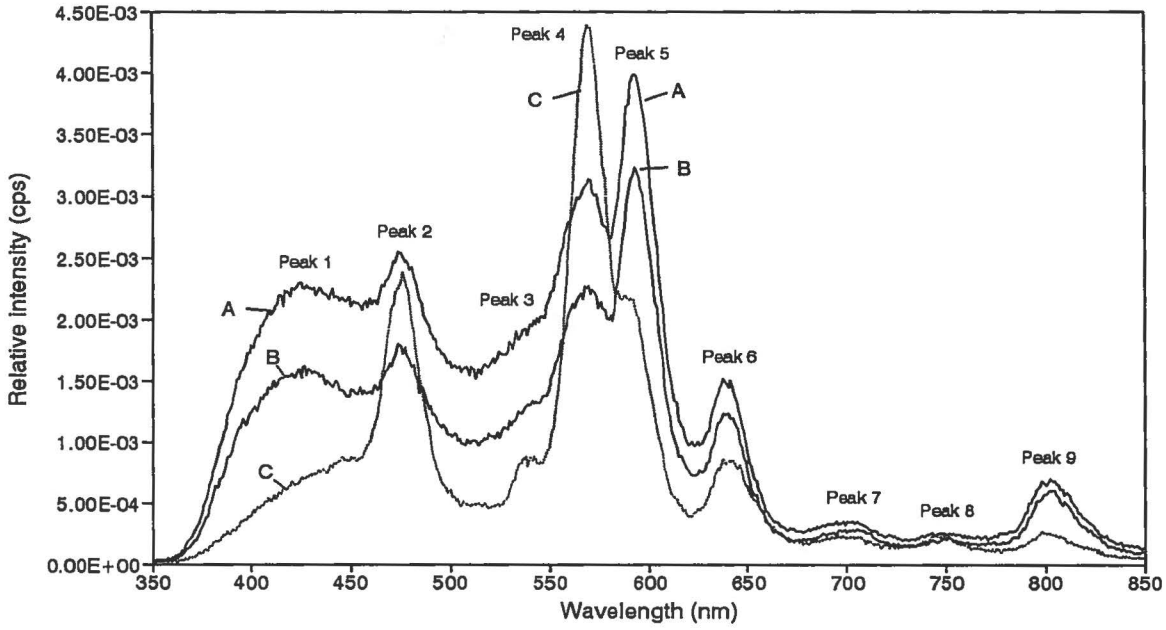

Fig. 10.2-3a. CL spectra of mantled apatite crystal in the layered ferroaugite syenite (C58), Center I. Spectrum (A) is from the pink luminescent core. Spectrum (B) is from the brownish pink luminescent intermediate mantle. Spectrum (C) is from the yellow luminescent rim. CL conditions: 10 kV, 0.8 mA.

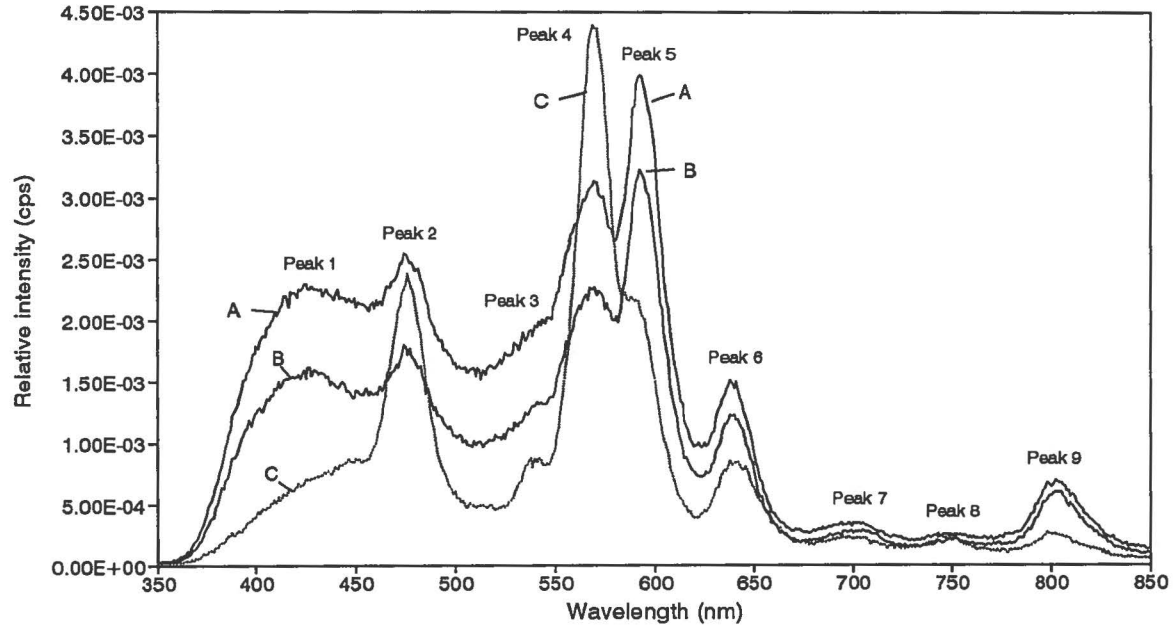

Fig. 10.2-3b. CL spectra of mantled apatite crystal in the layered ferroaugite syenite (C58), Center I. Spectrum (A) is from the pink luminescent core. Spectrum (B×1.4) is the spectrum B from the brownish pink luminescent intermediate mantle and mutiplied by 1.4 factor. Spectrum (C) is from the yellow luminescent rim. CL conditions: 10 kV, 0.8 mA.

Nd) with 0.12-0.13 apfu Si (Appendix 4-1). The brownish pink intermediate mantle contains 0.26-0.85 apfu total REE (0.07-0.18 apfu La, 0.12-0.42 apfu Ce, n.d.-0.08 apfu Pr and 0.06-0.14 apfu Nd) with 0.25-0.62 apfu Si. The yellow rim contains 0.02-0.16 total REE (n.d.-0.03 apfu La, n.d.-0.08 apfu Ce, n.d.-0.03 apfu Pr and n.d.-0.05 apfu Nd) with n.d.-0.27 apfu Si. Generally, the detectable REE (La, Ce and Pr) in the yellow rim are relatively lower than that in the pink cores and the brownish pink mantles, but the latter contains highest total REE and Si.

10.2.2. Apatite crystals in unlayered ferroaugite syenites

a. Pink luminescent apatite crystals

In sample C188, most apatite crystals are euhedral (Fig. 10.2-4a), and exhibit a homogeneous pink luminescence (Fig. 10.2-4b). Some of them are mantled, with a narrow brownish pink core, and a broad, pink rim which is similar to the mantled apatite found in the lower series of layered syenite. However, some of the mantled apatite grains show an irregular, narrow, bronze rim. This bronze rim may have formed during late-stage fluid alteration, because these mantled apatite grains occur within aenigmatite grains and are surrounded by many small calcite veins. In comparison with other syenite samples in the unlayered ferroaugite syenites, this syenite (sample C188) may only be affected by very minor fluid alteration, because most of the optically homogeneous alkali feldspar crystals in the sample are not surrounded by a deuteric coarsened antiperthitic rim.

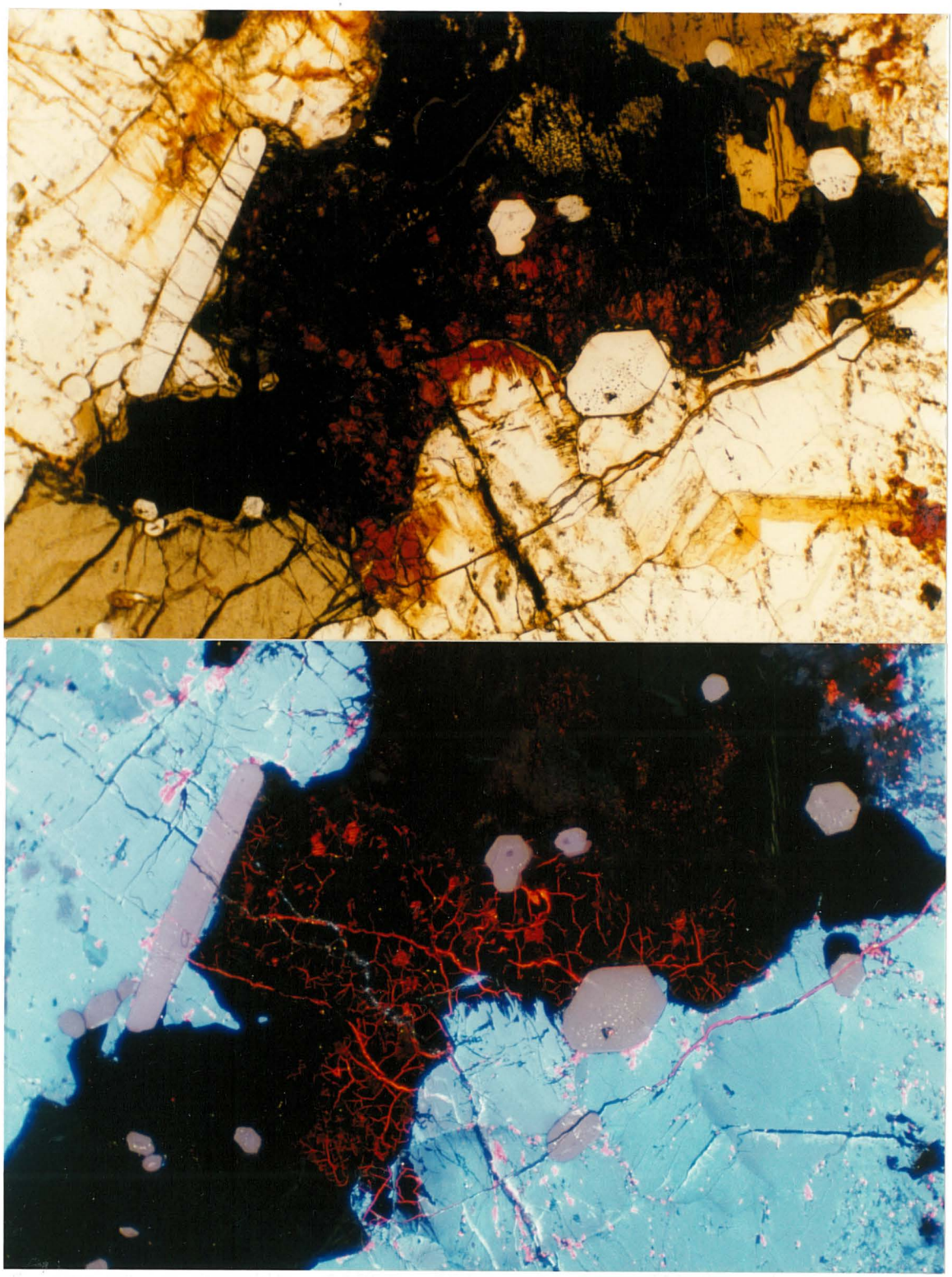

Fig. 10.2-4. Pink luminescent apatite crystals in the unlayered ferroaugite syenite (Sample C188), Center I. a. PoL. (Photographic conditions: 1.5s, ASA 400). b. CL. Most apatite crystals exhibit pink luminescence, and some apatite crystals are mantled with a small, brownish pink luminescent core and a broad, pink luminescent rim. The light blue luminescent crystals are the optically homogeneous alkali feldspar. Scale: 55 mm on photograph = 1 mm on thin section. (CL conditions: 10 kV, 0.8 Am. Photographic conditions: 15s, ASA 400).

The CL spectrum of the pink luminescent apatite is depicted in Fig. 10.2-5 which shows that peak 1 and peak 2 have high intensities, which are only slightly lower than peak 4 and peak 5. This CL spectral feature may indicate that the pink luminescent apatite has a high ratio of Eu^{2+} (or Ce^{2+}) activator to Dy^{3+}, Sm^{3+} and Pr^{3+} activator. SEM/EDS analyses show that pink luminescent apatite contains 0.09-0.1 apfu total REE (0.02-0.04 apfu La, 0.06 apfu Ce and n.d.-0.02 apfu Nd) with 0.13 apfu Si (Appendix 4-1).

In sample C302, the syenite is slightly affected by late-stage alteration, as the perthite crystals are mantled by a narrow deuteric coarsened perthitic to antiperthitic rim. The apatite crystals show a weakly zoned texture under CL, consisting of a light pink core and a pink rim. Some of these zoned crystals contain a few brown luminescent spots (Fig. 10.2-6). The light pink core has a similar CL spectrum to the pink apatite in sample C188, and contains very low contents of total REE from n.d.-0.06 apfu (n.d.-0.03 apfu La, n.d.-0.03 apfu Ce and n.d.-0.02 apfu Nd) and n.d-0.10 apfu Si (Appendix 4-1). The pink rim contains 0.20-0.34 apfu total REE (0.03 apfu La, 0.1-0.13 apfu Ce, n.d.-0.13 apfu Pr and 0.05-0.07 apfu Nd) with 0.10-0.17 apfu Si. The brown spots contain 0.40 apfu total REE (0.10 apfu La, 0.19 apfu Ce and 0.12 apfu Nd) with 0.25 apfu Si. The contents of the total REE and Si increase from the light pink core to the pink rim and to the brown spots. As the brown luminescent spots commonly occur along fractures within the apatite crystals, they may have formed during late-stage fluid alteration.

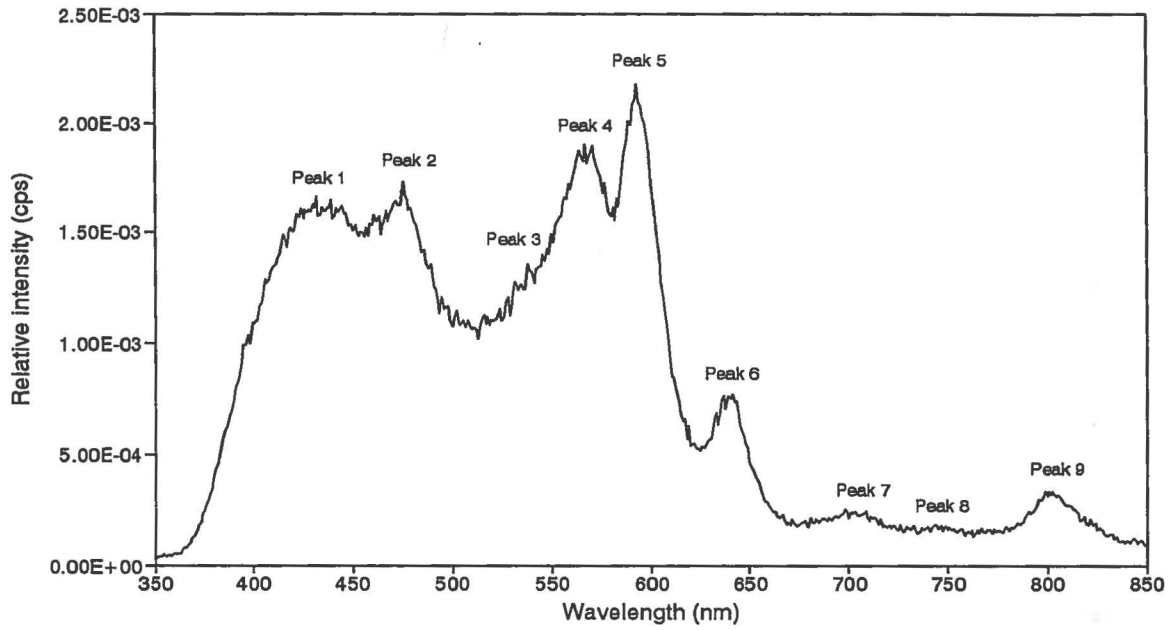

Fig. 10.2-5. CL spectrum of pink luminescent apatite in the unlayered ferroaugite syenite (C188), Center I. CL conditions: 10 kV, 0.8 mA.

b. Bronze luminescent apatite crystals

Syenite samples C100, C101 and C305 are strongly affected by late-stage fluid alteration, which is indicated by presence of optically homogeneous alkali feldspar or perthite are mantled by a deuteric coarsened antiperthitic rim. Under CL, the apatite crystals usually exhibit bronze luminescence. Some are mantled by an irregular-shaped, brownish pink luminescent rim. The CL spectra of the bronze luminescent apatite grains are different from those of the pink luminescent apatite. Bronze luminescent apatite (Fig. 10.2-7) has a relatively higher intensities of peaks 2, 4, 5 and 6, than those of the pink luminescent apatite (Fig. 10.2-5). Peak 1 is of very low intensity, and peak 3 is well-resolved on the left shoulder peak 4. These spectral features may indicate that the

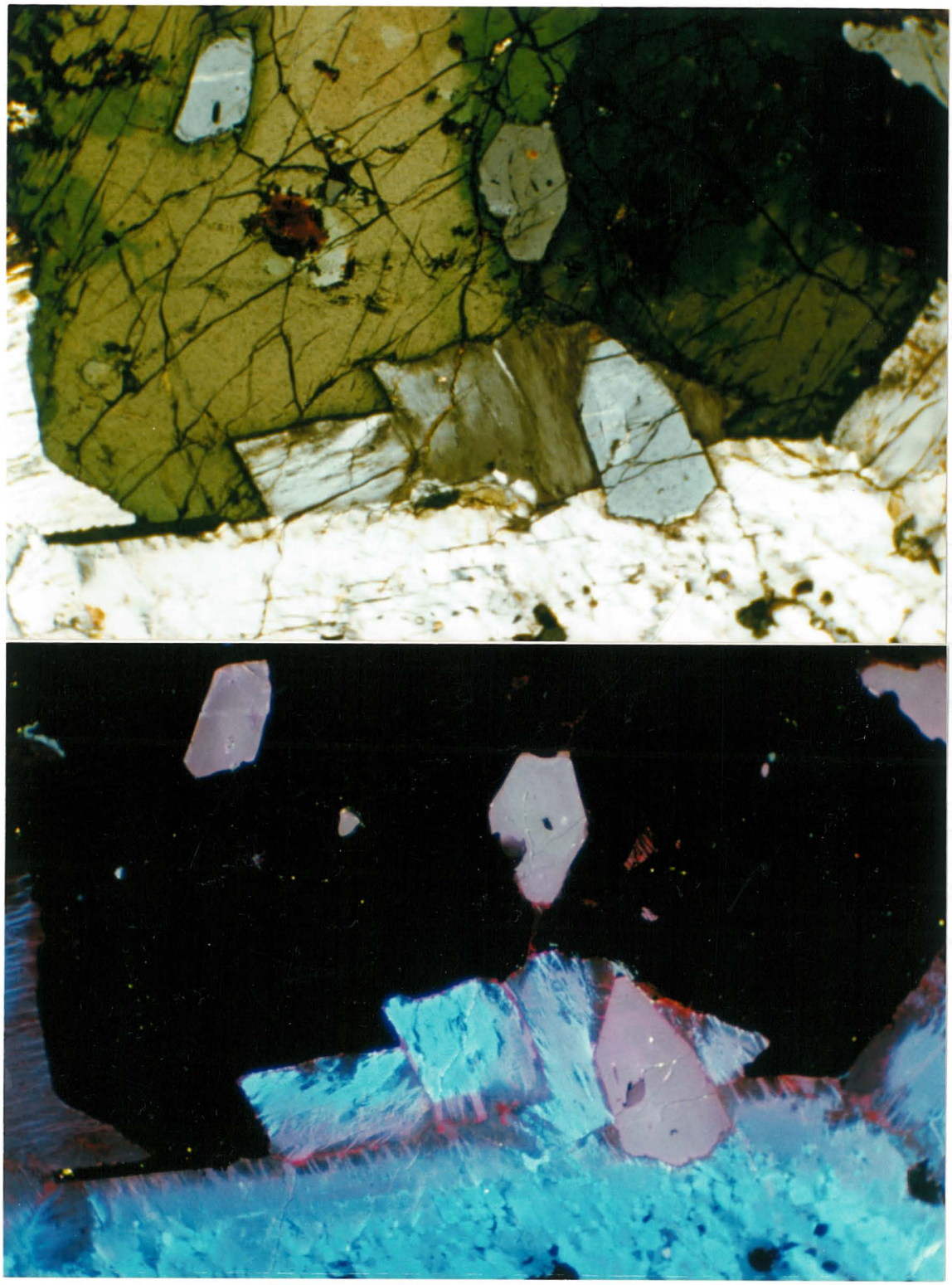

Fig. 10.2-6. Mantled apatite crystals in the unlayered ferroaugite syenite (Sample C302), Center I. a. TrL. (Photographic conditions: 2s, ASA 400). b. CL. The apatite crystals are slightly mantled with a light pink luminescent core and pink luminescent rim, and contain some brown luminescent spots. The light blue and dull blue luminescent perthite crystals are mantled by a deuteric coarsened perthitic rim. Scale: 55 mm on photograph = 1 mm on thin section. (CL conditions: 10 kV, 0.8 Am. Photographic conditions: 1m, ASA 400).

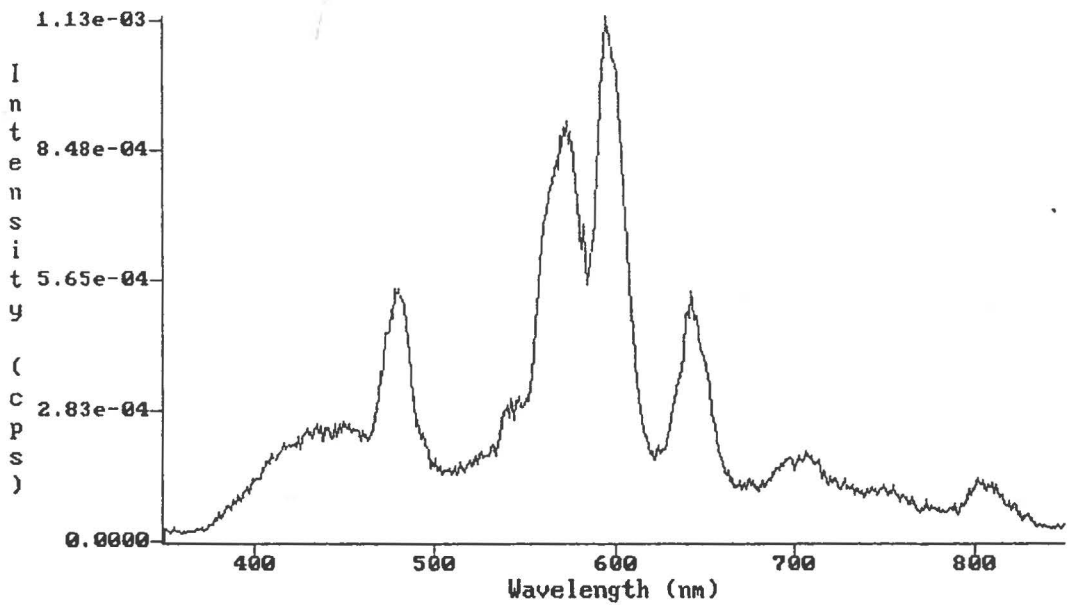

Fig. 10.2-7. CL spectrum of bronze luminescent apatite in the unlayered ferroaugite syenite (C305), Center I. CL conditions: 10 kV, 0.8 mA.

bronze luminescent apatite has a relatively higher proportion of Dy^{3+}, Tb^{3+}, Sm^{3+} and Pr^{3+} activators to Eu^{2+} (or Ce^{3+}) activators than the pink luminescent apatite.

10.2.3. Summary of apatite crystals in Center I syenites

Most apatite crystals in Center I syenite exhibit light pink to pink luminescence. Some apatite crystals show growth zones with a small brownish pink luminescent core and a light pink to pink luminescent rim.

The CL spectra of growth zoned apatites show that the brownish pink core has a relatively higher proportion of Eu^{2+} (or Ce^{3+}) to Dy^{3+}, Sm^{3+} and Pr^{3+} than the light pink rims demonstrating that LREE and Eu^{2+} are depleted during apatite crystallization. SEM/EDS

analyses show that the brownish pink cores have higher contents of total REE and Si than the light pink rims.

Apatite crystals affected by late-stage fluid alteration usually develop brownish pink to brown luminescent reaction rims or exhibit bronze luminescence, which have high total REE contents and Si. Apatites strongly affected by late-stage fluid alteration are found predominantly in the upper series syenite and in some unlayered syenite samples (C100, C101, C305). Some of the apatite reaction rims are in turn replaced by yellow or light pink luminescent secondary apatites. The secondary apatites have relatively lower contents of total REE and Si. The CL spectra show that the yellow luminescent secondary apatite is characterized by Dy^{3+} and Tb^{3+} activation indicating that the final late-stage fluid alteration produces MREE-HREE-rich secondary apatites.

The apatite crystals in Center I syenites generally are characterized by a LREE-enrichment. The REE substitution for Ca^{2+} in the apatite structure mainly may involve a coupled substitution of $Ca^{2+}+P^{5+}\rightleftarrows REE^{3+}+Si^{4+}$. This coupled substitution can be illustrated in a (Ca+P) versus (Si+REE) diagram (Fig 10.2-8b). The (Ca+P) shows a good correlation with (Si+REE) and the regression line has an intersection point (15.8) on the (Ca+P) axis and a slope of approximately 0.97. The intersection point 15.8 is approximately equal to the total cations (16) in a formula unit of apatite, and the slope of regression line of 0.97 indicates a 1:1 substitution between (Ca+P) and (Si+REE). However, the Ca^{2+} is also substituted by divalent REE such as Eu^{2+} activation as found in most CL spectra.

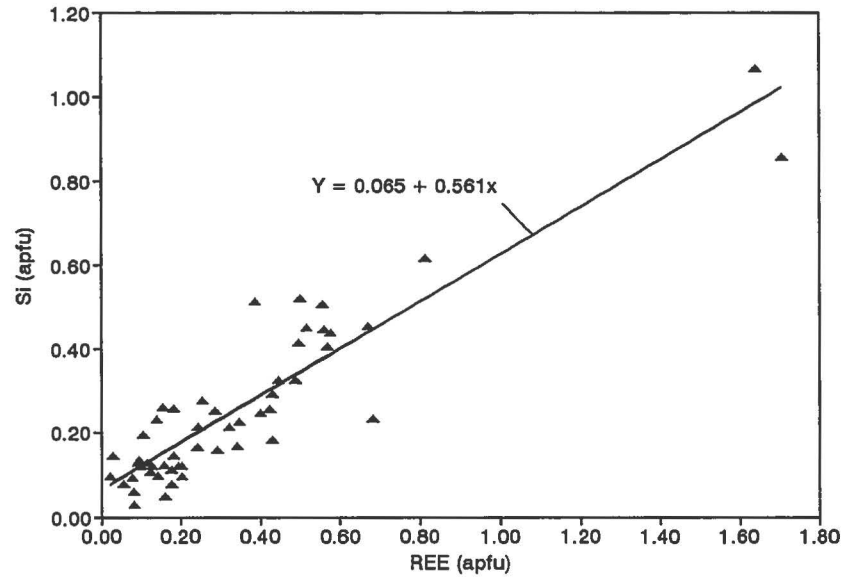

a

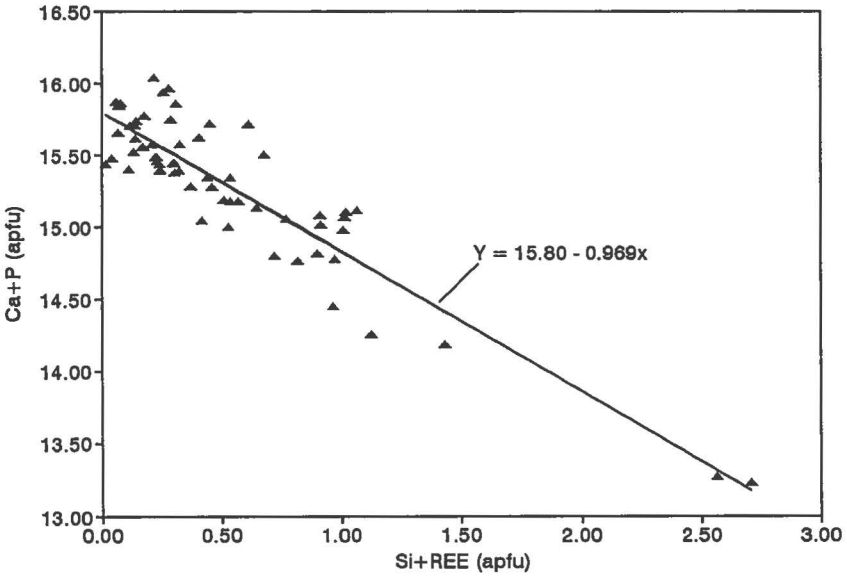

b

Fig. 10.2-8. Coupled substitutions involving REEs and Si in apatites in the ferroaugite syenites from Center I. (a) The variation in REE as a function of Si with a regression line slope of 0.561. (b) The variation in (Si+REE) as a function of (Ca+P) with a regression line slope of -0.969.

Figure 10.2-8a shows that the total REE have a good correlation with Si, with a slope of the regression line approximately equal to 0.56. This correlation indicates that the charge balance of REE substituted Ca^{2+} is maintained by approximately 1/2 Si^{4+}, which suggests that the substitution may be as follows: $2Ca^{2+}+P^{5+}\rightleftarrows(REE^{2+}+REE^{3+})+Si^{4+}$.

10.3. Apatite crystals in Center II

10.3.1. Apatite crystals in Pic Island layered syenite

In the amphibole nepheline syenite (samples C623, C629 and C630), apatite crystals are euhedral, short prismatic crystals (Fig. 6.1-1a, -2a). Under CL, most exhibit light pink or pink luminescence and some are mantled by a brownish pink rim (Fig. 6.1-1b, -2b). There are a few crystals which are mantled with a light pink core, a pink or brownish pink intermediate mantle and an oscillatory zoned rim. The oscillatory zoned rim usually consists of 2-4 concentric zones. Within each concentric zone, the luminescence colour gradually changes from core to rim from pink to brownish pink to outwards (Fig. 6.1-1b, -2b and Fig. 10.3-1b).

The CL spectra of the light pink core, the pink intermediate mantle and the brownish pink rim are shown in Fig. 10.3-2a and Fig. 10.3-2b. The ratios of peak 4, peak 5 and peak 6 to peak 1, peak 2 is a relatively lower for the light pink luminescent core (Fig. 10.3. -2a, spectrum A; -2b, spectrum A), moderately higher for the pink luminescent mantle (Fig. 10.2-2b, spectrum B) and are highest for the brownish pink luminescent rim (Fig. 10.2-2a, spectrum A). Which may indicate that the ratios of Dy^{3+}, Sm^{3+} and Pr^{3+} activators to Eu^{2+} (or Ce^{3+}) activators increase from the light pink core through to the pink mantle to the brownish pink luminescent rim.

The light pink cores contain 0.04-0.11 apfu total REE (n.d.-0.05 apfu La, 0.03-0.06 apfu Ce and n.d.-0.02 apfu Nd) with 0.05-0.18 apfu Si (Appendix 4-2). The pink and brownish pink mantles contain 0.16-0.40 apfu total REE (0.07-0.09 apfu La, 0.08-0.17 apfu Ce,

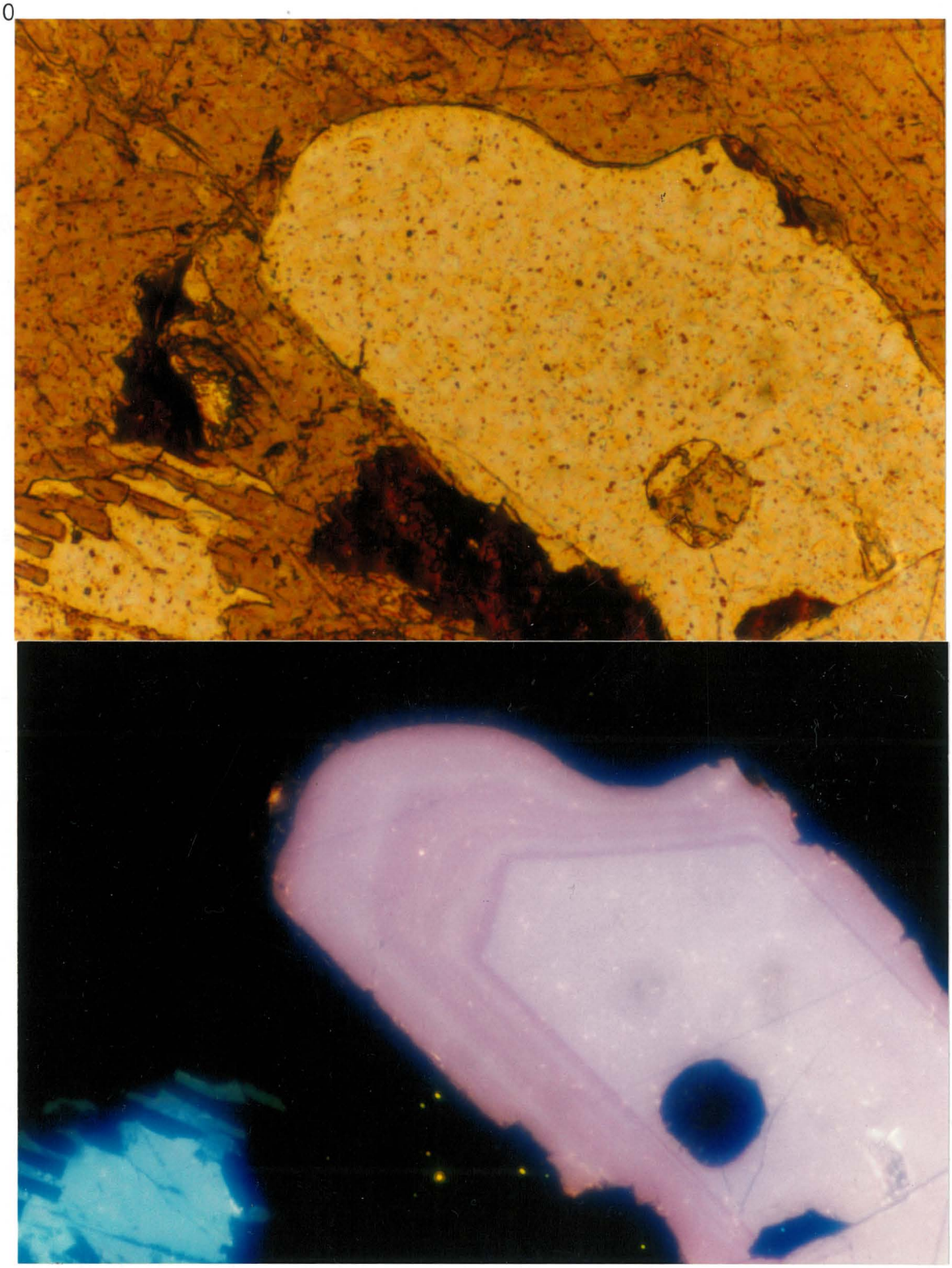

Fig. 10.3-1. An oscillatory zoned apatite crystal in the layered syenite (Sample C630), Pic Island, Center II. a. PoL. (Photographic conditions: 6s, ASA 400). b. CL. The apatite crystal is mantled with a light, a pink luminescent mantle and a light pink to pink luminescent oscillatory zoned rim. The light blue luminescent crystal is the optically homogeneous alkali feldspar. Scale: 140 mm on photograph = 1 mm on thin section. (CL conditions: 10 kV, 0.8 Am. Photographic conditions: 1m, ASA 400).

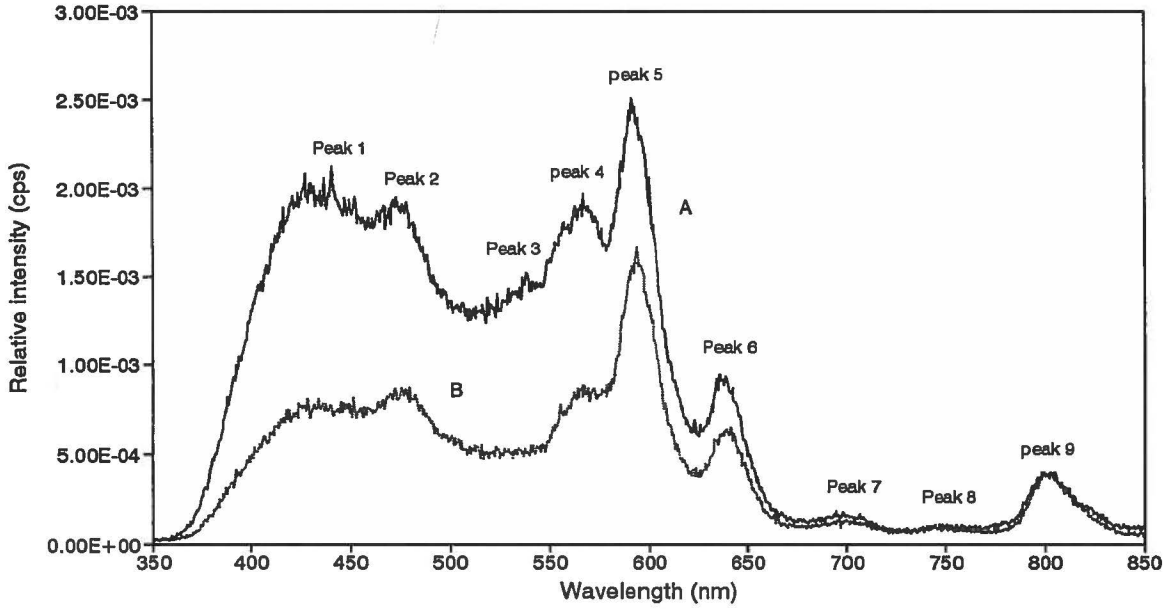

Fig. 10.3-2a. CL spectra of the mantled apatite in the layered amphibole nepheline syenite (C629), Pic Island, Center II. Spectrum (A) is from the light pink luminescent core. Spectrum (B) is from the brownish pink luminescent rim. CL conditions: 10 kV, 0.8 mA.

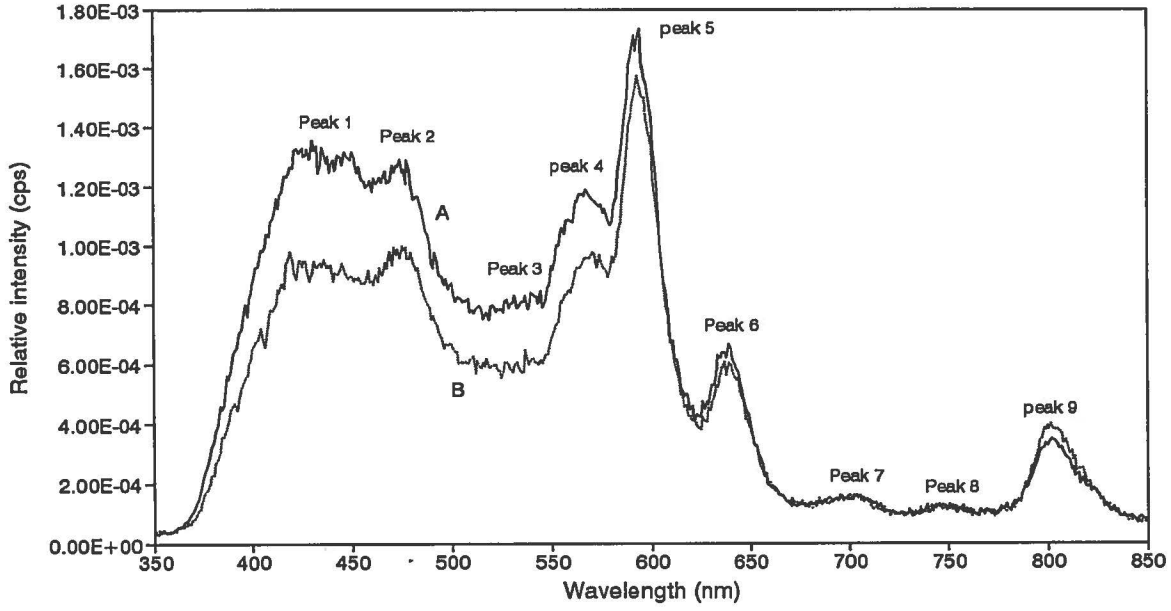

Fig. 10.3-2b. CL spectra of the mantled apatite in the layered amphibole nepheline syenite (C630), Pic Island, Center II. Spectrum (A) is from the pink luminescent core. Spectrum (B) is from the pink luminescent intermediate mantle. CL conditions: 10 kV, 0.8 mA.

n.d.-0.07 apfu Pr and 0.02-0.08 apfu Nd) with 0.11-0.30 apfu Si. In the oscillatory zoned rims, the pink zones contain 0.16-0.35 apfu total REE (0.03-0.07 apfu La, 0.05-0.16 apfu Ce, n.d.-0.08 apfu Pr and n.d.-0.06 apfu Nd) with 0.07-0.26 apfu Si. The brownish pink zones contain 0.20-0.47 apfu total REE (0.07-0.17 apfu La, 0.10-0.24 apfu Ce, n.d-0.05 apfu Pr and 0.03-0.07 apfu Nd) with 0.09-0.59 apfu Si. Generally, the contents of total REE and Si increase from the light pink rim through to the pink and brownish pink intermediate mantle, and to the pink and brownish pink oscillatory zoned rim.

In the miaskitic nepheline syenite (samples C624 and C626), some apatite crystals have different luminescence colours to the apatite crystals in the amphibole nepheline syenite. Thay are mantled with a yellow-pink core and a pink rim. The CL spectra of the yellow-pink core and the pink rim are illustrated in Fig. 10.3-3. The spectrum of the yellow-pink core has a relatively higher ratio of peaks 3, 4 and 5 to peak 1 than for the pink rim, which may indicate that the yellow-pink core has a relatively higher ratio of Dy^{3+} and Sm^{3+} activators to Eu^{2+} (Ce^{3+}) activators than the pink rim. This changing trend is different to the mantled apatite crystals in the amphibole nepheline syenite, and it may be caused by different late-stage fluid alteration (see section 6.1.4).

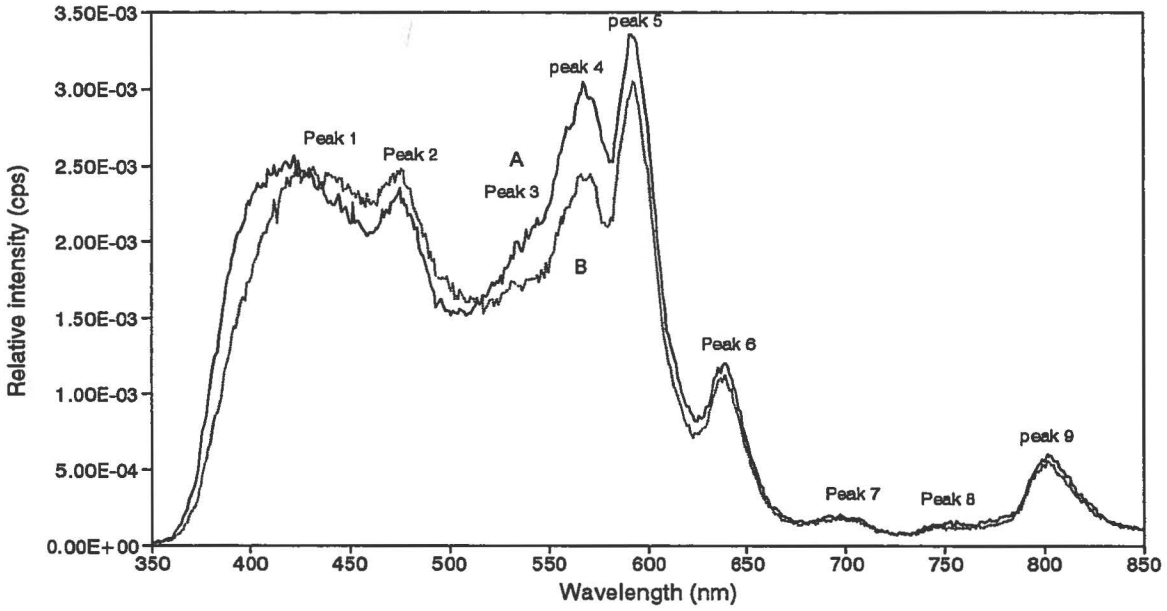

Fig. 10.3-3. CL spectra of the mantled apatite in the layered miaskitic nepheline syenite (C626), Pic Island, Center II. Spectrum (A) is from the yellow-pink luminescent core. Spectrum (B) is from the pink luminescent rim. CL conditions: 10 kV, 0.8 mA.

10.3.2. Apatite crystals in Neys Park syenite and gabbro

In the perthitic syenite (samples C97, C109, C111, C115, C3118A, C3118B, C3118C, C3118D, C1538B, C1863, N1A, N3B and N3C), most apatite crystals are fine-grained, anhedral crystals that usually exhibit brownish pink luminescence (Fig. 6.2-4b, -5b). A few slightly larger apatite crystals are euhedral, and are mantled with either a pink core and a brownish pink rim, or consist of a brownish pink core, a pink intermediate mantle and a brownish pink rim (Fig. 6.2-3). The CL spectrum of the pink mantle (Fig. 10.3-4a) shows that peak 5 has a highest luminescent intensity, and peak 1, 2 and 4 have moderate intensities. This spectrum is very similar that of the pink mantle in the amphibole nepheline syenite from Pic Island.

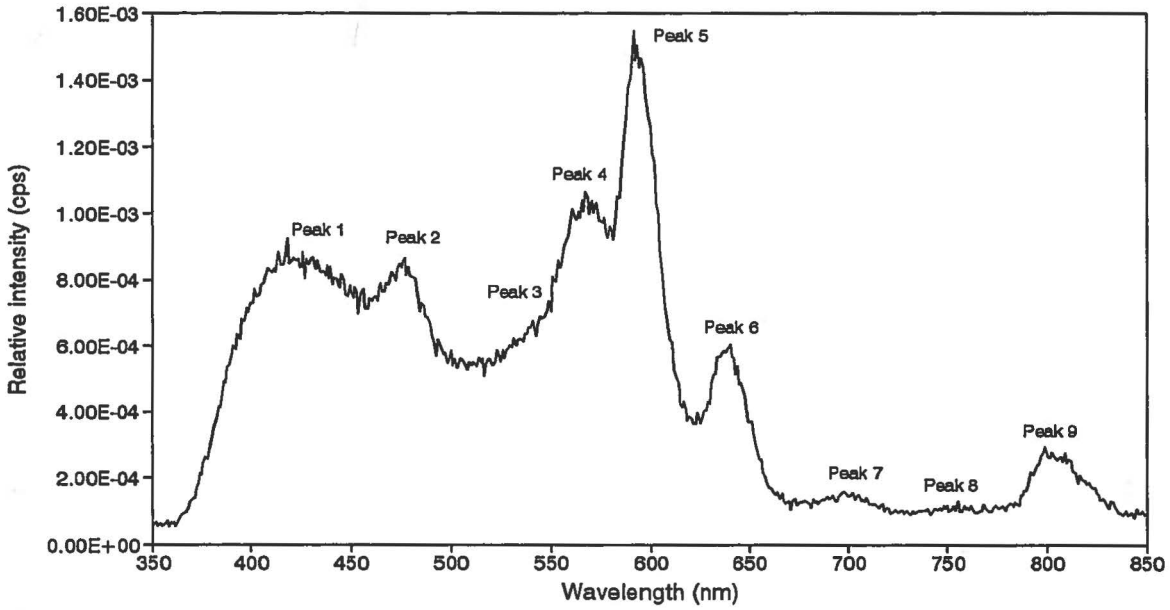

Fig. 10.3-4a. CL spectrum of the mantled apatite in the perthitic syenite (C97), Neys Park, Center II. The spectrum is from the pink luminescent intermediate mantle. CL conditions: 10 kV, 0.8 mA.

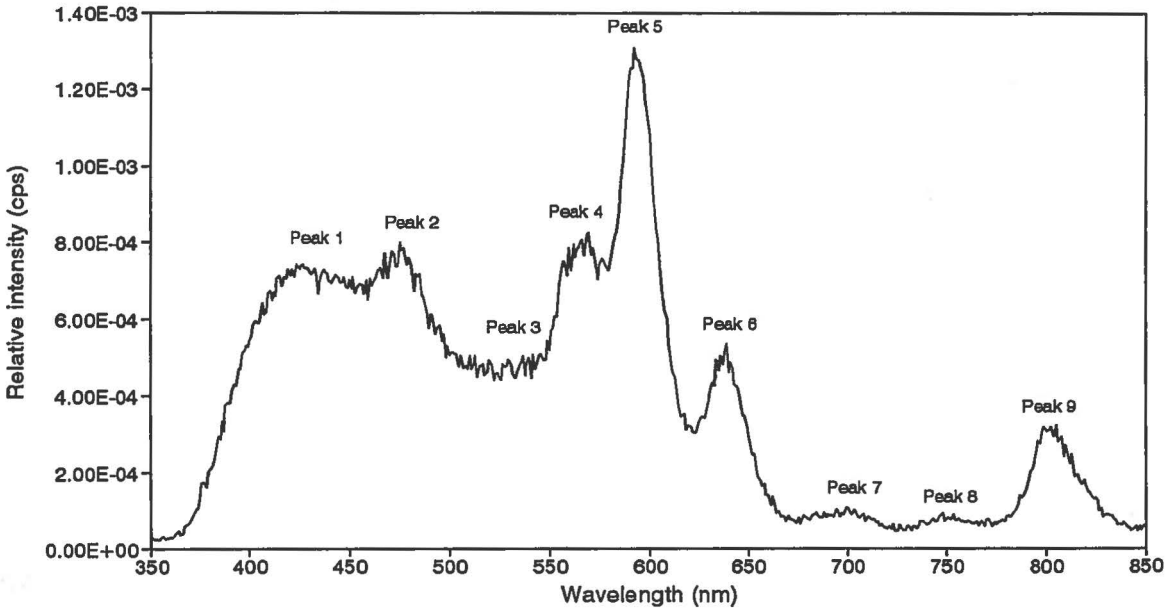

Fig. 10.3-4b. CL spectrum of pink luminescent apatite from the miaskitic nepheline syenite (C114), Neys Park, Center II. CL conditions: 10 kV, 0.8 mA.

The brownish pink cores contain 0.29-0.45 apfu total REE (0.06-0.10 apfu La, 0.23 apfu Ce, n.d.-0.03 apfu Pr and n.d.-0.10 apfu Nd) with 0.37-0.49 apfu Si (Appendix 4-2). The pink mantles contain 0.20-0.33 apfu total REE (0.04-0.06 apfu La, 0.08-0.18 apfu Ce, 0.03-0.07 apfu Pr and 0.04-0.05 apfu Nd). The brownish pink rims contain 0.26-0.46 apfu total REE (0.06-0.14 apfu La, 0.15-0.22 apfu Ce and 0.05-0.10 apfu Nd) with 0.26-0.36 apfu Si. The contents of the total REE and Si are relatively lower in the pink mantle than in the brownish pink core and rim.

The fine-grained, brownish pink crystals contain 0.22-0.38 apfu total REE (0.07-0.10 apfu La, 0.15-0.19 apfu Ce, n.d.-0.06 apfu Pr and n.d.-0.06 apfu Nd) with 0.20-0.30 apfu Si (Appendix 4-2). This apatite contains nearly the same amount of total REE and Si as the brownish pink rims of the mantled crystals.

In the miaskitic nepheline syenite (sample C114), most apatite crystals are euhedral, short prismatic crystals and exhibit pink luminescence. Some crystals are mantled with a small brownish pink core and a broad pink rim. Some of the cores are replaced by dull blue luminescent secondary alkali feldspar (Fig. 10.3-5b). The CL spectrum of the pink luminescent apatite (Fig. 10.3-4b) is very similar to that the apatite mantle found in the perthitic syenite (Fig. 10.3-4a).

SEM/EDS analyses show that the pink apatites (or the mantles) contain 0.12-0.25 apfu total REE (0.03-0.07 apfu La, 0.05-0.12 apfu Ce, n.d.-0.03 apfu Pr and 0.04 apfu Nd) with n.d-0.13 apfu Si (Appendix 4-2). The REE and Si content of in the pink luminescent

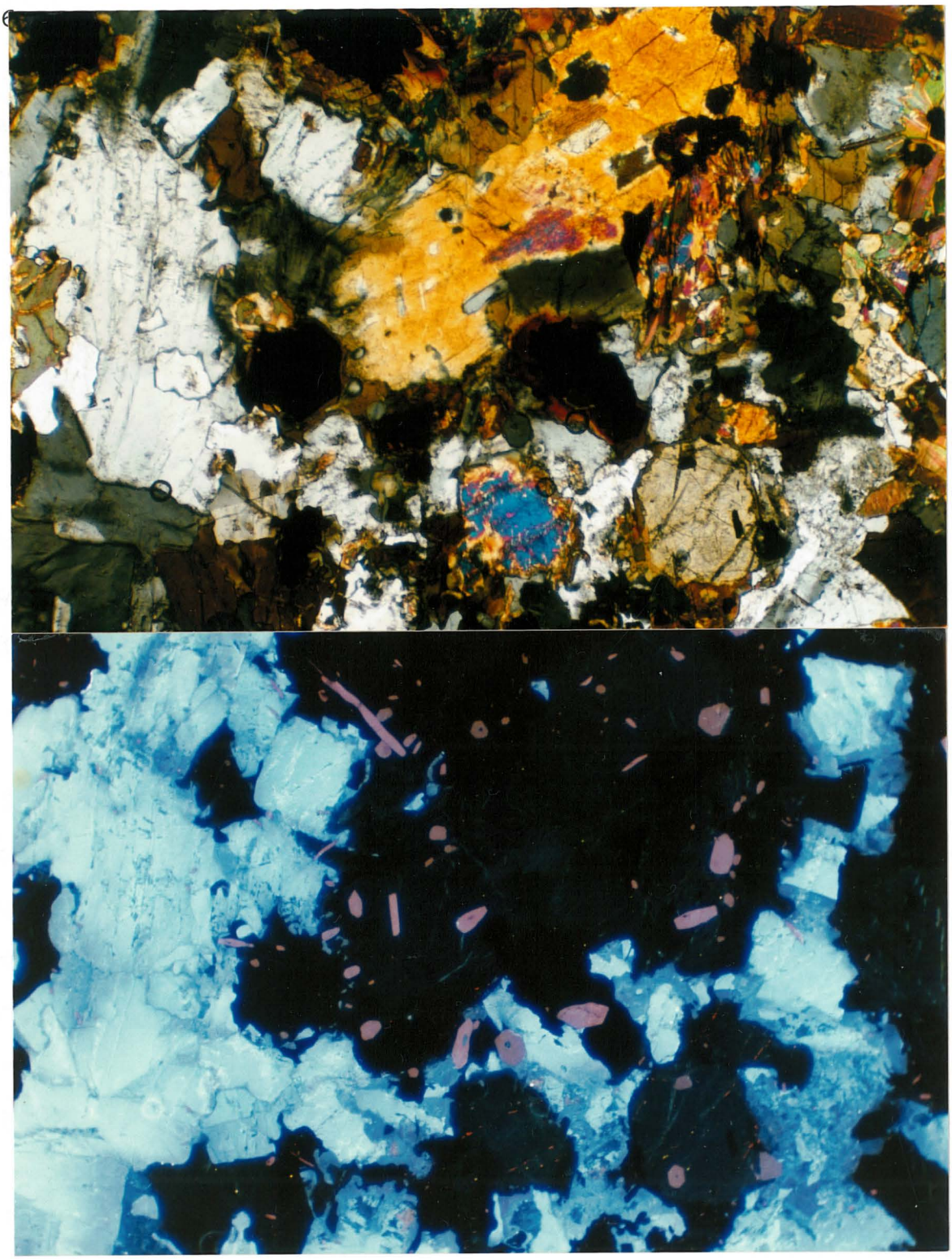

Fig. 10.3-5. Apatite crystals in the miaskitic nepheline syenite (Sample C114), Neys Park, Center II. a. PoL. (Photographic conditions: 1.8s, ASA 400). b. CL. Most the apatite crystals exhibit pink luminescence. Some apatite crystals are mantled with a small brownish pink luminescent core and a broad pink luminescent rim, and some of the core are replaced by a dull blue luminescent secondary K-feldspar. The light blue luminescent crystal is the optically homogeneous alkali feldspar which is mantled by dull blue luminescent secondary K-feldspar. Scale: 55 mm on photograph = 1 mm on thin section. (CL conditions: 10 kV, 0.8 Am. Photographic conditions: 45s, ASA 400).

crystals (or the mantles) are similar to those of the pink mantles in the perthitic syenite.

In the alkaline gabbro (sample C107), most apatite crystals are euhedral and commonly exhibit a homogeneous light violet or violet luminescence (Fig. 6.2-16, -20). The CL spectrum is shown in Fig. 10.3-6. Peak 1 has a higher intensity than other peaks. In comparison with the CL spectra of pink luminescent apatite in both perthitic syenite and miaskitic nepheline syenite, the violet luminescent apatite crystals in the gabbro may have a higher ratios of Eu^{2+} (or Ce^{3+}) activators to Dy^{3+}, Sm^{3+}, Pr^{3+} activators.

SEM/DES analyses show that the light violet and violet luminescent apatite crystals contain 0.03-0.2 apfu total REE (0.03-0.07 apfu La, n.d.-0.10 apfu Ce, n.d.-0.02 apfu Pr and n.d.-0.04 apfu Nd) with n.d.-0.09 apfu Si (Appendix 4-2).

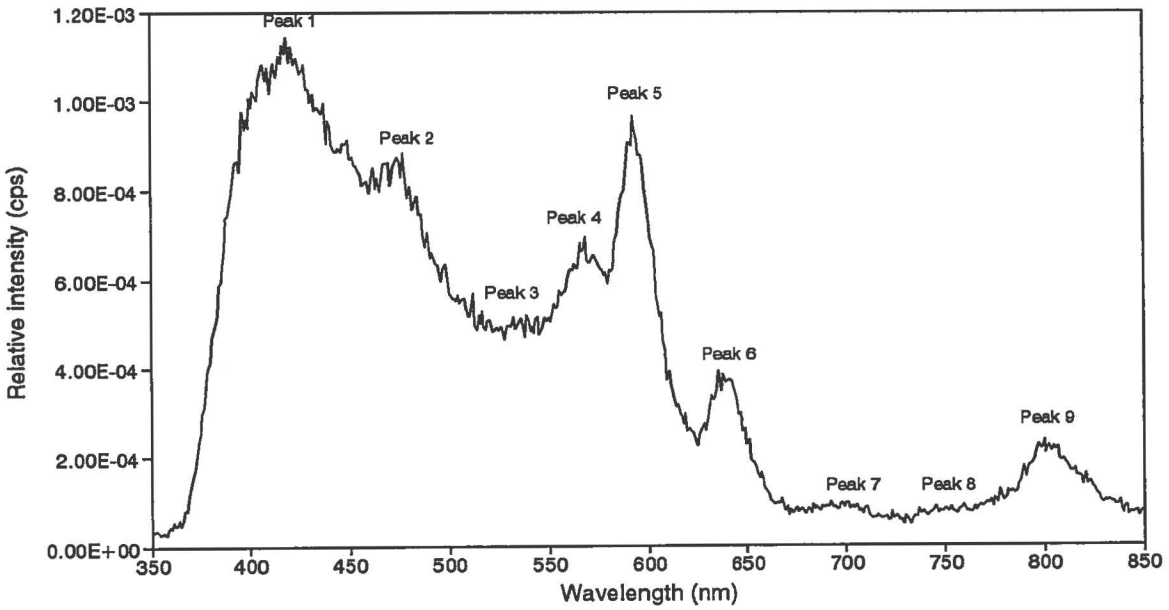

Fig. 10.3-6. CL spectrum of light violet luminescent apatite in the gabbro (C107), Neys Park, Center II. CL conditions: 10 kV, 0.8 mA.

10.3.3. Apatite crystals in recrystallized syenite

In the recrystallized syenite (samples C571, C572, C573 and C587), most apatite crystals exhibit pink luminescence (Fig. 6.3-1b and Fig. 10.3-7a). The CL spectrum is shown in Fig. 10.3-7b and has similar spectral features to both the spectra of the pink luminescent apatite mantles in the perthitic syenite and the pink luminescent apatite in the miaskitic nepheline syenite. In the recrystallized syenite, the pink luminescent apatite crystals contain relatively higher contents of total REE (0.18-0.34 apfu) and Si (n.d.-0.21 apfu) than the pink mantles and crystals of apatites in the perthitic syenites and the miaskitic nepheline syenites.

In the mosaic granuloblastic nepheline syenite (sample C587), a few light pink crystals (cores) are overgrown by a zoned apatite which is mantled with a brownish pink intermediate mantle and a brown rim (Fig. 10.3-8a, -8b). The brown rim is irregularly replaced by a light pink secondary apatite along the edges. The latter contains many small inclusions of allanite and REE-silicates (Fig. 10.3-8c).

SEM/EDS analyses show that the light pink cores contain 0.18-0.22 apfu total REE (0.03-0.06 apfu La, 0.10-0.12 apfu Ce and 0.03-0.04 apfu Nd) with 0.22-0.25 apfu Si (Appendix 4-2). The brownish pink mantle contains 0.53-0.60 apfu total REE (0.13-0.16 apfu La, 0.27 apfu Ce, 0.03-0.05 mole Pr and 0.10-0.12 apfu Nd) with 0.51-0.53 apfu Si, and the brown rim contains 0.82 apfu total REE (0.22 apfu La, 0.40 apfu Ce, 0.08 apfu Pr and 0.12 apfu Nd) with 0.82 apfu Si.

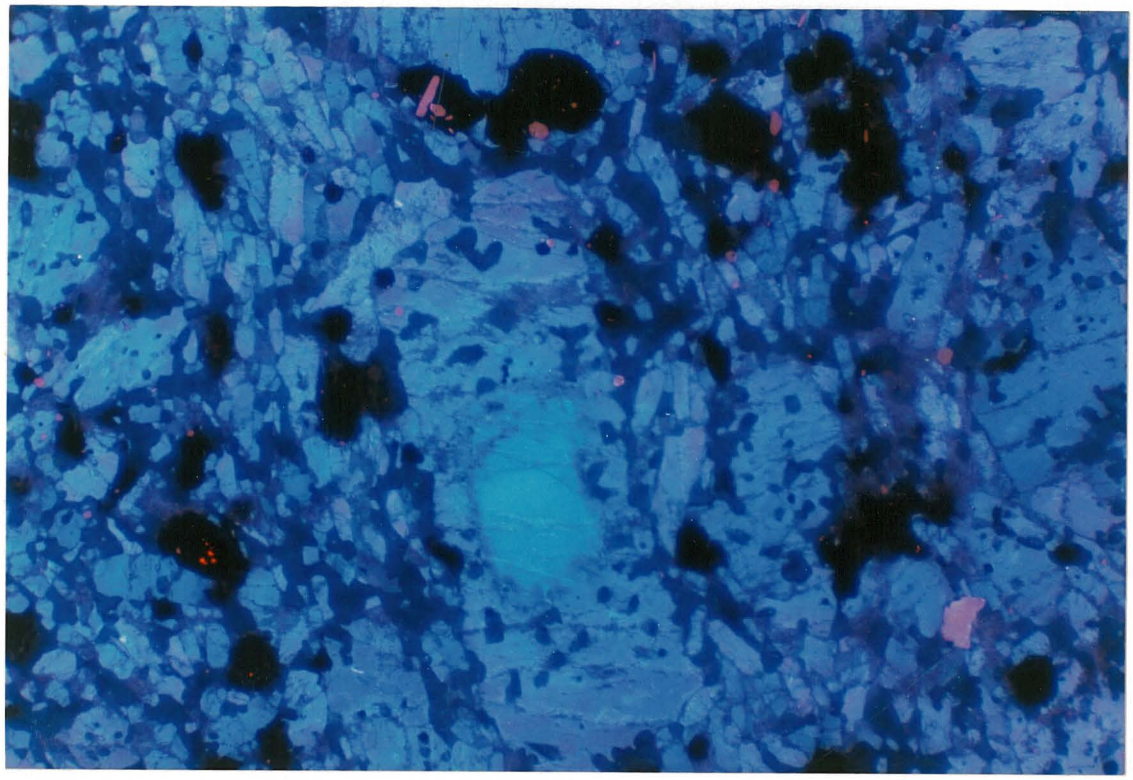

Fig. 10.3-7a. Pink luminescent apatite crystals in the porphyroblastic nepheline syenite (Sample C573) from Center II, Coldwell Complex. Scale: 55 mm on photograph = 1 mm on thin section. (CL conditions: 10 kV, 0.8 Am. Photographic conditions: 2 min, ASA 400).

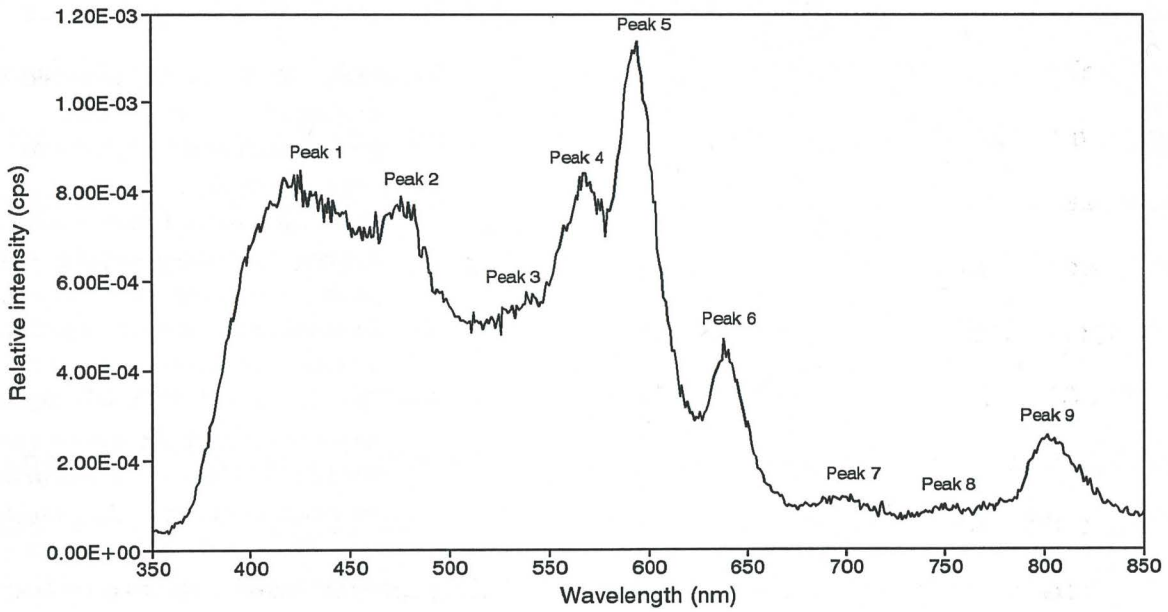

Fig. 10.3-7b. CL spectrum of the pink luminescent apatite in the porphyroblastic nepheline syenite (Sample C573) from Center II, Coldwell Complex. CL conditions: 10 kV, 0.8 mA.

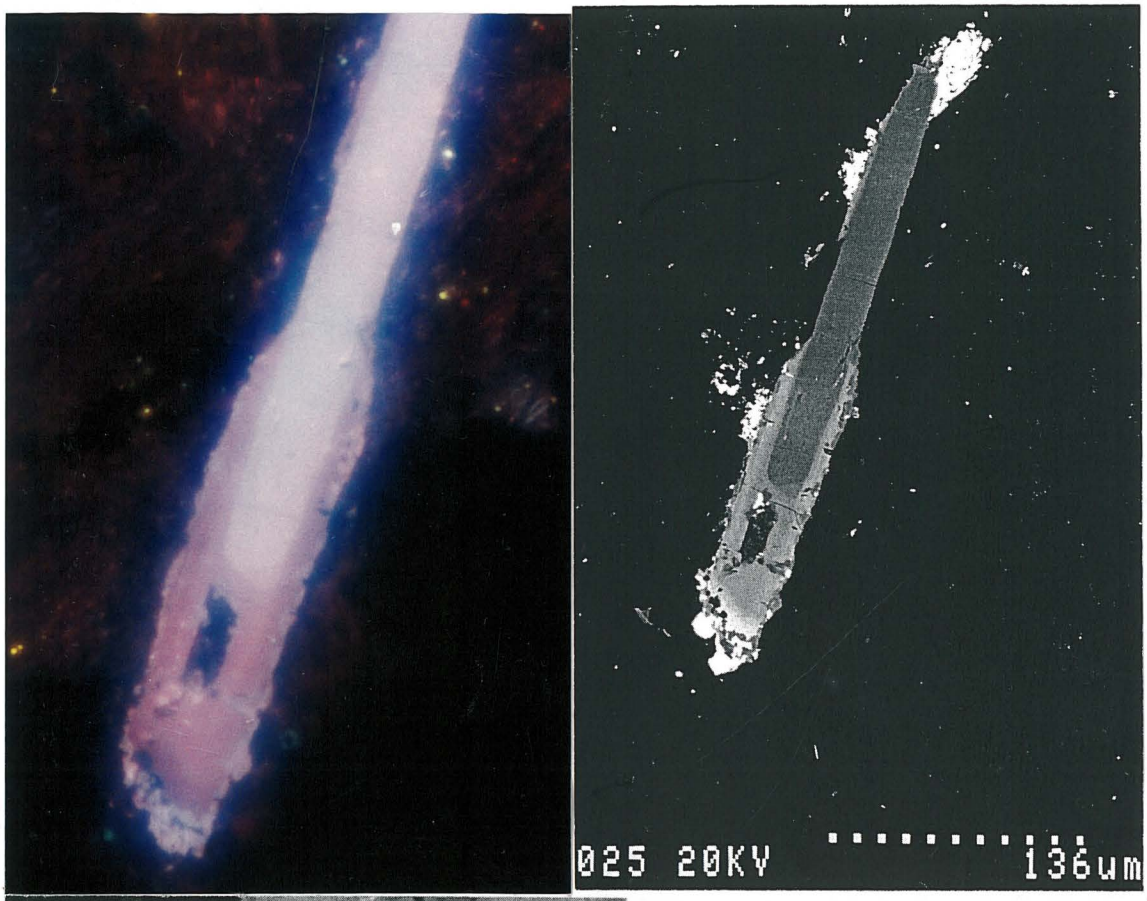

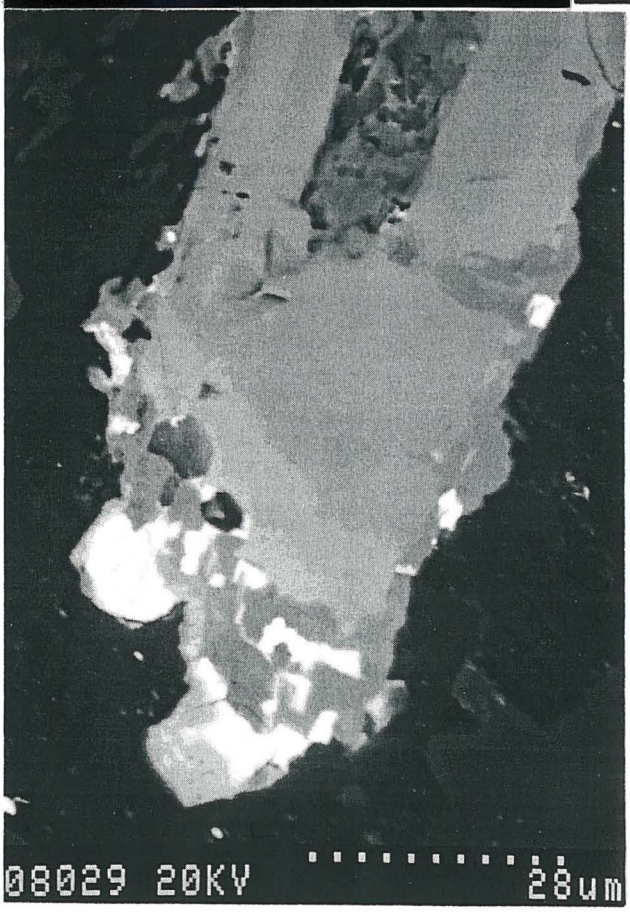

Fig. 10.3-8. A mantled apatite crystal in the mosaic granuloblastic nepheline syenite (Sample C587), Center II. a. CL. The light pink luminescent apatite (core) is over-grown by a brownish pink (mantle) to brown (rim) luminescent zoned apatite. The brown luminescent rim is replaced by a light pink luminescent secondary apatite along the edges. Scale: 140 mm on photograph=1 mm on thin section. (CL conditions: 10 kV, 0.8 mA. Photo-graphic conditions: 3m, ASA 400). b. and c. SEM/BSE images of the mantled apatite and show the same zoned features as the CL image. The white areas are the REEs-bearing minerals.

The total REE and Si contents increase from the core to the rim. The light pink secondary apatites contain relatively higher contents of total REE (0.25-0.30 apfu) and Si (0.30-0.34 apfu) than the light pink cores, but lower amounts than the brownish pink mantle and the brown rim.

10.3.4. Apatite crystals in unrecrystallized syenite

In unrecrystallized syenite, most apatite crystals show zoned textures under CL (Fig. 10.3-9b, -10b and -11b), which include: A brownish pink core zoned to a light pink intermediate mantle and a brownish pink rim (Fig. 10.3-9b); A pink luminescent core mantled to a light pink to pink oscillatory zoned rim (Fig. 10.3-10b); A light pink core zoned to a pink intermediate mantled and a brownish pink rim (Fig. 10.3-11b); A light pink core or zoned to a pink, or a brownish pink rim (Fig 10.3-9b, -10b, -11b).

The CL spectra of the light pink cores and pink luminescent rims (sample C293) are shown in Fig. 10-12. Although the light pink core has a relativey higher total intensity than the pink rim, the spectrum of the pink rim has a relatively higher ratio of peaks 4, 5 and 6 to peak 1 and 2 than the light pink luminescent core. This may indicate that the light pink luminescent rims have a relatively higher ratio of Dy^{3+}, Sm^{3+} and Pr^{3+} activators to Eu^{2+} (or Ce^{3+}) activators than the light pink core.

SEM/EDS analyses show that the light pink cores contain 0.04-0.16 apfu total REE (n.d.-0.04 apfu La, 0.05-0.07 apfu Ce, n.d.-0.04 apfu Pr and n.d.-0.09 apfu Nd) with n.d.-0.08 apfu Si (Appendix

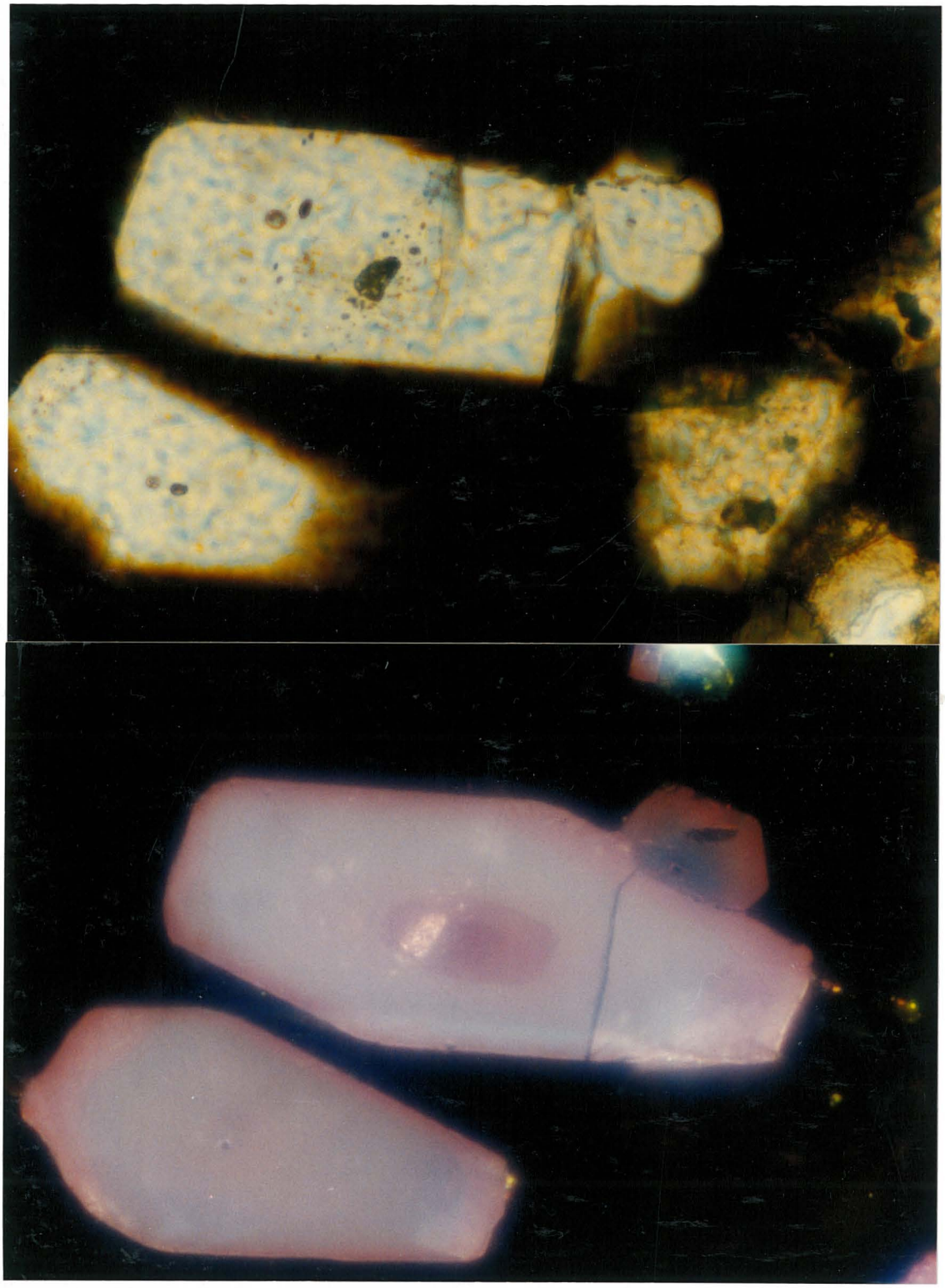

Fig. 10.3-9. Mantled apatite crystals in unrecrystallized nepheline syenite (Sample C279), Center II. a. Pol. (Photographic conditions: 4s, ASA 400). b. CL. The apatite crystals are mantled with a brownish pink luminescent core, a light pink luminescent intermediate mantled and a brownish pink luminescent rim, or are mantled with a light pink luminescent core and a brownish pink luminescent rim. Scale: 140 mm on photograph=1 mm on thin section. (CL conditions: 10 kV, 0.8 mA. Photographic conditions: 2m, ASA 400).

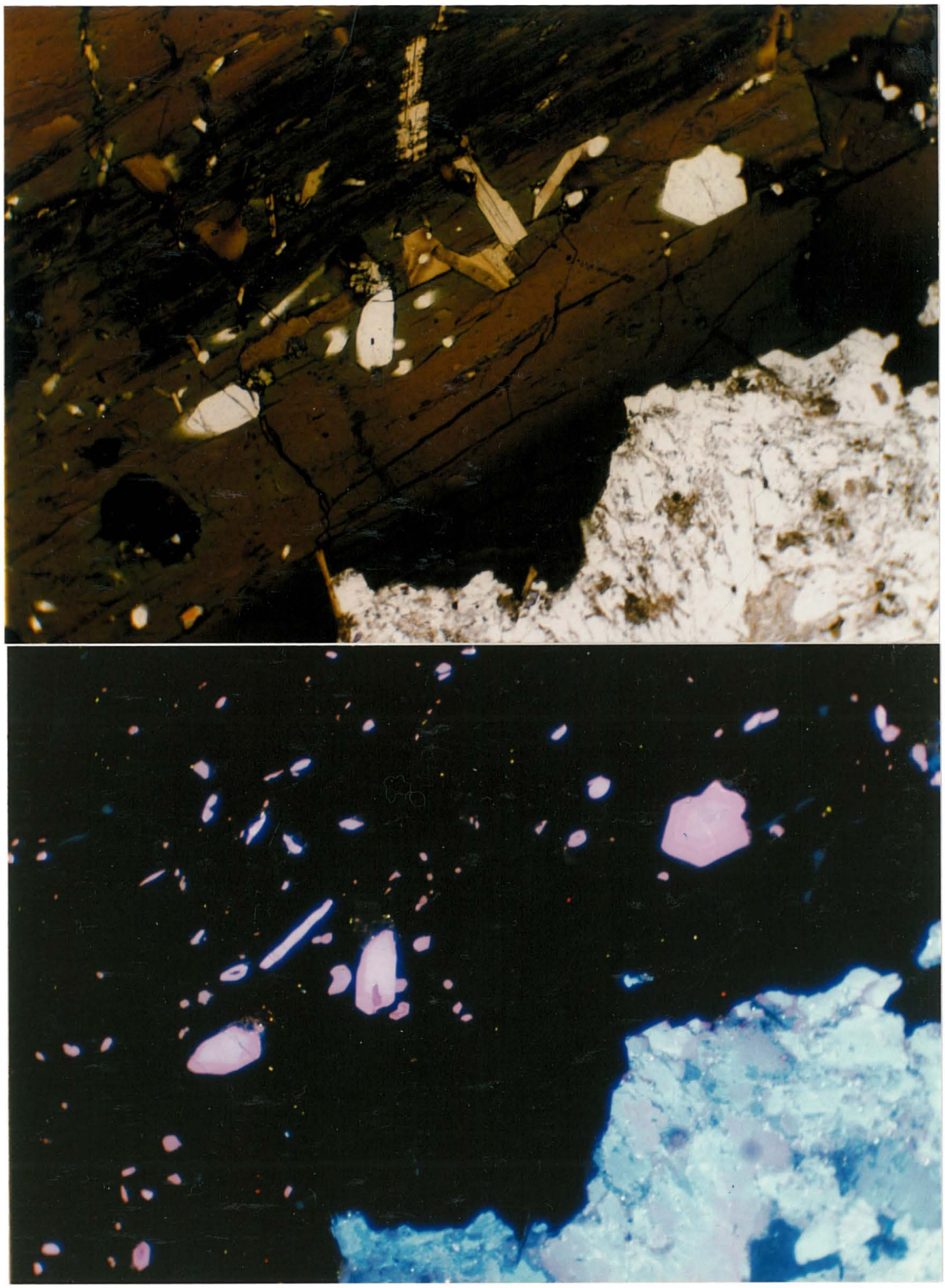

Fig. 10.3-10. Mantled apatite crystals in unrecrystallized nepheline syenite (Sample C293), Center II. a. Pol. (Photographic conditions: 2s, ASA 400). b. CL. The light pink luminescent apatite core is mantled by a pink luminescent rim, or is mantled by a light pink to pink luminescent oscillatory zoned rim. Scale: 55 mm on photograph=1 mm on thin section. (CL conditions: 10 kV, 0.8 mA. Photographic conditions: 1m, ASA 400).

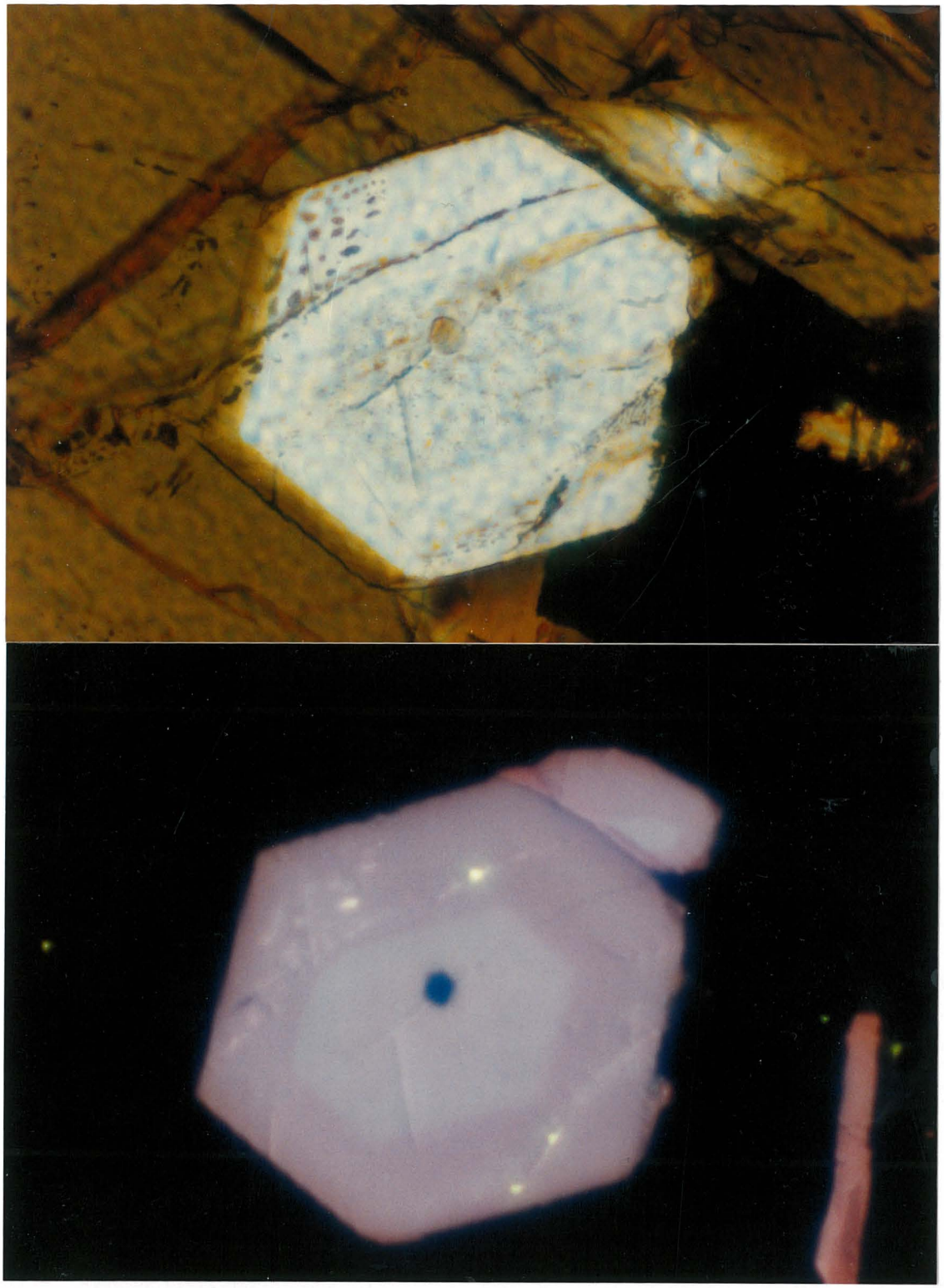

Fig. 10.3-11. A mantled apatite crystal in the unrecrystallized nepheline syenite (Sample C291), Center II. a. Pol. (Photographic conditions: 3s, ASA 400). b. CL. The apatite crystal is mantled with a light pink luminescent core, a pink luminescent intermediate mantle and a brownish pink luminescent rim. Scale: 140 mm on photograph=1 mm on thin section. (CL conditions: 10 kV, 0.8 mA. Photographic conditions: 2m, ASA 400).

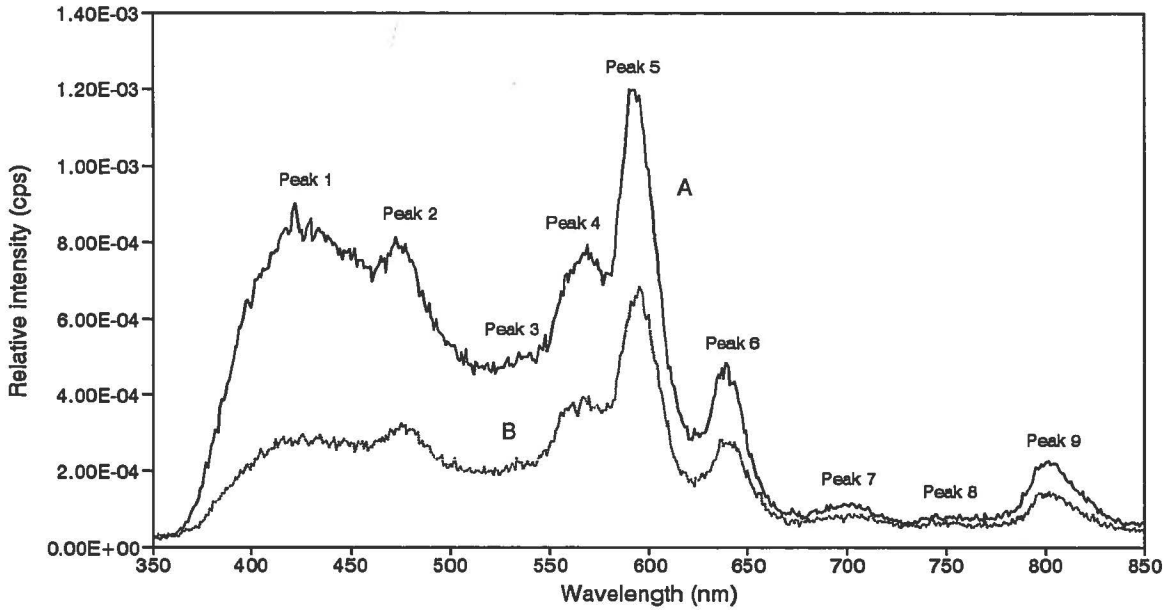

Fig. 10.3-12. CL spectra of the mantled apatite in the unrecrystallized nepheline syenite (C293), Center II. Spectrum (A) is from the light pink luminescent core. Spectrum (B) is from the pink luminescent rim. CL conditions: 10 kV, 0.8 mA.

4-2). The pink mantles contain 0.21-0.32 apfu total REE (0.04-0.09 apfu La, 0.11-0.18 apfu Ce, n.d.-0.03 apfu Pr and n.d.-0.06 apfu Nd) with 0.14-0.19 apfu Si, and the brownish pink luminescent rims contain 0.52-1.42 apfu total REE (0.14-0.33 apfu La, 0.30-0.66 apfu Ce, n.d.-0.19 apfu and 0.08-0.25 apfu Nd) with 0.43-0.85 apfu Si. The contents of total REE and Si increase from the light pink cores through to the pink mantles and to the brownish pink rims. In samples C276 and C472, however, some apatite crystals are mantled with a light pink to pink core and a brownish pink rim (Fig. 10.3-13a, -14). The brownish pink rim is replaced by an irregularly-shaped, light pink secondary apatite along the edges (Fig. 10.3-13a,b -14). These apatite crystals usually occur in the syenites which are strongly affected by late-stage fluid alteration. This is

recognized by the replacement of optically homogeneous alkali feldspar by secondary albite and K-feldspar. CL spectra of the light pink core and from the brownish pink rim are shown in Fig. 10.3-15b, and are similar to the spectra of mantled apatite from sample C293 in above.

SEM/EDS analyses show that the light pink to pink apatite cores contain 0.16-0.40 apfu total REE (0.03-0.10 apfu La, 0.09-0.21 apfu Ce, n.d-0.06 apfu Pr and n.d.-0.06 apfu Nd) with n.d.-0.27 apfu Si (Appendix 4-2), whereas the brownish pink rims contain 0.28-1.07 apfu total REE (0.08-0.30 apfu La, 0.15-0.50 apfu Ce, n.d.-0.09 apfu Pr and 0.09-0.46 apfu Nd) with 0.33-0.83 apfu Si. The light pink secondary apatite contents 0.14-0.46 apfu total REE (0.04-0.11 apfu La, 0.07-0.16 apfu Ce, n.d.-0.08 apfu Pr and n.d.-0.35 apfu Nd). The total REE and Si contents increase from the light pink cores to the brownish pink rims, then decrease in the light pink secondary apatite.

10.3.5. Summary of apatite crystals in Center II syenites

Most apatite crystals in Center II syenite exhibit light pink to pink luminescence. Some apatite crystals are mantled with a small brownish pink core and a light pink to pink rim which is similar to the mantled apatites found in Center I syenites. Some crystals are mantled with light pink to pink cores and brownish pink rims, or show light pink to pink alternating oscillatory zones.

Although, SEM/EDS analyses show that the pink or brownish pink zones (mantles or rims) have higher contents of total REE and Si

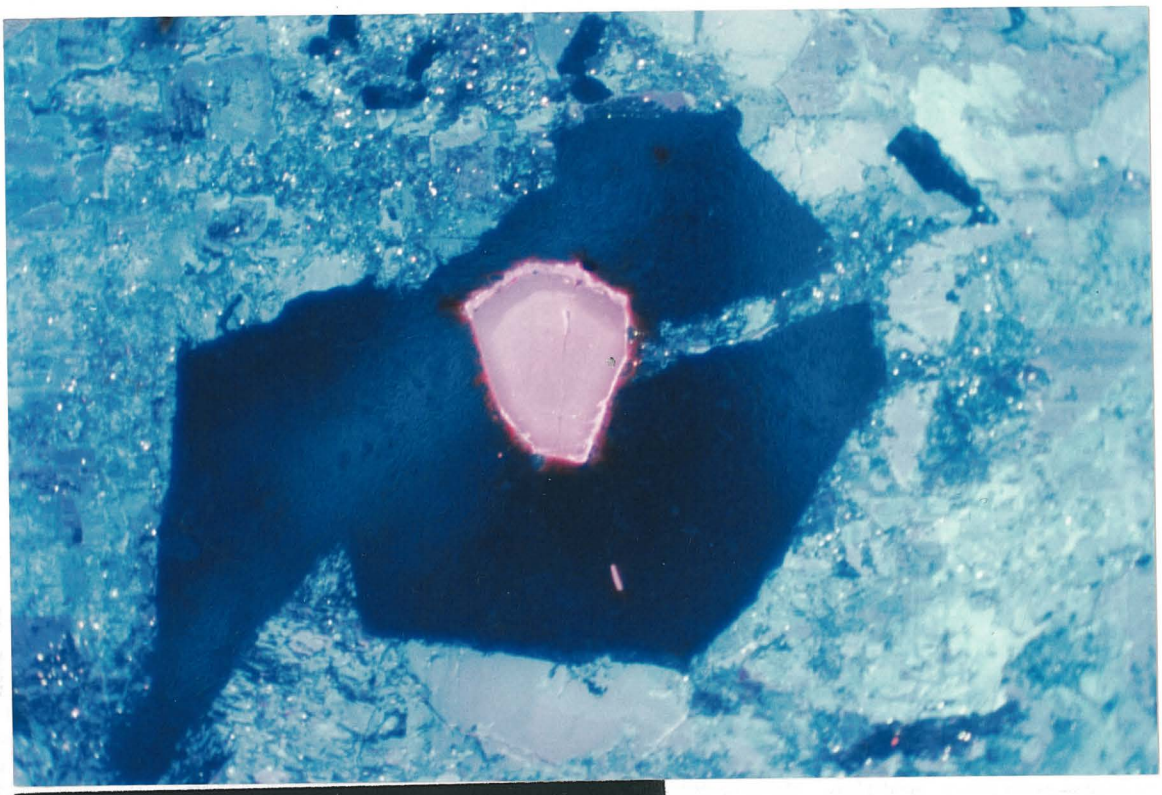

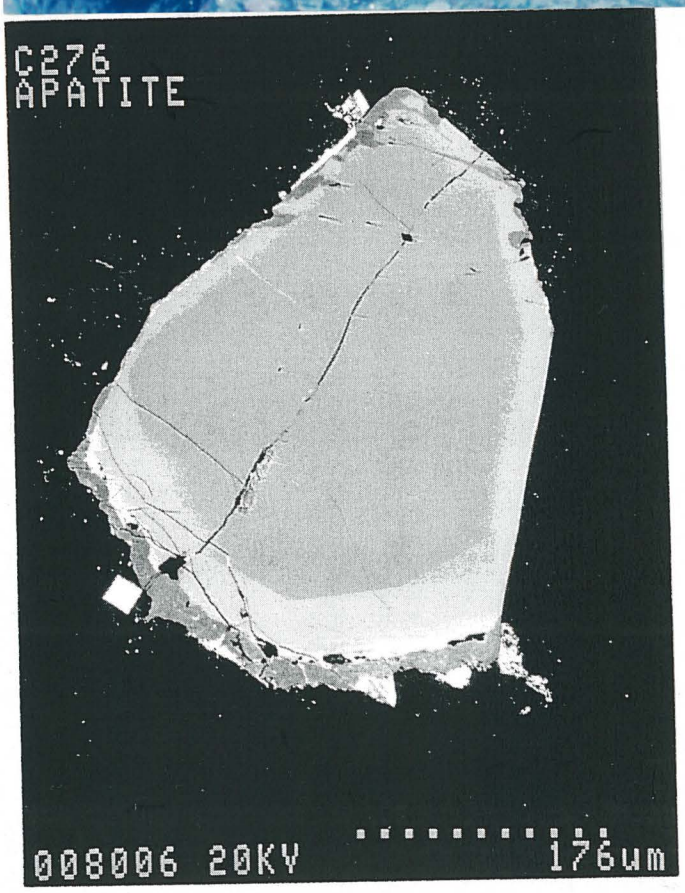

Fig. 10.3-13. A mantled apatite crystal in the unre-crystallized nepheline syenite (Sample C276), Center II. a. CL. The apatite crystal is mantled with a pink to light pink luminescent core and a brownish pink luminescent rim. The brownish pink luminescent rim is replaced by a light pink luminescent secondary apatite along the edges. Scale: 55 mm on photograph=1 mm on thin section. (CL conditions: 10 kV, 0.8 mA. Photographic conditions: 1m, ASA 400). b. SEM/BSE image shows the same zoned features as the CL image.

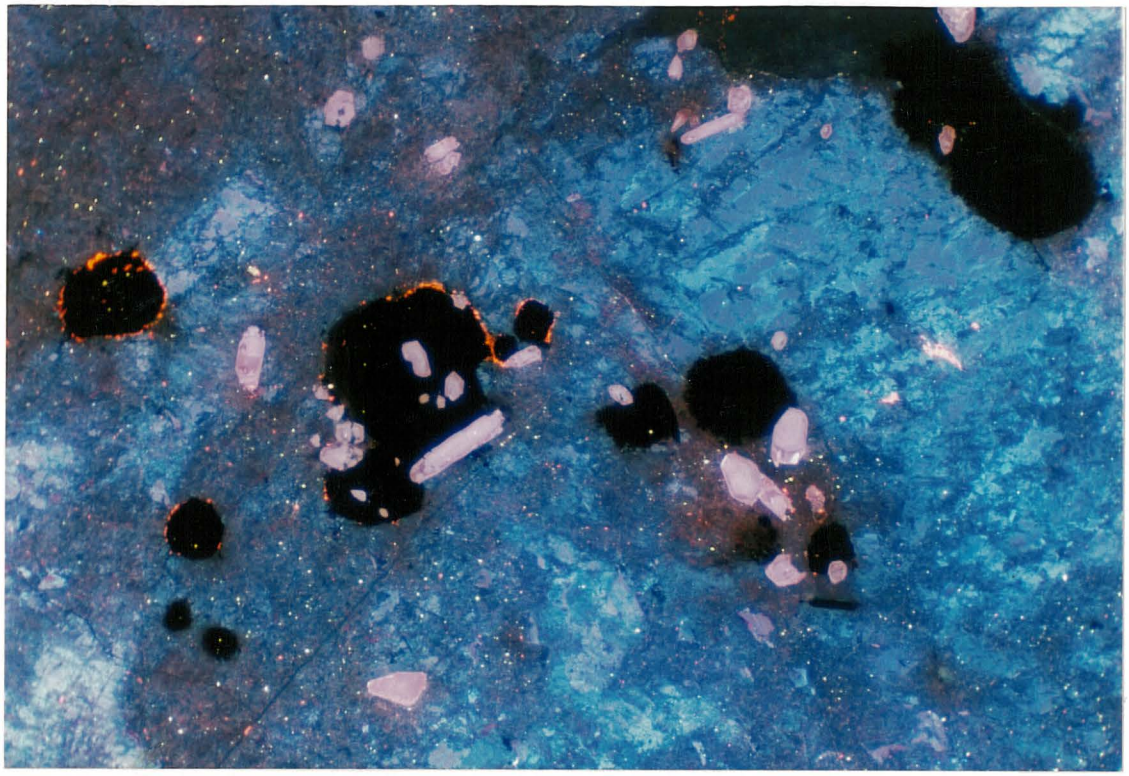

Fig. 10.3-14. Mantled apatite crystals in the unrecrystallized nepheline syenite (Sample C472), Center II. The apatite crystals are mantled with a pink to light pink luminescent core and a brownish pink luminescent rim. The brownish pink luminescent rim is relpaced by a light pink luminescent secondary apatite. Scale: 55 mm on photograph=1 mm on thin section. (CL conditions: 10 kV, 0.8 mA. Photographic conditions: 1.5m, ASA 400).

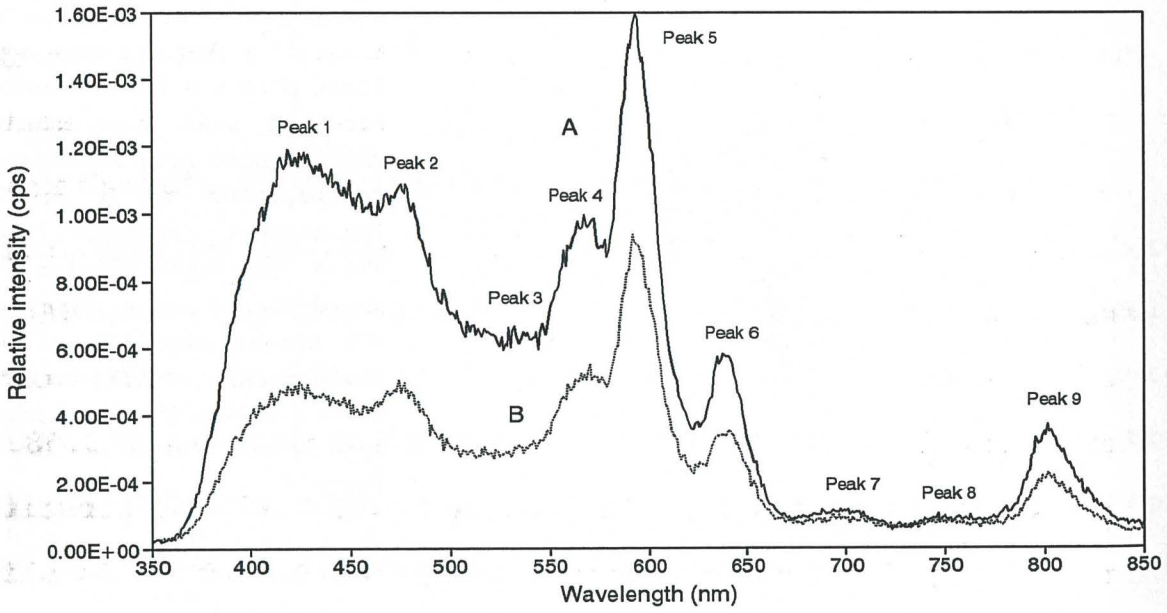

Fig. 10.3-15. CL spectra of the mantled apatite in the unrecrystallized nepheline syenite (Sample C472), Center II. Spectrum (A) is from the light pink luminescent core. Spectrum (B) is from the pink luminescent rim. CL conditions: 10 kV, 0.8 mA.

than the light pink zones (or cores), the CL spectra show that the pink or brownish pink zones have relatively higher ratios of Dy^{3+}, Sm^{3+} and Pr^{3+} to Eu^{2+} (or Ce^{3+}) than the light pink zones. This indicates that divalent REE, such as Eu^{2+} is depleted, and trivalent REE, such as Dy^{3+}, Sm^{3+} and Pr^{3+} are enriched during apatite crystallization.

During late-stage fluid alteration, apatite crystals usually develop irregular-shaped brownish pink luminescent reaction zones along the margins. The reaction rims have high total REE contents and Si. Some of the reaction rims are in turn replaced by light pink luminescent secondary apatites. The secondary apatites have relatively lower contents of total REE and Si than the original apatites.

The apatite crystals in Center II syenites generally are characterized by a LREE-enrichment, and are similar to those apatites as found in Center I syenites. The coupled substitution of $Ca^{2+}+P^{5+}\rightleftarrows REE^{3+}+Si^{4+}$ in apatites is also similar to Center I apatites. However, the regression line in the (Ca+P) vs. (Si+REE) diagram has a slope of approximately 1.03 (Fig 10.3-16b), which is slightly steeper than that in the Center I apatites. Figure 10.3-16a shows that the Ca^{2+} is also substituted by divalent REE, but the regression line of Si versus REE has a slope about 0.68. This correlation indicates that the charge balance of REE substitution for Ca^{2+} is maintained by approximately 2/3 Si^{4+} which is slightly higher than that in Center I apatites. This suggests that the content of the divalent REE in Center II apatites is relatively

lower than that in Center I apatites.

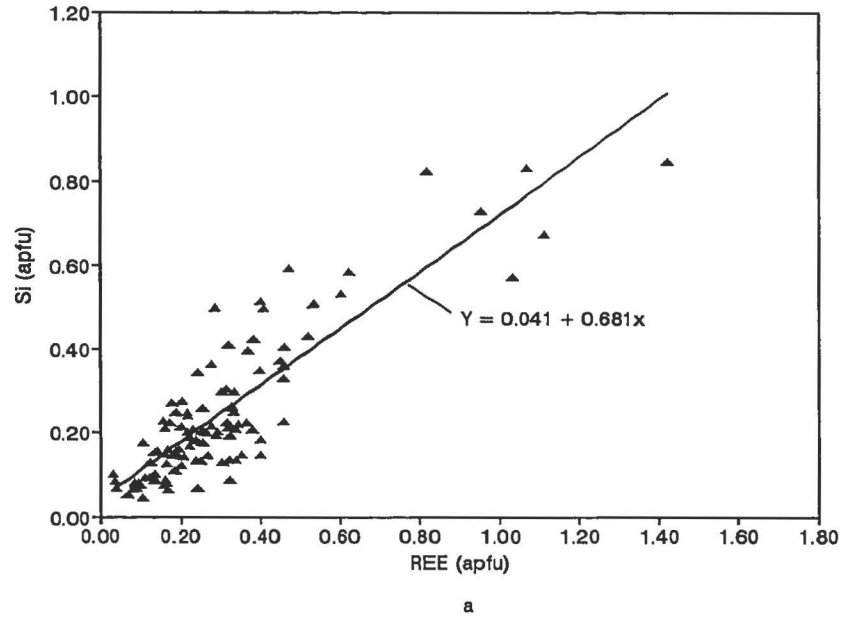

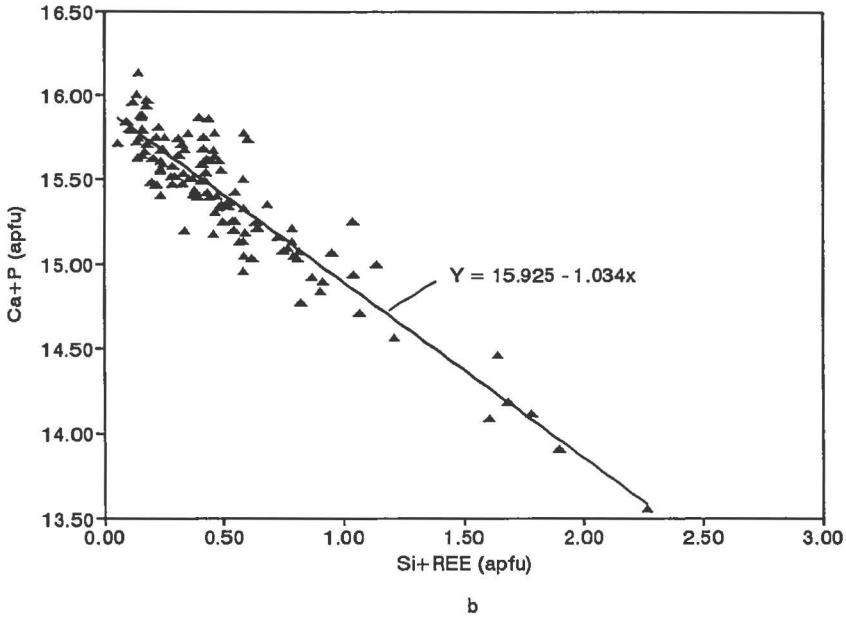

Fig. 10.3-16. Coupled substitutions involving REEs and Si in apatites from Center II syenites. (a) The variation in REE as a function of Si with a regression line slope of 0.681. (b) The variation in (Si+REE) as a function of (Ca+P) with a regression line slope of -1.034.

10.4. Apatite crystals in Center III

10.4.1. Apatite crystals in the magnesio-hornblende syenite

In the magnesio-hornblende syenite (samples C2123 and C180), apatite crystals commonly are euhedral, long prismatic crystals and exhibit uniform pink luminescence (Fig. 7.1-1b, -2b). The CL spectrum of the pink apatite is shown in Fig. 10.4-1, and is similar to that of the light pink apatite crystals from Center I and Center II. SEM/EDS analyses show that the pink apatite crystals contain 0.07-0.17 apfu total REE (n.d.-0.04 apfu La, 0.03-0.07 apfu Ce, n.d.-0.03 apfu Pr and n.d.-0.03 apfu Nd) with n.d.-0.09 apfu Si (Appendix 4-3).

10.4.2. Apatite crystals in the ferro-edenite syenite

In the ferro-edenite syenite (C2124, C2224, C2232, C2068, C294 and C322), most apatite crystals are fine-grained and usually exhibit pink or brownish pink luminescence. The CL spectrum of the pink apatite from sample C2068 (Fig. 10.4-2), consists of peak 1 and peak 2 with a moderate intensity, and peak 4 and peak 5 with a high intensity. In comparison with the pink apatite in the magnesio-hornblende syenite, the pink apatite in the ferro-edenite syenite has a relatively higher ratio of the peaks 4 and 5 to peaks 1 and 2. This may indicate that the apatite has a relatively higher ratio of Dy^{3+}, Sm^{3+} and Pr^{3+} activators to Eu^{2+} (Ce^{3+}) activators.

In some syenite samples (e.g., C1478), however, apatite crystals are mantled with a pink luminescent core and a brownish pink luminescent rim (Fig. 10.4-3a). The CL spectrum from the pink core

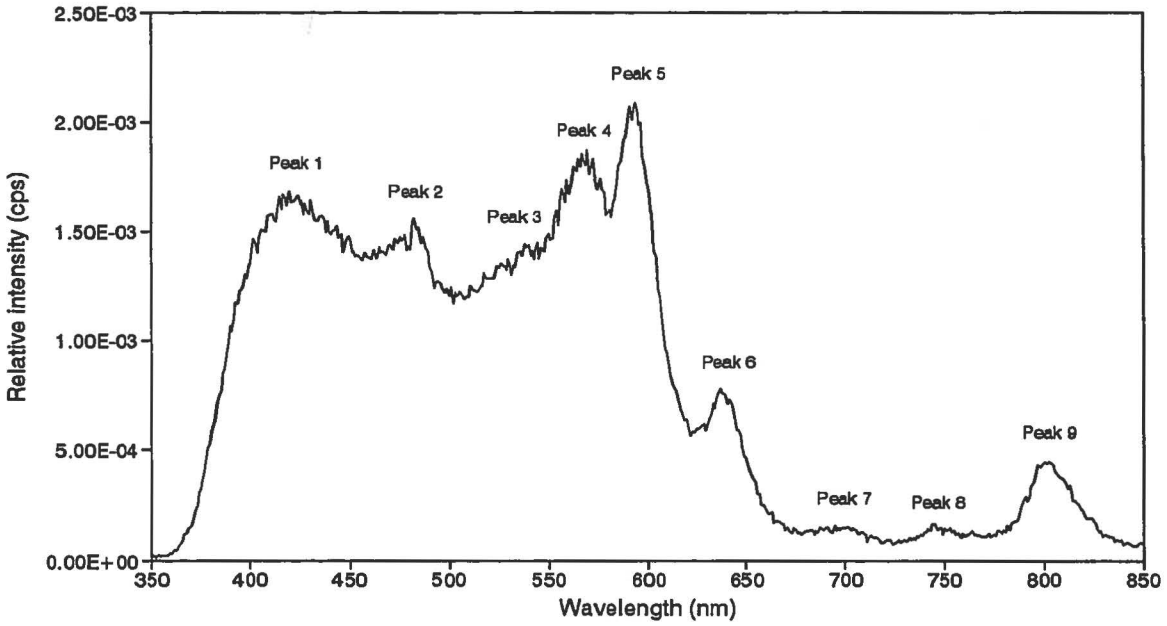

Fig. 10.4-1. CL spectrum of pink luminescent apatite in the magnsio-hornblende syenite (Sample C2123), Center III. CL conditions: 10 kV, 0.8 mA.

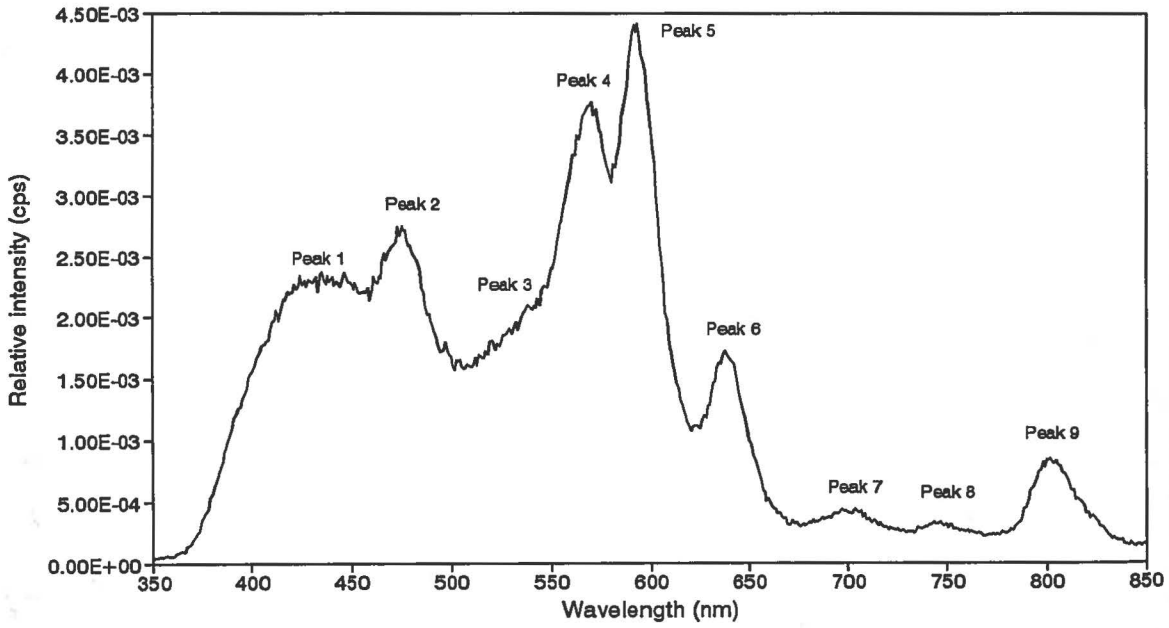

Fig. 10.4-2. CL spectrum of pink luminescent apatite in the ferro-edenite syenite (Sample C2068), Center III. CL conditions: 10 kV, 0.8 mA.

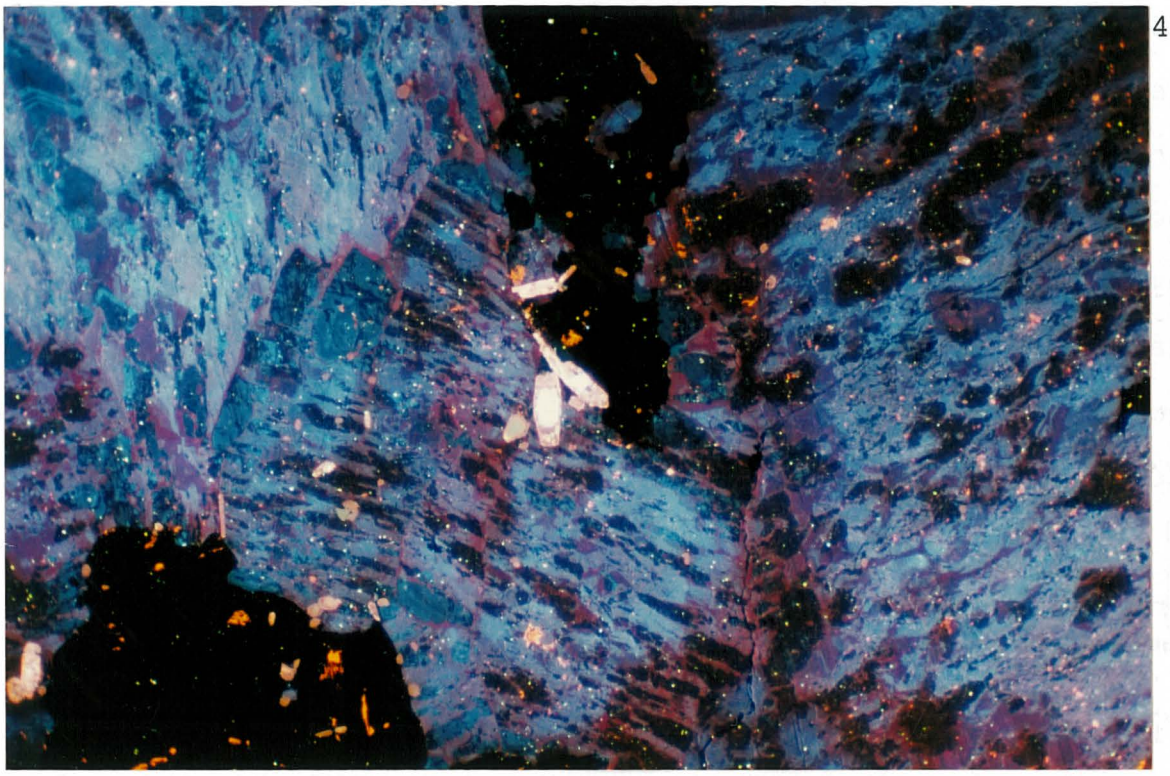

Fig. 10.4-3a. Mantled apatite crystals in the ferro-edenite syenite (Sample 1478), Center III. The apatite crystals are mantled with a light pink luminescent core and an irregular-shaped, brownish pink luminescent rim. Scale: 55 mm on photograph = 1 mm on thin section. (CL conditions: 10 kV, 0.8 Am. Photographic conditions: 50s, ASA 400).

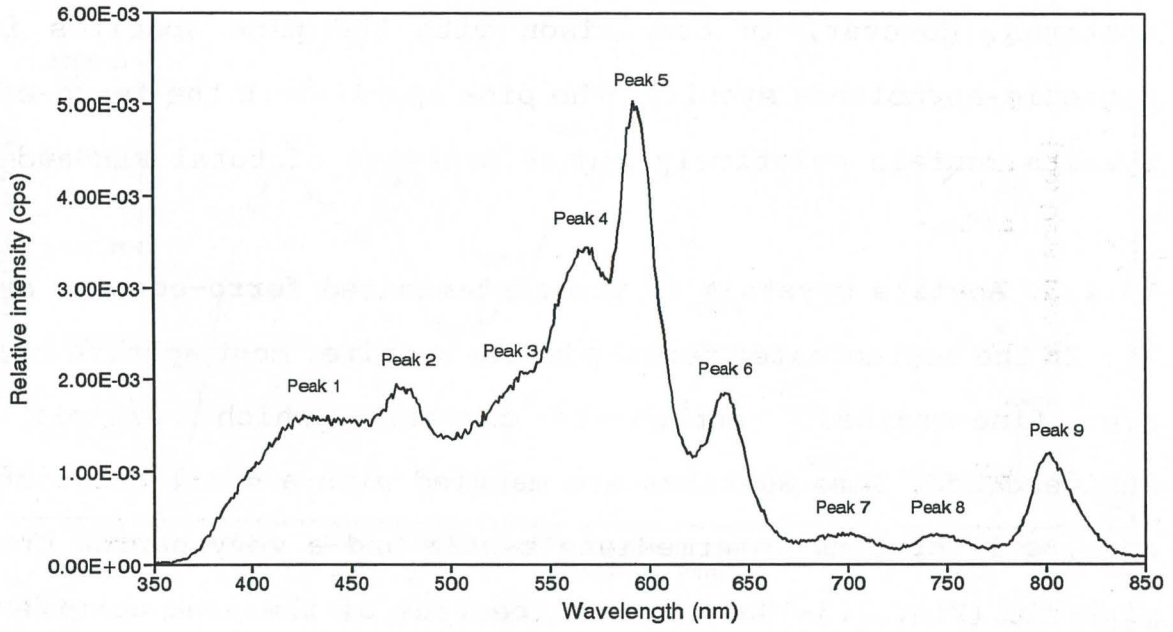

Fig. 10.4-3b. CL spectrum of a mantled apatite in the ferro-edenite syenite (Sample C1478), Center III. The spectrum is from the pink luminescent core. CL conditions: 10 kV, 0.8 mA.

is shown in Fig. 10.4-3b. In comparison with the pink apatite in the sample C2068, this spectrum has a relatively higher ratio of peaks 4 and 5 to peaks 1 and 2. This may indicate a higher ratio of Dy^{3+}, Sm^{3+} and Pr^{3+} activators to Eu^{2+} (Ce^{3+}) activators. Further, the data suggest that the proportions of Dy^{3+}, Sm^{3+} and Pr^{3+} activators to Eu^{2+} (Ce^{3+}) activators vary between individual samples of ferro-edenite syenite.

Pink apatite crystals (or cores) contain 0.09-0.34 apfu total REE (n.d.-0.09 apfu La, 0.05-0.21 apfu Ce, n.d.-0.05 apfu Pr and n.d.-0.34 apfu Nd) with n.d.-0.30 apfu Si (Appendix 4-3). The brownish pink apatite crystals (or rims) contain 0.50-0.80 apfu total REE (n.d-0.17 apfu La, 0.09-0.42 apfu Ce, n.d.-0.14 apfu Pr and 0.09-0.23 apfu Nd) with 0.36-0.69 apfu Si. The contents of total REE and Si in the pink apatites are higher than those of the browinsh pink apatites. However, in comparison with the pink apatites in the magnesio-hornblende syenite, the pink apatites in the ferro-edenite syenite contain relatively higher contents of total REE and Si.

10.4.3. Apatite crystals in the contaminated ferro-edenite syenite

In the contaminated ferro-edenite syenite, most apatite crystals are fine-grained, subhedral crystals which exhibit pink luminescence. Some apatites are mantled with a small brownish pink core, a light pink intermediate mantle and a very narrow brownish pink rim (Fig. 7.3-10b). The CL spectrum of the pink apatite (Fig. 10.4-4) shows that peaks 1 and 2 have lower luminescent intensities than peaks 4 and 5. In comparison with the spectrum of the pink

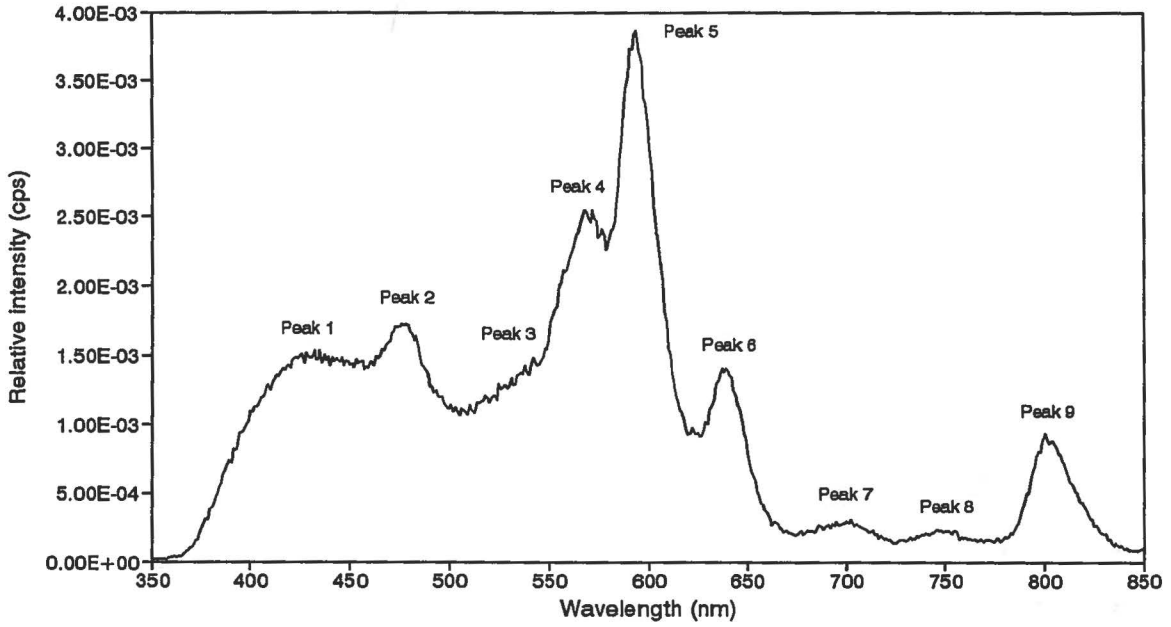

Fig. 10.4-4. CL spectrum of the pink luminescent apatite in the contaminated ferroedenite syenite (Sample C2036), Center III. CL conditions: 10 kV, 0.8 mA.

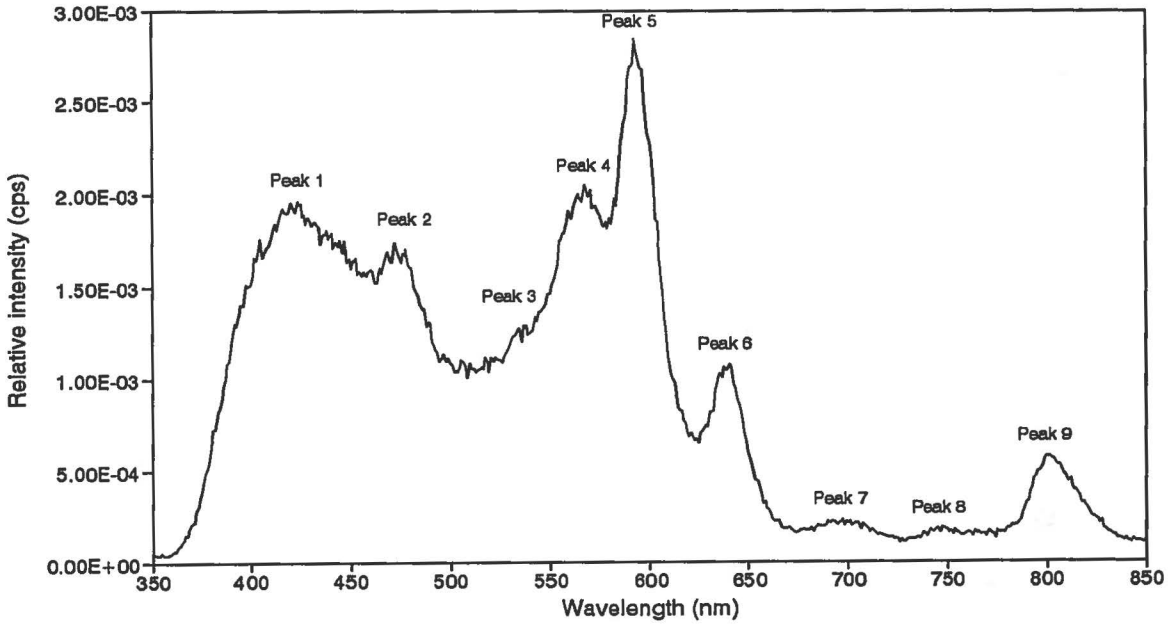

Fig. 10.4-5. CL spectrum of the pink luminescent apatite in the quartz syenite (Sample C2087), Center III. CL conditions: 10 kV, 0.8 mA.

apatite from the magnesio-hornblende syenite, this spectrum has a relatively higher ratio of peaks 4 and 5 to peaks 1 and 2. This may indicate that the pink apatite in the contaminated ferro-edenite syenite has a relatively higher ratio of Dy^{3+}, Sm^{3+} and Pr^{3+} activators to Eu^{2+} (or Ce^{3+}) activators. SEM/EDS analyses show that the pink apatite crystals contain 0.14-0.39 apfu total REE (0.03-0.10 apfu La, 0.08-0.17 apfu Ce and 0.02-0.08 apfu Nd) with 0.12-0.33 apfu Si. This pink apatite contains relatively higher contents of total REE and Si than the light pink luminescent apatite crystals in the magnesio-hornblende syenite and the ferro-edenite syenite.

10.4.4. Apatite crystals in the quartz syenite

The quartz syenite consists of two types of apatites, one is homogeneous pink luminescent apatite and other is mantled apatite which is effected by late-stage fluid alteration. In syenite samples C2087 and C2060, the apatite is euhedral, short prismatic crystals which exhibit homogeneous pink luminescence (Fig. 7.4-1b). The syenite is only slightly affected by late-stage fluid alteration as demonstrated by the presence of light blue homogeneous alkali feldspars and an absence of a deuteric coarsened secondary feldspar rim (see section 7.4.2). The CL spectrum of the homogeneous pink luminescent apatite consists of peak 1, 2 and 3 with moderate intensities and peak 5 with a high intensity (Fig. 10.4-5). The spectrum is similar to the pink apatite from the magnesio-hornblende syenite. These homogeneous pink apatites

contain 0.10-0.21 apfu total REE (0.03-0.05 apfu La, 0.05-0.10 apfu Ce, n.d.-0.03 apfu Pr and 0.02-0.03 apfu Nd) with n.d.-0.03 apfu Si. The total REE and Si contents in these apatites are also very similar to that in the pink apatite in the magnesio-hornblende syenite.

In syenite sample C2154, the apatite is also euhedral, short prismatic crystals, however, the CL reveals that the apatite consists of a pink core and an irregular-shaped, brownish pink rim (Fig. 10.4-6b). The syenite is strongly affected by late-stage fluid alteration as demonstrated by the presence of perthites which are mantled by deuteric coarsened antiperthic rims.

Both CL spectra of the pink core and brownish pink rim consist of peak 1 and peak 2 with low intensities, peak 4 with a moderote intensity and peak 5 with a high intensity (Fig. 10.4-7). This indicates that the ratio of Sm^{3+} and Pr^{3+} to Eu^{2+} and Dy^{3+} is relatively higher than the pink apatite in sample C2087.

10.4.5. Summary of apatite crystals in Center III syenites

Most apatite crystals in Center III syenite exhibit light pink to brownish pink luminescence. Some apatite crystals are mantled with a small brownish pink core, a light pink intermediate mantle and a brownish pink rim; or mantled with a pink core and an irregular-shaped brownish pink rim. In general, the brownish pink apatite (cores or rims) has higher contents of total REE and Si than the pink apatite (grains or cores).

The CL spectra show that the homogeneous pink luminescent

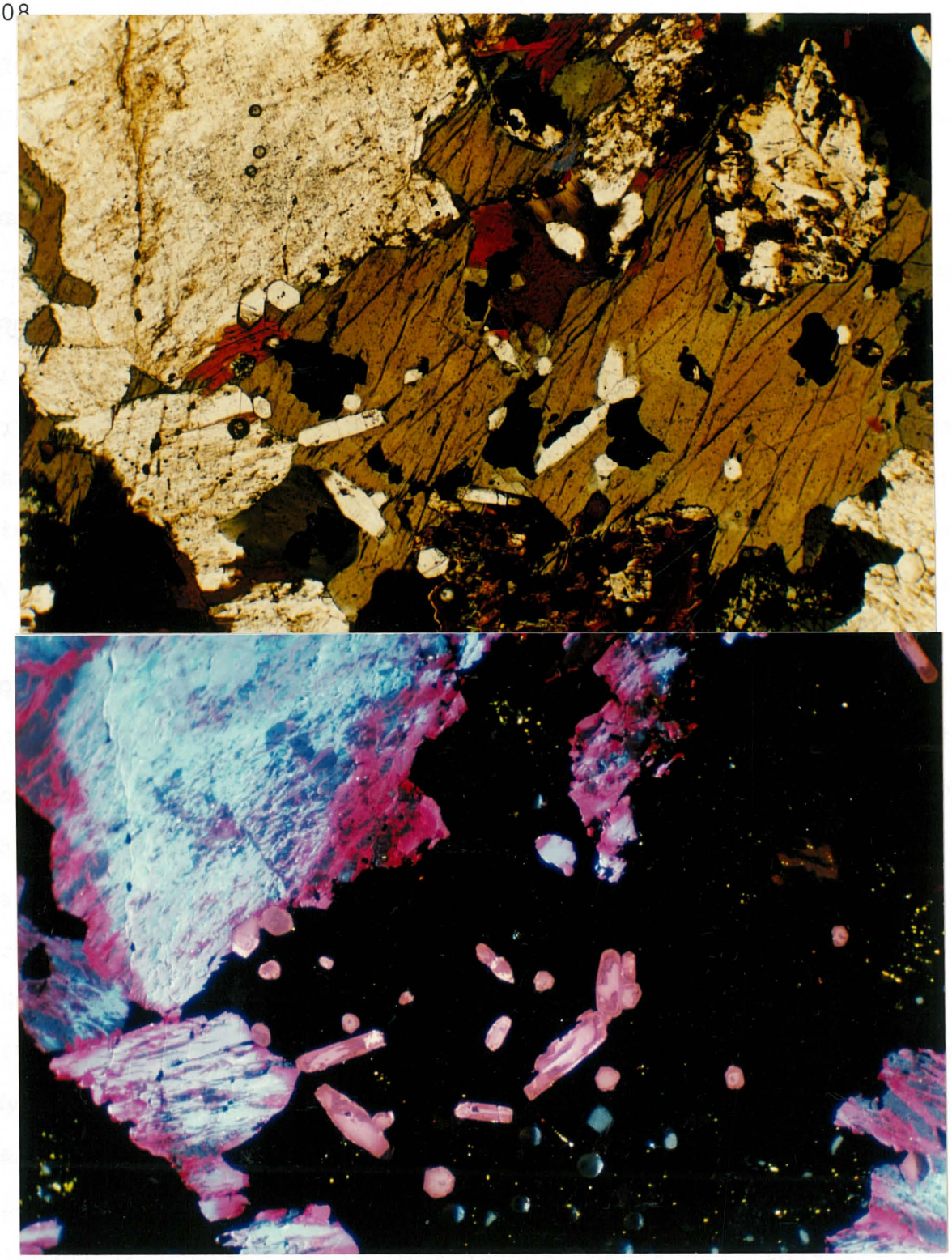

Fig. 10.4-6. Mantled apatite crystals in the quartz syenite (Sample C2154), Center III. a. PoL. (Photographic conditions: 1s, ASA 25). b. CL. The apatite crystals are mantled with a light pink luminescent core and an irregular-shaped brownish pink luminescent rim. The light blue and blue luminescent perthite grains are mantled by a deuteric coarsened antiperthitic rim with red and dull blue luminescence. Scale: 55 mm on photograph = 1 mm on thin section. (CL conditions: 10 kV, 0.8 Am. Photographic conditions: 25s, ASA 400).

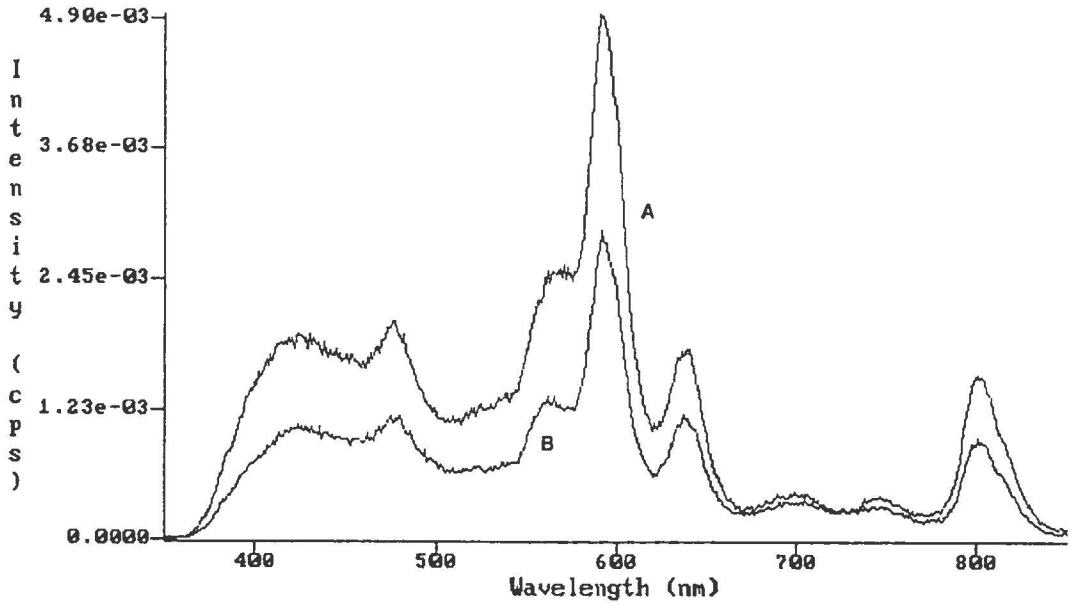

Fig. 10.4-7. CL spectrum of the mantled apatite in the quartz syenite (Sample C2154), Certer III. Spectrum (A) is from the pink luminescent core. Spectrum (B) is from the brownish pink luminescent rim. CL conditions: 10 kV, 0.8 mA.

apatites in the magnesio-hornblende syenite and in some the quartz syenite samples (C2087 and C2060) have relatively higher ratios of Eu^{2+} (or Ce^{3+}) to Dy^{3+}, Sm^{3+} and Pr^{3+} than the pink to brownish pink apatites in the ferro-edenite syenite and the contaminated ferro-edenite syenite.

Some apatites are affected by late-stage fluid alteration, and are zoned with a pink core and an irregular-shaped brownish pink luminescent reaction rim. The CL spectrum shows these apatites are characterized by Sm^{3+} or Pr^{3+} activation.

The apatite crystals in Center III syenites generally are characterized by a LREE-enrichment, and are similar to those apatites found in Center I and Center II syenites. Figure 10.4-8a shows that the total REE have a good correlation with Si, and the

Si versus REE regression line has a slope about 0.78. This indicates that the charge balance of REE substitution for Ca^{2+} is maintained by approximately 4/5 Si^{4+} which is higher than that in Center I and Center II apatites. This also suggests that the substitution of Ca^{2+} involves with both divalent and trivalent REE, but the latter is dominant in Center III apatites. Figure 10.4-8b shows that the REE substitution for Ca^{2+} in Center III apatites mainly involves a coupled substitution with Si^{4+}, but the regression line between (Ca+P) vs. (Si+REE) has a steeper slope of about 1.26 (Fig. 10.4-8b), which indicates that the charge balance may also involve other cations, such as Na^{+1}.

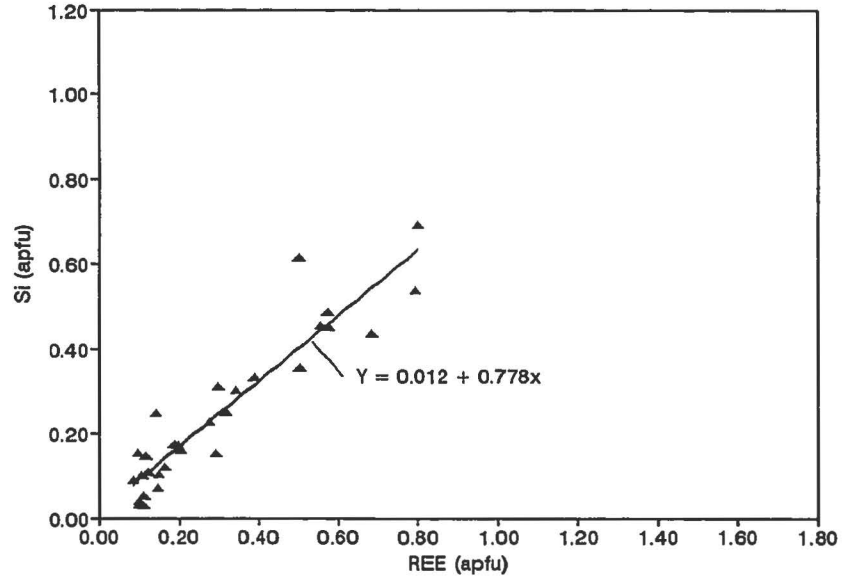

a

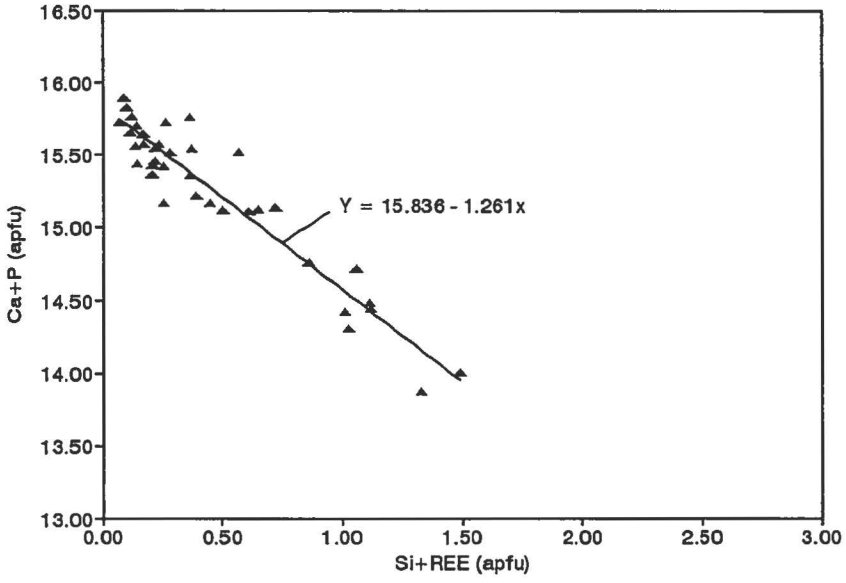

b

Fig. 10.4-8. Coupled substitutions involving REEs and Si in apatites from Center III syenites. (a) The variation in REE as a function of Si with a regression line slope of 0.0.778. (b) The variation in (Si+REE) as a function of (Ca+P) with a regression line slope of -1.261.

CHAPTER 11

CONCLUSIONS

11.1. Introduction

The Coldwell alkaline Complex is located on the north shore of Lake Superior, and is the largest alkaline intrusion in North America. The complex is divided into three Centers which represent three distinct magmatic episodes. Center I rocks consist of gabbro together with layered and massive ferroaugite syenites. The most abundant rocks are saturated ferroaugite syenites which are associated with Fe-rich oversaturated peralkaline syenitic residua. Center II rocks consist of alkali biotite gabbro and undersaturated syenites which include miaskitic nepheline syenite, amphibole nepheline syenite and recrystallized nepheline syenites. Center III syenites are associated with oversaturated residua. Four type syenites have been recognized; these are magnesio-hornblende syenite, ferro-edenite syenite, contaminated ferro-edenite syenite and quartz syenite.

Cathodoluminescence (CL) is a useful petrological tool as it can display textures which may not be seen by standard petrographic techniques. The luminescence colours that CL produces are related to impurities or defects in the minerals. For example, in feldspar crystals, a red luminescence is due to trace amounts of an Fe^{3+} activator whereas light blue luminescence is possibly due to a defect center in the feldspar crystal.

11.2. Feldspars and apatites in Center I syenites

11.2.1. Feldspars in Center I syenites

In the layered ferroaugite syenites, the feldspar crystals in the lower series syenite are mainly light violet blue luminescent optically homogeneous alkali feldspar crystals ($Or_{32-56}Ab_{41-62}An_{1-8}$). Some are mantled by light violet luminescent homogeneous K-rich alkali feldspar rims ($Or_{50-59}Ab_{38-49}An_{1-3}$), or incipient perthitic rims consisting of light blue luminescent exsolved Na-rich feldspar bands ($Ab_{54-64}Or_{29-43}An_{3-7}$) and light violet blue luminescent exsolved K-rich feldspar bands ($Or_{58-60}Ab_{39-41}An_1$). The light violet luminescent alkali feldspar rims usually have higher contents of Or than the light violet blue luminescent alkali feldspar crystals (or cores).

The feldspar crystals in the upper series syenite are mainly optically homogeneous alkali feldspar, irregular vein perthite and patch perthite. The optically homogeneous alkali feldspar is usually mantled and consists of a light blue luminescent core ($Or_{27-36}Ab_{63-72}An_{1-2}$ with 0.47-0.6 mole % $KFeSi_3O_8$), light violet blue luminescent intermediate mantle ($Or_{36-44}Ab_{55-63}An_1$ with 0.91-0.94 mole % $KFeSi_3O_8$) and a light violet rim ($Or_{40-41}Ab_{59-60}An_1$ with 0.9-1.21 mole % $KFeSi_3O_8$). The Or and Fe contents increase from the core through the mantle to the rim. The irregular vein and patch perthite crystals usually consist of light blue luminescent exsolved albite ($Ab_{87-97}Or_{1-10}An_{1-6}$), dull blue luminescent exsolved K-rich feldspar ($Or_{61-82}Ab_{17-38}An_{1-3}$), and light greyish blue to light bluish violet luminescent cryptoperthitic patches ($Or_{34-52}Ab_{47-64}An_{1-3}$ with 0.51-1.58 mole % $KFeSi_3O_8$) or are zoned with a light violet

luminescent cryptoperthite mantle ($Or_{37-50}Ab_{52-61}An_1$). However, a few individual light blue luminescent albite grains are found in sample C68.

In both series of syenites, the presence of the homogeneous alkali feldspars are mantled by the K-rich feldspar rims, which indicates that the residual liquids became richer in Na_2O as the magma continued to crystallize. The feldspars in the upper series syenite to be crystallized under more hydrous condition than in the lower series syenite, since the individual albite grains coexist with the homogeneous alkali feldspar are found in the upper series syenite. The more irregular vein and patch perthite which occur in the upper series syenite reflects a slower cooling rate than the lower series syenite.

The late-stage fluid induced deuteric coarsening and replacement of the alkali feldspar in the lower series syenite is different from that in the upper series syenite. In the lower series syenite, the alkali feldspar crystals are commonly replaced by two discrete secondary feldspars: violet luminescent secondary albite (Ab_{87-98} $Or_{0-7}An_{0-10}$) and purle luminescent secondary K-feldspar (Or_{85-99} $Ab_{0-14}An_{0-1}$), which are found along the margins or within the original feldspar crystals. A red luminescent (or non luminescence) secondary albite coarsened rim is rarely observed.

In the upper series syenite, most of the alkali feldspar crystals are mantled by an antiperthitic rim, which consists of the deep red luminescent secondary albite ($Ab_{87-97}Or_{1-10}An_{2-6}$) and the grey to brown luminescent secondary K-feldspar ($Ab_{96-99}Or_{1-3}An_1$). The grey to brown

luminescent secondary K-feldspar usually contains numerous micropores and Fe-bearing minerals. Both of the secondary feldspars contain higher Fe contents than the original feldspar, and especially red luminescent secondary albite. In the basal level of the lower series syenite, light blue luminescent homogeneous alkali feldspar crystals are replaced by dull blue luminescent oligoclase ($Ab_{71-77}An_{17-21}Or_{3-9}$), which has been further affected by late-stage fluids which result in the formtion of a dark blue to dark purple luminescent secondary oligoclase-albite rim ($Ab_{77-86}An_{12-16}Or_{2-8}$). This replacenemt is different from fluid-induced deuteric replacement and coarsening in both syenite series.

The late-stage fluid in upper series syenite appear to be more abundant than in the lower series syenite, as most of the alkali feldspar crystals in the upper series are mantled by an antiperthitic rim. In the upper series, the deep red luminescent secondary albite (2.58 mole % $KFeSi_3O_8$ in average) and the brown luminescent secondary K-feldspar (1.90 mole % $KFeSi_3O_8$ in average) have higher Fe contents than the violet to deep red luminescent secondary albite (0.48 mole % $KFeSi_3O_8$ in average) and the dull blue to purple luminescent secondary K-feldspar (0.38 mole % $KFeSi_3O_8$ in average) in the lower series syenite. Both the luminescence colour and Fe contents indicate that the late-stage fluid in the upper series syenite has a relatively higher oxygen fugacity than in the upper series syenite. Mitchell and Platt (1977) concluded that the trapped intercumulus liquids in the lower series syenite evolved in a closed system, whereas the trapped liquids in the upper series

syenite evolved in a relatively open system.

The thermal history of the alkali feldspars in the layered ferroaugite syenites can be divided into three principal events: (1) crystallization at high temperatures about ≥ 700 °C, (2) formation of incipient perthite or microperthite over a temperature range of 650-580 °C, and (3) fluid-induced replacement and deuteric coarsening of perthites at relatively low temperatures. These three thermal events differ in both series of syenites. In the lower series, the light blue to light violet optically homogeneous alkali feldspar (grains or the cores) crystallized at temperatures of about ≥700 °C, and were followed by light violet luminescent K-rich alkali feldspar rims crystallizing at about 720-680 °C. Light violet luminescent K-rich feldspar and light blue luminescent Na-rich feldspar in incipient perthite rims are formed at temperatures about 620-580 °C during cooling. The fluid-induced replacement may occur at about 500 °C to form purple luminescent secondary K-feldspar and violet luminescent secondary albite. Late-stage fluid-induced replacement may extended to temperatures <300 °C and precipitate deep red or non luminescent secondary albites in the interstices.

In the upper series syenite, the light blue to light violet luminescent homogeneous alkali feldspar cores and mantles, the light greyish blue to light bluish violet luminescent cryptoperthitic patches and mantles within in the perthite have crystallized at temperatures ≥700 °C. The microbraid texture of the cryptoperthitic patches developed at temperatures about 600-650 °C

during cooling. With continued cooling, dull blue luminescent exsolved K-feldspar and light blue luminescent exsolved Na-feldspar which occurs around the cryptoperthitic patches within the perthite formed at temperatures of about <580 °C. Deuteric coarsening occurs at low temperatures (<300 °C) to produce antiperthitic rims which consist of grey to brown luminescent secondary K-feldspar and the deep red luminescent secondary albite. Deuteric coarsening also occurs adjacent to fractures within the perthite.

The unlayered ferroaugite syenite unit generally has the same petrographic characteristics as the layered syenite unit. Most alkali feldspar crystals in the unlayered ferroaugite syenite unit consist of light violet blue luminescent homogeneous alkali feldspar, braid microperthite and incipient irregular vein perthite ($Or_{35-49}Ab_{50-64}An_{4-6}$). Some of these alkali feldspars are mantled by a light bluish violet to light violet luminescent alkali feldspar rim ($Or_{42-58}Ab_{42-57}An_{1}$) with high Or contents. These are similar to mantled alkali feldspar crystals found in the layered unit. Late-stage deuteric coarsening in the unlayered ferroaugite syenites mainly results in an antiperthitic rim which surrounds light violet blue luminescent homogeneous alkali feldspar or microperthite, similar to that in the upper series syenite. Deuteric coarsened antiperthitic rim consists of deep red luminescent secondary albite ($Ab_{99-100}Or_{0-1}An_{0-<1}$) and dark brown luminescent secondary K-feldspar ($Or_{91-100}Ab_{0-8}An_{0-1}$). These deuteric coarsened secondary feldspars usually have high average values of $KFeSi_8O_3$ contents, 1.89 (mole %) for the secondary albite and 1.74 (mole %) for secondary K-

feldspar. As the alkali feldspars in these unlayered ferroaugite syenites have similar petrographic and chemical characteristics to the alkali feldspars in the layered syenite unit, their genesis in both layered and unlayered syenites is similar.

Some unlayered ferroaugite syenite samples are porphyritic rocks contain mantled feldspar phenocrysts and groundmass. The mantled feldspar phenocrysts consist of microperthitic cores and light blue luminescent albite rims ($Ab_{80-94}Or_{1-4}An_{3-9}$), and the microperthitic cores consist of dull blue luminescent exsolved K-feldspar ($Or_{79-88}Ab_{11-12}An_1$) and the light blue luminescent exsolved albite ($Ab_{90-93}Or_{1-5}An_{5-7}$). The feldspar of groundmass consists of a light violet blue luminescent tweed microperthite core ($Or_{35-40}Ab_{60-64}An_1$) and a deuteric coarsened antiperthitic rim.

Some unlayered ferroaugite syenite samples contain recrystallized feldspar crystals. The crystals are mantled with light blue luminescent albite cores ($Ab_{79-91}An_{6-8}Or_{2-4}$), intermediate perthitic mantles and the deuteric coarsened antiperthitic rims. The intermediate perthitic mantles consist of light violet blue luminescent microperthitic patches ($Or_{48-53}Ab_{45-50}An_1$), light blue luminescent exsolved albite ($Ab_{93-96}Or_{1-3}An_{3-4}$) and dull blue luminescent exsolved K-feldspar ($Or_{81-93}Ab_{7-8}An_2$).

The thermal history of the alkali feldspars in the unlayered ferroaugite syenite unit is similar to the layered syenite unit. Alkali feldspar crystallized at temperatures ≥725 °C, and exsolved to braid and tweed microperthite at about 650-620 °C during cooling. With continued cooling, the exsolved K-feldspar and albite

formed at non-equilibrium temperatures below 420 and 520 °C, respectively. However, the albite rim of the phenocrysts may have formed at about 600-680 °C. The fluid-induced deuteric coarsening may have ocuurred at low temperatures <350 °C.

11.2.2. Apatites in Center I syenites

Most apatite crystals in Center I syenite exhibit light pink to pink luminescence. Some apatite crystals show growth zones with a small brownish pink luminescent core and a light pink to pink luminescent rim.

The CL spectra of growth zoned apatites show that the brownish pink core has a relatively higher proportion of Eu^{2+} (or Ce^{3+}) to Dy^{3+}, Sm^{3+} and Pr^{3+} than the light pink rims demonstrating that LREE and Eu^{2+} are depleted during apatite crystallization. SEM/EDS analyses show that the brownish pink cores have higher contents of total REE and Si than the light pink rims.

Apatite crystals affected by late-stage fluid alteration usually develop brownish pink to brown luminescent reaction rims or exhibit bronze luminescence, which have high total REE contents and Si. Apatites strongly affected by late-stage fluid alteration are found predominantly in the upper series syenite and in some unlayered syenite samples (C100, C101, C305). Some of the apatite reaction rims are in turn replaced by yellow or light pink luminescent secondary apatites. The secondary apatites have relatively lower contents of total REE and Si. The CL spectra show that the yellow luminescent secondary apatite is characterized by Dy^{3+} and Tb^{3+}

activation indicating that the final late-stage fluid alteration produces MREE-HREE-rich secondary apatites.

The apatite crystals in Center I syenites generally are characterized by a LREE-enrichment. The REE substitution for Ca^{2+} in the apatite structure mainly may involve a coupled substitution of $Ca^{2+}+P^{5+}\rightleftarrows REE^{3+}+Si^{4+}$. This coupled substitution can be illustrated in a (Ca+P) versus (Si+REE) diagram (Fig 10.2-8b). The (Ca+P) shows a good correlation with (Si+REE) and the regression line has an intersection point (15.8) on the (Ca+P) axis and a slope of approximately 0.97. The intersection point 15.8 is approximately equal to the total cations (16) in a formula unit of apatite, and the slope of regression line of 0.97 indicates a 1:1 substitution between (Ca+P) and (Si+REE). However, the Ca^{2+} is also substituted by divalent REE such as Eu^{2+} activation as found in most CL spectra. Figure 10.2-8a shows that the total REE have a good correlation with Si, with a slope of the regression line approximately equal to 0.56. This correlation indicates that the charge balance of REE substituted Ca^{2+} is maintained by approximately 1/2 Si^{4+}, which suggests that the substitution may be as follows: $2Ca^{2+}+P^{5+}\rightleftarrows(REE^{2+}+REE^{3+})+Si^{4+}$.

11.3. Feldspars and apatites in Center II syenites

11.3.1. Feldspars in Pic Island layered syenites

The layered syenites in Pic Island consist of amphibole nepheline syenite and miaskitic nepheline syenite. In the amphibole nepheline syenite, the feldspar crystals consist of light violet blue

luminescent homogeneous alkali feldspar ($Or_{39-50}Ab_{45-56}An_{2-6}$). The margins of the homogeneous alkali feldspar are usually exsolved into perthite which consists of light blue luminescent oligoclase ($Ab_{84-89}Or_{1-3}An_{9-15}$) and light violet luminescent K-feldspar ($Or_{61-66}Ab_{33-37}An_{1-2}$). In the miaskitic nepheline syenite, the feldspar crystals consist of light blue luminescent oligoclase ($Ab_{73-79}An_{19-22}Or_{1-6}$) and light violet blue luminescent homogeneous alkali feldspar ($Or_{56-70}Ab_{28-42}An_2$).

Late-stage, fluid-induced replacement of the feldspars in the amphibole nepheline syenite differ from the miaskitic nepheline syenite. As the fluid-feldspar interaction occurs in the amphibole nepheline syenite, the homogeneous alkali feldspar crystals are usually replaced by two discrete secondary feldspars which consist of light violet blue to light violet secondary albite ($Ab_{90-98}Or_{1-2}An_{4-9}$ with 0.4-0.75 mole % $KFeSi_3O_8$) and dull blue to dark brown luminescent secondary K-feldspar ($Or_{87-97}Ab_{2-12}An_1$ with 0.27-31 mole % $KFeSi_3O_8$). In the miaskitic nepheline syenite, however, the oligoclase crystals are replaced by greyish blue or grey luminescent secondary K-feldspars ($Or_{62-81}Ab_{17-35}An_{1-3}$ with 0.22-0.61 mole % $KFeSi_3O_8$) along the margins or within the crystals during late-stage fluid alteration. Since the secondary feldspars in both of the syenites contain very low Fe contents, and red luminescent secondary albite has not been observed, the late-stage fluid alteration may have occurred at a very low oxygen fugacity state, which is similar to that in the lower series layered ferroaugite syenite in Center I.

The thermal history of the feldspars in the amphibole nepheline syenite and the miaskitic nepheline syenite can be divided into four events: (1) the oligoclase and the homogeneous alkali feldspar crystallized at high temperatures about 750 °C and ≥710-620 °C, respectively. (2) The Na-feldspar and K-feldspar in the margins of the homogeneous alkali feldspar have exsolved at temperatures about 600-550 °C during cooling. (3) The secondary K-feldspar may have replaced the oligoclase at about 650-500 C° during an early fluid-feldspar interaction. (4) The two discrete secondary feldspars replacement may have occurred at very low temperatures <350 °C during late-stage fluid-induced deuteric alteration.

11.3.2. Feldspars in Neys Park syenites

Neys park syenites consist of perthitic nepheline syenite and miaskitic nepheline syenite. The perthitic nepheline syenite is light grey rock and contains many white to brick-red peralkaline pegmatitic patches. Alkali feldspars in the syenite consist of coarse-grained irregular vein and patch perthite; and fine-grained cross-hatched microcline and regular to irregular vein perthite. Both the coarse-grained and fine-grained perthites consist of light blue luminescent exsolved albite ($Ab_{95-99}Or_{1-2}An_{1-4}$) and dull blue luminescent K-feldspar host ($Or_{84-93}Ab_{6-15}An_1$). Some of the fine-grained perthite contains unexsolved, light violet or light violet blue luminescent alkali feldspar ($Or_{73-75}Ab_{24-26}An_1$) in the centre, and cross-hatched twinned, blue luminescent microcline ($Or_{93-96}Ab_{3-6}An_1$) at the margins. Alkali feldspars in the pegmatitic patches consist

of dull blue luminescent K-feldspar ($Or_{89-97}Ab_{3-10}An_{<1}$) and dull red luminescent albite ($Ab_{97-99}Or_{2-1}An_1$).

In the miaskitic nepheline syenite, most feldspar crystals are mantled with a bluish grey luminescent oligoclase core and a light blue luminescent alkali feldspar rim. However, some fine-grained alkali feldspar crystals are unmantled with light blue luminescence. For the mantled feldspar crystals, the oligoclase cores have a composition of $Ab_{73-76}An_{22-26}Or_{1-2}$, whereas the alkali feldspar rims range in composition from $Or_{38-48}Ab_{49-57}An_{3-6}$.

Late-stage fluid-induced deuteric coarsening and replacement in the perthitic syenite differ from the miaskitic nepheline syenite. In the perthitic syenite, late-stage fluid-induced alteration produces two discrete secondary feldspars by replaced and coarsened the coarse-grained perthite. The secondary feldspars usually occur at the margins of the coarse-grained perthite and consist of violet or red luminescent albite ($Ab_{97-98}Or_1An_{1-2}$) and dull blue or brown luminescent K-feldspar ($Or_{97-100}Ab_{0-3}An_{0-1}$). With continued replacement and coarsening, red to deep red luminescent secondary albites ($Ab_{97-99}Or_1An_{1-2}$) are formed which as a rim surrounding the fine- and coarse-grained perthite. The K-feldspar in the pegmatitic patches is also strongly replaced by dull red luminescent secondary albite ($Ab_{97-99}Or_{2-1}An_1$) during late-stage fluid alteration. In the miaskitic nepheline syenite, however, late-stage fluid alteration produces dull violet luminescent secondary K-feldspar ($Or_{48-50}Ab_{46-49}An_{3-4}$) and nepheline which replace the oligoclase core, and alters the light blue luminescent alkali feldspar rim into dull violet luminescent

secondary K-rich feldspar ($Or_{52-65}Ab_{33-45}An_{2-3}$). These CL and compositional characteristics indicate that the late-stage fluid in the perthitic syenite is Na-rich with a relatively high oxygen fugacity, whereas the late-stage fluid in maiskitic nepheline syenite is a K-rich fluid with a relatively low oxygen fugacity.

The thermal history of the alkali feldspars in the perthitic nepheline syenite can be divided into four events: (1) the unexsolved alkali feldspars in the centre of the fine-grained perthite may have formed at temperatures about 575-450 °C. (2) The perthite texture formed at temperatures about 450 °C during cooling. (3) The host K-feldspar may be converted to the cross-hatched microcline along margin areas at a temperature about 300 °C during cooling. However the time of formation of microcline is not very clear, it may be involved with late-stage fluid-feldspar interaction. (4) Since the deuteric coarsened or replaced secondary albite and K-feldspar have end member compositions, they may have formed at a low temperature below 300 °C during late-stage fluid alteration.

For the feldspars in the pegmatitic patches in the perthitic nepheline syenite, the crystallization of K-feldspar and albite may be only considered under the incoherent solvus producing two unmixed feldspars since no perthitic texture was observed in the pegmatitic patches. The crystallization temperatures of the K-feldspar range from 550 to 500 °C, whereas the albite range from 475 to 300 °C.

The thermal history of the feldspars in the miaskitic nepheline

syenite can be divided into three events: (1) the oligoclase crystallized at a high temperature about 800 °C, and (2) the alkali feldspar rim crystallized at temperatures ≤725 °C. (3) The secondary K-rich feldspar may have formed at temperatures about 700-500 °C. This temperature range agrees with the secondary K-rich feldspar-nepheline equilibrium temperatures which were determined by the nepheline geothemometer.

11.3.3. Feldspars in the recrystallized nepheline syenites

The recrystallized nepheline syenites consist of mosaic granuloblastic nepheline syenites and porphyroblastic nepheline syenites. The mosaic granuloblastic nepheline syenites contain non luminescent plagioclase relicts (bytownite, $An_{70-79}Ab_{21-29}Or_1$), light blue luminescent alkali feldspar relicts ($Or_{64-85}Ab_{13-35}An_{1-2}$) and light violet blue to light violet luminescent alkali feldspar neoblasts ($Or_{52-71}Ab_{27-47}An_{1-2}$).

The porphyroblastic nepheline syenites contain zoned alkali feldspar porphyroblasts, zoned plagioclase relicts and light blue to light violet blue luminescent relicts and neoblasts of alkali feldspar ($Or_{45-62}Ab_{39-51}An_{1-5}$) groundmass. The zoned alkali feldspar porphyroblasts are usually mantled with a relict feldspar core, a narrow reaction zone (intermediate mantle) and a broad recrystallized rim. In each porphyroblastic grain, the relict feldspar cores have a variety of luminescence colours and compositions, which are mainly light blue luminescent albite ($Ab_{84-88}Or_{5-7}An_{7-9}$), and light blue to light violet luminescent

unexsolved alkali feldspar ($Or_{28-55}Ab_{40-59}An_{3-7}$). Some of the unexsolved feldspar relict cores are exsolved into perthite along the edges. The perthite consists of light violet blue luminescent exsolved albite ($Ab_{89-93}Or_{2-5}An_{2-5}$) and light bluish violet luminescent exsolved alkali feldspar ($Or_{33-43}Ab_{55-63}An_{1-4}$). The reaction zone (mantle) usually consists of dull blue luminescent K-rich feldspar ($Or_{65-75}Ab_{25-34}An_{1}$) which is commonly hematitized; however, some mantles are intergrowths of K-rich feldspar ($Or_{68-94}Ab_{6-30}An_{1-2}$) and albite ($Ab_{87-90}Or_{5-10}An_{3-5}$) or oligoclase ($Ab_{73-77}An_{6-30}Or_{1-2}$). All of the recrystallized rims are unexsolved alkali feldspars with a range in composition from $Or_{45-65}Ab_{34-53}An_{1-2}$. Most of the recrystallized alkali feldspar rims generally reveal a range in luminescence colour from a dull blue inner rim to a light violet blue intremediate rim to a light violet luminescence outer rim with a decreasing Or content from the inner rim to the intermediate rim and then an increasing Or content in the outer rim. The zoned plagioclase relicts are mantled with small, blue luminescent andesine cores ($Ab_{48-58}An_{42-49}Or_{1-2}$) and larger light violet luminescent oligoclase rims ($Ab_{66-73}An_{25-33}Or_{1-6}$).

The neoblasts in the granuloblastic nepheline syenite has higher Or contents and is more recrystallized than the groundmass and recrystallized rims found in the porphyroblastic nepheline syenite. Mitchell and Platt (1982) also found that more evolved syenites in Center II are enriched in potassium.

After a detail study of recrystallization textures of felsic minerals, Mitchell and Platt (1982) suggested that the deformation

and recrystallization in Center II " must have occurred at temperatures which were high enough to promote rapid diffusion and to allow extensive grain boundary migration and bulge nucleation from subgrains ".

The process of initial recrystallization may involve a K_2O-rich metasomatic fluid which reacted with the original feldspars (alkali feldspars and plagioclase relicts) then crystallized along the margin of the relicts to form a K-rich feldspar mantle. The metasomatic fluid-feldspars interation caused a re-distribution of the K and Na contents of the original feldspars. After the mantles were formed, the K contents were depleted in the metasomatic fluid. The first recrystallized inner rims were formed under Na-rich conditions in comparison with the mantles. As the recrystallization progressed, the K content in the metasomatic fluid may have increased slightly again.

11.3.4. Apatites in Center II syenites

Most apatite crystals in Center II syenite exhibit light pink to pink luminescence. Some apatite crystals are mantled with a small brownish pink core and a light pink to pink rim which is similar to the mantled apatites found in Center I syenites. Some crystals are mantled with light pink to pink cores and brownish pink rims, or show light pink to pink alternating oscillatory zones.

Although, SEM/EDS analyses show that the pink or brownish pink zones (mantles or rims) have higher contents of total REE and Si than the light pink zones (or cores), the CL spectra show that the

pink or brownish pink zones have relatively higher ratios of Dy^{3+}, Sm^{3+} and Pr^{3+} to Eu^{2+} (or Ce^{3+}) than the light pink zones. This indicates that divalent REE, such as Eu^{2+} is depleted, and trivalent REE, such as Dy^{3+}, Sm^{3+} and Pr^{3+} are enriched during apatite crystallization.

During late-stage fluid alteration, apatite crystals usually develop irregular-shaped brownish pink luminescent reaction zones along the margins. The reaction rims have high total REE contents and Si. Some of the reaction rims are in turn replaced by light pink luminescent secondary apatites. The secondary apatites have relatively lower contents of total REE and Si than the original apatites.

The apatite crystals in Center II syenites generally are characterized by a LREE-enrichment, and are similar to those apatites as found in Center I syenites. The coupled substitution of $Ca^{2+}+P^{5+}\rightleftarrows REE^{3+}+Si^{4+}$ in apatites is also similar to Center I apatites. However, the regression line in the (Ca+P) vs. (Si+REE) diagram has a slope of approximately 1.03 (Fig 10.3-16b), which is slightly steeper than that in the Center I apatites. Figure 10.3-16a shows that the Ca^{2+} is also substituted by divalent REE, but the regression line of Si versus REE has a slope about 0.68. This correlation indicates that the charge balance of REE substitution for Ca^{2+} is maintained by approximately 2/3 Si^{4+} which is slightly higher than that in Center I apatites. This suggests that the content of the divalent REE in Center II apatites is relatively lower than that in Center I apatites.

11.4. Feldspars and apatites in Center III syenites

11.4.1. Feldspars in the magnesio-hornblende syenites

The magnesio-hornblende syenites contain light blue to blue luminescent, optically homogeneous K-feldspar crystals ($Or_{86-89}Ab_{10-14}An_{0-1}$), and zoned plagioclase crystals with light greenish blue luminescent cores and light violet blue luminescent rims. Although the composition of the plagioclase varies from grain to grain within each samples, the rims always ($Ab_{67-71}An_{28-32}Or_1$ and $Ab_{84-86}An_{12-13}Or_{2-3}$) have higher Ab contents than the cores ($Ab_{51-55}An_{44-48}Or_{1-2}$ and $Ab_{76-79}An_{19-21}Or_{2-3}$, respectively). Some oligoclase cores contain small, bright, light blue luminescent K-rich feldspar ($Or_{82-88}Ab_{12-18}An_{<1}$) inclusions with higher Ba contents (2.3-3.1 wt.% BaO) than the blue luminescent K-feldspar (0.5-0.8 wt.% BaO).

During late-stage fluid-feldspar interaction, the plagioclase and K-feldspar are replaced by dull violet luminescent secondary oligoclase ($Ab_{72-89}An_{9-25}Or_{1-4}$). The secondary oligoclases occurs as irregular patches in the core of the plagioclase, as an irregular rim surrounding the plagioclase and as an irregular vein cross cutting the K-feldspar grains.

The thermal history of the feldspars in the magnesio-hornblende syenite can be divided into three events: (1) fractional crystallization of the plagioclase at a temperature range from 900-750 °C, however, the initial crystallization temperature of the plagioclase may be higher than 900 °C. Since most of the light greenish blue luminescent plagioclase cores have been replaced by secondary plagioclase, the original composition of centre of the

core is unknown. (2) Crystallization of the K-feldspar at a temperature range from 580-450 °C. (3) The late-stage fluid-feldspar interaction may occur at a moderate temperature, since the secondary oligoclase contains a relatively high An content.

11.4.2. Feldspars in the ferro-edenite syenite

In ferro-edenite syenite, feldspars mainly consist of mantled alkali feldspar and irregular vein antiperthite. The mantled feldspar crystals usually consist of original alkali feldspar cores and deuteric coarsened perthitic or antiperthitic rims. The original alkali feldspar cores usually exhibit light blue to light violet blue luminescence. They mainly consist of unexsolved alkali feldspar, braid microperthite, oscillatory zoned alkali feldspar with a composition range from ($Or_{21-48}Ab_{51-78}An_{1-3}$), and rarely are albite with a composition of ($Ab_{90-95}Or_{2-3}An_{3-8}$). Some alkali feldspar crystals are mantled with a light blue luminescent braid microperthite core ($Or_{49-71}Ab_{28-49}An_{1-2}$), a narrow, bright, light blue luminescent albite intermediate mantle ($Ab_{92-97}Or_{1-4}An_{1-6}$), a light violet blue luminescent albite rim ($Ab_{95-98}Or_{1-3}An_{1-3}$) and a deuteric coarsened antiperthitic rim. The deuteric coarsened perthitic and antiperthitic rims consist of dull red to deep red luminescent secondary albite ($Ab_{97-100}Or_{0-2}An_{0-1}$) and dull blue to brown luminescent secondary K-feldspar ($Or_{85-100}Ab_{0-15}An_{0-1}$).

The irregular vein antiperthite crystals consist of light violet blue to dull violet blue luminescent albite host ($Ab_{91-97}Or_{2-7}An_{1-2}$) and dull blue luminescent exsolved K-feldspar ($Or_{88-90}Ab_{9-11}An_{1}$).

However, most irregular vein antiperthite crystals are strongly affected by late-stage fluid-feldspar interactions and have similar luminescence properties and compositions as the deuteric coarsened antiperthitic rim of the mantled feldspar crystals.

The thermal history of the alkali feldspars in the ferro-edenite syenite can be divided into five principle events: (1) the original alkali feldspar crystals crystallized at temperatures about ≥725-520 °C. (2) The braid microperthite textures formed at about 650-420 °C during cooling. (3) The grains with an albite core, and grains with an albite mantle and rim may have formed at a temperature range from 600-450 °C. (4) The exsolved K-feldspar and albite host in the irregular vein antiperthite may have formed during cooling at non-equilibrium temperatures below 370 °C and 520 °C, respectively. They may also be continually diffused at low temperatures during late-stage fluid-feldspar interaction. (5) Since the deuteric coarsened secondary albite and K-feldspar have end member compositions, they formed at very low temperatures about <350 °C.

11.4.3. Feldspars in the contaminated ferro-edenite syenite

In the contaminated ferro-edenite syenite, the feldspar phenocrysts mainly consist of zoned plagioclase, K-feldspar, irregular vein perthite and regular vein antiperthite. Groundmass feldspars mainly consist of K-feldspar, perthite, antiperthite and secondary Na-feldspar.

The zoned plagioclase phenocrysts consist of light greenish blue

luminescent andesine-oligoclase ($Ab_{52-77}An_{21-45}Or_{1-2}$) core and light blue to light violet blue luminescent albite ($Ab_{89-96}An_{3-4}Or_{1-2}$) rim.

Most irregular vein perthite phenocrysts are mantled with an incipient perthitic core, a braid microperthitic intermediate mantle may or may not be present and a deuteric coarsened perthitic rim. The incipient perthitic cores usually contain light blue to light violet luminescent unexsolved alkali feldspar patches ($Or_{30-46}Ab_{54-68}An_{1-3}$), light blue luminescent exsolved albite and light violet blue luminescent exsolved K-feldspar. Some irregular vein perthitic phenocrysts are unzoned and contain light blue luminescent exsolved albite ($Ab_{90-95}Or_{3-8}An_{2-4}$) and light violet blue luminescent exsolved K-feldspar ($Or_{82-94}Ab_{5-17}An_{1}$). The plagioclase and irregular vein perthite phenocrysts are usually surrounded by fine-grained perthite and K-rich feldspar groundmass. The perthite grains in the groundmass contains blue luminescent exsolved albite and violet blue luminescent K-feldspar host. Whereas, the K-rich feldspar grains in the groundmass are usually mantled with a blue luminescent core ($Or_{79-83}Ab_{15-20}An_{1-2}$) and a dull blue luminescent rim ($Or_{91}Ab_{8}An_{1}$).

Most regular vein antiperthite phenocrysts contain dull blue luminescent exsolved K-feldspar ($Or_{88-92}Ab_{7-12}An_{<1}$) and deep red luminescent albite host ($Ab_{97-99}Or_{1-2}An_{<1}$). Some regular vein antiperthite crystals are zoned with a light violet blue luminescent braid microperthitic core or mantle ($Or_{25-43}Ab_{56-74}An_{<1}$). These regular vein antiperthite are surrounded by some fine-grained antiperthite grains (groundmass) which consist of dull blue

luminescent exsolved K-feldspar and deep red luminescent albite host.

K-feldspar phenocrysts ($Or_{86-89}Ab_{11-14}An_{0-2}$) are uncommon, some of them exhibit dull blue luminescence and some have no luminescence.

During late-stage, fluid-induced, deuteric coarsening and replacement, the cores of the plagioclase grains are replaced by dull blue luminescent secondary K-feldspar ($Or_{75-100}Ab_{0-25}An_{0-1}$) and secondary albite ($Ab_{86-88}Or_{10-13}An_{1-2}$). Deuteric coarsening usually occurs at the margins of the unexsolved alkali feldspar and incipient perthitic core to form a secondary perthitic rim, which consists of light blue to light violet secondary albite ($Ab_{95-97}Or_{1}An_{2-5}$) and dull blue to dark blue luminescent secondary K-feldspar. In the feldspar groundmass, the late-stage fluid-feldspar interaction produces dull violet to deep red luminescent secondary albite ($Ab_{93-95}Or_{1-2}An_{4-7}$) as a rim surrounding feldspar grains in the groundmass.

The thermal history of the feldspars in the contaminated ferro-edenite syenite can be divided into seven events: (1) the plagioclase phenocrysts may have fractionally crystallized at a temperature range from 850 to 750 °C. However, initial crystallization temperature of the plagioclase phenocrysts may be higher than 850 °C because most the cores of the plagioclase phenocrysts have been replaced by secondary Na- and K-feldspar, compositions from the centre areas of the plagioclase are unknown. (2) The irregular vein perthite phenocrysts have crystallized at temperatures ≥700 °C. (3) The microperthite textures may have

formed at temperatures 650-620 °C. (4) The albite and K-feldspar in the irregular vein perthite and regular vein antiperthite may have exsolved during cooling at non-equilibrium temperatures below 400 °C and 520 °C, respectively. (5) The K-feldspar phenocrysts may have crystallized at temperatures about 440-360 °C. (6) The mantled K-rich feldspar in the groundmass formed temperatures about 530-350 °C. (7) Since the deuteric coarsened secondary albite and K-feldspar have end member compositions, they formed at a very low temperature below 350 °C.

11.4.4. Feldspars in the quartz syenite

Quartz syenites contain optically homogeneous alkali feldspar, mantled feldspar and irregular vein antiperthite. The optically homogeneous alkali feldspar crystals are usually zoned with a light blue to blue luminescent core ($Ab_{52-71}Or_{26-47}An_{1-3}$) and a light violet blue luminescent rim ($Or_{83}Ab_{15}An_2$) with an incipient perthitic texture along the edges of the rim. The mantled feldspar crystals commonly consist of a light blue luminescent albite core ($Ab_{91-99}Or_{1-9}An_{0-2}$) and a deuteric coarsened antiperthitic rim. Within the deuteric coarsened antiperthitic rim, the albite host ($Ab_{91-96}Or_{4-9}An_{0-1}$) usually exhibits dull red to deep red luminescence and the exsolved K-feldspar ($Or_{99}Ab_1$) exhibits dull blue to dark blue luminescence.

Most irregular vein antiperthite grains reveal alternating dull red, violet, and deep red luminescent oscillartory zones. Within these zones, the albite host ($Ab_{98}Or_{1-2}An_{0-1}$) usually exhibits violet

to deep red luminescence, whereas the exsolved K-feldspar ($Or_{91-100}Ab_{0-8}An_{0-1}$) exhibits dull blue to dark blue luminescence. Some irregular vein antiperthite grains are unzoned and contain deep red luminescent albite host ($Ab_{98-99}Or_{0-2}$) and dull red luminescent exsolved K-feldspar ($Or_{89-96}Ab_{3-9}An_{0-2}$). Both the albite host and the exsolved K-feldspar contain high Fe contents (1.5-4 mole % $KFeSi_3O_8$).

During late-stage fluid-induced deuteric coarsening and replacement, the albite cores are mainly coarsened by the antiperthite rim. Deuteric coarsening or replacement also occurs within the albite core to form dull blue luminescent secondary K-feldspar ($Or_{90-94}Ab_{6-9}An_{0-1}$), and occurs at interstices between the antiperthite grains to form deep red luminescent secondary albite ($Ab_{98-100}Or_{0-2}An_{0-1}$).

The thermal history of the alkali feldspars in the quartz syenite can be divided into four events: (1) the blue luminescent homogeneous alkali feldspar cores have crystallized at temperatures ≥700 °C. (2) The light violet blue luminescent Na-rich alkali feldspar rims may have crystallized at a temperature about 660 °C. (3) The light blue luminescent albite cores of the mantled feldspar formed at temperatures about 600-450 °C. (4) The zoned and unzoned irregular vein antiperthite and the deuteric coarsened antiperthite rims may have formed at a low temperature about <350 °C, since the exsolution products have end menbers compositions.

11.4.5. Apatites in Center III syenites

Most apatite crystals in Center III syenite exhibit light pink to brownish pink luminescence. Some apatite crystals are mantled with a small brownish pink core, a light pink intermediate mantle and a brownish pink rim; or mantled with a pink core and an irregular-shaped brownish pink rim. In general, the brownish pink apatite (cores or rims) has higher contents of total REE and Si than the pink apatite (grains or cores).

The CL spectra show that the homogeneous pink luminescent apatites in the magnesio-hornblende syenite and in some the quartz syenite samples (C2087 and C2060) have relatively higher ratios of Eu^{2+} (or Ce^{3+}) to Dy^{3+}, Sm^{3+} and Pr^{3+} than the pink to brownish pink apatites in the ferro-edenite syenite and the contaminated ferro-edenite syenite.

Some apatites are affected by late-stage fluid alteration, and are zoned with a pink core and an irregular-shaped brownish pink luminescent reaction rim. The CL spectrum shows these apatites are characterized by Sm^{3+} or Pr^{3+} activation.

The apatite crystals in Center III syenites generally are characterized by a LREE-enrichment, and are similar to those apatites found in Center I and Center II syenites. Figure 10.4-8a shows that the total REE have a good correlation with Si, and the Si versus REE regression line has a slope about 0.78. This indicates that the charge balance of REE substitution for Ca^{2+} is maintained by approximately 4/5 Si^{4+} which is higher than that in Center I and Center II apatites. This also suggests that the

substitution of Ca^{2+} involves with both divalent and trivalent REE, but the latter is dominant in Center III apatites. Figure 10.4-8b shows that the REE substitution for Ca^{2+} in Center III apatites mainly involves a coupled substitution with Si^{4+}, but the regression line between (Ca+P) vs. (Si+REE) has a steeper slope of about 1.26 (Fig. 10.4-8b), which indicates that the charge balance may also involve other cations, such as Na^{+1}.

REFERENCES

Axe, J.D., and Dieke, G.H., 1962. Calculation of crystal-field splitting of Sm^{3+} and Dy^{3+} levels in $LaCl_3$ with inclusion of J mixing. The journal of chemical physics. Vol. 37, No. 10, 2364-2371.

Beevers, A.C., and McIntyre, D.B., 1946. The atomic structure of fluor-apatite and its relation to that tooth and bone material. Mineralogical Magazine, vol 27, 254-257.

Binder, G., and Troll, G., 1989. Coupled anion substitution in natural carbon-bearing apatites. Contrib Mineral Petrol, Vol. 101, pp. 394-401.

Blasse, G., and Bril, A., 1967. Investigation of Ce^{3+}-activated phosphors. The journal of chemical physics. Vol. 47, No. 12, 5139-5145.

Brecher, C., Samelson, H., and Lempicki, A., 1967. The energy level structure of Eu^{3+} in YVO_4. In: Optical properties of ions in crystals. Crosswhite, H.M. and Moos, H.W., Interscience., 73-83.

Brown, W.L., and Parsons, I. 1989. Alkali feldspars: ordering rates, phase transformations and behaviour diagrams for igneous rock. Mineralogical magazine, March 1989, Vol. 53, pp. 25-42.

Bube, R.H. 1992. Electrons in solids: an introductory survey (Third edition). Academic press, Inc. London.

Caspers, H.H., and Rast, H.E. 1967. Optical absorption and fluorescence spectra of EuF_3. The journal of chemical physics. Vol. 47, No. 11, 4505-4514.

Crosswhite, H.M., and Dieke, G.H. 1961. Spectrum and magnetic properties of hexagonal $DyCl_3$. The journal of chemical and physics. Vol. 35, No. 5, 1535-1548.

Crosswhite, H.M., and Moos, H.W. 1967. Crystal spectroscopy at the Johns Hopkins University. In Optical Propertis of Ions in Crystals. Crosswhite, H.M., and Moos, H.W. (eds), Interscience Publishers, New York.

Deer, W.A., Howie, R.A., and Zussman, J. 1966. An introdution to the rock forminig minerals. Longman Scientific and Technical, New York.

Dieke, G.H., and Sarup, R. 1958. Fluorescence spectrum of $PrCl_3$ and the levels of the Pr^{+++} ion. The journal of chemical physics. Vol. 29, No. 4, 741-745.

Dieke, G.H., and Shobha Singh, 1961. Absorption and fluorescence spectra with magnetic properties of $ErCl_3$. The journal of chemical physics. Vol. 35, No. 2, 555-563.

Dieke, G.H., and Crosswhite, H.M., 1963. The spectra of the doubly and triply ionized rare earths. Applied optic. Vol. 2, No. 7, 675-686.

DeShazer, L.D., and Dieke, G.H., 1963. Spectra and energy levels of Eu^{3+} in $LaCl_3$. The journal of chemical physics. Vol. 38, No. 9, 2190-2199.

Edgar, A.D., 1984. Chemistry, occurrence and paragenesis of feldspathoids: A review. In Feldspars and Feldspathoids. Brown, W. L. (ed), D. Reidel Publishing Company. Dordrecht, Holland.

Faye, G.H. 1969. The optical absorption spectrum of tetrahedrally-bonded Fe^{3+} in the orthoclase. The Canadian Mineralogist. 10, 112-117.

Finch, A.A., and Walker, F. David L. 1991 Cathodoluminescence and microporosity in alkali feldspars from Blå Måne Sø perthosite, South Greenland. Mineralogist Magazine, Vol. 55. pp. 583-589.

Freed, S. 1931. Electronic transitions between an inner shell and the virtual outer shells of the ions of the rare earths in crystals. Physical review, Vol. 38, pp. 2122-2130.

Fry, J.L., 1968. Optical absorption and fluorescence spectra of Dy^{3+} in LaF_3. The journal of chemical physics. Vol. 48, No. 5, 2342-2348.

Fuhrman, M.L., and Lindsley, D.H. 1988. Ternary-feldspar modeling and thermometry. American Mineralogist, Vol. 73, pp. 201-215.

Geake, J.E., Walker, D.J., Telfer, D.J., Mills, A.A., garlick, G.F. 1973. Proc. 4th Lunar Sci. Conf., Geochim. cosmochim. Acta Suppl. 3, 4, 3181-3189.

Geake, J.E., Walker, D.J., Telfer, D.J., and Mills, A.A. 1977. The cause and significance of luminescence in lunar plagioclase. Phil. Trans. R. Soc. Lond. A. 285, pp. 403-408.

Görz, H., Bhalla, R.J.R.S.B., and White, E.W. 1970. Detailed cathodoluminescence characterization of common silicates. In Space science applications of solid state luminescence phenomena. Weber, J.N., and White, E. (eds), 62-70. MRL pub. 70-101. State College, Pa.: Penn. State University.

Gravely, Ben T., 1970. Absorption, fluorescence, and thermo-luminescence in gamma-irradiated Pr^{3+} : LaF_3. The journal of chemical physics. Vol. 52, No. 7, 3610-3613.

Hamilton, D.L., and MacKenzie, W.S., 1965. Phase-equilibrium studies in the system $NaAlSiO_4$(nepheline)-$KAlSiO_4$(kalsilite)-SiO_2-H_2O. Mineral. Mag. Vol. 34, pp.214-231.

Hamilton, D.L., 1961. Nephelines as crystallization temperature indicators. J. Geol. Vol. 69, pp. 321-329.

Hamilton, D.L., and MacKenzie, W.S., 1960. Nepheline solid solution in the system $NaAlSiO_4$-$KAlSiO_4$-SiO_2. J. Petrol. Vol. 1. pp. 56-72.

Hayward, C.L., and Jones, A.P., 1991. Cathodoluminescence petrography of Middle Proterozoic extrusive carbonatite from Qasiarsuk, South Greenland. Mineralogical Magazine. Vol. 55, pp. 591-603.

Henderson, C.M.B., and Gibb. F.G.F., 1972. Plagioclase-Ca-rich-nepheline intergrowths in a syenite from the Marangudzi copmlex, Rhodesia. Mineral. Mag. June 1972, Vol. 38, pp. 670-677.

Hogarth, D.D., 1988. Chemical composition of fluorapatite and associated minerals from skarn near Catineau, Quebec. Mineralogical Magazine, Vol. 52, pp. 347-358.

Holt, D.B. 1974. Quantitative scanning electron microscope studies of cathodoluminescence in adamantine semiconductors. In Quantitative Scanning Electron Microscopy. Holt, D.B.M., Grant, P.R., and Boswarva, I.M. (eds), Academic Press, London.

Hughes, J.M., Cameron, M., and Mariano, A.N., 1991a. Rare-earth-element ordering and structural variations in natural rare-earth-bearing apatites. American Mineralogist, Vol. 76, pp. 1165-1173.

Hughes, J.M., Cameron, M., and Crowley, K.D., 1991b. Ordering of divalent cations in the apatite structure: Crystal structure refinements of natural Mn- and Sr-bearing apatite. American Mineralogist, Vol. 76, pp. 1857-1862.

Hughes, J.M., Cameron, M., and Crowley, K.D., 1989. Structural variations in natural F, OH, and CL apatites. American Mineralogist, Vol. 74, pp. 870-876.

Hulcheon, I.D., Steel, I.M., Smith, J.V., and Clayton, R.N. 1978. Ion microprobe, electron microprobe and cathodoluminescence data for Allende inclusions with emphasis on plagioclase chemisty. In Proceedings of the Lunar Planetary Science Conference 9th, Geochimica et Cosmochimica Acta, Supplement 10. pp. 1345-1368. Pergamon Press, New York.

Jorre, L.D.S, and Simth, D.G.W. 1988. Cathodoluminescence gallium-enriched feldspars from the Thor Lake rare-metal deposits, Northwest Territories. Canadian Mineralogist, Vol. 26, pp. 301-308.

Keller, S.P. 1958. Fluorescence spectra, term assignments, and crystal field splitting of rare earth activated phosphors. The journal of chemical physics. Vol. 29, No. 1, 180-187.

Lang, R.J. 1936. The spectrum of trebly ionized cerium. Canadian Journal of Research. Vol. 14, pp.127-130.

Laud, K.R., Gibbons, E.F., Tien, T.Y., and Stadler, H.L. 1971. Cathodoluminescence of Ce^{3+}- and Eu^{3+}-activated alkaline earth feldspars. J. Electrochem. Soc., Solid state science, vol. 118, No. 6, pp. 918-923.

Liu, Yu and Comodi, P., 1993. Some aspects of the crystal-chemistry of apatites. Mineralogical Magazine, Vol 57, pp. 709-719.

Magno, M.S., and Dieke, G.H., 1962. Absorption and fluorescence spectra of hexagonal $SmCl_3$ and their Zeeman effects. The journal of chemical physics. Vol. 37, No. 10, 2354-2363.

Manning, P.G. 1970. Racah paramenters and their relationship to lengths and covalencies of Mn^{2+} and Fe^{3+} oxygen bonds in silicates. The Canadian Mineralogist. 10, 677-688.

Marfunin, A.S., 1979. Spectroscopy, Luminescence and Radiation Centers in Minerals. Springer-Verlag Berlin Heideberg.

Mariano, A.N. 1978. The application of cathodoluminescence for carbonatite exploration and characterization. Proceedings of the First International Symposium on Carbonatite, Pocos de Caldas, M.G., Brasil, 39-57.

Mariano, A.N. 1988. Some further geological applications of cathodoluminescence. In Cathodoluminescence of Geological Materials. Marshall, D.J. Unwin-Hyman, Boston.

Mariano, A.N. 1989. Cathdoluminescence emission spectra of rare earth element activators in minerals. In Geochemistry and mineralogy of rare earth elements. Mineralogical Society of America reviews in mineralogy vol. 21, pp 339-348.

Mariano, A.N., and Ito, J., and Ring, P.J. 1973. Cathodoluminescence of plagioclase. Geol. Soc. Amer., Abstract with prorams 5, pp. 726.

Mariano, A.N., and Ring, P.J., 1975. Europium-activated cathdo-luminescence in minerals. Geochimica et Cosmochimica Acta. Vol. 39, pp. 649-660.

Marshall, D.J., 1988. Cathodoluminescence of Geological Materials. Unwin-Hyman, Boston.

Mitchell, R.H., and Platt, R.G., 1978. Mafic mineralogy of ferroaugite syenite from the Coldwell alkaline Complex, Ontario, Canada. Journal of Petrology, Vol. 19, Part 4, pp. 627-651.

Mitchell, R.H., and Platt, R.G., 1979. Nepheline-plagioclase intergrowths of metasomatic origin from the Coldwell Complex, Ontario. Canadian Mineralogist. Vol. 17, pp. 537-540.

Mitchell, R.H., and Platt, R.G., 1982. Mineralogy and petrology of nepheline syenites from the Coldwell alkali Complex, Ontario, Canada. Journal of Petrology, Vol. 23, Part 2, pp. 186-214.

Mitchell, R.H. 1990. A review of the compositional variation of amphiboles in alkaline plutonic coplexs. Lithos, Vol. 26, pp. 135-156.

Mitchell, R.H., Platt, R.G., Lukosius-Sanders, J., Artist-Downey, M., and Moogk-Pickard, S., (1993). Petrology of syenite from Center III of the Coldwell alkaline Complex, Northwestern, Ontario, Canada. Can. J. Earth Sci. Vol. 30, pp. 145-158.

Morozov, A.M., Morozova, A.K., Trefimov, A.K., and Feolilov, P.P., 1970. Spectral and luminescent characteristics of fluorapatite single crystals activated by rera earth ions. Optical and spectrascopy. Vol. 29. 590-596.

Mulja, T., and Mitchell, R.H. 1991. The Geordie Lake Intrusion, Coldwell Complex, Ontario: A palladium- and tellurium-rich disseminated sulfide occurrence derived from an evolved tholeiitic magma. Economic Geology. Vol. 86, pp. 1050-1069.

Ozawa, J., 1990. Cathodoluminescence: theory and applications. Kodansha, Tokyo.

Powell, M., and Powell, R., 1977. A nepheline-alkali feldspar geothermometer. Contrib. Mineral. Petrol. Vol. 62, pp. 193-204.

Rae, D.A., and Chambers, D.A. 1988. Metasomatism in the North Qôroq centre, South Greenland: cathodoluminescence and mineral chemistry of alkali feldspars. Transactions of the Royal Society of the Edinburgh: Earth Sciences, 79, 1-2, pp. 1-12.

Rakovan, J., and Reeder, R.J., 1994. Differential incorporation of trace elements and dissymmetrization in apatite: The role of surface structure during growth. American Mineralogist, Vol. 79, pp. 892-903.

Rao, Y.J., and Murthy, I.S., 1974. Nepheline as a metasomatic product. American Mineralogist, Vol. 59, pp. 690-693.

Rast, H.E., Fry, J.L, and Caspers, H.H., 1967. Energy levels of Sm^{3+} in LaF_3. The journal of chemical physics. Vol. 46, No. 4, 1460-1466.

Remond, G., Cesbron, F. Chapoulie, R., Ohnenstetter, D., Roques-Carme, R., and Schvoerer, M. 1992. cathodoluminescence applied to the microcharacterization of mineral materials: A present status in experimentation and interpretation. Scanning Microscopy, Vol. 6, No. 1, pp. 23-68.

Roeder, P.L., MacArthur, D., Ma, Xin-Pei, Palmer, G.R., and Mariano, A.N., 1987. Cathodoluminescence and microprobe study of rare-earth elements in apatite. American mineralogist. Vol. 72, 801-811.

Rønsbo, J., 1989. Couled substitutions involving REEs and Na And Si in apatites in alkaline rocks from the Ilímaussaq intrusion, South Greenland, and the petrological implications. American mineralogist. Vol 74, pp. 896-901.

Ropp, R.C., 1964. Spectra properties of rare earth oxide phosphors. Journal of the electrochemical society. Vol. 111, No. 3, 311-317.

Sarup, R., and Crozier, M.H., 1965. Analysis of the eigenstate of Pr^{3+} in $LaCl_3$ using the Zeeman effect in high fields. The journal of chemical physics. Vol. 42, No. 1, 371-376.

Sayer, E.V., and Freed, S. 1955. Absorption spectrum and quantum states of the praseodymium ion. II. Anhydrous praseodymium fluoride in films. The journal of chemical physics. Vol. 23, No. 11, 2066-2068.

Sayre, E.V., Sancier, K.M., and Freed, S., 1955. Absorption spectrum and quantum states of the praseodymium ion. I. Single crystals of praseodymium chloride. The journal of chemical physics. Vol. 23, No. 11, 2060-2065.

Sippel, R.F. 1971. luminescence petrography of the Apollo 12 rocks and comparative features in terrestrial rocks and meteorites. In Proceedings of the Second Lunar Conference, Vol. 1, Levinson, A.A. (ed.), 247-263. Cambridge: Mass.: MIT.

Sippel, R.F., and Spener, A.B. 1970. Luminescence petrography and properties of lunar crystalline rocks and breccias. In Proceedings of the Apollo 11 Lunar Science Conference, Vol. 3. Geochimica et Cosmochimica Acta, Supplement 1, Levinson, A.A. (ed.), 2413-2426. New York, Pergamon.

Smith, J.V., and Stenstrom, R.C., 1965. Electron-excited luminescence as a petrologic tool. Journal of geology. Vol. 73, p. 627-635.

Telfer, D.J., and Walker, G., 1978. Ligand field bands of Mn^{2+} and Fe^{3+} luminescence centers and their site occupancy in plagioclase feldspars. Modern geology. Vol. 6, p. 199-210.

Tilley, C.E. 1954. Nepheline-alkali feldspar parageneses: Am. Jour. Sci., Vol. 252. pp. 65-75.

Van Uitert, L.G., and Soden, R.R. 1960. J. Appl. Phys. Vol. 31, pp. 328.

Van Uitert, L.G., and Johnson, L.F., 1966. Energy transfer between rare-earth ions. The journal of chemical physics. Vol. 44, No. 9, 3514-3522.

Varsanyi, F., and Dieke, G.H., 1962. Energy levels of Hexagonal $ErCl_3$. The journal of chemical physics. Vol. 36, No. 11, 2951-2961.

Waldron, K.A., and Parsons, I., 1992. Feldspar microtextures and multistage thermal history of syenites from the Coldwell Complex, Ontario. Contributions to Mineralogy and Petroology. Vol. 111, 222-234.

Weber, M.J., and Bierig, R.W., 1964. Paramagnetic resonance and relaxation of trivalent rare-earth ions in calcium fluoride. I. Resonance spectra and crystal fields. Physical review. Vol. 134, No. 6A, A1492-A1503.

Wenzel, T., and Ramseyer, K. 1992 Mineralogical and mineral-chemical changes in a fractionation-dominated diorite-monzodiorite-monzonite sequence: evidence from cathodo-luminescence. Eur. J. Mineral., 4, 1391-1399.

Wortman, D.E., and Sanders, D., 1971. Optical spectrum of trivalent dysprosium in calcium tungstate. The journal of chemical physics. Vol. 55, No. 7, 3212-3219.

Wybourne, B.G., 1962. Structure of f^n configurations. II. f^5 and f^9 configurations. The journal of chemical physics. Vol. 36. No. 9, 2301-2311.

Yacobi, B.G., and Holt, D.B., 1990. Cathodoluminescence microscopy of inorganic solids. Plenum Press, New York Lewis, N.Y.

Appendix 1. Representative compositions of feldspars in the lower series ferroaugite syenite (C35) in Center I, Coldwell Complex, Ontario

	Alkali feldspar										Oligoclase	
CL colour	Light blue										Dull blue	
Anal. No.	1	2	3	4	5	6	7	8	9	10	11	12
SiO2	63.70	64.59	63.36	63.44	64.32	63.16	62.06	62.63	62.68	62.33	61.03	61.40
Al2O3	19.59	20.19	20.25	20.46	19.96	19.11	19.43	20.07	19.23	19.65	23.31	23.68
Fe2O3	0.26	0.18	0.33	0.08	0.30	-	0.08	-	-	0.14	0.30	0.16
BaO	1.80	1.30	1.87	1.92	1.39	3.69	4.67	2.39	3.12	2.85	1.23	1.07
CaO	1.10	1.60	1.51	1.36	1.04	0.66	0.57	1.13	0.88	1.33	3.58	4.40
Na2O	5.83	5.81	6.08	5.02	5.52	4.92	4.35	6.31	5.29	6.59	8.88	8.07
K2O	7.59	6.35	6.64	7.41	7.00	8.45	8.85	7.28	8.39	6.77	1.62	1.24
STRUCTURAL FORMULA BASED ON 32 OXYGENS												
Si	11.667	11.678	11.560	11.604	11.711	11.722	11.622	11.541	11.661	11.541	10.998	11.001
Al	4.230	4.303	4.356	4.412	4.284	4.181	4.290	4.360	4.218	4.289	4.952	5.002
Fe+3	0.035	0.024	0.046	0.011	0.041	-	0.011	-	-	0.020	0.041	0.021
Ca	0.216	0.310	0.295	0.267	0.203	0.131	0.114	0.223	0.175	0.264	0.691	0.845
Na	2.070	2.037	2.151	1.780	1.949	1.770	1.580	2.254	1.908	2.366	3.103	2.804
K	1.774	1.465	1.546	1.729	1.626	2.001	2.114	1.711	1.991	1.599	0.372	0.283
Ba	0.129	0.092	0.134	0.138	0.099	0.268	0.343	0.173	0.227	0.207	0.087	0.075
MOL PERCENT END MEMBERS												
Celsian	3.06	2.34	3.20	3.51	2.53	6.43	8.23	3.96	5.29	4.64	2.02	1.86
Fe-Or	0.83	0.62	1.10	0.27	1.05	-	0.26	-	-	0.45	0.95	0.52
Anorthite	5.11	7.89	7.08	6.79	5.18	3.15	2.75	5.12	4.08	5.92	16.10	20.97
Albite	49.01	51.86	51.57	45.37	49.74	42.45	37.95	51.69	44.35	53.10	72.26	69.60
Orthoclase	41.99	37.29	37.05	44.06	41.50	47.97	50.80	39.24	46.28	35.89	8.67	7.04
MOL PERCENT IN AN-AB-OR SYSTEM												
An	5.32	8.13	7.40	7.06	5.37	3.36	3.00	5.33	4.30	6.24	16.59	21.48
Ab	51.00	53.44	53.88	47.15	51.59	45.37	41.48	53.82	46.83	55.94	74.47	71.31
Or	43.69	38.43	38.72	45.79	43.04	51.27	55.52	40.86	48.87	37.82	8.94	7.21

Appendix 1. continued

	Oligoclase										Secondary albite		
CL colour	Dull blue										Purple		
Anal. No.	13	14	15	16	17	18	19	20	21	22	23	24	25
SiO2	61.14	61.16	61.58	60.76	61.01	60.83	61.51	60.94	61.06	61.29	62.38	61.65	61.66
Al2O3	22.69	23.68	23.06	23.01	23.64	23.90	23.12	23.35	23.62	23.39	23.13	23.27	23.02
Fe2O3	0.24	0.13	-	-	0.12	0.17	-	0.11	0.16	0.21	-	0.23	0.33
BaO	1.36	1.13	1.32	0.71	0.72	0.40	0.69	0.94	-	0.70	-	0.47	0.53
CaO	3.74	4.08	3.94	3.96	3.74	4.51	3.83	3.99	4.44	3.82	2.81	3.62	3.00
Na2O	9.18	8.48	8.38	9.60	9.23	9.47	9.21	9.29	9.40	9.42	11.09	9.37	10.03
K2O	1.59	1.35	1.63	1.75	1.27	0.65	1.65	1.38	0.94	0.97	0.45	1.33	1.46
STRUCTURAL FORMULA BASED ON 32 OXYGENS													
Si	11.045	10.980	11.080	10.975	10.967	10.893	11.042	10.966	10.944	11.000	11.108	11.039	11.055
Al	4.832	5.012	4.892	4.900	5.010	5.046	4.893	4.954	4.991	4.949	4.856	4.912	4.866
Fe+3	0.033	0.018	-	-	0.017	0.022	-	0.015	0.021	0.029	-	0.031	0.045
Ca	0.724	0.785	0.760	0.766	0.720	0.865	0.737	0.769	0.853	0.735	0.536	0.695	0.576
Na	3.216	2.952	2.924	3.362	3.217	3.288	3.206	3.241	3.267	3.278	3.829	3.253	3.487
K	0.366	0.309	0.374	0.403	0.291	0.148	0.378	0.317	0.215	0.222	0.102	0.304	0.334
Ba	0.096	0.079	0.093	0.050	0.051	0.028	0.049	0.066	-	0.049	-	0.033	0.037
MOL PERCENT END MEMBERS													
Celsian	2.17	1.92	2.24	1.10	1.18	0.64	1.11	1.50	-	1.14	-	0.76	0.83
Fe-Or	0.75	0.43	-	-	0.38	0.52	-	0.34	0.48	0.66	-	0.73	1.00
Anorthite	16.32	18.94	18.30	16.73	16.77	19.88	16.86	17.45	19.58	17.03	12.00	16.09	12.87
Albite	72.50	71.24	70.44	73.38	74.89	75.55	73.38	73.52	75.00	76.01	85.71	75.38	77.84
Orthoclase	8.26	7.46	9.02	8.80	6.78	3.41	8.65	7.19	4.94	5.15	2.29	7.04	7.46
MOL PERCENT IN AN-AB-OR SYSTEM													
An	16.81	19.40	18.72	16.91	17.04	20.12	17.05	17.78	19.67	17.35	12.00	16.34	13.11
Ab	74.68	72.96	72.06	74.19	76.08	76.43	74.20	74.90	75.37	77.41	85.71	76.52	79.30
Or	8.51	7.64	9.22	8.90	6.89	3.45	8.75	7.32	4.96	5.24	2.29	7.15	7.60

Appendix 1. Representative compositions of feldspars in the lower series ferroaugite syenite (C40, C58) in Center I, Coldwell Complex, Ontario

	Alkali feldspar, core							Incipient perthite, rim						
CL colour	Light violet blue							Light blue				Light violet		
Anal. No.	C40-1	C40-2	C40-3	C40-4	C40-5	C58-1	C58-2	C40-6	C40-7	C40-8	C40-9	C40-10	C40-11	C40-12
SiO2	65.47	64.56	64.69	65.31	65.25	64.32	64.5	64.31	65.98	65.24	64.88	65.89	64.90	65.98
Al2O3	19.32	19.24	20.43	20.27	19.54	20.21	20.24	19.72	19.85	19.42	19.73	18.58	18.30	18.31
FE2O3	0.38	0.38	0.29	0.26	0.13	0.18	0.17	0.23	-	0.14	-	0.31	0.14	0.26
BaO	0.68	0.26	-	-	0.89	0.33	0.64	-	-	0.25	-	-	-	-
CaO	1.08	1.27	1.23	0.73	1.19	0.89	0.91	1.08	1.45	0.66	0.66	0.3	0.26	0.29
Na2O	7.27	7.42	7.19	6.17	7.03	7.27	7.01	7.58	7.48	6.51	7.03	4.59	4.91	4.6
K2O	5.75	6.90	6.19	7.29	5.98	6.44	6.55	5.99	5.08	7.80	7.71	10.37	11.49	10.24
STRUCTURAL FORMULA BASED ON 32 OXYGENS														
Si	11.792	11.696	11.625	11.730	11.766	11.640	11.649	11.687	11.788	11.790	11.724	11.955	11.888	12.001
Al	4.102	4.109	4.328	4.292	4.154	4.312	4.309	4.225	4.181	4.137	4.203	3.974	3.952	3.926
Fe+3	0.051	0.052	0.039	0.035	0.018	0.025	0.023	0.032	-	0.020	-	0.042	0.020	0.035
Ca	0.208	0.247	0.237	0.140	0.230	0.173	0.176	0.210	0.278	0.128	0.128	0.058	0.051	0.057
Na	2.539	2.607	2.505	2.149	2.458	2.551	2.455	2.671	2.591	2.281	2.463	1.615	1.744	1.622
K	1.321	1.595	1.419	1.670	1.376	1.487	1.509	1.389	1.158	1.798	1.777	2.400	2.685	2.376
Ba	0.048	0.018	-	-	0.063	0.023	0.045	-	-	0.018	-	-	-	-
MOL PERCENT END MEMBERS														
Celsian	1.15	0.41	-	-	1.52	0.55	1.08	-	-	0.42	-	-	-	-
Fe-Or	1.23	1.14	0.93	0.87	0.44	0.58	0.55	0.74	-	0.46	-	1.03	0.44	0.86
Anorthite	5.00	5.46	5.64	3.52	5.55	4.05	4.18	4.89	6.89	3.01	2.93	1.42	1.13	1.38
Albite	60.92	57.69	59.64	53.80	59.31	59.91	58.33	62.09	64.35	53.74	56.39	39.23	38.75	39.66
Orthoclase	31.70	35.30	33.79	41.82	33.19	34.92	35.86	32.28	28.76	42.37	40.69	58.32	59.67	58.10
MOL PERCENT IN AN-AB-OR SYSTEM														
An	5.12	5.54	5.69	3.55	5.66	4.10	4.25	4.93	6.89	3.04	2.93	1.43	1.14	1.39
Ab	62.40	58.60	60.20	54.27	60.49	60.59	59.29	62.55	64.35	54.22	56.39	39.64	38.93	40.01
Or	32.47	35.86	34.10	42.19	33.85	35.31	36.45	32.52	28.76	42.74	40.69	58.93	59.94	58.60

Appendix 1. continued

	Perthite, rim		Secondary Na-feldspar						Secondary K-feldspar			
CL colour	Light violet		Dull blue		Dull violet blue		Dull red			Purple		
Anal. No.	C40-13	C58-3	C40-14	C40-15	C40-16	C40-17	C40-18	C40-19	C40-20	C40-21	C40-22	C40-23	C40-24
SiO2	66.82	65.63	62.52	62.53	63.74	63.9	62.11	63.33	63.95	64.42	63.02	65.03	64.18
Al2O3	17.88	19.23	22.76	22.37	22.53	23.13	22.47	21.88	22.47	17.33	18.2	17.29	17.89
Fe2O3	-	0.25	-	-	0.16	0.20	0.81	0.22	0.28	-	0.17	-	0.18
BaO	-	-	-	-	-	-	-	-	-	0.35	0.6	0.27	0.57
CaO	0.22	0.31	1.71	1.69	0.71	0.81	1.37	0.48	0.5	0.29	0.22	0.27	-
Na2O	4.85	5.78	12.62	12.75	11.58	11.31	12.25	13.31	12.27	1.41	1.75	-	0.99
K2O	10.24	8.73	0.4	0.33	1.03	0.67	0.32	0.79	0.57	16.13	15.53	16.87	16.22
STRUCTURAL FORMULA BASED ON 32 OXYGENS													
Si	12.099	11.862	11.139	11.178	11.323	11.285	11.140	11.288	11.322	12.014	11.829	12.113	11.959
Al	3.817	4.097	4.781	4.715	4.718	4.816	4.751	4.598	4.690	3.810	4.027	3.797	3.930
Fe+3	-	0.034	-	-	0.021	0.027	0.110	0.030	0.037	-	0.024	-	0.025
Ca	0.043	0.060	0.326	0.324	0.135	0.153	0.263	0.092	0.095	0.058	0.044	0.054	-
Na	1.703	2.026	4.360	4.419	3.989	3.873	4.260	4.600	4.212	0.510	0.637	-	0.358
K	2.366	2.013	0.091	0.075	0.233	0.151	0.073	0.180	0.129	3.838	3.719	4.009	3.856
Ba	-	-	-	-	-	-	-	-	-	0.026	0.044	0.020	0.042
MOL PERCENT END MEMBERS													
Celsian	-	-	-	-	-	-	-	-	-	0.58	0.99	0.48	0.97
Fe-Or	-	0.82	-	-	0.48	0.63	2.33	0.61	0.83	-	0.53	-	0.58
Anorthite	1.04	1.45	6.83	6.72	3.09	3.65	5.59	1.87	2.12	1.31	0.99	1.32	-
Albite	41.42	49.01	91.26	91.72	91.11	92.13	90.52	93.86	94.17	11.51	14.26	-	8.36
Orthoclase	57.54	48.71	1.90	1.56	5.33	3.59	1.56	3.67	2.88	86.61	83.24	98.20	90.09
MOL PERCENT IN AN-AB-OR SYSTEM													
An	1.04	1.46	6.83	6.72	3.10	3.67	5.73	1.88	2.14	1.32	1.01	1.33	-
Ab	41.42	49.42	91.26	91.72	91.54	92.72	92.68	94.43	94.96	11.57	14.47	-	8.49
Or	57.54	49.11	1.90	1.56	5.36	3.61	1.59	3.69	2.90	87.11	84.52	98.67	91.51

Appendix 1. Representative compositions of feldspars in the lower series ferroaugite syenite (C47) in Center I, Coldwell Complex, Ontario

	Alkali feldspar, core			Alkali feldspar, rim			Secondary Na-feldspar					Secondary K-feldspar		
CL colour	Light blue			Light violet blue			Dull red					Purple		
Anal. No.	1	2	3	4	5	6	7	8	9	10	11	12	13	14
SiO2	65.08	64.62	64.41	65.56	65.96	66.36	65.73	63.54	65.70	65.08	64.04	63.66	62.37	63.31
Al2O3	19.22	19.37	18.60	18.42	18.26	17.65	22.43	22.17	22.82	22.52	22.92	17.26	17.33	17.23
Fe2O3	0.24	0.19	0.29	0.23	0.17	0.19	0.53	0.50	-	0.09	-	0.16	0.08	-
BaO	-	-	1.36	-	-	-	-	0.27	-	0.27	-	-	0.99	0.38
CaO	1.04	0.95	0.92	0.26	0.66	0.29	0.41	1.68	0.44	0.43	2.13	0.13	0.28	0.18
Na2O	6.50	7.38	5.96	6.10	4.49	5.50	10.03	11.09	10.67	10.80	10.62	1.64	0.36	0.95
K2O	7.72	7.50	8.51	9.32	10.48	10.02	0.91	0.80	0.21	0.82	0.29	16.98	18.60	17.76
STRUCTURAL FORMULA BASED ON 32 OXYGENS														
Si	11.782	11.705	11.794	11.914	11.983	12.053	11.527	11.295	11.507	11.465	11.299	11.942	11.853	11.940
Al	4.102	4.136	4.015	3.946	3.911	3.779	4.637	4.646	4.712	4.677	4.767	3.817	3.883	3.831
Fe+3	0.033	0.026	0.040	0.032	0.023	0.026	0.070	0.067	-	0.012	-	0.022	0.011	-
Ca	0.202	0.184	0.181	0.051	0.128	0.056	0.077	0.320	0.083	0.081	0.403	0.026	0.057	0.036
Na	2.282	2.592	2.116	2.149	1.582	1.937	3.411	3.822	3.624	3.689	3.633	0.597	0.133	0.347
K	1.783	1.733	1.988	2.161	2.429	2.322	0.204	0.181	0.047	0.184	0.065	4.064	4.510	4.273
Ba	-	-	0.098	-	-	-	-	0.019	-	0.019	-	-	0.074	0.028
MOL PERCENT END MEMBERS														
Celsian	-	-	2.21	-	-	-	-	0.43	-	0.47	-	-	1.54	0.60
Fe-Or	0.77	0.57	0.90	0.73	0.55	0.59	1.87	1.52	-	0.30	-	0.47	0.23	-
Anorthite	4.69	4.07	4.08	1.15	3.09	1.30	2.05	7.26	2.20	2.04	9.82	0.55	1.19	0.78
Albite	53.06	57.15	47.85	48.93	38.00	44.62	90.67	86.68	96.55	92.57	88.59	12.67	2.77	7.41
Orthoclase	41.47	38.22	44.96	49.19	58.36	53.49	5.41	4.11	1.25	4.62	1.59	86.31	94.26	91.21
MOL PERCENT IN AN-AB-OR SYSTEM														
An	4.73	4.09	4.21	1.16	3.10	1.31	2.09	7.40	2.20	2.05	9.82	0.56	1.21	0.78
Ab	53.48	57.48	49.39	49.29	38.21	44.89	92.40	88.40	96.55	93.29	88.59	12.73	2.82	7.46
Or	41.79	38.43	46.40	49.55	58.68	53.81	5.52	4.20	1.25	4.66	1.59	86.71	95.96	91.76

Appendix 1. Representative compositions of feldspars in the lower series ferroaugite syenite (C53, C55) in Center I, Coldwell Complex, Ontario

	Homogeneous alkali feldspar							Secondary K-feldspars							
CL colour	Light blue							Purple							
Anal. No.	C53-1	C53-2	C55-1	C55-2	C55-3	C55-4	C55-5	C53-3	C53-4	C55-6	C55-7	C55-8	C55-9	C55-10	C55-11
SiO2	66.07	65.36	64.74	65.16	66.06	65.78	65.31	63.12	62.96	61.64	63.39	64.37	63.04	62.98	62.23
Al2O3	18.69	19.17	19.20	18.93	18.91	18.67	18.82	17.87	17.48	17.14	16.38	17.13	16.85	16.92	17.30
Fe2O3	0.32	0.24	0.41	0.13	-	0.17	0.24	0.47	0.08	0.37	-	0.10	0.13	-	0.13
BaO	0.39	-	-	0.70	-	-	-	0.32	1.00	0.78	0.50	0.51	-	0.82	1.23
CaO	0.24	0.41	0.66	0.52	0.92	0.68	0.67	0.17	-	0.23	0.11	0.19	0.15	0.13	-
Na2O	5.93	5.72	6.21	6.08	6.46	6.30	5.86	0.58	0.53	1.55	1.55	1.47	0.50	-	0.85
K2O	8.30	9.12	8.51	8.23	7.04	8.41	9.13	16.85	17.96	17.83	18.07	16.24	19.34	19.16	18.26
STRUCTURAL FORMULA BASED ON 32 OXYGENS															
Si	11.944	11.837	11.767	11.853	11.923	11.895	11.848	11.882	11.902	11.781	11.996	12.022	11.936	11.956	11.842
Al	3.983	4.093	4.114	4.059	4.024	3.980	4.025	3.966	3.896	3.862	3.655	3.772	3.761	3.787	3.881
Fe+3	0.044	0.033	0.056	0.018	-	0.023	0.033	0.066	0.011	0.053	-	0.014	0.019	-	0.019
Ca	0.046	0.080	0.129	0.101	0.178	0.132	0.130	0.034	-	0.047	0.022	0.038	0.030	0.026	-
Na	2.079	2.009	2.189	2.144	2.261	2.209	2.061	0.212	0.194	0.574	0.569	0.532	0.184	-	0.314
K	1.914	2.107	1.973	1.910	1.621	1.940	2.113	4.047	4.331	4.348	4.363	3.870	4.672	4.640	4.433
Ba	0.028	-	-	0.050	-	-	-	0.024	0.074	0.058	0.037	0.037	-	0.061	0.092
MOL PERCENT END MEMBERS															
Celsian	0.67	-	-	1.18	-	-	-	0.54	1.61	1.15	0.74	0.83	-	1.29	1.89
Fe-Or	1.07	0.79	1.29	0.43	-	0.53	0.77	1.51	0.24	1.04	-	0.31	0.39	-	0.39
Anorthite	1.13	1.88	2.96	2.40	4.38	3.06	3.00	0.78	-	0.93	0.45	0.85	0.62	0.56	-
Albite	50.56	47.50	50.35	50.77	55.69	51.33	47.52	4.83	4.21	11.31	11.40	11.85	3.74	-	6.46
Orthoclase	46.57	49.83	45.40	45.22	39.93	45.08	48.71	92.34	93.94	85.58	87.41	86.16	95.25	98.15	91.26
MOL PERCENT IN AN-AB-OR SYSTEM															
An	1.15	1.90	3.00	2.44	4.38	3.08	3.03	0.80	-	0.95	0.45	0.86	0.62	0.57	-
Ab	51.46	47.88	51.01	51.60	55.69	51.60	47.89	4.93	4.29	11.56	11.48	11.99	3.76	-	6.61
Or	47.39	50.23	45.99	45.96	39.93	45.32	49.09	94.27	95.71	87.49	88.07	87.15	95.62	99.43	93.39

Appendix 1. continued

	Secondary Na-feldspar											Secondary albite		
CL colour	Light violet, violet							Deep red					Non luminescence		
Anal. No.	C53-5	C53-6	C55-12	C55-13	C55-14	C55-15	C55-16	C53-7	C53-8	C55-17	C55-18	C55-19	C55-20	C55-21	C55-22
SiO2	63.41	63.53	65.91	65.23	64.23	64.36	63.56	63.50	63.76	65.27	63.91	64.30	65.51	65.42	65.28
Al2O3	22.50	22.43	22.62	22.77	21.96	22.32	22.85	22.63	22.10	23.35	23.35	22.27	23.39	23.02	22.95
Fe2O3	-	-	0.23	-	0.09	-	-	0.13	0.34	-	0.12	0.27	-	0.11	0.11
BaO	-	-	-	-	0.99	-	-	0.23	-	-	-	0.82	-	-	-
CaO	1.11	0.73	0.14	0.61	1.28	1.12	1.17	0.17	0.17	0.14	0.61	0.96	0.40	0.28	0.22
Na2O	11.38	11.28	10.71	10.74	10.29	10.81	10.69	13.01	13.24	11.06	11.90	10.38	10.50	11.04	11.34
K2O	1.39	2.03	0.41	0.48	1.17	1.28	1.01	0.33	0.43	0.18	0.11	0.70	0.10	0.14	0.12
STRUCTURAL FORMULA BASED ON 32 OXYGENS															
Si	11.291	11.311	11.533	11.463	11.427	11.398	11.313	11.272	11.317	11.425	11.267	11.422	11.452	11.454	11.442
Al	4.723	4.708	4.666	4.717	4.606	4.660	4.795	4.736	4.625	4.818	4.853	4.664	4.820	4.752	4.742
Fe+3	-	-	0.031	-	0.012	-	-	0.018	0.046	-	0.016	0.036	-	0.015	0.015
Ca	0.212	0.139	0.026	0.115	0.244	0.213	0.223	0.032	0.032	0.026	0.115	0.183	0.075	0.053	0.041
Na	3.929	3.894	3.634	3.659	3.549	3.712	3.689	4.478	4.557	3.754	4.068	3.575	3.559	3.748	3.854
K	0.316	0.461	0.092	0.108	0.266	0.289	0.229	0.075	0.097	0.040	0.025	0.159	0.022	0.031	0.027
Ba	-	-	-	-	0.069	-	-	0.016	-	-	-	0.057	-	-	-
MOL PERCENT END MEMBERS															
Celsian	-	-	-	-	1.67	-	-	0.35	-	-	-	1.42	-	-	-
Fe-Or	-	-	0.81	-	0.29	-	-	0.39	0.97	-	0.38	0.89	-	0.38	0.37
Anorthite	4.75	3.10	0.69	2.96	5.89	5.04	5.39	0.70	0.68	0.69	2.73	4.56	2.05	1.37	1.05
Albite	88.16	86.64	96.07	94.27	85.74	88.09	89.07	96.95	96.29	98.26	96.30	89.17	97.34	97.44	97.90
Orthoclase	7.09	10.26	2.42	2.77	6.41	6.86	5.54	1.62	2.06	1.05	0.59	3.96	0.61	0.81	0.68
MOL PERCENT IN AN-AB-OR SYSTEM															
An	4.75	3.10	0.70	2.96	6.01	5.04	5.39	0.71	0.69	0.69	2.74	4.67	2.05	1.37	1.05
Ab	88.16	86.64	96.86	94.27	87.45	88.09	89.07	97.66	97.23	98.26	96.67	91.28	97.34	97.81	98.26
Or	7.09	10.26	2.44	2.77	6.54	6.86	5.54	1.63	2.08	1.05	0.59	4.05	0.61	0.82	0.68

Appendix 1. Representative compositions of feldspars in the upper series ferroaugite syenite (C65) in Center I, Coldwell Complex, Ontario

Irregular vein perthite

	Cryptoperthitic patches (braid microperthite)									Exsolved Na-feldspar			
CL colour	Light greyish blue, light violet blue, light bluish violet									Light blue			
Anal. No.	1	2	3	4	5	6	7	8	9	10	11	12	13
SiO2	66.00	64.56	65.80	65.01	65.79	65.97	65.04	66.41	66.35	65.28	65.10	64.79	64.95
Al2O3	19.53	20.42	20.30	19.86	19.44	19.48	20.20	18.20	19.25	22.66	22.56	21.62	23.45
Fe2O3	0.32	0.16	0.18	0.18	0.47	-	0.38	0.37	0.20	0.34	0.13	0.13	0.40
BaO	-	0.87	-	0.54	0.44	-	-	-	-	0.19	0.45	0.60	-
CaO	0.13	0.57	0.53	0.30	0.40	0.16	0.28	0.22	0.08	0.81	1.04	0.62	0.77
Na2O	6.09	6.83	7.12	6.01	6.16	5.76	5.96	5.38	5.91	9.68	10.16	10.39	10.20
K2O	7.96	6.61	5.76	7.46	7.35	8.68	7.50	8.93	8.13	1.07	0.43	1.87	0.15
STRUCTURAL FORMULA BASED ON 32 OXYGENS													
Si	11.864	11.659	11.773	11.789	11.844	11.881	11.753	12.036	11.930	11.476	11.468	11.510	11.380
Al	4.139	4.348	4.282	4.246	4.126	4.136	4.303	3.889	4.081	4.696	4.685	4.528	4.844
Fe+3	0.044	0.021	0.024	0.024	0.063	-	0.051	0.050	0.027	0.046	0.018	0.018	0.053
Ca	0.025	0.110	0.102	0.058	0.077	0.031	0.054	0.043	0.015	0.153	0.196	0.118	0.145
Na	2.123	2.392	2.470	2.113	2.150	2.011	2.088	1.891	2.060	3.300	3.470	3.579	3.465
K	1.825	1.523	1.315	1.726	1.688	1.995	1.729	2.065	1.865	0.240	0.097	0.424	0.034
Ba	-	0.062	-	0.038	0.031	-	-	-	-	0.013	0.031	0.042	-
MOL PERCENT END MEMBERS													
Celsian	-	1.50	-	0.97	0.77	-	-	-	-	0.35	0.81	1.00	-
Fe-Or	1.09	0.51	0.61	0.61	1.58	-	1.31	1.24	0.68	1.22	0.46	0.43	1.43
Anorthite	0.62	2.69	2.60	1.47	1.92	0.76	1.38	1.06	0.39	4.07	5.15	2.82	3.91
Albite	52.84	58.22	63.17	53.36	53.62	49.82	53.23	46.70	51.93	87.97	91.04	85.61	93.75
Orthoclase	45.45	37.08	33.62	43.58	42.10	49.42	44.08	51.01	47.00	6.40	2.54	10.14	0.91
MOL PERCENT IN AN-AB-OR SYSTEM													
An	0.63	2.74	2.61	1.50	1.97	0.76	1.40	1.07	0.39	4.13	5.22	2.86	3.97
Ab	53.42	59.42	63.56	54.22	54.92	49.82	53.94	47.29	52.28	89.37	92.22	86.85	95.11
Or	45.95	37.84	33.83	44.28	43.11	49.42	44.66	51.64	47.32	6.50	2.57	10.29	0.92

Appendix 1. continued

	Irregular vein perthite												
	Exsolved Na-feldspar										Exsolved K-feldspar		
CL colour	Light blue										Blue		
Anal. No.	14	15	16	17	18	19	20	21	22	23	24	25	26
SiO2	64.43	64.67	65.90	64.69	64.24	65.55	63.61	63.45	63.16	63.47	66.94	66.96	64.95
Al2O3	22.95	23.30	22.77	23.29	22.99	22.90	23.03	23.02	21.98	22.88	18.30	18.00	18.20
Fe2O3	0.10	0.20	-	-	0.16	0.26	0.10	0.21	-	0.19	0.13	0.28	0.19
BaO	0.75	0.30	-	-	0.58	-	0.33	0.29	1.33	-	-	-	-
CaO	0.68	0.58	0.21	0.71	0.66	0.43	1.00	1.22	0.94	1.08	0.18	0.17	0.29
Na2O	10.50	10.19	10.72	10.74	10.95	10.62	11.70	11.21	12.03	12.18	4.20	2.64	3.21
K2O	0.36	0.20	0.25	0.42	0.31	0.27	0.25	0.62	0.58	0.21	10.08	11.81	12.90
STRUCTURAL FORMULA BASED ON 32 OXYGENS													
Si	11.392	11.401	11.533	11.374	11.354	11.474	11.261	11.247	11.307	11.239	12.096	12.151	11.948
Al	4.784	4.843	4.698	4.827	4.790	4.726	4.806	4.811	4.639	4.776	3.899	3.851	3.947
Fe+3	0.013	0.027	-	-	0.021	0.034	0.013	0.028	-	0.025	0.018	0.038	0.026
Ca	0.129	0.110	0.039	0.134	0.125	0.081	0.190	0.232	0.180	0.205	0.035	0.033	0.057
Na	3.600	3.483	3.638	3.661	3.752	3.604	4.016	3.853	4.176	4.182	1.472	0.929	1.145
K	0.081	0.045	0.056	0.094	0.070	0.060	0.056	0.140	0.132	0.047	2.324	2.734	3.028
Ba	0.052	0.021	-	-	0.040	-	0.023	0.020	0.093	-	-	-	-
MOL PERCENT END MEMBERS													
Celsian	1.34	0.56	-	-	1.00	-	0.53	0.47	2.04	-	-	-	-
Fe-Or	0.34	0.72	-	-	0.52	0.89	0.31	0.66	-	0.56	0.47	1.02	0.61
Anorthite	3.32	2.97	1.05	3.44	3.12	2.13	4.41	5.42	3.94	4.60	0.91	0.89	1.34
Albite	92.90	94.52	97.45	94.14	93.62	95.38	93.43	90.17	91.14	93.78	38.24	24.88	26.90
Orthoclase	2.10	1.22	1.50	2.42	1.74	1.60	1.31	3.28	2.89	1.06	60.38	73.22	71.14
MOL PERCENT IN AN-AB-OR SYSTEM													
An	3.38	3.01	1.05	3.44	3.17	2.15	4.45	5.48	4.02	4.62	0.91	0.89	1.35
Ab	94.49	95.75	97.45	94.14	95.06	96.24	94.22	91.20	93.03	94.31	38.42	25.13	27.07
Or	2.13	1.24	1.50	2.42	1.77	1.61	1.32	3.32	2.95	1.07	60.67	73.97	71.58

Appendix 1. continued

	Irregular vein perthite Exsolved K-feldspar Blue						Secondary K-feldspar in fracture Dull greenish blue				Deuteric coarsened rim 2nd. K-feldspar Dull grey,		
CL colour													
Anal. No.	27	28	29	30	31	32	33	34	35	36	37	38	39
SiO2	65.19	65.18	65.40	64.62	64.71	65.42	64.91	63.85	63.85	64.36	64.93	64.45	65.46
Al2O3	18.46	18.15	18.10	18.06	17.82	18.14	17.65	17.93	17.36	17.51	17.45	17.65	17.41
Fe2O3	0.19	0.14	-	0.30	0.21	0.09	0.28	-	-	-	0.30	0.39	0.46
BaO	-	-	0.17	-	-	0.20	-	-	0.36	-	-	0.76	-
CaO	0.59	0.14	0.21	0.29	0.13	0.26	0.18	0.08	-	0.15	-	-	-
Na2O	3.93	2.04	3.59	3.31	2.03	2.10	1.05	0.81	0.48	-	-	0.65	1.13
K2O	11.53	14.36	12.42	13.45	14.61	13.81	15.96	17.12	17.94	17.74	17.35	16.13	15.46
STRUCTURAL FORMULA BASED ON 32 OXYGENS													
Si	11.918	11.994	11.993	11.910	11.997	12.016	12.025	11.935	11.987	12.033	12.071	12.007	12.096
Al	3.979	3.937	3.913	3.924	3.895	3.928	3.855	3.951	3.842	3.859	3.825	3.876	3.793
Fe+3	0.026	0.020	-	0.042	0.029	0.012	0.039	-	-	-	0.042	0.055	0.063
Ca	0.116	0.028	0.041	0.057	0.026	0.051	0.036	0.016	-	0.030	-	-	-
Na	1.393	0.728	1.276	1.183	0.730	0.748	0.377	0.294	0.175	-	-	0.235	0.405
K	2.689	3.371	2.906	3.163	3.456	3.236	3.772	4.083	4.297	4.231	4.115	3.834	3.645
Ba	-	-	0.012	-	-	0.014	-	-	0.026	-	-	0.055	-
MOL PERMOL PERCENT END MEMBERS													
Celsian	-	-	0.29	-	-	0.35	-	-	0.59	-	-	1.33	-
Fe-Or	0.62	0.48	-	0.94	0.69	0.30	0.92	-	-	-	1.01	1.31	1.54
Anorthite	2.74	0.67	0.97	1.29	0.61	1.26	0.85	0.36	-	0.71	-	-	-
Albite	32.98	17.55	30.14	26.61	17.21	18.41	8.93	6.68	3.88	-	-	5.62	9.84
Orthoclase	63.67	81.30	68.60	71.16	81.49	79.67	89.31	92.95	95.53	99.29	98.99	91.75	88.62
MOL PERCENT IN AN-AB-OR SYSTEM													
An	2.75	0.67	0.98	1.30	0.61	1.27	0.85	0.36	-	0.71	-	-	-
Ab	33.19	17.64	30.22	26.87	17.33	18.53	9.01	6.68	3.91	-	-	5.77	10.00
Or	64.06	81.69	68.80	71.83	82.06	80.20	90.13	92.95	96.09	99.29	100.00	94.23	90.00

Appendix 1. continued

Deuteric coarsened antiperthitic rim

CL colour	Secondary K-feldspar to violet blue						Secondary K-feldspar Brown							
Anal. No.	40	41	42	43	44	45	46	47	48	49	50	51	52	53
SiO2	64.33	64.99	64.92	65.24	64.52	64.50	65.06	65.29	64.89	65.53	65.47	65.16	65.33	65.49
Al2O3	18.06	17.81	17.17	17.76	17.52	17.88	17.95	17.61	18.06	17.17	17.09	17.64	17.26	17.73
Fe2O3	0.50	0.59	0.40	0.58	0.59	0.67	0.16	-	0.39	0.62	0.13	0.57	0.34	0.17
BaO	-	-	-	-	0.62	0.32	-	-	0.32	0.25	0.67	-	-	-
CaO	0.11	0.09	0.06	0.09	0.13	0.09	-	0.24	-	0.18	-	0.25	0.14	0.17
Na2O	1.11	-	0.62	-	-	-	0.34	-	-	-	-	-	0.57	-
K2O	15.47	16.58	16.88	16.39	16.29	16.23	16.35	16.87	16.38	16.19	16.34	16.19	16.39	16.46
STRUCTURAL FORMULA BASED ON 32 OXYGENS														
Si	11.953	12.034	12.072	12.061	12.041	12.004	12.048	12.095	12.022	12.139	12.181	12.070	12.103	12.100
Al	3.956	3.888	3.764	3.871	3.855	3.923	3.919	3.846	3.944	3.750	3.748	3.852	3.770	3.862
Fe+3	0.070	0.082	0.056	0.080	0.083	0.093	0.022	-	0.054	0.087	0.019	0.079	0.048	0.023
Ca	0.022	0.018	0.012	0.018	0.026	0.018	-	0.048	-	0.036	-	0.050	0.028	0.034
Na	0.400	-	0.224	-	-	-	0.122	-	-	-	-	-	0.205	-
K	3.667	3.917	4.005	3.866	3.879	3.854	3.863	3.987	3.871	3.826	3.878	3.826	3.874	3.880
Ba	-	-	-	-	0.045	0.023	-	-	0.023	0.018	0.049	-	-	-
MOL PERCENT END MEMBERS														
Celsian	-	-	-	-	1.12	0.59	-	-	0.59	0.46	1.24	-	-	-
Fe-Or	1.68	2.04	1.30	2.03	2.05	2.34	0.54	-	1.37	2.19	0.47	2.00	1.16	0.59
Anorthite	0.53	0.44	0.28	0.45	0.64	0.45	-	1.18	-	0.90	-	1.25	0.67	0.85
Albite	9.62	-	5.20	-	-	-	3.05	-	-	-	-	-	4.93	-
Orthoclase	88.18	97.51	93.22	97.52	96.18	96.62	96.41	98.82	98.04	96.45	98.29	96.75	93.25	98.56
MOL PERCENT IN AN-AB-OR SYSTEM														
An	0.54	0.45	0.28	0.46	0.67	0.46	-	1.18	-	0.93	-	1.28	0.68	0.86
Ab	9.78	-	5.27	-	-	-	3.06	-	-	-	-	-	4.99	-
Or	89.68	99.55	94.45	99.54	99.33	99.54	96.94	98.82	100.00	99.07	100.00	98.72	94.34	99.14

Appendix 1. continued

Deuteric coarsened antiperthitic rim

Secondary Na-feldspar

CL colour	Deep red											
Anal. No.	54	55	56	57	58	59	60	61	62	63	64	65
SiO2	65.69	65.30	65.71	64.01	65.52	66.00	66.64	66.79	65.82	66.14	64.89	66.89
Al2O3	22.20	22.34	22.71	21.78	22.18	22.24	21.31	22.29	22.27	22.09	22.96	22.33
Fe2O3	0.57	0.52	0.37	0.87	0.84	0.87	1.90	1.04	0.67	0.62	0.54	0.89
BaO	0.55	-	-	-	-	-	-	-	-	-	-	-
CaO	-	0.11	-	0.06	-	-	0.16	-	0.24	-	0.15	-
Na2O	10.93	11.53	10.71	13.23	11.26	10.53	9.41	9.71	10.67	10.92	10.91	9.70
K2O	0.12	0.16	0.30	0.14	0.28	0.22	0.39	0.27	0.40	0.29	0.26	0.27
STRUCTURAL FORMULA BASED ON 32 OXYGENS												
Si	11.539	11.475	11.517	11.348	11.500	11.563	11.675	11.631	11.533	11.577	11.415	11.643
Al	4.598	4.628	4.693	4.552	4.590	4.593	4.401	4.576	4.600	4.558	4.762	4.582
Fe+3	0.075	0.069	0.048	0.116	0.112	0.114	0.251	0.137	0.088	0.082	0.072	0.116
Ca	-	0.021	-	0.011	-	-	0.030	-	0.045	-	0.028	-
Na	3.723	3.929	3.640	4.548	3.832	3.577	3.197	3.279	3.625	3.706	3.721	3.274
K	0.027	0.036	0.067	0.032	0.063	0.049	0.087	0.060	0.089	0.065	0.058	0.060
Ba	0.038	-	-	-	-	-	-	-	-	-	-	-
MOL PERCENT END MEMBERS												
Celsian	0.98	-	-	-	-	-	-	-	-	-	-	-
Fe-Or	1.94	1.70	1.29	2.46	2.78	3.06	7.03	3.94	2.29	2.13	1.86	3.38
Anorthite	-	0.51	-	0.24	-	-	0.84	-	1.17	-	0.73	-
Albite	96.38	96.90	96.93	96.63	95.65	95.63	89.68	94.33	94.22	96.19	95.91	94.89
Orthoclase	0.70	0.88	1.79	0.67	1.57	1.31	2.45	1.73	2.32	1.68	1.50	1.74
MOL PERCENT IN AN-AB-OR SYSTEM												
An	-	0.52	-	0.25	-	-	0.91	-	1.20	-	0.74	-
Ab	99.28	98.58	98.19	99.06	98.39	98.64	96.46	98.20	96.42	98.28	97.73	98.20
Or	0.72	0.90	1.81	0.69	1.61	1.36	2.63	1.80	2.38	1.72	1.53	1.80

Appendix 1. Representative compositions of feldspars in the upper series ferroaugite syenites (C68) in Center I, Coldwell Complex, Ontario

	Optical homogeneous alkali feldspar											Albite twinned	
	at centre areas				at intermediate areas			at margin areas				albite	
CL colour	Light blue				Light violet blue			Light violet				Violet, red	
Anal. No.	1	2	3	4	5	6	7	8	9	10	11	12	13
SiO2	65.35	65.47	65.02	65.02	65.41	65.50	65.65	65.72	65.52	65.42	65.65	65.21	65.52
Al2O3	20.60	20.37	20.73	20.49	19.73	19.65	19.92	19.31	19.37	19.77	19.22	22.40	22.66
Fe2O3	0.14	0.18	0.19	0.18	0.28	0.30	0.28	0.38	0.34	0.28	0.33	0.47	0.57
BaO	0.24	-	0.20	-	-	-	-	0.10	0.17	-	-	0.15	-
CaO	0.17	0.25	0.39	0.22	0.15	0.13	0.16	0.07	0.11	0.12	0.11	-	-
Na2O	8.44	7.24	8.62	8.21	6.47	7.69	7.24	7.10	7.15	7.11	7.09	11.49	11.07
K2O	5.07	6.37	4.87	5.80	7.78	6.76	6.78	7.37	7.35	7.15	7.55	0.27	0.24
STRUCTURAL FORMULA BASED ON 32 OXYGENS													
Si	11.684	11.736	11.632	11.665	11.798	11.776	11.779	11.834	11.813	11.781	11.837	11.470	11.480
Al	4.342	4.305	4.372	4.334	4.195	4.165	4.213	4.099	4.117	4.197	4.086	4.645	4.681
Fe+3	0.019	0.024	0.025	0.024	0.038	0.041	0.038	0.051	0.047	0.038	0.045	0.062	0.075
Ca	0.033	0.048	0.075	0.042	0.029	0.025	0.031	0.014	0.021	0.023	0.021	-	-
Na	2.926	2.516	2.990	2.856	2.263	2.681	2.519	2.479	2.500	2.483	2.479	3.919	3.761
K	1.156	1.457	1.112	1.328	1.790	1.550	1.552	1.693	1.691	1.643	1.737	0.061	0.054
Ba	0.017	-	0.014	-	-	-	-	0.007	0.012	-	-	0.010	-
MOL PERCENT END MEMBERS													
Celsian	0.41	-	0.33	-	-	-	-	0.17	0.28	-	-	0.26	-
Fe-Or	0.47	0.59	0.60	0.56	0.92	0.94	0.91	1.21	1.09	0.90	1.06	1.53	1.92
Anorthite	0.78	1.19	1.77	1.00	0.70	0.58	0.74	0.32	0.50	0.55	0.50	-	-
Albite	70.48	62.21	70.93	67.20	54.92	62.39	60.85	58.41	58.53	59.31	57.89	96.72	96.70
Orthoclase	27.86	36.01	26.37	31.24	43.46	36.09	37.50	39.90	39.59	39.24	40.56	1.50	1.38
MOL PERCENT IN AN-AB-OR SYSTEM													
An	0.79	1.19	1.79	1.00	0.71	0.59	0.75	0.32	0.50	0.56	0.50	-	-
Ab	71.10	62.58	71.60	67.58	55.43	62.98	61.41	59.23	59.35	59.84	58.51	98.48	98.59
Or	28.10	36.23	26.61	31.42	43.86	36.43	37.84	40.45	40.14	39.60	40.99	1.52	1.41

Appendix 1. continued

	Albite twinned albite		Deuteric coarsened antiperthitic rim									Secondary K-feldspar in albite		
			Secondary K-feldspar					Secondary Na-feldsar						
CL colour	Violet, red		Dark grey, brown					Deep red				Brown		
Anal. No.	14	15	16	17	18	19	20	21	22	23	24	25	26	27
SiO2	64.68	64.59	64.50	65.02	64.24	64.97	64.88	64.30	64.40	64.48	63.82	64.50	64.19	64.65
Al2O3	22.27	21.41	17.11	17.65	17.29	17.02	17.33	22.30	22.06	22.41	22.23	17.11	17.36	17.18
Fe2O3	0.82	0.72	1.33	0.81	1.46	0.80	1.09	0.78	0.79	0.53	0.90	1.33	1.39	1.40
BaO	-	-	-	-	0.70	-	-	-	0.13	0.30	-	-	-	1.40
CaO	-	-	-	-	0.09	0.12	0.14	0.05	0.08	0.06	-	-	-	-
Na2O	12.01	13.20	0.67	0.96	1.08	1.14	0.81	12.29	12.17	11.97	12.53	0.67	1.10	0.06
K2O	0.29	0.14	16.38	15.65	15.29	16.03	15.71	0.30	0.45	0.14	0.15	16.38	15.82	0.92
STRUCTURAL FORMULA BASED ON 32 OXYGENS														
Si	11.404	11.435	12.010	12.021	11.961	12.059	12.029	11.363	11.390	11.396	11.333	12.010	11.956	12.735
Al	4.629	4.469	3.756	3.847	3.795	3.724	3.788	4.646	4.600	4.669	4.654	3.756	3.812	3.990
Fe+3	0.109	0.096	0.187	0.113	0.204	0.112	0.152	0.103	0.105	0.071	0.120	0.187	0.195	0.208
Ca	-	-	-	-	0.018	0.024	0.028	0.009	0.015	0.011	-	-	-	-
Na	4.106	4.531	0.242	0.344	0.390	0.410	0.291	4.211	4.174	4.102	4.314	0.242	0.397	0.023
K	0.065	0.032	3.891	3.691	3.632	3.796	3.716	0.068	0.102	0.032	0.034	3.891	3.759	0.231
Ba	-	-	-	-	0.051	-	-	-	0.009	0.021	-	-	-	0.108
MOL PERCENT END MEMBERS														
Celsian	-	-	-	-	1.19	-	-	-	0.20	0.49	-	-	-	18.96
Fe-Or	2.55	2.07	4.33	2.72	4.75	2.57	3.63	2.36	2.38	1.67	2.69	4.33	4.48	36.43
Anorthite	-	-	-	-	0.42	0.55	0.66	0.22	0.34	0.27	-	-	-	-
Albite	95.93	97.26	5.60	8.30	9.08	9.45	6.95	95.89	94.76	96.82	96.55	5.60	9.13	4.02
Orthoclase	1.52	0.68	90.07	88.98	84.57	87.43	88.75	1.54	2.31	0.75	0.76	90.07	86.40	40.58
MOL PERCENT IN AN-AB-OR SYSTEM														
An	-	-	-	-	0.44	0.56	0.69	0.22	0.35	0.27	-	-	-	-
Ab	98.44	99.31	5.85	8.53	9.65	9.70	7.22	98.20	97.28	98.96	99.22	5.85	9.56	9.02
Or	1.56	0.69	94.15	91.47	89.90	89.74	92.09	1.58	2.37	0.76	0.78	94.15	90.44	90.98

Appendix 1. Representative compositions of feldspars in the upper series ferroaugite syenite (C70) in Center I, Coldwell Complex, Ontario

	Microperthite, core		Albite, core				Exsol. albite, core		Antiperthite, rim, 2nd K-feldspar		2nd albite		2nd K-feldspar, core		
CL colour	Light blue		Violet blue - red				Light blue		Brown		Violet-red		Dull violet		
Anal. No.	1	2	3	4	5	6	7	8	9	10	11	12	13	14	15
SiO2	65.07	65.60	64.76	65.48	65.57	65.20	64.81	64.43	61.24	61.63	66.56	64.88	61.72	60.45	61.23
Al2O3	19.32	18.60	21.64	21.51	22.07	21.41	21.89	21.62	16.76	16.88	21.05	21.13	15.77	16.22	16.37
Fe2O3	0.44	0.42	0.41	0.54	0.74	0.28	0.68	1.41	2.22	0.58	0.74	0.82	2.55	3.88	3.43
BaO	-	-	-	0.33	-	0.88	-	-	0.26	0.63	-	-	-	-	0.65
CaO	0.18	0.12	0.16	0.06	-	0.23	0.11	0.22	0.16	0.15	0.07	0.06	0.19	0.07	0.24
Na2O	7.64	6.51	12.84	11.77	11.34	11.60	12.25	12.23	-	-	11.32	12.85	-	0.62	-
K2O	7.36	8.84	0.27	0.41	0.42	0.23	0.39	0.36	19.43	20.24	0.26	0.24	20.26	19.50	18.78
STRUCTURAL FORMULA BASED ON 32 OXYGENS															
Si	11.757	11.884	11.447	11.546	11.512	11.555	11.437	11.390	11.714	11.804	11.677	11.488	11.803	11.578	11.678
Al	4.115	3.972	4.509	4.471	4.568	4.473	4.554	4.506	3.779	3.811	4.354	4.411	3.556	3.662	3.681
Fe+3	0.060	0.058	0.055	0.072	0.098	0.037	0.090	0.188	0.320	0.083	0.098	0.110	0.366	0.559	0.493
Ca	0.035	0.023	0.030	0.011	-	0.044	0.021	0.042	0.033	0.031	0.013	0.011	0.039	0.014	0.049
Na	2.677	2.287	4.400	4.024	3.860	3.986	4.191	4.192	-	-	3.851	4.412	-	0.230	-
K	1.697	2.043	0.061	0.092	0.094	0.052	0.088	0.081	4.742	4.946	0.058	0.054	4.943	4.765	4.570
Ba	-	-	-	0.023	-	0.061	-	-	0.019	0.047	-	-	-	-	0.049
MOL PERCENT END MEMBERS															
Celsian	-	-	-	0.54	-	1.46	-	-	0.38	0.93	-	-	-	-	0.94
Fe-Or	1.35	1.31	1.20	1.71	2.43	0.89	2.05	4.17	6.26	1.63	2.45	2.39	6.85	10.04	9.55
Anorthite	0.78	0.53	0.67	0.27	-	1.04	0.47	0.93	0.64	0.60	0.33	0.25	0.73	0.26	0.95
Albite	59.90	51.84	96.79	95.30	95.25	95.36	95.48	93.10	-	-	95.78	96.18	-	4.13	-
Orthoclase	37.97	46.32	1.34	2.18	2.32	1.24	2.00	1.80	92.72	96.84	1.45	1.18	92.42	85.57	88.56
MOL PERCENT IN AN-AB-OR SYSTEM															
An	0.79	0.54	0.67	0.27	-	1.07	0.48	0.97	0.69	0.62	0.34	0.25	0.78	0.29	1.06
Ab	60.72	52.53	97.97	97.49	97.62	97.66	97.47	97.15	-	-	98.18	98.53	-	4.60	-
Or	38.49	46.93	1.36	2.23	2.38	1.27	2.04	1.88	99.31	99.38	1.48	1.21	99.22	95.12	98.94

Appendix 1. Representative compositions of feldspars in the upper series ferroaugite syenite (C72) in Center I, Coldwell Complex, Ontario

	Irregular vein perthitic core						Cryptoperthitic mantle					
	Exsolved Na-feldspar			Exsolved K-feldspar			Alkali feldspar					
CL colour	Light blue			Dull blue			L. violet blue		Light violet			
Anal. No.	1	2	3	4	5	6	7	8	9	10	11	12
SiO2	63.93	64.05	63.79	65.80	66.35	65.66	65.32	65.07	65.22	65.19	66.62	67.05
Al2O3	22.18	22.12	23.41	18.26	17.83	17.97	19.97	18.99	19.05	18.38	18.31	18.31
Fe2O3	0.18	0.10	0.10	0.12	0.08	-	0.13	0.14	0.30	0.47	0.24	0.28
BaO	0.41	-	0.41	-	-	-	-	0.66	-	0.64	-	-
CaO	0.38	0.65	1.35	0.09	0.09	0.19	0.29	0.24	-	0.16	0.07	0.09
Na2O	12.34	12.45	10.63	3.86	3.04	3.59	7.38	6.31	6.38	6.03	5.76	5.42
K2O	0.50	0.28	0.31	11.78	12.28	12.49	6.85	8.60	8.99	9.19	8.61	8.35
STRUCTURAL FORMULA BASED ON 32 OXYGENS												
Si	11.357	11.369	11.265	12.006	12.119	12.024	11.747	11.831	11.832	11.884	12.041	12.090
Al	4.645	4.629	4.874	3.928	3.839	3.879	4.234	4.070	4.074	3.950	3.902	3.892
Fe+3	0.024	0.013	0.013	0.017	0.011	-	0.018	0.020	0.041	0.064	0.033	0.038
Ca	0.072	0.124	0.255	0.018	0.018	0.037	0.056	0.047	-	0.031	0.014	0.017
Na	4.250	4.285	3.640	1.366	1.077	1.275	2.573	2.224	2.244	2.131	2.019	1.895
K	0.113	0.063	0.070	2.742	2.862	2.918	1.572	1.995	2.081	2.137	1.985	1.921
Ba	0.029	-	0.028	-	-	-	-	0.047	-	0.046	-	-
MOL PERCENT END MEMBERS												
Celsian	0.64	-	0.71	-	-	-	-	1.09	-	1.04	-	-
Fe-Or	0.53	0.30	0.33	0.41	0.27	-	0.43	0.46	0.94	1.45	0.82	0.97
Anorthite	1.61	2.76	6.38	0.42	0.44	0.88	1.32	1.08	-	0.71	0.33	0.45
Albite	94.70	95.53	90.84	32.97	27.14	30.13	61.00	51.34	51.40	48.33	49.83	48.95
Orthoclase	2.52	1.41	1.74	66.20	72.14	68.98	37.25	46.04	47.66	48.47	49.01	49.62
MOL PERCENT IN AN-AB-OR SYSTEM												
An	1.63	2.76	6.44	0.43	0.45	0.88	1.33	1.10	-	0.73	0.34	0.45
Ab	95.81	95.82	91.80	33.10	27.22	30.13	61.26	52.14	51.89	49.57	50.24	49.43
Or	2.55	1.42	1.76	66.47	72.34	68.98	37.41	46.76	48.11	49.71	49.42	50.11

Appendix 1. continued

	Deuteric coarsened antiperthitic rim									Albite twinned			
	Secondary K-feldspar						Secondary Na-feldspar			secondary albite			
CL colour	Dark grey				Brown		Red			Purple		Light blue	
Anal. No.	13	14	15	16	17	18	19	20	21	22	23	24	25
SiO2	64.85	65.01	64.89	64.91	64.80	65.45	65.28	65.20	64.12	63.79	62.78	63.80	64.07
Al2O3	18.05	17.57	17.49	17.53	17.25	17.03	22.51	21.86	21.64	22.41	22.86	23.00	22.86
Fe2O3	0.33	0.50	0.43	0.29	0.38	0.34	0.71	0.50	0.83	0.16	0.12	0.41	0.24
BaO	-	-	-	-	-	-	-	-	-	-	-	-	-
CaO	0.07	0.26	0.06	0.17	0.14	0.25	-	-	-	0.31	0.56	0.76	0.73
Na2O	1.63	0.88	-	-	0.87	1.02	11.08	12.16	13.22	12.99	13.31	11.66	11.80
K2O	15.10	15.84	17.17	17.12	16.46	15.94	0.16	0.33	0.26	0.37	0.21	0.24	0.32
STRUCTURAL FORMULA BASED ON 32 OXYGENS													
Si	11.976	12.033	12.057	12.059	12.054	12.118	11.477	11.488	11.372	11.306	11.176	11.279	11.311
Al	3.930	3.834	3.831	3.839	3.783	3.717	4.666	4.541	4.525	4.683	4.798	4.794	4.758
Fe+3	0.046	0.070	0.061	0.040	0.053	0.048	0.094	0.066	0.111	0.021	0.016	0.055	0.032
Ca	0.014	0.052	0.012	0.034	0.028	0.050	-	-	-	0.059	0.107	0.144	0.138
Na	0.584	0.316	-	-	0.314	0.366	3.777	4.154	4.546	4.464	4.594	3.997	4.039
K	3.558	3.740	4.070	4.058	3.906	3.765	0.036	0.074	0.059	0.084	0.048	0.054	0.072
Ba	-	-	-	-	-	-	-	-	-	-	-	-	-
MOL PERCENT END MEMBERS													
Celsian	-	-	-	-	-	-	-	-	-	-	-	-	-
'Fe-Or	1.10	1.67	1.46	0.98	1.23	1.14	2.41	1.54	2.36	0.45	0.34	1.29	0.76
Anorthite	0.33	1.23	0.29	0.82	0.65	1.17	-	-	-	1.27	2.24	3.39	3.23
Albite	13.89	7.56	-	-	7.30	8.66	96.67	96.73	96.39	96.47	96.41	94.05	94.33
Orthoclase	84.68	89.54	98.25	98.20	90.83	89.03	0.92	1.73	1.25	1.81	1.00	1.27	1.68
MOL PERCENT IN AN-AB-OR SYSTEM													
An	0.33	1.26	0.29	0.83	0.66	1.19	-	-	-	1.28	2.25	3.43	3.25
Ab	14.05	7.69	-	-	7.39	8.76	99.06	98.25	98.72	96.91	96.75	95.28	95.05
Or	85.62	91.06	99.71	99.17	91.96	90.06	0.94	1.75	1.28	1.82	1.00	1.29	1.70

Appendix 1. Representative compositions of feldspars in the unlayered ferroaugite syenite (C100) in Center I, Coldwell Complex, Ontario

	Microperthitic, core				oscillatory zone			Deuteric coarsened antiperthite, rim				2nd. albite		
CL colour	Light violet blue				Light violet			Deep red				2nd. K-feldspar Brown	Dull blue	
Anal. No.	1	2	3	4	5	6	7	8	9	10	11	12	13	14
SiO2	65.62	66.12	65.67	65.43	66.20	65.76	65.88	65.09	65.02	64.13	64.05	64.73	67.32	65.62
Al2O3	20.04	19.05	19.82	19.64	19.42	19.23	19.18	22.38	22.51	22.47	22.58	17.89	16.07	17.59
Fe2O3	0.18	0.34	0.36	0.36	0.30	0.43	0.40	1.12	0.84	0.46	0.76	0.53	0.39	0.22
BaO	0.48	-	-	-	-	-	-	-	-	-	-	-	-	-
CaO	0.11	0.10	0.10	0.10	-	0.14	0.06	-	-	-	-	-	0.20	0.21
Na2O	6.86	6.49	6.96	6.48	5.95	6.82	5.86	11.34	11.71	12.87	12.04	-	-	0.83
K2O	6.73	7.93	7.06	7.68	8.16	7.51	8.66	0.08	-	0.12	0.15	16.58	15.93	15.54
STRUCTURAL FORMULA BASED ON 32 OXYGENS														
Si	11.788	11.902	11.796	11.810	11.897	11.851	11.884	11.440	11.423	11.334	11.346	12.024	12.390	12.100
Al	4.244	4.043	4.197	4.179	4.115	4.086	4.079	4.637	4.662	4.682	4.715	3.918	3.487	3.824
Fe+3	0.024	0.047	0.048	0.048	0.041	0.059	0.054	0.148	0.112	0.061	0.101	0.075	0.054	0.031
Ca	0.021	0.019	0.019	0.019	-	0.027	0.012	-	-	-	-	-	0.039	0.041
Na	2.389	2.265	2.424	2.268	2.073	2.383	2.050	3.865	3.989	4.410	4.135	-	-	0.297
K	1.542	1.821	1.618	1.769	1.871	1.727	1.993	0.018	-	0.027	0.034	3.929	3.740	3.656
Ba	0.034	-	-	-	-	-	-	-	-	-	-	-	-	-
MOL PERCENT END MEMBERS														
Celsian	0.84	-	-	-	-	-	-	-	-	-	-	-	-	-
Fe-Or	0.60	1.12	1.17	1.18	1.02	1.40	1.32	3.68	2.72	1.35	2.36	1.86	1.41	0.77
Anorthite	0.53	0.46	0.47	0.47	-	0.64	0.28	-	-	-	-	-	1.03	1.03
Albite	59.57	54.55	58.99	55.26	52.03	56.80	49.89	95.87	97.28	98.05	96.85	-	-	7.37
Orthoclase	38.46	43.86	39.37	43.09	46.95	41.15	48.51	0.45	-	0.60	0.79	98.14	97.57	90.83
MOL PERCENT IN AN-AB-OR SYSTEM														
An	0.54	0.47	0.47	0.48	-	0.65	0.29	-	-	-	-	-	1.04	1.04
Ab	60.45	55.17	59.69	55.92	52.57	57.61	50.56	99.54	100.00	99.39	99.19	-	-	7.43
Or	39.02	44.36	39.84	43.61	47.43	41.74	49.16	0.46	-	0.61	0.81	100.00	98.96	91.53

Appendix 1. continued

	Secondary alibte, between core and rim			Secondary feldspars, in fractures		
CL colour	Purple			Dark blue		L. blue
Anal. No.	18	19	20	15	16	17
SiO2	64.97	64.49	64.27	64.60	64.01	64.45
Al2O3	23.12	23.03	23.07	17.74	17.96	22.40
Fe2O3	0.18	-	0.08	0.60	0.39	0.40
BaO	-	-	-	0.31	0.36	0.28
CaO	0.35	0.10	0.15	0.22	0.13	0.05
Na2O	11.09	12.07	11.86	-	2.23	11.77
K2O	0.22	0.30	0.16	16.60	14.88	0.21
Si	11.405	11.357	11.351	12.005	11.898	11.415
Al	4.785	4.781	4.804	3.887	3.936	4.677
Fe+3	0.023	-	0.010	0.084	0.054	0.053
Ca	0.066	0.019	0.028	0.044	0.026	0.009
Na	3.775	4.121	4.061	-	0.804	4.042
K	0.049	0.067	0.036	3.936	3.529	0.047
Ba	-	-	-	0.023	0.026	0.019
Celsian	-	-	-	0.55	0.59	0.47
Fe-Or	0.60	-	0.25	2.05	1.23	1.28
Anorthite	1.68	0.45	0.69	1.07	0.58	0.23
Albite	96.46	97.95	98.19	-	18.11	96.89
Orthoclase	1.26	1.60	0.87	96.32	79.49	1.14
An	1.69	0.45	0.69	1.10	0.59	0.23
Ab	97.04	97.95	98.44	-	18.44	98.61
Or	1.27	1.60	0.87	98.90	80.96	1.16

Appendix 1. Representative compositions of feldspars in the unlayered ferroaugite syenite (C101) in Center I, Coldwell Complex, Ontario

	Phenocryst, microperthite core						Phenocryst, rim				
	Na-feldspar				K-feldspar		Albite				
CL colour	Light blue				Dull blue		Light blue				
Anal. No.	1-1	1-2	1-3	1-4	1-5	1-6	1-7	1-8	1-9	1-10	1-11
SiO2	63.25	63.21	62.88	63.27	64.60	64.08	62.68	62.98	63.60	63.35	64.43
Al2O3	22.63	24.04	23.28	23.50	18.18	18.60	22.13	23.23	20.70	24.01	23.82
Fe2O3	0.13	-	-	-	0.29	0.07	0.19	0.12	0.23	0.08	0.11
BaO	0.80	-	0.83	0.74	0.38	-	1.66	1.63	2.02	-	-
CaO	1.67	1.37	1.13	0.96	0.23	0.32	0.70	0.87	1.24	1.82	0.97
Na2O	11.33	11.05	11.38	10.62	1.25	2.40	12.02	9.91	9.64	10.03	10.08
K2O	0.18	0.34	0.31	0.92	15.10	14.36	0.64	1.26	2.59	0.31	0.21
STRUCTURAL FORMULA BASED ON 32 OXYGEN											
Si	11.253	11.155	11.198	11.229	11.955	11.856	11.258	11.249	11.486	11.193	11.325
Al	4.746	5.002	4.887	4.917	3.966	4.057	4.686	4.892	4.407	5.001	4.936
Fe+3	0.018	-	-	-	0.040	0.009	0.026	0.016	0.032	0.010	0.015
Ca	0.318	0.259	0.216	0.183	0.046	0.063	0.135	0.167	0.240	0.345	0.183
Na	3.908	3.781	3.929	3.655	0.449	0.861	4.186	3.432	3.376	3.436	3.435
K	0.041	0.077	0.070	0.208	3.565	3.390	0.147	0.287	0.597	0.070	0.047
Ba	0.056	-	0.058	0.051	0.028	-	0.117	0.114	0.143	-	-
MOL PERCENT END MEMBERS											
Celsian	1.28	-	1.36	1.26	0.67	-	2.53	2.84	3.26	-	-
Fe-Or	0.41	-	-	-	0.98	0.21	0.55	0.41	0.72	0.27	0.40
Anorthite	7.33	6.29	5.05	4.46	1.11	1.47	2.92	4.15	5.47	8.92	4.96
Albite	90.03	91.85	91.95	89.20	10.87	19.91	90.81	85.46	76.95	89.00	93.36
Orthoclase	0.94	1.86	1.65	5.08	86.38	78.40	3.18	7.15	13.60	1.81	1.28
MOL PERCENT IN AN-AB-OR SYSTEM											
An	7.46	6.29	5.12	4.51	1.12	1.47	3.02	4.29	5.70	8.95	4.98
Ab	91.58	91.85	93.21	90.34	11.05	19.96	93.70	88.33	80.14	89.24	93.73
Or	0.96	1.86	1.67	5.15	87.83	78.57	3.28	7.39	14.17	1.81	1.28

The analyses from No. 1-1 to 1-24 are in the coares graind feldspar crystal and the analyses from No. 2-1 to 2-6 are in the fine grained feldspar crystals.

Appendix 1. continued

	Secondary feldspar, core					Antiperthite groundmass							
	Alkali feldspar					K-feldspar					Na-feldspar		
CL colour	Dull blue					Dull blue			Brown		Red		
Anal. No.	1-12	1-13	1-14	1-15	1-16	1-17	1-18	1-19	1-21	1-22	1-23	1-24	1-25
SiO2	64.37	63.62	64.52	65.02	63.84	64.52	65.68	64.97	65.18	64.79	64.08	62.48	64.61
Al2O3	19.20	19.61	19.09	19.31	19.01	17.59	17.91	17.93	18.30	17.62	22.72	22.49	22.91
Fe2O3	-	0.16	0.14	0.10	0.12	0.60	0.29	0.13	0.44	0.13	0.68	0.66	0.31
BaO	0.69	1.24	1.90	1.57	2.62	-	-	0.34	-	-	0.35	-	-
CaO	0.46	0.14	0.23	0.23	0.31	-	0.12	0.07	0.07	0.10	-	-	-
Na2O	4.13	4.78	4.12	4.94	3.31	0.95	-	-	-	0.48	12.07	13.91	12.02
K2O	11.15	9.55	10.02	8.85	10.80	16.40	16.04	16.58	15.67	16.88	0.16	0.11	0.17
STRUCTURAL FORMULA BASED ON 32 OXYGEN													
Si	11.799	11.737	11.843	11.849	11.816	11.989	12.099	12.047	12.036	12.038	11.326	11.168	11.370
Al	4.149	4.265	4.131	4.149	4.148	3.853	3.889	3.919	3.984	3.860	4.734	4.739	4.753
Fe+3	-	0.022	0.020	0.014	0.017	0.084	0.040	0.019	0.062	0.019	0.090	0.088	0.041
Ca	0.090	0.028	0.045	0.045	0.061	-	0.024	0.014	0.014	0.020	-	-	-
Na	1.468	1.710	1.466	1.746	1.188	0.342	-	-	-	0.173	4.137	4.821	4.101
K	2.608	2.248	2.346	2.058	2.550	3.888	3.770	3.922	3.692	4.001	0.036	0.025	0.038
Ba	0.050	0.090	0.137	0.112	0.190	-	-	0.025	-	-	0.024	-	-
MOL PERCENT END MEMBERS													
Celsian	1.18	2.19	3.40	2.82	4.74	-	-	0.62	-	-	0.57	-	-
Fe-Or	-	0.53	0.50	0.35	0.42	1.95	1.04	0.47	1.64	0.44	2.10	1.79	0.99
Anorthite	2.14	0.68	1.13	1.13	1.53	-	0.62	0.35	0.37	0.47	-	-	-
Albite	34.82	41.74	36.52	43.93	29.65	7.93	-	-	-	4.10	96.49	97.70	98.10
Orthoclase	61.86	54.87	58.45	51.78	63.65	90.12	98.34	98.56	97.99	94.98	0.84	0.51	0.91
MOL PERCENT IN AN-AB-OR SYSTEM													
An	2.17	0.69	1.17	1.17	1.62	-	0.62	0.35	0.37	0.47	-	-	-
Ab	35.24	42.90	38.01	45.36	31.26	8.09	-	-	-	4.12	99.14	99.48	99.08
Or	62.59	56.40	60.82	53.47	67.12	91.91	99.38	99.65	99.63	95.40	0.86	0.52	0.92

Appendix 1. continued

	Groungmass, core			Groundmass, antiperthite rim			
	Microperthite			K-feldspar		Na-feldspar	
CL colour	Light violet blue			Brown		Red	
Anal. No.	2-1	2-2	2-3	2-4	2-4	2-5	2-6
SiO2	65.35	64.88	64.98	64.61	65.07	64.68	64.81
Al2O3	19.63	20.37	19.24	17.73	17.55	22.35	22.41
Fe2O3	0.20	0.21	0.27	0.43	0.58	0.59	0.62
BaO	-	-	-	0.34	-	-	0.21
CaO	0.14	0.22	0.08	-	-	-	0.07
Na2O	7.34	7.78	7.64	0.88	0.35	12.25	11.86
K2O	7.36	6.56	7.61	15.95	16.23	0.20	0.09
STRUCTURAL FORMULA BASED ON 32 OXYGEN							
Si	11.776	11.666	11.774	12.008	12.074	11.405	11.421
Al	4.170	4.318	4.110	3.885	3.839	4.646	4.656
Fe+3	0.024	0.026	0.033	0.055	0.073	0.070	0.074
Ca	0.027	0.042	0.016	-	-	-	0.013
Na	2.565	2.713	2.684	0.317	0.126	4.188	4.052
K	1.692	1.505	1.759	3.782	3.842	0.045	0.020
Ba	-	-	-	0.025	-	-	0.014
MOL PERCENT END MEMBERS							
Celsian	-	-	-	0.59	-	-	0.35
Fe-Or	0.57	0.60	0.73	1.31	1.80	1.63	1.78
Anorthite	0.63	0.99	0.35	-	-	-	0.32
Albite	59.53	63.29	59.76	7.59	3.12	97.32	97.07
Orthoclase	39.28	35.12	39.17	90.51	95.09	1.05	0.48
MOL PERCENT IN AN-AB-OR SYSTEM							
An	0.63	1.00	0.35	-	-	-	0.32
Ab	59.87	63.68	60.20	7.74	3.17	98.94	99.18
Or	39.50	35.33	39.45	92.26	96.83	1.06	0.50

Appendix 1. Representative compositions of feldspars in the unlayered ferroaugite syenite (C188) in Center I, Coldwell Complex, Ontario

	Alkali feldspar		Secondary K-feldspar			Secondary oligoclase			Secondary albite	
CL colour	L. violet blue		Dull blue			Purple			Deep purple	
Anal. No.	1	2	3	4	5	6	7	8	10	11
SiO2	64.67	64.85	64.70	64.58	64.50	63.28	63.18	63.37	64.95	64.33
Al2O3	20.09	19.90	17.65	17.89	18.08	23.13	23.19	23.02	22.82	22.90
Fe2O3	0.13	0.12	0.09	-	0.24	0.14	0.14	0.18	0.16	0.12
BaO	0.36	0.64	1.40	1.00	1.42	0.35	0.15	0.27	-	0.17
CaO	1.14	0.90	0.40	0.22	0.30	2.86	2.65	3.14	0.73	0.78
Na2O	5.83	5.71	2.66	2.82	3.32	9.83	9.88	9.17	11.01	11.37
K2O	7.46	7.83	13.11	13.39	11.96	0.42	0.56	0.79	0.31	0.34
STRUCTURAL FORMULA BASED ON 32 OXYGENS										
Si	11.706	11.739	11.993	11.966	11.932	11.211	11.209	11.234	11.414	11.346
Al	4.287	4.247	3.857	3.908	3.943	4.831	4.850	4.811	4.728	4.762
Fe+3	0.018	0.017	0.012	-	0.034	0.019	0.019	0.024	0.021	0.016
Ca	0.221	0.175	0.079	0.044	0.059	0.543	0.504	0.596	0.137	0.147
Na	2.046	2.004	0.956	1.013	1.191	3.377	3.399	3.152	3.752	3.888
K	1.723	1.808	3.100	3.165	2.823	0.095	0.127	0.179	0.070	0.077
Ba	0.026	0.045	0.102	0.073	0.103	0.024	0.010	0.019	-	0.012
MOL PERCENT END MEMBERS										
Celsian	0.63	1.12	2.39	1.69	2.44	0.60	0.26	0.47	-	0.28
Fe-Or	0.45	0.41	0.29	-	0.81	0.47	0.48	0.60	0.52	0.39
Anorthite	5.48	4.31	1.87	1.02	1.41	13.38	12.41	15.03	3.45	3.56
Albite	50.73	49.50	22.50	23.59	28.29	83.21	83.73	79.40	94.28	93.92
Orthoclase	42.71	44.66	72.95	73.70	67.05	2.34	3.12	4.50	1.75	1.85
MOL PERCENT IN AN-AB-OR SYSTEM										
An	5.54	4.38	1.92	1.03	1.46	13.52	12.50	15.19	3.47	3.58
Ab	51.28	50.27	23.12	24.00	29.24	84.11	84.35	80.26	94.77	94.55
Or	43.18	45.35	74.96	74.97	69.30	2.36	3.15	4.55	1.76	1.86

Appendix 1. Representative compositions of feldspars in the unlayred ferroaugite syenite (C302) in Center I, Coldwell Complex, Ontario

	Na-feldspar, core				Exsolved albite, mantle							K-feldspar, mantle		
CL colour	Light blue				Ligth blue							Dull blue		
Anal. No.	1	2	3	4	5	6	7	8	9	10	11	12	13	14
SiO2	63.15	62.54	62.39	62.54	63.96	63.64	64.38	64.75	64.68	64.42	64.04	65.62	64.73	64.37
Al2O3	23.52	24.33	24.44	23.81	23.34	22.73	23.43	23.22	23.14	23.62	23.32	17.61	18.33	17.72
Fe2O3	-	-	0.17	0.23	0.20	0.26	-	0.18	0.22	0.12	0.24	0.51	-	1.23
BaO	-	-	0.60	0.74	-	-	-	-	-	0.22	-	-	-	0.43
CaO	1.43	3.02	3.41	1.92	0.87	0.86	0.67	0.58	0.58	0.68	0.56	-	0.05	0.18
Na2O	11.16	9.56	8.49	9.72	11.03	11.68	11.03	10.87	11.13	10.41	11.48	2.02	2.12	0.77
K2O	0.40	0.32	0.53	0.66	0.50	0.40	0.35	0.26	0.28	0.33	0.38	14.29	14.16	15.42
STRUCTURAL FORMULA BASED ON 32 OXYGENS														
Si	11.196	11.068	11.052	11.140	11.285	11.297	11.330	11.379	11.365	11.335	11.287	12.066	11.972	11.947
Al	4.916	5.076	5.104	5.000	4.855	4.757	4.861	4.811	4.793	4.900	4.845	3.817	3.997	3.877
Fe+3	-	-	0.022	0.031	0.027	0.034	-	0.024	0.029	0.016	0.032	0.071	-	0.172
Ca	0.272	0.573	0.647	0.366	0.164	0.164	0.126	0.109	0.109	0.128	0.106	-	0.010	0.036
Na	3.836	3.281	2.916	3.357	3.773	4.020	3.764	3.704	3.792	3.552	3.923	0.720	0.760	0.277
K	0.090	0.072	0.120	0.150	0.113	0.091	0.079	0.058	0.063	0.074	0.085	3.352	3.341	3.651
Ba	-	-	0.042	0.052	-	-	-	-	-	0.015	-	-	-	0.031
MOL PERCENT END MEMBERS														
Celsian	-	-	1.11	1.31	-	-	-	-	-	0.40	-	-	-	0.75
Fe-Or	-	-	0.59	0.79	0.65	0.79	-	0.60	0.74	0.43	0.78	1.71	-	4.13
Anorthite	6.47	14.59	17.27	9.26	4.03	3.80	3.18	2.80	2.73	3.39	2.55	-	0.24	0.86
Albite	91.37	83.57	77.82	84.85	92.55	93.31	94.84	95.10	94.96	93.83	94.61	17.38	18.49	6.65
Orthoclase	2.15	1.84	3.20	3.79	2.76	2.10	1.98	1.50	1.57	1.96	2.06	80.91	81.27	87.61
MOL PERCENT IN AN-AB-OR SYSTEM														
An	6.47	14.59	17.57	9.46	4.06	3.83	3.18	2.82	2.75	3.42	2.57	-	0.24	0.90
Ab	91.37	83.57	79.17	86.67	93.16	94.05	94.84	95.67	95.66	94.61	95.35	17.68	18.49	6.99
Or	2.15	1.84	3.25	3.87	2.78	2.12	1.98	1.51	1.58	1.97	2.08	82.32	81.27	92.11

Appendix 1. continued

	Exsolved K-feldspar, mantle					Microperthite, mantle					2nd albite, rim		
CL colour	Dull blue					Light violet blue					Purple		
Anal. No.	15	16	17	18	19	20	21	22	23	24	25	26	27
SiO2	64.50	64.93	63.71	64.11	63.97	66.10	65.82	67.43	66.89	67.31	64.18	64.50	64.13
Al2O3	18.24	18.42	18.03	17.79	17.56	19.02	18.54	18.40	18.56	18.82	22.88	23.53	22.49
Fe2O3	0.19	0.08	0.14	0.69	1.34	0.22	0.30	0.27	0.23	0.24	-	0.08	0.22
BaO	0.44	0.35	0.20	-	0.58	-	0.57	-	-	0.17	-	-	0.36
CaO	0.16	0.10	0.12	0.13	0.09	0.26	0.20	0.22	0.18	0.20	0.24	0.23	0.09
Na2O	1.58	0.76	0.35	-	-	5.07	5.55	5.47	5.55	5.36	12.08	11.45	12.39
K2O	14.68	15.38	17.04	17.24	17.17	9.04	8.69	8.24	8.38	7.82	0.31	0.22	0.34
STRUCTURAL FORMULA BASED ON 32 OXYGENS													
Si	11.951	11.988	11.930	11.956	11.916	11.947	11.959	12.089	12.040	12.057	11.348	11.329	11.354
Al	3.984	4.010	3.980	3.911	3.856	4.053	3.971	3.889	3.938	3.974	4.769	4.872	4.694
Fe+3	0.026	0.011	0.020	0.097	0.189	0.030	0.041	0.036	0.032	0.033	-	0.010	0.030
Ca	0.032	0.020	0.024	0.026	0.018	0.050	0.039	0.042	0.035	0.038	0.045	0.043	0.017
Na	0.568	0.272	0.127	-	-	1.777	1.955	1.901	1.937	1.862	4.141	3.899	4.253
K	3.470	3.623	4.071	4.102	4.080	2.085	2.014	1.885	1.924	1.787	0.070	0.049	0.077
Ba	0.032	0.025	0.015	-	0.042	-	0.041	-	-	0.012	-	-	0.025
MOL PERCENT END MEMBERS													
Celsian	0.77	0.64	0.34	-	0.98	-	0.99	-	-	0.32	-	-	0.57
Fe-Or	0.64	0.27	0.48	2.29	4.35	0.77	1.00	0.93	0.80	0.88	-	0.26	0.67
Anorthite	0.77	0.50	0.57	0.61	0.41	1.28	0.95	1.09	0.88	1.03	1.07	1.08	0.39
Albite	13.75	6.89	2.99	-	-	45.07	47.80	49.20	49.32	49.88	97.29	97.43	96.63
Orthoclase	84.07	91.70	95.63	97.10	94.25	52.88	49.25	48.77	49.00	47.89	1.64	1.23	1.74
MOL PERCENT IN AN-AB-OR SYSTEM													
An	0.78	0.51	0.57	0.63	0.44	1.29	0.97	1.10	0.89	1.04	1.07	1.08	0.39
Ab	13.95	6.95	3.01	-	-	45.42	48.78	49.67	49.72	50.49	97.29	97.68	97.84
Or	85.27	92.54	96.42	99.37	99.56	53.29	50.25	49.23	49.39	48.47	1.64	1.23	1.77

Appendix 1. continued

	Secondary albite, antiperthitic rim						Secondary K-feldspar, antiperthitic rim							
CL colour	Violet blue			Red			Grey				Brown			
Anal. No.	28	29	30	31	32	33	34	35	36	37	38	39	40	41
SiO2	65.29	64.59	64.48	63.93	63.63	64.27	64.74	64.99	64.76	63.83	64.23	64.18	63.63	63.83
Al2O3	23.13	21.84	21.76	22.39	22.34	22.20	17.90	17.59	17.37	17.87	17.86	18.09	18.04	17.75
Fe2O3	0.42	0.83	0.61	0.88	0.98	0.81	0.47	0.76	1.01	0.56	0.79	0.81	0.22	0.36
BaO	-	-	-	0.49	0.17	-	-	-	-	-	-	-	-	0.36
CaO	-	-	0.10	-	0.07	-	0.09	0.08	0.07	0.23	0.09	0.07	0.09	0.16
Na2O	10.90	12.68	12.81	12.19	12.65	12.58	-	0.95	0.89	0.37	0.63	-	0.65	0.59
K2O	0.18	-	0.13	0.22	0.26	0.15	16.49	15.71	15.89	16.84	16.28	16.85	16.76	16.67
STRUCTURAL FORMULA BASED ON 32 OXYGENS														
Si	11.439	11.417	11.416	11.328	11.284	11.362	12.025	12.024	12.017	11.928	11.948	11.934	11.919	11.947
Al	4.778	4.551	4.542	4.677	4.671	4.627	3.920	3.837	3.800	3.937	3.917	3.966	3.984	3.917
Fe+3	0.056	0.111	0.081	0.117	0.131	0.108	0.065	0.105	0.141	0.078	0.110	0.114	0.031	0.050
Ca	-	-	0.019	-	0.013	-	0.018	0.016	0.014	0.046	0.018	0.014	0.018	0.032
Na	3.703	4.346	4.398	4.188	4.350	4.312	-	0.341	0.320	0.134	0.227	-	0.236	0.214
K	0.040	-	0.029	0.050	0.059	0.034	3.908	3.708	3.762	4.015	3.864	3.997	4.005	3.981
Ba	-	-	-	0.034	0.012	-	-	-	-	-	-	-	-	0.026
MOL PERCENT END MEMBERS														
Celsian	-	-	-	0.78	0.26	-	-	-	-	-	-	-	-	0.61
Fe-Or	1.47	2.49	1.80	2.67	2.86	2.42	1.63	2.52	3.33	1.83	2.62	2.75	0.73	1.16
Anorthite	-	-	0.42	-	0.29	-	0.45	0.38	0.33	1.08	0.43	0.34	0.42	0.75
Albite	97.48	97.51	97.13	95.42	95.30	96.82	-	8.17	7.56	3.14	5.39	-	5.50	4.98
Orthoclase	1.06	-	0.65	1.13	1.29	0.76	97.92	88.92	88.78	93.96	91.57	96.91	93.35	92.50
MOL PERCENT IN AN-AB-OR SYSTEM														
An	-	-	0.43	-	0.30	-	0.46	0.39	0.34	1.10	0.44	0.35	0.42	0.76
Ab	98.93	100.00	98.91	98.83	98.37	99.22	-	8.38	7.82	3.20	5.53	-	5.54	5.07
Or	1.07	-	0.66	1.17	1.33	0.78	99.54	91.23	91.84	95.71	94.03	99.65	94.03	94.18

Appendix 1. Representative compositions of feldspars in the unlayered ferroaugite syenite (C305) in Center I, Coldwell Complex, Ontario

	Optically homogeneous alkali feldspar, core							Optically homogeneous alkali feldspar host, mantle				Exsolved albite, mantle		
CL colour	Light violet blue							Bluish violet to violet blue				Dull red		
Anal. No.	1	2	3	4	5	6	7	8	9	10	11	12	13	14
SiO2	65.47	65.06	64.60	64.76	64.86	65.58	64.81	66.13	65.72	66.70	65.25	63.43	64.35	64.34
Al2O3	20.23	20.03	20.12	19.73	19.86	20.29	20.12	19.99	19.96	19.09	19.72	22.55	22.99	22.53
Fe2O3	0.29	0.30	0.29	0.23	0.16	0.20	0.29	0.60	0.68	1.59	1.00	0.40	0.48	0.39
BaO	0.54	-	0.21	0.76	0.65	0.53	0.44	-	0.25	0.17	0.15	-	-	-
CaO	0.10	0.33	0.25	0.18	0.93	0.21	0.07	0.08	0.08	0.09	0.11	0.26	-	-
Na2O	6.39	7.23	7.86	7.60	6.85	5.93	7.42	5.99	6.04	4.03	6.41	12.71	11.96	12.65
K2O	7.02	6.95	6.60	6.78	7.21	7.07	6.69	7.27	7.03	8.50	7.07	0.24	0.20	0.13
STRUCTURAL FORMULA BASED ON 32 OXYGENS														
Si	11.768	11.718	11.660	11.717	11.692	11.792	11.702	11.834	11.813	11.961	11.770	11.280	11.338	11.356
Al	4.287	4.253	4.281	4.209	4.221	4.301	4.283	4.217	4.230	4.036	4.194	4.728	4.776	4.688
Fe+3	0.039	0.041	0.039	0.032	0.022	0.027	0.039	0.081	0.092	0.214	0.136	0.054	0.063	0.052
Ca	0.019	0.064	0.048	0.035	0.180	0.040	0.014	0.015	0.015	0.017	0.021	0.050	-	-
Na	2.227	2.525	2.751	2.666	2.394	2.068	2.598	2.078	2.105	1.401	2.242	4.383	4.086	4.329
K	1.610	1.597	1.520	1.565	1.658	1.622	1.541	1.660	1.612	1.945	1.627	0.054	0.045	0.029
Ba	0.038	-	0.015	0.054	0.046	0.037	0.031	-	0.018	0.012	0.011	-	-	-
MOL PERCENT END MEMBERS														
Celsian	0.97	-	0.34	1.24	1.07	0.98	0.74	-	0.46	0.33	0.26	-	-	-
Fe-Or	0.99	0.96	0.90	0.73	0.50	0.71	0.93	2.11	2.39	5.97	3.36	1.18	1.51	1.17
Anorthite	0.49	1.51	1.11	0.80	4.18	1.07	0.32	0.40	0.40	0.48	0.53	1.09	-	-
Albite	56.62	59.74	62.90	61.27	55.68	54.49	61.52	54.20	54.79	39.04	55.54	96.53	97.42	98.16
Orthoclase	40.93	37.79	34.75	35.96	38.57	42.75	36.50	43.29	41.96	54.17	40.31	1.20	1.07	0.66
MOL PERCENT IN AN-AB-OR SYSTEM														
An	0.50	1.52	1.12	0.82	4.24	1.08	0.33	0.41	0.41	0.51	0.55	1.10	-	-
Ab	57.75	60.32	63.69	62.50	56.57	55.43	62.56	55.37	56.40	41.66	57.63	97.68	98.91	99.33
Or	41.75	38.15	35.19	36.69	39.18	43.48	37.11	44.22	43.19	57.82	41.82	1.21	1.09	0.67

Appendix 1. continued

	Exsolved K-feldspar, mantle			Deuteric coarsened antiperthitic rim, 2nd. albite			2nd K-feldspar				Secondary feldspars, in fractures			
CL colour	Blue			Red			Brown				Non CL			
Anal. No.	15	16	17	18	19	20	21	22	23	24	25	26	27	28
SiO2	65.15	64.85	65.39	64.36	64.18	64.58	64.94	64.48	63.86	64.70	62.90	62.34	64.56	64.74
Al2O3	18.17	17.98	18.04	22.70	22.76	22.61	17.96	18.07	18.15	17.73	22.28	22.56	17.97	18.34
Fe2O3	0.11	0.20	0.18	0.41	0.42	0.42	0.51	-	1.92	0.70	0.21	0.24	-	-
BaO	-	0.58	-	-	-	-	-	0.58	-	-	-	-	0.88	-
CaO	0.13	0.18	0.38	-	-	0.11	0.12	0.06	0.15	0.17	1.51	0.12	-	0.06
Na2O	-	-	-	12.32	12.41	12.07	0.27	0.26	-	-	11.79	12.66	0.67	0.86
K2O	16.34	16.13	15.96	0.26	0.26	0.24	16.02	16.48	15.79	16.54	0.87	1.50	15.91	15.89
STRUCTURAL FORMULA BASED ON 32 OXYGENS														
Si	12.043	12.035	12.062	11.351	11.329	11.380	12.024	11.998	11.866	12.018	11.242	11.194	12.008	11.979
Al	3.960	3.934	3.923	4.720	4.736	4.697	3.920	3.964	3.976	3.883	4.695	4.776	3.941	4.001
Fe+3	0.015	0.028	0.025	0.055	0.056	0.056	0.071	-	0.269	0.098	0.028	0.033	-	-
Ca	0.026	0.036	0.075	-	-	0.021	0.024	0.012	0.030	0.034	0.289	0.023	-	0.012
Na	-	-	-	4.213	4.247	4.124	0.097	0.094	-	-	4.086	4.408	0.242	0.309
K	3.853	3.819	3.756	0.059	0.059	0.054	3.784	3.912	3.743	3.920	0.198	0.344	3.775	3.751
Ba	-	0.042	-	-	-	-	-	0.042	-	-	-	-	0.064	-
MOL PERCENT END MEMBERS														
Celsian	-	1.07	-	-	-	-	-	1.04	-	-	-	-	1.57	-
Fe-Or	0.40	0.71	0.64	1.26	1.29	1.32	1.79	-	6.65	2.42	0.62	0.69	-	-
Anorthite	0.66	0.91	1.95	-	-	0.49	0.60	0.29	0.74	0.84	6.28	0.48	-	0.29
Albite	-	-	-	97.39	97.37	96.93	2.44	2.31	-	-	88.79	91.68	5.92	7.58
Orthoclase	98.94	97.30	97.41	1.35	1.34	1.27	95.17	96.35	92.61	96.75	4.31	7.15	92.51	92.13
MOL PERCENT IN AN-AB-OR SYSTEM														
An	0.66	0.93	1.96	-	-	0.49	0.61	0.30	0.79	0.86	6.32	0.48	-	0.29
Ab	-	-	-	98.63	98.64	98.22	2.48	2.33	-	-	89.34	92.32	6.02	7.58
Or	99.34	99.07	98.04	1.37	1.36	1.29	96.91	97.37	99.21	99.14	4.34	7.20	93.98	92.13

Appendix 2. Representative compositions of feldspars in the early layered nepheline syenite (C623) in Center II, Pic Island, Coldwell Complex, Ontario

	Homogeneous alkali feldspars							Secondary Na-feldspars					
CL colour	Light blue							Light violet		Light violet-blue			
Anal. No.	1-1	1-2	1-3	1-4	1-5	2-1	2-2	1-6	1-7	1-8	1-9	2-3	2-4
SiO2	65.46	65.99	65.64	66.09	66.27	65.74	66.87	65.13	64.97	64.37	64.50	63.91	64.20
Al2O3	19.71	20.02	20.12	19.84	19.54	19.84	19.22	22.95	23.54	23.38	23.44	23.45	23.41
Fe2O3	0.20	0.13	-	-	0.19	0.32	0.23	0.21	0.11	-	0.16	0.18	-
BaO	-	0.44	0.55	0.26	-	-	0.68	-	-	-	-	-	-
CaO	0.55	0.53	0.38	0.38	0.36	0.64	0.46	0.73	1.08	0.93	1.18	1.48	1.77
Na2O	5.93	5.50	5.47	5.38	5.24	5.44	5.32	10.54	10.18	10.91	10.50	10.62	10.36
K2O	7.86	7.39	7.78	8.05	8.21	7.96	7.24	0.31	0.13	0.22	0.24	0.14	0.26
STRUCTURAL FORMULA BASED ON 32 OXYGENS													
Si	11.811	11.842	11.817	11.873	11.913	11.821	11.986	11.434	11.373	11.330	11.327	11.270	11.294
Al	4.193	4.235	4.270	4.202	4.141	4.206	4.061	4.750	4.858	4.852	4.853	4.875	4.855
Fe+3	0.027	0.018	-	-	0.026	0.044	0.031	0.028	0.015	-	0.021	0.024	-
Ca	0.106	0.102	0.073	0.073	0.069	0.123	0.088	0.137	0.203	0.175	0.222	0.280	0.334
Na	2.075	1.914	1.909	1.874	1.826	1.897	1.849	3.588	3.455	3.723	3.575	3.631	3.534
K	1.809	1.692	1.787	1.845	1.883	1.826	1.657	0.069	0.029	0.049	0.054	0.031	0.058
Ba	-	0.031	0.039	0.018	-	-	0.048	-	-	-	-	-	-
MOL PERCENT END MEMBERS													
Celsian	-	0.82	1.02	0.48	-	-	1.30	-	-	-	-	-	-
Fe-Or	0.68	0.48	-	-	0.67	1.12	0.86	0.73	0.40	-	0.53	0.60	-
Anorthite	2.65	2.71	1.92	1.92	1.82	3.17	2.41	3.59	5.47	4.44	5.74	7.05	8.50
Albite	51.64	50.94	50.14	49.18	48.01	48.76	50.34	93.86	93.35	94.31	92.35	91.56	90.01
Orthoclase	45.04	45.04	46.92	48.42	49.50	46.95	45.10	1.82	0.78	1.25	1.39	0.79	1.49
MOL PERCENT IN AN-AB-OR SYSTEM													
An	2.66	2.75	1.94	1.93	1.84	3.21	2.46	3.62	5.49	4.44	5.77	7.09	8.50
Ab	51.99	51.62	50.65	49.42	48.34	49.31	51.45	94.55	93.72	94.31	92.84	92.11	90.01
Or	45.34	45.63	47.40	48.65	49.83	47.48	46.09	1.83	0.79	1.25	1.40	0.80	1.49

Appendix 2. continued

2nd Na-fspars		Secondary K-feldspars			
Non CL		Dull blue			
1-10	1-11	1-12	1-13	2-5	2-6
65.42	65.05	64.64	64.97	64.48	64.20
23.22	23.49	18.21	18.05	17.80	18.04
-	0.21	-	0.09	-	0.08
0.23	-	-	0.48	0.85	0.71
0.16	0.77	0.14	0.17	0.20	0.14
10.64	10.23	1.42	1.08	0.22	0.28
0.24	0.26	15.31	15.17	16.25	16.31
STRUCTURAL FORMULA BASED ON 32 OXYGENS					
11.463	11.388	11.972	12.014	12.027	11.979
4.796	4.848	3.976	3.935	3.914	3.969
-	0.028	-	0.012	-	0.011
0.030	0.144	0.028	0.034	0.040	0.028
3.615	3.473	0.510	0.387	0.080	0.101
0.054	0.058	3.618	3.579	3.867	3.883
0.016	-	-	0.035	0.062	0.052
MOL PERCENT END MEMBERS					
0.43	-	-	0.86	1.53	1.27
-	0.75	-	0.31	-	0.27
0.81	3.90	0.67	0.83	0.99	0.69
97.32	93.78	12.27	9.57	1.97	2.49
1.44	1.57	87.06	88.43	95.51	95.28
MOL PERCENT IN AN-AB-OR SYSTEM					
0.81	3.93	0.67	0.84	1.00	0.70
97.74	94.49	12.27	9.68	2.00	2.53
1.45	1.58	87.06	89.48	97.00	96.78

Appendix 2. Represntive compositions of feldspars in the early layered nephline syenites (C624, C626) in Center II, Pic Island, Coldwell Complex, Ontario

	Oligoclase, core								Secondary K-feldspar, rim			
CL colour	Light blue								Dull blue to grey			
Anal. No.	C626-1	C626-2	C626-3	C626-4	C626-5	C626-6	C624-1	C624-2	C626-7	C626-8	C626-9	C626-10
SiO2	63.06	63.52	63.03	63.45	64.00	62.08	62.14	63.06	65.49	65.69	65.58	64.67
Al2O3	24.50	23.32	23.84	24.38	23.66	23.54	23.61	23.96	18.34	18.84	18.42	18.07
Fe2O3	-	0.28	0.16	-	0.18	0.13	-	0.20	-	0.07	-	-
BaO	-	-	-	-	-	1.17	1.06	-	0.72	0.73	1.30	1.05
CaO	4.04	3.85	4.21	3.41	3.92	4.16	4.15	3.86	0.20	0.44	0.37	0.44
Na2O	7.90	8.67	8.01	7.89	7.63	8.27	8.03	7.78	2.69	3.75	3.18	1.95
K2O	0.22	0.29	0.29	0.46	0.49	0.66	1.01	0.85	12.56	10.08	11.07	13.82
STRUCTURAL FORMULA BASED ON 32 OXYGENS												
Si	11.114	11.213	11.153	11.180	11.257	11.081	11.089	11.154	12.008	11.972	12.007	11.970
Al	5.090	4.853	4.973	5.064	4.906	4.954	4.967	4.996	3.964	4.048	3.976	3.943
Fe+3	-	0.033	0.019	-	0.021	0.016	-	0.024	-	0.008	-	-
Ca	0.763	0.728	0.798	0.644	0.739	0.796	0.794	0.732	0.039	0.086	0.073	0.087
Na	2.700	2.968	2.748	2.696	2.602	2.862	2.778	2.668	0.956	1.325	1.129	0.700
K	0.049	0.065	0.065	0.103	0.110	0.150	0.230	0.192	2.938	2.344	2.586	3.264
Ba	-	-	-	-	-	0.082	0.074	-	0.052	0.052	0.093	0.076
MOL PERCENT END MEMBERS												
Celsian	-	-	-	-	-	2.09	1.91	-	1.30	1.37	2.40	1.85
Fe-Or	-	0.88	0.51	-	0.61	0.41	-	0.66	-	0.22	-	-
Anorthite	21.72	19.19	21.99	18.70	21.28	20.37	20.47	20.23	0.99	2.25	1.87	2.11
Albite	76.87	78.21	75.70	78.30	74.95	73.28	71.68	73.80	24.00	34.73	29.09	16.96
Orthoclase	1.41	1.72	1.80	3.00	3.17	3.85	5.93	5.31	73.72	61.43	66.63	79.08
MOL PERCENT IN AN-AB-OR SYSTEM												
An	21.72	19.36	22.10	18.70	21.41	20.89	20.87	20.37	1.00	2.29	1.92	2.15
Ab	76.87	78.90	76.09	78.30	75.41	75.16	73.08	74.29	24.31	35.29	29.81	17.28
Or	1.41	1.74	1.81	3.00	3.19	3.95	6.05	5.34	74.69	62.42	68.28	80.57

Appendix 2. continued

	Secondary K-feldspar, rim				Alkali feldspars				
CL colour	Dull blue to grey				Light violet blue				
Anal. No.	C626-11	C626-12	C624-3	C624-4	C626-13	C626-14	C626-15	C626-16	C624-5
SiO2	65.89	64.69	64.11	64.84	64.25	66.20	66.15	65.84	64.84
Al2O3	18.72	19.09	18.27	17.72	19.27	18.16	18.75	18.67	19.20
Fe2O3	0.17	0.16	0.20	-	0.31	0.26	0.10	0.08	0.19
BaO	1.03	0.78	1.31	0.89	1.08	0.95	0.64	0.59	1.13
CaO	0.56	0.52	0.46	0.36	0.44	0.35	0.43	0.30	0.30
Na2O	3.14	2.96	2.02	1.71	4.56	3.50	2.84	3.50	3.30
K2O	10.32	11.29	13.30	14.31	9.19	10.61	10.91	10.72	10.83
STRUCTURAL FORMULA BASED ON 32 OXYGENS									
Si	12.002	11.881	11.915	12.026	11.811	12.058	12.028	12.001	11.877
Al	4.020	4.134	4.003	3.875	4.176	3.900	4.019	4.012	4.146
Fe+3	0.021	0.019	0.025	-	0.039	0.032	0.012	0.010	0.023
Ca	0.109	0.102	0.092	0.072	0.087	0.068	0.084	0.059	0.059
Na	1.109	1.054	0.728	0.615	1.625	1.236	1.001	1.237	1.172
K	2.398	2.645	3.154	3.386	2.155	2.466	2.531	2.493	2.531
Ba	0.074	0.056	0.095	0.065	0.078	0.068	0.046	0.042	0.081
MOL PERCENT END MEMBERS									
Celsian	1.98	1.45	2.33	1.56	1.95	1.75	1.24	1.10	2.10
Fe-Or	0.55	0.50	0.61	-	0.97	0.81	0.34	0.25	0.61
Anorthite	2.95	2.64	2.24	1.73	2.18	1.77	2.28	1.53	1.52
Albite	29.89	27.19	17.78	14.86	40.80	31.95	27.25	32.21	30.31
Orthoclase	64.63	68.23	77.04	81.84	54.10	63.72	68.89	64.92	65.46
MOL PERCENT IN AN-AB-OR SYSTEM									
An	3.02	2.69	2.31	1.76	2.24	1.81	2.32	1.55	1.57
Ab	30.66	27.73	18.32	15.10	42.03	32.79	27.69	32.65	31.16
Or	66.31	69.58	79.37	83.14	55.73	65.40	69.99	65.80	67.28

Appendix 2. Represntive compositions of feldspars in the early layered nephline syenites (C629, C630) in Center II, Pic Island, Coldwell complex, Ontario

	Homogeneous alkali feldspars						Na-rich feldspars						K-rich feldspars		
CL colour	Light blue and light violet blue						Light blue						Light violet		
Anal. No.	C630-1	C630-1	C630-3	C629-1	C629-2	C629-3	C630-4	C630-5	C630-6	C629-4	C629-5	C629-6	C629-7	C629-8	C629-9
SiO2	65.41	65.28	65.19	66.31	66.09	66.68	64.79	64.52	65.42	64.92	65.06	64.83	66.12	65.68	65.85
Al2O3	19.86	20.95	19.75	20.05	19.99	18.98	22.75	23.76	23.39	23.13	22.68	23.06	18.13	18.71	18.67
Fe2O3	0.14	0.14	0.28	-	-	0.10	0.27	0.31	0.18	0.18	0.22	0.19	0.51	0.18	0.19
BaO	0.62	0.37	-	0.64	0.62	1.47	0.72	0.57	-	-	0.84	-	0.80	0.78	0.97
CaO	0.91	1.00	1.18	0.62	0.80	0.81	1.76	2.56	2.02	2.24	1.76	2.29	0.17	0.27	0.32
Na2O	4.93	5.93	5.11	5.06	4.99	5.59	9.22	8.07	8.28	8.91	9.03	8.88	4.06	3.51	3.98
K2O	8.14	6.34	8.52	7.32	7.51	6.38	0.23	0.24	0.43	0.48	0.23	0.31	10.26	10.77	10.04
STRUCTURAL FORMULA BASED ON 32 OXYGENS															
Si	11.807	11.686	11.770	11.883	11.864	11.990	11.433	11.324	11.449	11.398	11.466	11.405	12.036	11.976	11.980
Al	4.226	4.421	4.204	4.236	4.231	4.024	4.733	4.917	4.826	4.787	4.712	4.783	3.891	4.022	4.004
Fe+3	0.018	0.018	0.034	-	-	0.012	0.032	0.037	0.021	0.021	0.027	0.023	0.063	0.022	0.023
Ca	0.176	0.192	0.228	0.119	0.154	0.156	0.333	0.481	0.379	0.421	0.332	0.432	0.033	0.053	0.062
Na	1.725	2.058	1.789	1.758	1.737	1.949	3.155	2.746	2.810	3.033	3.086	3.029	1.433	1.241	1.404
K	1.875	1.448	1.962	1.674	1.720	1.464	0.052	0.054	0.096	0.108	0.052	0.070	2.383	2.505	2.330
Ba	0.044	0.026	-	0.045	0.044	0.104	0.050	0.039	-	-	0.058	-	0.057	0.056	0.069
MOL PERCENT END MEMBERS															
Celsian	1.14	0.69	-	1.25	1.19	2.81	1.37	1.17	-	-	1.63	-	1.44	1.44	1.78
Fe-Or	0.46	0.47	0.85	-	-	0.33	0.88	1.10	0.64	0.59	0.75	0.63	1.59	0.57	0.60
Anorthite	4.59	5.13	5.69	3.31	4.21	4.24	9.19	14.34	11.46	11.76	9.35	12.15	0.84	1.36	1.60
Albite	44.96	55.01	44.57	48.90	47.53	52.90	87.12	81.79	85.00	84.65	86.82	85.26	36.10	32.01	36.10
Orthoclase	48.85	38.70	48.90	46.54	47.07	39.72	1.43	1.60	2.90	3.00	1.45	1.96	60.03	64.63	59.92
MOL PERCENT IN AN-AB-OR SYSTEM															
An	4.66	5.19	5.74	3.35	4.26	4.37	9.40	14.67	11.53	11.83	9.58	12.23	0.86	1.39	1.64
Ab	45.70	55.66	44.95	49.52	48.10	54.61	89.13	83.69	85.54	85.15	88.93	85.80	37.23	32.66	36.98
Or	49.64	39.15	49.31	47.13	47.64	41.01	1.46	1.64	2.92	3.02	1.49	1.97	61.91	65.95	61.38

Appendix 2. Representative compositions of feldspars in the perthitic nepheline syenite (N1A) in Center II, Neys Park

	Perthite, core						Antiperthite, margins							
	Exsolved K-feldspar				Exso. albite		Secondary K-feldspar			Secondary albite				
CL colour	Light violet blue				Light blue		Dull blue			Dull red		Deep red		
Anal. No.	N1A-1	N1A-2	N1A-3	N1A-4	N1A-5	N1A-6	N1A-7	N1A-8	N1A-9	N1A-10	N1A-11	N1A-12	N1A-13	N1A-14
SiO2	65.90	65.73	66.46	66.30	60.77	60.85	66.58	67.24	66.70	61.71	61.25	61.70	61.59	61.73
Al2O3	20.27	20.23	19.96	20.36	23.41	24.23	20.36	20.50	20.27	23.63	23.59	23.76	23.66	23.78
Fe2O3	-	0.10	-	-	0.07	0.06	-	-	0.10	0.06	0.07	0.09	0.22	0.14
BaO	0.36	0.28	0.32	0.09	-	0.10	-	-	0.14	-	-	-	-	-
CaO	0.09	0.09	-	0.11	0.28	0.30	0.08	0.06	-	0.14	0.08	0.08	-	0.18
Na2O	1.46	2.09	1.61	1.64	15.16	14.34	0.68	-	0.58	14.47	14.95	14.01	14.40	14.07
K2O	11.92	11.49	11.65	11.50	0.19	0.13	12.06	12.20	12.22	-	0.07	0.11	0.10	0.11
STRUCTURAL FORMULA BASED ON 32 OXYGENS														
Si	11.921	11.889	11.993	11.940	10.917	10.881	11.996	12.049	12.006	11.004	10.955	11.014	10.992	11.000
Al	4.323	4.314	4.246	4.323	4.958	5.108	4.325	4.331	4.302	4.968	4.974	5.000	4.978	4.996
Fe+3	-	0.014	-	-	0.009	0.007	-	-	0.014	0.007	0.009	0.012	0.030	0.019
Ca	0.017	0.017	-	0.021	0.054	0.057	0.015	0.012	-	0.027	0.015	0.015	-	0.034
Na	0.512	0.733	0.563	0.573	5.280	4.972	0.238	-	0.202	5.003	5.185	4.849	4.983	4.861
K	2.751	2.652	2.682	2.642	0.044	0.030	2.772	2.789	2.806	-	0.016	0.025	0.023	0.025
Ba	0.026	0.020	0.023	0.006	-	0.007	-	-	0.010	-	-	-	-	-
MOL PERCENT IN END MEMBERS														
Celsian	0.77	0.58	0.69	0.20	-	0.14	-	-	0.33	-	-	-	-	-
Fe-Or	-	0.40	-	-	0.17	0.15	-	-	0.45	0.15	0.17	0.24	0.59	0.39
Anorthite	0.53	0.51	-	0.65	1.00	1.13	0.51	0.41	-	0.53	0.29	0.31	-	0.70
Albite	15.49	21.34	17.24	17.66	98.02	98.00	7.85	-	6.68	99.32	99.23	98.93	98.96	98.41
Orthoclase	83.21	77.18	82.07	81.49	0.81	0.58	91.64	99.59	92.55	-	0.31	0.51	0.45	0.51
MOL PERCENT IN AN-AB-OR SYSTEM														
An	0.53	0.51	-	0.66	1.00	1.14	0.51	0.41	-	0.53	0.29	0.31	-	0.70
Ab	15.61	21.55	17.36	17.70	98.19	98.28	7.85	-	6.73	99.47	99.40	99.17	99.55	98.79
Or	83.86	77.94	82.64	81.65	0.81	0.59	91.64	99.59	93.27	-	0.31	0.51	0.45	0.51

Appendix 2. Representative compositions of feldspars in the perthitic nepheline syenite (N2A) in Center II, Neys Park

	Exsolved Na-feldspar		Exsolved K-feldspar			Microcline			Secondary albite, margins	
CL colour	Light blue		Light violet blue			Light violet blue			Dull red	
Anal. No.	1	2	3	4	5	6	7	8	9	10
SiO2	65.31	64.80	63.78	63.96	63.68	64.50	64.14	64.25	64.05	63.97
Al2O3	22.98	23.04	17.82	17.94	18.22	17.73	17.88	17.86	23.13	22.89
Fe2O3	-	-	0.11	0.07	-	-	0.09	0.12	-	-
BaO	-	-	-	0.28	-	-	0.24	-	0.23	-
CaO	0.08	0.52	0.17	0.18	0.12	0.22	0.11	0.25	0.29	0.19
Na2O	11.20	11.18	1.32	1.32	1.33	0.76	0.37	0.73	11.60	12.57
K2O	0.43	0.32	16.81	16.26	16.65	16.79	17.07	16.80	0.39	0.24
STRUCTURAL FORMULA BASED ON 32 OXYGENS										
Si	11.453	11.397	11.909	11.922	11.874	11.997	11.971	11.959	11.330	11.312
Al	4.751	4.777	3.923	3.942	4.005	3.888	3.934	3.919	4.824	4.772
Fe+3	-	-	0.016	0.009	-	-	0.012	0.017	-	-
Ca	0.015	0.098	0.034	0.036	0.024	0.044	0.022	0.050	0.055	0.036
Na	3.808	3.813	0.478	0.477	0.481	0.274	0.134	0.263	3.979	4.310
K	0.096	0.072	4.004	3.867	3.961	3.984	4.064	3.990	0.088	0.054
Ba	-	-	-	0.020	-	-	0.018	-	0.016	-
MOL PERCENT IN END MEMBERS										
Celsian	-	-	-	0.46	-	-	0.41	-	0.39	-
Fe-Or	-	-	0.34	0.21	-	-	0.29	0.40	-	-
Anorthite	0.38	2.46	0.75	0.82	0.54	1.02	0.52	1.15	1.33	0.82
Albite	97.16	95.74	10.55	10.82	10.77	6.37	3.15	6.10	96.16	97.95
Orthoclase	2.45	1.80	88.36	87.69	88.70	92.61	95.63	92.35	2.13	1.23
MOL PERCENT IN AN-AB-OR SYSTEM										
An	0.38	2.46	0.75	0.82	0.54	1.02	0.52	1.16	1.33	0.82
Ab	97.16	95.74	10.58	10.89	10.77	6.37	3.17	6.12	96.53	97.95
Or	2.45	1.80	88.67	88.29	88.70	92.61	96.31	92.72	2.14	1.23

Appendix 2. Representative compositions of feldspars within the brick-red irregular pegmatitic patches (N3A) in the perthitic syenite in Center II, Neys Park, Coldwell Complex, Ontario

	K-feldspar							Secondary albite					
CL colour	Dull blue							Dull red					
Anal. No.	1	2	3	4	5	6	7	8	9	10	11	12	13
SiO2	63.53	64.36	64.14	63.96	64.33	63.65	63.70	63.96	64.04	63.96	63.91	63.87	63.64
Al2O3	18.30	17.78	17.88	17.58	17.81	17.65	17.95	22.95	22.63	22.83	23.26	23.21	22.83
Fe2O3	-	0.10	-	0.11	0.13	-	-	-	0.17	0.10	0.13	-	-
BaO	-	-	0.23	-	-	0.15	-	-	-	0.54	-	0.45	-
CaO	0.12	-	0.15	-	0.16	0.12	0.10	0.18	0.21	0.18	0.19	0.30	0.16
Na2O	0.42	0.36	1.00	0.62	0.37	1.32	0.89	12.68	12.59	12.21	12.37	12.03	13.02
K2O	17.31	17.32	16.60	17.60	17.00	17.11	17.36	0.14	0.38	0.19	0.15	0.14	0.35
STRUCTURAL FORMULA BASED ON 32 OXYGENS													
Si	11.889	11.997	11.953	11.972	11.991	11.919	11.907	11.303	11.324	11.322	11.274	11.290	11.272
Al	4.037	3.907	3.928	3.879	3.914	3.896	3.956	4.781	4.718	4.765	4.838	4.837	4.767
Fe+3	-	0.014	-	0.016	0.019	-	-	-	0.022	0.013	0.018	-	-
Ca	0.024	-	0.030	-	0.032	0.024	0.020	0.034	0.040	0.034	0.036	0.057	0.030
Na	0.152	0.130	0.361	0.225	0.134	0.479	0.323	4.345	4.317	4.191	4.231	4.123	4.471
K	4.133	4.119	3.947	4.203	4.043	4.087	4.140	0.032	0.086	0.043	0.034	0.032	0.079
Ba	-	-	0.017	-	-	0.011	-	-	-	0.037	-	0.031	-
MOL PERCENT IN END MEMBERS													
Celsian	-	-	0.39	-	-	0.24	-	-	-	0.87	-	0.73	-
Fe-Or	-	0.33	-	0.35	0.44	-	-	-	0.50	0.31	0.41	-	-
Anorthite	0.56	-	0.69	-	0.76	0.52	0.45	0.77	0.89	0.79	0.83	1.34	0.66
Albite	3.54	3.05	8.30	5.06	3.16	10.41	7.20	98.51	96.69	97.04	97.98	97.18	97.61
Orthoclase	95.91	96.62	90.63	94.58	95.64	88.82	92.36	0.72	1.92	0.99	0.78	0.74	1.73
MOL PERCENT IN AN-AB-OR SYSTEM													
An	0.56	-	0.69	-	0.76	0.52	0.45	0.77	0.90	0.80	0.84	1.35	0.66
Ab	3.54	3.06	8.33	5.08	3.18	10.44	7.20	98.51	97.17	98.19	98.38	97.90	97.61
Or	95.91	96.94	90.98	94.92	96.06	89.04	92.36	0.72	1.93	1.01	0.78	0.75	1.73

Appendix 2. Representative compositions of feldspars in the perthitic nepheline syenite (N3B) in Center II, Neys Park

	Perthite												
	Exsolved Na-feldspar							Exsolved K-feldspar					
CL colour	Light blue							Light violet blue					
Anal. No.	1-1	1-2	1-3	2-1	2-2	2-3	2-4	1-4	1-5	1-6	1-7	2-5	2-6
SiO2	64.51	64.30	65.42	64.98	65.49	64.85	64.74	64.23	64.79	64.82	64.39	65.55	64.40
Al2O3	22.26	22.77	23.05	23.27	23.49	22.96	22.54	17.77	18.02	17.41	17.52	17.98	17.69
Fe2O3	0.16	0.19	0.11	-	-	0.13	0.09	-	0.10	0.09	-	-	0.08
BaO	0.78	-	-	-	-	0.36	-	-	-	0.33	0.23	-	0.24
CaO	0.26	0.14	0.71	0.43	0.51	0.51	0.44	0.15	0.11	0.11	0.21	0.18	0.21
Na2O	11.84	12.46	10.47	10.18	10.29	10.97	11.87	1.36	1.00	0.71	1.8	1.72	1.30
K2O	0.21	0.16	0.25	0.23	0.22	0.23	0.19	16.11	15.99	16.54	15.85	14.45	16.09
STRUCTURAL FORMULA BASED ON 32 OXYGENS													
Si	11.420	11.342	11.452	11.451	11.440	11.407	11.412	11.975	11.995	12.059	11.984	12.057	11.980
Al	4.646	4.735	4.757	4.834	4.838	4.761	4.684	3.906	3.933	3.818	3.844	3.899	3.880
Fe+3	0.021	0.025	0.015	-	-	0.018	0.012	-	0.014	0.012	-	-	0.011
Ca	0.049	0.026	0.133	0.081	0.095	0.096	0.083	0.030	0.022	0.022	0.042	0.035	0.042
Na	4.064	4.262	3.554	3.478	3.485	3.741	4.057	0.492	0.359	0.256	0.650	0.613	0.469
K	0.047	0.036	0.056	0.052	0.049	0.052	0.043	3.832	3.777	3.926	3.764	3.391	3.819
Ba	0.054	-	-	-	-	0.025	-	-	-	0.024	0.017	-	0.017
MOL PERCENT IN END MEMBERS													
Celsian	1.28	-	-	-	-	0.63	-	-	-	0.57	0.38	-	0.40
Fe-Or	0.49	0.58	0.39	-	-	0.45	0.28	-	0.33	0.29	-	-	0.25
Anorthite	1.16	0.61	3.54	2.25	2.63	2.44	1.98	0.69	0.52	0.52	0.94	0.88	0.96
Albite	95.95	97.99	94.58	96.32	96.02	95.16	96.72	11.29	8.61	6.04	14.53	15.18	10.76
Orthoclase	1.12	0.83	1.49	1.43	1.35	1.31	1.02	88.02	90.54	92.58	84.16	83.94	87.63
MOL PERCENT IN AN-AB-OR SYSTEM													
An	1.19	0.61	3.56	2.25	2.63	2.47	1.99	0.69	0.52	0.52	0.94	0.88	0.97
Ab	97.67	98.56	94.95	96.32	96.02	96.20	96.99	11.29	8.63	6.09	14.58	15.18	10.83
Or	1.14	0.83	1.49	1.43	1.35	1.33	1.02	88.02	90.84	93.39	84.48	83.94	88.20

Analyses 1-1 to 1-13 are from phenocrsyts of the feldspar grains and 2-1 to 2-13 are from groundmass of the feldspar grains.

Appendix 2. continued

	Perthite			2nd. K-feldspar		Antiperthite, margins							
	Exsolved K-feldspar					Scondary Na-feldspar							
CL colour	Light violet blue			Brown		Dull red							
Anal. No.	2-7	2-8	2-9	1-8	1-9	1-10	1-11	1-12	1-13	2-10	2-11	2-12	2-13
SiO2	65.12	64.48	65.69	64.48	64.83	65.11	64.74	65.35	64.83	64.89	65.03	64.64	65.50
Al2O3	17.62	17.76	18.11	17.58	17.52	22.81	23.15	23.01	22.72	22.65	22.55	22.97	22.74
Fe2O3	0.14	-	-	0.21	-	0.29	0.19	-	0.17	0.09	0.19	0.12	-
BaO	-	0.52	-	0.27	-	-	-	-	-	-	-	-	-
CaO	0.21	0.28	0.19	-	0.07	0.15	0.31	0.13	0.17	0.28	0.15	0.35	0.20
Na2O	1.07	0.74	1.27	0.4	-	11.42	11.5	11.31	12	11.84	11.93	11.82	11.38
K2O	15.85	16.22	14.56	17.01	17.58	0.25	0.05	0.2	0.13	0.16	0.17	0.11	0.18
STRUCTURAL FORMULA BASED ON 32 OXYGENS													
Si	12.050	12.001	12.072	12.022	12.066	11.431	11.374	11.451	11.403	11.421	11.435	11.369	11.480
Al	3.844	3.897	3.924	3.864	3.844	4.721	4.795	4.753	4.711	4.700	4.675	4.763	4.699
Fe+3	0.020	-	-	0.030	-	0.038	0.025	-	0.022	0.012	0.025	0.016	-
Ca	0.042	0.056	0.037	-	0.014	0.028	0.058	0.024	0.032	0.053	0.028	0.066	0.038
Na	0.384	0.267	0.453	0.145	-	3.887	3.917	3.843	4.093	4.041	4.067	4.031	3.867
K	3.742	3.851	3.414	4.046	4.174	0.056	0.011	0.045	0.029	0.036	0.038	0.025	0.040
Ba	-	0.038	-	0.020	-	-	-	-	-	-	-	-	-
MOL PERCENT IN END MEMBERS													
Celsian	-	0.90	-	0.47	-	-	-	-	-	-	-	-	-
Fe-Or	0.48	-	-	0.70	-	0.95	0.62	-	0.53	0.28	0.60	0.39	-
Anorthite	0.99	1.33	0.96	-	0.33	0.70	1.45	0.62	0.77	1.28	0.68	1.59	0.95
Albite	9.17	6.34	11.59	3.41	-	96.95	97.64	98.23	98.01	97.57	97.80	97.42	98.03
Orthoclase	89.36	91.43	87.45	95.43	99.67	1.40	0.28	1.14	0.70	0.87	0.92	0.60	1.02
MOL PERCENT IN AN-AB-OR SYSTEM													
An	1.00	1.34	0.96	-	0.33	0.71	1.46	0.62	0.77	1.28	0.68	1.60	0.95
Ab	9.21	6.40	11.59	3.45	-	97.88	98.26	98.23	98.53	97.85	98.39	97.80	98.03
Or	89.79	92.26	87.45	96.55	99.67	1.41	0.28	1.14	0.70	0.87	0.92	0.60	1.02

Appendix 2. Representative compositions of feldspars in the perthitic nepheline syenite (N3C) from Center II, Neys Park

	Unexsolved alkali feldspar, core			Perthite: Exsolved Na-feldspar				Perthite: Exsolved K-feldspar				Secondary albite, margins			
CL colour	Light violet blue			Light blue				Light violet blue				Dull red			
Anal. No.	1	2	3	4	5	6	7	8	9	10	11	12	13	14	15
SiO2	66.41	65.62	65.71	65.29	65.28	64.26	64.55	65.52	65.08	64.56	64.59	65.46	64.95	65.28	65.82
Al2O3	17.51	17.92	17.84	22.77	22.99	22.60	22.11	17.71	17.56	18.00	17.42	22.68	23.28	23.00	22.90
Fe2O3	0.26	-	0.14	0.08	0.28	0.09	0.21	0.17	0.18	-	0.13	0.09	0.32	-	0.16
BaO	-	0.53	0.53	-	-	-	-	-	-	-	0.39	-	-	-	-
CaO	0.23	0.12	0.25	0.38	0.47	0.45	0.22	0.14	0.18	0.09	0.15	0.35	0.19	0.09	0.23
Na2O	2.69	2.99	2.82	11.22	10.70	12.23	12.82	1.51	0.78	1.54	1.16	11.23	11.14	11.39	10.74
K2O	12.93	12.82	12.72	0.27	0.16	0.27	0.11	14.97	16.24	15.81	16.17	0.20	0.15	0.16	0.17
STRUCTURAL FORMULA BASED ON 32 OXYGENS															
Si	12.131	12.044	12.053	11.455	11.446	11.355	11.401	12.070	12.057	11.968	12.025	11.477	11.387	11.448	11.505
Al	3.771	3.878	3.858	4.710	4.752	4.708	4.604	3.846	3.835	3.934	3.823	4.688	4.812	4.755	4.719
Fe+3	0.035	-	0.020	0.010	0.037	0.012	0.028	0.023	0.025	-	0.019	0.012	0.043	-	0.020
Ca	0.045	0.024	0.049	0.071	0.088	0.085	0.042	0.028	0.036	0.018	0.030	0.066	0.036	0.017	0.043
Na	0.953	1.064	1.003	3.817	3.638	4.190	4.390	0.539	0.280	0.554	0.419	3.818	3.787	3.873	3.640
K	3.013	3.002	2.977	0.060	0.036	0.061	0.025	3.518	3.839	3.739	3.841	0.045	0.034	0.036	0.038
Ba	-	0.038	0.038	-	-	-	-	-	-	-	0.028	-	-	-	-
MOL PERCENT IN END MEMBERS															
Celsian	-	0.92	0.93	-	-	-	-	-	-	-	0.66	-	-	-	-
Fe-Or	0.87	-	0.49	0.26	0.97	0.27	0.63	0.56	0.59	-	0.43	0.30	1.09	-	0.55
Anorthite	1.11	0.57	1.20	1.80	2.32	1.96	0.93	0.67	0.85	0.41	0.69	1.67	0.92	0.43	1.15
Albite	23.55	25.78	24.54	96.41	95.77	96.37	97.89	13.13	6.70	12.84	9.66	96.90	97.13	98.66	97.29
Orthoclase	74.47	72.73	72.84	1.53	0.94	1.40	0.55	85.64	91.85	86.74	88.57	1.14	0.86	0.91	1.01
MOL PERCENT IN AN-AB-OR SYSTEM															
An	1.12	0.58	1.22	1.81	2.35	1.96	0.93	0.68	0.86	0.41	0.70	1.67	0.93	0.43	1.16
Ab	23.75	26.02	24.89	96.66	96.70	96.63	98.51	13.20	6.74	12.84	9.76	97.19	98.20	98.66	97.82
Or	75.12	73.40	73.89	1.53	0.95	1.40	0.56	86.12	92.40	86.74	89.54	1.14	0.87	0.91	1.02

Appendix 2. Representative compositions of feldspars in the perthitic nepheline syenites in Center I Coldwell Complex, Neys Park, Ontario

	Exsolved albite in the perthite												
CL colour	Light blue												
Anal. No.	C3118D -1	C3118D -2	C3118A -1	C3118A -2	C109 -1	C109 -2	C111 -1	C111 -2	C1863 -1	C1863 -2	C97 -1	C97 -2	C97 -3
SiO2	62.53	62.01	61.70	62.22	62.99	62.71	63.01	63.04	62.41	62.71	61.92	64.11	63.97
Al2O3	22.54	22.84	23.05	22.49	22.99	22.70	22.48	22.77	22.50	22.69	22.94	22.54	22.88
Fe2O3	-	0.09	-	0.18	-	0.16	-	0.10	0.10	-	0.07	-	0.09
BaO	-	-	-	-	-	-	-	0.37	0.32	-	0.49	-	-
CaO	0.33	0.39	0.54	0.52	0.36	0.35	0.29	0.37	0.41	0.58	0.28	0.34	0.42
Na2O	14.49	14.40	14.45	14.38	13.35	13.96	13.67	13.15	14.05	13.46	14.17	12.44	12.35
K2O	0.11	0.17	0.13	0.16	0.31	0.14	0.28	0.21	0.22	0.56	0.14	0.49	0.18
STRUCTURAL FORMULA BASED ON 32 OXYGENS													
Si	11.154	11.086	11.041	11.122	11.188	11.165	11.232	11.214	11.154	11.175	11.082	11.346	11.307
Al	4.740	4.814	4.863	4.740	4.814	4.765	4.724	4.775	4.741	4.767	4.840	4.703	4.768
Fe+3	-	0.012	-	0.024	-	0.021	-	0.013	0.013	-	0.009	-	0.012
Ca	0.063	0.075	0.104	0.100	0.069	0.067	0.055	0.071	0.079	0.111	0.054	0.064	0.080
Na	5.012	4.992	5.013	4.984	4.598	4.819	4.725	4.536	4.869	4.651	4.917	4.269	4.233
K	0.025	0.039	0.030	0.036	0.070	0.032	0.064	0.048	0.050	0.127	0.032	0.111	0.041
Ba	-	-	-	-	-	-	-	0.026	0.022	-	0.034	-	-
MOL PERCENT IN END MEMBERS													
Celsian	-	-	-	-	-	-	-	0.55	0.45	-	0.68	-	-
Fe-Or	-	0.23	-	0.47	-	0.42	-	0.29	0.27	-	0.18	-	0.27
Anorthite	1.24	1.46	2.01	1.94	1.45	1.35	1.14	1.50	1.56	2.27	1.06	1.45	1.82
Albite	98.27	97.55	97.41	96.89	97.07	97.58	97.54	96.65	96.73	95.13	97.44	96.06	96.98
Orthoclase	0.49	0.76	0.58	0.71	1.48	0.64	1.31	1.02	1.00	2.60	0.63	2.49	0.93
MOL PERCENT IN AN-AB-OR SYSTEM													
An	1.24	1.46	2.01	1.95	1.45	1.36	1.14	1.52	1.57	2.27	1.07	1.45	1.83
Ab	98.27	97.78	97.41	97.34	97.07	98.00	97.54	97.46	97.43	95.13	98.29	96.06	97.24
Or	0.49	0.76	0.58	0.71	1.48	0.65	1.31	1.02	1.00	2.60	0.64	2.49	0.93

Appendix 2. continued

	Exsolved K-feldspar in the perthite										
CL colour	Light violet blue										
Anal. No.	C3118D -3	C3118D -4	C3118A -3	C109 -3	C109 -4	C111 -3	C111 -4	C1863 -3	C97 -4	C97 -5	C97 -6
SiO2	65.91	65.22	65.39	65.21	65.16	64.29	64.55	64.99	64.89	64.00	63.77
Al2O3	18.17	18.55	18.75	18.32	18.52	18.77	18.72	18.35	18.19	17.40	17.82
Fe2O3	0.06	-	-	-	0.09	0.09	-	0.09	0.10	0.09	-
BaO	-	-	0.60	-	-	0.47	-	0.27	0.51	0.35	0.25
CaO	0.08	0.08	0.12	0.15	-	0.25	0.08	0.12	0.21	0.13	0.13
Na2O	0.87	1.28	1.32	1.01	0.87	1.53	0.93	1.31	1.11	1.52	1.12
K2O	14.92	14.79	13.82	15.31	15.37	14.45	15.09	14.88	15.00	16.52	16.91
STRUCTURAL FORMULA BASED ON 32 OXYGENS											
Si	12.089	11.994	11.998	12.012	11.996	11.890	11.952	11.985	11.994	11.966	11.922
Al	3.929	4.022	4.056	3.978	4.020	4.093	4.087	3.989	3.964	3.835	3.928
Fe+3	0.008	-	-	-	0.012	0.012	-	0.012	0.014	0.013	-
Ca	0.016	0.016	0.024	0.030	-	0.050	0.016	0.024	0.042	0.026	0.026
Na	0.309	0.456	0.470	0.361	0.311	0.549	0.334	0.468	0.398	0.551	0.406
K	3.491	3.470	3.235	3.598	3.610	3.409	3.565	3.501	3.537	3.940	4.033
Ba	-	-	0.043	-	-	0.034	-	0.020	0.037	0.026	0.018
MOL PERCENT IN END MEMBERS											
Celsian	-	-	1.14	-	-	0.84	-	0.48	0.92	0.56	0.41
Fe-Or	0.20	-	-	-	0.31	0.31	-	0.31	0.35	0.27	-
Anorthite	0.41	0.40	0.63	0.74	-	1.22	0.41	0.59	1.03	0.57	0.58
Albite	8.09	11.58	12.45	9.04	7.90	13.53	8.53	11.64	9.88	12.10	9.06
Orthoclase	91.30	88.02	85.78	90.21	91.79	84.10	91.06	86.98	87.83	86.50	89.96
MOL PERCENT IN AN-AB-OR SYSTEM											
An	0.41	0.40	0.63	0.74	-	1.24	0.41	0.59	1.05	0.58	0.58
Ab	8.11	11.58	12.60	9.04	7.92	13.69	8.53	11.73	10.00	12.20	9.09
Or	91.48	88.02	86.77	90.21	92.08	85.07	91.06	87.68	88.95	87.23	90.32

Appendix 2. continued

Secondary albite in the margins of perthite

CL colour	Dull red												Deep red,	
Anal. No.	C3118D -5	C3118D -6	C3118A -4	C3118A -5	C109 -5	C109 -6	C111 -5	C111 -6	C1863 -4	C1863 -5	C97 -7	C97 -8	C3118D -7	C3118D -8
SiO2	63.00	62.38	62.04	62.18	62.69	62.84	62.13	63.01	62.68	62.73	62.87	63.68	62.40	62.25
Al2O3	22.99	22.44	22.60	22.66	22.70	23.16	23.48	23.05	22.72	22.92	22.91	22.47	23.14	22.86
Fe2O3	-	0.22	0.23	0.09	0.07	-	-	0.08	0.14	0.11	-	0.18	0.07	0.08
BaO	-	-	-	0.29	-	-	-	-	-	-	-	0.37	-	0.14
CaO	0.20	0.45	0.51	0.29	0.28	0.15	0.26	0.12	0.38	0.11	0.07	0.25	0.16	0.22
Na2O	13.70	14.43	14.34	14.32	14.06	13.53	13.31	13.66	13.75	13.99	13.67	12.76	14.12	14.22
K2O	0.11	0.10	0.15	0.18	0.21	0.13	0.18	0.09	0.34	0.15	0.25	0.24	0.12	0.16
STRUCTURAL FORMULA BASED ON 32 OXYGENS														
Si	11.186	11.137	11.100	11.119	11.166	11.172	11.102	11.183	11.164	11.159	11.193	11.306	11.110	11.117
Al	4.812	4.723	4.767	4.777	4.767	4.854	4.946	4.823	4.771	4.807	4.809	4.703	4.857	4.813
Fe+3	-	0.030	0.031	0.012	0.009	-	-	0.010	0.019	0.015	-	0.024	0.009	0.010
Ca	0.038	0.086	0.098	0.056	0.053	0.029	0.050	0.023	0.073	0.021	0.013	0.048	0.031	0.042
Na	4.717	4.995	4.975	4.965	4.856	4.664	4.612	4.701	4.749	4.825	4.719	4.393	4.874	4.924
K	0.025	0.023	0.034	0.041	0.048	0.029	0.041	0.020	0.077	0.034	0.057	0.054	0.027	0.036
Ba	-	-	-	0.020	-	-	-	-	-	-	-	0.026	-	0.010
MOL PERCENT IN END MEMBERS														
Celsian	-	-	-	0.40	-	-	-	-	-	-	-	0.57	-	0.20
Fe-Or	-	0.58	0.61	0.23	0.18	-	-	0.22	0.39	0.30	-	0.52	0.18	0.21
Anorthite	0.80	1.68	1.90	1.09	1.08	0.61	1.06	0.48	1.47	0.43	0.28	1.05	0.62	0.84
Albite	98.68	97.30	96.82	97.47	97.78	98.77	98.07	98.87	96.56	98.57	98.54	96.67	98.65	98.03
Orthoclase	0.52	0.44	0.67	0.81	0.96	0.62	0.87	0.43	1.57	0.70	1.19	1.20	0.55	0.73
MOL PERCENT IN AN-AB-OR SYSTEM														
An	0.80	1.69	1.91	1.10	1.08	0.61	1.06	0.48	1.48	0.43	0.28	1.06	0.62	0.84
Ab	98.68	97.87	97.41	98.09	97.96	98.77	98.07	99.09	96.94	98.87	98.54	97.73	98.83	98.43
Or	0.52	0.45	0.67	0.81	0.96	0.62	0.87	0.43	1.58	0.70	1.19	1.21	0.55	0.73

Appendix 2. Representative compositions of nephelines occur inside the brick-red irregular pegmatitic patches in the perthitic pheneline syenite (N3A), the miaskitic nepheline syenite (non-patch) (C114) and the late pegmatitic syenite (C472).

	Ne inside patch			Ne in non patch syenite			Ne in late pegmatitic syenite			
CL colour	Dark blue			Dark blue			Dark blue			
Anal. No.	N3A-1	N3A-2	N3A-3	C114-1	C114-2	C114-3	C472-1	C472-2	C472-3	C472-4
SiO2	46.01	46.31	47.01	44.28	46.22	44.17	45.03	44.44	44.75	44.55
Al203	31.24	32.17	31.09	32.96	31.75	32.73	33.54	33.25	32.86	33.04
Fe203	0.16	0.18	0.20	0.04	0.20	0.18	0.00	0.08	0.00	0.04
CaO	0.05	0.17	0.16	1.15	0.89	1.13	1.01	1.08	1.11	1.11
Na20	16.97	15.26	16.09	16.51	16.79	16.55	15.07	15.91	16.09	15.92
K2O	5.03	5.37	5.47	4.91	4.17	4.55	5.35	5.25	5.19	5.34
Total	99.46	99.46	100.02	99.85	100.02	99.31	100.00	100.01	100.00	100.00
STRUCTURAL FORMULA BASED ON 32 OXYGENS										
Si	8.809	8.816	8.929	8.472	8.768	8.486	8.554	8.481	8.540	8.507
Al	7.049	7.218	6.960	7.432	7.099	7.411	7.509	7.479	7.390	7.435
Fe+3	0.022	0.025	0.029	0.006	0.029	0.026	0.000	0.011	0.000	0.006
Ca	0.010	0.035	0.033	0.236	0.181	0.233	0.206	0.221	0.227	0.227
Na	6.300	5.632	5.926	6.125	6.175	6.165	5.550	5.887	5.953	5.894
K	1.229	1.304	1.326	1.198	1.009	1.115	1.296	1.278	1.263	1.301
Wt PERCENT END MEMBER MOLECULES										
Ne	76.32	70.77	72.33	74.53	75.18	75.05	69.86	72.41	72.85	72.23
Ks	16.63	18.33	18.10	16.26	13.74	15.18	18.17	17.54	17.21	17.77
Fe-Ne	0.33	0.39	0.42	0.09	0.42	0.38	0.00	0.17	0.00	0.09
An	0.24	0.86	0.78	5.62	4.33	5.57	5.07	5.33	5.44	5.46
Qtz	6.48	9.66	8.37	3.49	6.32	3.83	6.90	4.56	4.50	4.45
RECALCULATED Wt% IN Ne-Ks-Qtz SYSTEM										
Ne	76.75	71.66	73.21	79.06	78.94	79.79	73.59	76.62	77.04	76.47
Ks	16.73	18.56	18.32	17.24	14.43	16.14	19.14	18.56	18.20	18.81
Qtz	6.52	9.78	8.47	3.70	6.64	4.07	7.27	4.82	4.76	4.71

Total FeO calculated as Fe203. Ne=NaAlSiO4; Ks=KAlSiO4; Fe-Ne=NaFeSiO4; An=CaAl2Si208; Qtz=SiO2.

Appendix 2. Representative compositions of feldspars in the miaskitic nepheline syenite (C114) in Center II, Neys Park, Coldwell Complex, Ontario

	Oligoclase, core		Alkali feldspar, rim				Secondary alkali feldspar, margins of the rim				core		Relict olig., core	
CL colour	Bluish grey		Light blue				Dull violet				Dull violet		Dull blue	
Anal. No.	1	2	3	4	5	6	7	8	9	10	11	12	13	14
SiO2	58.46	58.89	64.75	65.86	64.74	64.98	65.30	65.87	65.36	65.56	65.26	64.96	61.03	61.18
Al2O3	24.53	24.18	19.42	19.62	19.69	19.73	18.59	19.02	18.81	19.54	19.27	20.28	23.79	23.36
Fe2O3	0.12	0.17	-	-	-	-	0.19	-	0.16	0.22	0.17	0.13	0.18	0.23
BaO	0.63	0.34	-	0.34	0.31	0.47	-	-	0.25	0.39	0.26	-	-	0.38
CaO	5.53	6.26	0.59	0.71	1.00	1.21	0.40	0.65	0.67	0.54	0.64	0.76	3.09	2.77
Na2O	10.43	9.77	6.46	5.43	6.79	6.78	3.86	5.25	5.40	4.29	5.86	5.20	11.77	11.74
K2O	0.31	0.31	8.78	8.04	7.36	6.83	11.43	9.21	9.37	9.48	8.56	8.68	0.16	0.36
STRUCTURAL FORMULA BASED ON 32 OXYGENS														
Si	10.574	10.632	11.750	11.860	11.720	11.731	11.930	11.906	11.871	11.862	11.817	11.723	10.901	10.958
Al	5.231	5.147	4.155	4.165	4.202	4.199	4.004	4.053	4.028	4.168	4.114	4.315	5.010	4.933
Fe+3	0.017	0.023	-	-	-	-	0.026	-	0.021	0.030	0.023	0.018	0.024	0.031
Ca	1.072	1.211	0.115	0.137	0.194	0.234	0.078	0.126	0.130	0.105	0.124	0.147	0.591	0.532
Na	3.658	3.420	2.273	1.896	2.383	2.373	1.367	1.840	1.902	1.505	2.058	1.819	4.076	4.077
K	0.072	0.071	2.033	1.847	1.700	1.573	2.664	2.124	2.171	2.188	1.978	1.998	0.036	0.082
Ba	0.045	0.024	-	0.024	0.022	0.033	-	-	0.018	0.028	0.018	-	-	0.027
MOL PERCENT END MEMBERS														
Celsian	0.92	0.51	-	0.61	0.51	0.79	-	-	0.42	0.72	0.44	-	-	0.56
Fe-Or	0.34	0.48	-	-	-	-	0.63	-	0.50	0.78	0.54	0.45	0.51	0.66
Anorthite	22.04	25.50	2.60	3.51	4.51	5.55	1.89	3.08	3.07	2.72	2.96	3.69	12.51	11.19
Albite	75.23	72.01	51.42	48.56	55.44	56.32	33.06	44.99	44.83	39.03	48.98	45.68	86.22	85.85
Orthoclase	1.47	1.50	45.98	47.31	39.54	37.33	64.42	51.93	51.18	56.75	47.08	50.17	0.77	1.73
MOL PERCENT IN AN-AB-OR SYSTEM														
An	22.32	25.75	2.60	3.53	4.54	5.60	1.91	3.08	3.10	2.76	2.99	3.71	12.57	11.33
Ab	76.19	72.73	51.42	48.86	55.72	56.77	33.27	44.99	45.24	39.63	49.47	45.89	86.65	86.91
Or	1.49	1.52	45.98	47.61	39.74	37.63	64.82	51.93	51.65	57.62	47.55	50.40	0.78	1.75

Appendix 2. Representative compositions of feldspars in gabbro in Center II, Neys Park, Coldwell Complex, Ontario

	Plagioclases					Secondary K-feldspars, margins						
CL colour	Light blue					Light violet-blue						
Anal. No.	C107-1	C107-2	C107-3	C107-4	C107-5	C107-6	C107-7	C107-8	C107-9	C107-10	C107-11	C107-12
SiO2	56.36	56.29	54.80	54.76	56.67	64.29	64.84	63.61	63.77	62.17	60.57	61.89
Al2O3	27.77	27.34	28.42	28.61	27.64	18.01	18.09	17.47	18.07	19.20	18.78	18.25
Fe2O3	-	0.19	0.18	0.20	-	-	-	0.18	-	-	-	0.08
BaO	0.43	0.85	0.62	0.58	-	0.37	1.06	-	1.35	3.79	2.75	2.95
CaO	10.00	9.77	10.70	10.80	9.41	0.17	0.15	0.14	0.17	0.38	0.30	0.25
Na2O	5.33	5.48	5.20	4.94	5.64	1.25	3.43	1.25	1.24	3.11	3.80	3.61
K2O	0.11	0.10	0.10	0.05	0.28	15.81	12.43	17.20	15.40	11.35	13.21	12.94
STRUCTURAL FORMULA BASED ON 32 OXYGENS												
Si	10.135	10.158	9.915	9.902	10.191	11.957	11.959	11.928	11.917	11.672	11.547	11.697
Al	5.887	5.817	6.062	6.099	5.860	3.949	3.933	3.862	3.981	4.250	4.221	4.066
Fe+3	-	0.026	0.024	0.027	-	-	-	0.025	-	-	-	0.011
Ca	1.927	1.889	2.074	2.093	1.813	0.034	0.030	0.028	0.034	0.076	0.061	0.051
Na	1.858	1.918	1.824	1.732	1.967	0.451	1.227	0.454	0.449	1.132	1.405	1.323
K	0.025	0.023	0.023	0.012	0.064	3.751	2.925	4.115	3.672	2.719	3.213	3.120
Ba	0.030	0.060	0.044	0.041	-	0.027	0.077	-	0.099	0.279	0.205	0.218
MOL PERCENT END MEMBERS												
Celsian	0.79	1.54	1.10	1.05	-	0.63	1.80	-	2.32	6.63	4.21	4.63
Fe-Or	-	0.66	0.61	0.70	-	-	-	0.54	-	-	-	0.23
Anorthite	50.17	48.25	51.99	53.59	47.17	0.79	0.70	0.61	0.80	1.82	1.25	1.07
Albite	48.39	48.97	45.72	44.36	51.16	10.57	28.81	9.83	10.56	26.92	28.76	28.01
Orthoclase	0.66	0.59	0.58	0.30	1.67	88.00	68.70	89.02	86.31	64.64	65.78	66.06
MOL PERCENT IN AN-AB-OR SYSTEM												
An	50.57	49.33	52.89	54.55	47.17	0.80	0.71	0.61	0.82	1.95	1.31	1.13
Ab	48.77	50.07	46.52	45.15	51.16	10.64	29.34	9.89	10.81	28.83	30.02	29.44
Or	0.66	0.60	0.59	0.30	1.67	88.56	69.95	89.50	88.37	69.23	68.67	69.43

Appendix 2. Representive composition of feldspars in the mosaic granuloblastic nephline syenite (C587) in Center II, Coldwell Complex, Ontario

	Relict alkali feldspars												
CL colour	Light blue												
Anal. No.	1	2	3	4	5	6	7	8	9	10	11	12	13
SiO2	65.83	66.02	66.04	65.84	65.83	65.95	67.51	66.43	65.67	67.08	65.33	64.93	66.00
Al2O3	18.01	17.63	17.44	17.91	18.38	18.10	17.74	18.60	18.37	17.59	17.79	17.94	18.30
Fe2O3	0.13	0.19	0.29	0.59	-	0.21	0.18	0.27	0.16	0.26	0.34	0.17	0.23
BaO	0.76	0.61	0.62	1.16	1.07	0.62	-	0.85	0.99	0.26	0.79	1.14	1.25
CaO	0.20	0.18	0.23	0.37	0.34	0.17	0.22	0.21	0.31	0.29	0.32	0.46	0.17
Na2O	3.28	2.32	2.11	1.27	3.24	3.95	2.97	2.95	3.60	2.59	1.88	2.97	3.02
K2O	11.72	12.95	13.17	12.92	11.13	11.02	11.25	10.75	10.81	11.70	13.58	12.40	11.05
STRUCTURAL FORMULA BASED ON 32 OXYGENS													
Si	12.050	12.117	12.135	12.089	12.025	12.031	12.215	12.058	12.002	12.202	12.042	11.977	12.052
Al	3.887	3.815	3.778	3.877	3.958	3.893	3.784	3.980	3.958	3.772	3.866	3.901	3.939
Fe+3	0.017	0.023	0.036	0.073	-	0.026	0.022	0.033	0.019	0.031	0.043	0.021	0.029
Ca	0.039	0.035	0.045	0.073	0.067	0.033	0.043	0.041	0.061	0.057	0.063	0.091	0.033
Na	1.164	0.826	0.752	0.452	1.148	1.397	1.042	1.038	1.276	0.914	0.672	1.062	1.069
K	2.737	3.032	3.087	3.027	2.594	2.565	2.597	2.489	2.521	2.715	3.193	2.918	2.574
Ba	0.055	0.044	0.045	0.083	0.077	0.044	-	0.060	0.071	0.019	0.057	0.082	0.089
MOL PERCENT END MEMBERS													
Celsian	1.36	1.11	1.13	2.25	1.97	1.09	-	1.65	1.80	0.50	1.42	1.97	2.36
Fe-Or	0.41	0.59	0.91	1.97	-	0.64	0.59	0.90	0.49	0.84	1.07	0.50	0.76
Anorthite	0.98	0.89	1.14	1.96	1.71	0.82	1.15	1.12	1.54	1.51	1.57	2.18	0.88
Albite	29.02	20.85	18.96	12.19	29.54	34.37	28.14	28.35	32.32	24.46	16.68	25.45	28.17
Orthoclase	68.23	76.56	77.87	81.62	66.77	63.09	70.12	67.98	63.86	72.69	79.27	69.90	67.83
MOL PERCENT IN AN-AB-OR SYSTEM													
An	1.00	0.91	1.17	2.05	1.75	0.83	1.16	1.14	1.57	1.53	1.61	2.23	0.90
Ab	29.54	21.21	19.35	12.73	30.14	34.97	28.30	29.09	33.08	24.79	17.10	26.09	29.08
Or	69.46	77.88	79.48	85.22	68.12	64.20	70.54	69.76	65.35	73.68	81.29	71.68	70.01

Analysis No. 16 is from the light violet luminescent core of the neoblast alkali feldspar, and analysis No. 17 is from the light violet-blue luminescent rim of the neoblast alkali feldspar.

Appendix 2. continued

	Neoblast alkali feldspars								Relict plagioclase				
CL colour	Light violet-blue								Non luminescence				
Anal. No.	14	15	16	17	18	19	20	21	22	23	24	25	26
SiO2	67.60	65.80	66.87	67.31	65.23	67.03	66.07	67.32	45.40	44.74	44.31	45.68	47.16
Al2O3	18.32	18.86	18.95	18.85	18.39	18.88	18.40	18.28	34.19	33.94	34.15	34.28	34.03
Fe2O3	0.12	0.18	0.19	0.16	0.27	-	0.31	0.23	0.12	0.32	0.06	0.16	0.39
BaO	-	1.14	0.47	-	1.46	0.60	1.04	-	0.14	-	0.22	0.17	-
CaO	0.36	0.18	0.28	0.30	0.43	0.26	0.33	0.21	17.60	17.76	16.80	16.88	14.34
Na2O	2.72	4.98	4.31	3.62	3.68	3.81	3.40	3.27	2.55	3.13	3.57	2.86	3.22
K2O	10.82	8.50	8.95	9.55	10.56	9.33	10.46	10.46	-	0.09	-	-	0.17
STRUCTURAL FORMULA BASED ON 32 OXYGENS													
Si	12.177	11.962	12.034	12.098	11.956	12.077	12.032	12.152	8.409	8.326	8.311	8.446	8.699
Al	3.891	4.042	4.020	3.994	3.974	4.010	3.950	3.890	7.466	7.446	7.551	7.473	7.400
Fe+3	0.015	0.022	0.023	0.019	0.033	-	0.038	0.029	0.015	0.041	0.007	0.019	0.049
Ca	0.069	0.035	0.054	0.058	0.084	0.050	0.064	0.041	3.493	3.542	3.376	3.344	2.834
Na	0.950	1.755	1.504	1.262	1.308	1.331	1.201	1.145	0.916	1.129	1.298	1.025	1.152
K	2.487	1.971	2.055	2.190	2.469	2.145	2.430	2.409	-	0.021	-	-	0.040
Ba	-	0.081	0.033	-	0.105	0.042	0.074	-	0.010	-	0.016	0.012	-
MOL PERCENT END MEMBERS													
Celsian	-	2.10	0.90	-	2.62	1.19	1.95	-	0.23	-	0.34	0.28	-
Fe-Or	0.42	0.57	0.63	0.54	0.83	-	1.01	0.79	0.35	0.86	0.15	0.44	1.19
Anorthite	1.97	0.91	1.47	1.64	2.11	1.41	1.69	1.12	78.77	74.83	71.87	75.98	69.56
Albite	26.98	45.42	40.99	35.76	32.70	37.30	31.53	31.59	20.65	23.86	27.64	23.30	28.26
Orthoclase	70.62	51.01	56.01	62.07	61.74	60.10	63.82	66.50	-	0.45	-	-	0.98
MOL PERCENT IN AN-AB-OR SYSTEM													
An	1.98	0.93	1.49	1.65	2.19	1.42	1.74	1.13	79.23	75.47	72.23	76.53	70.40
Ab	27.10	46.66	41.63	35.95	33.87	37.75	32.49	31.84	20.77	24.07	27.77	23.47	28.61
Or	70.92	52.41	56.88	62.40	63.95	60.83	65.77	67.03	-	0.46	-	-	0.99

Appendix 2. continued

Relict and neoblast alkali feldspars (undivided)

CL colour	Light blue and light violet-blue													
Anal. No.	27	28	29	30	31	32	33	34	35	36	37	38	39	40
SiO2	64.93	65.48	65.46	65.59	65.31	65.25	65.75	65.87	65.65	65.62	65.75	66.08	65.04	65.72
Al2O3	18.20	18.11	18.73	18.23	18.56	19.14	18.56	18.14	18.66	18.62	18.38	17.97	18.57	18.11
Fe2O3	0.16	0.09	0.16	0.16	0.12	0.16	0.26	0.24	0.19	0.24	0.12	0.12	0.16	0.18
BaO	0.56	0.50	0.28	0.80	0.52	0.84	-	0.48	0.54	0.50	-	-	-	0.65
CaO	0.29	0.11	0.22	0.25	0.16	0.39	0.15	0.24	0.20	0.15	0.19	0.19	0.14	0.22
Na2O	2.34	2.76	3.93	3.21	2.93	5.39	4.56	2.68	4.21	4.83	3.52	3.46	3.83	3.97
K2O	13.53	12.95	11.02	11.78	12.41	8.68	9.86	12.38	10.56	10.05	11.76	11.62	11.50	10.78
STRUCTURAL FORMULA BASED ON 32 OXYGENS														
Si	11.966	12.020	11.944	12.008	11.963	11.863	11.992	12.044	11.954	11.940	12.006	12.081	11.942	12.027
Al	3.954	3.919	4.029	3.935	4.008	4.102	3.991	3.910	4.006	3.994	3.957	3.873	4.020	3.907
Fe+3	0.019	0.011	0.019	0.019	0.015	0.019	0.032	0.030	0.023	0.030	0.015	0.015	0.019	0.022
Ca	0.057	0.022	0.043	0.049	0.031	0.076	0.029	0.047	0.039	0.029	0.037	0.037	0.028	0.043
Na	0.836	0.982	1.390	1.140	1.041	1.900	1.613	0.950	1.486	1.704	1.246	1.227	1.364	1.409
K	3.181	3.033	2.565	2.752	2.900	2.013	2.294	2.888	2.453	2.333	2.740	2.710	2.694	2.517
Ba	0.040	0.036	0.020	0.057	0.037	0.060	-	0.034	0.039	0.036	-	-	-	0.047
MOL PERCENT END MEMBERS														
Celsian	0.98	0.88	0.50	1.43	0.93	1.47	-	0.87	0.95	0.86	-	-	-	1.15
Fe-Or	0.47	0.27	0.48	0.48	0.38	0.47	0.80	0.77	0.58	0.73	0.37	0.38	0.47	0.55
Anorthite	1.39	0.53	1.07	1.22	0.78	1.87	0.74	1.19	0.97	0.71	0.92	0.93	0.67	1.07
Albite	20.22	24.05	34.43	28.37	25.86	46.70	40.64	24.06	36.79	41.24	30.86	30.75	33.22	34.89
Orthoclase	76.94	74.26	63.53	68.50	72.06	49.49	57.82	73.12	60.72	56.46	67.84	67.94	65.64	62.34
MOL PERCENT IN AN-AB-OR SYSTEM														
An	1.41	0.54	1.08	1.24	0.79	1.90	0.74	1.21	0.98	0.72	0.92	0.94	0.67	1.09
Ab	20.52	24.34	34.77	28.92	26.20	47.63	40.97	24.46	37.36	41.91	30.98	30.86	33.38	35.50
Or	78.07	75.13	64.15	69.83	73.01	50.47	58.29	74.33	61.66	57.37	68.10	68.20	65.95	63.42

Appendix 2. continued

	Secondary albite									
CL colour	Dull red									
Anal.no	41	42	43	44	45	46	47	48	49	50
SiO2	66.39	65.37	65.41	64.33	65.18	66.00	66.43	64.89	65.07	64.23
Al2O3	23.22	22.86	22.95	22.48	22.39	23.15	22.97	22.47	22.73	22.47
Fe2O3	0.17	0.26	0.19	-	-	0.08	-	0.06	0.19	-
BaO	-	-	-	-	-	-	-	-	-	0.08
CaO	0.19	0.44	0.42	0.79	0.95	0.10	0.46	0.21	0.25	0.51
Na2O	9.69	10.46	10.47	10.37	10.95	10.15	9.98	12.22	11.47	12.23
K2O	0.09	0.22	0.16	0.12	0.09	0.09	0.17	0.09	0.21	0.16
STRUCTURAL FORMULA BASED ON 32 OXYGENS										
Si	11.567	11.482	11.482	11.475	11.483	11.540	11.568	11.428	11.438	11.372
Al	4.769	4.734	4.749	4.728	4.650	4.772	4.716	4.665	4.710	4.690
Fe+3	0.020	0.030	0.022	-	-	0.009	-	0.007	0.022	-
Ca	0.035	0.083	0.079	0.151	0.179	0.019	0.086	0.040	0.047	0.097
Na	3.273	3.562	3.564	3.587	3.740	3.441	3.370	4.173	3.909	4.199
K	0.020	0.049	0.036	0.027	0.020	0.020	0.038	0.020	0.047	0.036
Ba	-	-	-	-	-	-	-	-	-	0.006
MOL PERCENT END MEMBERS										
Celsian	-	-	-	-	-	-	-	-	-	0.13
Fe-Or	0.59	0.82	0.61	-	-	0.26	-	0.16	0.56	-
Anorthite	1.06	2.22	2.13	4.01	4.55	0.54	2.46	0.93	1.17	2.23
Albite	97.76	95.64	96.29	95.26	94.93	98.62	96.46	98.43	97.10	96.81
Orthoclase	0.60	1.32	0.97	0.73	0.51	0.58	1.08	0.48	1.17	0.83
MOL PERCENT IN AN-AB-OR SYSTEM										
An	1.07	2.24	2.15	4.01	4.55	0.54	2.46	0.94	1.18	2.23
Ab	98.33	96.42	96.88	95.26	94.93	98.88	96.46	98.59	97.65	96.93
Or	0.60	1.33	0.97	0.73	0.51	0.58	1.08	0.48	1.18	0.83

Appendix 2. Representive composition of feldspars in the porphyroblastic nephline syenite (C571) in Center II, Redsucker Cove, Coldwell Complex, Ontario

	Porphyroblaste Alkali feldspar, core			2nd. Na-feldspar, core			Porphyroblaste Alkali feldspar, rim				Groundmass Alkali feldspar				
CL colour	Light violet			Dull blue			Light violet blue				Light violet blue				
Anal. No.	1-1	1-2	1-3	1-4	1-5	1-6	1-7	1-8	1-9	1-10	1-11	1-12	1-13	1-14	1-15
SiO2	66.80	66.36	66.61	65.01	64.76	63.89	65.43	66.70	65.71	65.59	65.77	66.08	66.06	66.15	66.23
Al2O3	18.51	18.08	18.35	23.40	23.17	23.21	19.71	19.36	19.29	19.22	20.27	19.56	19.86	19.41	19.03
Fe2O3	0.20	0.13	-	-	-	0.19	0.10	0.11	0.18	0.08	0.11	-	-	0.17	0.09
BaO	0.40	0.42	-	-	-	-	0.38	0.74	1.04	1.30	-	0.91	0.68	0.61	0.82
CaO	0.20	0.18	0.13	0.31	0.17	0.10	0.71	0.45	0.68	0.75	0.54	0.51	0.79	0.96	0.72
Na2O	3.97	3.54	3.30	11.03	11.69	11.31	4.12	4.06	4.31	3.75	4.84	5.16	4.68	4.76	4.29
K2O	9.95	11.32	11.33	0.25	0.21	0.29	9.11	8.60	8.72	9.35	8.47	7.50	7.93	7.83	8.83
STRUCTURAL FORMULA BASED ON 32 OXYGENS															
Si	12.070	12.077	12.095	11.394	11.377	11.341	11.861	11.995	11.907	11.915	11.812	11.917	11.879	11.914	11.968
Al	3.943	3.879	3.928	4.835	4.799	4.857	4.212	4.105	4.121	4.116	4.292	4.159	4.210	4.121	4.054
Fe+3	0.024	0.016	-	-	-	0.023	0.012	0.014	0.022	0.010	0.014	-	-	0.020	0.011
Ca	0.039	0.035	0.025	0.058	0.032	0.019	0.138	0.087	0.132	0.146	0.104	0.099	0.152	0.185	0.139
Na	1.391	1.249	1.162	3.748	3.982	3.893	1.448	1.416	1.514	1.321	1.685	1.804	1.632	1.662	1.503
K	2.294	2.628	2.625	0.056	0.047	0.066	2.107	1.973	2.016	2.167	1.941	1.726	1.819	1.799	2.036
Ba	0.028	0.030	-	-	-	-	0.027	0.052	0.074	0.093	-	0.064	0.048	0.043	0.058
MOL PERCENT IN END MEMBERS															
Celsian	0.75	0.76	-	-	-	-	0.72	1.47	1.96	2.48	-	1.74	1.31	1.16	1.55
Fe-Or	0.65	0.42	-	-	-	0.57	0.33	0.38	0.58	0.26	0.36	-	-	0.55	0.29
Anorthite	1.03	0.89	0.66	1.51	0.79	0.48	3.70	2.45	3.51	3.91	2.78	2.67	4.17	4.99	3.72
Albite	36.83	31.55	30.48	97.05	98.05	97.31	38.80	39.98	40.30	35.36	45.02	48.86	44.69	44.80	40.11
Orthoclase	60.74	66.39	68.86	1.45	1.16	1.64	56.45	55.72	53.64	58.00	51.84	46.73	49.83	48.49	54.33
MOL PERCENT IN AB-OR-AN SYSTEM															
An	1.04	0.90	0.66	1.51	0.79	0.48	3.73	2.49	3.61	4.02	2.79	2.72	4.22	5.08	3.79
Ab	37.36	31.93	30.48	97.05	98.05	97.87	39.21	40.73	41.35	36.35	45.18	49.73	45.29	45.58	40.87
Or	61.60	67.18	68.86	1.45	1.16	1.65	57.05	56.77	55.05	59.63	52.03	47.56	50.49	49.34	55.34

Appendix 2. continued

	Porphyroblaste Alkali feldspar, core			rim		Groundmass Alkali feldspar				
CL colour	Light blue			L. violet blue		Light violet blue				
Anal. No.	2-1	2-2	2-3	2-4	2-5	2-6	2-7	2-8	2-9	2-10
SiO2	66.01	64.61	65.40	66.36	66.30	65.89	66.16	65.37	66.27	66.01
Al2O3	18.61	19.33	18.86	18.73	18.54	18.95	19.12	19.27	18.75	18.50
Fe2O3	-	0.12	0.10	0.10	0.13	0.14	0.17	0.13	0.17	0.27
BaO	0.80	1.37	1.62	0.95	0.77	0.97	0.51	0.97	0.92	-
CaO	0.56	1.03	1.00	0.86	0.76	0.82	0.78	0.85	0.68	0.66
Na2O	4.58	4.33	4.51	4.78	4.41	4.30	4.61	5.73	3.96	3.91
K2O	9.08	9.14	8.52	8.25	9.09	8.94	8.44	7.68	9.27	10.62
STRUCTURAL FORMULA BASED ON 32 OXYGENS										
Si	11.997	11.801	11.907	11.988	12.006	11.941	11.948	11.839	12.001	11.983
Al	3.987	4.162	4.048	3.989	3.958	4.049	4.071	4.114	4.003	3.959
Fe+3	-	0.015	0.012	0.012	0.016	0.018	0.020	0.016	0.020	0.033
Ca	0.109	0.202	0.195	0.166	0.147	0.159	0.151	0.165	0.132	0.128
Na	1.614	1.533	1.592	1.674	1.548	1.511	1.614	2.012	1.390	1.376
K	2.105	2.130	1.979	1.901	2.100	2.067	1.945	1.774	2.142	2.460
Ba	0.057	0.098	0.116	0.067	0.055	0.069	0.036	0.069	0.065	-
MOL PERCENT IN END MEMBERS										
Celsian	1.47	2.46	2.97	1.76	1.41	1.80	0.96	1.71	1.74	-
Fe-Or	-	0.38	0.32	0.32	0.42	0.46	0.54	0.41	0.55	0.82
Anorthite	2.81	5.07	5.01	4.36	3.81	4.16	4.01	4.09	3.52	3.21
Albite	41.54	38.55	40.89	43.81	40.04	39.51	42.86	49.85	37.08	34.43
Orthoclase	54.19	53.54	50.82	49.75	54.31	54.06	51.63	43.96	57.11	61.54
MOL PERCENT IN AB-OR-AN SYSTEM										
An	2.85	5.22	5.18	4.45	3.88	4.26	4.07	4.17	3.60	3.24
Ab	42.16	39.68	42.27	44.74	40.79	40.43	43.51	50.92	37.95	34.72
Or	54.99	55.11	52.55	50.81	55.32	55.31	52.42	44.91	58.45	62.04

Appendix 2. Representive composition of feldspars in the porphyroblastic nephline syenite (C572) in Center II, Redsucker Cove, Coldwell Complex, Ontario

	Porphyroblaste													
	Alkali feldspar, core									Alkali feldspar, mantle				
										K-feldspar			oligoclase	
CL colour	Light violet-blue					Light blue				Dull bull			Light blue	
Anal. No.	1-1	1-2	1-3	1-4	1-5	1-6	1-7	1-8	1-9	1-10	1-11	1-12	1-13	1-14
SiO2	65.84	66.10	66.23	64.90	64.84	65.51	65.45	65.35	65.80	64.63	64.38	65.13	62.68	62.59
Al2O3	19.21	19.30	19.81	19.57	20.04	19.28	19.56	19.50	19.52	17.81	18.32	18.48	24.26	24.06
Fe2O3	0.16	0.14	0.10	0.14	-	0.11	0.09	-	0.16	-	0.29	-	0.09	0.23
BaO	0.92	-	-	1.46	1.60	1.22	1.09	1.38	1.35	-	1.46	1.53	-	0.38
CaO	0.95	1.03	0.87	0.89	0.93	1.10	1.37	1.36	0.95	-	0.20	0.44	4.84	4.32
Na2O	5.11	4.66	4.98	5.32	4.89	5.05	5.39	5.32	4.66	0.72	2.25	3.22	7.81	8.25
K2O	7.85	8.22	7.78	7.72	7.70	7.53	7.07	7.01	7.59	16.84	13.11	11.19	0.22	0.18
STRUCTURAL FORMULA BASED ON 32 OXYGENS														
Si	11.893	11.927	11.885	11.789	11.763	11.872	11.819	11.827	11.884	12.011	11.924	11.959	11.066	11.074
Al	4.091	4.106	4.191	4.191	4.286	4.119	4.164	4.161	4.156	3.902	4.000	4.001	5.050	5.019
Fe+3	0.019	0.018	0.012	0.018	-	0.014	0.011	-	0.019	-	0.036	-	0.011	0.028
Ca	0.184	0.199	0.167	0.173	0.181	0.214	0.265	0.264	0.184	-	0.040	0.087	0.916	0.819
Na	1.790	1.630	1.733	1.874	1.720	1.774	1.887	1.867	1.632	0.259	0.808	1.146	2.674	2.830
K	1.809	1.892	1.781	1.789	1.782	1.741	1.629	1.619	1.749	3.993	3.098	2.621	0.050	0.041
Ba	0.065	-	-	0.104	0.114	0.087	0.077	0.098	0.096	-	0.106	0.110	-	0.026
MOL PERCENT IN END MEMBERS														
Celsian	1.68	-	-	2.63	3.00	2.26	1.99	2.54	2.60	-	2.59	2.78	-	0.70
Fe-Or	0.49	0.47	0.33	0.45	-	0.36	0.28	-	0.52	-	0.89	-	0.29	0.75
Anorthite	4.76	5.33	4.53	4.38	4.76	5.58	6.85	6.86	5.00	-	0.97	2.18	25.09	21.87
Albite	46.28	43.60	46.92	47.34	45.30	46.34	48.78	48.53	44.35	6.10	19.77	28.92	73.26	75.59
Orthoclase	46.78	50.60	48.23	45.20	46.94	45.46	42.10	42.07	47.53	93.90	75.78	66.12	1.36	1.09
MOL PERCENT IN AB-OR-AN SYSTEM														
An	4.86	5.35	4.54	4.52	4.91	5.73	7.01	7.03	5.16	-	1.01	2.25	25.16	22.20
Ab	47.31	43.81	47.07	48.85	46.70	47.59	49.91	49.79	45.78	6.10	20.48	29.74	73.48	76.70
Or	47.82	50.84	48.39	46.64	48.39	46.69	43.08	43.17	49.06	93.90	78.51	68.01	1.36	1.10

Appendix 2. continued

	Porphyroblaste Alkali feldspar, rim					Groundmass Alkali feldspar							
CL colour	Light blue					Light violet-blue							
Anal. No.	1-15	1-16	1-17	1-18	1-19	1-20	1-21	1-22	1-23	2-1	2-2	2-3	2-4
SiO2	65.85	65.73	65.54	65.63	65.58	65.41	65.17	66.26	65.70	65.33	66.52	64.53	64.65
Al2O3	19.58	19.08	19.60	19.72	19.16	19.58	19.41	18.89	19.18	19.34	19.27	19.57	19.79
Fe2O3	0.14	0.14	0.26	0.24	0.14	0.14	0.10	0.08	0.09	0.29	-	1.11	0.20
BaO	0.72	0.82	0.80	1.52	1.34	-	1.44	1.02	1.30	1.35	0.81	1.41	1.22
CaO	0.98	1.16	0.63	0.91	0.87	0.55	0.80	0.69	0.20	0.78	0.83	0.89	1.07
Na2O	4.76	4.99	4.46	4.73	4.43	5.24	4.66	4.09	4.09	4.39	4.36	4.81	4.68
K2O	7.98	7.75	8.62	7.27	8.48	8.79	8.43	8.84	9.43	8.55	8.23	7.96	8.40
STRUCTURAL FORMULA BASED ON 32 OXYGENS													
Si	11.871	11.904	11.862	11.854	11.900	11.834	11.844	11.996	11.938	11.863	11.972	11.730	11.753
Al	4.161	4.074	4.182	4.199	4.099	4.176	4.159	4.032	4.109	4.140	4.089	4.194	4.242
Fe+3	0.018	0.018	0.031	0.030	0.018	0.018	0.012	0.010	0.011	0.036	-	0.137	0.025
Ca	0.189	0.225	0.122	0.176	0.169	0.107	0.156	0.134	0.039	0.152	0.160	0.173	0.208
Na	1.664	1.752	1.565	1.656	1.559	1.838	1.642	1.436	1.441	1.546	1.521	1.695	1.650
K	1.835	1.791	1.990	1.675	1.963	2.029	1.955	2.042	2.186	1.981	1.890	1.846	1.948
Ba	0.051	0.058	0.057	0.108	0.095	-	0.103	0.072	0.093	0.096	0.057	0.100	0.087
MOL PERCENT IN END MEMBERS													
Celsian	1.35	1.51	1.51	2.95	2.50	-	2.65	1.96	2.46	2.52	1.57	2.54	2.22
Fe-Or	0.47	0.46	0.83	0.82	0.47	0.44	0.32	0.26	0.29	0.93	-	3.46	0.63
Anorthite	5.04	5.86	3.24	4.83	4.45	2.67	4.03	3.62	1.03	3.98	4.41	4.39	5.32
Albite	44.29	45.59	41.56	45.44	40.97	46.05	42.46	38.87	38.23	40.57	41.93	42.90	42.11
Orthoclase	48.85	46.58	52.85	45.96	51.61	50.83	50.54	55.28	57.99	51.99	52.08	46.71	49.73
MOL PERCENT IN AB-OR-AN SYSTEM													
An	5.13	5.97	3.32	5.02	4.58	2.68	4.15	3.71	1.06	4.13	4.48	4.67	5.48
Ab	45.11	46.50	42.56	47.22	42.23	46.26	43.76	39.76	39.31	42.02	42.60	45.64	43.34
Or	49.76	47.52	54.12	47.76	53.19	51.06	52.09	56.54	59.63	53.85	52.91	49.70	51.18

Appendix 2. continued

	Groundmass				Porphyroblaste						
	Two feldspars, margins of the groundmass				Porphyroblastic plagioclase, core			rim			
CL colour	Dull blue		Light blue		Light blue			Light violet			
Anal. No.	2-5	2-6	2-7	2-8	2-9	2-10	2-11	2-12	2-13	2-14	2-15
SiO2	64.14	65.73	61.89	62.34	57.94	57.15	57.93	62.96	61.63	61.77	61.79
Al2O3	18.45	18.58	24.23	24.16	25.29	26.43	26.37	23.88	24.42	24.42	25.03
Fe2O3	0.10	0.17	0.19	0.20	0.16	-	-	0.18	0.18	-	0.18
BaO	1.60	0.66	-	0.75	1.41	1.01	0.47	-	-	-	-
CaO	0.28	0.27	5.47	4.44	8.30	9.16	9.26	4.75	5.35	5.79	6.05
Na2O	2.83	2.31	7.95	7.95	6.35	5.38	5.01	7.32	8.12	7.85	6.74
K2O	12.61	12.30	0.29	0.18	0.13	0.35	0.34	0.94	0.17	0.18	0.13
STRUCTURAL FORMULA BASED ON 32 OXYGENS											
Si	11.883	12.011	10.968	11.053	10.508	10.350	10.434	11.124	10.936	10.942	10.917
Al	4.030	4.003	5.062	5.050	5.407	5.643	5.599	4.974	5.109	5.100	5.213
Fe+3	0.013	0.021	0.023	0.024	0.019	-	-	0.021	0.021	-	0.021
Ca	0.056	0.053	1.039	0.844	1.613	1.778	1.787	0.899	1.017	1.099	1.145
Na	1.017	0.818	2.732	2.733	2.233	1.889	1.750	2.508	2.794	2.696	2.309
K	2.981	2.867	0.066	0.041	0.030	0.081	0.078	0.212	0.038	0.041	0.029
Ba	0.116	0.047	-	0.052	0.100	0.072	0.033	-	-	-	-
MOL PERCENT IN END MEMBERS											
Celsian	2.78	1.24	-	1.41	2.51	1.88	0.91	-	-	-	-
Fe-Or	0.30	0.54	0.59	0.65	0.48	-	-	0.58	0.55	-	0.61
Anorthite	1.33	1.39	26.92	22.84	40.37	46.54	48.99	24.70	26.28	28.65	32.68
Albite	24.31	21.50	70.79	74.00	55.89	49.46	47.96	68.89	72.17	70.29	65.88
Orthoclase	71.28	75.33	1.70	1.10	0.75	2.12	2.14	5.82	0.99	1.06	0.84
MOL PERCENT IN AB-OR-AN SYSTEM											
An	1.37	1.41	27.08	23.32	41.61	47.43	49.44	24.85	26.42	28.65	32.88
Ab	25.08	21.89	71.21	75.56	57.61	50.41	48.40	69.30	72.58	70.29	66.28
Or	73.54	76.70	1.71	1.13	0.78	2.16	2.16	5.86	1.00	1.06	0.84

Appendix 2. Representive composition of feldspars in the porphyroblastic nephline syenite (C267) in Center II, Pic Island, Coldwell Complex, Ontario

	Phorphyroblast														
	Na-feldspar, core					Secondary alkali feldspar, core				K-feldspar, mantle		Alkali feldspar, rim			
CL colour	Light blue					Dull blue				Dull blue		Light violet			
Anal. No.	1-1	1-2	1-3	1-4	1-5	1-6	1-7	1-8	1-9	1-10	1-11	1-12	1-13	1-14	1-15
SiO2	64.11	64.56	64.24	63.38	64.95	65.11	65.65	65.50	66.35	66.73	66.49	68.34	67.14	67.47	66.53
Al2O3	22.97	23.31	23.24	22.60	22.88	19.85	19.38	19.27	18.71	18.24	17.77	18.17	17.80	17.71	18.56
Fe2O3	0.09	-	-	0.26	-	0.12	-	-	0.11	0.17	0.13	0.22	0.33	0.30	-
BaO	1.43	1.52	1.46	1.48	0.61	0.94	1.53	1.36	0.65	-	0.67	-	-	-	-
CaO	1.61	1.50	1.48	1.42	1.63	0.76	0.32	0.95	0.24	0.14	0.08	0.18	0.26	0.13	0.13
Na2O	8.92	7.95	8.82	9.44	8.48	4.37	4.77	3.41	3.91	3.23	2.62	3.87	3.86	3.92	4.96
K2O	0.75	1.09	0.67	0.85	1.14	8.47	8.13	9.50	9.71	11.26	12.16	9.25	10.38	10.51	9.61
STRUCTURAL FORMULA BASED ON 32 OXYGENS															
Si	11.376	11.417	11.375	11.344	11.464	11.820	11.914	11.910	12.037	12.109	12.145	12.225	12.156	12.184	12.031
Al	4.805	4.860	4.852	4.769	4.761	4.248	4.146	4.131	4.001	3.902	3.827	3.832	3.800	3.770	3.957
Fe+3	0.011	-	-	0.031	-	0.015	-	-	0.014	0.020	0.016	0.027	0.041	0.037	-
Ca	0.306	0.284	0.281	0.272	0.308	0.148	0.062	0.185	0.047	0.027	0.016	0.035	0.050	0.025	0.025
Na	3.069	2.726	3.028	3.276	2.902	1.538	1.679	1.202	1.375	1.136	0.928	1.342	1.355	1.373	1.739
K	0.170	0.246	0.151	0.194	0.257	1.962	1.882	2.204	2.247	2.607	2.834	2.111	2.398	2.421	2.217
Ba	0.099	0.105	0.101	0.104	0.042	0.067	0.109	0.097	0.046	-	0.048	-	-	-	-
MOL PERCENT IN END MEMBERS															
Celsian	2.72	3.13	2.84	2.68	1.20	1.79	2.92	2.63	1.24	-	1.25	-	-	-	-
Fe-Or	0.29	-	-	0.80	-	0.40	-	-	0.37	0.54	0.43	0.77	1.06	0.95	-
Anorthite	8.38	8.46	7.88	7.02	8.78	3.96	1.67	5.02	1.25	0.72	0.41	0.98	1.31	0.65	0.63
Albite	83.97	81.10	85.02	84.49	82.70	41.24	44.98	32.60	36.88	29.98	24.15	38.19	35.25	35.60	43.68
Orthoclase	4.65	7.32	4.25	5.01	7.32	52.60	50.44	59.76	60.26	68.76	73.76	60.06	62.37	62.80	55.69
MOL PERCENT IN AB-OR-AN SYSTEM															
An	8.64	8.73	8.11	7.28	8.89	4.05	1.72	5.15	1.27	0.72	0.41	0.99	1.33	0.66	0.63
Ab	86.57	83.72	87.51	87.54	83.70	42.17	46.33	33.48	37.48	30.14	24.57	38.49	35.63	35.94	43.68
Or	4.79	7.55	4.37	5.19	7.40	53.78	51.95	61.37	61.25	69.14	75.02	60.53	63.04	63.40	55.69

Appendix 2. continued

	Phorphyroblast														
	Alkali feldspar, core			Two feldspars, mantle				inner rim		middle			outer rim			
CL colour	Light violet blue			Blue	Light blue			L. violet blue		Light violet blue			Light violet			
Anal. No.	2-1	2-2	2-3	2-4	2-5	2-6	2-7	2-8	2-9	2-10	2-11	2-12	2-13	2-14	2-15	2-16
SiO2	67.06	67.28	66.13	65.08	65.43	66.30	66.73	66.71	66.79	66.61	66.34	66.50	67.46	67.52	67.65	68.21
Al2O3	20.06	20.26	20.10	17.71	23.19	22.76	22.40	19.34	19.29	20.04	20.18	19.60	17.83	18.11	17.92	17.77
Fe2O3	0.24	-	0.36	0.40	0.24	0.32	-	0.38	0.26	0.33	0.12	0.23	0.23	0.20	0.20	0.30
BaO	-	-	0.88	-	0.35	-	-	-	0.40	-	-	0.30	-	0.41	0.23	-
CaO	0.78	0.63	0.52	0.13	0.96	0.76	0.58	0.17	0.17	0.22	0.49	0.40	0.13	0.08	0.21	-
Na2O	5.44	5.12	5.87	2.37	8.73	9.10	8.64	5.04	4.71	5.35	5.74	5.62	3.65	3.55	3.41	3.75
K2O	6.33	6.70	6.18	13.99	0.67	0.79	1.44	8.41	8.41	7.48	6.80	7.17	10.64	10.16	10.41	9.81
STRUCTURAL FORMULA BASED ON 32 OXYGENS																
Si	11.922	11.941	11.842	12.021	11.493	11.573	11.669	11.963	11.992	11.895	11.865	11.924	12.186	12.177	12.199	12.260
Al	4.205	4.239	4.243	3.857	4.802	4.684	4.618	4.089	4.083	4.219	4.255	4.143	3.797	3.850	3.810	3.765
Fe+3	0.029	-	0.043	0.050	0.029	0.038	-	0.046	0.031	0.040	0.015	0.028	0.029	0.024	0.024	0.037
Ca	0.149	0.120	0.100	0.026	0.181	0.142	0.109	0.033	0.033	0.042	0.094	0.077	0.025	0.015	0.041	-
Na	1.875	1.762	2.038	0.849	2.973	3.080	2.930	1.753	1.640	1.852	1.991	1.954	1.278	1.241	1.192	1.307
K	1.436	1.517	1.412	3.297	0.150	0.176	0.321	1.924	1.926	1.704	1.552	1.640	2.452	2.338	2.395	2.249
Ba	-	-	0.062	-	0.024	-	-	-	0.028	-	-	0.021	-	0.029	0.016	-
MOL PERCENT IN END MEMBERS																
Celsian	-	-	1.69	-	0.72	-	-	-	0.77	-	-	0.57	-	0.79	0.44	-
Fe-Or	0.84	-	1.18	1.19	0.87	1.11	-	1.22	0.85	1.11	0.41	0.76	0.75	0.67	0.67	1.02
Anorthite	4.26	3.52	2.73	0.61	5.38	4.14	3.23	0.87	0.89	1.16	2.57	2.07	0.66	0.42	1.11	-
Albite	53.75	51.84	55.77	20.11	88.56	89.63	87.20	46.67	44.82	50.91	54.52	52.52	33.78	34.03	32.50	36.37
Orthoclase	41.15	44.64	38.63	78.10	4.47	5.12	9.56	51.24	52.66	46.83	42.50	44.09	64.80	64.08	65.28	62.61
MOL PERCENT IN AB-OR-AN SYSTEM																
An	4.29	3.52	2.81	0.62	5.47	4.18	3.23	0.88	0.91	1.17	2.58	2.09	0.67	0.43	1.12	-
Ab	54.20	51.84	57.42	20.35	89.99	90.64	87.20	47.25	45.56	51.48	54.74	53.23	34.04	34.54	32.87	36.75
Or	41.50	44.64	39.77	79.03	4.54	5.18	9.56	51.87	53.53	47.35	42.67	44.68	65.29	65.03	66.02	63.25

Appendix 3. Representative compositions of feldspars in the magnesio-hornblende syenite (C180) in Center III, Coldwell Complex, Ontario

	K-feldspar			Oligoclase, core			K-feldspar spots, core		Oligoclase, rim			Secondary oligoclase, margins		
CL colour	Blue			Light greenish blue			Light blue		Light violet blue			Dull violet		
Anal. No.	1	2	3	4	5	6	7	8	9	10	11	12	13	14
SiO2	63.55	64.62	64.33	62.30	63.86	62.36	63.45	62.54	62.84	63.22	63.42	63.63	62.73	62.96
Al2O3	18.03	17.50	17.89	23.43	24.35	23.42	17.80	17.98	23.26	23.56	23.04	23.13	23.75	22.60
Fe2O3	0.07	-	0.17	0.23	-	0.21	0.13	0.17	0.26	0.42	0.43	0.23	0.18	0.14
BaO	0.79	0.70	0.45	0.33	-	0.40	2.29	3.10	-	-	-	-	-	-
CaO	0.13	0.12	-	4.30	3.72	3.95	0.07	0.09	2.83	2.79	2.47	2.30	3.40	2.07
Na2O	1.64	1.12	1.18	9.04	7.42	9.19	2.01	1.28	10.16	9.62	10.19	10.40	9.74	11.64
K2O	15.35	15.93	15.91	0.37	0.51	0.32	14.26	14.87	0.35	0.43	0.37	0.33	0.22	0.49
STRUCTURAL FORMULA BASED ON 32 OXYGENS														
Si	11.900	12.034	11.972	11.073	11.211	11.094	11.905	11.835	11.159	11.167	11.223	11.238	11.097	11.201
Al	3.980	3.842	3.925	4.910	5.039	4.912	3.937	4.011	4.869	4.906	4.807	4.816	4.953	4.740
Fe+3	0.009	-	0.023	0.031	-	0.028	0.019	0.024	0.034	0.056	0.058	0.031	0.024	0.019
Ca	0.026	0.024	-	0.819	0.700	0.753	0.014	0.018	0.538	0.528	0.468	0.435	0.644	0.395
Na	0.595	0.404	0.426	3.116	2.526	3.170	0.731	0.470	3.498	3.295	3.496	3.561	3.341	4.015
K	3.667	3.785	3.777	0.084	0.114	0.073	3.414	3.590	0.079	0.097	0.084	0.074	0.050	0.111
Ba	0.058	0.051	0.033	0.023	-	0.028	0.168	0.230	-	-	-	-	-	-
MOL PERCENT END MEMBERS														
Celsian	1.33	1.20	0.77	0.56	-	0.69	3.87	5.31	-	-	-	-	-	-
Fe-Or	0.22	-	0.55	0.77	-	0.70	0.43	0.55	0.82	1.41	1.41	0.76	0.58	0.43
Anorthite	0.60	0.56	-	20.11	20.95	18.58	0.32	0.42	12.97	13.28	11.41	10.61	15.88	8.69
Albite	13.67	9.48	10.00	76.50	75.63	78.24	16.83	10.84	84.29	82.87	85.15	86.82	82.31	88.43
Orthoclase	84.19	88.76	88.69	2.06	3.42	1.79	78.54	82.88	1.91	2.44	2.03	1.81	1.22	2.45
MOL PERCENT IN AN-AB-OR SYSTEM														
An	0.61	0.57	-	20.38	20.95	18.84	0.34	0.45	13.08	13.47	11.57	10.69	15.97	8.73
Ab	13.88	9.60	10.13	77.53	75.63	79.34	17.58	11.52	84.99	84.06	86.37	87.48	82.80	88.81
Or	85.51	89.83	89.87	2.09	3.42	1.82	82.08	88.04	1.93	2.47	2.06	1.83	1.23	2.46

Appendix 3. Representative compositions of feldspars in the magnesio-hornblende syenite (C2123) in Center III, Coldwell Complex, Ontario

	K-feldspar				Plagioclase							
					Labradorite, core			Oligoclase, rim				
CL colour	Light blue				Light greenish blue			Light violet blue				
Anal. No.	1	2	3	4	5	6	7	8	9	10	11	12
SiO2	63.99	65.18	64.94	63.18	54.38	54.97	56.12	61.29	61.69	59.98	60.85	61.95
Al2O3	17.63	17.27	17.99	17.93	27.78	27.24	26.81	24.49	24.18	24.64	24.32	24.24
Fe2O3	0.16	-	0.16	0.12	0.27	0.38	0.23	0.13	0.27	0.32	0.32	0.49
BaO	0.29	-	0.37	0.24	-	-	-	0.28	-	-	-	0.24
CaO	0.24	0.13	0.22	0.07	12.03	11.60	10.78	5.95	5.72	6.84	6.10	5.28
Na2O	1.59	1.71	2.79	2.36	5.40	5.71	5.63	7.36	7.94	7.89	7.66	7.36
K2O	16.12	15.71	13.55	15.62	0.17	0.13	0.30	0.34	0.23	0.29	0.42	0.49
STRUCTURAL FORMULA BASED ON 32 OXYGENS												
Si	11.938	12.076	11.971	11.849	9.864	9.961	10.139	10.904	10.942	10.719	10.860	10.982
Al	3.878	3.772	3.910	3.964	5.940	5.820	5.711	5.136	5.056	5.191	5.117	5.066
Fe+3	0.022	-	0.022	0.017	0.036	0.052	0.032	0.018	0.036	0.043	0.043	0.065
Ca	0.048	0.026	0.043	0.014	2.338	2.252	2.087	1.134	1.087	1.310	1.167	1.003
Na	0.575	0.614	0.997	0.858	1.899	2.006	1.972	2.539	2.731	2.734	2.651	2.530
K	3.837	3.713	3.187	3.737	0.039	0.030	0.069	0.077	0.052	0.066	0.096	0.111
Ba	0.021	-	0.027	0.018	-	-	-	0.020	-	-	-	0.017
MOL PERCENT END MEMBERS												
Celsian	0.47	-	0.63	0.38	-	-	-	0.52	-	-	-	0.45
Fe-Or	0.49	-	0.50	0.37	0.84	1.19	0.76	0.47	0.91	1.04	1.09	1.75
Anorthite	1.07	0.59	1.02	0.30	54.21	51.90	50.17	29.95	27.84	31.54	29.49	26.92
Albite	12.77	14.11	23.32	18.48	44.03	46.23	47.41	67.03	69.92	65.83	67.00	67.91
Orthoclase	85.21	85.30	74.53	80.47	0.91	0.69	1.66	2.04	1.33	1.59	2.42	2.97
MOL PERCENT IN AN-AB-OR SYSTEM												
An	1.08	0.59	1.03	0.31	54.67	52.52	50.55	30.24	28.09	31.87	29.81	27.53
Ab	12.90	14.11	23.59	18.62	44.41	46.78	47.77	67.70	70.56	66.52	67.74	69.43
Or	86.03	85.30	75.38	81.08	0.92	0.70	1.68	2.06	1.34	1.61	2.44	3.04

Appendix 3. continued

	Secondary oligclase, margins					Na-feldspar, interstice	
CL colour	Dull violet					Non-CL	
Anal. No.	13	14	15	16	17	18	19
SiO2	62.06	61.04	61.44	61.91	61.46	63.60	62.83
Al2O3	23.62	23.68	23.92	23.26	23.64	23.67	24.79
Fe2O3	0.17	-	0.41	0.39	0.27	-	0.20
BaO	0.58	-	-	-	-	-	-
CaO	5.04	5.17	5.05	4.77	4.79	0.15	1.16
Na2O	8.01	9.17	8.92	8.59	9.52	11.88	9.05
K2O	0.54	0.67	0.30	0.36	0.34	0.70	2.00
STRUCTURAL FORMULA BASED ON 32 OXYGENS							
Si	11.044	10.924	10.929	11.064	10.950	11.233	11.107
Al	4.956	4.996	5.016	4.901	4.966	4.929	5.166
Fe+3	0.022	-	0.055	0.052	0.036	-	0.027
Ca	0.961	0.991	0.963	0.913	0.914	0.028	0.220
Na	2.764	3.182	3.077	2.977	3.289	4.068	3.102
K	0.123	0.153	0.068	0.082	0.077	0.158	0.451
Ba	0.040	-	-	-	-	-	-
MOL PERCENT END MEMBERS							
Celsian	1.03	-	-	-	-	-	-
Fe-Or	0.57	-	1.32	1.30	0.83	-	0.70
Anorthite	24.58	22.92	23.13	22.70	21.19	0.67	5.78
Albite	70.68	73.55	73.92	73.96	76.19	95.63	81.64
Orthoclase	3.14	3.54	1.64	2.04	1.79	3.71	11.87
MOL PERCENT IN AN-AB-OR SYSTEM							
An	24.98	22.92	23.44	23.00	21.36	0.67	5.82
Ab	71.84	73.55	74.91	74.94	76.83	95.63	82.22
Or	3.19	3.54	1.66	2.07	1.81	3.71	11.96

Appendix 3. Representative compositions of feldspars in the ferro-edenite syenite (C182) in Center III, Coldwell Complex, Ontario

	Microperthite						Antiperthite, rim							
	core				mantle		Na-feldspar			K-feldspar				
CL colour	Light violet blue				Light violet		Dull red			Dull blue				
Anal. No.	1	2	3	4	5	6	7	8	9	10	11	12	13	14
SiO2	65.84	65.87	65.87	65.53	65.83	65.70	65.29	65.81	64.21	64.72	65.67	65.26	65.43	64.91
Al2O3	20.05	21.20	19.92	20.36	19.20	19.91	22.98	23.30	22.97	17.67	17.42	18.05	17.41	17.42
Fe2O3	0.34	0.31	0.33	0.29	0.29	0.30	0.23	0.27	0.22	0.32	0.21	-	0.24	0.47
BaO	-	0.51	-	-	-	-	-	-	-	-	-	-	-	-
CaO	0.15	0.14	0.16	0.14	0.12	0.15	-	0.13	0.03	-	0.09	0.13	0.19	0.07
Na2O	7.63	8.49	7.63	8.33	6.02	7.13	11.36	10.22	11.95	1.48	0.42	0.70	1.39	0.79
K2O	5.95	3.52	6.38	5.38	8.57	6.78	0.17	0.30	0.21	15.85	16.03	15.33	15.37	16.15
STRUCTURAL FORMULA BASED ON 32 OXYGENS														
Si	11.778	11.684	11.777	11.712	11.877	11.788	11.442	11.485	11.349	11.999	12.139	12.069	12.083	12.056
Al	4.229	4.433	4.199	4.290	4.084	4.212	4.748	4.794	4.787	3.862	3.796	3.935	3.790	3.814
Fe+3	0.046	0.042	0.045	0.039	0.039	0.041	0.031	0.035	0.030	0.045	0.029	-	0.034	0.065
Ca	0.029	0.027	0.031	0.027	0.023	0.029	-	0.024	0.006	-	0.018	0.026	0.038	0.014
Na	2.647	2.920	2.645	2.887	2.106	2.481	3.860	3.458	4.095	0.532	0.151	0.251	0.498	0.284
K	1.358	0.797	1.455	1.227	1.973	1.552	0.038	0.067	0.047	3.749	3.780	3.617	3.621	3.827
Ba	-	0.035	-	-	-	-	-	-	-	-	-	-	-	-
MOL PERCENT END MEMBERS														
Celsian	-	0.93	-	-	-	-	-	-	-	-	-	-	-	-
Fe-Or	1.14	1.09	1.07	0.93	0.95	0.99	0.78	0.98	0.71	1.04	0.74	-	0.81	1.56
Anorthite	0.70	0.70	0.73	0.64	0.56	0.70	-	0.68	0.14	-	0.45	0.66	0.90	0.33
Albite	64.87	76.44	63.34	69.07	50.86	60.47	98.25	96.48	98.02	12.30	3.78	6.45	11.88	6.79
Orthoclase	33.29	20.85	34.85	29.35	47.64	37.84	0.97	1.86	1.13	86.66	95.03	92.89	86.41	91.32
MOL PERCENT IN AN-AB-OR SYSTEM														
An	0.71	0.71	0.74	0.65	0.57	0.71	-	0.68	0.14	-	0.45	0.66	0.90	0.34
Ab	65.62	78.01	64.03	69.72	51.34	61.08	99.02	97.43	98.72	12.43	3.81	6.45	11.97	6.90
Or	33.67	21.28	35.23	29.63	48.09	38.21	0.98	1.88	1.14	87.57	95.74	92.89	87.12	92.77

Appendix 3. Representative compositions of feldspars in the ferro-edenite syenite (C294) in Center III, Coldwell Complex, Ontario

	Microperthite, core											Albite,		
	Alkali feldspar					Secondary K-feldspar						mantle		
CL colour	Light blue					Dull blue						Light blue		
Anal. No.	1	2	3	4	5	6	7	8	9	10	11	12	13	14
SiO2	64.89	64.57	65.41	65.38	66.37	63.77	64.87	62.12	64.27	64.00	62.55	62.80	62.73	62.89
Al2O3	18.55	18.07	19.41	18.02	18.79	18.22	17.60	17.60	17.57	17.87	17.80	22.96	22.93	22.98
Fe2O3	1.12	1.40	0.94	0.29	0.79	0.80	0.79	2.81	1.16	0.80	2.51	0.30	0.63	0.21
BaO	-	0.19	0.15	-	-	0.25	0.27	-	-	0.31	0.14	-	-	-
CaO	0.38	0.18	0.40	0.11	0.25	0.16	0.19	0.13	0.13	0.08	0.12	1.01	1.06	1.13
Na2O	5.09	3.93	5.49	3.25	3.84	1.03	-	0.85	-	0.58	0.57	12.56	11.71	12.43
K2O	9.57	12.21	8.41	12.53	10.00	15.30	16.27	16.22	16.99	16.44	16.38	0.39	0.71	0.32
STRUCTURAL FORMULA BASED ON 32 OXYGENS														
Si	11.845	11.838	11.800	12.009	11.984	11.886	12.038	11.704	11.965	11.924	11.733	11.161	11.173	11.173
Al	3.992	3.906	4.128	3.902	4.000	4.003	3.850	3.909	3.856	3.925	3.936	4.811	4.815	4.813
Fe+3	0.154	0.193	0.128	0.040	0.107	0.112	0.110	0.399	0.162	0.112	0.355	0.040	0.085	0.028
Ca	0.074	0.035	0.077	0.022	0.048	0.032	0.038	0.026	0.026	0.016	0.024	0.192	0.202	0.215
Na	1.802	1.397	1.920	1.157	1.344	0.372	-	0.311	-	0.210	0.207	4.328	4.044	4.282
K	2.229	2.856	1.936	2.936	2.304	3.638	3.852	3.899	4.035	3.908	3.920	0.088	0.161	0.073
Ba	-	0.014	0.011	-	-	0.018	0.020	-	-	0.023	0.010	-	-	-
MOL PERCENT END MEMBERS														
Celsian	-	0.30	0.26	-	-	0.44	0.49	-	-	0.53	0.23	-	-	-
Fe-Or	3.62	4.30	3.15	0.96	2.82	2.69	2.74	8.60	3.83	2.63	7.85	0.86	1.89	0.61
Anorthite	1.75	0.79	1.90	0.52	1.27	0.77	0.94	0.57	0.61	0.37	0.53	4.14	4.50	4.68
Albite	42.30	31.08	47.16	27.86	35.35	8.92	-	6.70	-	4.91	4.59	93.10	90.02	93.13
Orthoclase	52.33	63.53	47.53	70.66	60.56	87.19	95.83	84.13	95.55	91.56	86.80	1.90	3.59	1.58
MOL PERCENT IN AN-AB-OR SYSTEM														
An	1.81	0.82	1.97	0.53	1.31	0.79	0.97	0.62	0.64	0.39	0.58	4.17	4.59	4.71
Ab	43.89	32.58	48.82	28.13	36.37	9.21	-	7.33	-	5.07	4.99	93.91	91.75	93.71
Or	54.30	66.60	49.21	71.35	62.32	90.00	99.03	92.05	99.36	94.54	94.43	1.92	3.66	1.59

Appendix 3. continued

	Na-feldspar, mantle					Albite, rim							
CL colour	Light blue					Light violet blue							
Anal. No.	15	16	17	18	19	20	21	22	23	24	25	26	27
SiO2	62.40	62.36	64.74	63.85	64.26	64.15	63.52	63.74	62.60	62.40	62.34	63.17	63.42
Al2O3	22.92	22.47	23.75	23.34	23.59	23.36	23.17	23.14	22.99	22.35	22.56	22.85	23.00
Fe2O3	0.22	0.19	0.10	0.16	0.19	0.09	0.13	0.22	-	0.19	0.19	0.11	0.19
BaO	-	0.40	0.39	0.70	0.25	-	-	0.23	-	0.20	0.15	-	-
CaO	1.08	0.34	1.12	1.23	1.14	0.11	0.48	0.58	0.79	0.64	0.70	0.61	0.66
Na2O	13.16	13.95	9.59	10.42	10.27	12.05	12.39	11.65	13.23	13.89	13.69	12.77	12.25
K2O	0.24	0.31	0.31	0.33	0.32	0.25	0.31	0.47	0.29	0.35	0.40	0.41	0.49
STRUCTURAL FORMULA BASED ON 32 OXYGENS													
Si	11.115	11.154	11.355	11.285	11.303	11.300	11.237	11.272	11.147	11.156	11.137	11.220	11.236
Al	4.813	4.738	4.911	4.863	4.892	4.851	4.832	4.824	4.826	4.711	4.751	4.785	4.804
Fe+3	0.030	0.025	0.013	0.021	0.025	0.012	0.018	0.030	-	0.025	0.025	0.015	0.025
Ca	0.206	0.065	0.210	0.233	0.215	0.021	0.091	0.110	0.151	0.123	0.134	0.116	0.125
Na	4.545	4.838	3.261	3.571	3.503	4.115	4.250	3.995	4.568	4.815	4.742	4.398	4.208
K	0.055	0.071	0.069	0.074	0.072	0.056	0.070	0.106	0.066	0.080	0.091	0.093	0.111
Ba	-	0.028	0.027	0.048	0.017	-	-	0.016	-	0.014	0.010	-	-
MOL PERCENT END MEMBERS													
Celsian	-	0.56	0.75	1.23	0.45	-	-	0.37	-	0.28	0.21	-	-
Fe-Or	0.62	0.51	0.37	0.52	0.65	0.28	0.40	0.70	-	0.50	0.51	0.32	0.56
Anorthite	4.26	1.30	5.88	5.90	5.61	0.49	2.05	2.58	3.15	2.42	2.68	2.51	2.80
Albite	93.99	96.23	91.07	90.46	91.42	97.89	95.96	93.86	95.47	95.22	94.78	95.16	94.15
Orthoclase	1.13	1.41	1.94	1.89	1.87	1.34	1.58	2.49	1.38	1.58	1.82	2.01	2.48
MOL PERCENT IN AN-AB-OR SYSTEM													
An	4.29	1.31	5.94	6.01	5.67	0.50	2.06	2.61	3.15	2.44	2.70	2.52	2.82
Ab	94.58	97.27	92.10	92.08	92.43	98.16	96.35	94.87	95.47	95.97	95.47	95.46	94.69
Or	1.13	1.42	1.96	1.92	1.90	1.34	1.59	2.52	1.38	1.59	1.84	2.02	2.49

Appendix 3. continued

	Secondary albite, antiperthite rim			Na-feldspar, antiperthite rim				K-feldspar, antiperthite, rim					
CL colour	Purple			Deep red				Dark brown					
Anal. No.	28	29	30	31	32	33	34	35	36	37	38	39	40
SiO2	63.80	63.38	64.09	64.18	64.52	64.93	62.99	64.65	63.74	64.54	64.81	64.70	64.93
Al2O3	23.11	23.21	22.91	23.09	22.84	22.96	22.65	17.90	17.61	18.14	18.37	17.78	17.96
Fe2O3	0.20	0.20	0.22	0.22	0.44	0.28	0.36	0.10	-	0.07	-	-	-
BaO	0.12	-	-	-	-	-	-	-	-	-	-	-	-
CaO	0.14	0.45	0.83	0.17	-	0.11	-	0.19	-	0.10	-	0.13	0.08
Na2O	12.32	12.49	11.53	12.05	12.13	11.51	13.71	-	1.27	-	1.07	-	-
K2O	0.32	0.29	0.20	0.31	0.11	0.24	0.17	16.75	16.68	17.00	15.53	17.39	17.04
STRUCTURAL FORMULA BASED ON 32 OXYGENS													
Si	11.277	11.217	11.322	11.315	11.359	11.403	11.208	12.031	11.963	11.995	11.985	12.032	12.040
Al	4.816	4.843	4.771	4.799	4.741	4.754	4.751	3.927	3.897	3.974	4.005	3.898	3.926
Fe+3	0.027	0.027	0.030	0.029	0.059	0.037	0.048	0.014	-	0.009	-	-	-
Ca	0.027	0.085	0.157	0.032	-	0.021	-	0.038	-	0.020	-	0.026	0.016
Na	4.222	4.286	3.949	4.119	4.141	3.919	4.730	-	0.462	-	0.384	-	-
K	0.072	0.065	0.045	0.070	0.025	0.054	0.039	3.977	3.994	4.031	3.664	4.126	4.031
Ba	0.008	-	-	-	-	-	-	-	-	-	-	-	-
MOL PERCENT END MEMBERS													
Celsian	0.19	-	-	-	-	-	-	-	-	-	-	-	-
Fe-Or	0.61	0.60	0.71	0.69	1.39	0.91	0.99	0.35	-	0.23	-	-	-
Anorthite	0.61	1.91	3.76	0.76	-	0.51	-	0.94	-	0.49	-	0.62	0.39
Albite	96.93	96.02	94.46	96.91	98.02	97.24	98.21	-	10.37	-	9.48	-	-
Orthoclase	1.66	1.47	1.08	1.64	0.58	1.33	0.80	98.71	89.63	99.28	90.52	99.38	99.61
MOL PERCENT IN AN-AB-OR SYSTEM													
An	0.61	1.92	3.78	0.76	-	0.52	-	0.94	-	0.49	-	0.62	0.39
Ab	97.72	96.60	95.13	97.59	99.41	98.14	99.19	-	10.37	-	9.48	-	-
Or	1.67	1.48	1.09	1.65	0.59	1.35	0.81	99.06	89.63	99.51	90.52	99.38	99.61

Appendix 3. continued

	Antiperthite					
	K-feldspar			Na-feldspar		
CL colour	Dull blue			Dull red		
Anal. No.	41	43	44	45	46	47
SiO2	64.48	64.25	64.04	63.20	64.86	63.72
Al2O3	17.80	18.14	17.90	22.84	23.25	23.21
Fe2O3	0.27	0.13	-	0.23	0.14	0.20
BaO	-	0.18	0.78	-	-	-
CaO	0.09	0.16	0.14	0.11	0.26	0.42
Na2O	1.61	1.39	0.53	13.45	11.32	12.23
K2O	15.69	15.76	16.63	0.19	0.18	0.24
STRUCTURAL FORMULA BASED ON 32 OXYGENS						
Si	11.968	11.928	11.962	11.215	11.381	11.255
Al	3.895	3.970	3.942	4.778	4.810	4.833
Fe+3	0.037	0.019	-	0.031	0.019	0.027
Ca	0.018	0.032	0.028	0.021	0.049	0.079
Na	0.579	0.500	0.192	4.628	3.851	4.188
K	3.715	3.733	3.963	0.043	0.040	0.054
Ba	-	0.013	0.057	-	-	-
MOL PERCENT END MEMBERS						
Celsian	-	0.30	1.35	-	-	-
Fe-Or	0.86	0.43	-	0.66	0.48	0.61
Anorthite	0.41	0.74	0.66	0.44	1.23	1.83
Albite	13.32	11.65	4.53	97.99	97.27	96.32
Orthoclase	85.41	86.88	93.47	0.91	1.02	1.24
MOL PERCENT IN AN-AB-OR SYSTEM						
An	0.42	0.75	0.67	0.45	1.24	1.84
Ab	13.44	11.73	4.59	98.64	97.74	96.91
Or	86.15	87.52	94.74	0.92	1.02	1.25

Appendix 3. Representative compositions of feldspars in the ferro-edenite syenite (C322) in Center III, Coldwell Complex, Ontario

	Na-feldspar host, antiperthitic, core			Exsolved K-feldspar, antiperthitic, core				Alkali feldspar, Microperthite, mantle			Albite, antiperthitic rim	
CL colour	Light blue			Dull blue				Light violet blue			Red	
Anal. No.	1	2	3	4	5	6	7	8	9	10	11	12
SiO2	63.39	63.31	62.89	64.66	64.86	65.85	65.30	64.50	65.33	64.74	65.69	64.60
Al2O3	22.79	23.46	22.73	18.00	17.96	17.86	18.18	20.76	19.95	20.23	23.25	23.00
Fe2O3	0.38	-	0.13	0.13	-	0.23	0.20	0.33	0.22	0.10	0.60	0.48
BaO	-	-	0.10	0.19	-	-	-	-	-	-	-	-
CaO	-	0.51	0.15	0.06	0.17	0.13	0.12	0.25	0.08	0.08	-	0.05
Na2O	12.70	12.52	13.41	0.84	2.44	1.27	0.49	8.33	6.74	7.97	10.37	11.67
K2O	0.13	0.21	0.16	16.03	14.57	14.68	15.65	5.73	7.63	6.72	0.14	0.14
STRUCTURAL FORMULA BASED ON 32 OXYGENS												
Si	11.275	11.198	11.216	11.996	11.975	12.091	12.040	11.590	11.766	11.674	11.467	11.366
Al	4.779	4.892	4.779	3.937	3.909	3.866	3.952	4.398	4.236	4.300	4.785	4.771
Fe+3	0.051	-	0.018	0.019	-	0.032	0.028	0.045	0.030	0.014	0.079	0.063
Ca	-	0.097	0.029	0.012	0.034	0.026	0.024	0.048	0.015	0.015	-	0.009
Na	4.380	4.294	4.637	0.302	0.873	0.452	0.175	2.902	2.354	2.786	3.510	3.981
K	0.030	0.047	0.036	3.794	3.432	3.439	3.681	1.314	1.753	1.546	0.031	0.031
Ba	-	-	0.007	0.014	-	-	-	-	-	-	-	-
MOL PERCENT END MEMBERS												
Celsian	-	-	0.15	0.33	-	-	-	-	-	-	-	-
Fe-Or	1.13	-	0.38	0.45	-	0.82	0.71	1.05	0.73	0.31	2.18	1.55
Anorthite	-	2.18	0.61	0.29	0.78	0.65	0.61	1.12	0.37	0.35	-	0.23
Albite	98.20	96.75	98.10	7.30	20.13	11.45	4.48	67.35	56.68	63.89	96.96	97.45
Orthoclase	0.66	1.07	0.77	91.63	79.09	87.09	94.20	30.48	42.22	35.44	0.86	0.77
MOL PERCENT IN AN-AB-OR SYSTEM												
An	-	2.18	0.61	0.29	0.78	0.65	0.61	1.13	0.37	0.36	-	0.23
Ab	99.33	96.75	98.62	7.36	20.13	11.54	4.51	68.06	57.10	64.09	99.12	98.98
Or	0.67	1.07	0.77	92.35	79.09	87.80	94.87	30.81	42.53	35.56	0.88	0.78

Appendix 3. continued

	Albite, antiperthitic rim			K-feldspar, antiperthitic rim				Scondary feldspars, within biotite		
CL colour	Red			Brown				Dark brown		
Anal. No.	13	14	15	16	17	18	19	20	21	22
SiO2	64.58	63.71	64.78	65.44	65.65	64.70	65.31	64.80	64.55	63.49
Al2O3	22.50	22.55	22.72	17.71	17.73	17.81	18.31	17.42	18.36	22.17
Fe2O3	0.51	0.53	0.42	0.24	0.42	0.31	0.14	0.50	0.32	0.83
BaO	-	-	0.18	-	-	0.57	-	-	0.42	-
CaO	-	-	-	0.08	-	0.11	0.15	0.18	0.12	-
Na2O	12.38	13.03	11.71	1.19	0.85	1.70	-	0.67	-	13.41
K2O	0.08	0.15	0.12	15.36	15.38	14.84	16.09	16.40	16.26	0.18
STRUCTURAL FORMULA BASED ON 32 OXYGENS										
Si	11.381	11.287	11.408	12.069	12.090	11.988	12.040	12.037	11.968	11.272
Al	4.675	4.710	4.717	3.851	3.849	3.890	3.979	3.815	4.013	4.640
Fe+3	0.068	0.071	0.056	0.034	0.059	0.043	0.020	0.070	0.045	0.111
Ca	-	-	-	0.016	-	0.022	0.030	0.036	0.024	-
Na	4.230	4.476	3.998	0.426	0.304	0.611	-	0.241	-	4.616
K	0.018	0.034	0.027	3.614	3.613	3.508	3.784	3.886	3.846	0.041
Ba	-	-	0.012	-	-	0.041	-	-	0.031	-
MOL PERCENT END MEMBERS										
Celsian	-	-	0.30	-	-	0.98	-	-	0.77	-
Fe-Or	1.57	1.55	1.37	0.83	1.47	1.03	0.52	1.65	1.14	2.34
Anorthite	-	-	-	0.39	-	0.52	0.77	0.85	0.60	-
Albite	98.01	97.71	97.67	10.41	7.63	14.45	-	5.70	-	96.81
Orthoclase	0.42	0.74	0.66	88.38	90.89	83.02	98.70	91.80	97.48	0.86
MOL PERCENT IN AN-AB-OR SYSTEM										
An	-	-	-	0.39	-	0.53	0.78	0.86	0.62	-
Ab	99.58	99.25	99.33	10.49	7.75	14.75	-	5.80	-	99.12
Or	0.42	0.75	0.67	89.12	92.25	84.72	99.22	93.34	99.38	0.88

Appendix 3. Representative compositions of feldspars in the ferro-edenite syenite (C371) in Center III, Coldwell Complex, Ontario

	Antiperthite, core								Antiperthite, rim							
	Na-feldspar host				Exsolved K-feldspar				Na-feldspar host				Exsolved K-feldspar			
CL colour	Light violet				Dull blue				Deep red				Brown			
Anal. No.	1	2	3	4	5	6	7	8	9	10	11	12	13	14	15	16
SiO2	64.62	63.38	65.03	65.01	65.12	65.71	65.74	65.34	63.37	64.05	64.29	63.53	65.18	65.24	65.18	65.72
Al2O3	23.20	22.28	23.04	23.37	17.92	18.68	17.50	18.26	22.31	22.41	22.57	21.90	17.75	17.57	17.81	17.75
Fe2O3	0.29	0.23	0.31	0.26	0.31	0.27	0.24	0.17	0.59	1.06	0.88	1.29	0.61	0.47	0.34	0.44
BaO	-	-	0.15	-	-	-	-	0.33	-	-	-	-	0.23	-	-	-
CaO	-	-	0.05	0.05	0.12	-	0.13	0.09	-	-	-	0.04	0.13	0.15	0.11	0.08
Na2O	11.82	14.00	11.36	11.26	1.85	0.78	1.42	1.27	13.64	12.50	12.21	13.18	0.52	1.48	0.60	1.17
K2O	0.10	0.06	0.09	0.08	14.64	14.59	14.99	14.56	0.10	0.05	0.14	0.20	15.64	14.85	15.98	14.89
STRUCTURAL FORMULA BASED ON 32 OXYGENS																
Si	11.355	11.265	11.413	11.389	12.008	12.028	12.105	12.023	11.257	11.319	11.340	11.282	12.046	12.057	12.047	12.083
Al	4.806	4.669	4.767	4.827	3.896	4.031	3.799	3.961	4.672	4.669	4.694	4.585	3.867	3.828	3.881	3.847
Fe+3	0.038	0.031	0.041	0.034	0.043	0.037	0.034	0.023	0.079	0.140	0.117	0.172	0.085	0.065	0.048	0.062
Ca	-	-	0.009	0.009	0.024	-	0.026	0.018	-	-	-	0.008	0.026	0.030	0.022	0.016
Na	4.027	4.825	3.866	3.825	0.661	0.277	0.507	0.453	4.698	4.283	4.176	4.538	0.186	0.530	0.215	0.417
K	0.022	0.014	0.020	0.018	3.444	3.407	3.522	3.418	0.023	0.011	0.032	0.045	3.688	3.501	3.768	3.493
Ba	-	-	0.010	-	-	-	-	0.024	-	-	-	-	0.017	-	-	-
MOL PERCENT END MEMBERS																
Celsian	-	-	0.26	-	-	-	-	0.60	-	-	-	-	0.42	-	-	-
Fe-Or	0.93	0.64	1.04	0.87	1.03	0.99	0.83	0.59	1.64	3.17	2.70	3.62	2.12	1.57	1.18	1.54
Anorthite	-	-	0.24	0.24	0.57	-	0.63	0.45	-	-	-	0.16	0.64	0.72	0.54	0.40
Albite	98.52	99.08	97.95	98.43	15.85	7.44	12.40	11.51	97.89	96.58	96.58	95.27	4.66	12.85	5.31	10.46
Orthoclase	0.55	0.28	0.51	0.46	82.54	91.57	86.14	86.85	0.47	0.25	0.73	0.95	92.16	84.85	92.97	87.60
MOL PERCENT IN AN-AB-OR SYSTEM																
An	-	-	0.24	0.24	0.57	-	0.63	0.46	-	-	-	0.17	0.66	0.73	0.54	0.40
Ab	99.45	99.72	99.24	99.29	16.02	7.51	12.51	11.65	99.52	99.74	99.25	98.85	4.78	13.06	5.37	10.63
Or	0.55	0.28	0.52	0.46	83.41	92.49	86.86	87.89	0.48	0.26	0.75	0.99	94.56	86.21	94.09	88.97

Appendix 3. Representative compositions of feldspars in the ferro-edenite syenite (C2025) in Center III, Coldwell Complex, Ontario

	Perthite, core							Antiperthite, rim						
	Na-feldspar				K-feldspar			Exsolved K-feldspar				Na-feldspar host		
CL colour	Light blue				Dull blue			Dull blue				Dull red		
Anal. No.	1	2	4	5	6	7	8	9	10	11	12	13	14	15
SiO2	63.37	63.27	63.86	63.69	64.89	64.48	65.65	65.23	65.10	64.78	64.20	64.75	63.49	63.75
Al2O3	23.48	23.92	23.75	23.57	18.44	17.34	18.63	17.72	17.47	17.88	17.86	23.13	22.19	23.08
Fe2O3	0.11	0.13	0.16	0.14	-	-	0.19	0.22	0.18	0.30	0.13	0.22	0.31	0.18
BaO	0.35	0.32	-	-	0.59	0.24	-	-	-	-	-	-	-	-
CaO	1.61	1.51	1.22	1.13	0.14	0.07	0.18	-	-	0.16	0.22	0.10	-	0.15
Na2O	10.59	10.31	10.63	11.10	1.55	2.43	2.73	1.07	0.98	0.87	1.31	11.64	13.43	12.63
K2O	0.45	0.43	0.29	0.36	14.40	15.43	12.33	15.79	16.11	16.05	16.29	0.19	0.19	0.23
STRUCTURAL FORMULA BASED ON 32 OXYGENS														
Si	11.216	11.186	11.247	11.234	11.971	11.997	11.993	12.055	12.075	11.998	11.942	11.374	11.305	11.267
Al	4.899	4.986	4.931	4.901	4.011	3.803	4.012	3.861	3.820	3.904	3.917	4.790	4.658	4.809
Fe+3	0.015	0.018	0.021	0.019	-	-	0.026	0.031	0.025	0.042	0.019	0.029	0.042	0.024
Ca	0.305	0.286	0.230	0.214	0.028	0.014	0.035	-	-	0.032	0.044	0.019	-	0.028
Na	3.634	3.534	3.630	3.796	0.554	0.877	0.967	0.383	0.352	0.312	0.472	3.965	4.637	4.328
K	0.102	0.097	0.065	0.081	3.389	3.663	2.874	3.723	3.812	3.793	3.866	0.043	0.043	0.052
Ba	0.024	0.022	-	-	0.043	0.017	-	-	-	-	-	-	-	-
MOL PERCENT END MEMBERS														
Celsian	0.59	0.56	-	-	1.06	0.38	-	-	-	-	-	-	-	-
Fe-Or	0.36	0.45	0.52	0.47	-	-	0.67	0.75	0.59	1.00	0.42	0.72	0.88	0.53
Anorthite	7.48	7.23	5.83	5.20	0.69	0.31	0.90	-	-	0.76	1.00	0.46	-	0.64
Albite	89.07	89.31	91.99	92.37	13.81	19.18	24.78	9.27	8.41	7.48	10.74	97.76	98.20	97.66
Orthoclase	2.49	2.45	1.65	1.97	84.44	80.13	73.65	89.99	90.99	90.76	87.84	1.05	0.91	1.17
MOL PERCENT IN AN-AB-OR SYSTEM														
An	7.56	7.30	5.87	5.22	0.70	0.31	0.91	-	-	0.77	1.00	0.47	-	0.64
Ab	89.93	90.22	92.47	92.80	13.96	19.25	24.95	9.34	8.46	7.55	10.78	98.47	99.08	98.18
Or	2.51	2.48	1.66	1.98	85.34	80.44	74.14	90.66	91.54	91.68	88.22	1.06	0.92	1.18

Appendix 3. continued

	Oscillatory zoned antiperthite					
	Exsolved K-feldspar			Na-feldspar host		
CL colour	Dull blue			Dull red		
Anal. No.	16	17	18	19	20	21
SiO2	65.03	65.91	63.99	63.79	64.12	63.56
Al2O3	17.85	18.09	17.92	23.23	22.82	23.00
Fe2O3	0.07	0.13	0.12	0.33	0.11	0.11
BaO	-	-	-	-	-	-
CaO	0.15	0.07	0.08	0.31	-	0.12
Na2O	1.01	-	1.73	12.03	12.75	12.80
K2O	15.74	15.80	16.17	0.32	0.21	0.18
Si	12.037	12.113	11.913	11.263	11.323	11.264
Al	3.895	3.920	3.933	4.836	4.751	4.805
Fe+3	0.009	0.018	0.017	0.044	0.015	0.015
Ca	0.030	0.014	0.016	0.059	-	0.023
Na	0.362	-	0.624	4.119	4.365	4.398
K	3.717	3.705	3.841	0.072	0.047	0.041
Ba	-	-	-	-	-	-
Celsian	-	-	-	-	-	-
Fe-Or	0.23	0.49	0.38	1.03	0.33	0.33
Anorthite	0.72	0.37	0.35	1.37	-	0.51
Albite	8.80	-	13.88	95.92	98.60	98.25
Orthoclase	90.25	99.14	85.38	1.68	1.07	0.91
An	0.72	0.37	0.36	1.38	-	0.51
Ab	8.82	-	13.94	96.92	98.93	98.58
Or	90.45	99.63	85.71	1.70	1.07	0.91

Appendix 3. Representative compositions of feldspars in the ferro-edenite syenite (C2124) in Center III, Coldwell Complex, Ontario

	Homogeneous alkali feldspar, core						Exsolved Na-feldspar, perthite rim			K-feldspar host, Perthite rim		
CL colour	Light violet blue						Dull violet			Dull blue		
Anal. No.	1	2	3	4	5	6	7	8	9	10	11	12
SiO2	65.00	65.32	65.05	65.07	65.38	65.36	64.18	64.35	64.09	64.77	64.29	64.59
Al2O3	20.22	20.07	20.12	19.79	20.25	19.90	22.87	23.45	22.99	17.83	18.02	18.04
Fe2O3	0.21	0.23	0.24	0.21	0.26	0.16	0.19	0.21	0.21	-	0.16	0.17
BaO	-	-	0.26	-	-	-	-	-	-	-	-	0.81
CaO	0.32	0.20	0.29	0.38	0.19	0.18	0.17	0.12	0.12	0.37	0.24	0.08
Na2O	6.80	6.33	7.02	7.00	6.63	7.17	12.47	11.66	12.21	1.66	2.17	0.70
K2O	7.29	7.78	7.03	7.56	7.33	7.25	0.14	0.23	0.25	14.95	15.14	15.50
STRUCTURAL FORMULA BASED ON 32 OXYGENS												
Si	11.713	11.762	11.717	11.738	11.743	11.760	11.323	11.315	11.318	12.007	11.917	12.000
Al	4.296	4.261	4.272	4.209	4.288	4.221	4.757	4.861	4.787	3.897	3.938	3.951
Fe+3	0.029	0.032	0.033	0.029	0.035	0.021	0.025	0.028	0.028	-	0.022	0.023
Ca	0.062	0.039	0.056	0.073	0.037	0.035	0.032	0.023	0.023	0.073	0.048	0.016
Na	2.376	2.210	2.452	2.448	2.309	2.501	4.266	3.975	4.181	0.597	0.780	0.252
K	1.676	1.787	1.615	1.740	1.680	1.664	0.032	0.052	0.056	3.536	3.580	3.674
Ba	-	-	0.018	-	-	-	-	-	-	-	-	0.059
MOL PERCENT END MEMBERS												
Celsian	-	-	0.44	-	-	-	-	-	-	-	-	1.47
Fe-Or	0.69	0.78	0.79	0.67	0.85	0.50	0.58	0.69	0.65	-	0.49	0.58
Anorthite	1.49	0.95	1.34	1.71	0.90	0.82	0.74	0.55	0.53	1.75	1.08	0.40
Albite	57.36	54.33	58.73	57.07	56.87	59.26	97.96	97.49	97.50	14.19	17.61	6.27
Orthoclase	40.46	43.94	38.70	40.55	41.37	39.42	0.72	1.27	1.31	84.07	80.83	91.29
MOL PERCENT IN AN-AB-OR SYSTEM												
An	1.50	0.96	1.36	1.72	0.91	0.83	0.74	0.56	0.53	1.75	1.08	0.40
Ab	57.76	54.76	59.46	57.45	57.36	59.55	98.53	98.17	98.14	14.19	17.69	6.40
Or	40.74	44.28	39.18	40.83	41.73	39.62	0.73	1.27	1.32	84.07	81.23	93.20

Appendix 3. continued

	Secondary albite, interstice					2nd Na-feldspar, in xenolith			2nd K-feldspar, in xenolith	
CL colour	Dull red					Dull red			Dull blue	
Anal. No.	13	14	15	16	17	18	19	20	21	22
SiO2	63.04	62.86	64.44	63.04	62.96	65.20	63.73	63.70	64.02	64.93
Al2O3	23.32	23.20	23.61	23.26	23.13	23.01	22.66	22.84	18.08	17.88
Fe2O3	0.20	0.30	0.16	0.07	0.13	0.28	0.28	0.18	0.36	0.10
BaO	-	-	-	-	-	-	0.27	0.45	-	-
CaO	1.07	0.95	0.83	0.96	0.97	0.07	0.75	0.97	-	0.14
Na2O	12.06	12.49	10.68	12.42	12.48	11.35	11.94	11.59	1.48	0.64
K2O	0.36	0.22	0.30	0.17	0.25	0.12	0.39	0.28	15.88	16.31
STRUCTURAL FORMULA BASED ON 32 OXYGENS										
Si	11.169	11.153	11.315	11.178	11.176	11.429	11.293	11.285	11.912	12.026
Al	4.871	4.853	4.887	4.862	4.840	4.755	4.734	4.771	3.966	3.904
Fe+3	0.027	0.040	0.021	0.009	0.018	0.037	0.037	0.024	0.050	0.014
Ca	0.203	0.181	0.156	0.182	0.184	0.013	0.142	0.184	-	0.028
Na	4.143	4.297	3.636	4.270	4.295	3.858	4.103	3.981	0.534	0.230
K	0.081	0.050	0.067	0.038	0.057	0.027	0.088	0.063	3.770	3.854
Ba	-	-	-	-	-	-	0.019	0.031	-	-
MOL PERCENT END MEMBERS										
Celsian	-	-	-	-	-	-	0.43	0.73	-	-
Fe-Or	0.60	0.88	0.53	0.20	0.39	0.93	0.84	0.55	1.14	0.34
Anorthite	4.56	3.95	4.02	4.05	4.05	0.33	3.24	4.30	-	0.67
Albite	93.01	94.08	93.71	94.89	94.31	98.05	93.47	92.94	12.27	5.57
Orthoclase	1.83	1.09	1.73	0.85	1.24	0.68	2.01	1.48	86.59	93.42
MOL PERCENT IN AN-AB-OR SYSTEM										
An	4.59	3.99	4.05	4.06	4.07	0.34	3.29	4.35	-	0.68
Ab	93.57	94.91	94.21	95.08	94.69	98.97	94.68	94.15	12.41	5.59
Or	1.84	1.10	1.74	0.86	1.25	0.69	2.03	1.50	87.59	93.73

Appendix 3. continued

Xenolith, Na-feldspar,

	margins					core				
CL colour	Light blue					Light blue				
Anal. No.	23	24	25	26	27	28	29	30	31	32
SiO2	64.27	64.55	63.30	62.88	63.23	62.05	62.73	62.61	61.86	62.08
Al2O3	23.87	23.48	22.50	23.32	23.50	23.70	23.79	23.73	23.84	23.64
Fe2O3	0.22	0.26	0.17	0.14	0.17	0.19	0.07	0.17	0.10	0.16
BaO	0.35	0.49	0.24	0.59	0.25	0.25	-	-	0.55	-
CaO	1.35	0.53	0.66	0.97	0.55	1.84	1.73	2.23	3.22	2.64
Na2O	9.73	10.40	12.91	11.46	12.11	11.56	11.36	10.99	10.16	11.00
K2O	0.27	0.25	0.23	0.28	0.21	0.43	0.32	0.29	0.27	0.26
STRUCTURAL FORMULA BASED ON 32 OXYGENS										
Si	11.288	11.355	11.251	11.196	11.193	11.045	11.110	11.094	11.017	11.049
Al	4.943	4.869	4.715	4.895	4.904	4.973	4.967	4.957	5.005	4.960
Fe+3	0.029	0.034	0.022	0.019	0.022	0.025	0.009	0.022	0.013	0.021
Ca	0.254	0.100	0.126	0.185	0.104	0.351	0.328	0.423	0.614	0.503
Na	3.314	3.547	4.449	3.956	4.157	3.990	3.901	3.776	3.508	3.796
K	0.061	0.056	0.052	0.064	0.047	0.098	0.072	0.066	0.061	0.059
Ba	0.024	0.034	0.017	0.041	0.017	0.017	-	-	0.038	-
MOL PERCENT END MEMBERS										
Celsian	0.65	0.90	0.36	0.96	0.40	0.39	-	-	0.91	-
Fe-Or	0.80	0.90	0.48	0.45	0.51	0.56	0.21	0.52	0.32	0.48
Anorthite	6.90	2.65	2.69	4.34	2.40	7.83	7.62	9.88	14.51	11.50
Albite	90.00	94.07	95.35	92.75	95.60	89.04	90.50	88.08	82.82	86.68
Orthoclase	1.64	1.49	1.12	1.49	1.09	2.18	1.68	1.53	1.45	1.35
MOL PERCENT IN AN-AB-OR SYSTEM										
An	7.00	2.70	2.72	4.40	2.42	7.91	7.63	9.93	14.69	11.55
Ab	91.33	95.79	96.16	94.09	96.48	89.89	90.69	88.54	83.85	87.09
Or	1.67	1.52	1.13	1.51	1.10	2.20	1.68	1.54	1.47	1.35

Appendix 3. Representative compositions of feldspars in the ferro-edenite syenite (C2224) in Center III, Coldwell Complex, Ontario

	Antiperthite											Secondary albite		
	Na-feldspar host						Exsolved K-feldspar							
CL colour	Blue			Light violet blue			Dull blue					Dull red		
Anal. No.	1	2	4	5	6	7	8	9	10	11	12	13	14	15
SiO2	63.75	63.76	64.91	65.15	64.80	64.47	64.65	65.03	64.81	65.00	64.57	62.48	63.69	64.28
Al2O3	22.90	22.71	23.48	23.18	22.87	23.73	18.24	17.94	18.04	17.73	18.02	23.13	23.33	23.67
Fe2O3	0.13	0.11	0.18	0.16	0.14	0.18	0.06	0.20	-	0.08	-	0.16	0.13	0.18
BaO	0.49	0.51	-	0.68	-	0.83	-	-	0.81	-	0.32	-	-	-
CaO	0.21	0.22	0.37	0.32	0.18	0.30	0.16	0.12	0.15	0.23	0.20	0.62	0.61	0.60
Na2O	12.16	11.70	10.50	9.46	11.35	10.26	1.14	1.28	1.29	1.20	1.04	13.45	12.11	10.97
K2O	0.37	0.90	0.43	1.06	0.41	1.26	15.39	15.21	15.70	15.68	15.60	0.18	0.25	0.18
STRUCTURAL FORMULA BASED ON 32 OXYGENS														
Si	11.296	11.325	11.388	11.460	11.414	11.304	11.978	12.023	11.970	12.033	11.992	11.116	11.239	11.301
Al	4.784	4.756	4.857	4.807	4.749	4.905	3.984	3.910	3.928	3.870	3.945	4.852	4.854	4.906
Fe+3	0.018	0.015	0.023	0.021	0.019	0.023	0.008	0.028	-	0.011	-	0.021	0.018	0.024
Ca	0.040	0.042	0.070	0.060	0.034	0.056	0.032	0.024	0.030	0.046	0.040	0.118	0.115	0.113
Na	4.178	4.029	3.572	3.226	3.877	3.488	0.410	0.459	0.462	0.431	0.374	4.640	4.143	3.740
K	0.084	0.204	0.096	0.238	0.092	0.282	3.638	3.588	3.699	3.703	3.696	0.041	0.056	0.040
Ba	0.034	0.035	-	0.047	-	0.057	-	-	0.059	-	0.023	-	-	-
MOL PERCENT END MEMBERS														
Celsian	0.78	0.82	-	1.30	-	1.46	-	-	1.38	-	0.56	-	-	-
Fe-Or	0.41	0.34	0.62	0.57	0.48	0.60	0.19	0.68	-	0.26	-	0.43	0.41	0.60
Anorthite	0.92	0.97	1.85	1.68	0.84	1.44	0.78	0.58	0.70	1.09	0.96	2.45	2.66	2.89
Albite	95.97	93.15	94.97	89.82	96.39	89.28	10.02	11.20	10.87	10.28	9.06	96.27	95.63	95.48
Orthoclase	1.92	4.71	2.56	6.62	2.29	7.21	89.01	87.54	87.05	88.37	89.41	0.85	1.30	1.03
MOL PERCENT IN AN-AB-OR SYSTEM														
An	0.93	0.98	1.86	1.71	0.85	1.47	0.78	0.58	0.71	1.09	0.97	2.46	2.67	2.90
Ab	97.13	94.25	95.56	91.54	96.85	91.16	10.04	11.27	11.02	10.31	9.11	96.69	96.02	96.06
Or	1.94	4.77	2.58	6.75	2.30	7.37	89.18	88.14	88.27	88.60	89.92	0.85	1.30	1.04

Appendix 3. Representative compositions of feldspars in the ferro-edenite syenite (C2232) in Center III, Coldwell Complex, Ontario

	Alkali feldspar (microperthite), core			Alkali feldspar (microperthite), mantle 1						Alkali feldspar (microperthite), mantle 2		
CL colour	Light bluish violet			Light violet blue						Light blue		
Anal. No.	1-1	1-2	1-3	1-4	1-5	1-6	1-7	1-8	1-9	1-10	1-11	1-12
SiO2	65.85	66.15	66.15	66.08	66.24	65.47	65.50	65.79	65.93	66.01	65.84	64.84
Al2O3	19.25	19.83	20.27	20.35	19.65	19.95	20.24	20.45	20.43	20.47	20.14	20.62
Fe2O3	0.20	0.26	0.26	0.17	0.33	0.13	0.36	0.28	0.21	0.21	0.29	0.27
BaO	0.21	-	-	-	-	0.38	-	-	-	-	0.15	0.64
CaO	0.18	0.09	0.20	0.26	0.18	0.18	0.25	0.47	0.30	0.22	0.37	0.26
Na2O	6.08	5.70	5.87	6.25	5.57	6.55	6.38	7.21	7.01	6.37	6.93	7.57
K2O	8.06	7.92	7.28	6.52	7.84	7.34	6.83	5.72	6.14	6.75	6.32	5.83
STRUCTURAL FORMULA BASED ON 32 OXYGENS												
Si	11.886	11.870	11.827	11.824	11.895	11.787	11.775	11.748	11.769	11.789	11.782	11.654
Al	4.096	4.195	4.272	4.293	4.160	4.234	4.290	4.305	4.300	4.310	4.249	4.369
Fe+3	0.027	0.035	0.034	0.022	0.045	0.018	0.048	0.037	0.028	0.028	0.039	0.036
Ca	0.035	0.017	0.038	0.050	0.035	0.035	0.048	0.090	0.057	0.042	0.071	0.050
Na	2.128	1.983	2.035	2.168	1.939	2.286	2.224	2.496	2.426	2.206	2.404	2.638
K	1.856	1.813	1.661	1.488	1.796	1.686	1.566	1.303	1.398	1.538	1.443	1.337
Ba	0.015	-	-	-	-	0.027	-	-	-	-	0.011	0.045
MOL PERCENT END MEMBERS												
Celsian	0.37	-	-	-	-	0.66	-	-	-	-	0.27	1.10
Fe-Or	0.67	0.90	0.91	0.60	1.18	0.45	1.24	0.95	0.73	0.74	0.98	0.88
Anorthite	0.86	0.45	1.02	1.34	0.91	0.86	1.24	2.29	1.47	1.10	1.79	1.22
Albite	52.40	51.54	54.00	58.15	50.83	56.43	57.22	63.57	62.05	57.83	60.60	64.25
Orthoclase	45.71	47.12	44.07	39.91	47.08	41.61	40.30	33.19	35.76	40.32	36.36	32.56
MOL PERCENT IN AN-AB-OR SYSTEM												
An	0.87	0.45	1.03	1.34	0.92	0.87	1.25	2.31	1.48	1.11	1.81	1.24
Ab	52.95	52.00	54.50	58.50	51.44	57.06	57.94	64.18	62.50	58.26	61.37	65.54
Or	46.19	47.54	44.47	40.15	47.64	42.07	40.81	33.50	36.02	40.62	36.82	33.21

Appendix 3. continued

	Alkali feldspar (microperthite), core				Albite (albite twinned) core			2nd. albite, antiperthite rim	
CL colour	Light blue				Light blue			Purple	
Anal. No.	2-1	2-2	2-3	2-4	2-5	2-6	2-7	2-8	2-9
SiO2	64.80	65.60	66.06	65.32	63.88	63.71	63.77	64.72	64.11
Al2O3	21.24	21.38	20.23	20.65	22.78	22.97	23.24	22.80	22.90
Fe2O3	0.20	0.42	0.17	0.20	0.14	0.09	0.14	0.09	0.13
BaO	-	-	0.43	-	-	-	-	-	-
CaO	0.40	0.60	0.50	0.31	1.05	1.00	0.73	0.34	0.43
Na2O	8.07	7.58	6.30	7.19	11.70	11.59	11.83	11.51	11.42
K2O	5.04	4.29	6.34	5.81	0.29	0.47	0.31	0.43	0.16
STRUCTURAL FORMULA BASED ON 32 OXYGENS									
Si	11.594	11.648	11.814	11.717	11.302	11.279	11.259	11.401	11.366
Al	4.480	4.476	4.265	4.367	4.752	4.794	4.837	4.735	4.786
Fe+3	0.027	0.056	0.022	0.027	0.019	0.012	0.019	0.012	0.018
Ca	0.077	0.114	0.096	0.060	0.199	0.190	0.138	0.064	0.082
Na	2.800	2.610	2.185	2.501	4.014	3.979	4.050	3.931	3.926
K	1.150	0.972	1.446	1.330	0.065	0.106	0.070	0.097	0.036
Ba	-	-	0.030	-	-	-	-	-	-
MOL PERCENT END MEMBERS									
Celsian	-	-	0.80	-	-	-	-	-	-
Fe-Or	0.66	1.50	0.59	0.69	0.45	0.28	0.45	0.29	0.44
Anorthite	1.89	3.04	2.54	1.52	4.63	4.43	3.23	1.56	2.01
Albite	69.06	69.55	57.80	63.84	93.40	92.82	94.69	95.79	96.66
Orthoclase	28.38	25.90	38.27	33.95	1.52	2.48	1.63	2.35	0.89
MOL PERCENT IN AN-AB-OR SYSTEM									
An	1.90	3.09	2.57	1.53	4.65	4.44	3.24	1.57	2.02
Ab	69.53	70.61	58.62	64.29	93.82	93.08	95.12	96.07	97.08
Or	28.57	26.30	38.81	34.18	1.53	2.48	1.64	2.36	0.89

Appendix 3. continued

	Deuteric coarsened albite, antiperthite rim						Deuteric coarsened K-feldspar, antiperthite rim					
CL colour	Red						Dark brown					
Anal. No.	1-13	1-14	1-15	2-10	2-11	2-12	1-16	1-17	1-18	2-13	2-14	2-15
SiO2	65.89	65.51	64.84	65.21	65.50	65.29	64.10	63.35	64.57	64.23	64.26	64.04
Al2O3	22.49	22.62	22.65	23.12	22.46	22.39	17.73	17.76	17.42	17.32	17.47	17.42
Fe2O3	0.14	0.38	0.41	0.31	0.34	0.46	0.27	0.23	0.18	0.30	0.28	0.41
BaO	-	-	-	-	-	-	0.17	-	-	-	-	-
CaO	0.07	0.11	-	0.10	-	-	0.13	0.18	-	0.08	-	0.07
Na2O	11.16	11.23	11.93	11.05	11.53	11.62	0.74	0.94	0.82	0.56	0.97	1.33
K2O	0.12	0.19	0.20	0.23	0.20	0.28	16.80	17.18	17.03	17.45	17.04	16.69
STRUCTURAL FORMULA BASED ON 32 OXYGENS												
Si	11.542	11.482	11.407	11.426	11.490	11.471	11.961	11.894	12.027	12.007	11.988	11.959
Al	4.644	4.674	4.698	4.776	4.645	4.638	3.900	3.931	3.825	3.817	3.842	3.835
Fe+3	0.019	0.050	0.054	0.041	0.045	0.060	0.037	0.033	0.025	0.042	0.039	0.058
Ca	0.013	0.021	-	0.019	-	-	0.026	0.036	-	0.016	-	0.014
Na	3.790	3.816	4.070	3.754	3.922	3.959	0.268	0.342	0.296	0.203	0.351	0.482
K	0.027	0.042	0.045	0.051	0.045	0.063	3.999	4.115	4.047	4.162	4.055	3.976
Ba	-	-	-	-	-	-	0.012	-	-	-	-	-
MOL PERCENT END MEMBERS												
Celsian	-	-	-	-	-	-	0.29	-	-	-	-	-
Fe-Or	0.49	1.27	1.31	1.06	1.13	1.48	0.86	0.73	0.57	0.95	0.88	1.28
Anorthite	0.34	0.53	-	0.49	-	-	0.60	0.80	-	0.36	-	0.31
Albite	98.47	97.12	97.62	97.12	97.75	96.99	6.16	7.56	6.78	4.59	7.89	10.63
Orthoclase	0.70	1.08	1.08	1.33	1.12	1.54	92.09	90.91	92.65	94.09	91.23	87.78
MOL PERCENT IN AN-AB-OR SYSTEM												
An	0.34	0.53	-	0.49	-	-	0.61	0.81	-	0.37	-	0.31
Ab	98.96	98.37	98.91	98.16	98.87	98.44	6.24	7.62	6.82	4.63	7.96	10.77
Or	0.70	1.10	1.09	1.34	1.13	1.56	93.16	91.58	93.18	95.00	92.04	88.92

Appendix 3. Representative compositions of feldspars in the contaminated ferro-edenite syenite (C2036) in Center III, Coldwell Complex, Ontario

	Phenocryst, core												
	Oligoclase-Andesine			Secondary Na-feldspar					Secondary K-feldspar				
CL colour	Light greenish blue			Dull blue					Dull blue				
Anal. No.	2-1	2-2	2-3	1-1	1-2	1-3	2-4	2-5	1-4	1-5	1-6	2-6	2-7
SiO2	60.22	58.17	58.10	62.23	61.80	62.07	61.07	61.00	64.13	63.60	64.08	63.82	63.88
Al2O3	24.63	25.81	26.04	23.28	23.65	23.48	23.95	23.56	18.45	18.86	18.16	18.83	18.51
Fe2O3	0.07	0.10	0.13	0.08	0.14	0.07	0.10	0.10	-	0.09	0.04	-	-
BaO	-	-	-	0.24	0.19	0.23	0.12	0.32	2.40	2.28	2.45	1.83	1.81
CaO	4.81	8.32	7.67	2.31	2.96	2.64	2.89	2.72	0.19	0.14	0.14	0.18	0.22
Na2O	9.83	7.51	7.62	11.39	11.01	11.26	11.63	12.06	1.17	2.12	1.45	0.60	1.29
K2O	0.31	0.10	0.22	0.33	0.19	0.26	0.20	0.25	13.66	12.55	13.40	14.17	13.96
STRUCTURAL FORMULA BASED ON 32 OXYGENS													
Si	10.768	10.437	10.436	11.092	11.009	11.051	10.908	10.925	11.940	11.849	11.964	11.910	11.913
Al	5.192	5.459	5.514	4.892	4.967	4.928	5.043	4.975	4.050	4.143	3.997	4.143	4.070
Fe+3	0.009	0.014	0.018	0.010	0.019	0.009	0.013	0.013	-	0.012	0.006	-	-
Ca	0.922	1.599	1.476	0.441	0.565	0.504	0.553	0.522	0.038	0.028	0.028	0.036	0.044
Na	3.408	2.613	2.654	3.936	3.803	3.887	4.028	4.188	0.422	0.766	0.525	0.217	0.466
K	0.071	0.023	0.050	0.075	0.043	0.059	0.046	0.057	3.245	2.983	3.192	3.374	3.321
Ba	-	-	-	0.017	0.013	0.016	0.008	0.022	0.175	0.166	0.179	0.134	0.132
MOL PERCENT END MEMBERS													
Celsian	-	-	-	0.37	0.30	0.36	0.18	0.47	4.51	4.21	4.56	3.56	3.34
Fe-Or	0.20	0.32	0.43	0.23	0.44	0.20	0.29	0.28	-	0.32	0.16	-	-
Anorthite	20.90	37.65	35.16	9.85	12.71	11.26	11.90	10.87	0.98	0.71	0.71	0.96	1.11
Albite	77.29	61.49	63.21	87.87	85.58	86.87	86.65	87.19	10.89	19.36	13.36	5.77	11.77
Orthoclase	1.60	0.54	1.20	1.68	0.97	1.32	0.98	1.19	83.63	75.41	81.21	89.71	83.79
MOL PERCENT IN AN-AB-OR SYSTEM													
An	20.94	37.77	35.31	9.91	12.81	11.32	11.96	10.95	1.02	0.74	0.75	0.99	1.15
Ab	77.45	61.69	63.48	88.41	86.21	87.35	87.06	87.85	11.40	20.28	14.02	5.99	12.17
Or	1.61	0.54	1.21	1.69	0.98	1.33	0.99	1.20	87.58	78.98	85.23	93.02	86.68

Appendix 3. continued

	Phenocryst, inner rim								Phenocryst, outer rim				
	Na-feldspar				Secondary K-feldspar				Na-feldspar				
CL colour	Light blue				Dull blue				Light violet blue				
Anal. No.	1-7	1-8	2-8	2-9	1-9	1-10	2-10	2-11	1-11	1-12	1-13	2-12	2-13
SiO2	61.64	61.93	62.58	61.82	64.32	63.43	61.46	62.36	63.13	64.08	63.80	63.47	62.97
Al2O3	23.61	23.73	23.50	23.92	18.55	18.64	19.11	18.55	23.37	23.59	23.45	23.01	23.02
Fe2O3	0.12	0.12	0.13	0.12	0.08	0.07	-	0.08	0.16	0.24	0.13	0.17	0.22
BaO	0.48	0.34	0.51	-	1.68	2.39	5.18	3.71	-	0.40	-	-	0.31
CaO	1.51	2.30	1.89	1.92	0.11	0.08	0.08	0.14	0.88	0.73	0.75	0.70	0.78
Na2O	12.52	11.47	11.16	12.05	1.78	2.74	1.60	2.14	12.11	10.81	11.45	12.19	12.26
K2O	0.13	0.12	0.24	0.18	13.49	12.52	12.27	12.86	0.27	0.17	0.18	0.35	0.22
STRUCTURAL FORMULA BASED ON 32 OXYGENS													
Si	11.007	11.025	11.121	10.994	11.922	11.831	11.692	11.773	11.185	11.287	11.265	11.245	11.202
Al	4.971	4.980	4.924	5.015	4.054	4.099	4.286	4.129	4.881	4.898	4.881	4.806	4.828
Fe+3	0.016	0.016	0.018	0.016	0.011	0.009	-	0.011	0.021	0.032	0.018	0.022	0.030
Ca	0.289	0.439	0.360	0.366	0.022	0.016	0.016	0.028	0.167	0.138	0.142	0.133	0.149
Na	4.335	3.959	3.845	4.155	0.640	0.991	0.590	0.783	4.160	3.692	3.920	4.188	4.229
K	0.030	0.027	0.054	0.041	3.190	2.979	2.978	3.098	0.061	0.038	0.041	0.079	0.050
Ba	0.034	0.024	0.036	-	0.122	0.175	0.386	0.274	-	0.028	-	-	0.022
MOL PERCENT END MEMBERS													
Celsian	0.71	0.53	0.82	-	3.06	4.19	9.72	6.54	-	0.70	-	-	0.48
Fe-Or	0.35	0.37	0.41	0.36	0.27	0.22	-	0.26	0.47	0.83	0.43	0.50	0.66
Anorthite	6.14	9.83	8.34	7.99	0.55	0.38	0.41	0.68	3.79	3.51	3.44	3.01	3.32
Albite	92.16	88.67	89.16	90.76	16.06	23.76	14.86	18.68	94.36	93.99	95.14	94.70	94.42
Orthoclase	0.63	0.61	1.26	0.89	80.06	71.44	75.00	73.84	1.38	0.97	0.98	1.79	1.11
MOL PERCENT IN AN-AB-OR SYSTEM													
An	6.21	9.91	8.45	8.02	0.57	0.40	0.45	0.72	3.81	3.56	3.46	3.02	3.36
Ab	93.15	89.47	90.27	91.08	16.61	24.86	16.46	20.04	94.80	95.45	95.55	95.18	95.51
Or	0.64	0.62	1.28	0.90	82.82	74.74	83.08	79.24	1.39	0.99	0.99	1.80	1.13

Appendix 3. continued

	Groundmass								Aplitic dike					
	Secondary Na-feldspar				K-feldspar				Na-feldspar			K-feldspar		
CL colour	Dull violet				Blue		Dull blue		Dull violet			Dull blue		
Anal. No.	2-14	2-15	1-14	1-15	2-16	2-17	1-16	1-17	1-18	1-19	1-20	1-21	1-22	1-23
SiO2	62.94	62.56	61.90	62.39	65.28	65.95	64.92	65.20	63.34	63.11	62.58	65.14	64.63	65.66
Al2O3	23.07	22.87	22.93	23.41	18.49	18.06	18.06	18.11	23.34	23.58	23.09	18.12	18.55	18.18
Fe2O3	0.08	0.18	0.22	0.07	0.18	0.27	0.10	-	0.07	0.09	0.13	0.10	0.09	-
BaO	-	0.11	-	-	0.54	0.18	0.48	0.26	-	-	0.15	-	-	0.33
CaO	0.50	0.32	0.88	1.26	0.26	0.30	0.29	0.21	0.92	0.97	0.72	0.26	0.15	0.09
Na2O	13.15	13.81	13.42	12.65	2.20	1.64	0.87	0.85	11.94	11.73	13.13	0.40	0.95	0.44
K2O	0.22	0.17	0.25	0.18	13.07	13.63	15.29	15.03	0.35	0.30	0.13	15.75	15.31	15.30
STRUCTURAL FORMULA BASED ON 32 OXYGENS														
Si	11.178	11.144	11.084	11.093	11.977	12.072	12.009	12.049	11.210	11.181	11.139	12.039	11.954	12.084
Al	4.830	4.803	4.840	4.907	3.999	3.897	3.939	3.945	4.870	4.925	4.845	3.948	4.045	3.944
Fe+3	0.010	0.024	0.030	0.009	0.025	0.037	0.014	-	0.009	0.012	0.018	0.014	0.012	-
Ca	0.095	0.061	0.169	0.240	0.051	0.059	0.057	0.042	0.174	0.184	0.137	0.051	0.030	0.018
Na	4.528	4.770	4.659	4.361	0.783	0.582	0.312	0.305	4.097	4.029	4.531	0.143	0.341	0.157
K	0.050	0.039	0.057	0.041	3.059	3.183	3.609	3.543	0.079	0.068	0.030	3.714	3.613	3.592
Ba	-	0.008	-	-	0.039	0.013	0.035	0.019	-	-	0.010	-	-	0.024
MOL PERCENT END MEMBERS														
Celsian	-	0.16	-	-	0.98	0.33	0.86	0.48	-	-	0.22	-	-	0.63
Fe-Or	0.22	0.49	0.61	0.19	0.62	0.95	0.35	-	0.20	0.28	0.38	0.35	0.31	-
Anorthite	2.03	1.25	3.44	5.16	1.29	1.52	1.43	1.06	4.00	4.29	2.91	1.31	0.74	0.47
Albite	96.68	97.32	94.79	93.77	19.78	15.03	7.75	7.79	93.98	93.86	95.87	3.65	8.53	4.14
Orthoclase	1.06	0.79	1.16	0.88	77.33	82.17	89.61	90.66	1.81	1.58	0.62	94.68	90.42	94.76
MOL PERCENT IN AN-AB-OR SYSTEM														
An	2.04	1.25	3.46	5.17	1.31	1.54	1.44	1.07	4.01	4.30	2.92	1.32	0.75	0.47
Ab	96.90	97.95	95.37	93.95	20.10	15.22	7.84	7.83	94.17	94.12	96.45	3.67	8.55	4.17
Or	1.07	0.79	1.17	0.88	78.58	83.24	90.71	91.10	1.82	1.58	0.63	95.02	90.70	95.36

Appendix 3. Representative compositions of feldspars in the contaminated ferro-edenite syenites (C2065, C2063) in Center III, Coldwell Complex, Ontario

Phenocryst

	Secondary K-feldspar, core					Andesine				K-feldspar		
CL colour	Non-luminescence					Light greenish blue				Dull blue		
Anal. No.	1-1	1-2	1-3	1-4	1-5	1-6	1-7	1-8	1-9	1-10	1-11	1-12
SiO2	64.91	64.63	64.39	65.23	64.59	59.64	56.19	57.94	56.85	64.82	64.16	64.98
Al2O3	17.43	17.26	17.55	17.31	17.94	25.28	26.81	26.56	26.74	17.84	18.38	17.25
Fe2O3	0.08	0.78	0.12	0.10	0.14	-	-	0.09	0.50	0.32	-	0.26
BaO	0.27	0.48	1.04	0.34	0.50	-	-	-	-	-	-	0.31
CaO	0.17	0.18	0.19	0.09	0.24	7.00	9.73	8.58	9.47	-	0.38	-
Na2O	-	-	-	-	-	7.58	6.90	6.20	6.05	1.29	1.32	1.67
K2O	17.15	16.57	16.72	16.94	16.60	0.29	0.31	0.39	0.37	15.64	15.05	15.48
STRUCTURAL FORMULA BASED ON 32 OXYGENS												
Si	12.079	12.051	12.033	12.120	12.009	10.661	10.153	10.393	10.232	12.005	11.929	12.063
Al	3.824	3.794	3.867	3.792	3.932	5.327	5.711	5.617	5.674	3.895	4.029	3.775
Fe+3	0.011	0.109	0.017	0.014	0.020	-	-	0.012	0.068	0.045	-	0.036
Ca	0.034	0.036	0.038	0.018	0.048	1.341	1.884	1.649	1.826	-	0.076	-
Na	-	-	-	-	-	2.627	2.417	2.156	2.111	0.463	0.476	0.601
K	4.072	3.942	3.986	4.016	3.938	0.066	0.071	0.089	0.085	3.696	3.570	3.666
Ba	0.020	0.035	0.076	0.025	0.036	-	-	-	-	-	-	0.023
MOL PERCENT END MEMBERS												
Celsian	0.48	0.85	1.85	0.61	0.90	-	-	-	-	-	-	0.52
Fe-Or	0.26	2.65	0.42	0.34	0.50	-	-	0.31	1.66	1.07	-	0.83
Anorthite	0.82	0.87	0.92	0.44	1.18	33.24	43.08	42.21	44.65	-	1.84	-
Albite	-	-	-	-	-	65.12	55.28	55.20	51.62	11.02	11.55	13.90
Orthoclase	98.44	95.63	96.81	98.61	97.42	1.64	1.63	2.28	2.08	87.91	86.62	84.76
MOL PERCENT IN AN-AB-OR SYSTEM												
An	0.83	0.90	0.95	0.44	1.20	33.24	43.08	42.34	45.40	-	1.84	-
Ab	-	-	-	-	-	65.12	55.28	55.37	52.49	11.14	11.55	14.09
Or	99.17	99.10	99.05	99.56	98.80	1.64	1.63	2.29	2.11	88.86	86.62	85.91

Analyses 1-1 to 1-17 are from sample C2065 and analyses 2-1 to 2-7 are from sample C2063.

Appendix 3. continued

	Groundmass					Phenocryst						
						Homogeneous, core					Perthite, rim	
	Secondary Na-feldspar					alkali feldspar					Na-feldspar	
CL colour	Light violet			Dull blue		Light blue			L. violet blue		Light blue	
Anal. No.	1-13	1-14	1-15	1-16	1-17	2-1	2-2	2-3	2-4	2-5	2-6	2-7
SiO2	63.77	63.49	64.39	62.94	62.74	64.50	64.71	64.82	64.66	64.77	62.87	62.85
Al2O3	23.18	23.16	23.05	23.51	23.16	20.44	20.16	20.34	19.63	19.52	22.81	22.70
Fe2O3	0.20	0.13	0.21	0.34	0.41	0.19	0.07	0.16	0.10	0.12	0.13	0.30
BaO	-	0.18	-	-	0.22	-	-	-	0.29	0.18	-	-
CaO	1.10	1.07	0.81	0.94	1.49	0.59	0.63	0.58	0.37	0.10	1.11	0.54
Na2O	11.44	11.76	11.29	12.07	11.76	8.46	7.00	7.21	7.26	6.64	12.83	13.13
K2O	0.28	0.21	0.28	0.23	0.17	5.68	7.38	6.91	7.23	8.57	0.13	0.28
STRUCTURAL FORMULA BASED ON 32 OXYGENS												
Si	11.261	11.235	11.336	11.146	11.148	11.607	11.678	11.666	11.736	11.758	11.181	11.194
Al	4.826	4.832	4.784	4.908	4.852	4.337	4.289	4.316	4.200	4.178	4.782	4.766
Fe+3	0.027	0.018	0.028	0.046	0.055	0.026	0.009	0.021	0.014	0.017	0.018	0.040
Ca	0.208	0.203	0.153	0.178	0.284	0.114	0.122	0.112	0.072	0.019	0.212	0.103
Na	3.917	4.035	3.854	4.144	4.052	2.952	2.449	2.516	2.555	2.337	4.424	4.534
K	0.063	0.047	0.063	0.052	0.039	1.304	1.699	1.587	1.674	1.985	0.029	0.064
Ba	-	0.012	-	-	0.015	-	-	-	0.021	0.013	-	-
MOL PERCENT END MEMBERS												
Celsian	-	0.29	-	-	0.34	-	-	-	0.48	0.29	-	-
Fe-Or	0.63	0.41	0.68	1.04	1.24	0.58	0.21	0.50	0.32	0.38	0.38	0.85
Anorthite	4.94	4.70	3.73	4.03	6.38	2.59	2.85	2.64	1.66	0.45	4.52	2.17
Albite	92.93	93.50	94.05	93.75	91.17	67.16	57.24	59.40	58.93	53.47	94.47	95.64
Orthoclase	1.50	1.10	1.53	1.18	0.87	29.67	39.71	37.46	38.62	45.41	0.63	1.34
MOL PERCENT IN AN-AB-OR SYSTEM												
An	4.97	4.73	3.75	4.08	6.49	2.60	2.85	2.65	1.67	0.45	4.53	2.19
Ab	93.52	94.16	94.70	94.74	92.63	67.55	57.36	59.70	59.40	53.83	94.83	96.45
Or	1.51	1.11	1.55	1.19	0.88	29.84	39.79	37.65	38.92	45.72	0.63	1.35

Appendix 3. continued

	Perthitic phenocryst						Groundmass							
	Perthite, core													
	Na-feldspar		K-feldspar				K-feldspar				Na-feldspar			
CL colour	Light blue		Light violet blue				Dull blue				Dull red			
Anal. No.	15	16	17	18	19	20	21	22	23	24	25	26	27	28
SiO2	63.43	64.38	64.72	64.05	64.19	64.62	64.24	63.65	63.29	64.61	64.80	65.18	65.21	64.40
Al2O3	23.35	23.00	17.53	17.59	18.06	18.32	17.45	17.37	18.32	17.46	22.84	23.04	23.03	22.46
Fe2O3	0.07	0.20	0.14	0.13	0.26	0.17	0.28	0.30	0.29	0.28	0.32	0.31	0.39	0.27
BaO	0.42	0.62	-	0.72	0.51	0.31	-	-	0.23	-	0.17	-	-	0.23
CaO	0.55	0.37	0.19	0.21	0.24	-	-	0.14	0.15	0.14	0.06	-	0.07	0.12
Na2O	11.68	10.90	0.63	1.05	2.01	0.96	1.65	2.53	1.88	1.65	11.61	11.28	11.17	12.42
K2O	0.51	0.55	16.62	16.26	14.54	15.64	16.32	15.86	14.68	15.90	0.23	0.14	0.17	0.14
STRUCTURAL FORMULA BASED ON 32 OXYGENS														
Si	11.237	11.369	12.040	11.968	11.922	11.963	11.975	11.906	11.862	11.999	11.400	11.430	11.428	11.375
Al	4.877	4.788	3.845	3.875	3.955	3.998	3.835	3.830	4.048	3.823	4.737	4.763	4.758	4.677
Fe+3	0.009	0.027	0.020	0.019	0.036	0.023	0.039	0.042	0.041	0.039	0.043	0.041	0.051	0.035
Ca	0.104	0.070	0.038	0.042	0.048	-	-	0.028	0.030	0.028	0.011	-	0.013	0.023
Na	4.012	3.732	0.227	0.380	0.724	0.345	0.596	0.918	0.683	0.594	3.960	3.835	3.796	4.254
K	0.115	0.124	3.944	3.876	3.445	3.694	3.881	3.785	3.510	3.767	0.052	0.031	0.038	0.032
Ba	0.029	0.043	-	0.053	0.037	0.022	-	-	0.017	-	0.012	-	-	0.016
MOL PERCENT END MEMBERS														
Celsian	0.68	1.07	-	1.21	0.87	0.55	-	-	0.39	-	0.29	-	-	0.37
Fe-Or	0.21	0.67	0.48	0.43	0.83	0.57	0.86	0.89	0.95	0.88	1.05	1.05	1.32	0.81
Anorthite	2.45	1.75	0.90	0.96	1.11	-	-	0.59	0.70	0.63	0.28	-	0.34	0.52
Albite	93.96	93.41	5.37	8.70	16.87	8.44	13.20	19.23	15.96	13.42	97.12	98.15	97.37	97.58
Orthoclase	2.70	3.10	93.25	88.70	80.31	90.44	85.93	79.30	81.99	85.08	1.27	0.80	0.98	0.72
MOL PERCENT IN AN-AB-OR SYSTEM														
An	2.47	1.78	0.90	0.98	1.13	-	-	0.59	0.71	0.63	0.28	-	0.34	0.53
Ab	94.81	95.06	5.40	8.85	17.17	8.53	13.32	19.40	16.18	13.54	98.44	99.19	98.67	98.74
Or	2.72	3.16	93.70	90.17	81.70	91.47	86.68	80.01	83.11	85.83	1.28	0.81	0.99	0.73

Appendix 3. Representative compositions of feldspars in the quartz syenite (C173) in Center III, Coldwell Complex, Ontario

	Albite, core		Oscillatory Antiperthite						Secondary albite	
			Exsolved albite,			K-feldspar host,				
			rim	core	rim	rim	core	rim		
CL colour	Light blue		Dull red			Dull blue			Deep red	
Anal. No.	C173-1	C173-2	C173-3	C173-4	C173-5	C173-6	C173-7	C173-9	C173-10	C173-11
SiO2	64.39	64.07	64.97	64.90	64.91	65.23	63.81	64.56	64.74	64.81
Al2O3	23.05	23.15	22.37	22.76	22.76	17.06	17.10	17.04	22.68	22.38
Fe2O3	-	0.22	0.62	0.21	0.32	0.33	0.23	0.20	0.49	0.58
BaO	0.33	-	-	-	-	-	-	-	-	-
CaO	1.19	1.08	-	-	-	-	0.22	0.10	-	-
Na2O	10.68	11.15	11.95	12.01	11.93	0.50	1.09	0.98	11.78	11.86
K2O	0.16	0.26	0.16	0.14	0.12	16.91	17.57	16.97	0.13	0.35
STRUCTURAL FORMULA BASED ON 32 OXYGENS										
Si	11.359	11.298	11.430	11.410	11.408	12.116	11.967	12.056	11.405	11.422
Al	4.794	4.813	4.640	4.717	4.716	3.736	3.781	3.751	4.710	4.650
Fe+3	-	0.029	0.082	0.028	0.043	0.047	0.033	0.028	0.065	0.077
Ca	0.225	0.204	-	-	-	-	0.044	0.020	-	-
Na	3.653	3.812	4.076	4.094	4.065	0.180	0.396	0.355	4.024	4.053
K	0.036	0.058	0.036	0.031	0.027	4.007	4.204	4.043	0.029	0.079
Ba	0.023	-	-	-	-	-	-	-	-	-
MOL PERCENT END MEMBERS										
Celsian	0.58	-	-	-	-	-	-	-	-	-
Fe-Or	-	0.72	1.96	0.67	1.03	1.10	0.70	0.63	1.57	1.82
Anorthite	5.71	4.97	-	-	-	-	0.95	0.45	-	-
Albite	92.79	92.88	97.18	98.57	98.32	4.25	8.47	7.98	97.72	96.31
Orthoclase	0.91	1.43	0.86	0.76	0.65	94.65	89.88	90.94	0.71	1.87
MOL PERCENT IN AN-AB-OR SYSTEM										
An	5.75	5.01	-	-	-	-	0.95	0.45	-	-
Ab	93.33	93.56	99.13	99.24	99.34	4.30	8.53	8.03	99.28	98.10
Or	0.92	1.44	0.87	0.76	0.66	95.70	90.51	91.52	0.72	1.90

Appendix 3. Representative compositions of feldspars in quartz syenite (C369) from Center III, Coldwell Complex, Ontario

	Antiperthite					
	Albite host,			Exsolved K-feldspar,		
	core	mantle	rim	core	mantle	rim
CL colour	Red	Violet	Dull red	Dark blue	Dull blue	Dark blue
Anal. No.	C369-1	C369-2	C369-3	C369-4	C369-5	C369-6
SiO2	65.42	64.56	63.85	64.41	64.99	65.52
Al2O3	21.96	21.91	20.79	17.29	17.40	17.59
Fe2O3	1.76	0.89	2.78	0.19	0.38	0.26
BaO	-	0.74	-	0.42	-	-
CaO	-	0.10	0.12	0.15	0.15	-
Na2O	10.47	11.52	12.40	0.84	0.92	-
K2O	0.29	0.20	0.19	16.73	16.20	16.54
STRUCTURAL FORMULA BASED ON 32 OXYGENS						
Si	11.503	11.442	11.359	12.024	12.052	12.120
Al	4.552	4.578	4.360	3.805	3.804	3.836
Fe+3	0.232	0.119	0.372	0.027	0.053	0.036
Ca	-	0.019	0.023	0.030	0.030	-
Na	3.570	3.959	4.277	0.304	0.331	-
K	0.065	0.045	0.043	3.984	3.833	3.904
Ba	-	0.051	-	0.031	-	-
MOL PERCENT END MEMBERS						
Celsian	-	1.23	-	0.70	-	-
Fe-Or	6.01	2.83	7.89	0.61	1.24	0.90
Anorthite	-	0.45	0.49	0.69	0.70	-
Albite	92.31	94.41	90.71	6.95	7.79	-
Orthoclase	1.68	1.08	0.91	91.06	90.27	99.10
MOL PERCENT IN AN-AB-OR SYSTEM						
An	-	0.47	0.53	0.69	0.71	-
Ab	98.21	98.40	98.48	7.04	7.89	-
Or	1.79	1.12	0.99	92.26	91.40	100.00

Appendix 3. Representative compositions of feldspars in the quartz syenite (C2087) in Center III, Coldwell Complex, Ontario

	Homogeneous alkali feldspar, core				rim
CL colour	Blue				L. violet blue
Anal. No.	C2087-1	C2087-2	C2087-3	C2087-4	C2087-5
SiO2	65.07	65.26	64.71	64.69	64.27
Al2O3	19.27	19.66	21.56	20.22	21.19
Fe2O3	0.10	0.10	0.18	-	-
BaO	0.61	-	0.78	1.20	0.89
CaO	0.38	0.23	0.51	0.47	0.52
Na2O	6.56	6.24	7.84	6.97	10.28
K2O	8.02	8.52	4.43	6.35	2.85
STRUCTURAL FORMULA BASED ON 32 OXYGENS					
Si	11.801	11.790	11.567	11.701	11.509
Al	4.120	4.187	4.543	4.312	4.473
Fe+3	0.014	0.014	0.024	-	-
Ca	0.074	0.045	0.098	0.091	0.100
Na	2.307	2.186	2.717	2.444	3.569
K	1.856	1.964	1.010	1.465	0.651
Ba	0.043	-	0.055	0.085	0.062
MOL PERCENT END MEMBERS					
Celsian	1.01	-	1.40	2.08	1.42
Fe-Or	0.32	0.32	0.61	-	-
Anorthite	1.72	1.06	2.50	2.23	2.28
Albite	53.73	51.95	69.61	59.83	81.44
Orthoclase	43.22	46.67	25.88	35.86	14.86
MOL PERCENT IN AN-AB-OR SYSTEM					
An	1.74	1.06	2.55	2.28	2.31
Ab	54.45	52.12	71.04	61.10	82.62
Or	43.80	46.82	26.41	36.63	15.07

Appendix 3. Representative compositions of feldspars in the quartz syenite (C330) in Center III, Coldwell Complex, Ontario

	Perthitic core,					Antiperthite, rim			
	Albite			2nd. K-feldspar		Albite		K-feldspar	
CL colour	Light blue			Dull blue		Red		Dark blue	
Anal. No.	C330-1	C330-2	C330-3	C330-4	C330-5	C330-6	C330-7	C330-8	C330-9
SiO2	63.53	64.58	63.90	64.65	64.30	62.32	63.83	64.60	64.62
Al2O3	22.41	21.80	21.81	17.39	17.46	22.33	22.68	17.31	17.31
Fe2O3	-	0.36	0.50	0.18	0.21	0.39	0.48	0.13	0.27
BaO	-	-	-	-	-	0.47	-	-	0.22
CaO	0.43	-	0.16	-	0.21	-	-	0.07	0.23
Na2O	13.05	11.65	13.10	0.75	1.14	13.53	12.39	1.04	0.81
K2O	0.21	1.66	0.16	16.84	16.69	0.15	0.12	16.85	16.57
STRUCTURAL FORMULA BASED ON 32 OXYGENS									
Si	11.298	11.451	11.366	12.047	11.984	11.206	11.323	12.033	12.034
Al	4.699	4.557	4.573	3.820	3.836	4.734	4.743	3.801	3.800
Fe+3	-	0.047	0.067	0.025	0.030	0.053	0.064	0.019	0.037
Ca	0.082	-	0.030	-	0.042	-	-	0.014	0.046
Na	4.500	4.005	4.518	0.271	0.412	4.717	4.262	0.376	0.292
K	0.048	0.376	0.036	4.004	3.969	0.034	0.027	4.004	3.937
Ba	-	-	-	-	-	0.033	-	-	0.016
MOL PERCENT END MEMBERS									
Celsian	-	-	-	-	-	0.68	-	-	0.37
Fe-Or	-	1.07	1.44	0.58	0.67	1.09	1.47	0.42	0.86
Anorthite	1.77	-	0.66	-	0.94	-	-	0.32	1.06
Albite	97.20	90.45	97.12	6.30	9.25	97.52	97.91	8.51	6.76
Orthoclase	1.03	8.48	0.78	93.12	89.14	0.71	0.62	90.75	90.95
MOL PERCENT IN AN-AB-OR SYSTEM									
An	1.77	-	0.67	-	0.95	-	-	0.32	1.07
Ab	97.20	91.43	98.54	6.34	9.32	99.28	99.37	8.55	6.84
Or	1.03	8.57	0.79	93.66	89.74	0.72	0.63	91.13	92.09

Appendix 3. Representative compositions of feldspars in the quartz syenite (C2092) in Center III, Coldwell Complex, Ontario

	Perthite, in xenolith											Antiperthite		
	Exsolved Na-feldspar						K-feldspar host					Na-feldspar host		
CL colour	Light blue						Blue					Deep red		
Anal. No.	1	2	3	4	5	6	7	8	9	10	11	12	13	14
SiO2	64.98	64.38	64.31	63.41	62.83	63.90	64.57	64.41	64.92	64.17	65.04	65.10	65.56	65.22
Al2O3	22.72	23.14	22.48	22.79	22.53	22.70	18.07	18.11	17.93	18.22	17.97	22.06	21.78	21.74
Fe2O3	0.17	-	-	0.21	-	-	-	0.18	-	-	-	0.46	0.77	0.76
CaO	0.14	0.22	0.16	0.12	0.33	0.24	0.28	0.13	0.17	0.07	-	-	-	-
Na2O	11.74	12.16	12.51	12.11	13.33	12.94	-	1.65	1.77	1.71	0.89	11.58	11.30	11.63
K2O	0.37	0.15	0.31	0.13	0.35	0.22	16.41	14.82	15.21	15.30	16.10	0.05	0.19	0.15
STRUCTURAL FORMULA BASED ON 32 OXYGENS														
Si	11.419	11.332	11.378	11.316	11.232	11.304	12.023	11.967	11.998	11.935	12.031	11.510	11.554	11.524
Al	4.707	4.802	4.689	4.795	4.748	4.734	3.967	3.967	3.907	3.995	3.919	4.598	4.525	4.529
Fe+3	0.022	-	-	0.028	-	-	-	0.025	-	-	-	0.061	0.102	0.100
Ca	0.026	0.041	0.030	0.023	0.063	0.045	0.056	0.026	0.034	0.014	-	-	-	-
Na	4.000	4.150	4.291	4.190	4.621	4.439	-	0.594	0.634	0.617	0.319	3.970	3.861	3.984
K	0.083	0.034	0.070	0.030	0.080	0.050	3.898	3.513	3.586	3.630	3.800	0.011	0.043	0.034
MOL PERCENT END MEMBERS														
Fe-Or	0.53	-	-	0.66	-	-	-	0.60	-	-	-	1.50	2.54	2.44
Anorthite	0.64	0.98	0.69	0.54	1.33	1.00	1.41	0.62	0.79	0.33	-	-	-	-
Albite	96.82	98.22	97.72	98.11	97.00	97.90	-	14.30	14.91	14.47	7.75	98.22	96.39	96.74
Orthoclase	2.01	0.80	1.59	0.69	1.68	1.10	98.59	84.48	84.30	85.20	92.25	0.28	1.07	0.82
MOL PERCENT IN AN-AB-OR SYSTEM														
An	0.64	0.98	0.69	0.54	1.33	1.00	1.41	0.63	0.79	0.33	-	-	-	-
Ab	97.34	98.22	97.72	98.76	97.00	97.90	-	14.38	14.91	14.47	7.75	99.72	98.91	99.16
Or	2.02	0.80	1.59	0.70	1.68	1.10	98.59	84.99	84.30	85.20	92.25	0.28	1.09	0.84

Appendix 3. continued

	Antiperthite Na-feldspar host			Antiperthite Exsolved K-feldspar						Secondary Na-feldspar,				
CL colour	Deep red			Dull red						Deep red				
Anal. No.	15	16	17	18	19	20	21	22	23	24	25	26	27	28
SiO2	65.35	65.07	65.17	64.36	64.76	64.86	64.63	64.41	64.60	65.37	65.46	65.26	65.75	64.97
Al2O3	21.66	22.01	22.17	17.16	17.17	17.29	17.11	17.09	16.94	21.72	22.49	22.01	21.59	21.73
Fe2O3	0.82	1.01	1.22	0.92	0.74	0.61	0.66	0.52	0.51	1.09	1.12	1.06	1.13	0.93
CaO	-	-	-	0.21	0.35	0.20	0.25	-	0.16	-	-	-	0.12	-
Na2O	11.31	11.87	11.22	0.34	1.02	0.58	0.71	0.67	0.64	11.05	11.03	10.77	11.40	12.19
K2O	0.28	0.14	0.16	16.62	15.46	15.51	15.45	15.94	16.10	0.21	-	0.19	-	0.27
STRUCTURAL FORMULA BASED ON 32 OXYGENS														
Si	11.549	11.453	11.464	12.025	12.052	12.091	12.090	12.092	12.103	11.543	11.468	11.525	11.552	11.460
Al	4.513	4.567	4.598	3.780	3.767	3.800	3.773	3.783	3.742	4.521	4.645	4.583	4.472	4.519
Fe+3	0.109	0.134	0.162	0.130	0.104	0.086	0.092	0.074	0.072	0.145	0.148	0.140	0.150	0.124
Ca	-	-	-	0.042	0.070	0.040	0.050	-	0.032	-	-	-	0.023	-
Na	3.875	4.051	3.827	0.123	0.368	0.210	0.258	0.244	0.232	3.783	3.747	3.688	3.883	4.169
K	0.063	0.031	0.036	3.962	3.671	3.689	3.687	3.818	3.848	0.047	-	0.043	-	0.061
MOL PERCENT END MEMBERS														
Fe-Or	2.70	3.18	4.02	3.05	2.48	2.13	2.26	1.78	1.72	3.64	3.80	3.62	3.70	2.85
Anorthite	-	-	-	0.99	1.66	0.99	1.23	-	0.77	-	-	-	0.56	-
Albite	95.74	96.08	95.09	2.89	8.74	5.21	6.30	5.90	5.56	95.17	96.20	95.27	95.75	95.76
Orthoclase	1.56	0.75	0.89	93.07	87.13	91.67	90.21	92.32	91.95	1.19	-	1.11	-	1.40
MOL PERCENT IN AN-AB-OR SYSTEM														
An	-	-	-	1.02	1.70	1.01	1.25	-	0.78	-	-	-	0.58	-
Ab	98.40	99.23	99.07	2.98	8.96	5.32	6.45	6.00	5.65	98.76	100.00	98.85	99.42	98.56
Or	1.60	0.77	0.93	96.00	89.34	93.66	92.30	94.00	93.57	1.24	-	1.15	-	1.44

Appendix 4-1. Representive compositions of apatites in ferroaugite syenites from Center I, Coldwell Complex

Layered ferroaugite syenite of lower series

CL color	Pink						Brownish pink core					Light pink rim				
Anal. No.	C35-1	C35-2	C35-3	C35-4	C35-5	C35-6	C47-1	C47-2	C47-3	C47-4	C47-5	C47-6	C47-7	C47-8	C47-9	C47-10
SiO2	1.26	0.72	0.87	0.60	0.57	0.36	2.49	2.89	2.99	2.37	2.54	0.47	0.73	0.66	0.96	0.71
FeO (T)	0.11	0.10	0.07	0.10	0.65	0.03	0.16	0.32	0.53	0.21	0.36	0.48	n.d.	0.14	0.76	n.d.
CaO	52.62	52.54	54.12	53.17	54.22	54.25	51.30	52.11	52.18	51.34	50.48	56.32	56.76	55.35	54.47	57.43
SrO	n.d.	0.45	0.11	0.18	0.53	0.42	0.93	n.d.	n.d.	n.d.	0.19	n.d.	n.d.	n.d.	n.d.	n.d.
Na2O	n.d.	n.d.	n.d.	0.79	n.d.	0.53	n.d.	n.d.	n.d.	0.82	n.d.	n.d.	n.d.	1.61	1.23	0.94
K2O	0.36	0.13	0.23	0.24	0.25	0.13	n.d.	0.18	n.d.	0.25	0.32	n.d.	n.d.	0.30	0.28	0.22
P2O5	40.35	42.45	41.51	42.50	42.88	42.83	36.03	35.69	36.26	36.53	36.59	39.85	39.92	38.98	38.11	38.90
La2O3	0.72	0.62	0.78	0.79	0.15	0.33	1.19	1.88	1.85	1.76	1.74	0.69	n.d.	0.80	1.13	n.d.
Ce2O3	2.10	1.82	1.66	1.12	0.58	0.98	4.50	4.64	3.95	4.13	3.87	1.32	1.22	1.42	2.70	1.02
Pr2O3	1.32	0.39	n.d.	n.d.	n.d.	n.d.	0.73	n.d.	n.d.	n.d.	0.84	n.d.	0.73	n.d.	n.d.	n.d.
Nd2O3	1.08	0.51	0.53	0.44	0.59	0.06	2.53	2.17	2.04	1.86	2.27	0.87	0.64	0.63	n.d.	0.62
NUMBERS OF THE IONS ON THE BASIS OF 25 (O, CL)																
P	5.791	5.996	5.877	5.976	5.982	5.999	5.379	5.309	5.353	5.428	5.454	5.714	5.702	5.629	5.561	5.592
Si	0.214	0.120	0.145	0.100	0.094	0.060	0.439	0.508	0.521	0.416	0.447	0.080	0.123	0.113	0.165	0.121
Ca	9.558	9.393	9.698	9.462	9.573	9.616	9.693	9.810	9.750	9.655	9.523	10.221	10.261	10.117	10.059	10.449
Fe2+	0.016	0.014	0.010	0.014	0.090	0.004	0.024	0.047	0.077	0.031	0.053	0.068		0.020	0.110	
Sr		0.044	0.011	0.017	0.050	0.040	0.095				0.019					
Na				0.254		0.170				0.279				0.532	0.411	0.309
K	0.078	0.028	0.049	0.051	0.053	0.027		0.040		0.056	0.072			0.065	0.062	0.048
La	0.045	0.038	0.048	0.048	0.009	0.020	0.077	0.122	0.119	0.114	0.113	0.043		0.050	0.072	
Ce	0.130	0.111	0.102	0.068	0.035	0.059	0.291	0.298	0.252	0.265	0.249	0.082	0.075	0.089	0.170	0.063
Pr	0.082	0.024					0.047				0.054		0.045			
Nd	0.065	0.030	0.032	0.026	0.035	0.004	0.159	0.136	0.127	0.117	0.143	0.053	0.039	0.038		0.038
REEs (T)	0.322	0.203	0.181	0.143	0.079	0.083	0.574	0.557	0.498	0.496	0.559	0.178	0.159	0.177	0.242	0.101
Ca site	9.97	9.68	9.95	9.94	9.84	9.94	10.39	10.45	10.33	10.52	10.23	10.47	10.42	10.91	10.88	10.91
P site	6.00	6.12	6.02	6.08	6.08	6.06	5.82	5.82	5.87	5.84	5.90	5.79	5.83	5.74	5.73	5.71

Appendix 4-1. continued

Layered ferroaugite syenite of lower series

CL color	Brownish pink			Yellow		Pink		Brownish pink		Yellow			B. pink	Pink
	core			rim		core		mantal		rim			core	rim
Anal. No.	C58-1	C58-2	C58-3	C58-4	C58-5	C58-6	C58-7	C58-8	C58-9	C58-10	C58-11	C58-12	C58-13	C58-14
SiO2	1.50	1.67	1.73	0.49	n.d.	0.73	0.77	1.93	3.53	1.58	1.18	n.d.	3.04	0.65
FeO (T)	0.11	0.18	0.21	n.d.	0.12	n.d.	0.30	n.d.	n.d.	0.22	n.d.	0.37	n.d.	0.11
CaO	51.67	50.92	48.88	53.78	54.21	52.80	52.99	48.93	45.99	51.04	52.83	52.84	50.23	53.36
SrO	n.d.	n.d.	n.d.	n.d.	n.d.	n.d.	n.d.	n.d.	n.d.	0.35	0.28	1.02	n.d.	n.d.
Na2O	n.d.	0.68	n.d.	n.d.	n.d.	n.d.	0.60	n.d.	n.d.	0.72	n.d.	1.86	n.d.	n.d.
K2O	0.26	n.d.	n.d.	0.20	n.d.	n.d.	0.31	n.d.	0.32	0.38	0.38	0.33	0.11	n.d.
P2O5	41.52	42.38	41.68	44.53	44.36	44.02	42.94	41.22	37.42	42.60	42.77	42.94	39.80	43.81
La2O3	1.24	1.14	1.42	0.25	n.d.	0.58	0.35	1.45	2.77	0.48	n.d.	n.d.	1.58	0.72
Ce2O3	2.51	2.04	3.46	0.69	0.44	0.92	1.09	4.06	6.49	1.32	0.95	n.d.	3.16	1.04
Pr2O3	n.d.	n.d.	0.89	n.d.	0.43	n.d.	n.d.	0.92	1.28	n.d.	n.d.	n.d.	n.d.	n.d.
Nd2O3	0.94	1.00	1.19	n.d.	0.35	0.64	0.47	1.48	2.19	0.82	0.83	0.32	1.52	0.32
NUMBERS OF THE IONS ON THE BASIS OF 25 (O, CL)														
P	5.895	5.952	5.959	6.140	6.147	6.115	6.008	5.900	5.550	5.980	6.000	6.035	5.706	6.083
Si	0.252	0.277	0.292	0.080		0.120	0.127	0.326	0.618	0.262	0.196		0.515	0.107
Ca	9.285	9.051	8.845	9.385	9.507	9.282	9.383	8.864	8.632	9.068	9.380	9.399	9.114	9.377
Fe2+	0.015	0.025	0.030		0.016		0.041			0.031		0.051		0.015
Sr										0.034	0.027	0.098		
Na		0.219					0.192			0.231		0.599		
K	0.056			0.042			0.065		0.072	0.080	0.080	0.070	0.024	
La	0.077	0.070	0.088	0.015		0.035	0.021	0.090	0.179	0.029			0.099	0.044
Ce	0.154	0.124	0.214	0.041	0.026	0.055	0.066	0.251	0.416	0.080	0.058		0.196	0.062
Pr			0.055		0.026			0.057	0.082					
Nd	0.056	0.059	0.072		0.020	0.038	0.028	0.089	0.137	0.049	0.049	0.019	0.092	0.019
REEs (T)	0.287	0.253	0.429	0.056	0.072	0.128	0.115	0.488	0.814	0.158	0.107	0.019	0.387	0.125
Ca site	9.64	9.55	9.30	9.48	9.60	9.41	9.80	9.35	9.52	9.60	9.59	10.24	9.52	9.52
P site	6.15	6.23	6.25	6.22	6.15	6.23	6.14	6.23	6.17	6.24	6.20	6.04	6.22	6.19

Appendix 4-1. continued

Layered ferroaugite syenite of upper series

CL color	Brownish pink		Light pink		Brownish pink		Light pink		Pink		Brownish pink		Light pink		
	core		rim		core		rim		core		mantle		rim		
Anal. No.	C65-1	C65-2	C65-3	C65-4	C65-5	C65-6	C65-7	C65-8	C70-1	C70-2	C70-3	C70-4	C70-5	C70-6	C70-7
SiO2	1.26	1.34	n.d.	n.d.	1.90	2.60	n.d.	n.d.	1.32	1.47	5.52	4.44	0.92	1.04	0.70
FeO (T)	0.37	0.17	n.d.	0.22	n.d.	n.d.	n.d.	0.38	n.d.	n.d.	0.38	0.08	n.d.	0.21	0.20
CaO	52.39	51.50	54.60	55.38	51.14	47.48	54.33	52.23	49.92	53.67	40.97	40.65	54.53	54.82	55.75
SrO	0.85	n.d.	n.d.	n.d.	n.d.	n.d.	n.d.	0.33	0.24	0.18	n.d.	n.d.	0.24	0.23	1.04
Na2O	0.91	n.d.	n.d.	n.d.	0.84	2.32	n.d.	n.d.	0.92	n.d.	n.d.	0.75	n.d.	1.13	n.d.
K2O	n.d.	n.d.	0.20	0.23	n.d.	0.32	0.20	0.15	0.19	0.12	n.d.	n.d.	0.32	0.30	0.25
P2O5	40.17	41.25	42.78	42.36	38.92	38.41	43.01	41.98	36.79	37.83	28.99	29.79	38.66	35.59	38.95
La2O3	0.94	0.99	0.75	0.44	1.81	1.63	n.d.	0.77	1.80	1.51	4.47	4.68	0.68	0.56	n.d.
Ce2O3	2.10	2.78	1.68	0.84	3.37	3.75	1.71	2.18	4.63	2.73	12.31	10.99	1.83	3.00	1.79
Pr2O3	n.d.	0.70	n.d.	n.d.	n.d.	0.80	n.d.	0.85	1.66	0.48	1.85	3.25	0.73	0.81	n.d.
Nd2O3	0.93	1.18	n.d.	n.d.	1.93	1.97	0.61	1.14	2.45	2.01	4.65	5.37	1.43	2.34	1.32
NUMBERS OF THE IONS ON THE BASIS OF 25 (O, CL)															
P	5.763	5.883	6.016	5.976	5.655	5.635	6.043	5.999	5.526	5.546	4.744	4.867	5.644	5.327	5.639
Si	0.214	0.226			0.326	0.451			0.234	0.255	1.067	0.857	0.159	0.184	0.120
Ca	9.512	9.296	9.717	9.888	9.404	8.815	9.661	9.446	9.490	9.958	8.484	8.405	10.075	10.385	10.215
Fe2+	0.052	0.024		0.031				0.054			0.061	0.013		0.031	0.029
Sr	0.084							0.032	0.025	0.018			0.024	0.024	0.103
Na	0.299				0.280	0.779			0.316			0.281		0.387	
K			0.042	0.049		0.071	0.042	0.032	0.043	0.027			0.070	0.068	0.055
La	0.059	0.062	0.046	0.027	0.115	0.104		0.048	0.118	0.096	0.319	0.333	0.043	0.037	
Ce	0.130	0.171	0.102	0.051	0.212	0.238	0.104	0.135	0.301	0.173	0.871	0.776	0.116	0.194	0.112
Pr		0.043				0.051		0.052	0.107	0.030	0.130	0.229	0.046	0.052	
Nd	0.056	0.071			0.118	0.122	0.036	0.069	0.155	0.124	0.321	0.370	0.088	0.148	0.081
REEs (T)	0.245	0.347	0.148	0.078	0.445	0.515	0.140	0.304	0.681	0.424	1.641	1.708	0.293	0.431	0.193
Ca site	10.19	9.67	9.91	10.05	10.13	10.18	9.84	9.87	10.56	10.43	10.19	10.41	10.46	11.33	10.59
P site	5.98	6.11	6.02	5.98	5.98	6.09	6.04	6.00	5.76	5.80	5.81	5.72	5.80	5.51	5.76

Appendix 4-1. continued

	LFAS of upper series		Unlayered ferroaugite syenite													
CL color	Bronze		Bronze core	B. pink rim	Pink core	B. pink mamtle	Light pink rim		Pink		Light pink core			Pink rim		Brown spot
Anal. No.	C72-1	C72-2	C100-1	C100-2	C101-1	C101-2	C101-3	C101-4	C188-1	C188-2	C302-1	C302-2	C302-3	C302-4	C302-5	C302-6
SiO2	1.40	1.55	0.88	2.35	0.30	2.63	0.18	n.d.	0.81	0.78	n.d.	0.59	0.44	0.99	0.58	1.45
FeO (T)	0.31	0.42	0.13	n.d.	0.50	0.43	0.23	0.57	0.14	0.30	0.20	0.40	0.24	0.25	0.19	0.30
CaO	52.83	53.11	55.76	49.18	53.57	45.55	52.75	52.75	53.50	53.45	55.75	55.27	55.70	51.31	52.99	50.97
SrO	n.d.	n.d.	0.43	n.d.	n.d.	0.36	0.69	2.20	0.31	n.d.	n.d.	n.d.	n.d.	n.d.	n.d.	n.d.
Na2O	0.64	n.d.	n.d.	n.d.	n.d.	n.d.	1.78	n.d.	n.d.	n.d.	n.d.	n.d.	n.d.	n.d.	0.80	n.d.
K2O	n.d.	0.19	n.d.	0.23	0.19	0.32	0.23	0.15	n.d.	0.27	0.16	0.18	n.d.	0.35	n.d.	0.07
P2O5	42.43	41.52	42.09	38.95	42.46	39.48	42.62	43.45	43.19	43.11	42.88	43.16	42.78	41.53	41.79	40.20
La2O3	0.58	0.75	n.d.	1.83	0.79	1.95	n.d.	n.d.	0.38	0.58	0.44	n.d.	n.d.	0.51	0.46	1.54
Ce2O3	1.32	1.43	n.d.	4.05	1.52	5.02	n.d.	n.d.	0.97	0.96	0.57	n.d.	n.d.	1.78	2.03	2.96
Pr2O3	n.d.	n.d.	n.d.	1.36	n.d.	1.18	0.44	n.d.	n.d.	n.d.	n.d.	n.d.	n.d.	2.12	n.d.	n.d.
Nd2O3	0.44	0.81	0.53	1.80	0.34	2.46	0.96	0.71	0.28	n.d.	n.d.	0.40	n.d.	1.17	0.82	1.95
NUMBERS OF THE IONS ON THE BASIS OF 25 (O, CL)																
P	5.933	5.859	5.891	5.688	5.997	5.795	6.002	6.102	6.032	6.029	5.998	5.994	5.984	5.926	5.931	5.811
Si	0.231	0.258	0.145	0.405	0.050	0.456	0.030		0.134	0.129		0.097	0.073	0.167	0.097	0.248
Ca	9.349	9.485	9.876	9.090	9.575	8.462	9.401	9.376	9.456	9.460	9.869	9.714	9.861	9.266	9.518	9.325
Fe2+	0.043	0.059	0.018		0.070	0.062	0.032	0.079	0.019	0.041	0.028	0.055	0.033	0.035	0.027	0.043
Sr			0.041			0.036	0.067	0.212	0.030							
Na	0.205						0.574								0.260	
K		0.040		0.051	0.040	0.071	0.049	0.032		0.057	0.034	0.038		0.075		0.015
La	0.035	0.046		0.116	0.049	0.125			0.023	0.035	0.027			0.032	0.028	0.097
Ce	0.080	0.087		0.256	0.093	0.319			0.059	0.058	0.034			0.110	0.125	0.185
Pr				0.085		0.075	0.027							0.130		
Nd	0.026	0.048	0.031	0.111	0.020	0.152	0.057	0.042	0.016			0.023		0.070	0.049	0.119
REEs (T)	0.141	0.182	0.031	0.569	0.162	0.670	0.084	0.042	0.098	0.093	0.061	0.023		0.342	0.202	0.401
Ca site	9.74	9.77	9.97	9.71	9.85	9.30	10.21	9.74	9.60	9.65	9.99	9.83	9.89	9.72	10.01	9.78
P site	6.16	6.12	6.04	6.09	6.05	6.25	6.03	6.10	6.17	6.16	6.00	6.09	6.06	6.09	6.03	6.06

Appendix 4-2. Representive compositions of apatites in syenites from Center II, Coldwell Complex

	Pic Island layered syenite														
CL color	L. pink	B. pink	Pink	B.pink	L. pink	Pink	Pink	B.pink	Dull pink		L. pink	Pink	L. pink	Pink	Pink
	core	mantle	rim 1	rim 2	core	mantle	rim 1	rim 2					core	mantle	rim 1
Anal. No.	C623-1	C623-2	C623-3	C623-4	C623-4	C623-5	C623-6	C623-7	C623-7	C623-8	C623-10	C624-1	C629-1	C629-2	C629-3
SiO2	0.41	0.85	0.40	0.72	0.41	0.88	0.52	0.51	0.45	0.41	n.d.	n.d.	n.d.	1.61	1.27
FeO (T)	0.18	0.23	n.d.	n.d.	n.d.	n.d.	0.21	0.39	n.d.	n.d.	0.18	n.d.	0.12	n.d.	n.d.
CaO	55.75	51.59	54.69	54.83	56.07	54.76	54.52	53.40	56.38	55.88	53.91	57.29	54.71	55.00	53.54
SrO	0.18	n.d.	n.d.	0.21	n.d.	0.21	n.d.	n.d.	n.d.	n.d.	0.92	n.d.	1.05	n.d.	n.d.
Na2O	1.06	0.81	n.d.	n.d.	n.d.	0.87	n.d.	n.d.	n.d.	n.d.	0.62	0.43	1.08	n.d.	0.63
K2O	0.35	0.23	0.26	0.39	0.27	0.31	0.19	0.24	0.31	0.21	0.21	0.22	n.d.	0.09	0.18
P2O5	41.32	39.73	40.60	40.54	41.73	40.27	41.69	39.84	41.00	41.73	41.07	39.66	42.04	40.12	41.68
La2O3	n.d.	1.40	0.56	1.15	0.46	1.06	0.50	1.67	0.71	0.73	0.94	0.92	0.31	1.07	1.12
Ce2O3	0.64	2.64	1.36	1.54	0.65	1.23	0.76	2.17	0.96	0.77	1.45	1.38	0.64	1.27	1.53
Pr2O3	n.d.	1.12	1.23	n.d.	n.d.	n.d.	0.84	0.66	n.d.	n.d.	n.d.	n.d.	n.d.	n.d.	n.d.
Nd2O3	n.d.	1.24	0.81	0.57	0.40	0.34	0.59	0.66	n.d.	n.d.	1.45	n.d.	n.d.	0.58	n.d.
NUMBERS OF IONS ON THE BASIS OF 25 (O, CL)															
P	5.836	5.772	5.820	5.792	5.880	5.748	5.904	5.781	5.816	5.889	5.865	5.704	5.937	5.710	5.869
Si	0.068	0.146	0.068	0.121	0.068	0.148	0.087	0.087	0.075	0.068				0.271	0.211
Ca	9.965	9.485	9.921	9.914	9.998	9.893	9.771	9.806	10.122	9.980	9.744	10.429	9.778	9.906	9.541
Fe2+	0.025	0.033					0.029	0.056			0.025		0.017		
Sr	0.017			0.021		0.021					0.090		0.102		
Na	0.343	0.269				0.284					0.203	0.142	0.349		0.203
K	0.074	0.050	0.056	0.084	0.057	0.067	0.041	0.052	0.066	0.045	0.045	0.048		0.019	0.038
La		0.089	0.035	0.072	0.028	0.066	0.031	0.106	0.044	0.045	0.058	0.058	0.019	0.066	0.069
Ce	0.039	0.166	0.084	0.095	0.040	0.076	0.047	0.136	0.059	0.047	0.090	0.086	0.039	0.078	0.093
Pr		0.070	0.076				0.051	0.041							
Nd		0.076	0.049	0.034	0.024	0.020	0.035	0.040			0.087			0.035	
REEs (T)	0.039	0.400	0.244	0.201	0.092	0.162	0.164	0.323	0.103	0.092	0.235	0.143	0.058	0.179	0.162
Ca site	10.46	10.24	10.22	10.22	10.15	10.43	10.01	10.24	10.29	10.12	10.34	10.76	10.30	10.10	9.94
P site	5.90	5.92	5.89	5.91	5.95	5.90	5.99	5.87	5.89	5.96	5.87	5.70	5.94	5.98	6.08

Appendix 4-2. continued

	Pic Island layered syenite													Neys Park syenite	
CL color	Brownish pink			L. pink	Pink	B. pink	Brown	L. pink	Pink		Pink		Dull pink		Brownish pink	
	rim 2			core	mantle	rim 1	rim 2	core	mantle		rim 1	rim 3	core		core	
Anal. No.	C629-4	C629-5	C629-6	C629-7	C629-8	C629-9	C629-10	C630-1	C630-5	C630-1	C630-2	C630-3	C630-6	C630-7	C97-1	C97-2
SiO2	3.48	3.02	2.96	1.05	1.80	2.91	2.36	0.31	0.65	0.79	1.55	0.86	n.d.	1.00	2.91	2.18
FeO (T)	0.28	0.20	0.08	0.09	0.14	0.10	0.18	0.15	n.d.	n.d.	1.46	0.14	0.11	n.d.	0.17	n.d.
CaO	50.02	51.05	52.77	53.96	51.21	50.37	50.50	55.40	53.52	52.46	50.97	51.68	55.49	53.09	50.95	49.48
SrO	n.d.	0.20	n.d.	0.71	n.d.	0.21	0.57	n.d.	0.22	n.d.	n.d.	n.d.	n.d.	0.19	n.d.	0.32
Na2O	n.d.	0.40	n.d.	0.43	1.16	0.54	0.41	n.d.	0.95	n.d.	n.d.	0.57	0.47	1.00	n.d.	1.26
K2O	n.d.	0.16	n.d.	0.27	0.20	0.12	n.d.	0.15	0.19	0.42	0.13	0.06	0.12	n.d.	n.d.	0.14
P2O5	38.60	38.45	39.47	41.46	40.39	38.81	38.59	42.75	41.08	40.67	40.55	40.97	42.20	40.99	38.89	39.39
La2O3	2.66	1.41	1.47	0.87	1.24	1.83	2.05	0.23	1.06	1.07	0.82	1.18	0.40	1.27	0.96	1.52
Ce2O3	3.83	3.26	2.37	0.92	2.36	3.44	3.29	0.49	1.34	2.75	2.15	2.65	0.83	2.03	3.59	3.60
Pr2O3	n.d.	0.60	n.d.	n.d.	0.73	0.42	0.81	n.d.	n.d.	0.70	1.30	1.07	n.d.	n.d.	n.d.	0.46
Nd2O3	1.07	1.16	0.81	n.d.	0.77	0.82	1.17	0.39	0.64	0.92	1.02	0.82	0.33	0.34	n.d.	1.65
NUMBERS OF IONS ON THE BASIS OF 25 (O, CL)																
P	5.572	5.558	5.621	5.861	5.771	5.614	5.618	5.981	5.858	5.851	5.809	5.873	5.945	5.834	5.662	5.703
Si	0.593	0.516	0.498	0.175	0.304	0.497	0.406	0.051	0.109	0.134	0.262	0.146		0.168	0.500	0.373
Ca	9.137	9.340	9.511	9.653	9.261	9.222	9.304	9.809	9.659	9.552	9.242	9.376	9.893	9.562	9.389	9.066
Fe2+	0.040	0.029	0.011	0.013	0.020	0.014	0.026	0.021			0.207	0.020	0.015		0.024	
Sr		0.020		0.069		0.021	0.057		0.021					0.019		0.032
Na		0.132		0.139	0.380	0.179	0.137		0.310			0.187	0.152	0.326		0.418
K		0.035		0.058	0.043	0.026		0.032	0.041	0.091	0.028	0.013	0.025			0.031
La	0.167	0.089	0.091	0.054	0.077	0.115	0.130	0.014	0.066	0.067	0.051	0.074	0.025	0.079	0.061	0.096
Ce	0.239	0.204	0.146	0.056	0.146	0.215	0.207	0.030	0.083	0.171	0.133	0.164	0.051	0.125	0.226	0.225
Pr		0.037			0.045	0.026	0.051			0.043	0.080	0.066				0.029
Nd	0.065	0.071	0.049		0.046	0.050	0.072	0.023	0.039	0.056	0.062	0.050	0.020	0.020		0.101
REEs (T)	0.472	0.401	0.286	0.110	0.314	0.407	0.460	0.067	0.187	0.337	0.326	0.354	0.095	0.224	0.287	0.451
Ca site	9.65	9.96	9.81	10.04	10.02	9.87	9.98	9.93	10.22	9.98	9.80	9.95	10.18	10.13	9.70	10.00
P site	6.16	6.07	6.12	6.04	6.08	6.11	6.02	6.03	5.97	5.99	6.07	6.02	5.94	6.00	6.16	6.08

Appendix 4-2. continued

	Neys Park syenite											Neys Park gabbro				
CL color	Pink mantle		Brownish pink rim		Light pink				Brownish pink			Violet				
Anal. No.	C97-3	C97-4	C97-5	C97-6	C114-1	C114-2	C114-3	C114-4	C3118a-1	C3118a-2	C3118d-1	C107-1	C107-2	C107-3	C107-4	C107-5
SiO2	n.d.	n.d.	1.54	2.09	0.77	0.60	0.77	n.d.	1.40	1.76	1.20	0.45	n.d.	0.48	0.62	0.38
FeO (T)	0.24	n.d.	n.d.	n.d.	0.08	0.05	n.d.	0.07	0.19	n.d.	0.11	n.d.	n.d.	0.21	0.09	n.d.
CaO	50.69	52.65	53.02	50.97	53.07	54.79	55.03	53.88	51.45	52.35	50.14	53.87	54.25	54.64	55.33	52.88
SrO	n.d.	1.35	n.d.	n.d.	n.d.	0.21	n.d.	n.d.	n.d.	n.d.	0.26	n.d.	0.25	0.26	0.26	n.d.
Na2O	2.21	0.71	n.d.	n.d.	1.20	0.82	n.d.	n.d.	1.76	n.d.	1.90	0.60	n.d.	n.d.	n.d.	1.53
K2O	0.22	n.d.	0.12	0.17	0.17	0.25	0.34	0.18	0.31	n.d.	n.d.	n.d.	0.32	0.17	0.26	0.15
P2O5	40.91	41.90	41.12	38.86	40.41	41.01	41.10	43.53	40.02	40.39	40.29	42.41	42.12	42.62	42.87	42.25
La2O3	0.91	0.69	1.02	2.19	1.10	0.50	0.52	0.63	1.15	1.62	1.27	1.04	0.79	0.59	0.56	0.80
Ce2O3	2.79	1.30	2.41	3.52	1.95	1.10	0.82	0.95	2.36	3.04	2.88	1.56	1.50	0.98	n.d.	1.60
Pr2O3	1.07	0.50	n.d.	n.d.	0.41	n.d.	n.d.	n.d.	n.d.	n.d.	0.97	n.d.	0.67	n.d.	n.d.	0.40
Nd2O3	0.59	0.80	0.76	1.56	0.59	0.61	0.69	0.71	n.d.	0.75	0.97	n.d.	n.d.	n.d.	n.d.	n.d.
NUMBERS OF IONS ON THE BASIS OF 25 (O, CL)																
P	5.918	5.977	5.830	5.667	5.799	5.824	5.845	6.090	5.777	5.774	5.808	5.968	5.973	5.973	5.971	5.963
Si			0.258	0.360	0.131	0.101	0.129		0.239	0.297	0.204	0.075		0.079	0.102	0.063
Ca	9.280	9.506	9.513	9.408	9.638	9.848	9.905	9.540	9.399	9.471	9.148	9.595	9.736	9.692	9.753	9.446
Fe2+	0.034				0.011	0.007		0.010	0.027		0.016			0.029	0.012	
Sr		0.132				0.020					0.026		0.024	0.025	0.025	
Na	0.732	0.232			0.394	0.267			0.582		0.627	0.193				0.495
K	0.048		0.026	0.037	0.037	0.054	0.073	0.038	0.067				0.068	0.036	0.055	0.032
La	0.057	0.043	0.063	0.139	0.069	0.031	0.032	0.038	0.072	0.101	0.080	0.064	0.049	0.036	0.034	0.049
Ce	0.175	0.080	0.148	0.222	0.121	0.068	0.050	0.057	0.147	0.188	0.180	0.095	0.092	0.059		0.098
Pr	0.067	0.031			0.025						0.060		0.041			0.024
Nd	0.036	0.048	0.045	0.096	0.036	0.037	0.041	0.042		0.045	0.059					
REEs (T)	0.334	0.202	0.256	0.457	0.251	0.135	0.124	0.138	0.220	0.334	0.378	0.159	0.182	0.095	0.034	0.171
Ca site	10.43	10.07	9.79	9.90	10.33	10.33	10.10	9.73	10.30	9.80	10.20	9.95	10.01	9.88	9.88	10.14
P site	5.92	5.98	6.09	6.03	5.93	5.92	5.97	6.09	6.02	6.07	6.01	6.04	5.97	6.05	6.07	6.03

Appendix 4-2. continued

	Neys Park gabbro							Recrystallized syenite								
CL color	Violet			Light violet				Pink						Light pink core		
Anal. No.	C107-6	C107-7	C107-8	C107-9	C107-10	C107-11	C107-12	C572-1	C572-2	C572-3	C572-4	C572-5	C572-6	C587-1	C587-2	C587-3
SiO2	0.51	0.75	n.d.	n.d.	0.47	0.55	0.54	1.20	0.78	1.26	n.d.	1.26	1.20	1.31	1.45	1.45
FeO (T)	0.16	n.d.	0.12	0.12	n.d.	0.12	0.28	0.09	0.12	n.d.	n.d.	0.09	0.25	n.d.	n.d.	n.d.
CaO	52.99	53.42	53.81	52.78	54.02	55.00	54.24	53.21	54.36	55.19	55.77	54.23	54.73	56.28	56.41	55.95
SrO	n.d.	n.d.	0.62	1.13	0.37	0.33	0.33	n.d.	n.d.	0.27	1.49	n.d.	n.d.	n.d.	n.d.	n.d.
Na2O	0.64	n.d.	n.d.	0.51	0.68	n.d.	0.73	1.04	n.d.	n.d.	n.d.	0.49	n.d.	n.d.	n.d.	n.d.
K2O	0.19	0.16	0.17	0.18	0.27	0.20	n.d.	0.32	0.28	0.25	0.25	0.18	0.37	n.d.	n.d.	n.d.
P2O5	42.61	42.93	42.92	40.96	41.40	41.38	41.57	38.59	39.16	39.76	39.39	39.24	39.33	39.00	38.70	39.05
La2O3	0.95	1.06	0.82	0.74	0.89	0.81	0.57	1.41	1.03	0.89	1.44	1.08	1.51	0.42	0.83	1.00
Ce2O3	1.27	1.67	1.45	1.83	1.33	1.18	1.26	2.32	2.47	1.79	1.44	2.25	2.02	1.87	1.65	1.90
Pr2O3	n.d.	n.d.	n.d.	0.63	n.d.	n.d.	n.d.	0.69	0.87	n.d.	n.d.	0.40	n.d.	n.d.	n.d.	n.d.
Nd2O3	n.d.	n.d.	n.d.	0.57	0.50	n.d.	n.d.	0.97	0.78	0.58	n.d.	0.72	0.59	0.54	0.55	0.59
NUMBERS OF IONS ON THE BASIS OF 25 (O, CL)																
P	6.009	6.009	6.043	5.911	5.882	5.873	5.892	5.620	5.685	5.689	5.721	5.658	5.663	5.615	5.575	5.607
Si	0.085	0.124			0.079	0.092	0.090	0.206	0.134	0.213		0.215	0.204	0.223	0.247	0.246
Ca	9.458	9.464	9.589	9.639	9.713	9.879	9.730	9.808	9.988	9.995	10.251	9.897	9.974	10.254	10.285	10.167
Fe2+	0.022		0.017	0.017		0.017	0.039	0.013	0.017			0.013	0.036			
Sr			0.060	0.112	0.036	0.032	0.032			0.026	0.148					
Na	0.207			0.169	0.221		0.237	0.347				0.162				
K	0.040	0.034	0.036	0.039	0.058	0.043		0.070	0.061	0.054	0.055	0.039	0.080			
La	0.058	0.065	0.050	0.047	0.055	0.050	0.035	0.089	0.065	0.055	0.091	0.068	0.095	0.026	0.052	0.063
Ce	0.077	0.101	0.088	0.114	0.082	0.072	0.077	0.146	0.155	0.111	0.090	0.140	0.126	0.116	0.103	0.118
Pr				0.039				0.043	0.054			0.025				
Nd				0.035	0.030			0.060	0.048	0.035		0.044	0.036	0.033	0.033	0.036
REEs (T)	0.136	0.166	0.139	0.235	0.167	0.123	0.112	0.338	0.322	0.201	0.182	0.277	0.256	0.176	0.188	0.216
Ca site	9.86	9.66	9.84	10.21	10.19	10.09	10.15	10.58	10.39	10.28	10.64	10.39	10.35	10.43	10.47	10.38
P site	6.09	6.13	6.04	5.91	5.96	5.97	5.98	5.83	5.82	5.90	5.72	5.87	5.87	5.84	5.82	5.85

Appendix 4-2. continued

	Recrystallized syenite					Unrecrystallized syenite								
CL color	Brownish pink mantle		Brown rim	Light pink 2nd. apatite rim		Light pink core		Pink mantle		Brownish pink rim		Light pink core		
Anal. No.	C587-4	C587-5	C587-6	C587-7	C587-8	C291-1	C291-2	C291-3	C291-4	C291-5	C291-6	C293-1	C293-2	C293-3
SiO2	2.89	3.03	4.62	1.73	1.98	n.d.	0.46	1.14	1.11	4.49	4.02	0.26	n.d.	0.39
FeO (T)	n.d.	n.d.	n.d.	n.d.	n.d.	n.d.	0.45	0.09	n.d.	0.14	n.d.	0.21	n.d.	n.d.
CaO	52.97	51.21	48.89	55.49	55.75	53.86	56.20	54.44	55.49	42.16	46.33	55.42	56.51	55.19
SrO	n.d.	n.d.	n.d.	n.d.	n.d.	0.79	n.d.	n.d.	n.d.	0.40	n.d.	n.d.	n.d.	0.41
Na2O	n.d.	n.d.	n.d.	n.d.	n.d.	1.46	n.d.	n.d.	n.d.	n.d.	0.74	n.d.	n.d.	1.00
K2O	n.d.	n.d.	n.d.	n.d.	n.d.	0.28	0.10	0.14	0.20	n.d.	0.22	0.27	n.d.	0.15
P2O5	35.66	35.99	33.82	37.48	37.21	40.63	41.39	39.52	39.56	31.56	33.72	41.21	41.30	41.36
La2O3	2.05	2.50	3.36	1.18	1.37	n.d.	n.d.	1.32	1.06	4.68	3.50	0.68	0.49	n.d.
Ce2O3	4.14	4.19	6.07	2.20	2.15	0.79	1.08	2.92	2.58	9.52	7.47	1.06	0.80	0.94
Pr2O3	0.47	0.73	1.17	0.54	n.d.	0.67	n.d.	n.d.	n.d.	2.79	1.03	n.d.	0.46	n.d.
Nd2O3	1.63	1.98	1.92	0.89	0.35	1.17	0.32	0.43	n.d.	3.64	2.38	n.d.	0.45	0.41
NUMBERS OF IONS ON THE BASIS OF 25 (O, CL)														
P	5.295	5.355	5.111	5.476	5.447	5.843	5.842	5.691	5.675	5.038	5.180	5.876	5.860	5.856
Si	0.507	0.533	0.825	0.299	0.342		0.077	0.194	0.188	0.847	0.729	0.044		0.065
Ca	9.954	9.643	9.350	10.260	10.329	9.802	10.040	9.921	10.075	8.517	9.007	10.002	10.148	9.889
Fe2+							0.063	0.013		0.022		0.030		
Sr						0.078				0.044				0.040
Na						0.481					0.260			0.324
K						0.061	0.021	0.030	0.043		0.051	0.058		0.032
La	0.133	0.162	0.221	0.075	0.087			0.083	0.066	0.325	0.234	0.042	0.030	
Ce	0.266	0.270	0.397	0.139	0.136	0.049	0.066	0.182	0.160	0.657	0.496	0.065	0.049	0.058
Pr	0.030	0.047	0.076	0.034		0.041				0.192	0.068		0.028	
Nd	0.102	0.124	0.122	0.055	0.022	0.071	0.019	0.026		0.245	0.154		0.027	0.024
REEs (T)	0.531	0.603	0.816	0.303	0.245	0.162	0.085	0.291	0.226	1.419	0.953	0.108	0.134	0.082
Ca site	10.48	10.25	10.17	10.56	10.57	10.58	10.21	10.26	10.34	10.00	10.27	10.20	10.28	10.37
P site	5.80	5.89	5.94	5.77	5.79	5.84	5.92	5.88	5.86	5.88	5.91	5.92	5.86	5.92

Appendix 4-2. continued

Unrecrystallized syenite

CL color		Pink		Brownish pink			Light pink		Pink		Light pink	Light pink			
		mantle		rim			core		rim			core			
Anal. No.	C293-4	C293-5	C293-6	C293-7	C293-8	C293-9	C275-1	C275-2	C275-3	C275-4	C275-5	C472-1	C472-2	C472-3	C472-4
SiO2	1.06	0.84	1.12	2.46	3.70	3.12	0.50	0.46	0.76	0.94	0.49	1.52	0.87	1.08	n.d.
FeO (T)	0.11	n.d.	n.d.	n.d.	0.08	0.15	n.d.	n.d.	n.d.	0.15	n.d.	0.08	0.17	n.d.	0.12
CaO	53.73	55.35	52.65	51.77	45.50	44.31	56.95	55.62	54.04	53.98	55.73	52.81	54.91	54.49	54.63
SrO	0.39	n.d.	0.39	n.d.	n.d.	1.14	n.d.	n.d.	n.d.	0.21	n.d.	n.d.	n.d.	n.d.	0.77
Na2O	n.d.	n.d.	1.02	1.52	n.d.	n.d.	0.61	n.d.	n.d.	0.68	0.84	0.70	0.57	n.d.	n.d.
K2O	0.13	0.19	n.d.	n.d.	0.20	0.19	0.15	0.27	0.22	0.24	n.d.	0.12	0.23	0.17	0.25
P2O5	40.24	40.11	39.39	36.12	33.81	34.52	41.19	42.23	40.01	40.78	41.57	39.34	40.10	40.24	40.31
La2O3	0.69	0.97	1.37	2.09	3.67	3.46	n.d.	0.52	1.04	0.95	0.29	1.58	0.66	1.19	1.09
Ce2O3	2.14	1.70	2.82	4.73	7.95	7.49	0.61	0.90	1.79	1.83	1.09	2.79	1.50	2.71	1.84
Pr2O3	0.44	n.d.	n.d.	n.d.	1.84	1.79	n.d.	n.d.	0.84	n.d.	n.d.	n.d.	n.d.	n.d.	n.d.
Nd2O3	0.65	0.69	1.01	1.31	3.20	2.63	n.d.	n.d.	1.28	n.d.	n.d.	0.91	0.91	n.d.	0.69
NUMBERS OF IONS ON THE BASIS OF 25 (O, CL)															
P	5.778	5.742	5.707	5.355	5.222	5.368	5.803	5.925	5.763	5.808	5.856	5.680	5.736	5.756	5.822
Si	0.180	0.142	0.192	0.431	0.675	0.573	0.083	0.076	0.129	0.158	0.082	0.259	0.147	0.182	
Ca	9.764	10.029	9.654	9.713	8.895	8.721	10.155	9.877	9.851	9.729	9.936	9.649	9.941	9.864	9.986
Fe2+	0.016				0.012	0.023				0.021		0.011	0.024		0.017
Sr	0.038		0.039			0.121				0.020					0.076
Na			0.338	0.516			0.197			0.222	0.271	0.231	0.187		
K	0.028	0.041			0.047	0.045	0.032	0.057	0.048	0.052		0.026	0.050	0.037	0.054
La	0.043	0.061	0.086	0.135	0.247	0.234		0.032	0.065	0.059	0.018	0.099	0.041	0.074	0.069
Ce	0.133	0.105	0.177	0.303	0.531	0.504	0.037	0.055	0.111	0.113	0.066	0.174	0.093	0.168	0.115
Pr	0.027				0.122	0.120			0.052						
Nd	0.039	0.042	0.062	0.082	0.209	0.173			0.078			0.055	0.055		0.042
REEs (T)	0.243	0.207	0.325	0.520	1.109	1.030	0.037	0.086	0.307	0.172	0.084	0.329	0.189	0.242	0.226

Appendix 4-2. continued

Unrecrystallized syenite

CL color	Brownish pink rim				Light pink 2nd. apatite rim				Light pink core							
Anal. No.	C472-5	C472-6	C472-7	C472-8	C472-9	C472-10	C472-11	C472-12	C276-1	C276-2	C276-3	C276-4	C276-5	C276-6	C276-7	C276-8
SiO2	4.53	2.91	3.29	2.02	0.85	n.d.	1.45	1.31	1.05	1.34	1.20	1.20	1.32	1.32	1.20	1.24
FeO (T)	n.d.	0.32	n.d.	0.17	n.d.	0.52	n.d.	n.d.	n.d.	n.d.	n.d.	n.d.	n.d.	n.d.	n.d.	n.d.
CaO	44.53	50.49	48.30	51.08	53.32	53.43	53.58	52.49	53.15	52.49	52.49	52.69	51.44	51.90	53.76	53.16
SrO	n.d.	n.d.	0.33	0.21	0.47	1.72	n.d.	n.d.	n.d.	n.d.	n.d.	n.d.	n.d.	n.d.	n.d.	n.d.
Na2O	0.64	n.d.	1.36	0.77	0.67	n.d.	n.d.	n.d.	n.d.	n.d.	n.d.	n.d.	n.d.	1.05	n.d.	n.d.
K2O	n.d.	0.07	0.15	n.d.	0.19	0.27	0.12	n.d.	n.d.	n.d.	n.d.	n.d.	n.d.	0.27	0.21	0.24
P2O5	33.08	36.84	35.68	38.54	39.99	39.48	39.02	38.95	41.62	41.44	42.03	41.25	41.11	40.32	41.13	41.47
La2O3	4.38	2.11	2.08	1.78	1.33	1.32	1.57	1.74	0.95	0.48	1.48	1.60	1.05	0.97	0.95	1.26
Ce2O3	7.48	4.61	4.96	3.14	2.47	2.16	3.00	3.60	2.45	1.56	2.32	3.01	3.17	2.51	1.79	1.69
Pr2O3	1.38	n.d.	n.d.	n.d.	n.d.	n.d.	n.d.	0.88	0.31	n.d.	n.d.	n.d.	0.88	0.64	n.d.	n.d.
Nd2O3	2.67	1.63	2.59	1.41	0.47	0.38	0.74	1.05	0.47	0.50	0.51	0.18	0.87	1.03	0.80	0.88
NUMBERS OF IONS ON THE BASIS OF 25 (O, CL)																
P	5.143	5.461	5.367	5.633	5.763	5.781	5.661	5.674	5.895	5.925	5.932	5.867	5.878	5.782	5.838	5.873
Si	0.832	0.510	0.584	0.349	0.145		0.248	0.225	0.176	0.226	0.200	0.202	0.223	0.224	0.201	0.207
Ca	8.763	9.473	9.194	9.448	9.726	9.902	9.838	9.678	9.528	9.499	9.376	9.485	9.308	9.419	9.657	9.527
Fe2+		0.047		0.025		0.075										
Sr			0.034	0.021	0.046	0.173										
Na	0.228		0.468	0.258	0.221									0.345		
K		0.016	0.034		0.041	0.060	0.026							0.058	0.045	0.051
La	0.297	0.136	0.136	0.113	0.084	0.084	0.099	0.110	0.059	0.030	0.091	0.099	0.065	0.061	0.059	0.078
Ce	0.503	0.296	0.323	0.198	0.154	0.137	0.188	0.227	0.150	0.096	0.142	0.185	0.196	0.156	0.110	0.103
Pr	0.092							0.055	0.019				0.054	0.040		
Nd	0.175	0.102	0.164	0.087	0.029	0.023	0.045	0.065	0.028	0.030	0.030	0.011	0.052	0.062	0.048	0.053
REEs (T)	1.067	0.534	0.623	0.399	0.266	0.244	0.333	0.457	0.256	0.157	0.263	0.295	0.368	0.318	0.217	0.234
Ca site	10.06	10.07	10.35	10.15	10.30	10.45	10.20	10.13	9.78	9.66	9.64	9.78	9.68	10.14	9.92	9.81
P site	5.98	5.97	5.95	5.98	5.91	5.78	5.91	5.90	6.07	6.15	6.13	6.07	6.10	6.01	6.04	6.08

Appendix 4-2. continued

Unrecrystallized syenite

CL color	Light pink				Brownish pink					Light pink				
	core				rim					2nd. apatite rim				
Anal. No.	C276-9	C276-10	C276-11	C276-12	C276-13	C276-14	C276-15	C276-16	C276-17	C276-18	C276-19	C276-20	C276-21	C276-20
SiO2	1.08	0.96	1.65	1.26	2.50	2.32	2.43	1.94	2.17	1.29	0.79	0.92	0.86	0.93
FeO (T)	n.d.	n.d.	n.d.	n.d.	0.11	n.d.	n.d.	n.d.	n.d.	0.19	n.d.	n.d.	n.d.	n.d.
CaO	50.79	53.52	53.17	52.06	51.47	51.43	52.42	52.82	52.57	51.11	53.46	54.40	52.66	52.84
SrO	0.69	n.d.	n.d.	n.d.	n.d.	n.d.	n.d.	n.d.	n.d.	0.52	n.d.	n.d.	n.d.	n.d.
Na2O	n.d.	n.d.	n.d.	n.d.	n.d.	n.d.	n.d.	n.d.	n.d.	n.d.	n.d.	n.d.	n.d.	n.d.
K2O	n.d.	n.d.	n.d.	n.d.	n.d.	n.d.	n.d.	n.d.	n.d.	0.26	n.d.	n.d.	n.d.	n.d.
P2O5	40.89	41.84	41.81	41.47	39.62	39.59	39.98	39.33	40.63	41.02	41.70	42.45	41.88	41.88
La2O3	1.32	0.70	0.89	0.96	1.85	1.54	1.66	2.06	1.33	0.93	0.88	0.62	0.98	0.76
Ce2O3	3.41	1.72	1.70	2.82	3.68	3.08	3.51	3.83	2.49	2.65	1.91	1.14	1.70	1.52
Pr2O3	0.98	n.d.	n.d.	0.79	n.d.	0.49	n.d.	0.46	n.d.	1.27	0.44	n.d.	n.d.	n.d.
Nd2O3	0.72	0.74	0.78	0.66	0.65	0.86	n.d.	1.03	0.67	0.76	0.73	0.47	0.29	n.d.
NUMBERS OF IONS ON THE BASIS OF 25 (O, CL)														
P	5.885	5.922	5.876	5.893	5.686	5.708	5.699	5.633	5.767	5.872	5.912	5.942	5.972	5.974
Si	0.184	0.160	0.274	0.211	0.424	0.395	0.409	0.328	0.364	0.218	0.132	0.152	0.145	0.157
Ca	9.252	9.586	9.457	9.363	9.348	9.384	9.456	9.575	9.443	9.259	9.592	9.638	9.504	9.540
Fe2+					0.016					0.027				
Sr	0.068									0.051				
Na														
K										0.056				
La	0.083	0.043	0.054	0.059	0.116	0.097	0.103	0.129	0.082	0.058	0.054	0.038	0.061	0.047
Ce	0.212	0.105	0.103	0.173	0.228	0.192	0.216	0.237	0.153	0.164	0.117	0.069	0.105	0.094
Pr	0.061			0.048		0.030		0.028		0.078	0.027			
Nd	0.044	0.044	0.046	0.040	0.039	0.052		0.062	0.040	0.046	0.044	0.028	0.017	
REEs (T)	0.399	0.193	0.204	0.321	0.383	0.371	0.319	0.456	0.275	0.346	0.242	0.135	0.183	0.141
Ca site	9.72	9.78	9.66	9.68	9.75	9.76	9.78	10.03	9.72	9.74	9.83	9.77	9.69	9.68
P site	6.07	6.08	6.15	6.10	6.11	6.10	6.11	5.96	6.13	6.09	6.04	6.09	6.12	6.13

Appendix 4-3. Representive compositions of apatites in syenites from Center III, Coldwell Complex

	Magnesio-hornblende syenite							Contaminated ferro-edenite syenite				Ferro-edenite syenite			
CL color	Pink							Pink				Pink core		Brownish pink rim	
Anal. No.	C2123-1	C2123-2	C2123-3	C2123-4	C180-1	C180-2	C180-3	C2036-1	C2036-3	C2036-4	C2036-2	C2224-1	C2224-2	C2224-3	C2224-4
SiO2	n.d.	n.d.	0.20	0.54	0.32	0.25	n.d.	1.83	1.95	1.48	0.72	1.37	1.79	3.98	2.62
FeO (T)	0.14	0.17	0.30	0.07	0.15	0.33	0.15	n.d.	0.25	0.10	0.09	0.14	n.d.	n.d.	0.17
CaO	53.00	54.17	53.70	54.40	54.20	52.91	53.95	51.47	51.68	52.65	53.36	51.26	51.54	45.12	46.55
SrO	0.29	0.69	n.d.	n.d.	n.d.	0.16	0.48	n.d.	0.27	n.d.	n.d.	n.d.	n.d.	n.d.	1.30
Na2O	n.d.	n.d.	1.09	n.d.	n.d.	0.60	n.d.	0.73	n.d.	2.45	n.d.	n.d.	n.d.	n.d.	n.d.
K2O	n.d.	0.31	0.18	0.14	0.22	0.26	0.20	0.29	0.11	0.14	0.24	0.17	0.17	n.d.	0.07
P2O5	43.03	42.66	42.53	43.03	43.03	43.66	43.17	40.33	39.49	40.63	42.33	42.50	40.94	38.13	39.41
La2O3	0.66	0.20	0.55	0.44	0.39	0.46	n.d.	1.30	1.54	0.48	0.86	1.19	1.32	2.71	2.38
Ce2O3	1.20	0.71	0.79	0.96	0.55	0.75	0.79	2.72	3.36	1.26	1.55	2.28	3.37	6.60	5.01
Pr2O3	0.43	n.d.	n.d.	n.d.	0.45	0.26	0.43	n.d.	n.d.	n.d.	n.d.	n.d.	n.d.	0.57	n.d.
Nd2O3	0.54	0.24	0.35	n.d.	0.51	0.24	0.67	0.83	1.35	0.62	0.31	1.09	0.88	2.72	1.38
NUMBERS OF IONS ON THE BASIS OF 25 (O, CL)															
P	6.084	6.031	5.989	6.017	6.028	6.093	6.062	5.779	5.697	5.764	5.976	5.983	5.831	5.608	5.781
Si			0.033	0.089	0.053	0.041		0.310	0.332	0.248	0.120	0.228	0.301	0.691	0.454
Ca	9.484	9.693	9.570	9.627	9.609	9.346	9.587	9.333	9.436	9.452	9.534	9.133	9.290	8.399	8.643
Fe2+	0.020	0.024	0.042	0.010	0.021	0.045	0.021		0.036	0.014	0.013	0.019			0.025
Sr	0.028	0.067				0.015	0.046		0.027						0.131
Na			0.352			0.192		0.240		0.796					
K		0.066	0.038	0.030	0.046	0.055	0.042	0.063	0.024	0.030	0.051	0.036	0.036		0.015
La	0.041	0.012	0.034	0.027	0.024	0.028		0.081	0.097	0.030	0.053	0.073	0.082	0.174	0.152
Ce	0.073	0.043	0.048	0.058	0.033	0.045	0.048	0.169	0.210	0.077	0.095	0.139	0.208	0.420	0.318
Pr	0.026				0.027	0.016	0.026							0.036	
Nd	0.032	0.014	0.021		0.030	0.014	0.040	0.050	0.082	0.037	0.018	0.065	0.053	0.169	0.085
REEs (T)	0.172	0.070	0.103	0.085	0.114	0.103	0.114	0.300	0.389	0.144	0.166	0.277	0.342	0.798	0.555
Ca site	9.70	9.92	10.10	9.75	9.79	9.76	9.81	9.94	9.91	10.44	9.76	9.47	9.67	9.20	9.37
P site	6.08	6.03	6.02	6.11	6.08	6.13	6.06	6.09	6.03	6.01	6.10	6.21	6.13	6.30	6.24

Appendix 4-3. continued

Ferro-edenite syenite

CL color	Pink								Brownish pink		Pink			B. pink
Anal. No.	C2224-5	C2224-6	C2224-7	C2224-8	C2224-9	C2224-10	C2224-11	C2224-12	C2224-13	C2224-14	C322-1	C322-2	C322-3	C322-4
SiO2	n.d.	n.d.	0.43	n.d.	0.94	0.91	0.61	0.94	2.48	3.04	0.66	1.02	0.88	2.58
FeO (T)	n.d.	n.d.	0.10	n.d.	0.11	0.12	0.24	0.23	0.20	0.10	0.29	0.27	0.25	0.72
CaO	55.70	54.68	53.88	52.31	53.35	51.07	52.83	55.23	47.35	43.99	53.90	53.69	55.35	46.85
SrO	0.28	1.39	n.d.	1.45	n.d.	0.87	n.d.	n.d.	n.d.	0.28	0.41	n.d.	n.d.	0.29
Na2O	n.d.	0.80	1.57	n.d.	n.d.	n.d.	n.d.	n.d.	1.69	2.63	n.d.	n.d.	n.d.	2.91
K2O	0.27	0.22	0.20	0.46	0.19	n.d.	0.20	0.41	0.18	0.25	0.15	0.21	n.d.	n.d.
P2O5	42.17	40.80	41.34	42.25	43.67	42.18	43.78	39.54	37.33	37.22	42.26	40.85	41.50	37.40
La2O3	0.57	0.60	0.98	1.16	0.34	1.37	n.d.	0.90	1.69	1.68	0.63	0.75	n.d.	n.d.
Ce2O3	0.92	1.31	1.41	1.90	0.83	2.68	0.77	1.64	5.10	4.96	1.05	1.69	1.95	1.43
Pr2O3	n.d.	n.d.	n.d.	n.d.	n.d.	n.d.	0.43	n.d.	1.61	2.11	n.d.	n.d.	n.d	4.79
Nd2O3	n.d.	n.d.	n.d.	0.45	0.50	0.75	0.63	0.78	2.30	3.58	0.33	0.79	n.d	2.85
NUMBERS OF IONS ON THE BASIS OF 25 (O, CL)														
P	5.947	5.846	5.867	6.020	6.057	5.990	6.104	5.692	5.546	5.561	5.955	5.836	5.849	5.534
Si			0.072		0.154	0.153	0.100	0.160	0.435	0.536	0.110	0.172	0.146	0.451
Ca	9.941	9.916	9.677	9.434	9.365	9.178	9.322	10.063	8.902	8.318	9.613	9.707	9.872	8.774
Fe2+			0.014		0.015	0.017	0.033	0.033	0.029	0.015	0.040	0.038	0.035	0.105
Sr	0.027	0.136		0.142		0.085				0.029	0.040			0.029
Na		0.263	0.510						0.575	0.900				0.986
K	0.057	0.048	0.043	0.099	0.040		0.042	0.089	0.040	0.056	0.032	0.045		
La	0.035	0.037	0.061	0.072	0.021	0.085		0.056	0.109	0.109	0.039	0.047		
Ce	0.056	0.081	0.087	0.117	0.050	0.165	0.046	0.102	0.328	0.320	0.064	0.104	0.119	0.092
Pr							0.026		0.103	0.136				0.305
Nd				0.027	0.029	0.045	0.037	0.047	0.144	0.226	0.020	0.048		0.178
REEs (T)	0.091	0.119	0.147	0.216	0.100	0.294	0.109	0.206	0.684	0.791	0.122	0.199	0.119	0.574
Ca site	10.12	10.48	10.39	9.89	9.52	9.57	9.51	10.39	10.23	10.11	9.85	9.99	10.03	10.47
P site	5.95	5.85	5.94	6.02	6.21	6.14	6.20	5.85	5.98	6.10	6.07	6.01	6.00	5.98

Appendix 4-3. continued

	Ferro-edenite syenite					Quartz syenite			
CL color	Brownish pink			Pink in xonelith		Pink			
Anal. No.	C2124-1	C2124-2	C2124-3	C2124-4	C2124-5	C2087-1	C2087-2	C2087-3	C173-1
SiO2	2.09	2.79	3.57	0.63	1.46	n.d.	n.d.	0.18	1.05
FeO (T)	n.d.	0.30	0.25	0.14	0.16	n.d.	n.d.	n.d.	0.12
CaO	49.04	49.21	48.05	51.34	53.93	51.78	55.36	54.22	52.79
SrO	n.d.	0.96	n.d.	n.d.	n.d.	0.65	n.d.	n.d.	0.22
Na2O	n.d.	n.d.	n.d.	0.75	n.d.	1.42	n.d.	n.d.	n.d.
K2O	0.21	0.08	0.33	0.24	0.31	0.27	0.23	0.41	0.45
P2O5	40.52	37.58	38.81	44.39	38.94	42.04	42.73	42.70	42.26
La2O3	1.48	2.04	1.33	1.28	1.26	0.78	0.41	0.49	0.84
Ce2O3	3.42	4.56	4.69	1.22	2.44	1.67	0.80	0.98	1.64
Pr2O3	0.80	n.d.	n.d.	n.d.	0.58	0.40	n.d.	n.d.	n.d.
Nd2O3	2.45	2.41	1.97	n.d.	0.79	0.47	0.47	0.35	0.63
NUMBERS OF IONS ON THE BASIS OF 25 (O, CL)									
P	5.831	5.538	5.643	6.157	5.636	6.004	5.996	6.021	5.950
Si	0.355	0.486	0.613	0.103	0.250			0.030	0.175
Ca	8.932	9.178	8.843	9.012	9.879	9.359	9.832	9.677	9.407
Fe2+		0.044	0.036	0.019	0.023				0.017
Sr		0.097				0.064			0.021
Na				0.238		0.464			
K	0.046	0.018	0.072	0.050	0.068	0.058	0.049	0.087	0.095
La	0.093	0.131	0.084	0.077	0.079	0.049	0.025	0.030	0.052
Ce	0.213	0.291	0.295	0.073	0.153	0.103	0.049	0.060	0.100
Pr	0.050				0.036	0.025			
Nd	0.149	0.150	0.121		0.048	0.028	0.028	0.021	0.037
REEs (T)	0.504	0.571	0.500	0.151	0.317	0.205	0.101	0.111	0.189
Ca site	9.48	9.91	9.45	9.47	10.29	10.15	9.98	9.87	9.73
P site	6.19	6.02	6.26	6.26	5.89	6.00	6.00	6.05	6.12